



## Durham E-Theses

---

### *Shear strength, consolidation and drainage of colliery tailing lagoons*

Kirby, J. M.

#### How to cite:

---

Kirby, J. M. (1980) *Shear strength, consolidation and drainage of colliery tailing lagoons*, Durham theses, Durham University. Available at Durham E-Theses Online: <http://etheses.dur.ac.uk/7803/>

#### Use policy

---

The full-text may be used and/or reproduced, and given to third parties in any format or medium, without prior permission or charge, for personal research or study, educational, or not-for-profit purposes provided that:

- a full bibliographic reference is made to the original source
- a [link](#) is made to the metadata record in Durham E-Theses
- the full-text is not changed in any way

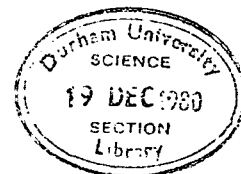
The full-text must not be sold in any format or medium without the formal permission of the copyright holders.

Please consult the [full Durham E-Theses policy](#) for further details.

SHEAR STRENGTH, CONSOLIDATION AND  
DRAINAGE OF COLLIERY TAILINGS LAGOONS

by

J. M. Kirby, B.Sc.



being a thesis presented in fulfilment of requirements for the degree of Doctor of Philosophy at the Department of Geological Sciences in the Faculty of Science of the University of Durham.

The copyright of this thesis rests with the author.  
No quotation from it should be published without  
his prior written consent and information derived  
from it should be acknowledged.

September 1980

ABSTRACT

Colliery tailings are laminated sediments which vary from coal-rich horizons of coarse sand size, to fine silt horizons composed mainly of quartz, illite and kaolinite. The proportion of finer laminae increases away from the inlet of the containing lagoon, although both fine and coarse bands are found everywhere in the lagoon. Coal itself has a low specific gravity and high friction coefficient. The density increases and the shear strength decreases away from the inlet. Both the average coal content (47%) and friction angle ( $35^{\circ}$ ) are higher for tailings than for coarse colliery discard (14% and  $31^{\circ}$  respectively).

The permeability of the contrasting laminae differs greatly, and consolidation and drainage in lagoons is therefore dominated by the horizontally laminated structure. Much of the water in lagoons drains laterally to the embankments. This water contains dissolved solids which reflect the groundwater chemistry of the Coal Measures at depth, being both saline and rich in sulphates.

Overtipping lagoons with coarse discard is being used increasingly for waste disposal purposes. It is possible to overtip with a 1.5m high layer of discard using a D6 vehicle at a sediment shear strength of  $3 \text{ KN/m}^2$ . However, to include a safety margin,  $4.5 \text{ KN/m}^2$  should be the lower bound. An effective stress stability study of overtipping indicates that a desiccated surface is necessary; the operation cannot progress where supernatant water remains on the lagoon. In terms of liquefaction hazards, vehicle vibration levels are not high enough to be of concern. Similarly, measured ground vibrations produced by explosives did not liquefy a lagoon being overtipped. It is suggested that a 200-year return period earthquake will not cause problems in this respect.

## ACKNOWLEDGEMENTS

I wish to thank my supervisor, Dr. R.K. Taylor, for the many useful discussions throughout this project, and Mr. G.R. Morrell for discussions and assistance in the field. The following technical staff of the Department of Geological Sciences rendered assistance: Mr. R.G. Hardy (Senior Experimental Officer), Mr. A.G. Swann, Mr. C.B. McEleavey and Mr. P. Kay.

I am indebted to the National Coal Board for the opportunity to pursue this research and in particular, the Chief Civil Engineer, Mr. A.R. Taylor. The views expressed in this thesis are those of the writer and not necessarily those of the N.C.B. Many of the N.C.B. staff have helped with information and access to the lagoons; Mr. A.R. Bacon (Senior Soils Engineer) deserves especial mention in this respect.

Thanks are also due to Mr. J. Van Der Merwe and Mr. M.J. Henderson for the use of their data.

The writer was supported by a grant from the Natural Environment Research Council. Much of the fieldwork was supported by N.C.B. research grants to Dr. Taylor.

TABLE OF CONTENTS

	Page
CHAPTER 1 INTRODUCTION	
1.1 Background (including Figs.1.1 to 1.3)	1
1.2 Previous Work	3
1.3 Aims of Current Investigation	7
1.4 Field Work Site Descriptions (including Figs.1.4 to 1.11)	8
1.5 Methods of Testing (including Fig.1.12)	14
1.6 Statistical Treatment of Results	16
1.7 Published Material	17
CHAPTER 2 THE USE OF THE FIELD VANE SHEAR TEST IN COLLIERY LAGOONS	
2.1 Introduction (including Fig.2.1)	18
2.2 Theoretical Considerations (including Figs.2.2 to 2.16 and Table 2.1)	20
2.3 Conclusions	38
CHAPTER 3 THE USE OF CONE PENETRATION TESTS IN COLLIERY LAGOONS	
3.1 Introduction	42
3.2 Field Testing Rig (Mark 1) (including Figs.3.1 and 3.2)	42
3.3 Field Penetration Results (including Figs 3.3 to 3.7 and Tables 3.1 and 3.2)	46
3.4 Field Testing Rig (Mark 2) (including Figs. 3.8 and 3.9)	53
3.5 Interpretation of Static Cone Penetration Tests (including Figs.3.10 and 3.11 and Table 3.3)	59
3.6 An Investigation into the Applicability of Vesic's Model to Cone Penetration Tests (including Figs.3.12 to 3.15 and Tables 3.4 to 3.6)	63
3.7 Conclusions	74
CHAPTER 4 THE GEOCHEMISTRY AND SEMINENTOLOGY OF COLLIERY LAGOONS	
4.1 Introduction	76
4.2 The Determination of Mineralogy (including Fig. 4.1)	76
4.3 The Determination of Chemistry (including Tables 4.1 and 4.2)	78

	Page
4.4 The Use of Burnt Samples for Analysis (including Figs.4.2 and 4.3)	81
4.5 The Recalculation of Mineralogy from Chemistry (including Table 4.3)	85
4.6 The Chemistry and Mineralogy of Colliery Tailings Lagoons (including Figs.4.4 to 4.17 and Table 4.4)	88
4.7 The Sedimentology of Colliery Tailings Lagoons (including Figs.4.18 to 4.22)	107
4.8 A Note on Sampling and Bias in Studies on Colliery Lagoons	116
4.9 The Relationship Between Organic Carbon Content and Specific Gravity (including Fig.4.23)	117
4.10 On the Difference Between Tailings and Slurry Lagoons (including Table 4.5)	118
4.11 Comparison of Lagoon and Tip Geochemistry	124
4.12 The Stabilisation of Fine Colliery Discard with Cement (including Figs.4.24 to 4.26 and Tables 4.6 to 4.10)	124
4.13 The Groundwater Chemistry of Tailings Lagoons (including Fig.4.27 and Tables 4.11 and 4.12)	131
4.14 Conclusions	139
CHAPTER 5 THE SHEAR STRENGTH OF COLLIERY LAGOONS	
5.1 Introduction	142
5.2 A Note on Stress Paths (including Figs.5.1 to 5.3)	142
5.3 The Comparison of Field Vane Test Data and Laboratory Shear Strength Envelopes	146
5.4 The Investigation at Peckfield Colliery (including Figs.5.4 to 5.16 and Tables 5.1 to 5.4)	148
5.5 East Hetton (including Figs.5.17 to 5.21 and Table 5.5)	179
5.6 Maltby (including Figs.5.22 to 5.25)	189
5.7 Silverhill (including Figs.5.26 and 5.27)	197

	Page
5.8 The Comparison of the Shear Strength of Coarse and Fine Discard (including Fig.5.28)	200
5.9 A Note on the Young's Modulus of Fine Colliery Discard (including Fig.5.29)	202
5.10 The Coefficient of Earth Pressure at Rest ( $K_o$ ) (Including Fig.5.30)	204
5.11 Conclusions	204
<b>CHAPTER 6 THE CONSOLIDATION AND DRAINAGE OF COLLIERY TAILINGS LAGOONS</b>	
6.1 Introduction	209
6.2 Theoretical Considerations	210
6.3 The Measurement of Consolidation Parameters (including Fig.6.1 and Table 6.1)	214
6.4 The Measurement of Permeability <u>In-Situ</u> (including Figs.6.2 to 6.6)	218
6.5 The Consolidation and Drainage of Lagoon 109B at East Hetton Colliery (including Figs.6.7 to 6.11 and Table 6.2)	226
6.6 The Consolidation and Drainage of Lagoon 16 at Silverhill (including Figs.6.12 to 6.16 and Table 6.3)	237
6.7 A Note on Gibson's Consolidation Model for an Accreting Deposit (including Fig.6.17)	242
6.8 The Comparison of <u>In-Situ</u> Measured Permeability Values for East Hetton and Silverhill Lagoons (including Fig.6.18)	246
6.9 The Consolidation and Drainage of Lagoons 6 and 7 at Peckfield Colliery (including Figs.6.19 to 6.23 and Tables 6.4 and 6.5)	246
6.10 The Consolidation and Drainage of Lagoon 6 at Maltby Colliery (including Fig.6.24 and Table 6.6)	254
6.11 The Compressibility of Colliery Lagoon Sediments (including Fig.6.25)	254
6.12 The Drainage of Colliery Lagoons (including Figs.6.26 to 6.31 and Table 6.7)	257
6.13 Conclusions	272

	Page
CHAPTER 7 THE OVERTIPPING OF COLLIERY LAGOONS	
7.1 Introduction (including Figs.7.1 to 7.4)	275
7.2 The Maltby Overtipping Trial (including Figs.7.5 to 7.10 and Tables 7.1 and 7.2)	276
7.3 The Overtipping Operation at Silverhill (including Figs.7.11 to 7.16 and Table 7.3)	292
7.4 The Bearing Capacity of Lagoon Sediments (including Figs.7.17 to 7.22 and Tables 7.4 to 7.6)	299
7.5 The Stability of an Excavated Face in a Lagoon (including Fig.7.23)	313
7.6 Conclusions	315
CHAPTER 8 CONCLUSIONS	318
REFERENCES	330
APPENDIX 2.1 THE STRESS DISTRIBUTIONS AT THE ENDS OF A VANE	337
APPENDIX 2.2 EQUATIONS OF TORQUE FOR VANES	342
APPENDIX 4.1 MINERALOGY DETERMINED BY X-RAY DIFFRACTION	345
APPENDIX 4.2 STANDARDS CALIBRATIONS AND THE REGRESSION EQUATIONS USED TO DETERMINE THE COMPOSITION OF SAMPLES	346
APPENDIX 4.3 THE REPEATABILITY OF COUNTS OBTAINED FROM THE XRF EQUIPMENT	351
APPENDIX 4.4 CHEMISTRY DETERMINED BY X-RAY FLOURESCENCE	354
APPENDIX 4.5 MINERALOGY RECALCULATED FROM THE XRF ANALYSIS	358
APPENDIX 4.6 ANALYSIS AND RESULTS OF THE WATER CHEMISTRY OF LAGOONS	350
APPENDIX 5.1 IN-SITU VANE TEST SHEAR STRENGTH DATA	362
APPENDIX 6.1 LABORATORY CONSOLIDATION DATA	365
APPENDIX 6.2 IN-SITU PERMEABILITY DETERMINATION, EAST HETTON	375
APPENDIX 6.3 IN-SITU PERMEABILITY MEASUREMENTS, SILVERHILL	377



## CHAPTER 1 INTRODUCTION

### 1.1 Background

The operation involved in winning coal generates a considerable amount of waste. Much of the waste from development roads in modern pits is segregated and taken out of the mine separately. The remainder is conveyed with the coal and is known as 'run of mine'. Prior to the Second World War the quantity of waste material in the run of mine was small, because the coal was sorted efficiently by hand at the face. In 1930, 200M tonnes of coal were produced with 7M tonnes of waste. Modern, mechanised mining techniques have produced a great increase in the output of waste. In 1966/67, 107M tonnes of coal were produced, with 50M tonnes of waste, of which 5M tonnes were fine discard. (Fine discard is described in the following paragraphs.)

Probably the most common treatment for separating the coal is the jig washer, as shown schematically in Fig.1.1. The raw product is first separated on screens at 125mm; the material coarser than 125mm is crushed. Some fine coal is usually extracted from the -125mm fraction as a dry product for blending later. The -125mm run of mine is customarily treated in Baum jigs which separate coal from discard according to their relative densities. Clean coal from the jigs is separated from the process water by vibrating screens and de-watered in dryers.

Small coal may be separated by froth flotation. The slurry of sand, silt and clay sized materials (- 0.5mm) remaining after the coal is skimmed off is known as tailings.

The coarse discard from the jigs is separated from process water by draining in perforated bucket elevators and high speed vibrating screens. The coarse discard is then delivered to the tip at about 10 per cent moisture content. Dirty water from the coarse discard de-watering process

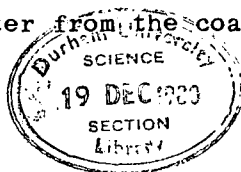
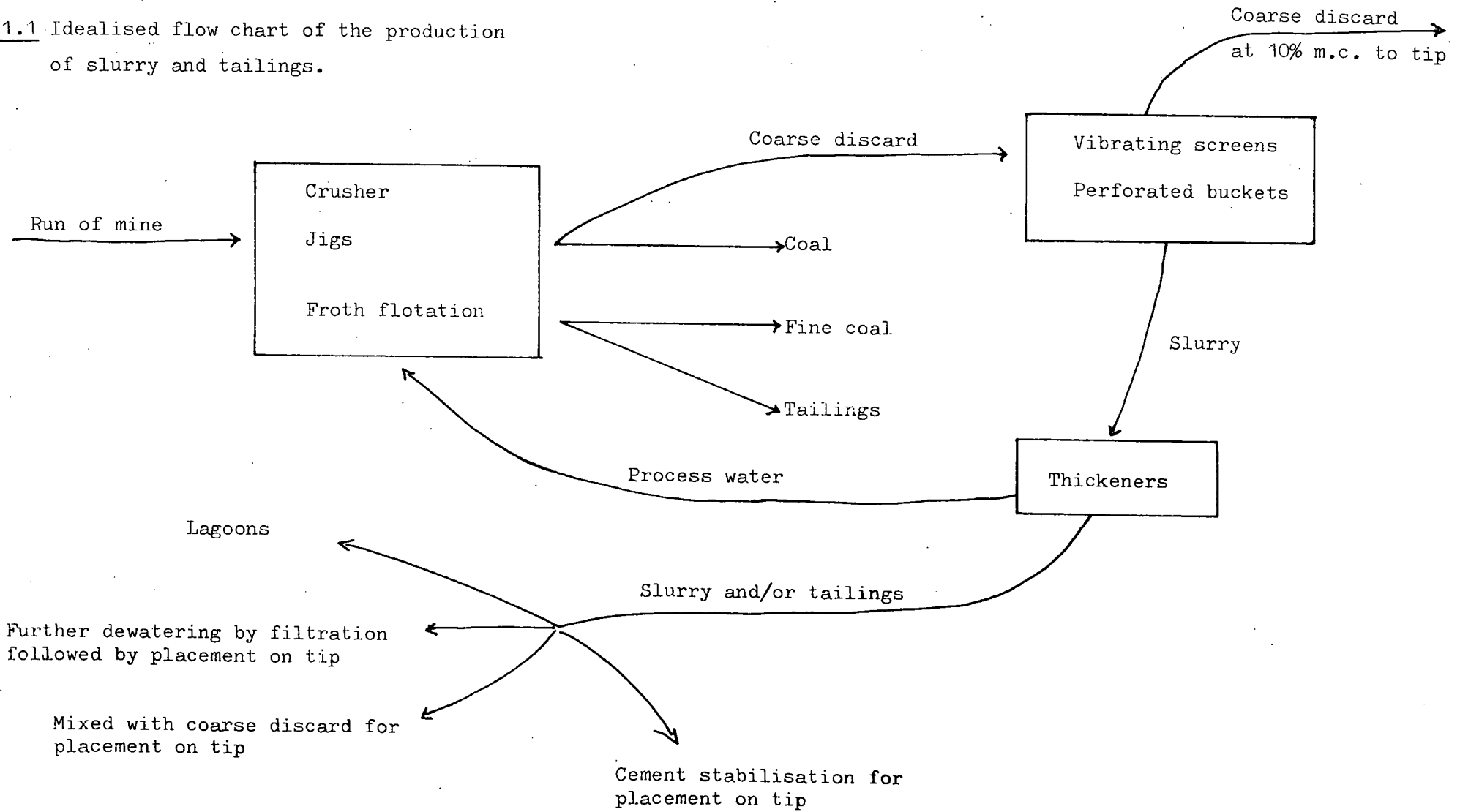


Fig.1.1 Idealised flow chart of the production of slurry and tailings.



and the tailings are treated with flocculents. Settlement in thickeners produces clean water for re-use and a thick, concentrated tailings pulp. Depending on whether there is a froth flotation plant in operation this is termed tailings or slurry, or collectively, fine discard.

At this stage the fine discard has a moisture content of several tens to a few hundred per cent, depending on the details of the process. This fine discard may be disposed of in several ways (Fig.1.1). Quantitatively the most important is disposal by pumping into impoundments referred to as lagoons. This is the cheapest method of disposal; comparative costs are given in Fig.1.2. Alternatively, the slurry or tailings may be filtered under pressure, either direct or vacuum, to produce a product dry enough for direct placement on the tip (c.20 per cent moisture content). The material may be mixed with coarse discard for direct placement on the tip, which can have the advantage of improving the grading characteristics of the coarse discard. Cement stabilisation for direct placement on the tip is not quantitatively important at the present time.

Lagoons themselves are composed of two parts. Firstly, there is the fine discard to be disposed of; secondly, the floor and embankments required to impound the fine discard. The floor and the embankments may be composed of various materials depending on local circumstances. The lagoon may be excavated into the local country rock, thus having natural materials for both the walls and the floor (see Fig.1.3.a). Alternatively, it may be formed in a valley with part man-made embankments, or on flat land with wholly artificially constructed containing embankments (Figs. 1.3. b-d). Finally it may be formed on the tip, this having both walls and floor of coarse discard, commonly with a view to over-tipping to produce a composite structure (Fig.1.3.e).

## 1.2 Previous work

Since the Aberfan disaster in 1966, there has been considerable

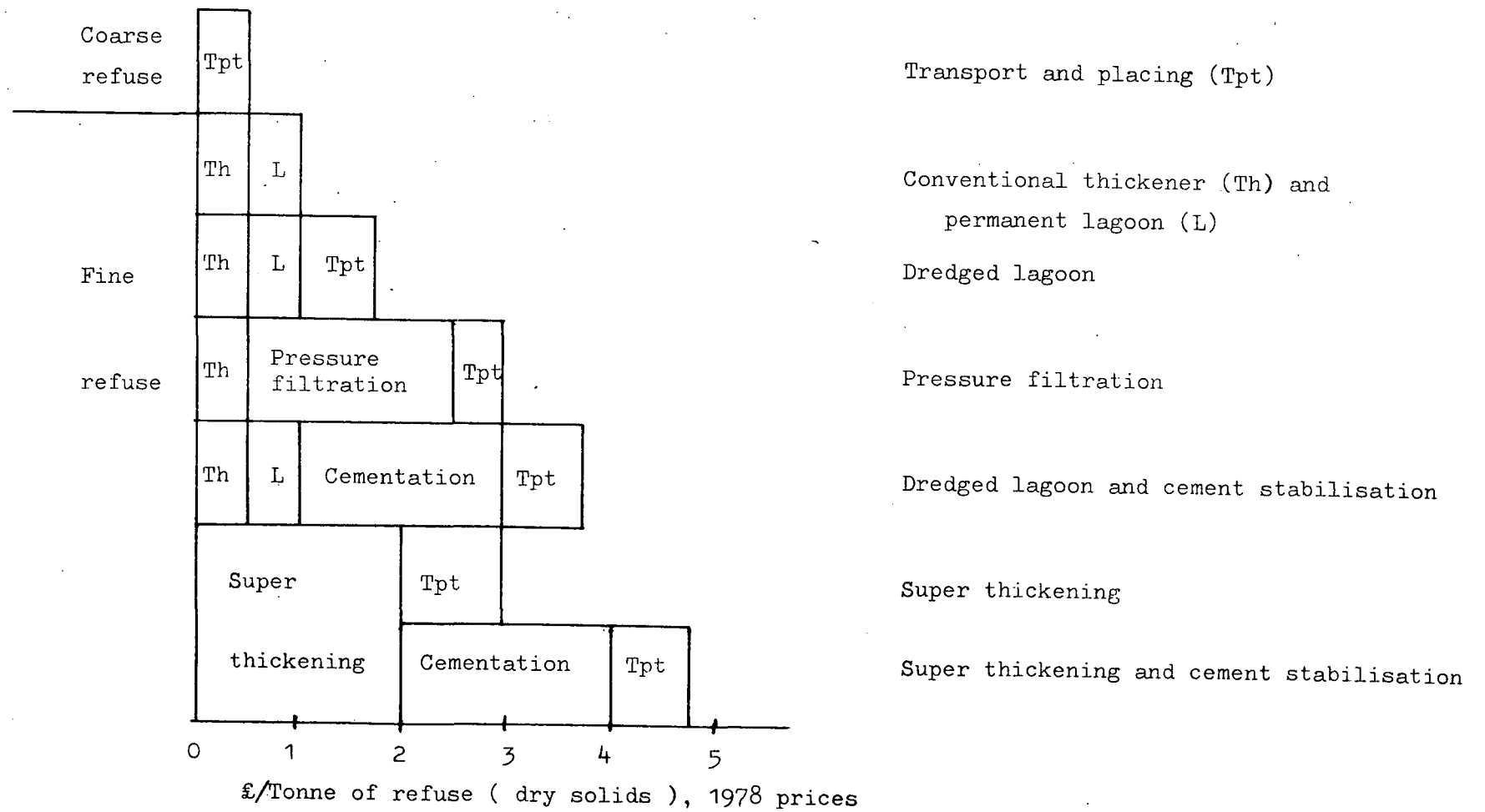
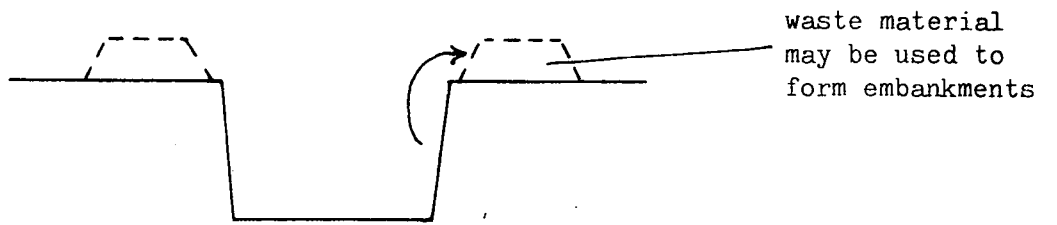


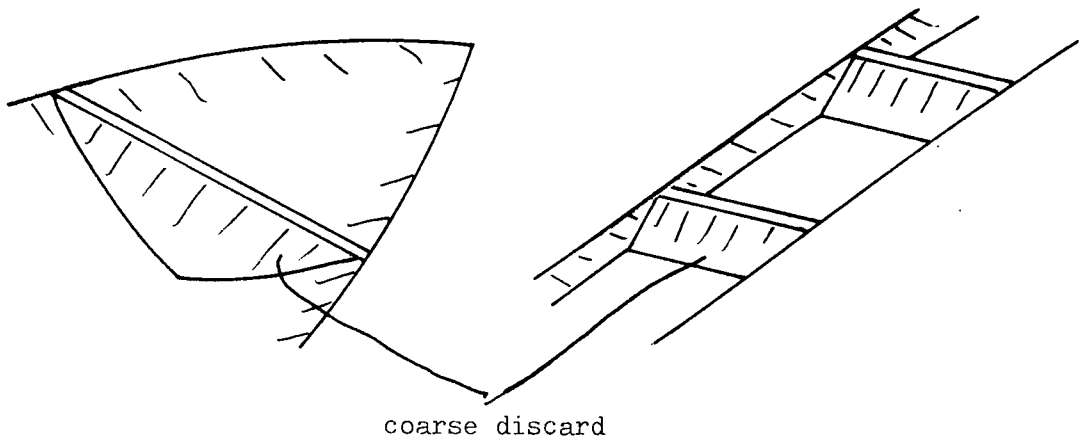
Fig.1.2 Relative costs of the different methods for the disposal of fine discard.

a. Excavated lagoon

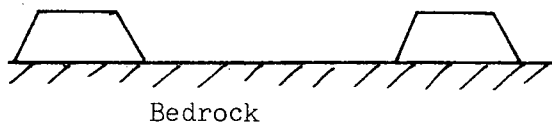


b. Partially constructed walls; cross valley

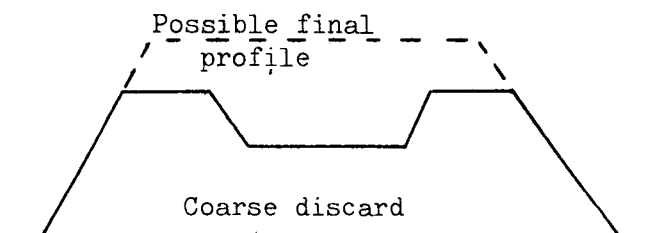
c. Partially constructed walls; in valley



d. All constructed walls



e. On tip



(N.B. Diagrammatic only)

research into the behaviour of tips and lagoons, McKechnie Thomson and Rodin, (1972); National Coal Board ('Red Book', 1972). Work on lagoons has concentrated on the geotechnical parameters. Lagoon sediments were found to vary from highly stratified to relatively homogenous deposits. The grain size of the material ranges from coarse sand to clay, generally with a fairly high coal content and therefore low specific gravity. Taylor and Cobb (1977) give the average organic carbon content of lagoons as 38.24 per cent. Lagoon sediments exist in a loose state, with high void ratios. National Coal Board (1972), Cobb (1977) and Taylor and Morrell (1978) quote void ratios from 0.4 to 1.4, with many values in the upper part of the range.

In-situ vane shear tests (NCB, 1972; Cobb, 1977) have proved the deposits to possess variable but generally low undrained shear strengths. The vane shear strength is often below  $40\text{kN/m}^2$ ; one lagoon at Williamthorpe colliery possesses no material stronger than  $1.5\text{ kN/m}^2$  in the top 8m of the deposit (NCB, 1972). Cobb (1977) showed that despite the variability of the in-situ shear strengths, much useful information may be extracted by comparing the results with various shear strength versus depth relationships. Laboratory shear strength tests indicate that the material has effective friction angles ranging from 22 to 40 degrees, with most values between 30 and 35 degrees. It is known that the coal content influences the friction angle of coarse discard (Taylor, 1974); this effect may be present in fine discard also (Cobb, 1977).

From oedometer tests, McKechnie Thomson and Rodin (1972) found that lagoon material generally has very low coefficients of consolidation, in the range 2 to  $30\text{ m}^2/\text{yr}$ . Cobb (1977) found that with the Rowe cell values of up to  $400\text{ m}^2/\text{yr}$  are measured. Tailings are generally incompressible, compression indices ranging from 0.02 to 0.27 (NCB, 1972). Cobb (1977) also found that the compressibility of lagoon sediments remained

fairly constant across a lagoon.

Few in-situ permeability measurements have been reported for lagoon deposits, despite a generally expressed preference for in-situ rather than laboratory measurements of this parameter. NCB (1972) find that the in-situ permeability values range from  $10^{-5}$  to  $10^{-8}$  m/sec, but fail to find a correlation with the type of deposit.

Previous work on the mineralogy and chemistry of colliery tailings has shown that the sediments consist of (in approximate order of abundance): clays (illite and kaolinite, the proportion of the latter increasing in the Northern coalfields, see Taylor and Spears, 1970), organic carbon, quartz, carbonates, pyrite and minor amounts of other constituents. The organic carbon is frequently the principal constituent, on occasion comprising up to 88 per cent by weight of the sample (Taylor and Morrell, 1979).

### 1.3 Aims of the Current Investigation

One of the major aims of this project has been to relate the shear strength and consolidation characteristics to the structure of lagoon deposits. In this respect a theoretical investigation of vane shear tests in layered media is outlined in Chapter 2. Cone penetration tests are considered as an alternative tool for measuring strengths in-situ in Chapter 3. Chapter 4 is concerned with the fundamental controls on the characteristics of lagoon sediments, namely the sedimentology, chemistry and mineralogy. The relationship of these fundamental controls to shear strength and consolidation parameters is investigated in Chapters 5 and 6. The in-situ permeability of lagoons is also investigated in Chapter 6 and the results used to investigate the drainage characteristics.

Finally, overtipping is a practice that will logically be used on an increasing scale as planning pressures on tipping sites continue to

increase. The bearing capacity of lagoon sediments and their behaviour with respect to liquefaction and drainage when overtipped is investigated in Chapter 7. Previous work has shown that fine colliery discard consists of the full range from sediments that liquefy readily to those that are very resistant to collapse under laboratory conditions (Kennedy, 1977; Taylor et al., 1978; Taylor and Morrell, 1979). This phenomenon is investigated in the field as well as in the laboratory in Chapter 7.

#### 1.4 Field Work Site Descriptions

Laboratory and field studies have mainly concentrated on lagoons at East Hetton Colliery (Northeastern Area, National Coal Board), Maltby (South Yorkshire), Peckfield (North Yorkshire) and Silverhill (North Nottinghamshire). Minor parts of the work involve lagoons at Gedling (South Nottinghamshire), Oakdale (South Wales) and Orgreave (South Yorkshire). The locations of these collieries are shown in Fig.1.4. The four main sites are described below.

##### 1. East Hetton

The lagoons at East Hetton are situated in a steep-sided, flat-bottomed valley which was originally formed as a glacial overflow channel (see Fig.1.5). Superficial deposits are generally thin along the valley sides; a thin layer of recent alluvial material covers the valley floor. A drain allows the Kelloe Beck to run beneath the lagoons and its flow is supplemented by waste from the overflow towers in the lagoons. Lagoon 109C was in use from 1950 onwards; in 1956/7 an embankment was constructed across the centre and the eastern wall raised to form lagoon 109B (see Fig 1.6). This continued to receive material until 1966 when lagoon 109A came into operation. In May 1977 repairs to the eastern bank of 109A necessitated a temporary excavation in 109B which removed some 6500 m<sup>3</sup> of material to a depth of 4m. This temporarily received material in the



Fig.1.4 Location of fieldwork sites.

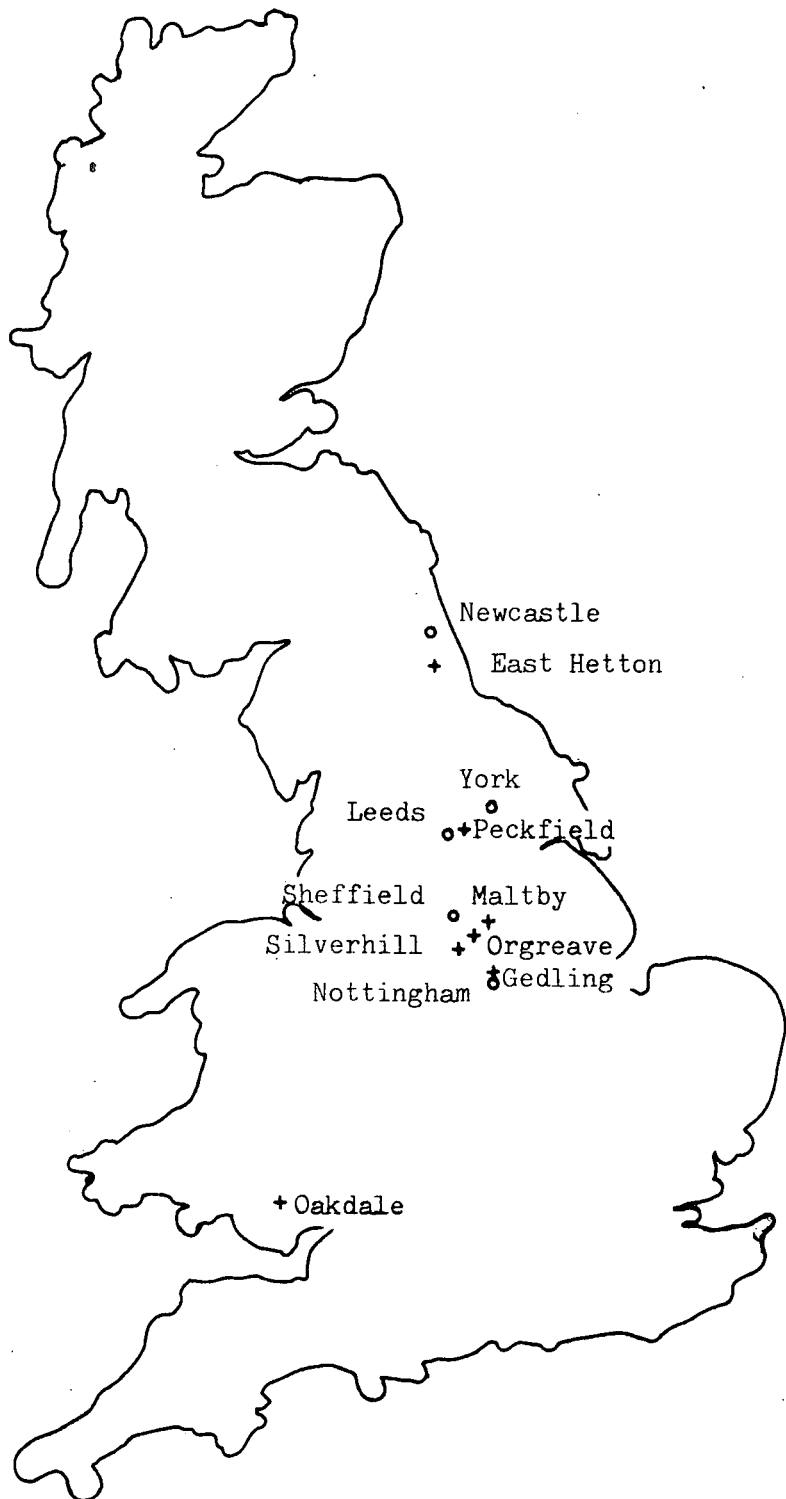


Fig.1.5 The lagoons at East Hetton.

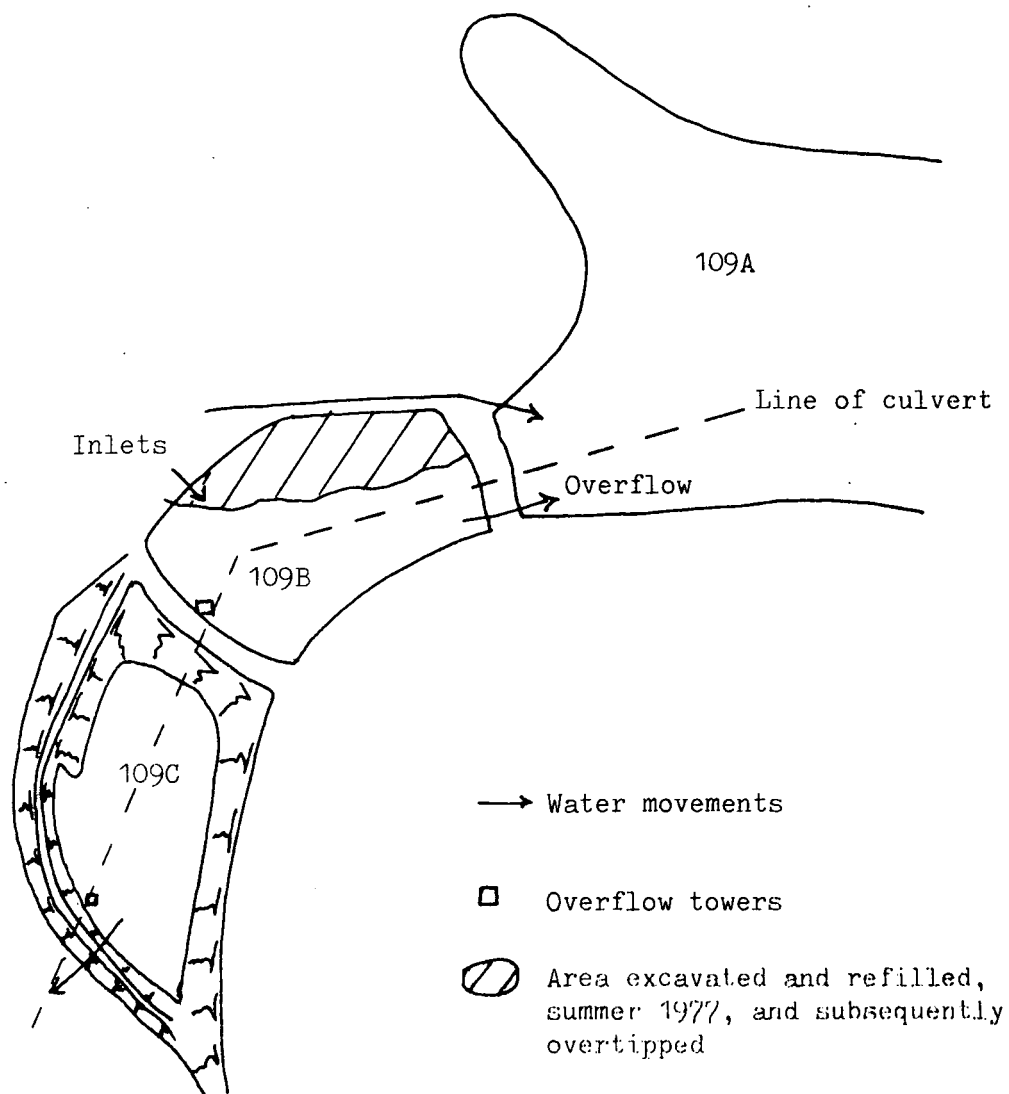
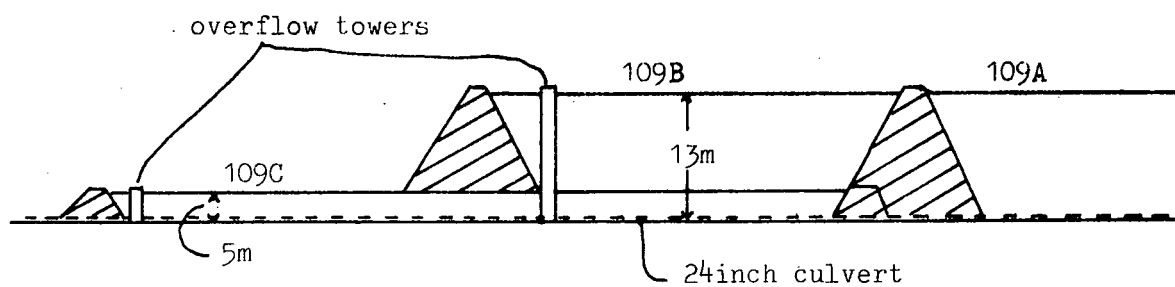


Fig.1.6 Cross section through the lagoons at East Hetton.

(not to scale)



summer of 1977, and subsequently was overtipped with coarse discard (Fig. 1.5).

## 2. Maltby

Lagoon No.6 at Maltby was chosen as the site for the overtipping operation described in Chapter 7. The lagoons are formed by building embankments from coarse discard both on top of the existing tip and abutting against its sides (see Figs. 1.7 and 1.8). The floor of lagoon 6 is Lower Magnesian Limestone covered with a red clay (varying from 0 to 700mm in thickness). The lagoon is approximately 12m deep and was filled from October 1967 to late 1969, and again for a period of a year in 1971-72. The lagoon now receives the overflow of lagoon No.5. The small embankments in the lagoon were emplaced by Wimpeys Ltd. for site access for testing and sampling and are approximately 300mm deep.

## 3. Peckfield

Peckfield colliery works the Beeston seam, but also disposes of waste from Ledston Luck colliery, which works the Flockton Thin and Middleton Little seams. The coal rank ranges from 702 to 802. Lagoons 6, 7 and 8 (see Fig.1.9) were dug into the local Lower Magnesian Limestone, the excavated material being heaped up to form embankments. The lagoons are 6m deep. They were filled with slurry from 1971 onwards; pumping continued intermittently until the summer of 1976, though by that time the lagoons were only receiving the overflow from lagoon 12.

## 4. Silverhill

Lagoon 16 at Silverhill is a cross valley type that abuts onto the tip of the shallow (up stream) end. (see Figs. 1.10 and 1.11). It incorporates an older lagoon (No.16A). On the north side of the valley the floor is a clay soil; on the south side the floor is a Coal Measures sandstone. The downstream embankment incorporates some internal drainage.

Fig.1.7 Sketch of the lagoons at Maltby.

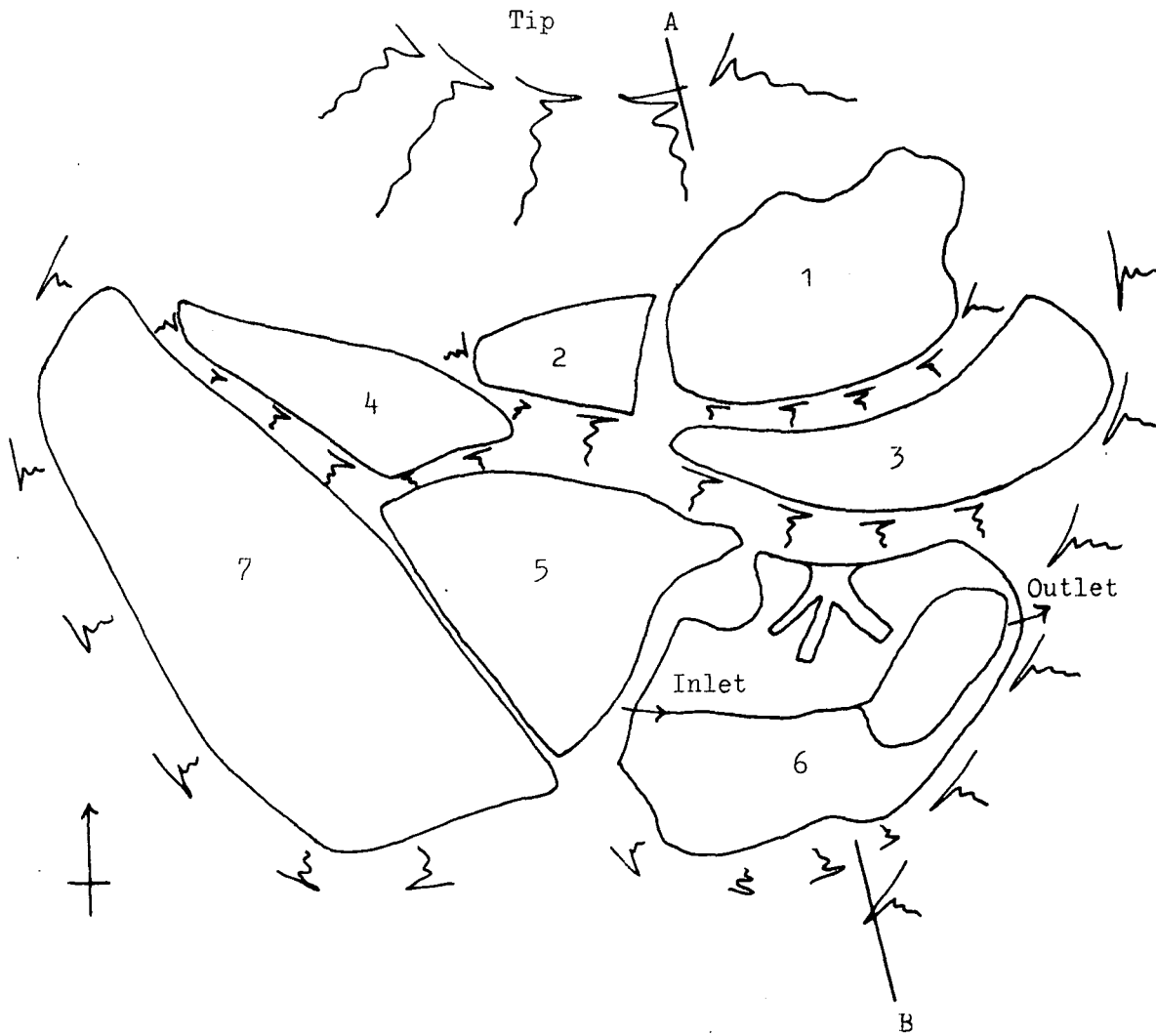


Fig.1.8 Cross section of the tip and lagoons at Maltby.

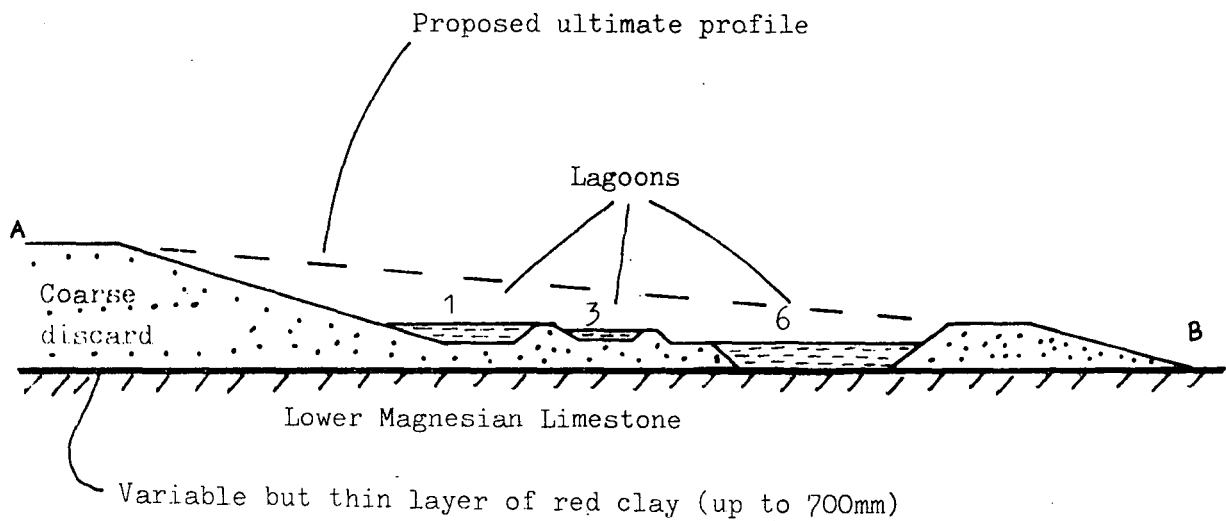


Fig.1.9 The lagoons at Peckfield.

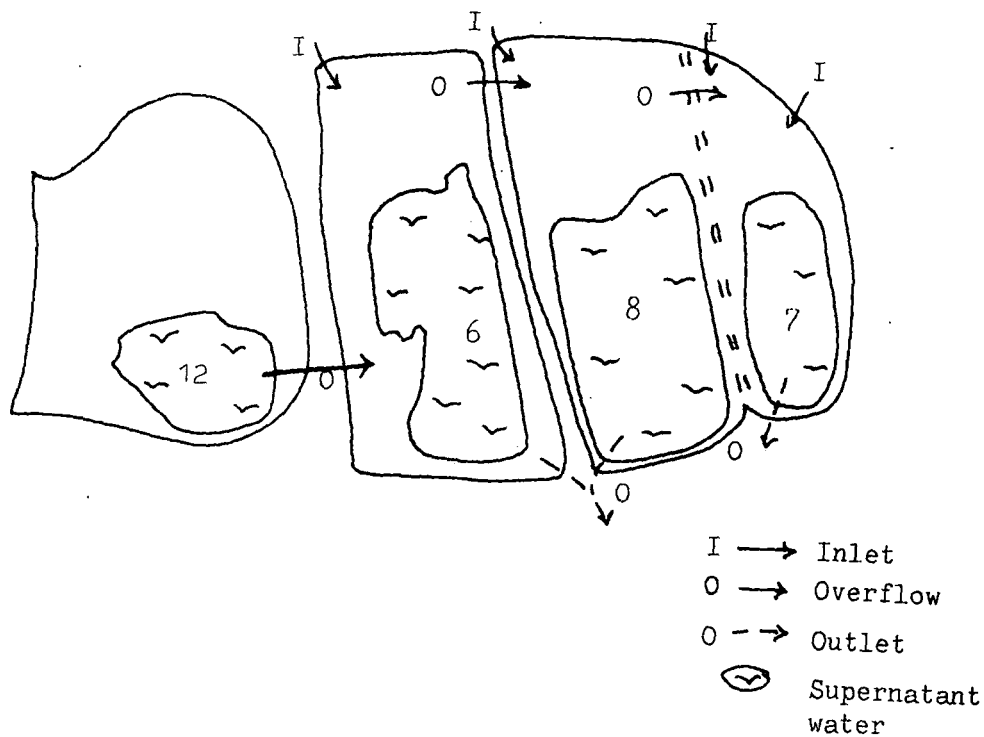


Fig.1.10 Lagoon 16 at Silverhill.

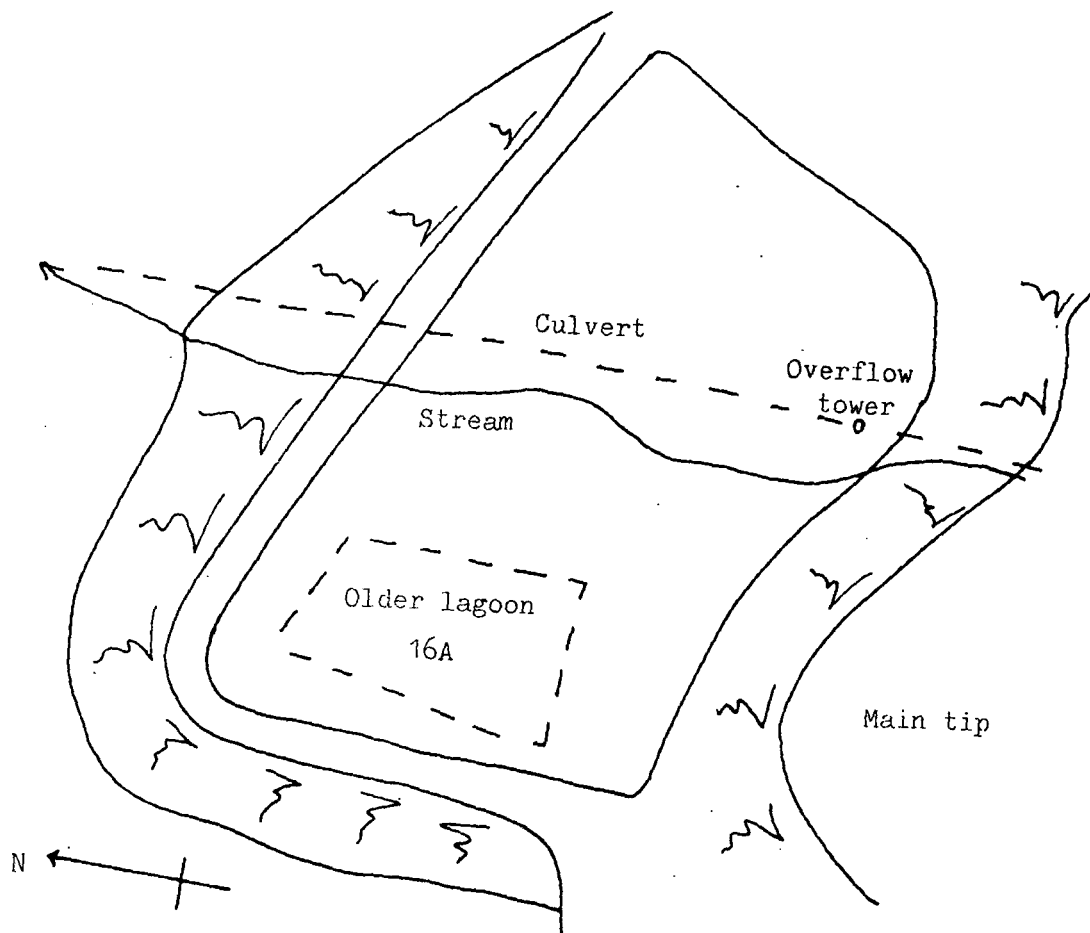
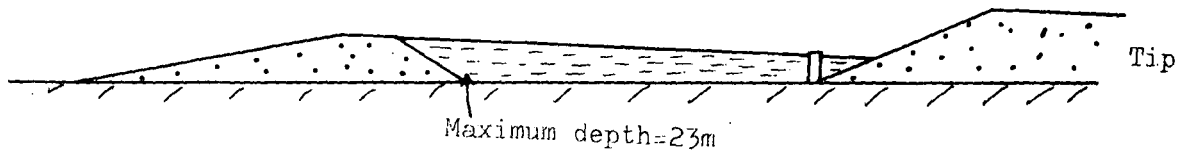


Fig.1.11 Section along the line of the culvert, lagoon 16, Silverhill.



The lagoon was filled between April 1969 and September 1978, the maximum depth being 22.7m. The supernatant water is drawn off periodically into the overflow tower which connects with a culvert running beneath the lagoon.

### 1.5 Methods of Testing

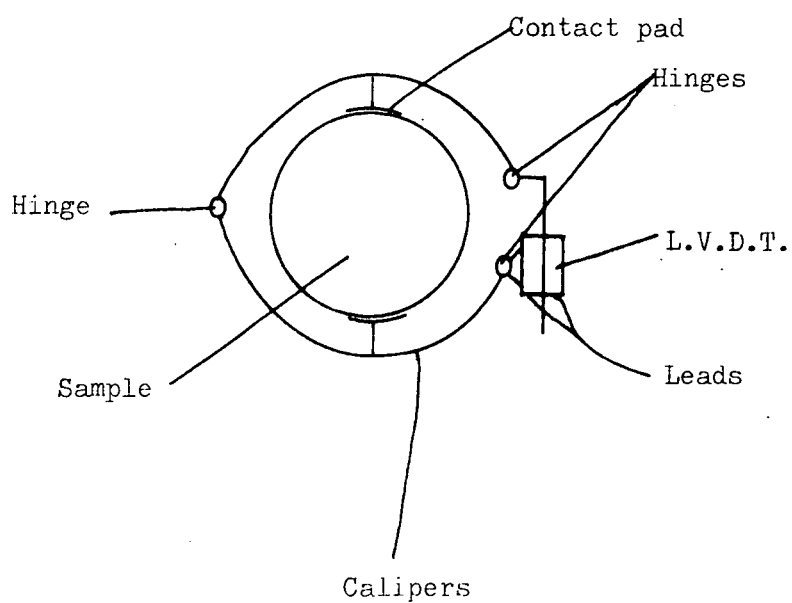
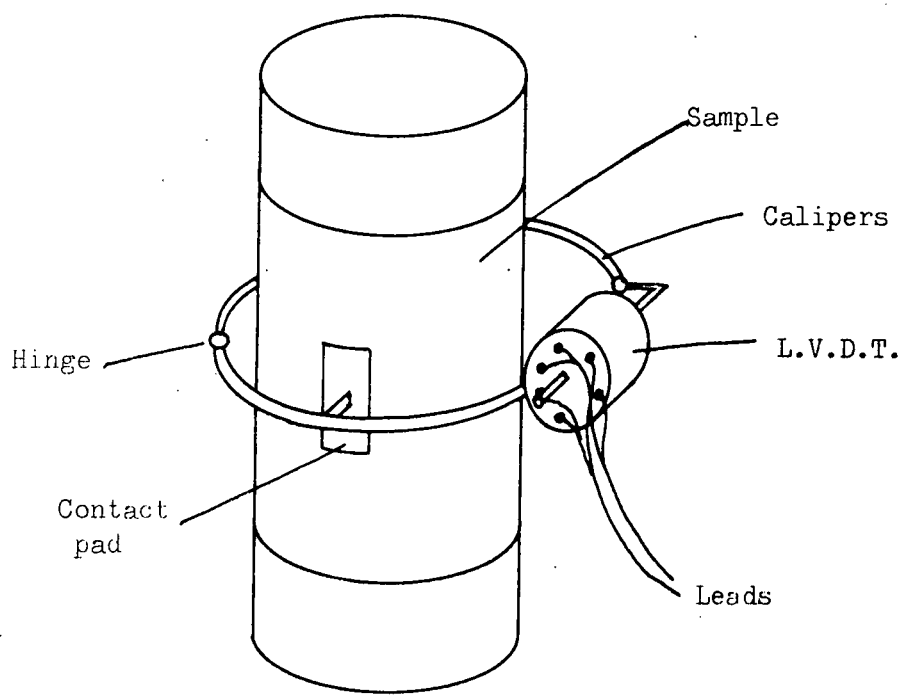
#### 1. Soils Tests

The methods of testing standard soil mechanics parameters follow BS1377 (1975). The Casagrande apparatus was used for the liquid limit test; particle size determination in the silt size range was by the pipette method.

Shear-box tests were performed using a Wykeham-Farrance 60 x 60mm shear-box. The choice of testing rates is described in the appropriate sections of chapter 5.

Triaxial tests were performed using Wykeham-Farrance 5 ton triaxial equipment. Pore pressure measurement was by Elechromechanisms pressure transducers (model P721-0002), which were calibrated against a Budenberg Standard Test Gauge. Initially the pressure system (cell and pore) was a standard mercury pot system as described by Bishop and Henkel (1962). Most tests, however, were performed with a compressed air system which supplied pressure to the cell and pore water. In the case of the pore water, an interface was required to maintain the integrity of the de-aired water. Pressure regulation was accomplished with Norgren valves, type 11-918-110. Volume change measurements were accomplished using a Wykeham Farrance volume change indicator (model 17083M).  $K_0$  tests (see Bishop and Henkel, p.140) were performed with calipers about the centre of the sample; an Elechromechanisms a.c. L.V.D.T. gave a null indication of caliper movement (see Fig.1.12). Resolution of this null indicator was approximately 0.001mm. As a change of cell pressure during the test is required, the thrust on the proving ring was measured and allowed for

Fig.1.12 Triaxial  $K_0$  measurement apparatus.



(see Bishop and Henkel, p.144). In all tests, the standard rubber membrane correction was applied (Bishop and Henkel, p.167).

Field vane shear tests were performed using a Farnell torsion head, and a rotation rate of 6 degrees per minute. The method of analysis is discussed in chapter 2.

Consolidation tests were performed using either Clockhouse type J 50mm oedometers or Armfield 6 or 10 inch Rowe cells with a mercury pot pressure system.

## 2. X-Ray Chemical and Mineralogical Tests

The equipment and methods employed are described in the appropriate sections of Chapter 4.

### 1.6 Statistical Treatment of Results

Statistical techniques have been used in this work where they are applicable. Most of the statistics ('t' tests, correlation coefficient, regression analysis) are described in Davies (1973). The linear regression technique used is the Reduced Major Axis method, in which both variables are assumed to be independent. The Fisher Least Significant Difference (LSD) Test is described by Till (1974) and is used as an alternative to the 't' test when the latter is not applicable. This condition arises if a variance ratio test (F test) indicates that the sample distributions are not from the same population. The Wilcoxon Matched Pairs Signed Ranks test, described by Siegel (1956), is applicable to paired data. It is used in Table 5 for strength data referring to matched depths in two separate profiles from the same lagoon. Significance levels for the various statistics were evaluated by the standard methods described in the above references, except for the significance level of the correlation coefficient which is taken from Table VI. of Fisher and Yates (1948). The statistics were evaluated by hand on a Hewlett Packard model 10 programmable



calculator, or by FORTRAN programs developed by the writer. The choice of method was determined by the size of the data set.

The multiple regression techniques referred to in Chapter 4 involved a pre-written suite of FORTRAN programs, the Statistical Package for the Social Sciences (SPSS) which is described by Nie et al. (1975).

### 1.7 Published Material

Some of the work relating to overtipping (Chapter 7) has already been published as "An Investigation of Overtipping a Colliery Lagoon" by Taylor R.K., Kirby J.M. and Lucas J.M. in the International Conference on Engineering for Protection from Natural Disasters, Asian Institute of Technology, Bangkok, Jan.1980 pp.629-642; Eds. Balasubramanian A.S., Karasudhi P. and Kanok-Nukulchai W.

## CHAPTER 2      THE USE OF THE FIELD VANE SHEAR TEST IN COLLIERY LAGOONS

### 2.1 Introduction

The vane shear test was first used between the wars, and gained widespread acceptance in the 1940's and 1950's. The test involves measuring the torque required to rotate a set of blades in the soil (see Fig.2.1); the torque is evidently directly proportional to the strength of the soil. The test is widely regarded as one of the best indicators of the in-situ strength properties of soils (particularly cohesive types). Use of the test in conjunction with laboratory testing programmes has led to considerable advances in the understanding of sampling procedures. A good review of these points is given by Cox (1965).

The test was originally devised to measure the strength of soft, sensitive clays, and therefore is a measure of the undrained strength of a soil. Extension of the test method in frictional soils, i.e. the use in soils that will drain during the test, is fraught with difficulties in interpretation. Many authorities therefore regard the test as being useful only in clays (e.g. Cox, op.cit). However, Blight (1965) has demonstrated that the test can be used to give drained strengths of frictional soils. Aas (1965) pointed out that the use of at least two vanes of different shapes allows an interpretation of the shear strengths of a soil on a vertical and horizontal plane. Hence, interpretation of this apparently simple test becomes a complex affair.

The loose and sensitive nature of colliery lagoon sediments makes them difficult to sample, and renders the samples obtained of dubious quality. It is quite easy, for instance, to liquefy a sample in a U100 at any one of several sampling and handling stages. Use of an in-situ shear strength test is therefore an attractive proposition. The vane test is that which has in the last 14 years been used by the National Coal

Fig. 2.1 The vane.

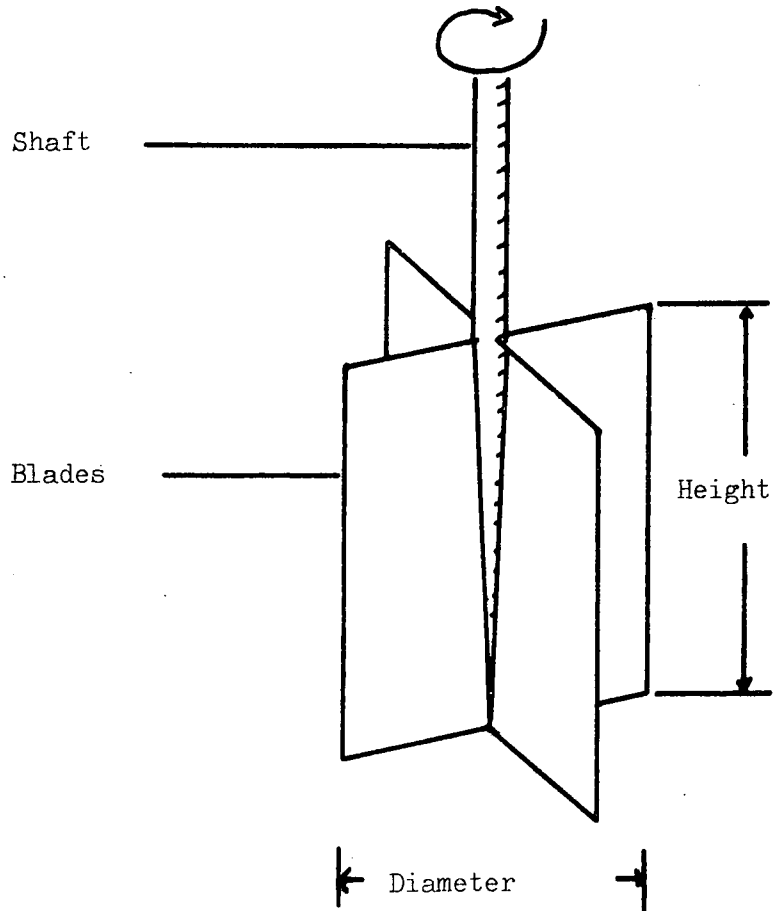
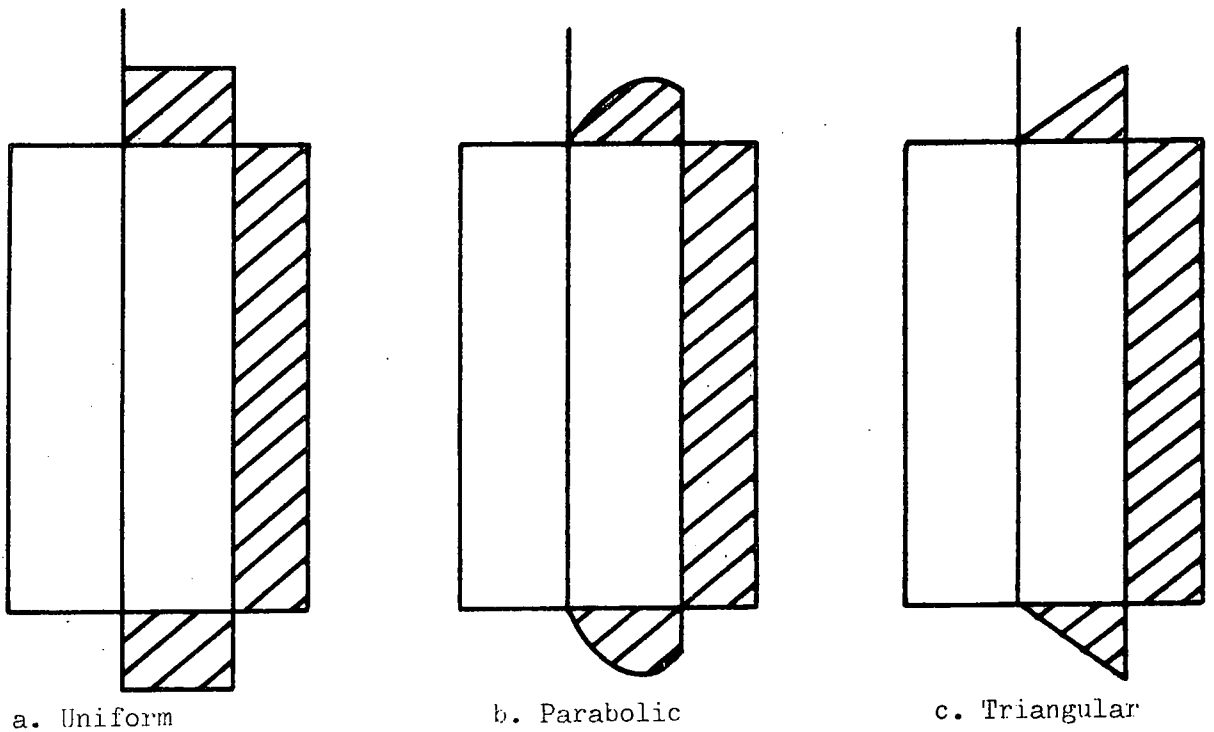


Fig. 2.2 Possible stress distributions around a vane.



Board. Although regarded as useful, the results from many tests carried out for the Board show a great deal of variation, and some difficulty has been experienced in extracting useful information (NCB, 1972; Hughes and Windle, 1976). A previous attempt to clarify the position of the test placed much emphasis on varying degrees of consolidation to explain the variability of the results (Cobb, 1976). Increasing pressure to overtip lagoons makes proper interpretation of the test of great concern. In Chapter 7, all aspects of overtipping practice, including the use of vane tests, are investigated. The purpose of the present chapter is to outline some fundamental theoretical considerations.

## 2.2 Theoretical Considerations

Cadling and Odenstad (1950) showed that the soil fails as a cylinder around the vane, and analyses are universally based on this type of failure surface. Other possibilities may exist (Cox, 1965) but are not usually considered. The rate of shear affects the test, but a rate of 6 degrees rotation per minute is fairly generally accepted, and has been adopted throughout the present field testing programmes. Four points are dealt with here in greater detail. In order they are:

1. The stress distribution around the vane;
  2. The use of paired tests to define anisotropy;
  3. Effect of drainage during the test;
  4. The effect of layering within the sediment (structural anisotropy).
1. The stress distribution around the vane

The simplest assumption is that the stresses at peak torque are uniformly distributed around the vane blades (see Fig. 2.2.a). From consideration of shear-force/displacement graphs it is clear that the distribution of stresses at the ends of the vane will more closely resemble that shown in Fig. 2.2.b. The triangular stress distribution

(Fig.2.2.c) also appears frequently in the literature (e.g. Donald et al, 1977). For vanes with a large height to diameter ratio the difference between the <sup>first</sup> two assumptions, in terms of the (vertical) strength calculated from the torque, is small. However, for vanes with a small height to diameter ratio the difference is critical. The assumptions of a curved or triangular stress distribution can be shown to give values of strength respectively 11% and 33% greater than the assumption of a uniform stress distribution along the horizontal edges of the vane (see for instance Aas, 1967; Menzies and Mailey, 1976). Donald et al., (1977) show empirically that the curved stress distribution is the best answer. This may be readily verified by simple numerical integration of a shear-force/displacement graph for various rotations until a maximum is obtained, as shown in Appendix 2.1. All results quoted herein assume this stress distribution unless otherwise stated.

One question that remains largely unanswered in the literature is the state of in-situ stresses in the ground after emplacement but prior to shear. From tests carried out by the present writer it is believed that the average value of  $K_0$  for most lagoons is about 0.5 (Chapter 5.10). Aas (1967) has shown that the value of  $K_0$  is indeed important. However, the state of stress in the soil is altered by emplacing the vane (Hansen and Gibson, 1949) and the ratio of the horizontal and vertical stresses may no longer be  $K_0$ . Since the amount by which the stresses in the soil are altered from the  $K_0$  condition is unknown, and may vary from soil to soil, the vane must remain an empirical tool, useful on a relative basis. Absolute values of strength can be obtained only by comparing the test with undisturbed samples, or by back analysing failures. Bjerrum (1972) compared the strengths derived by back analysis of failures in embankments, and showed that an empirical correction factor may be applied to the values

of strength from vane tests. This correction factor was derived for clay soils and becomes most significant in clays of high plasticity index.

As will be shown in Chapters 4 and 5, lagoons contain a mixture of non-plastic, sand-sized material, and silts and silty clays of low plasticity index. Consequently, this correction factor has not been applied to the results reported herein.

## 2. The use of paired vane tests to define anisotropy

Two or more vanes of different shape will have different combinations of torque from horizontal and vertical, or inclined, shear surfaces. This fact has been used to measure the anisotropy of soil by conducting vane shear tests with different vanes in the same soil horizon. Thus a set of simultaneous equations of torque are generated, which may be solved to give the strength of the soil on both vertical and horizontal surfaces. The method most commonly used is a graphical one originally devised by Aas (1965). The method was extended by Wiesel (1972) to cover the (usual) case of peak torque occurring on horizontal and vertical surfaces at different rotations. However, since readings have not been taken of torque vs rotation, this type of analysis has not been attempted here.

A slightly different method developed by Blight (1972) explicitly solves the simultaneous equations. This approach has been used here, and a computer program written to accept field torque readings and print out both the vertical and horizontal strengths, and the ratio of the vertical to the horizontal strength. This ratio, which Blight called  $R$ , is the inverse of the ratio usually quoted for a Wiesel-Aas analysis. However, it should be noted that  $\frac{S_v}{S_h} = R$  is directly proportional to  $K_o$ , and is to be preferred to the ratio  $\frac{S_h}{S_v} = \frac{1}{R} \propto \frac{1}{K_o}$ .

Vane tests have been conducted in pairs in the present work at

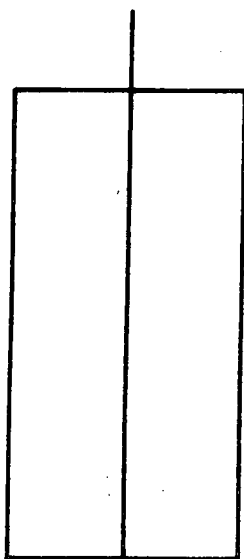
several locations, the combinations used being shown in Fig. 2.3. Also shown in Fig. 2.3 is a combination never used in the field; the reason for its inclusion will be explained later. The equations used to analyse the vane tests are developed in Appendix A.2.1. The relative merits of the combinations will be discussed later in the chapter.

### 3. The effect of drainage during the test

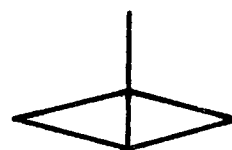
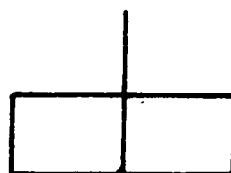
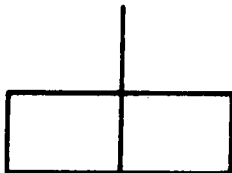
The test was originally designed to be used in sediments of low permeability. No drainage would occur during the shear stage of the test, which is therefore a test for undrained strength. Pore pressures generated by emplacement of the vane are assumed to have dissipated by <sup>having</sup> allowed a reasonable period to elapse before commencement of rotation. Furthermore, lack of a reasonable theory to account for the vane test in frictional soils (see Cox, 1965) retarded the extension of the test into such soils. However, as Blight (1965) pointed out, there is no reason why the test should not yield fully drained strengths of such soils. He therefore presents a method for estimating the degree of drainage during the test. However, because of the uncertainties of the stresses around the vane after emplacement, it cannot be assumed that the slope of a vane strength versus depth graph gives an angle of friction for the soil, in the conventional manner of Fig. 2.4.

It will be shown that lagoon sediments are a mixture of clays, silts and sands. The value of  $c_v$  for a "type" clay typically would be  $10-30\text{m}^2/\text{yr}$ . (see Chapter 6), a silt  $100-300\text{m}^2/\text{yr}$ , and a sand  $>1000\text{m}^2/\text{yr}$ . Three diameters of vane have been used in the field, these being 75mm, 100mm and 150mm. Taking typical time intervals to failure as being between 5 and 10 minutes, degrees of drainage can be estimated from Fig. 3 of Blight's (1965) paper. Table 2.1 shows the degree of drainage for the vanes used herein, for the  $c_v$  values indicated above. It can be

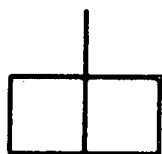
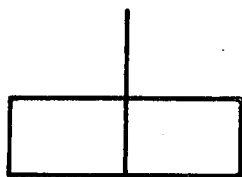
Fig. 2.3 The pairs of vanes.



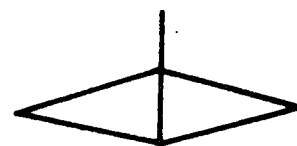
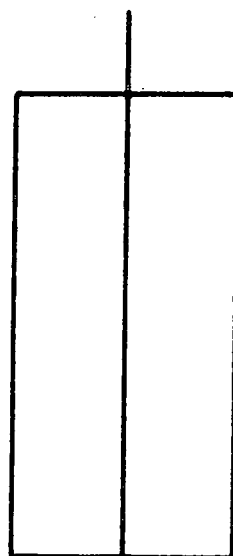
a. Pair 1, used in the field  
with  $D=75\text{mm}$ .



b. Pair 2, used in the field  
with  $D=75, 100, 150\text{mm}$ .



c. Pair 3, not used in the field.



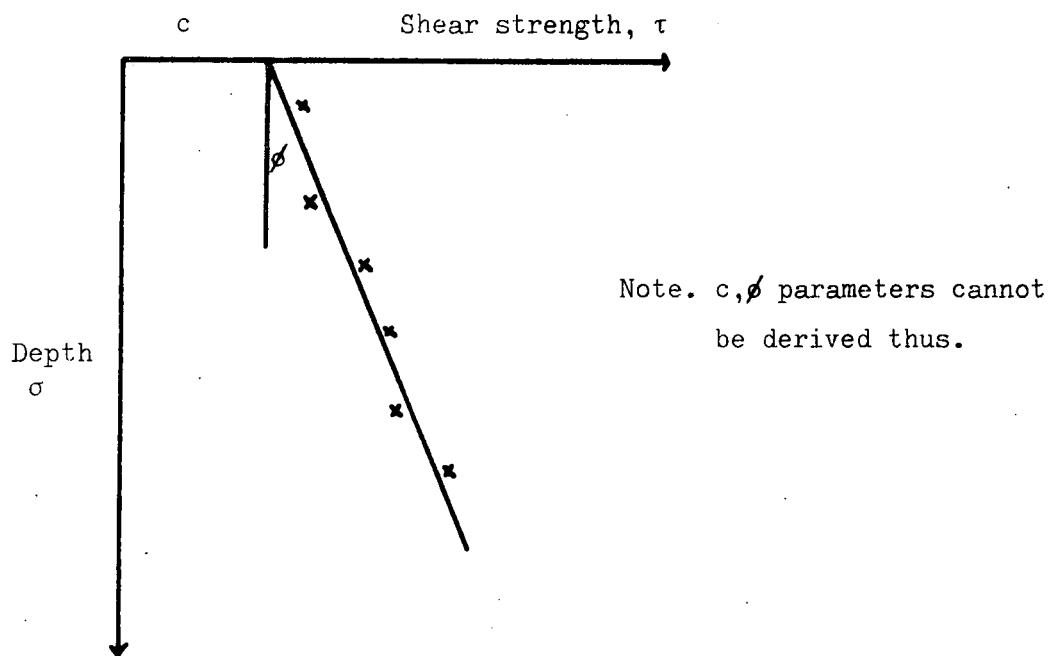
d. Pair 4, used in the field  
with  $D=75\text{mm}$  ( $H=2D$ ),  
 $D=100, 150\text{mm}$  (diamond).



Table 2.1 Degree of consolidation ( $U_c$ ) for vane tests, taking time to failure as 10 minutes.

Diameter of vane	$c_v$ ( $m^2/yr$ )	$U_c$ %
75 mm	10	5
	30	25
	100	67
	1000	100
100 mm	10	4
	30	15
	100	46
	1000	99
150 mm	10	0
	30	6
	100	19
	1000	95

Fig. 2.4 Strength -depth relationships from vane tests.



seen that the test is carried out under the full range of conditions from fully drained to completely undrained. However, as any field failure of the soil would probably occur under a similar range of conditions this is not necessarily unrealistic. In any event, since the  $c_v$  of a thin stratification or layer is not known in advance, it is not feasible to preselect the rate of shear as suggested by Blight (op.cit).

#### 4. The effect of layering within the sediment

The following distinction is necessary:

a) Structural anisotropy is the presence of layers within the soil which can be differentiated from one another on any given criterion (e.g. grading, permeability, etc.).

b) Strength anisotropy is the property of an individual layer having different strengths on planes of different orientations.

The fact that many colliery lagoons are layered is well known (Hughes and Windle, 1972; McKecknie Thompson and Rodin, 1972; Taylor and Cobb, 1977). Figure 2.5 shows the layering found at East Hetton colliery, one of the lagoons studied by the writer. Since even a vane of small height will probably affect more than one layer in many of the tests conducted, the effect of layers must be taken into account.

In lagoon number 7 at Peckfield Colliery, 81 paired vane tests were carried out using vanes of the combination shown in Fig.2.3.a, with the diameter being 75mm for each vane. This pair was chosen following Blight (1972). However, R values derived from the equations of torque outlined in Appendix 2.2 were extremely variable and were often negative (see Fig.5.8). U100 samples from this site taken during the early stages of testing revealed the fine nature of the layering and it was consequently decided to use vanes of similar heights because it was believed that these might produce "better" R values. The pair chosen

Fig.2.5 The layering in a U100 sample taken from lagoon 109B,  
East Hetton.



is shown in Fig.2.3.b., the diameter being 150mm. The R values were almost as variable as before (see Fig.5.8).

In the light of these results a computer simulation model was devised, with the intention of deciding the optimum vane pair for testing highly layered sediments. The model simulates paired vane shear tests conducted in soils of specified strength properties. The torques of the vanes are calculated according to equations 17 and 18 in Appendix 2.2. These torque values are then substituted in the equations for determining R (equations 19 - 22). This R value can then be compared to the  $S_v/S_h$  ratio of the soil as defined at the outset. A flow chart of the program is shown in Fig.2.6.

It is seen that in a structurally isotropic soil, the strength properties calculated will be the same as those defined (i.e.  $R_{calc} = R_{defined}$ ). However, when a soil boundary is introduced this is not necessarily so. Fig.2.7 shows that the H=2D vane would have a very high torque when compared to the H= D/3 vane, thus the parameter X (equation 5, Appendix 2.2) will be large, and hence R from equation 19 will be large (in fact it is 17.7 for the case considered). However, each individual layer actually has a value of R=1. Referring again to Fig.2.6, it can be seen that the computer program is an extension of this simple exercise to cover many combinations of vanes and soils, with soil boundaries placed in many positions with respect to the vanes. The vane combinations are those shown in Fig.2.3; vane pairs 1 and 2 had already been used in the field ; vane pairs 3 and 4 were under consideration for future use. Pair 3 would shear on nearly similar surfaces, while pair 4 consists of one vane measuring nearly vertical strength and the other measuring nearly horizontal strength. Shown in Fig.2.8 are the positions with respect to the vanes at which it was considered that there might be a soil boundary. As a further variation the possibility of vanes being emplaced at slightly different depths was also considered (see Fig.2.9).

Fig.2.6 Flow chart of the vane simulation program.

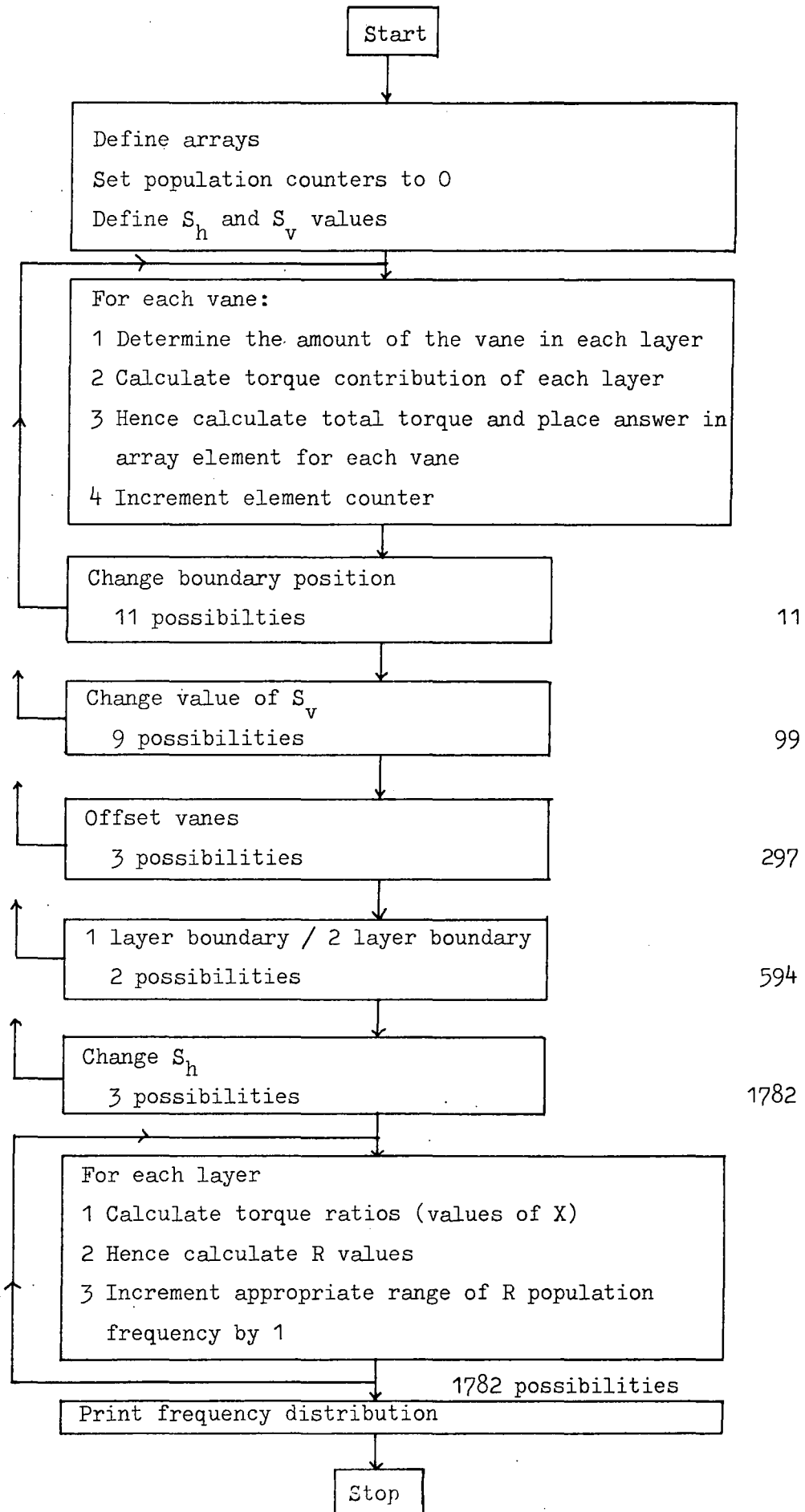
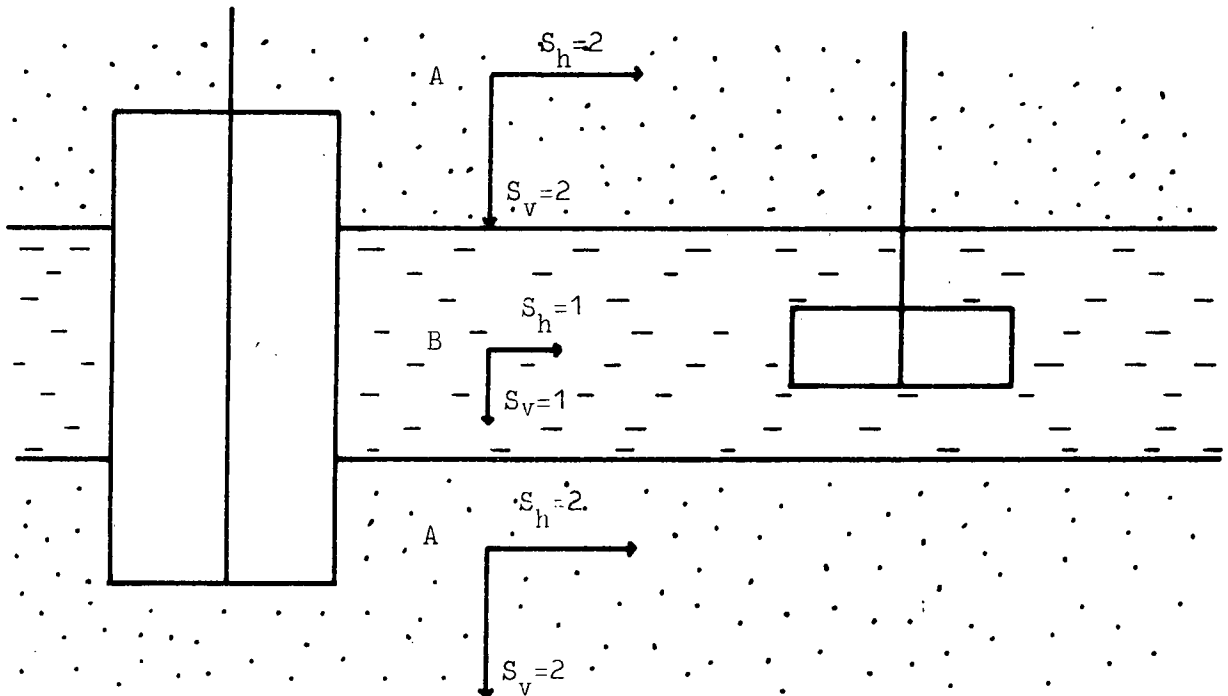


Fig. 2.7 A vane test in different layers.



$$T = \frac{\pi D^2 H \cdot S_v}{2} + \frac{\pi D^3 \cdot S_h}{7}$$

$$T = \frac{\pi D^2 H \cdot S_v}{2} + \frac{\pi D^3 \cdot S_h}{7}$$

Eliminate  $\pi$  for convenience, and let  $H$  of  $D/3$  vane be of unit length, i.e.  $D=3$ , Hof  $H=2D$  vane is 6.

$$T = \frac{27 \cdot 2}{2} + \frac{27 \cdot 1}{2} + \frac{27 \cdot 2}{7}$$

$$T = \frac{9 \cdot 1}{2} + \frac{27 \cdot 1}{7}$$

or,  $T = a + b + c$

$T = b + c$

where  $a$  is the vertical strength of layer A

$b$  is the vertical strength of layer B

$c$  is the horizontal strength at the top and bottom edges

$$T = 48.2$$

$$T = 8.36$$

Hence, from equation 5, Appendix 2.2,  $X=5.77$

From equation 19, Appendix 2.2,  $R=17.7$

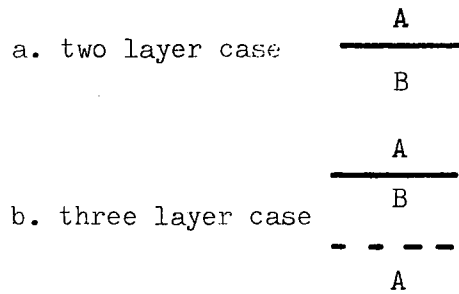
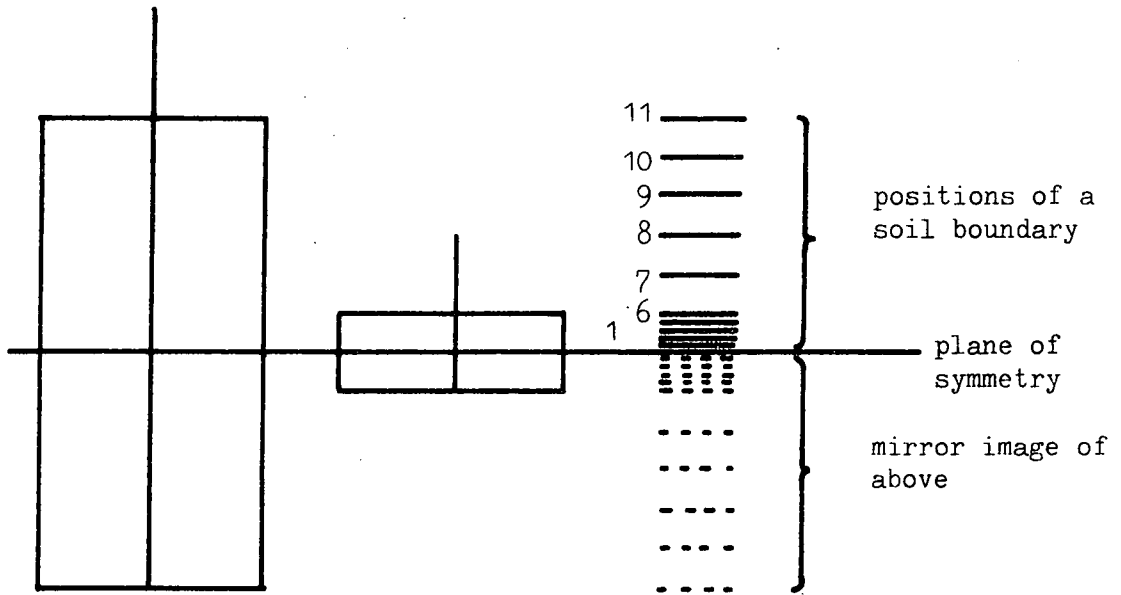
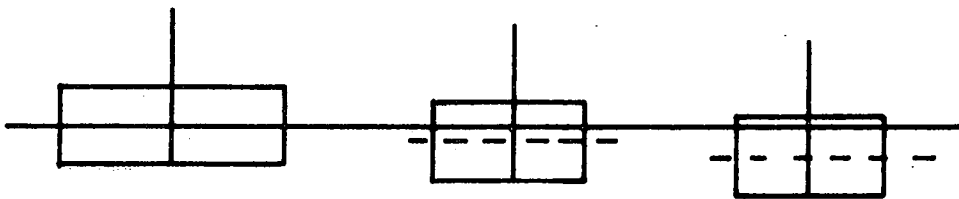


Fig.2.9 The offsetting of vanes.



Taking the height of the  $H=D/3$  vane as a unit length, the offsets are 0.2 and 0.4 unit lengths. With a vane of  $D=75\text{mm}$  this is equivalent to 5mm and 10mm respectively.

Shown in Fig.2.10 are all the possible soils used in the model. The nine soils depicted in Fig.2.10 were put through all the possible combinations of AB and ABA layer cases shown in Fig.2.8, except that for each AB pair, one of the soils always had  $S_h = 1$ . There are thus a total of 1782 possibilities (see Fig.2.6).

The population of R values that is calculated from this exercise, compared to the population that was specified at the outset should give an indication of the ability of each vane pair to define the strengths of structurally anisotropic soils. The frequency distribution of both the input population of R values, and the calculated values are shown in Fig.2.11.a-d. The following points arise:

- a) Pair 1 There are a large number of values outside the range 0.0-7.0, which reflects instability in the analytical equations. In this simple exercise the probability of such a value is approximately 20%, which ties in with the field evidence.
- b) Pair 2 This pair apparently reflects the input population very well, and seems to be the best pair within the limits of the model.
- c) Pair 3 This pair reflects the input population very faithfully indeed, except for the high proportion of spurious values (approximately 25% of all values). Close inspection of specific cases reveals that this occurs when the vanes are offset (i.e. not exactly in the same layer in equal proportion).
- d) Pair 4 This pair is moderately successful, with no wild values, but there is a spread around the true values.

On the basis of this model, pair 2 is the best choice, followed by pair 4.

A slightly different light is shed on these results if the strength ratio is considered rather than the torque ratio (i.e. X in equation 5,



Fig.2.10 The nine soil types, schematic representation.

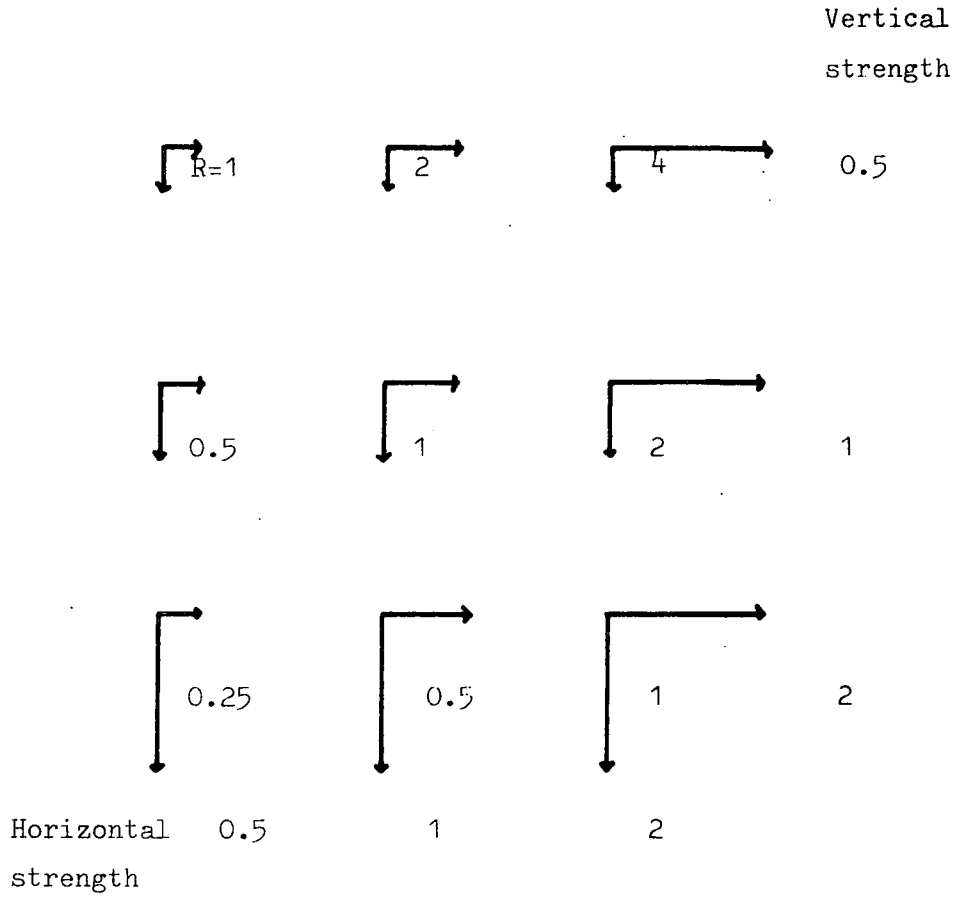
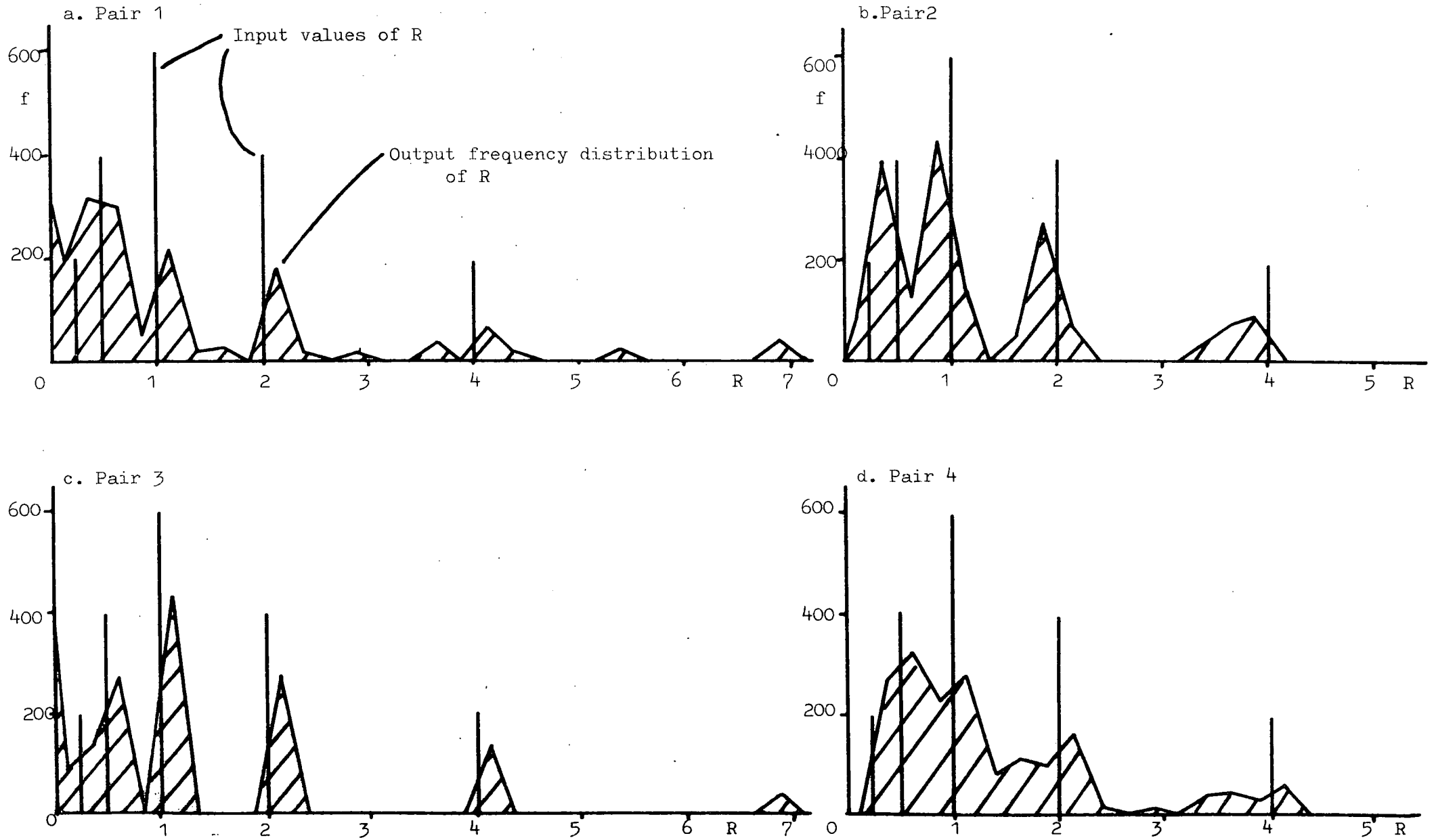


Fig. 2.11 Frequency distributions of R ( input and output ) from the vane simulation program.



Appendix 2.2). Thus, for the parabolic stress distribution, for the

$$H = 2D \text{ vane } S_{ave} = \frac{7}{8} S_v + \frac{1}{8} S_h \quad 1$$

$$H = d/3 \quad S_{ave} = \frac{7}{13} S_v + \frac{6}{13} S_h \quad 2$$

$$\text{dividing } \frac{S_{ave} 2D}{S_{ave} D/3} = Y = \frac{\frac{7}{8} S_v + \frac{1}{8} S_h}{\frac{7}{13} S_v + \frac{1}{13} S_h} \quad 3$$

substituting  $R S_h = S_v$ , and solving for R

$$R = \frac{\frac{6}{13} Y - \frac{1}{8}}{\frac{7}{8} - \frac{Y}{13}} \quad \dots \quad \text{Pair 1} \quad 4$$

similarly for pairs 2-4

$$R = \frac{\cos^2 \alpha - \frac{6Y}{13}}{\frac{7Y}{13} - \sin^2 \alpha} \quad \text{Pair 2} \quad 5$$

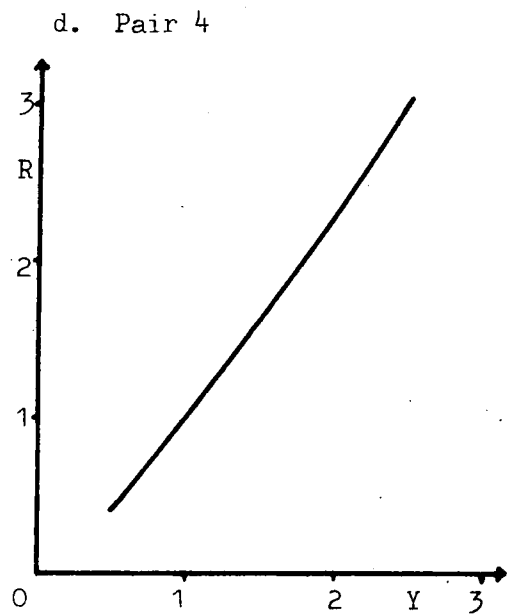
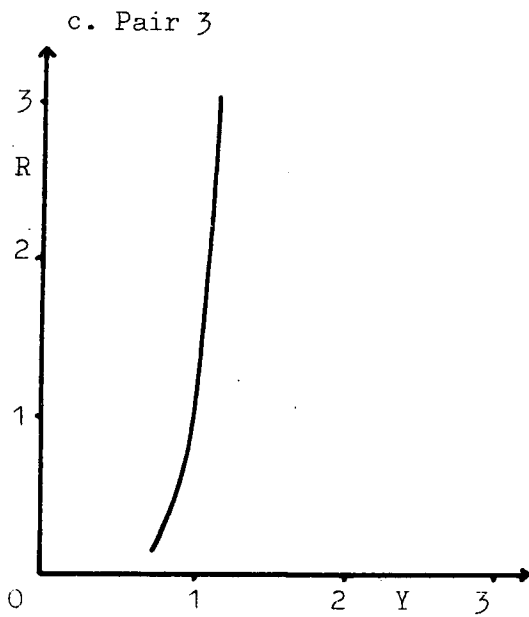
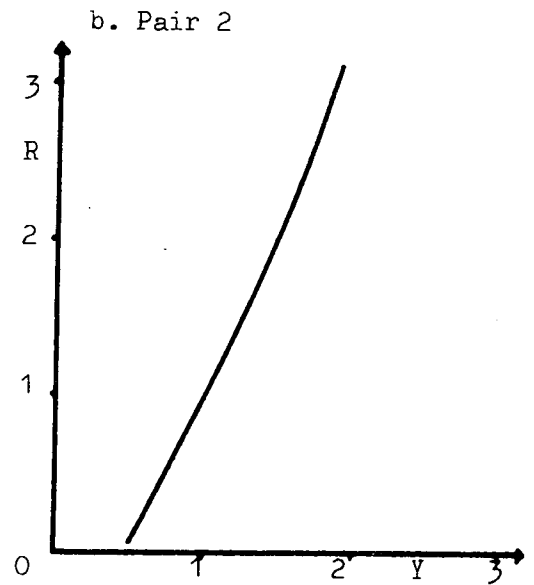
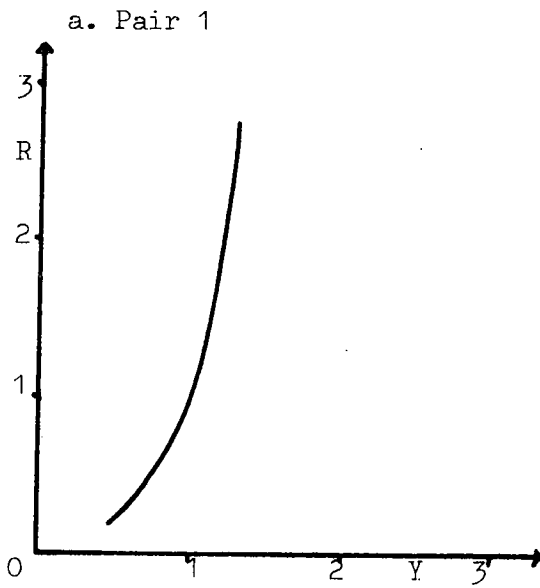
$$R = \frac{\frac{6}{13} - \frac{4Y}{13}}{\frac{9Y}{13} - \frac{7}{13}} \quad \text{Pair 3} \quad 6$$

$$R = \frac{\cos^2 \alpha Y - \frac{1}{8}}{\frac{7}{8} - \sin^2 \alpha Y} \quad \text{Pair 4} \quad 7$$

Equations 4-7 are plotted in Figs.2.12a-12d. Had these equations been used in the simulation, the results would have been the same, of course. However, inspection of Fig.2.12 shows that Pair 4 should be the best combination for resolving strength components. With the other three pairs a small error in Y (e.g. produced by operator error, or emplacement of the vanes to different depths), produces a very large error in R. However, for pair 4, the slope of the graph approaches an ideal 1:1 slope, and the results are thus insensitive to operator error, etc.

This approach, combined with the computer simulation, leads to the

Fig. 2.12 Curves of R versus Y.



following conclusion. From the field results, pairs 1 and 2 are known to yield variable results, and from Fig.2.12 can be seen to be very sensitive to small errors in reading; the simulation also showed pair 1 to yield variable results. Pair 3 also yields very variable results in the simulation, mainly because it is very sensitive to the exact relative emplacement depth of the two vanes. From Fig.2.12.c it would be expected to be very sensitive to operator error; no field tests were ever carried out with this pair. Pair 4 gives fairly variable answers in the simulation, but Fig.2.12.d suggests that it should perform better than the others.

No field tests had been performed with this pair specifically, however, the tests with pairs 1 and 2 at Peckfield had been carried out at coincident depths, although separated in time. As no great fluctuations of the water table were observed in piezometers monitored over this period, it is considered reasonable to combine the results of the H=2D vane and diamond vane. Values of R calculated for this pair show none of the extreme variability associated with pairs 1 and 2 (see Fig.5.9, Chapter 5). The vertical strength measured by this pair is that across layers, while the horizontal strength is the strength in a single layer, which accords with expected failure modes in a layered material. For these reasons, pair 4 was generally adopted for later work involving paired tests.

While installing a piezometer at the outlet end of lagoon No.6 at Peckfield, a particularly hard layer had been noticed at a depth of 880mm in a region where the sediments were generally very weak. A small series of vane tests was conducted in this layer in an attempt to produce experimental verification of the computer simulation model. It was intended to use the H=2D, H=D/3 and diamond vanes, but the H=2D vane in this layer exceeded the capacity of the torsion head. Only the two smaller vanes could therefore be used. There were 11 individual tests in this

series, and in each case the depth to the hard layer was measured. The contoured map is shown in Fig.2.13. The steep gradient of the layer (approximately 1 in 3) is obviously related to the greater consolidation settlement of the deeper layers away from the side of the lagoon. The exact profile of the hard layer was established from U100 samples, and is shown in Fig.2.14, along with the various parameters established in the laboratory. The grading curves are shown in Fig.2.15. Each layer was intrinsically nearly isotropic ( $R=1$ ) from the shear-box tests.

The vane tests were conducted at various depths of penetration into the hard layer itself, as shown schematically in Fig.2.16. Also shown on the figure are the  $R$  values obtained from the field tests and by calculation using the strength parameters shown in Fig.2.13. The match of the two sets of  $R$  values is not good, mostly due to the presence of the small upper hard layer. This was not noticed at the time of the field tests. Bearing in mind how critical the exact placement depth is, tests 1, 3, 4 and 6 show reasonable agreement of the measured and calculated values. This short experiment does not directly verify the computer simulation model, but it shows very reasonably how important layering is when conducting paired vane tests, even under carefully monitored conditions.

### 2.3 Conclusions

The nature of lagoon sediments renders the vane shear test a very useful empirical tool in site investigations. Theoretical uncertainties about the state of stress around the vane produce difficulties in relating the vane test to standard strength ( $c, \phi$ ) parameters in colliery lagoons. The vane test will take place under the full range of conditions from drained to undrained, but this will also be true of any failures

Fig. 2.13 Depths to the hard layer in lagoon 6 at Peckfield.

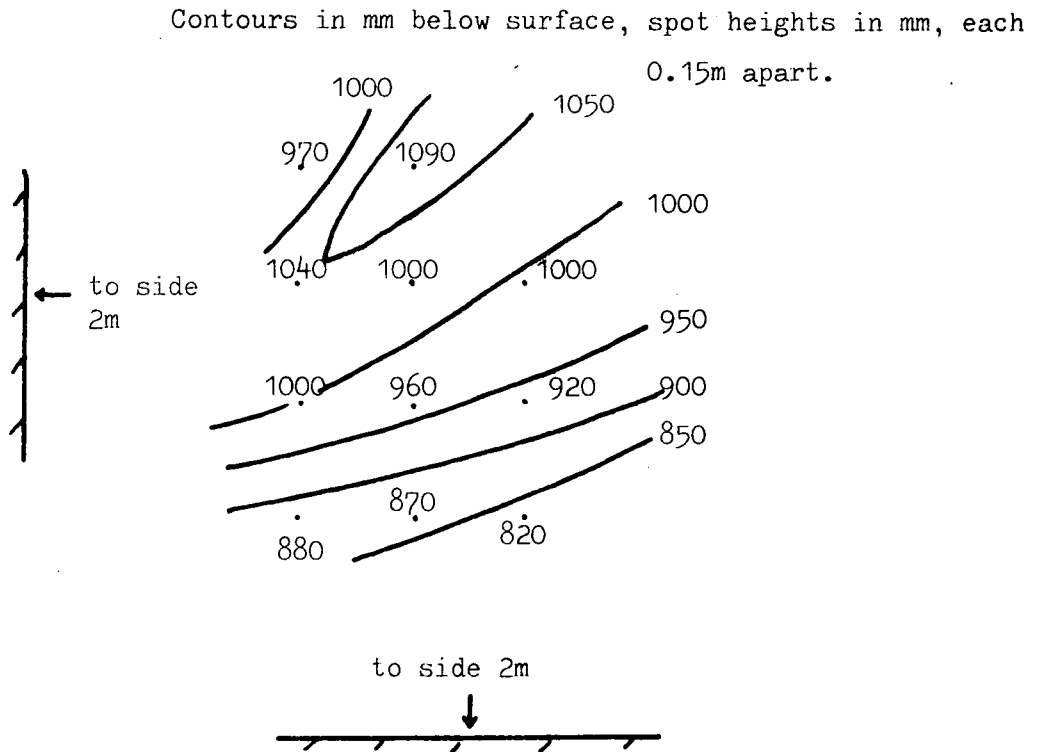
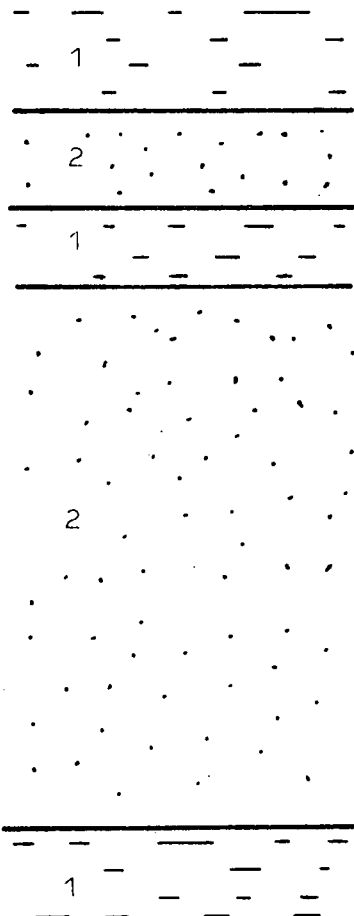


Fig. 2.14 The hard layer.

Layer type:



Layer type 1:

$c = 3 \text{ kN/m}^2$        $\phi = 2^\circ$   
 $c' = 3 \text{ kN/m}^2$        $\phi' = 26^\circ$   
 $m = 50\%$       Organic carbon = 38%  
 $LL = 47\%$       S.G. = 2.171  
 $e = 1.17$   
 Bulk density =  $1.42 \text{ Mg/m}^3$   
 $c_v = 5.61 \text{ m}^2/\text{yr}$

Layer type 2:

$c' = 3 \text{ kN/m}^2$        $\phi' = 38^\circ$   
 $c = 3 \text{ kN/m}^2$        $\phi = 38^\circ$   
 $m = 47\%$       Organic carbon = 79%

All tests in the shear box, horizontally oriented specimens.

Fig.2.15 Coarse and fine samples from the outlet of lagoon 6, Peckfield.

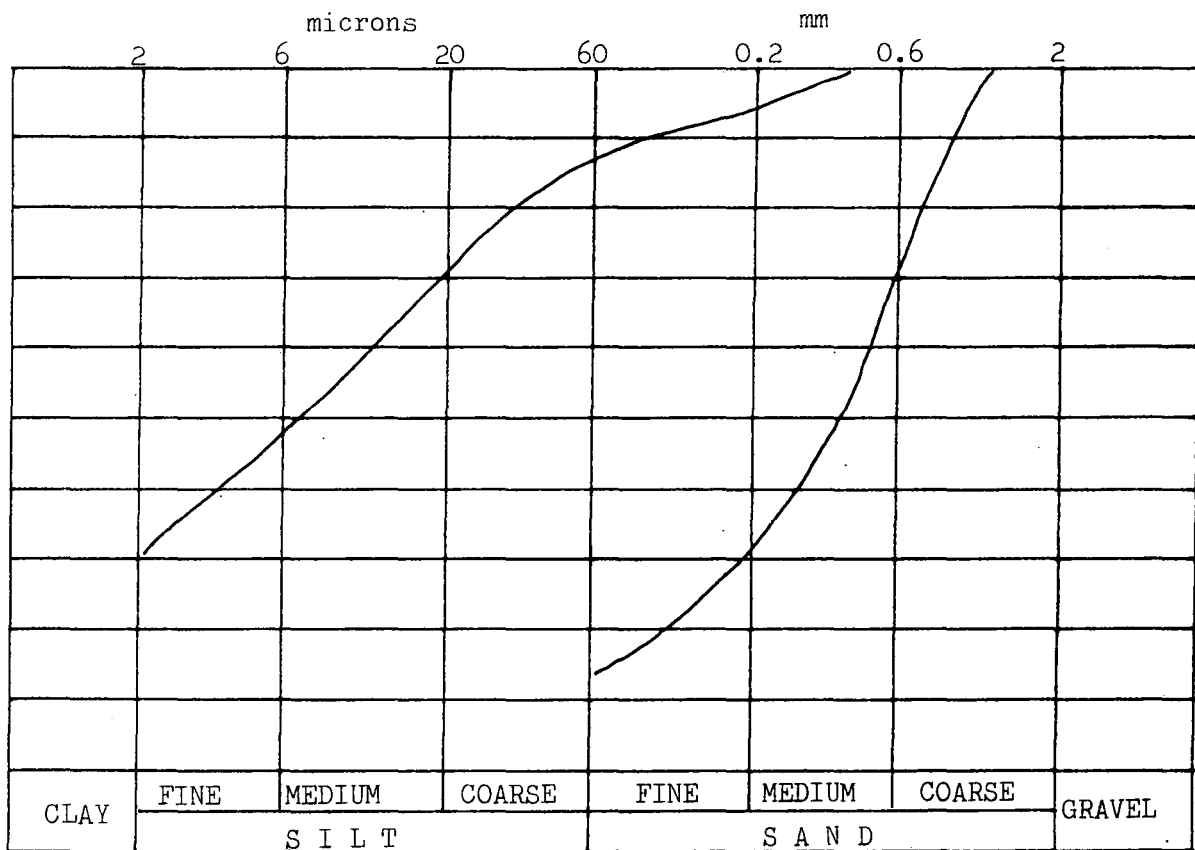
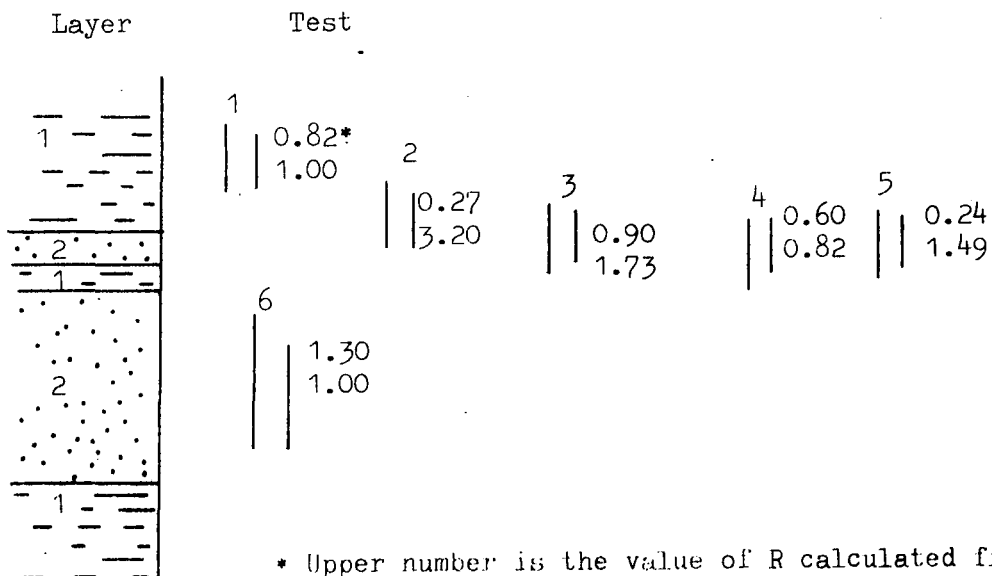


Fig.2.16 Vane tests in the hard layer of lagoon 6, Peckfield.



\* Upper number is the value of R calculated from the field vane tests  
 Lower number is the theoretically calculated value  
 In each case the vertical lines show the relative positions of the two vanes used to calculate R



(e.g. standing excavated faces or embankments).

The layered nature of lagoon sediments also makes for further difficulties in resolving vertical and horizontal strengths by the paired vanetest technique. In conjunction with field testing programme, the computer model which was devised allows a rational choice of the optimum vane pair for testing this type of sediment. The  $H=2D$  vane and a diamond vane with  $H=\frac{1}{2}D$  were found to be well suited to this task.

Although it is difficult to relate vane shear strengths to  $c, \phi$  parameters on a theoretical basis, it is possible to establish empirical relationships. These will be considered in Chapter 5.

## CHAPTER 3 THE USE OF CONE PENETRATION TESTS IN COLLIERY LAGOONS

### 3.1 Introduction

The limitations of vane shear tests in colliery lagoons (to wit, uncertainties concerning drainage, state of stress and the number of layers being sheared) led to the idea that a penetration test might be more useful in assessing the strength of these deposits.

Penetration testing is of two main types, dynamic or static. The former involves driving a penetration device by means of hammer blows for example. This type of test was discounted as being unsuitable for layered media with large variations in shear strength. Static penetration testing involves measuring the force required to advance the penetrometer at a constant rate. The test is usually performed with a 60 degree cone with a base area of  $100\text{mm}^2$ , although there is a lack of standardisation in cone testing (Begemann, 1974; Holden, 1974; Zweck, 1974).

### 3.2 Field Testing Rig (Mark 1)

The requirements for a cone penetrometer for use in colliery lagoons are as follows:-

1. It should be lightweight, due to the difficulty of movement on soft sediments.
2. It should generate only a small penetration resistance, as a great surface reaction (weight) cannot be supplied. In other words the cone tip and rods must be of small diameter.
3. Since, in general, commercial devices do not fulfil the first two criteria, it was decided to manufacture at Durham a device to assess the possibilities of penetration tests. Cheapness and ease of manufacture were also important for the preliminary device.

It was further decided to use two cones with different tip angles to assess the effect of this parameter. Accordingly a 60 degree cone

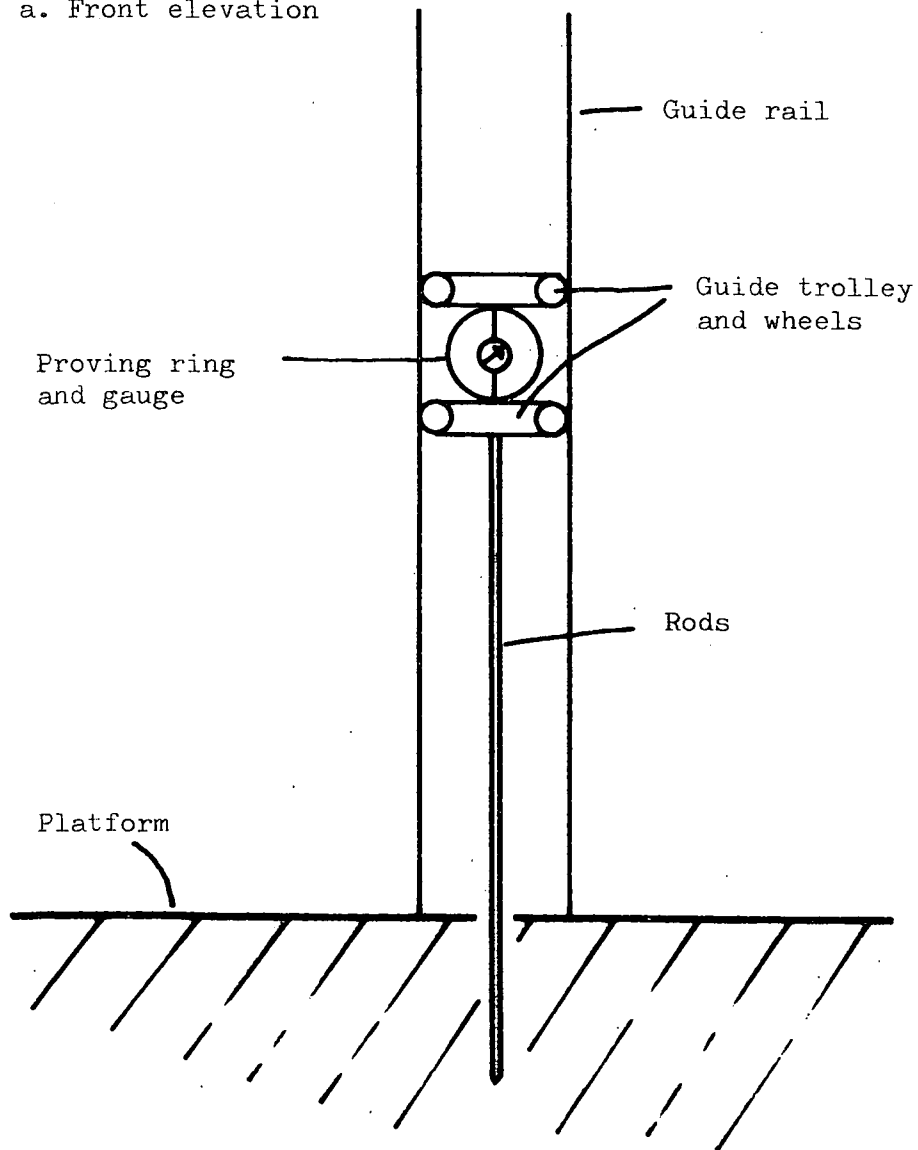
was not used initially, but one of 30 degrees and one of 90 degrees.

A suitable platform on which to stand any device existed at Durham in the form of the field vane platform. It was further decided to use the torsion head and tripod as the driving mechanism for cone penetration. With reference to Fig.3.1 the vane torsion head twists a dummy vane rod which draws in the pull wire. This in turn pulls downwards on the top of the proving ring, which then registers the force required to cause downward displacement of the rods and cone. The guide rails ensure a correct line of penetration, and are bolted to the vane tripod platform. The cone extension rods themselves are of 16mm stainless steel, this being a suitable commercially available size. The extension rods provide a penetration capability of up to 6m. A wire supports a weight from the top of the guide rail gantry, which counter-balances the weight of the proving ring plus extension rods. Thus there is no net downward force on the cone tip other than that registered by the proving ring. The complete device is shown in Fig.3.2.

Downward penetration resistance as measured by the proving ring in fact consists of two parts. Firstly there is the actual resistance at the cone tip, and secondly there is the resistance due to skin friction along the extension rods. The value of the skin friction was measured upon retraction of the rods (the proving ring being calibrated in tension for this purpose). It is assumed that the skin friction is a remoulded value on both insertion and retraction, and therefore the resistance to retraction is subtracted from the total penetration resistance to derive the net cone resistance. This assumption was considered adequate for the feasibility trials.

The penetration rate that was adopted for all trials was 40mm/minute.

a. Front elevation



b. Side elevation

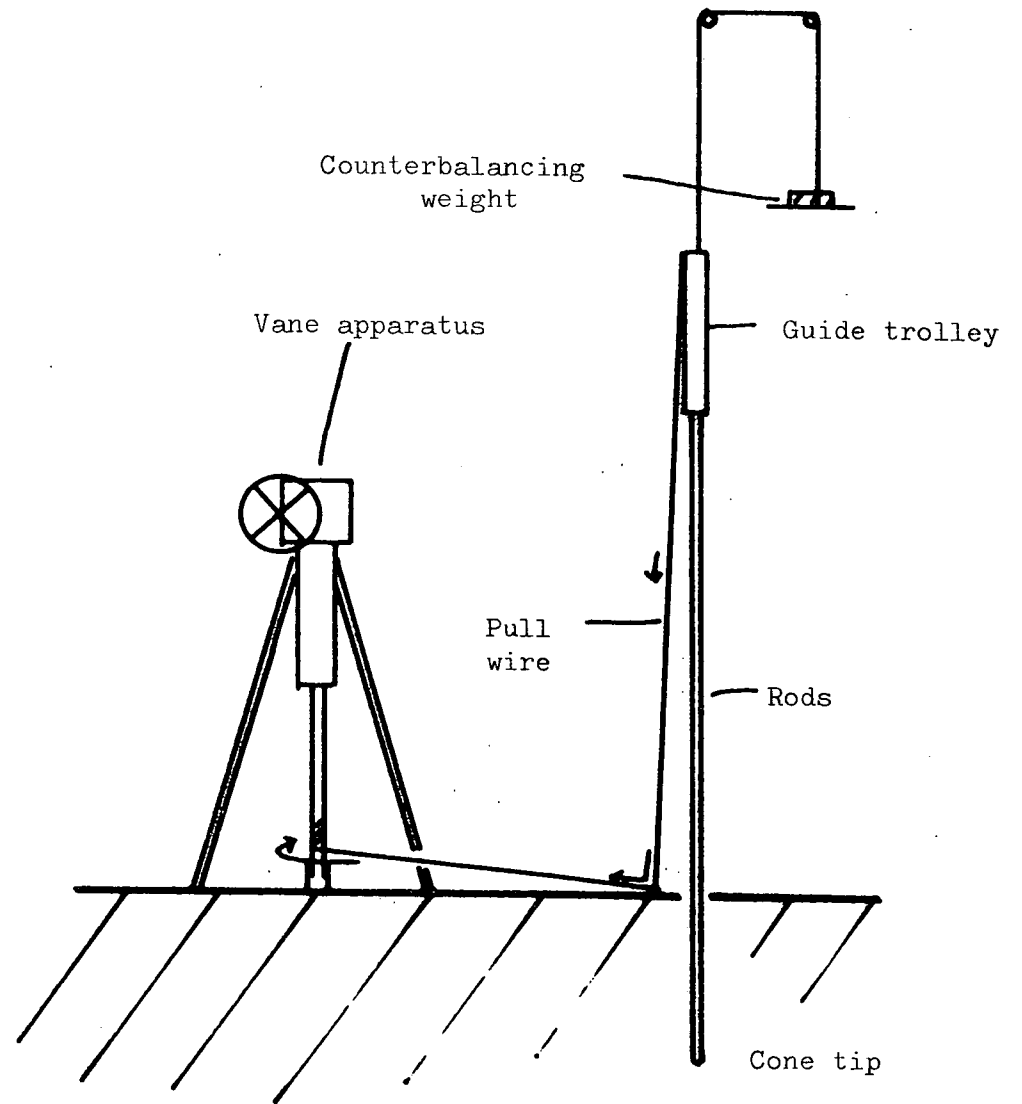
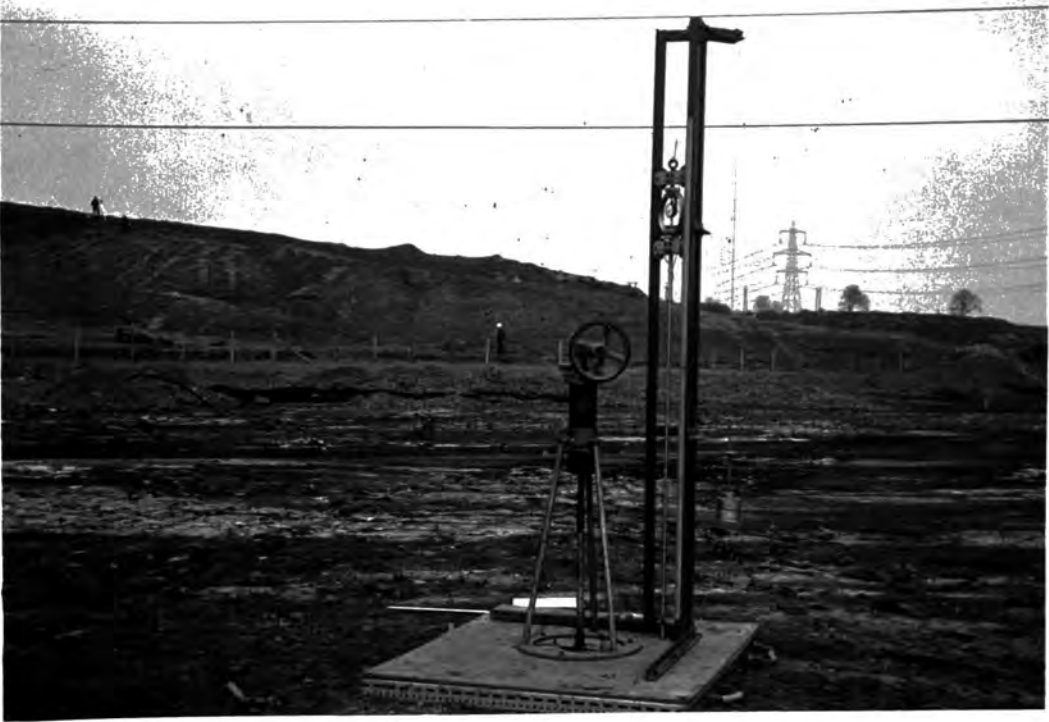


Fig.3.1 Schematic diagram of the cone penetration apparatus. Essential parts only are shown; not to scale.

Fig.3.2 The penetrometer rig, mark 1.



Faster rates were difficult to achieve, and at this rate readings could be taken manually at 10mm intervals. The resolution of the stress/strain readings was thus very good, but in view of the assumption stated above the graphs derived from work with this device should not be viewed as reflecting the same degree of accuracy as the precision with which they are drawn.

### 3.3 Field Penetration Results

With this penetrometer tests were performed in lagoon 109B at East Hetton Colliery (North East Area, NCB) and Lagoon 6 at Maltby Colliery (South Yorkshire Area, NCB); Taylor, Kirby and Lucas, 1980. The former was a straightforward feasibility study, the latter was linked to the overtipping exercise described in chapter 7.

The location of the tests at East Hetton are shown in Fig.3.3. Cone penetration tests and vane shear tests were performed at each location. Logs were also obtained, based on U100's recovered at each location. Figures 3.4, 3.5 and 3.6 show the profiles so obtained. It can be seen that the penetration resistance per unit area (curved surface area of the cone tip) is generally greater for the 90 degree cone, though the actual resistance load of the 30 degree cone is the greater. The 90 degree cone is apparently the more sensitive to fluctuations in resistance to penetration. It can further be seen that the lagoon is more layered with respect to penetration resistance at the inlet (location A, Fig.3.4) than it is nearer to the outlet (location B, Fig.3.5). This feature is probably linked to the more plastic, clay-rich nature of the sediments nearer to the outlet, which is reflected in the logs. Table 3.1 shows that there are considerably more fine grained layers at location B than there are at either of locations A or C. The lagoon sediments are extremely layered, stratifications being no thicker than 40mm on average.

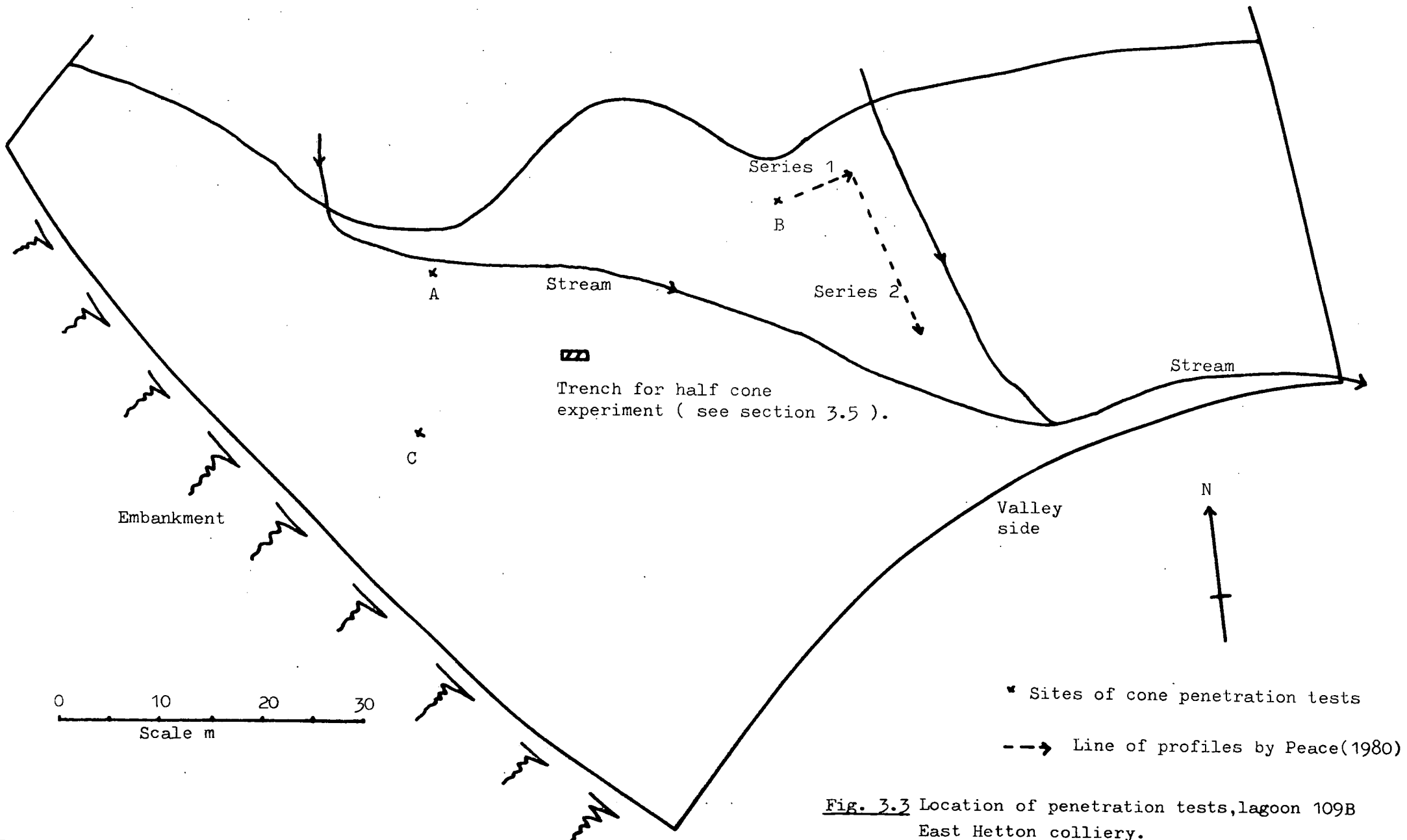

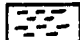

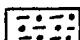
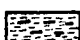
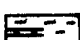


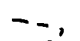




Fig. 3.3 Location of penetration tests, lagoon 109B East Hetton colliery.

## Explanation of symbols used in Figs. 3.4-3.6.

## a. Logs

	Coarse grained lamination
	Medium grained lamination
	Fine grained lamination
	Medium-coarse grained lamination
	Medium-fine grained lamination
	Parting (of coarse in medium)
	Disturbed sample
	30 degree cone
	90 degree cone
	Limits and natural moisture content
	Non-plastic

## b. Penetration resistance

Scale A- load per curved surface area of the cones. This scale is not standard, as resistance is usually quoted in terms of the base area of the cone. However, this scale has been shown in order to compare the two cones and also for comparison with Vesic's (1972) theory of cavity expansion (see sections 3.5 and 3.6).

Scale B- load per base area of the 90 degree cone.

Scale C- load per base area of the 30 degree cone.





Fig.3.5 Penetration resistance at location B, East Hetton.

(See key above for explanation of symbols and penetration scales.)

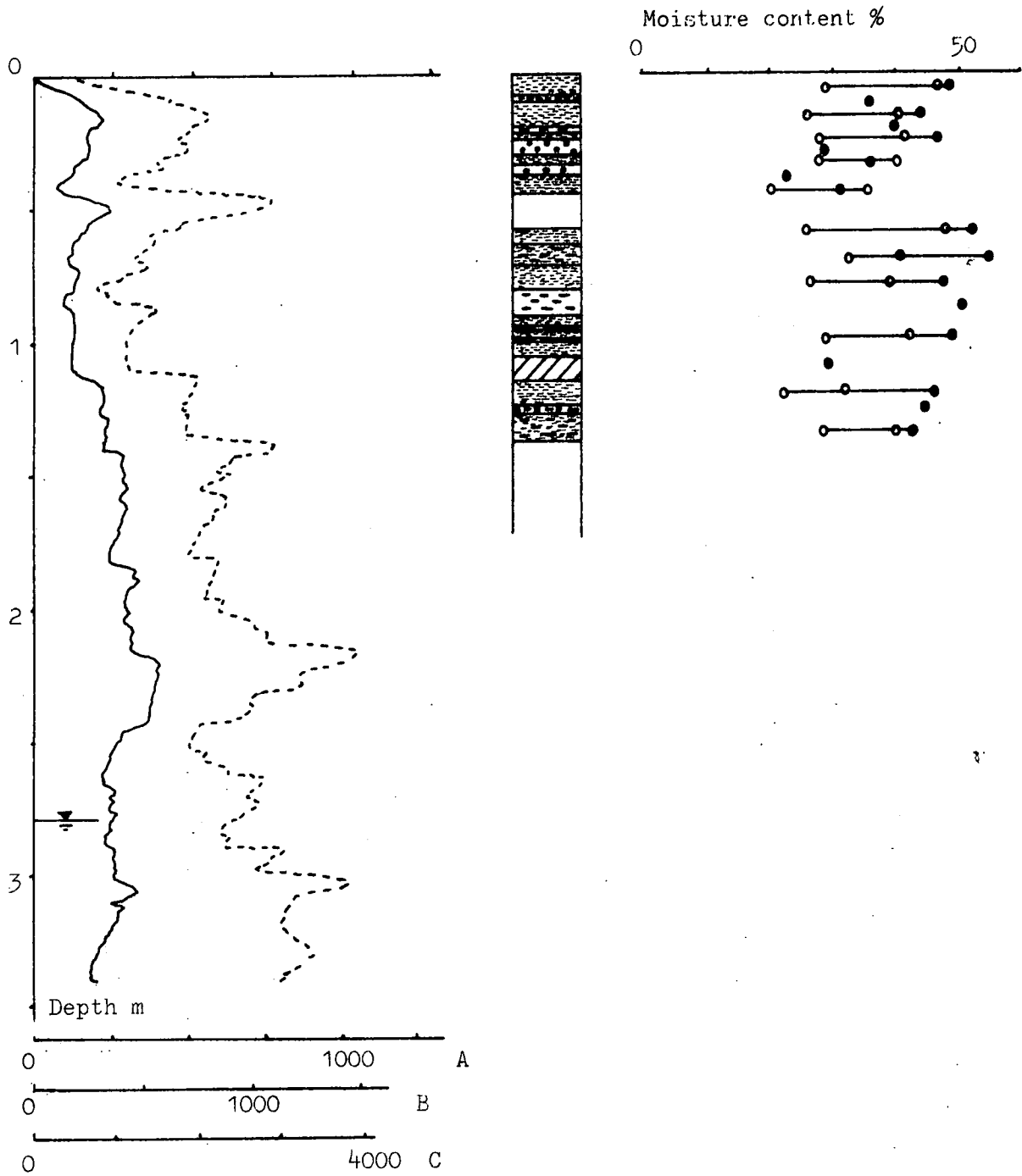


Fig.3.6 Penetration resistance at location C, East Hetton.

(See key above for explanation of symbols and penetration scales.)

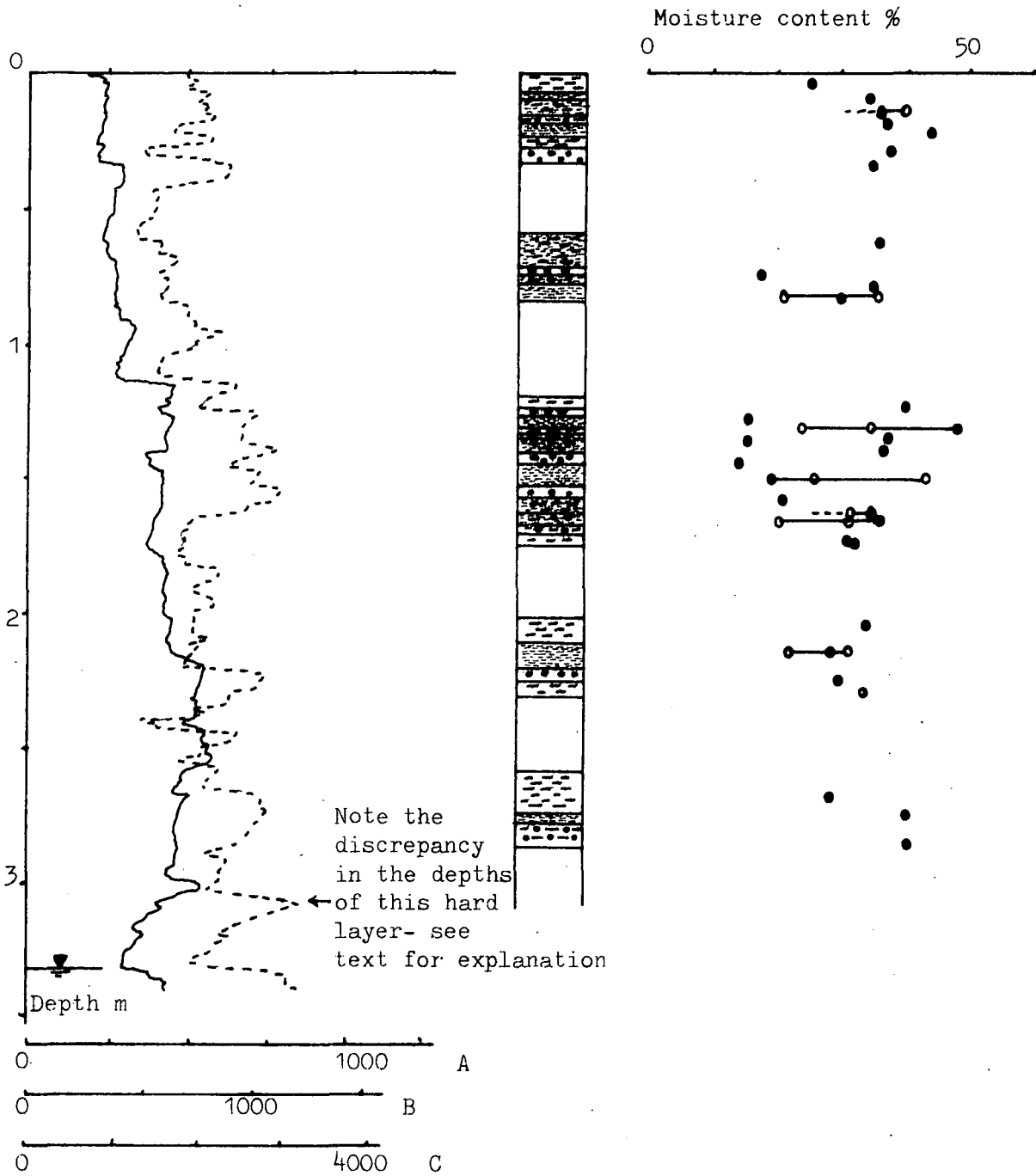


Table 3.1 East Hetton lagoon 109B, borehole logs.

Location	Borehole depth m	Recovered length m	Percentage recovery	Disturbed length m	Total undisturbed recovery m	.....of which	average no of units per m (all types)
A	2.60	1.55	59	0.24	1.31	Fine =28% Medium Fine =19% Medium =14% Fine/med/coarse =10% Med coarse =10% Coarse =19%	22 (NB many contained further subdivisions)
B	1.44	1.29	89	0.16	1.13	Fine =59% Med fine =15% Med =10% Med coarse =8% Coarse =8%	22
C	2.93	1.79	61	0.0	1.79	Fine =22% Med fine =38% Med =23% Med coarse =2% Coarse =15%	17

N.B. Fine, medium and coarse represent a visual log. Fine approximately represents a silty-clay, medium represents a medium to coarse silt, coarse represents a medium to coarse sand.

This feature precludes sensible correlations with the penetration resistance profiles. The problem is exacerbated by the tendency of the cone rods to deviate from a vertical line. This tendency is seen in the profile for location C (Fig.3.6) where the 90 degree cone and 30 degree cone record "apparent" depths 80mm apart for a hard band just below 3m depth. The finely layered nature of the lagoon also causes the correlation between the shear strength as measured by the field vane and penetration resistance to be very low. The correlation coefficients are given in Table 3.2.

The testing programme at Maltby also involved the same penetration device being used in conjunction with vane shear tests. Time permitted only one cone to be used; the 30 degree cone was adopted because it was felt that it would enable gross changes to be more readily assessed. The cone penetration resistance and vane shear strength profiles are given in Fig.37. It is apparent that over the depths of interest the sediments at Maltby are far weaker to both shear strength and penetration resistance than those at East Hetton. However, the increase in strength with depth at Maltby is more pronounced than at East Hetton. The greater depth of testing, and consequently greater importance of overburden effects probably accounts for the higher correlations between vane and cone tests at Maltby (see Table 3.2).

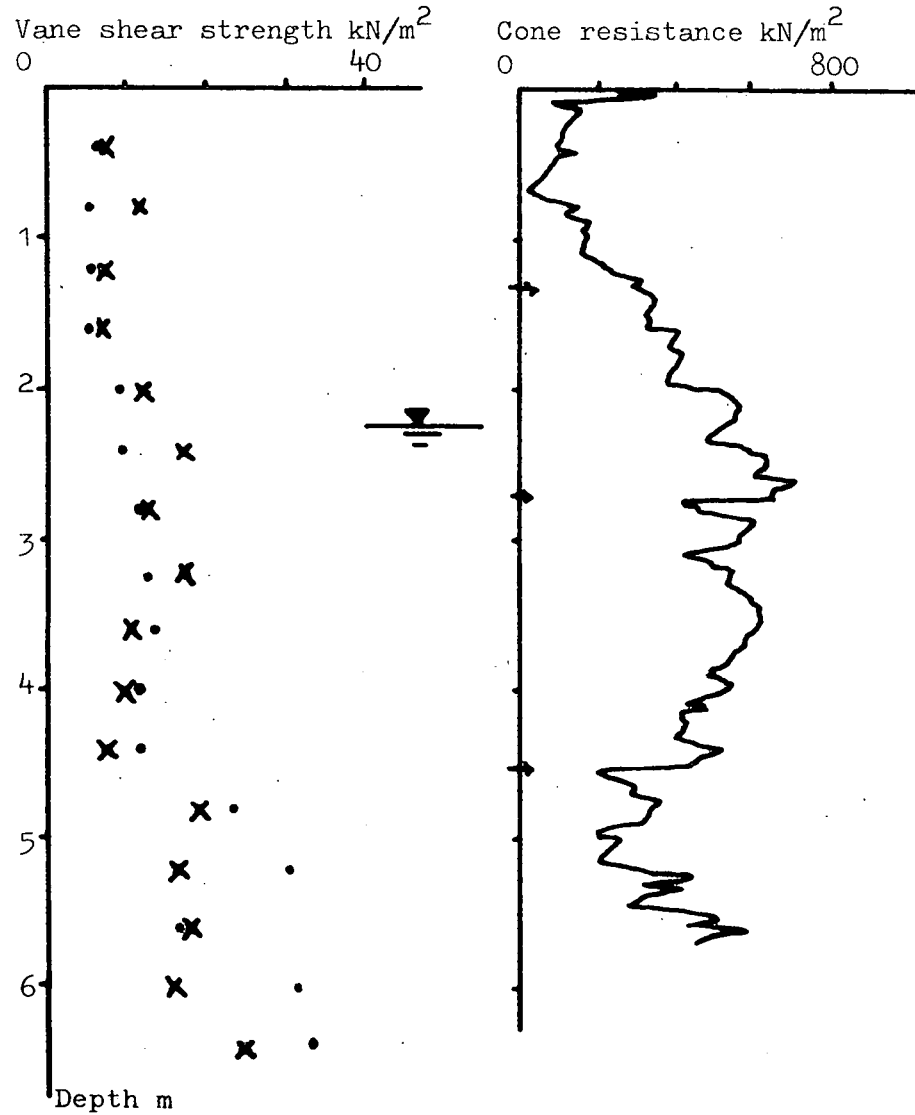
#### 3.4 Field Testing Rig (Mark 2)

The results discussed above were of a preliminary nature, but were felt to be sufficiently encouraging to undertake a second phase of study with an improved penetrometer. The details of design are explained by Peace (1980); it is sufficient to note here that the major differences are:-

a) the resistance to penetration is measured at the cone tip by an electrical load cell. This is both more accurate and eliminates the problem of measuring the skin friction.

Fig.3.7 Vane shear strength and cone penetration resistance, lagoon 6, Maltby colliery.

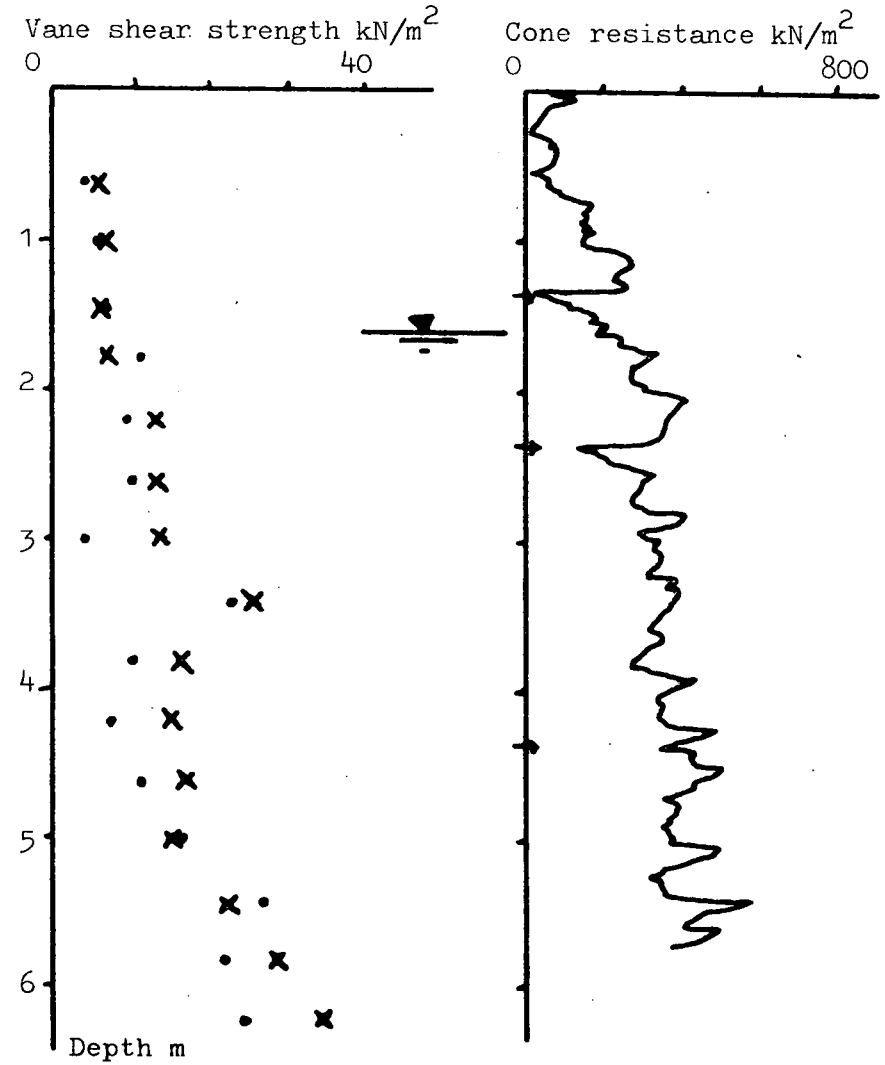
a. Profile 2



x H=2D vane, peak

• Diamond vane, peak

b. Profile 1



— 30 degree cone

→ Rod change on cone

b) the size of the load cell necessitated rods of 25mm diameter being used.

c) although the same guide rails were used as on the previous rig, the vane apparatus was replaced by a hand winch, as the driving mechanism. This enabled much faster penetration rates to be achieved. The penetration rate varied from 0.6 to 4cm/sec., compared to 4cm/min. in the previous trials.

With this improved cone penetrometer, Peace (op.cit.) conducted a series of tests in East Hetton lagoon 109B. Three tests were conducted in a first series of trials, and nine in a second series, spaced at 1.6m intervals in the directions indicated by Fig.3.3. It is apparent from Fig.3.8 that a much higher resolution of resistance is obtained by the improved penetrometer, compared to the original design. Correlations between the two are poor, but it should be pointed out that a full year had elapsed between the two sets of trials. A major difference between the profiles produced by the two types of rig in the base penetration line, which shows very little variation with depth in the case of the improved rig. This casts doubt on the assumption mentioned previously with regard to skin friction; to wit, that it was equal upon insertion and retraction.

The second series of trials by Peace (op.cit.) are reproduced in Fig.3.9., which shows a traverse from mid-lagoon (profile 1) towards the outlet (profile 9). It can be seen that the material is becoming weaker, and more homogenous with respect to strength. It is reasonable to assume that this is due to an increase in the proportion of clay towards the outlet. It can also be seen that layers are not continuous. The clearest example of this (though many exist) is found at a depth of 3.0m. Profiles 3 and 4 display a very strong layer at this depth, which is weaker in profiles 1,2,6 and 9 and is absent altogether from profiles 5,7 and 8. Only three factors could account for this; either a change

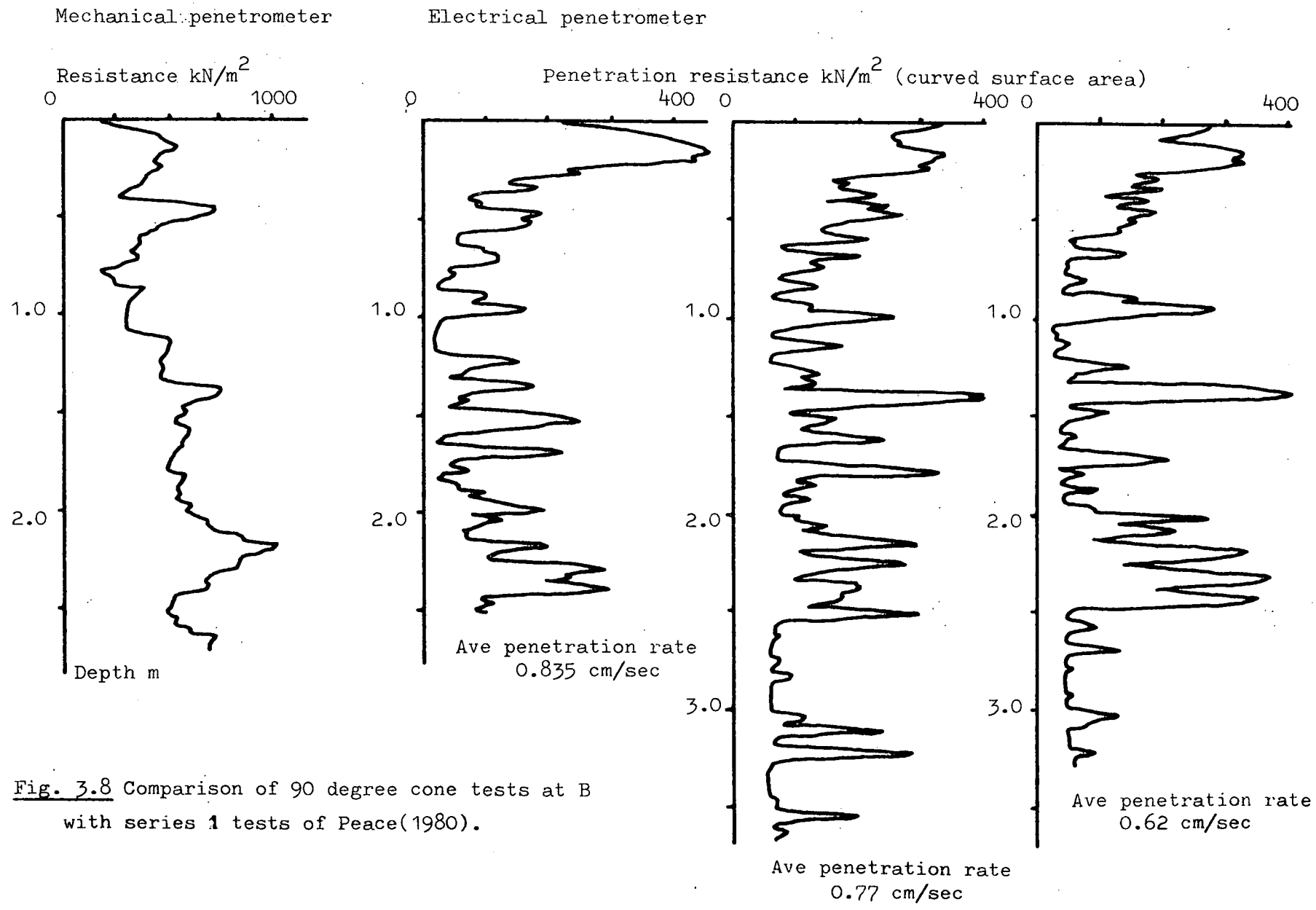


Fig. 3.8 Comparison of 90 degree cone tests at B with series 1 tests of Peace(1980).



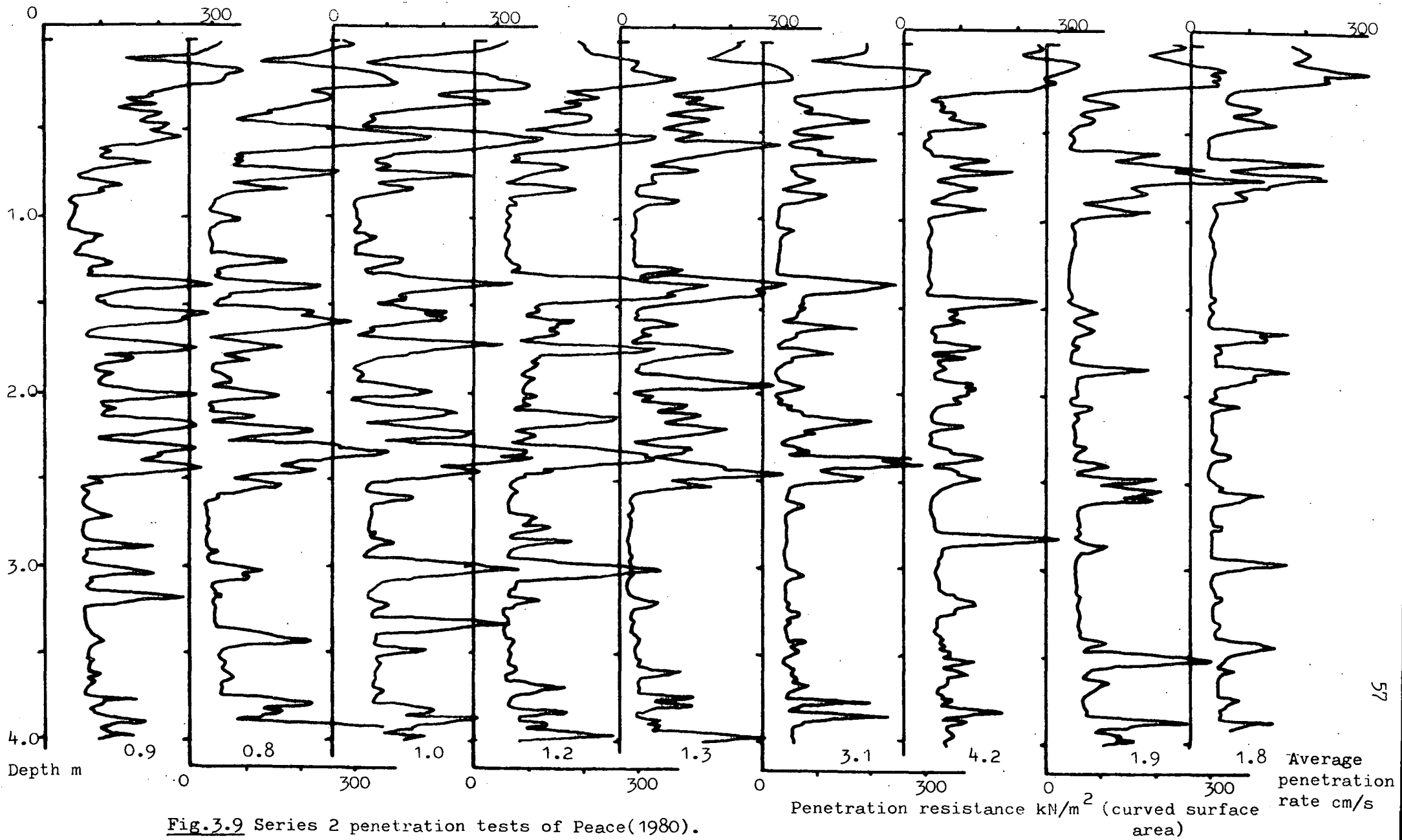


Fig.3.9 Series 2 penetration tests of Peace(1980).

Table 3.2 Correlation coefficients for vane shear tests and cone penetration tests.

Vane Cone	East Hetton <sup>1</sup>			Maltby <sup>2</sup>	
	Diamond	H=D/3	H=2D	Diamond	H=2D
30 degree tip	0.006	0.382	0.622 (99.9)	0.486 (95)	0.440 (95)
90 degree tip	0.227	-0.097	0.242		

Upper figures are product moment correlation coefficients.  
Figures in brackets are significance levels.

1 East Hetton based on 21 tests for each value.

2 Maltby based on 26 tests for each value.

Table 3.3 Correction factors from the field cone penetration and vane shear test results.

$$\text{Correction factor} = \frac{\text{cone resistance}^* - \text{depth} \times \text{density}}{\text{vane shear strength}}$$

(After Lunne *et. al.*, 1976)

Vane Cone	East Hetton <sup>1</sup>			Maltby <sup>2</sup>	
	Diamond	H=D/3	H=2D	Diamond	H=2D
30 degree tip	87 (mean)	70	52	132	119
	43 ( $\sigma$ )	32	19	48	53
90 degree tip	50	44	35		
	17	23	13		

\* In common with usual practice the resistance is taken as the load per unit base area.

1,2 As for Table 3.2 above.

in density (possibly due to desiccation); secondly, a change in the grading and material type within a layer; or thirdly, the layer might pinch out altogether towards the outlet. The first possibility is unlikely, as desiccation tends to affect large areas of a lagoon for similar time periods, and certainly there would not be another strong layer nearer to the outlet in profile 9. It is possible that the placement density could vary, but this is unlikely to produce a change in penetration resistance of a factor of ten between profiles 4 and 5. The second possibility not feasible in terms of sedimentary processes. The most likely alternative is that the layer dies out. There are numerous examples of this happening in the nine profiles.

### 3.5 Interpretation of Static Cone Penetration Tests

In the previous section, penetration profiles from colliery lagoons were briefly analysed on a qualitative basis. This section reviews the possibilities for more thorough interpretation of the test.

There are many methods of interpreting the results from static cone tests. A commonly sought parameter is a compressibility modulus, to be used in the computation of immediate settlements in sandy soils. Bachelier and Parez (1965), De Beer and Martens (1957) and Schultze and Metzger (1965) are amongst those who present methods for determining immediate settlements of foundations from cone test data. These are all for frictional (i.e.  $c=0$ ) soils, and as such are not readily applicable to lagoon deposits. Immediate settlements are not of much interest in any case.

Shear strength parameters have been derived from cone penetration tests by a number of authors. De Beer (1948) derives a method for estimating  $c$  and  $\phi$  values. Begemann (1969), based on De Beer's method, shows that for clay soils ( $\phi=0$ ):

$$\text{shear strength} \approx \text{cone resistance}/14.$$

Begemann (1965) also presents a method whereby measurement of the skin friction developed allows classification of soil types to be performed in-situ, and  $c, \phi$  values obtained. Durgonoglu (1972) utilises bearing capacity factors to derive  $c, \phi$  values, but states that the method is not valid for compressible soils, although an approximate correction is outlined. Durgonoglu (op.cit.) shows that it is possible to use results from two tests with different cones to derive  $c, \phi$  parameters. Application of the method to the East Hetton results does not yield sensible answers (cohesion is often negative).

All these approaches are based on bearing capacity factors derived theoretically from observed failure surfaces beneath model wedges or strip footings (see Fig 3.10). No failure surfaces have been observed for cones (see Durgonoglu, op.cit.; and Durgonoglu and Mitchell, 1975). The extension of the theory to cone tests is justified by the use of empirical shape factors according to some authors (e.g. Durgonoglu and Mitchell op.cit.).

A different type of approach to that outlined above considers empirical methods. Plantema (1957) showed that density is an important factor influencing the results. Lunne et.al. (1976) show that, for Norwegian clays:

$$\text{vane shear strength} \approx \text{cone resistance} / 17$$

This is based on a large number of field tests (cf. a factor of 14 from Begemann, 1969). Calculation of this factor for the East Hetton and Maltby data yields the results shown in Table 3.3. The high standard deviations reflect the fact that the correlation between the vane shear strength and the cone penetration resistance is poor. The values of 17 (Lunne et.al.) and 14 (Begemann) assume a 60 degree cone, and a vane of H=2D shape (Lunne et.al.), and refer to soils unlike the sediments found

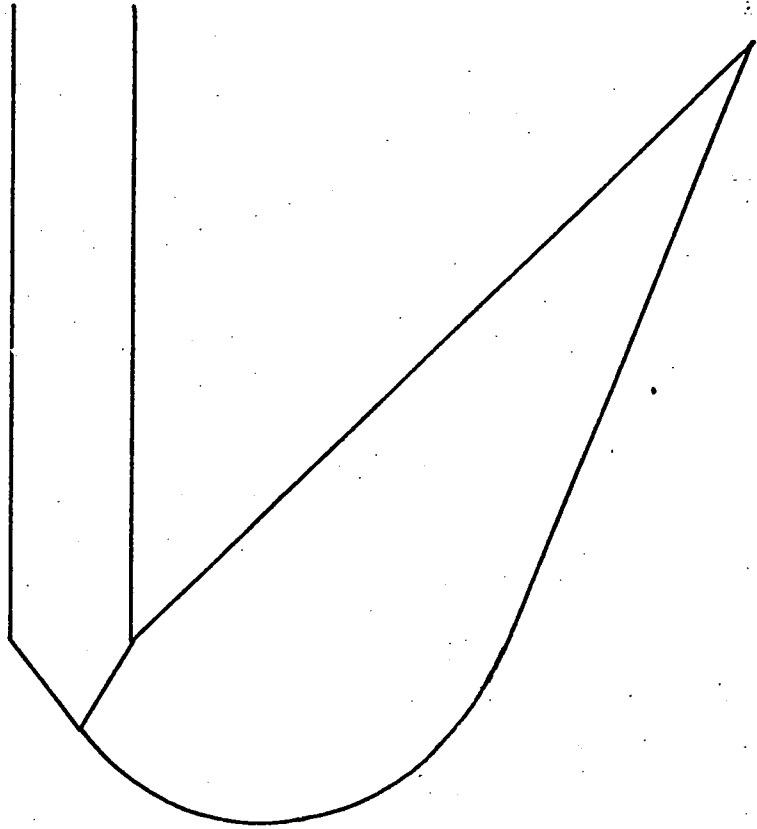


Fig.3.10 Generalised failure surface beneath a wedge, used to determine bearing capacity factors.

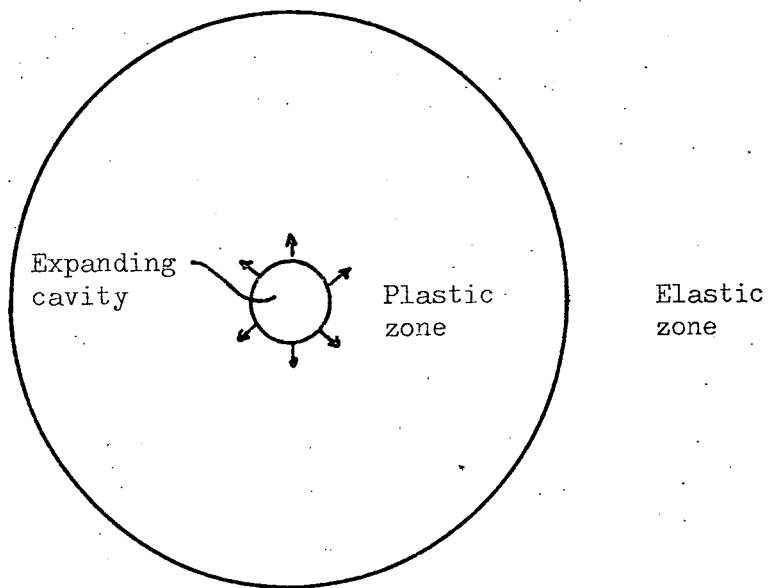


Fig.3.11 Deformation zones around an expanding cavity in Vesic's(1972) model.

in colliery tailings lagoons, so direct correspondence with Table 3.3. is not expected. Indeed, the values calculated in Table 3.3. are markedly higher than these calculated by Lunne et.al. It is significant that the values in Table 3.3. are different for the Maltby results, when compared to East Hetton, and it must be concluded that this empirical approach is not reliable when applied to colliery lagoons. The unreliability of the approach in general was pointed out by Billam (1977).

A different approach is adopted by Vesic (1972) in a theoretical study of the stresses around a cavity expanding into a soil that is governed by a limiting equilibrium. The case of expansion of a cylindrical cavity is applicable to cone penetration tests. No discrete failure surface is assumed, rather a plastic zone at limiting equilibrium within a zone of elastic deformation, Fig.3.11. The extent of the plastic zone, stresses within the body and pore water pressures can all be derived depending on the assumptions.

Basing his arguments on a Mohr-Coulomb equation for the plastic zone, and elastic behaviour in the elastic zone, Vesic (op.cit.) obtains the following equations:

$$P_u = c.F'_c + q.F'_q \quad \dots\dots\dots 3.1$$

$P_u$  is the pressure at the edge of the cavity; in other words, penetration resistance.

$c$  is the cohesion

$q$  is the overburden pressure (i.e.  $\gamma h$ ,  $h = \text{depth}$ )

$F'_c, F'_q$  are theoretical factors, the values of which are given graphically by Vesic (op.cit.).

The values depend on the values of  $\phi, I_{rr}'$ , where:

$$I_{rr}' = I_r \left\{ \begin{array}{l} \phi \\ v \end{array} \right\}, \text{ and:} \quad 3.2$$

$$I_r = E/2(1+\nu) (c + q \tan \phi) = G/(c+q \tan \phi) \quad 3.3$$

$\xi_v$  is a correction factor for  $I_r$ , and has a finite value  $\leq 1$ , depending on  $\Delta$ , the volumetric strain. Values are given graphically in Fig.4 of Vesic (op.cit.)

$E$ ,  $\nu$ ,  $G$  are the Young's modulus, Poisson's ratio and shear modulus of the material.

The radius of the plastic zone is found from

$$\frac{R_p}{R_u} = \sqrt{\frac{I' \sec \phi}{r r}}$$

where  $R_u$  is the radius of the cavity

$R_p$  is the radius of the plastic zone

Thus this method incorporates terms which include, or are dependent on, a large number of factors such as shear strength, density and compressibility all of which have been shown to influence the test results by the authors mentioned previously.

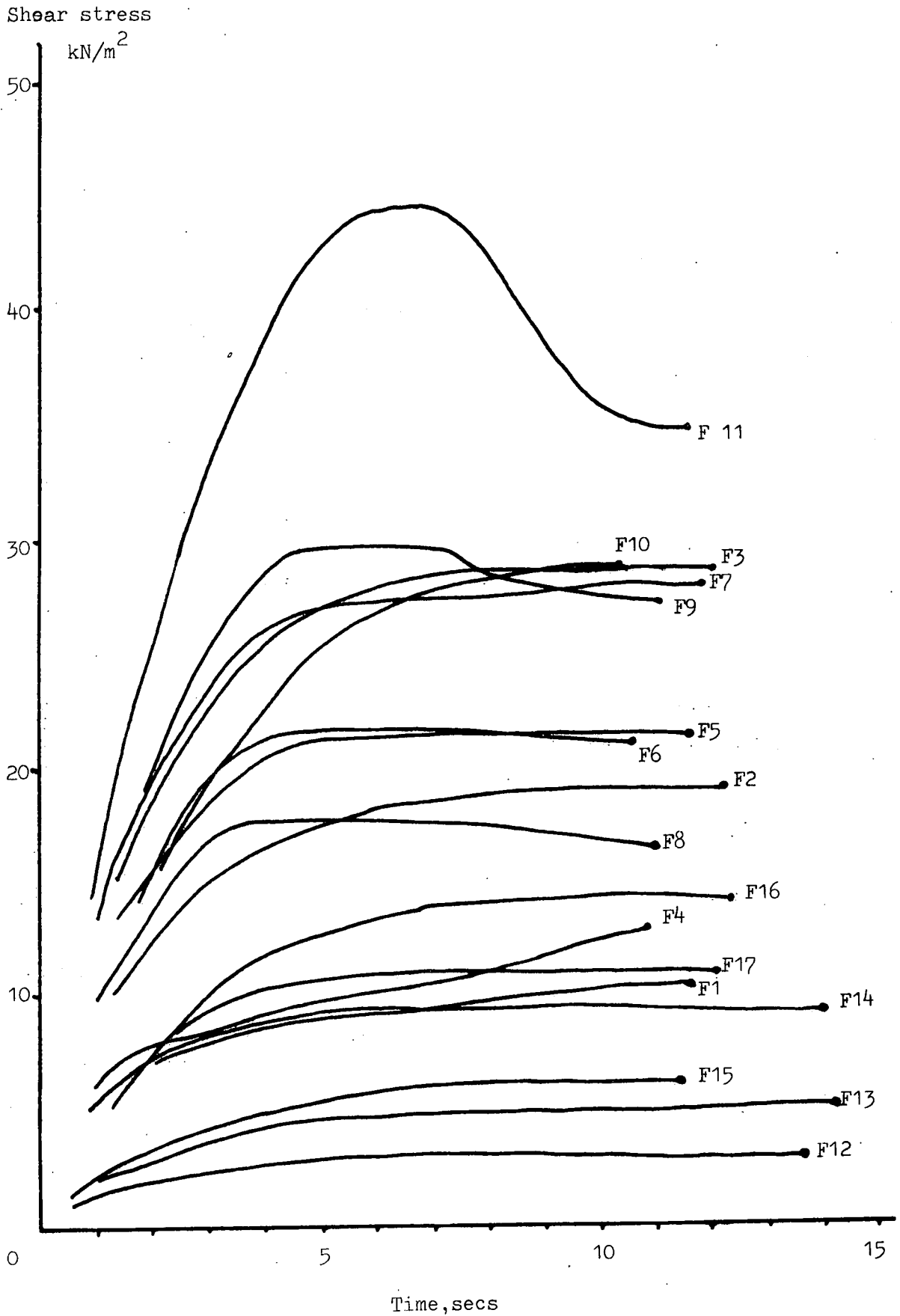
### 3.6 An Investigation into the Applicability of Vesic's Model to Cone Penetration Tests

The values of  $G$ ,  $\phi$  and  $c$  for various values of  $q$  (i.e. normal stress) can be found from shear-box data. In order to eliminate any rate effects, the values of  $G$  have been computed from shear box tests run at a rate of strain comparable to that in the soil during penetration by the cone. At a penetration rate of 40mm/min the 90 degree cone passes any point in 12 seconds. A particle of soil in the centre therefore moves outwards 8mm in 12 seconds, which is a strain rate of 40mm/min. Similarly, for the 30 degree cone the strain rate is 11mm/min. In fact shear takes place

in a zone, not on a discrete plane; furthermore, the path followed by any particle is not necessarily in a straight line from the centre of the outside, but probably curves downwards then outwards. These effects have been neglected. A number of shear-box tests have been conducted on undisturbed samples at comparable rates of shear, though it was necessary to hand-wind the shear-box. For the two rates of strain (i.e. 40mm/min and 11mm/min), the samples of each of the following East Hetton materials have been tested: a sandy layer; a silty layer; an over-consolidated clay; and a normally consolidated clay. Each of these materials has been sheared at three different normal stress levels, comparable to the levels of overburden stress that exist in the top few metres of a lagoon. The stress/time plots for the faster tests are shown in Fig.3.12, and for the slower tests in Fig.3.13. From these graphs the values of the shear modulus,  $G$ , have been calculated (taken as the secant modulus to 50% of peak shear stress). From the values of  $G$ , the values of  $I_r$  can be calculated according to equation 3.3. The value of  $(c+q \tan\phi)$  in this equation has been taken as  $\tau_f$ , the failure shear stress for each individual test, in order to eliminate differences between samples. The values of  $I$  and  $G$  are given in Table 3.4. for all the tests. It can be seen clearly in Fig.3.14 that these values  $I_r$  do not show any reasonable trends with soil type, or overburden pressure. The variation of values is too great for such trends to emerge. In contrast Vesic (1972) states that the magnitude of  $I_r$  should be inversely proportional to the square root of the confining pressure, though this was based on tests with up to  $10^4 \text{ kN/m}^2$  confining pressure. The lack of trends in the data presented here is probably due to the low confining pressures under consideration. Furthermore, there is no difference between the two rates of strain. The measured values of  $I_r$  therefore lie approximately between 20 and 40,



Fig.3.12 Stress-time curves for East Hetton material at approximately 50mm/min rate of displacement. Terminal strain is 10.8mm in each case. Numbers refer to entries in Table 3.3.



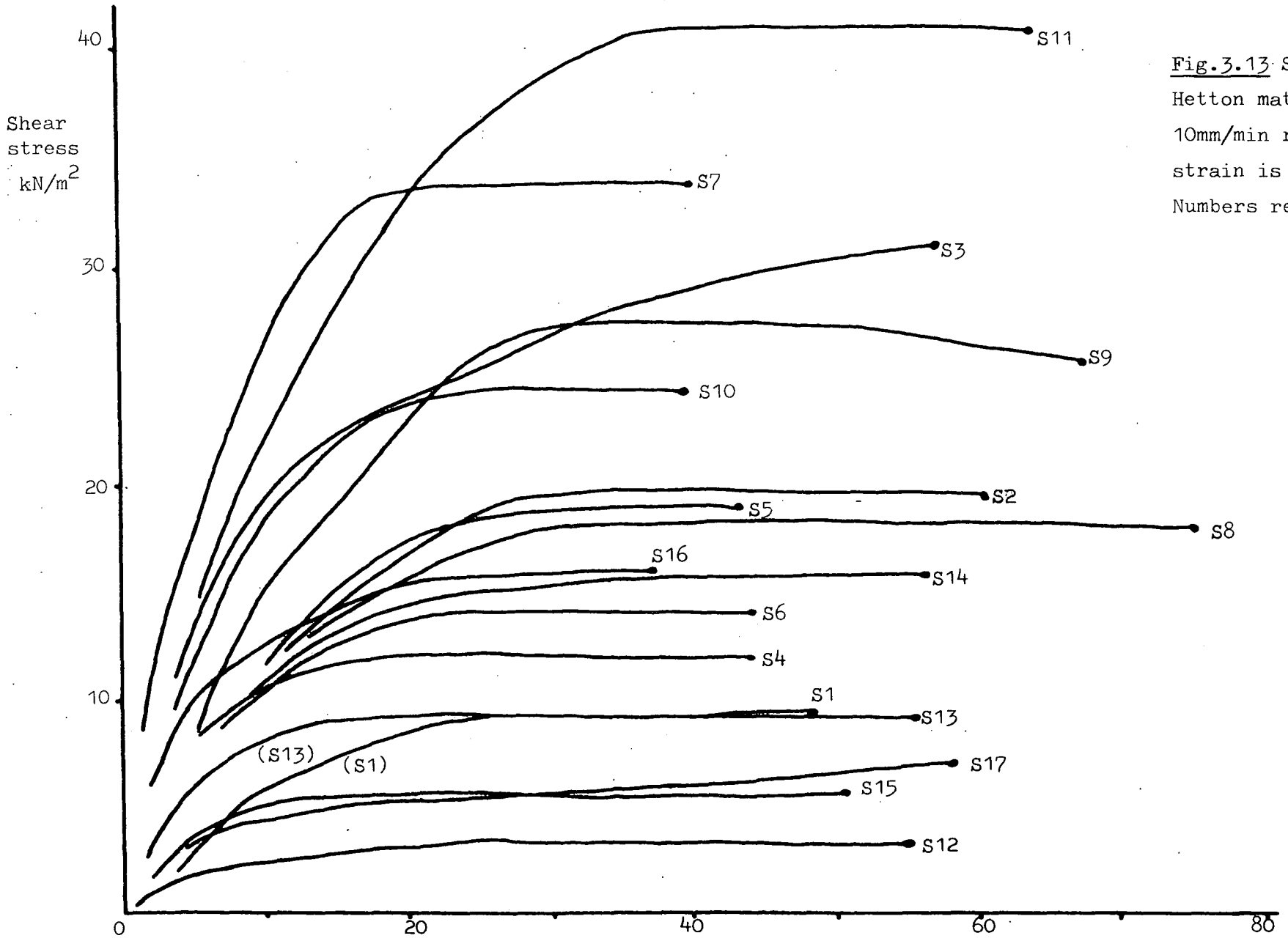
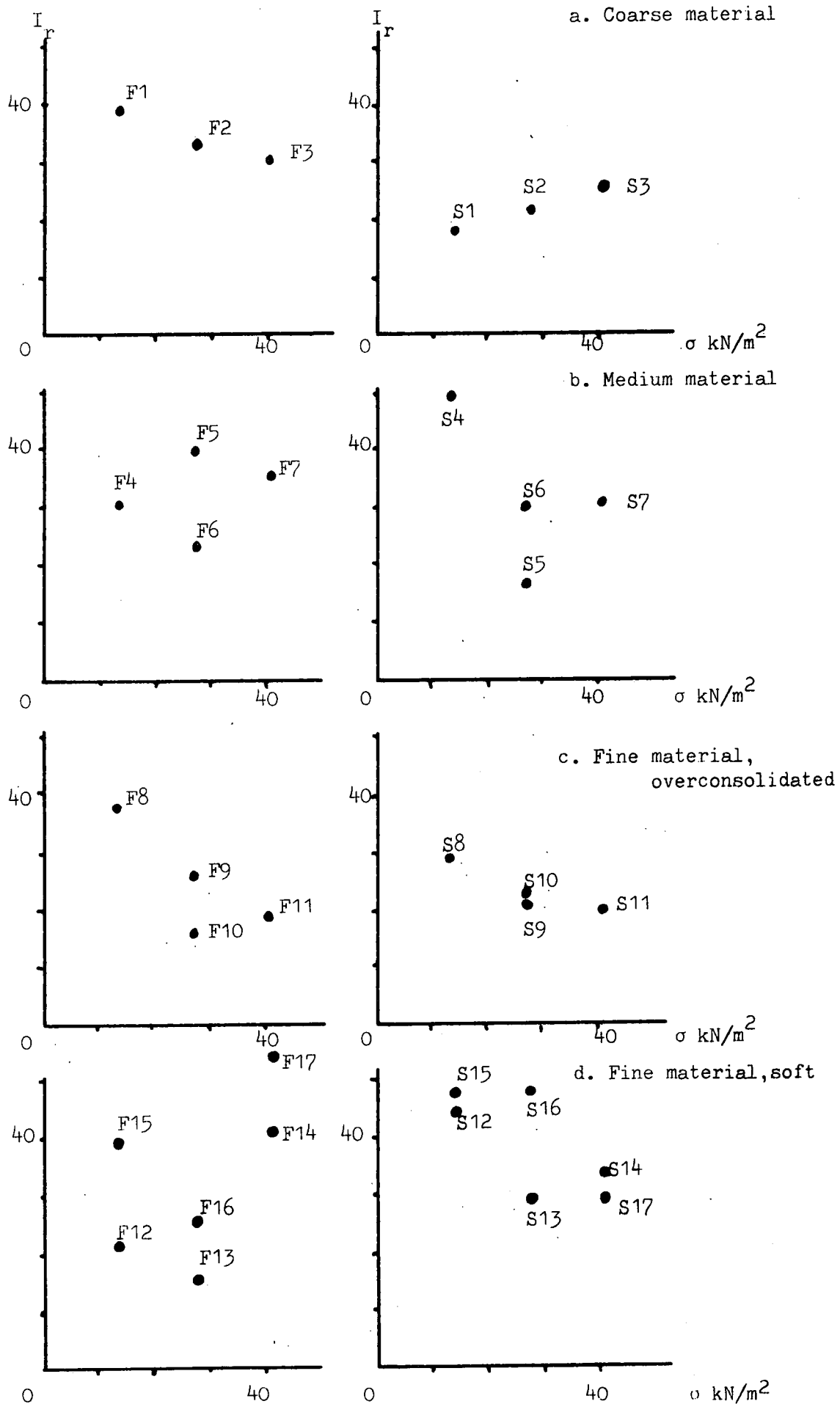


Fig.3.13 Stress-time curves for East Hetton material at approximately 10mm/min rate of displacement. Terminal strain is 10.8 mm in each case. Numbers refer to entries in Table 3.3.

Table 3.4 Shear box test data from East Hetton material.

Sample	Rate of shear mm/min	$\sigma$ kN/m <sup>2</sup>	$\tau_f$ kN/m <sup>2</sup>	$\epsilon_f$ kN/m <sup>2</sup>	$t_f$ kN/m <sup>2</sup>	$\tau_{\frac{1}{2}}$ kN/m <sup>2</sup>	$\epsilon_{\frac{1}{2}}$ kN/m <sup>2</sup>	$G_{\frac{1}{2}}$ kN/m <sup>2</sup>	$I_r$
S1	13	13.6	9.1	0.089	24	4.5	0.027	169	18.6
S2	11	27.2	19.4	0.085	28	9.7	0.023	425	21.9
S3	11	40.9	30.7	0.180	57	15.4	0.019	808	26.3
S4	15	13.6	12.0	0.058	14	6.0	0.010	598	49.8
S5	15	27.2	19.0	0.128	32	9.5	0.030	316	16.6
S6	15	27.2	13.9	0.090	22	7.0	0.016	427	30.7
S7	16	40.9	33.7	0.095	22	20.5	0.020	1035	30.7
S8	9	13.6	18.1	0.075	30	9.0	0.017	529	29.2
S9	9	7.2	27.2	0.075	28	13.6	0.023	580	21.3
S10	17	27.2	24.1	0.110	24	12.1	0.022	548	22.7
S11	9	40.9	41.2	0.101	36	20.6	0.025	832	20.2
S12	12	13.6	3.4	0.065	20	1.7	0.010	163	47.9
S13	12	27.2	9.5	0.050	19	4.8	0.010	458	48.2
S14	12	40.9	15.9	0.112	33	7.9	0.017	471	29.6
S15	13	13.6	15.7	0.053	15	2.9	0.011	255	44.8
S16	17	27.2	15.9	0.149	31	8.0	0.017	467	29.4
S17	11	40.9	7.0	0.180	58	3.5	0.015	233	33.3
F1	55	13.6	10.5	0.180	11	5.7	0.014	414	39.4
F2	54	27.2	19.0	0.135	9	9.5	0.015	633	33.3
F3	53	40.9	27.9	0.099	7	14.0	0.016	860	30.8
F4	59	13.6	12.7	0.171	11	6.4	0.016	393	30.9
F5	56	27.2	21.1	0.078	5	10.6	0.012	849	40.0
F6	59	27.2	21.2	0.072	4.4	10.6	0.021	497	23.4
F7	55	40.9	27.6	0.180	12	13.6	0.014	988	35.8
F8	59	13.6	17.4	0.056	3.4	8.7	0.013	665	38.2
F9	59	27.2	29.5	0.096	4.3	14.8	0.019	771	26.1
F10	59	27.2	28.2	0.139	8.5	13.6	0.030	461	16.3
F11	59	40.9	44.6	0.096	6	22.3	0.026	871	19.5
F12	47	13.6	2.9	0.061	5	1.5	0.013	115	39.7
F13	46	27.2	5.1	0.076	6	2.5	0.019	131	25.7
F14	46	40.9	9.3	0.060	5	4.6	0.009	509	54.7
F15	57	13.6	5.8	0.089	6	2.9	0.024	122	21.0
F16	51	27.2	14.1	0.110	8	7.1	0.032	219	15.5
F17	54	40.9	10.8	0.080	6	5.4	0.012	450	41.6

Fig.3.14 The variation of  $I_r$  with normal stress.



and these may be taken as lower and upper bounds.

The next step is to evaluate  $I'_{rr}$  from equation 3.2. In order to do this the value of  $\Delta$  (volumetric strain) has to be assumed from Table 3.5. It can be seen that clays ( $c_v = 20\text{m}^2/\text{yr}$ ) will behave essentially in an undrained fashion during penetration of the cone, while silts behave in a partially drained fashion and sands will be fully drained. Hence, the value of  $\Delta$  will be 0% for clays; 5% is a reasonable minimum estimate for a sand, and the value of  $\xi_v$  is not sensitive to the variation of above 5% (see Fig.4, Vesic, 1972).

It is now possible to construct Table 3.6. Values of the pressure at the edge of the cavity (i.e.  $P_u$ ) are presented in the table based on both the upper and lower bound estimates of  $I_r$ .

The values of  $P_u$  are, furthermore, given for depths of 1m and 3m, which spans the range tested at East Hetton. The Table shows that at any depth a sandy horizon should give a greater resistance to penetration than a normally consolidated clay, since even the lower estimate for sands exceeds the upper estimate for clays. In contrast the overconsolidated clay is more resistant than the sands at depths of a metre, but is less resistant at a depth of three metres.

The theoretical cavity pressures thus accord on a relative basis with normal expectations. Comparing the absolute values with the penetration resistance values (which are now taken as the resistance per curved surface area) measured by the first field device (see Figs.3.4 and 3.6) shows that the measured values exceed those given in Table 3.6 by factors of two or more. However, inspection of the resistance measured by the second device (Peace, 1980; and Figs.3.8 and 3.9) shows that the theoretical cavity pressures are of the same order. The agreement between the two for the measured "baseline" values of  $50\text{--}100\text{ kN/m}^2$  and the cavity

Table 3.5 Drainage of lagoon material during cone penetration tests.

$$C_r = \frac{T \cdot d^2}{t}, \quad \text{hence } T = \frac{C_r \cdot t}{d^2} *$$

t (secs)	$C_v$ ( $m^2/yr$ )	T	U (%)
45 (i.e. 30 degree cone)	5	0.012	15
12 (i.e. 90 degree cone)		0.003	5
2 (60 degree cone, Peace, 1072)		0.0002	0
45	10	0.023	22
12		0.006	10
2		0.0004	0
45	20	0.046	35
12		0.012	15
2		0.0008	0
45	40	0.092	56
12		0.024	23
2		0.0016	1
45	100	0.23	85
12		0.06	43
2		0.004	6
45	200	0.46	95+
12		0.12	65
2		0.008	12
45	400	0.91	95+
12		0.24	86
2		0.017	18
2	1000	0.04	33

\*Note Based on  $d=25mm$ , where  $d$  is the drainage path length.

Vesic (1972) shows that:

$$\delta u = ( 0.817 \alpha_f + 2 \ln R_p/r ) c$$

$$\text{where } \alpha_f = 0.707 ( 3A_f - 1 )$$

$A_f$  = Skempton's pore pressure parameter

$R_p$  = the radius of the plastic zone

$r$  = the radius at which the value of  $\delta u$  is required

$c$  = the cohesion

Thus the excess pore pressure falls logarithmically with distance from the cavity, and may be neglected beyond the plastic zone.

Table 3.6 The evaluation of cavity pressures for cone penetration tests in East Hetton lagoon sediments.

Material	$c^*$ kN/m <sup>2</sup>	$\phi^o$	$I_r$	$\xi_v^+$	$I'_{rr}$	$F'_c$	$F'_q$	$P_u$ at 1m <sup>†</sup> kN/m <sup>2</sup>	$P_u$ at 3m. <sup>†</sup> kN/m <sup>2</sup>	$R_p$ mm
Sand	0	35	20	0.5	10	4	4	52	156	28
			40	0.3	13	5	5	70	210	32
Clay	(0.58 x $\sigma'_v$ )	0	20	1.0	20	4	0	32	97	36
			40	1.0	40	4.5	0	37	110	51
Overconsol. clay	18 + (0.36 x $\sigma'_v$ )	0	20	1.0	20	4	0	92	132	36
			40	1.0	40	4.5	0	104	149	51
Clay (drained)	0	30	20	0.2	4	2.5	2.5	35	105	17
			40	0.1	4	2.5	2.5	35	105	17

\* Clays assumed undrained ( $\phi=0$ ), but their value of cohesion will depend on the effective stress during consolidation.

+  $\Delta=5\%$  for sands, 0% for undrained clays, 15% for drained clays; based on Vesic's (1972) chart for  $v$ .

†  $\gamma_b$  taken as 14 kN/m<sup>3</sup>.

pressures of a normally consolidated clay is good. The values of the peaks in the resistance graphs do not correspond so well to the calculated pressures for the overconsolidated clays or sands, but three points must be remembered. Firstly equation 3.1 shows that the calculated cavity pressure depends on the value of cohesion in a clay, and this may not be the same as that which was assumed in Table 3.6. Secondly, the effect of layering is unknown; and thirdly, Vesic's theory refers to a cylinder of infinite vertical extent. Since fine layers are the major constituent of the sediment near the outlet (see Table 3.1), these would be expected to give the best correspondence in any case.

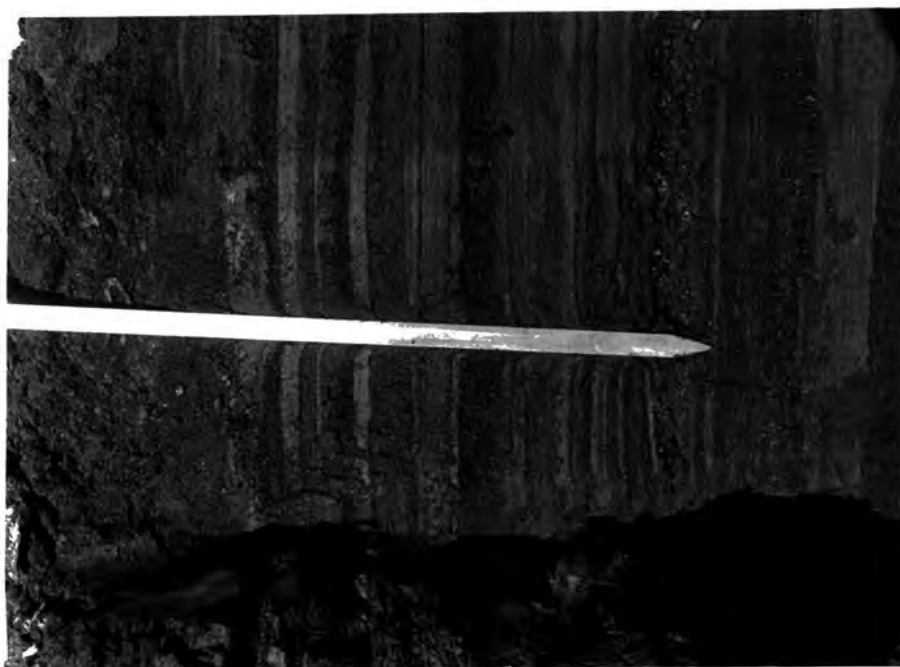
The radius of the plastic zone has also been calculated in Table 3.6. In order to check this directly in the field, a trench was dug in the sediment at the location shown in Fig.3.3, this area being dry enough to support a free face. A sheet of perspex was pushed hard against a flat vertical face of sediment. D section (half section) cones with 30 degree and 90 degree tips (these were readily available) were pushed vertically downwards by hand, flush with the perspex. The resulting deformation was photographed. It can be seen from Fig .3.15. that the edge of the plastic zone is fairly sharp and is between 17 and 25mm away from the centre line of the cone. No discrete failure surfaces are seen at all. During this exercise it could also be observed directly that sands were more resistant to penetration than the soft clays.

This observed radius for the plastic zone is comparable to that calculated in Table 3.6 for the sands, but not for the clays (the calculated value being too large). However, the known radius can be used to back-calculate other values. Thus taking  $R_p$  as 17mm,  $I_{rr}'$  must be 4; for  $I_r'$  to be 20,  $\xi$  must therefore be 0.2 and for  $I_r'$  to be 40,  $\xi$  must be 0.1. Each of these two cases gives a value of  $\Delta$  (volumetric change)



Fig. 3.15. Deformation in East Hetton tailings caused by passage of the cones.

a. 30 degree cone.



b. 90 degree cone.



of 15%, based on Fig.4 of Vesic (1972), which implies a degree of drainage for the clays.  $P_u$  is found as before, but does not change greatly with this change in assumption (see Table 3.6).

In section 3.3. it was shown that the more resistant penetration profiles correlated with those parts of the lagoon which contained coarser sediments. Vesic's (1972) model supports this conclusion with a theoretical treatment, although certain assumptions have had to be made in the application of the model to penetration tests in lagoons. It is therefore reasonable to conclude that layers that show little resistance to penetration consist of normally consolidated, fine, clay-rich sediments; on the other hand, a resistant stratum indicates a sandy horizon, or near the surface the stratum could consist of overconsolidated clay. Thus, in a general way the shear-strength properties associated with the various types of layer may be assigned to various portions of the resistance penetration log. Of particular interest will be the relative proportions of each type of layer at any location, as this will govern the behaviour of that location. For instance the stability of an over-tipping operation will depend on whether free draining sandy horizons, or impermeable clays are being overtipped (see chapter 7). The drainage properties at any location will also be linked to the distribution of the layers. In this context it is worth recalling that in Fig.3.9 many sandy horizons were observed to die out over short distances (i.e. there is evidence that layers are discontinuous).

### 3.7 Conclusions

A preliminary series of trials with a cheap, lightweight rig showed that cone penetration resistance could be used as a profiling tool for lagoons. However, the use of paired cone tests using two cones with different tip angles was found to offer no advantages over the use of a single cone.

A more sophisticated rig, using a load cell and a single 60 degree cone has been shown to produce a highly detailed picture of a lagoon very rapidly. It has been shown by comparison with known properties of the lagoon, by direct observation with hand pushed cones, and in a theoretical study, that horizons of different properties can be readily correlated against the profiles obtained from this field rig.

This is currently the "state of the art" with this rig. Possible future improvements could include a better guide rail system; more importantly a pore pressure transducer at the tip of the core would be a significant advance. Furthermore, it would be useful to correlate the cone resistance values obtained from such a device against some yardstick, say field vane tests, or better, bearing capacity observations from an overtipping exercise. Such a device could then be a very powerful field investigation tool for colliery lagoons.

## CHAPTER 4. THE GEOCHEMISTRY AND SEDIMENTOLOGY OF COLLIERY LAGOONS

### 4.1 Introduction

The importance of the geochemistry and sedimentology is threefold:

1. To understand the fundamental controls on shear strength and consolidation parameters.
2. To elucidate the controls on lagoon composition (e.g. type of washery) and the<sup>re</sup>fore arrive at general models.
3. To assess the constraints on alternative uses or alternative methods of disposal.

Consequently, the coal contents, mineralogy and major element geochemistry has been determined for a number of samples as follows:-

1. Peckfield lagoon 7 (series denoted as PL7...) 17 undisturbed samples from two vertical boreholes, split into  $<90\mu$  and  $>90\mu$  fractions.
2. Peckfield lagoon 6 (PL6...) 7 bulk samples from a depth of 1m taken at intervals from the inlet to the outlet, split into several fractions.
3. East Hetton lagoon 109B (EH....) 10 samples from three boreholes (locations A, B and C), representative layer types being taken at each location.
4. Maltby lagoon 6 (MA....) 6 samples from two boreholes, representative layer being taken. Also one coarse discard sample.
5. Oakdale Washery (OW....) 5 samples run as part of leaching experiments.
6. Silverhill lagoon 16 (SI....) Two representative layer types taken, mineralogy only being determined for these samples.

### 4.2 The Determination of Mineralogy

The mineralogy of the above specimens was analysed using a Phillips PW 1130 X-ray diffractometer. Cobalt  $K_{\alpha}$  radiation was used, this being preferred for samples with a high iron content (Taylor, 1977, pers.comm.).

The  $2\theta$  scans were measured with a CORIDA polar planimeter and interpreted according to the method and calibrations of Smith (1978) with a 10% boehmite internal standard. The mixed-layer clay content of the illite fraction was determined by adding ethylene glycol to the sample and warming at  $50^{\circ}\text{C}$  for a 24 hour period. Mixed-layer clay was taken as the difference in the area of the  $10\text{\AA}$  illite peak before and after this treatment.

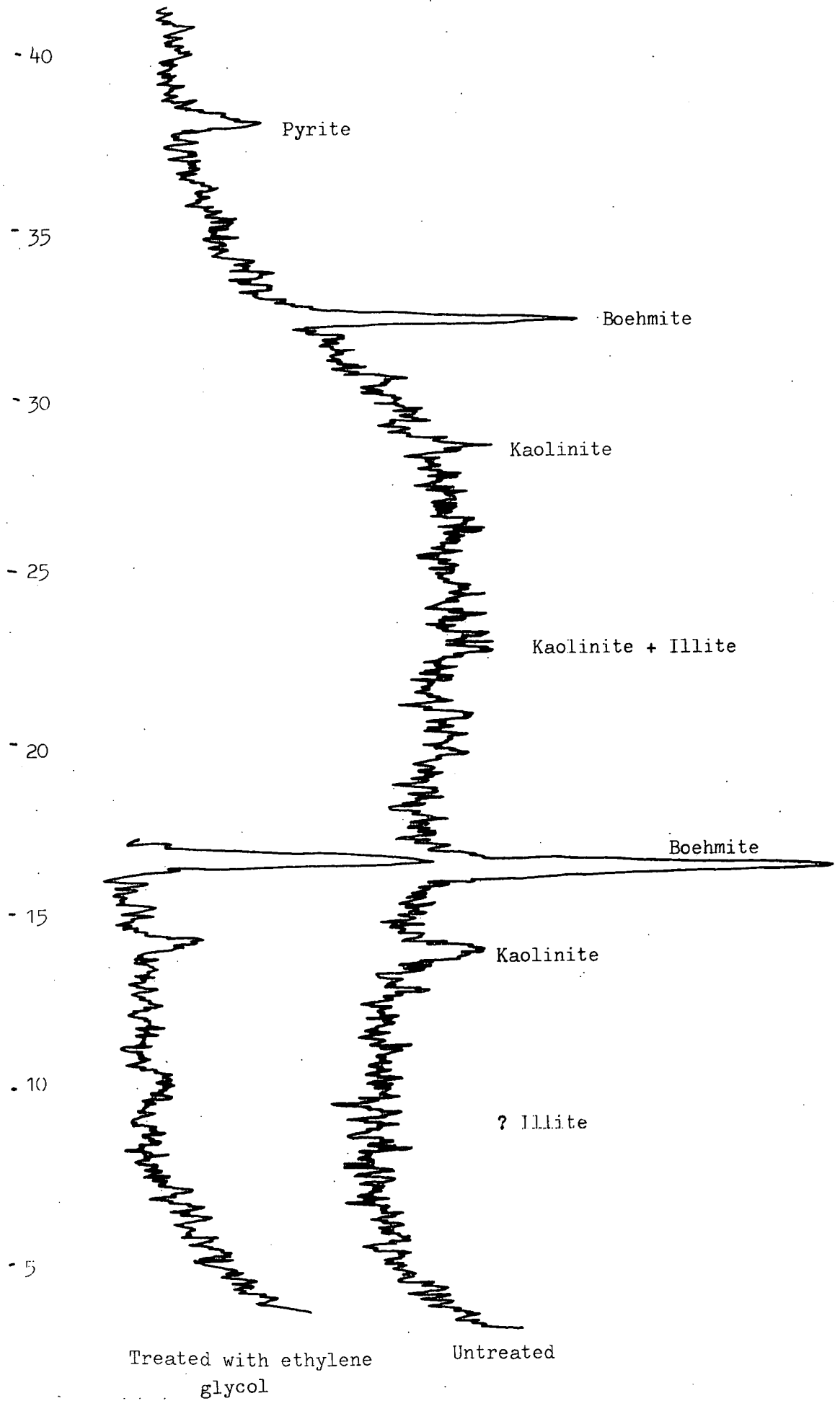
The samples under consideration are generally of a high organic carbon content. This may be taken as the coal content to a first approximation. High organic carbon produces a great deal of background scatter during X-ray diffraction (XRD) and interpretation of the scan is difficult. This can be seen from Fig.4.1. which shows the  $2\theta$  traces of a coal-rich sample. The interpretation of the mixed-layer clay fraction is impossible in this case. All the values of mineral weight-percent content reported herein must therefore be regarded as only semi-quantitative, the mixed-layer clay value being the least reliable parameter. Indeed it was found that the mixed-layer clay content was so difficult to determine that it was abandoned altogether after the Peckfield samples had been analysed. The accuracy of determinations decreases with increasing coal content.

The full results are reported in Appendix A4.1, and are discussed along with the chemistry in section 4.6.

#### 4.3 The Determination of Chemistry

Nicholls(1962) and Taylor (1971.a) have pointed out that the imprecise nature of X-ray diffraction work renders a chemical analysis desirable in addition. This is particularly true for the high carbon samples considered herein. Consequently major-element chemistry has been analysed for all samples (excepting two from Silverhill colliery) by

Fig.4.1 2 $\theta$  XRD scan of a coal rich sample (organic carbon=93%).



X-ray fluorescence (XRF). A pertinent example is given by the XRD analysis of sample 210C from Maltby lagoon No.6. There is no trace of pyrite or any other sulphur containing mineral, yet the chemistry of this sample revealed 49% by weight of sulphur, which is almost certainly in pyrite.

The chemistry was analysed using fully automatic prototype Phillips PW1400 X-ray fluorescence machine. The usual method was employed of running standards of known composition to obtain calibrations from which the sample compositions could be determined. The mass absorption correction procedure (Holland and Brindle, 1966) is customarily used at Durham but was considered inappropriate here for the following reason. The mass absorption correction depends on an accurate determination of all the major constituents including free carbon,  $\text{CO}_2$  and  $\text{H}_2\text{O}$ . As will be explained, accurate determinations of very high free carbon percentages are difficult to obtain.

Use was made instead of a non-linear, multiple regression model which does not require determination of all the constituents. The mass absorption correction is implied in the statistical relationships of the regression coefficients. The coefficients were determined using the procedure known as REGRESSION in the computer package "Statistical package for the social sciences" (Nie *et.al.*, 1975)

The regression equations used are given in Appendix A4.2 along with the "raw" plots of counts vs composition for the standards. Comparison of these equations with the mass absorption correction procedure is possible by considering the correlation coefficients produced by comparing the observed (i.e. actual) with expected (i.e. recomputed using the procedure adopted) chemistry for the standards. Table 4.1 indicates that the regression method is in fact superior for the standards considered

Table 4.1 Correlations of observed with expected chemistry of the standards used in the XRF analysis.

	XRFPL1 <sup>1</sup>		SPSS <sup>2</sup>	
	R <sup>3</sup>	SEE <sup>4</sup>	R	SEE
SiO <sub>2</sub>	0.980	Not quoted	0.997	1.607
Al <sub>2</sub> O <sub>3</sub>	0.994		0.997	0.778
Fe <sub>2</sub> O <sub>3</sub>	0.997		0.997	0.586
MgO	0.984		0.993	0.546
CaO	0.847		0.994	1.078
Na <sub>2</sub> O	0.921		0.997	0.153
K <sub>2</sub> O	0.993		0.995	0.184
TiO <sub>2</sub>	0.995		0.995	0.069
S	0.968		0.992	0.406
P <sub>2</sub> O <sub>5</sub>	0.976		0.979	0.044

1 Program based on Holland and Brindle (1966).

2 Regression model used in this work.

3 Correlation coefficient.

4 Standard error of the estimate

$$SEE = \sqrt{\frac{\sum (\text{obs} - \text{expected})^2}{N-1}}$$

The standard error of the total is

$$SEE_{\text{tot}} = \sqrt{\sum_{i=1}^{10} (SEE)^2} = 2.285$$

Table 4.2 Composition of the secondary standards.

$$SU1A = 2/3 \text{ SU1} + 1/3 \text{ NBS88A}$$

$$SU2A = 7/8 \text{ SU1} + 1/8 \text{ NBS88A}$$

	SiO <sub>2</sub>	Al <sub>2</sub> O <sub>3</sub>	Fe <sub>2</sub> O <sub>3</sub>	MgO	CaO	Na <sub>2</sub> O	K <sub>2</sub> O	TiO <sub>2</sub>	S	P <sub>2</sub> O <sub>5</sub>
SU1A	23.41	6.37	21.88	9.72	12.67	0.69	0.46	0.55	8.03	0.07
SU2A	30.35	8.30	28.62	6.10	7.23	0.90	0.57	0.71	10.54	0.09



by the writer.

The pyrite-rich nature of the lagoon samples dictated that the standards should have a wide range of sulphur compositions. This necessitated the making up of two secondary standards, the compositions of which are given in Table 4.2.

The XRF equipment was new at the time of use, and because it was a prototype there were teething problems. To check both these problems and the repeatability of the counts a number of checks were run. The details of these checks are given in Appendix A4.3. Bearing in mind the limitations to the accuracy of the analyses shown in Appendix A4.3 and Table 4.1 the results, which are given in detail in Appendix A4.4, can now be discussed.

#### 4.4 The Use of Burnt Samples for Analysis

In a trial run on a few samples it had been noticed that the sum of the elements and element oxides plus the coal content (as determined by thermal oxidation at 350°C) consistently exceeded 100% by a considerable margin. The cause of this was unclear and was investigated as follows. For 41 samples of lagoon material, duplicate subsamples were taken, making 82 subsamples. One of each pair was oxidised at 350°C, the carbon content being determined (and reported in the mineralogy, Table A.4.1.1). The 41 non-oxidised and the 41 oxidised samples were then made up into XRF pellets and analysed along with further non-oxidised samples as described above. The 41 non-oxidised samples are those from Peckfield lagoon 7, and from Maltby Colliery. They are denoted by the suffix "U" in Appendix A.4.4. The duplicate burnt samples are denoted by the suffix "B".

The chemistry analysed does not include free carbon, CO<sub>2</sub> or H<sub>2</sub>O, and hence in the case of the non-oxidised samples the sum of the components subtracted from 100% can to a first approximation be taken as the organic

carbon content;  $\text{CO}_2$  and  $\text{H}_2\text{O}+$  are much less significant. The sums of the components are given in the final column ("TOTAL") of Table A.4.4.1. Thus for the 41 non-oxidised samples (100-TOTAL) may be plotted against the carbon content determined by oxidised. It can be seen from Fig.4.2 that the thermal oxidation method gives a significantly higher estimate of free carbon than the XRF difference method. Although there is no statistical difference to separate the goodness of fit of the two regression lines in the figure, the curved fit is intuitively more realistic because:-

a) At 100% free carbon both methods should agree on a value of 100%. The curved fit extrapolated gives closer agreement. The 10% residuum on the XRF method may be due to background, but more likely it represents an amount of true ash in the coal.

b) At 0% free carbon there is still some chemistry unaccounted for by XRF analysis, i.e.  $\text{CO}_2$  and  $\text{H}_2\text{O}+$ . The curved regression line extrapolated suggests that this is of the order of 5%.

Keeling (1962) found that thermal oxidation at  $375^\circ\text{C}$  over-estimated carbon contents of up to 20% by as much as  $\times 1.5$ , a value which agrees with Fig.4.2. He attributed this mainly to loss of bonded water from gypsum and siderite. This mechanism cannot fully explain Fig.4.2, especially at the medium to high carbon contents.

Turning to the burnt samples, the sum of the chemistry in the TOTAL column again does not come to 100%, but rather to between 90 and 95%, generally. Thermogravimetric analysis to  $1000^\circ\text{C}$  (Zussman, 1967) was performed on two samples to determine the  $\text{CO}_2$  and  $\text{H}_2\text{O}+$  content. In the case of 1)90B these two results in 9.62%, and for 2)90B they result in 12.88% by weight. Adding these to the total value gives a grand total of 98.72% and 103.75% respectively, which are within the margin of error of the XRF analysis. Thus (100-TOTAL)% for the burnt samples is

Fig.4.2 Comparison of organic carbon contents as determined by XRF and thermal oxidation at 350°C.

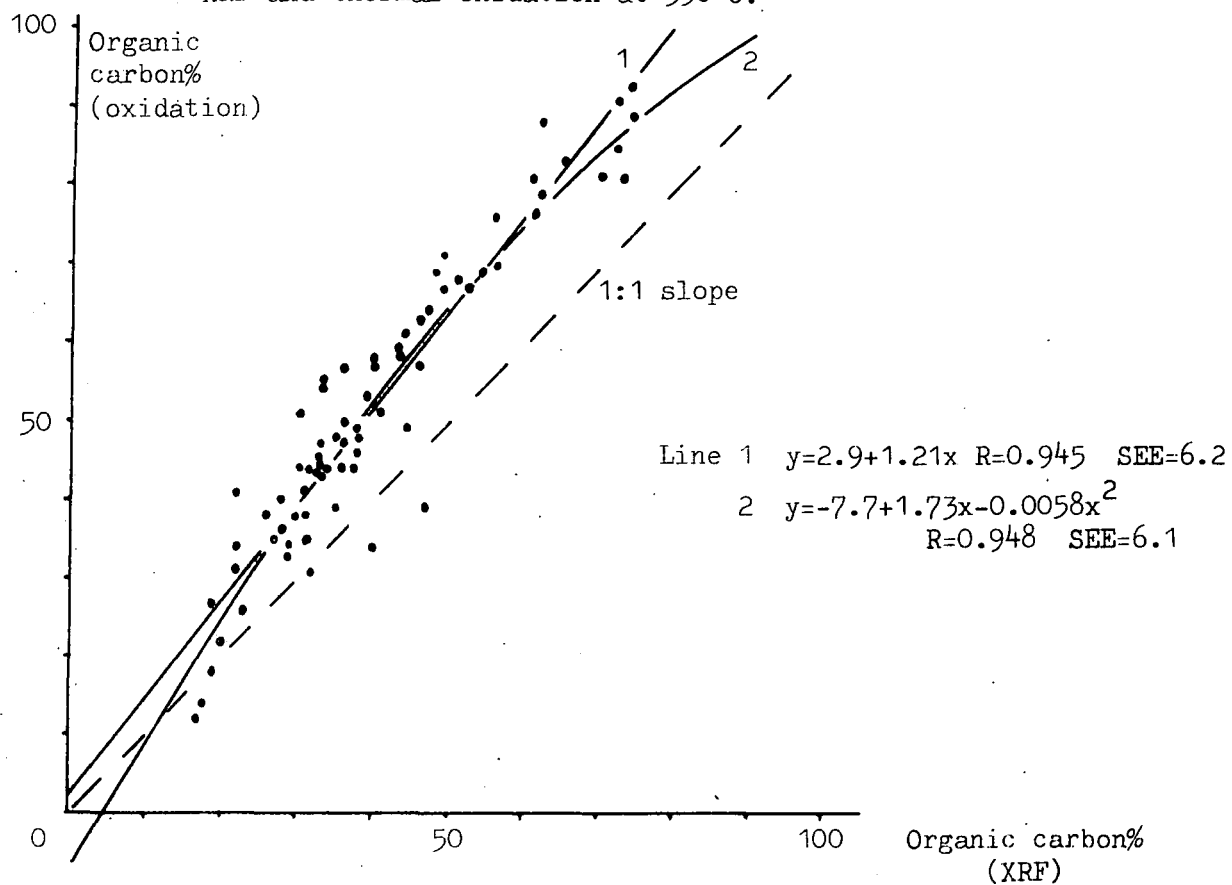
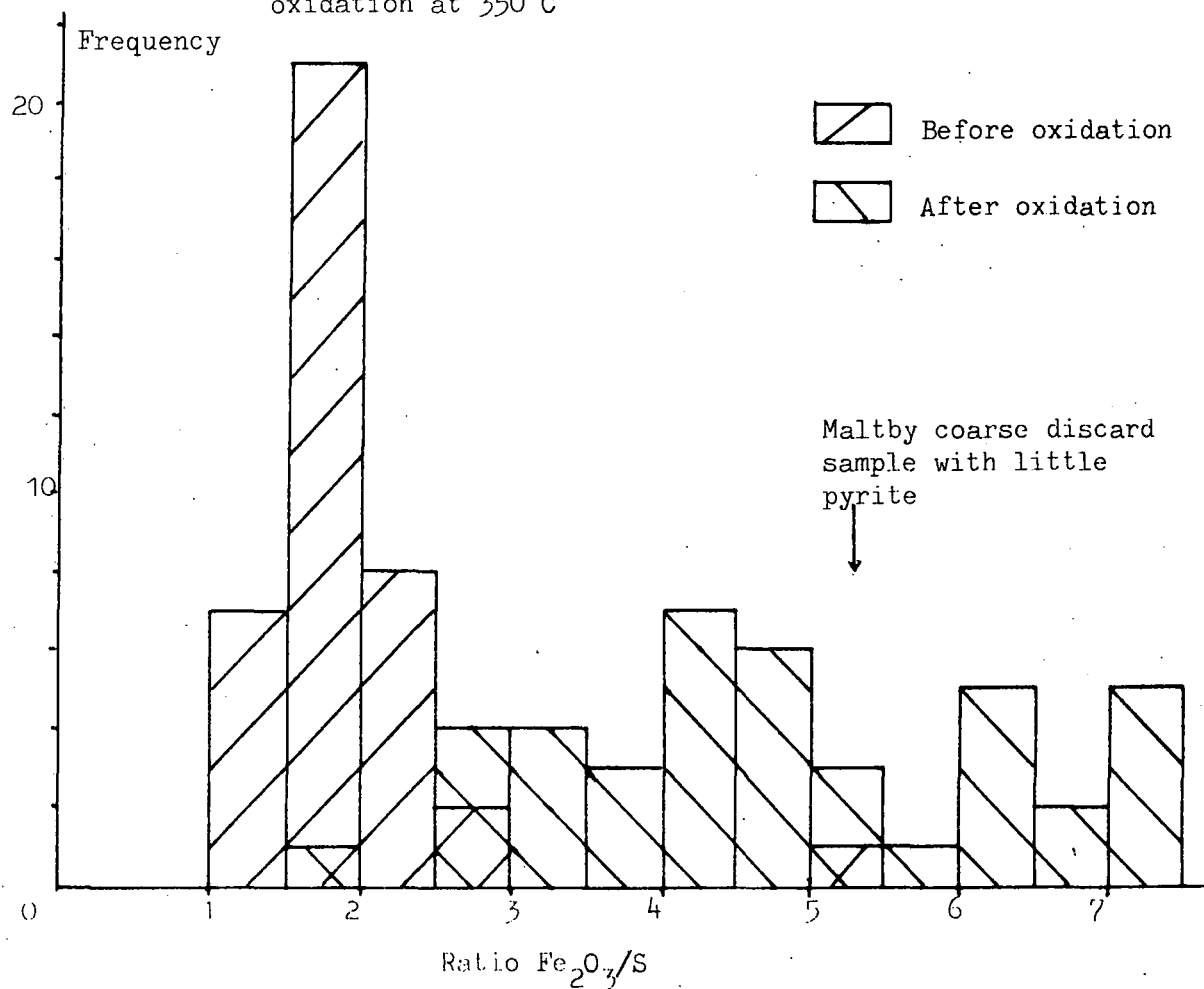


Fig.4.3 Comparison of iron:sulphur ratios before and after oxidation at 350°C



equivalent to the  $\text{CO}_2$  and  $\text{H}_2\text{O}$ , bearing in mind the errors of the analysis.

Inspection of Table A.4.2.1 reveals that upon burning the weight percentage of sulphur has fallen drastically. Since it is suspected that most of the sulphur is in pyrite, it is sensible to compare the iron: sulphur ratios before and after burning. Fig.4.3 shows that this ratio has risen from between about 1.0 and 3.0, to between about 2.5 and 7.5. In other words, the ratio has risen from a little above the theoretical ratio required for pyrite composition ( $\text{Fe}_2\text{O}_3$ : S is 1.25:1) to a ratio that reflects a much lower relative sulphur content.

The disappearance of the sulphur is in fact due to the oxidation of pyrite at the elevated temperature. That this can occur was checked by placing some pure iron pyrite in a furnace at  $350^\circ\text{C}$  for two days. On removal, the product was red, and an XRD determination proved it to be nearly pure haematite. The 41 ashed samples were also all red, and a quick XRD scan of the haematite  $2.69\text{\AA}$  and  $251\text{\AA}$  peaks proved their presence in the following samples: 11 90B, 1 90B and 16 90B from Peckfield lagoon 7; 210CB and 25CB from Maltby lagoon 6. No pyrite was present in any of these samples. The change from pyrite to haematite does involve a weight loss, but not enough to account for the full difference between the XRF and the thermal oxidation estimates of carbon content. The rest could be due to the loss of water from illite between  $100$  and  $350^\circ\text{C}$  (see Zussman, 1967).

It is therefore considered that the discrepancy in the estimates of free carbon by the oxidation method and the XRF difference method is due to material other than organic carbon being lost on oxidation at  $350^\circ\text{C}$ . It follows that the XRF difference method produces a somewhat more accurate estimation of free carbon, although the estimate will include  $\text{CO}_2$  and  $\text{H}_2\text{O}$ . It also follows that the non-oxidised pellets are to be preferred for

elucidating the chemistry of this type of sample, and attention is hereafter confined to non-oxidised specimens. However, unless otherwise stated, organic carbon values are taken as the estimate by thermal oxidation as this is the usual method employed.

#### 4.5 The Recalculation of Mineralogy from Chemistry

The minerals are of principal interest rather than the chemistry; the chemical analysis is performed because of its greater accuracy. It is possible to recalculate mineralogy from the chemistry, though as Nicholls (1962) points out the presence of some chemical species in several different minerals renders the problem insoluble unless certain simplifying assumptions are made. This is particularly true of clays which can have extremely variable chemical compositions, and a uniquely correct mineralogical recalculation would require an exact determination of the chemical make-up of each species of clay present.

The assumptions made here are a simplification of Nicholl's (1962) scheme, which requires a fuller chemical analysis than that presented in Appendix A.4.4; principally  $\text{FeO}$  and  $\text{Fe}_2\text{O}_3$ , S and  $\text{SO}_3$  must be reported separately and  $\text{H}_2\text{O}^+$ ,  $\text{H}_2\text{O}^-$  and  $\text{CO}_2$  must also be determined in order to apply Nicholl's scheme. The assumptions and procedure adopted are as follows: the calculation of EHCCL is provided in full as an example in Table 4.3.

1. The weight percentages of the chemical species are divided by their molecular weights to give molecular proportions, except for  $\text{CaO}$ ,  $\text{MgO}$  and  $\text{P}_2\text{O}_5$ .
2. Since sulphates were found in very few XRD analyses, it is assumed that all the sulphur is in the form of pyrite ( $\text{FeS}_2$ ). The molecular proportion of sulphur is divided by 2 and multiplied by 120 (the molecular weight of  $\text{FeS}_2$ ) to give the weight percentage of pyrites. For every 4 of S,

Table 4.3 The recalculation of mineralogy for sample EHCCL.

Step	Chemical species	SiO <sub>2</sub>	Al <sub>2</sub> O <sub>3</sub>	Fe <sub>2</sub> O <sub>3</sub>	MgO	CaO	Na <sub>2</sub> O	K <sub>2</sub> O	TiO <sub>2</sub>	S	P <sub>2</sub> O <sub>5</sub>
	XRF results	41.725	22.200	3.435	2.097	2.957	0.218	3.025	0.947	1.643	0.072
	Molecular weight	60	102	160	40	56	62	94	80	32	142
1	Molecular proportion	0.695	0.218	0.0215			0.00352	0.0322	0.0118	0.0513	
2	Pyrite=3.08%			<u>0.0128</u> in FeS <sub>2</sub> 0.00868 left						+2=0.02565 x120= <u>3.08%</u>	
3	Paragonite=2.68%	<u>0.021</u> 0.674 left	<u>0.011</u> 0.207 left				x764= <u>2.68%</u>				
4	Muscovite=25.62%	<u>0.193</u> 0.481 left	<u>0.097</u> 0.110 left					x796= <u>25.62%</u>			
5	Illite=2.68+25.62 =28.30% of which paragonite =9.49%										
6	Kaolinite=28.52%	<u>0.220</u> 0.261 left	x516+2= <u>28.52%</u>								
7	Quartz=15.61%	x60= <u>15.61%</u>									

N.B. The accuracy with which the arithmetic is quoted leads to 'apparent' small rounding errors in this table.

2 of Fe and therefore 1 of  $Fe_2O_3$  are required, and the molecular proportion of  $Fe_2O_3$  is adjusted accordingly.

3. Since the exact nature of the clays is unknown two theoretical end-member illites have been recalculated. Firstly all the  $Na_2O$  is assigned to paragonite, which has a composition of  $Na_2Al_4(Si_6Al_2)O_{20}(OH)_4$ . The weight percentage of paragonite is (mol prop  $Na_2O$ ) x 764.

4. Secondly the other end member is taken as muscovite, and all the  $K_2O$  is assigned to  $K_2Al_4(Si_6Al_2)O_{20}(OH)_4$ . The weight percentage of muscovite is (mol prop  $K_2O$ ) x 796.

5. Illite is taken to be the sum of the end members, paragonite and muscovite. The paragonite content is expressed as a percentage for comparison. In reality a considerable amount of  $Fe^{2+}$  and Mg can substitute for aluminium.

6. Remaining  $Al_2O_3$  after steps 5 and 6 is assigned to kaolinite, which has a formula of  $Al_4Si_4O_{10}(OH)_8$ ; the weight percentage is (remaining  $Al_2O_3 \div 2$ ) x 516. If chlorite is present this is an over-estimate; however chlorite was found but infrequently in the XRD work.

7. Remaining  $SiO_2$  is multiplied by 60 to give the weight percentage of free silica (quartz).

8. No recalculation is performed for  $P_2O_5$  because the mineral involved is not known and therefore no extra comparisons are possible than with the "raw" XRF results. No recalculation is performed for CaO, MgO or further recalculation for  $Fe_2O_3$  because the extent to which these chemical species are distributed between the carbonate mineral and the clays is not known.

The full results of this scheme are quoted in Appendix A.4.5. It is not suggested that recalculated mineralogy reflects the true chemical make-up of the minerals present in the samples; the least likely chemical constitutions are probably those of paragonite and muscovite. However, at the least, these recalculated mineral components should provide an

internally consistent method of comparing the chemistry of the various samples. For some recalculated minerals the comparison with real minerals should be reasonable, the best probably being pyrite, followed by free silica (quartz) and kaolinite.

The results of this procedure are discussed in the next section.

#### 4.6 The Chemistry and Mineralogy of Colliery Tailings Lagoons

##### 1. Grading

Chemical and mineralogical analyses have been performed on material from four lagoons, i.e. Lagoons 6 and 7 at Peckfield Colliery, N. Yorkshire Area; lagoon 109B at East Hetton Colliery, N. East Area and lagoon 6 at Maltby Colliery, S. Yorkshire Area. The locations of the samples in each lagoon are sketched in Figs. 4.4a-c. The grading curves of the samples are given in Figs. 4.5a-d, except in the case of the 17 samples from Peckfield lagoon 7 (Fig. 4.5.b) where log (median size in microns) has been plotted for reasons of clarity.

The samples from Peckfield lagoon 6 (Figs. 4.4.a and 4.5.a) were all bulk samples taken from 1m depth. It can be seen that the samples are finer and more plastic towards the outlet. The samples from lagoon 6 at Peckfield are plotted were simply in terms of a sample number vs log median size, as shown in Fig. 4.5.b. East Hetton lagoon 109B demonstrates again fining towards the outlet (Fig. 4.5.c), though the samples here are representative of "type" layers. The samples from Maltby lagoon 6 (Fig. 4.5d) are too close in terms of the size of the lagoon, and too few in number to discern any trends across the lagoon; again "type" layers have been chosen.

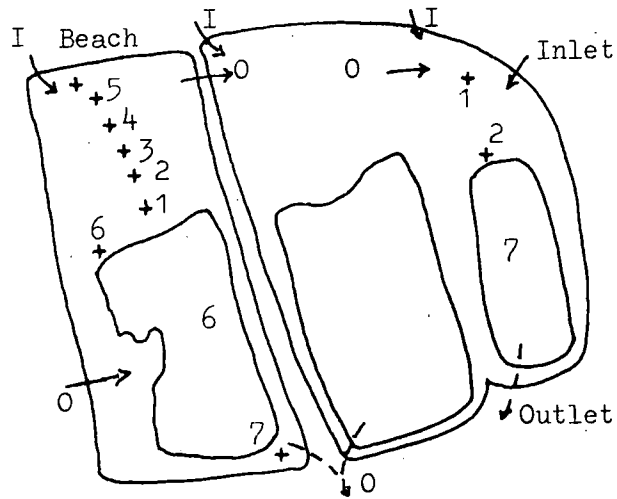
##### 2. Organic Carbon content

The organic carbon content (oxidation at 350<sup>o</sup>C) has been determined on all samples. Those from Peckfield lagoon 6 were split into different

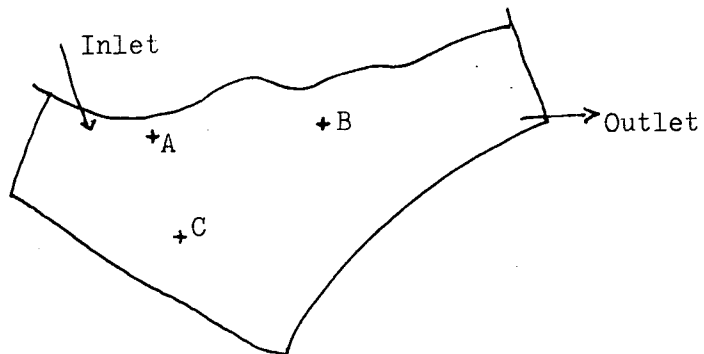


Fig.4.4 Sample locations.

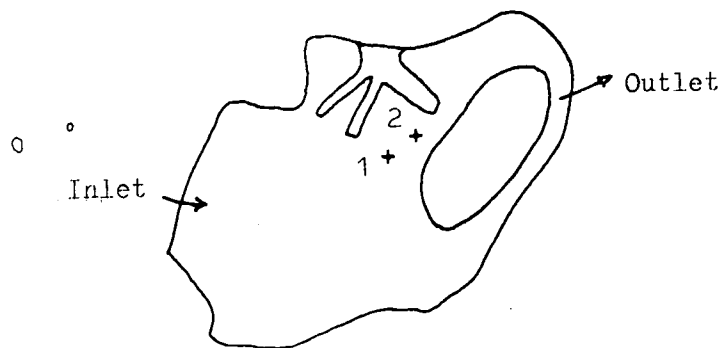
a. Peckfield lagoons 6 and 7 (series PL6 and PL7)



b. East Hetton lagoon 109B (EH series)



c. Maltby lagoon 6 (MA series)



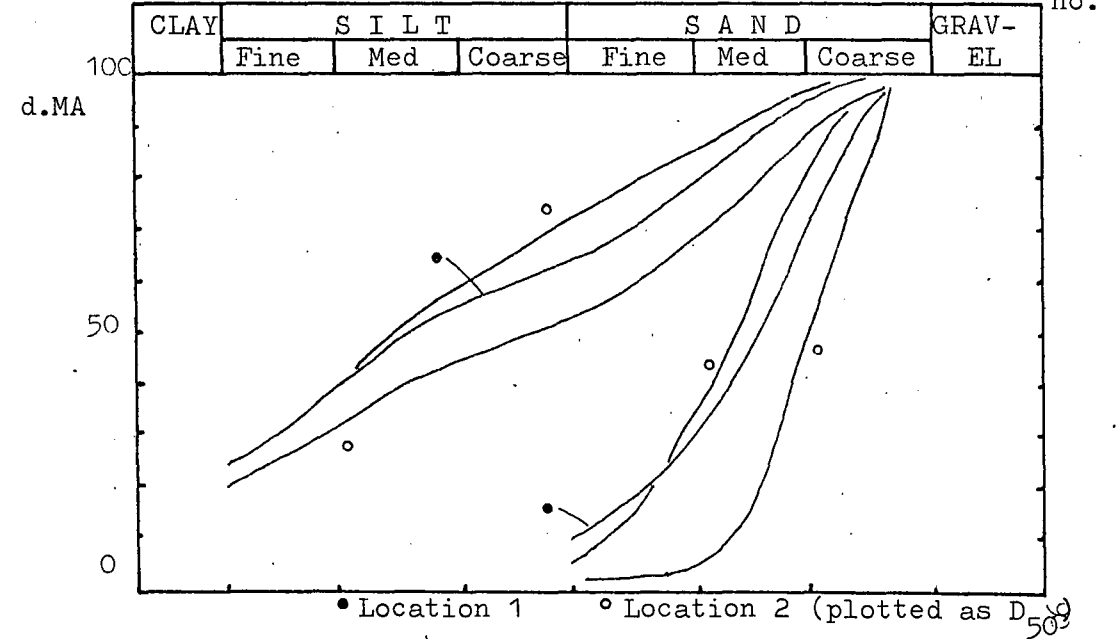
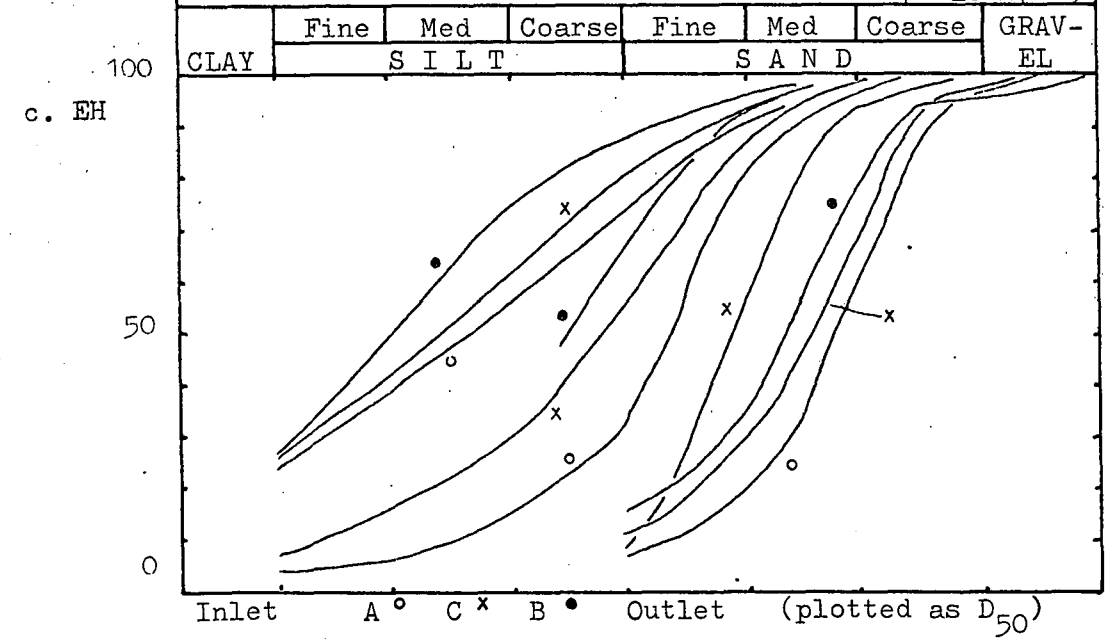
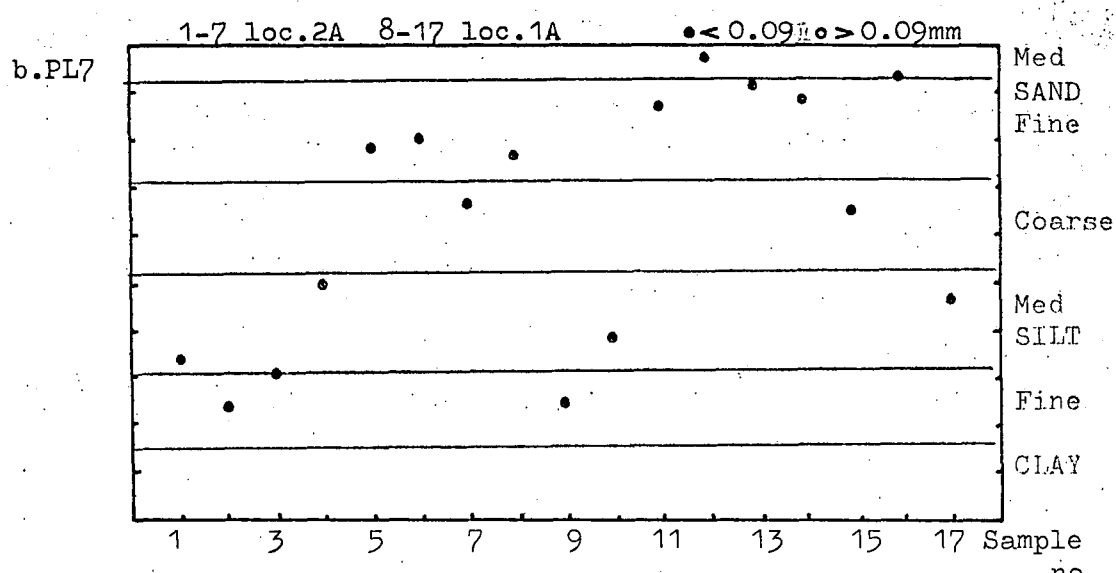
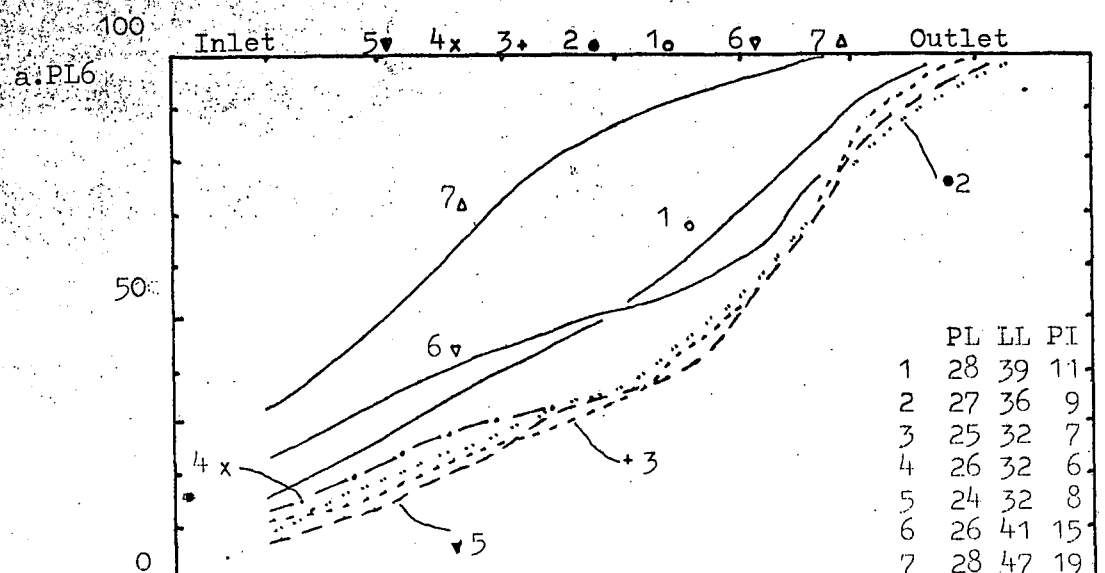


Fig.4.5 The grading of the materials analysed by XRF and XRD.

sieve sizes and the content determined for each sieve size. Fig.4.6a shows that in each sample there is an increase in coal with grade. Generally the samples further from the inlet are richer in coal in any given size range, except that the mid-lagoon samples are richest in big coal particles. The gross coal content of each whole sample increases towards the middle of the lagoon and then drops to the outlet. This is because, although sample 7 has a higher coal content in many size ranges, the bulk sample consists of the finer, coal-lean size ranges. The coal particles are carrying beyond the inlet, but the larger coal particles then settle out in the middle of the lagoon. Finer particles, especially of fine-sand size and below, settle generally over the whole lagoon.

The coal content of lagoon PL7 has been split into above and below 90 microns size fractions, Fig.4.6.b shows that the coal content increases with grade, and it will be shown in chapter 5 that it is correlated to the overall size of each sample. Fig.4.6.c. shows that the coal content increases with size, and further is generally higher nearer the outlet in any size range. In chapter 3 (Table 3.1) it was shown that at the outlet there is an increase in the finer coal-lean type of samples. Again the large coal particles are settling rapidly in the middle of the lagoon, but finer coal particles are being carried further. The Maltby samples again show an increase in coal content with size (Fig.4.6.d).

### 3. Quartz content

Quartz contents, both from the XRD and from the XRF mineralogical recalculation are plotted in Figs.4.7a-d for each sample. Fig.4.7a shows a decrease in quartz with grade, a reflection of the increase in coal content. The recalculated quartz content is higher than that determined from XRD analysis, but there is a much clearer trend of lower quartz away from the inlet in all size ranges. Fig.4.7b again shows that there

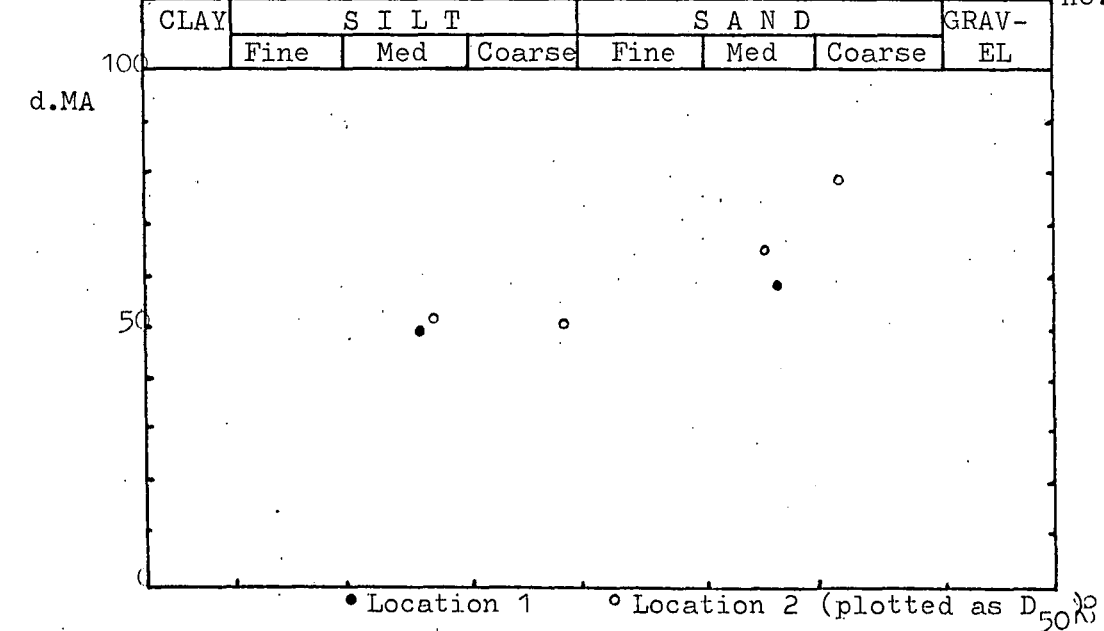
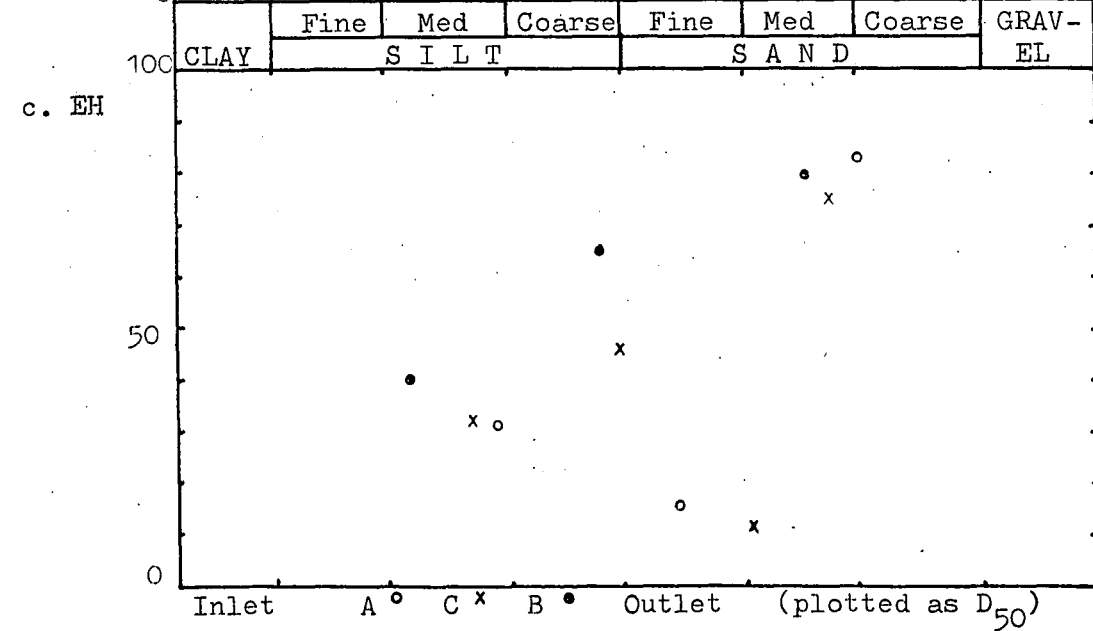
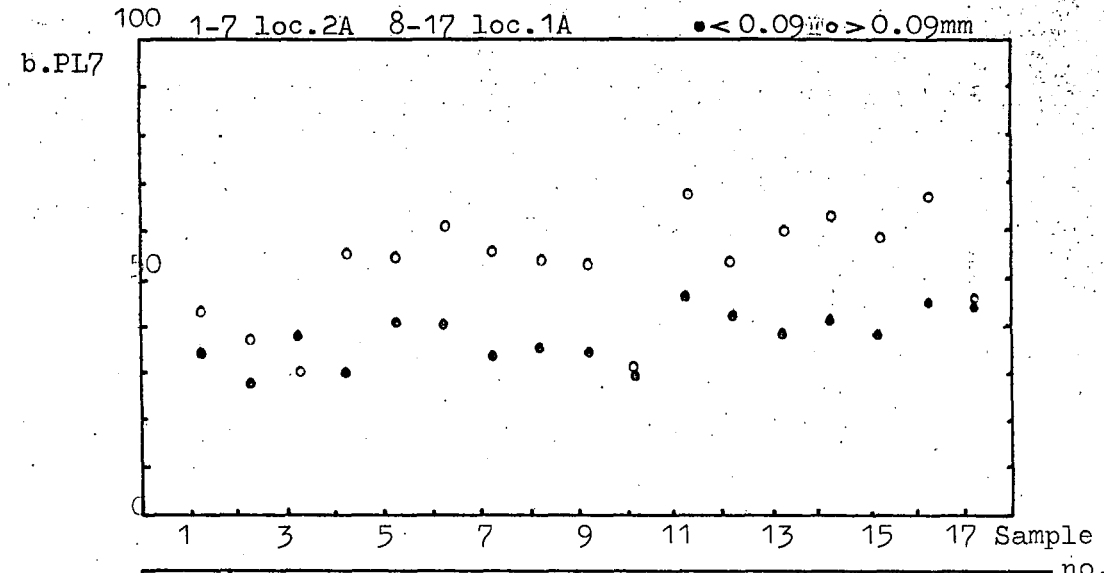
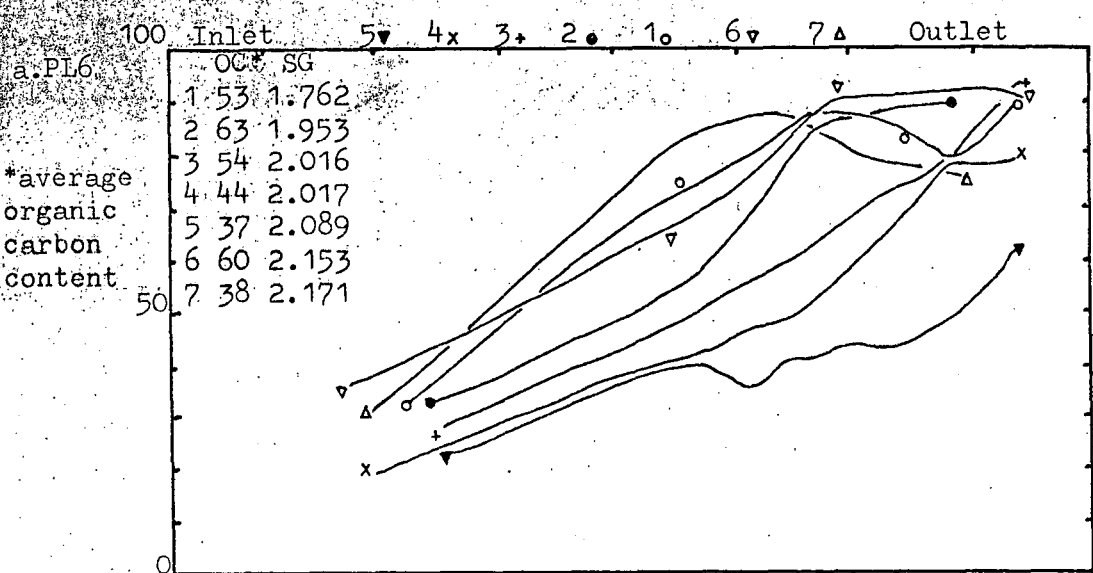
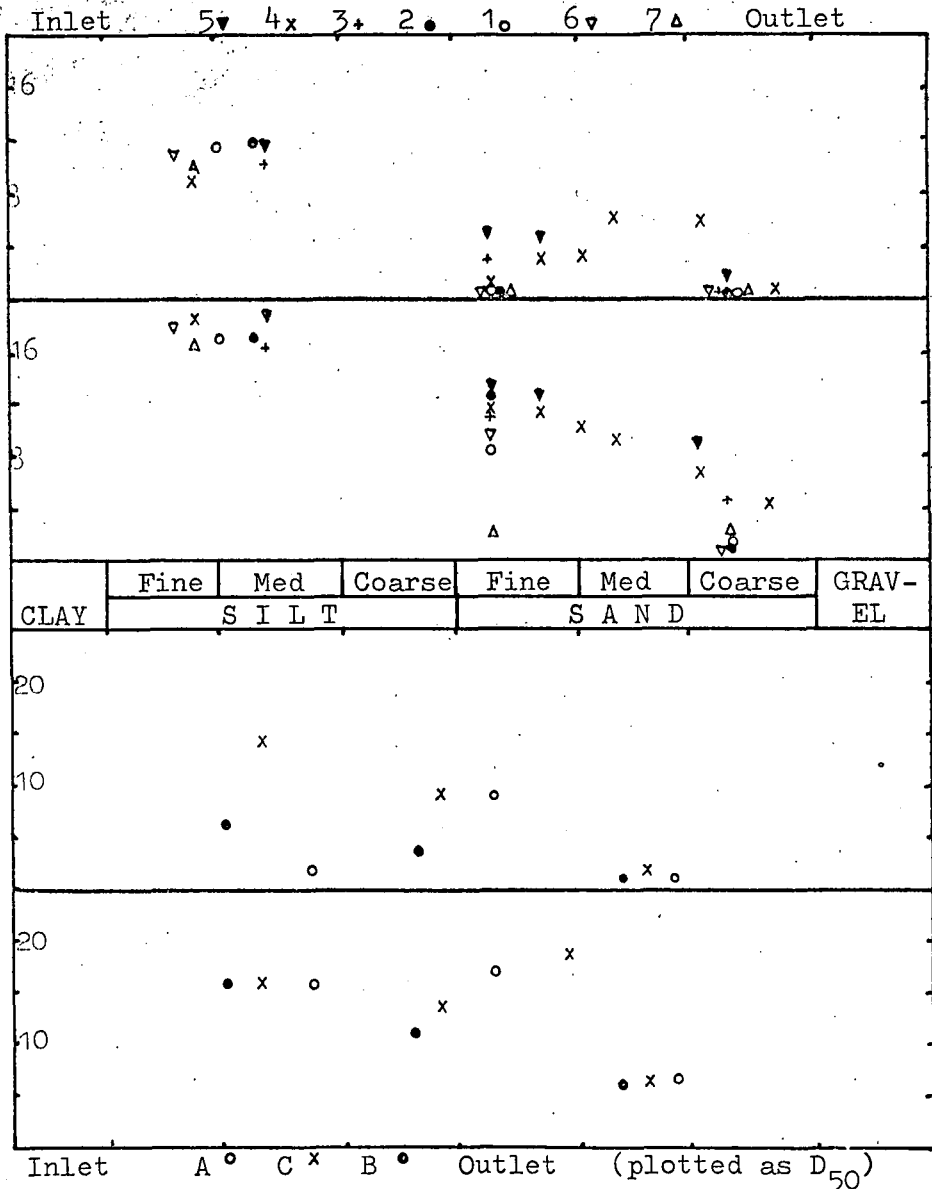
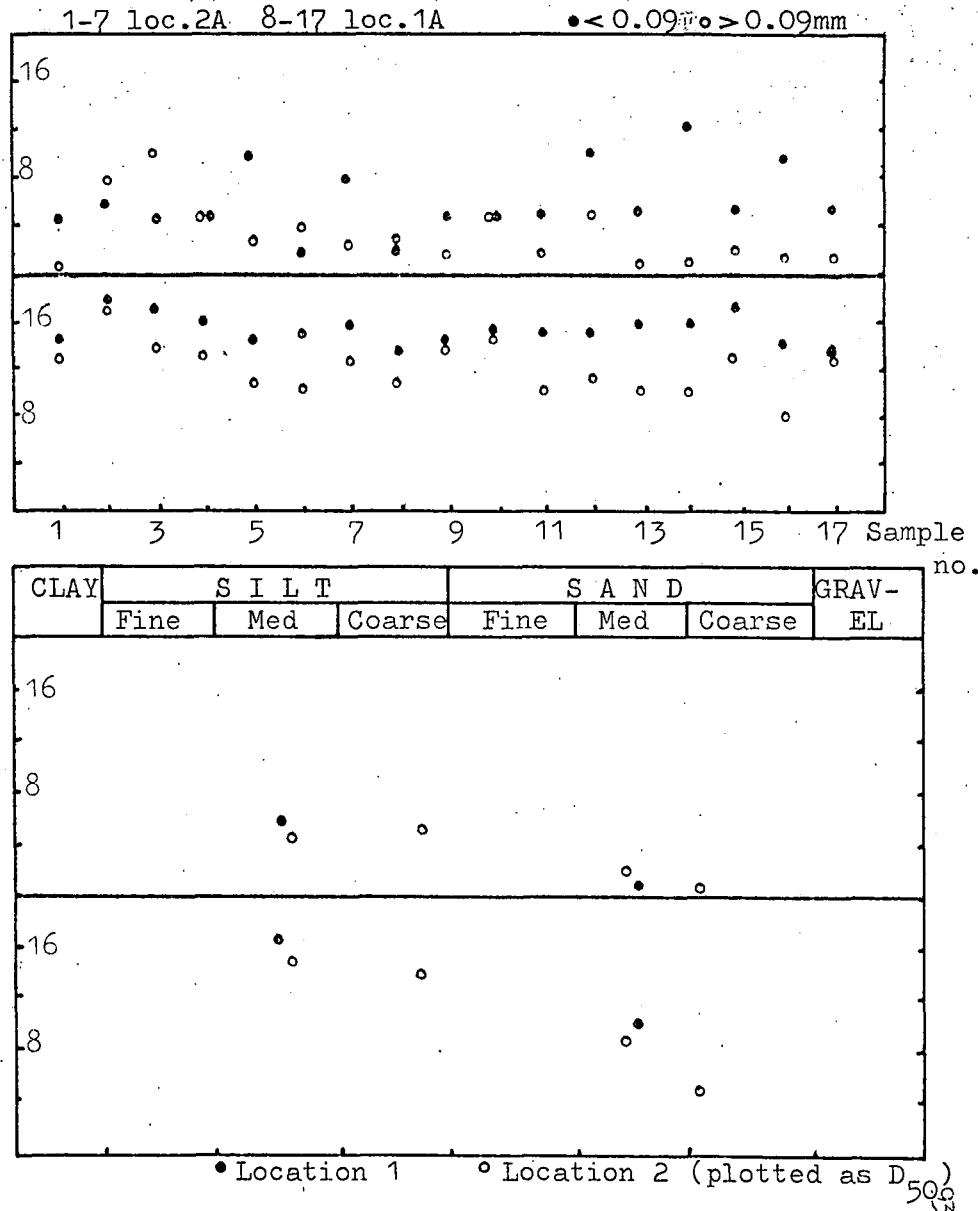


Fig.4.6 Organic carbon contents (thermal oxidation) of the XRF and XRD samples (in percent).

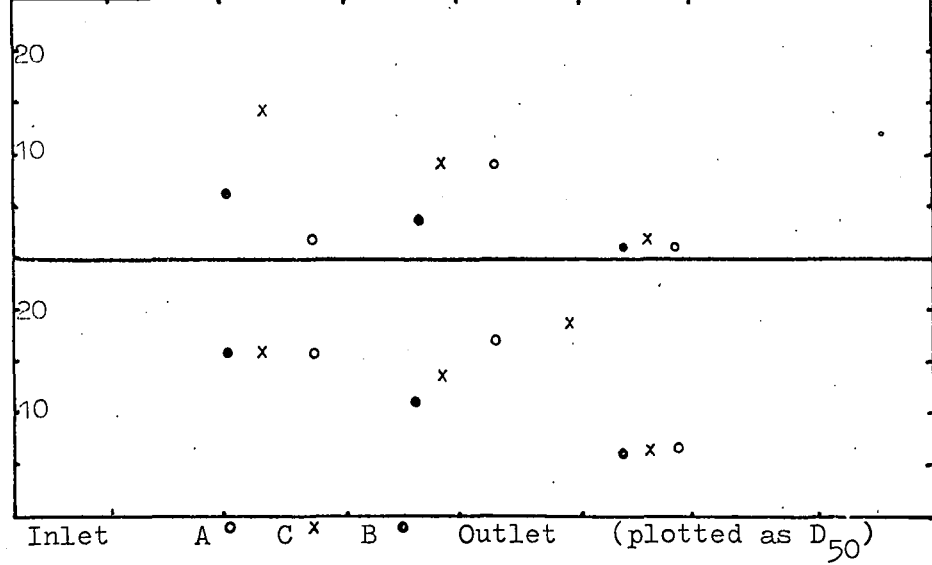
a.PL6



b.PL7



c. EH



d.MA

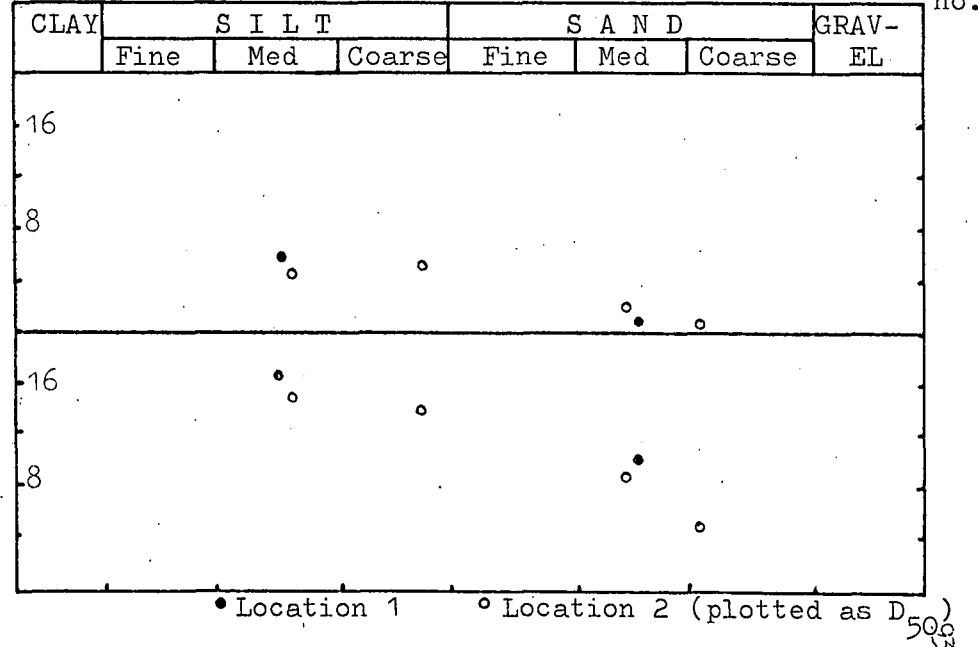


Fig.4.7 Distribution of quartz with grain size (in percent). Upper half = XRD, lower half = XRF recalculated.

is a decreasing quartz content with grade; again the recalculated determination gives a higher content and less random trends. Fig.4.7c again shows - less quartz with grade, less quartz away from the inlet and a steadier trend with the XRF recalculated analysis. Sample EHCMS is non-typical - with low coal and higher quartz. Excepting the trend with position in the lagoon, the same features found at Peckfield and East Hetton are repeated at Maltby (Fig.4.7d)

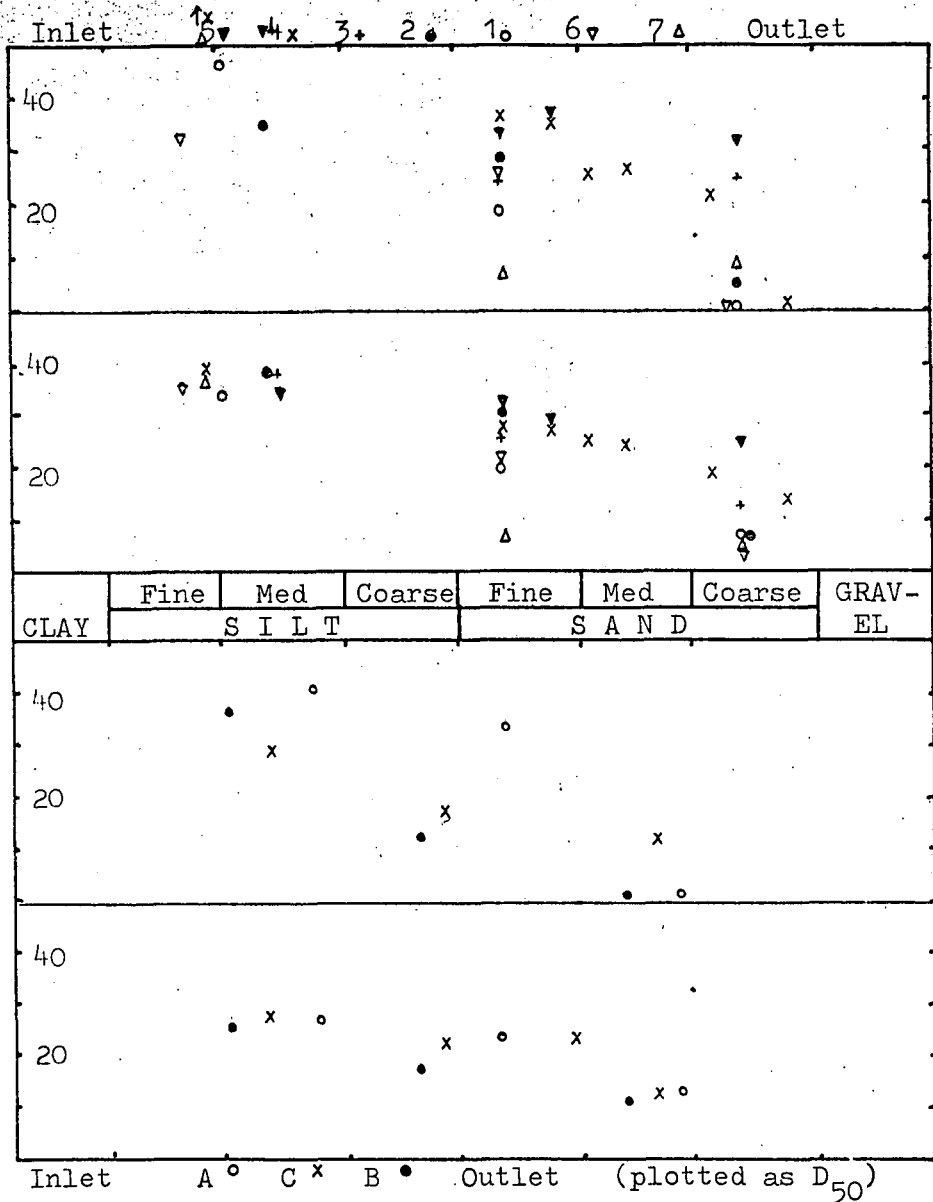
#### 4. Illite

The illite fraction is the total illite plus mixed layer clay in the XRD analysis, and muscovite plus paragonite theoretical end member in the XRF recalculation. The trends of illite content are fairly clear in both cases (Figs.4.8a-d). There is a decrease with increasing size, and a decrease away from the inlet in any one size range. Again, because there is more fine-grained material near the outlet the gross illite content is greater there. There is little difference between the two methods of determination: the recalculation method gives a lower illite content in the finer grades, but a higher one in the coarser grades.

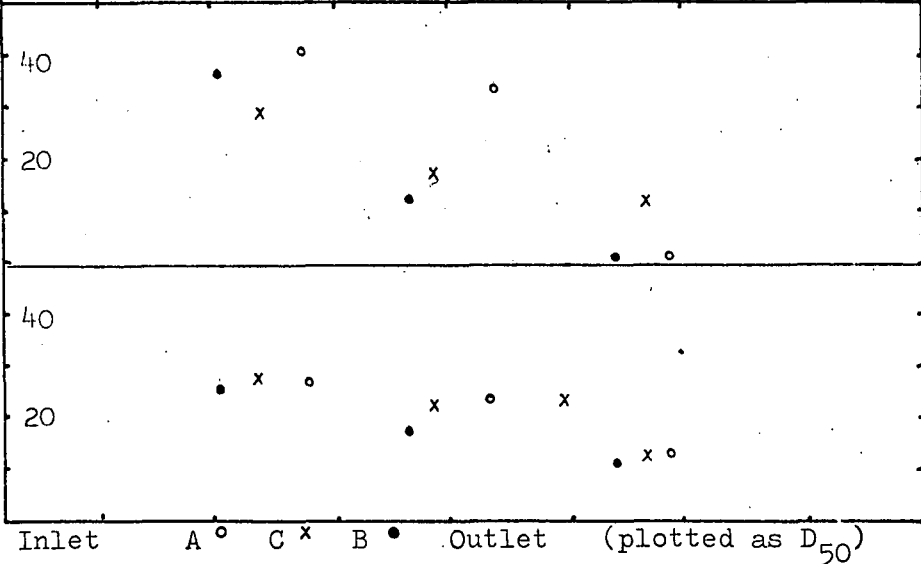
Turning to the illite composition, mixed-layer clay was analysed in all the Peckfield samples. As has been stated, the analysis is of dubious quality, and Figs.4.9a and 4.9b show that the greater the coal content, the more random is the nature of the determination. It was abandoned after these samples were analysed.

The paragonite percentage of the recalculated illite shows the relative importance of sodium to potassium. Fig.4.9a shows that in Peckfield lagoon 6 it generally lies between 10 and 20% in the near-inlet samples, but increases in the mid-lagoon and outlet samples, particularly in the coarser fractions. In lagoon 7 the paragonite content is always greater in the coarser grades, and the difference generally increases with samples

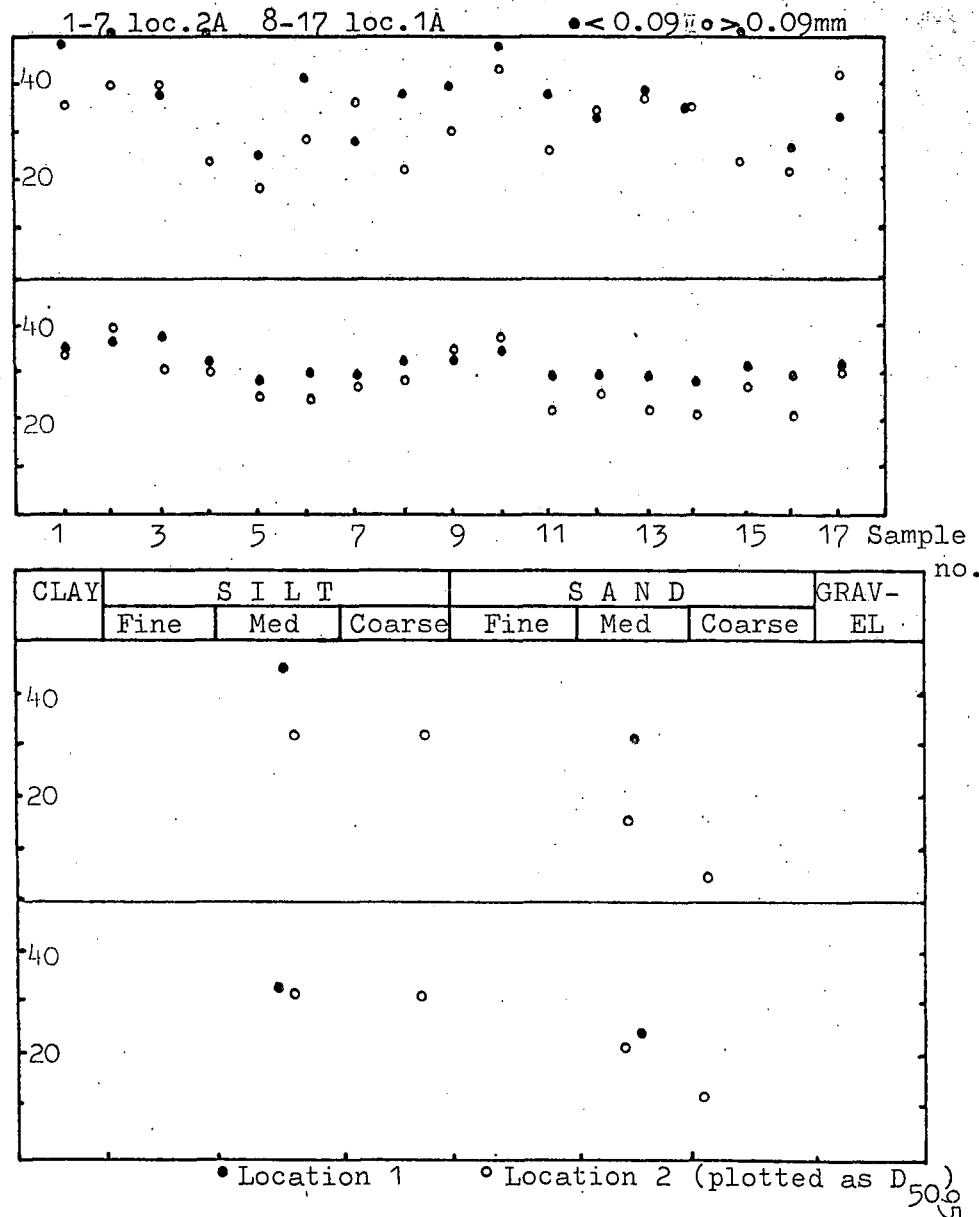
a.PL6



c. EH



b.PL7



d.MA

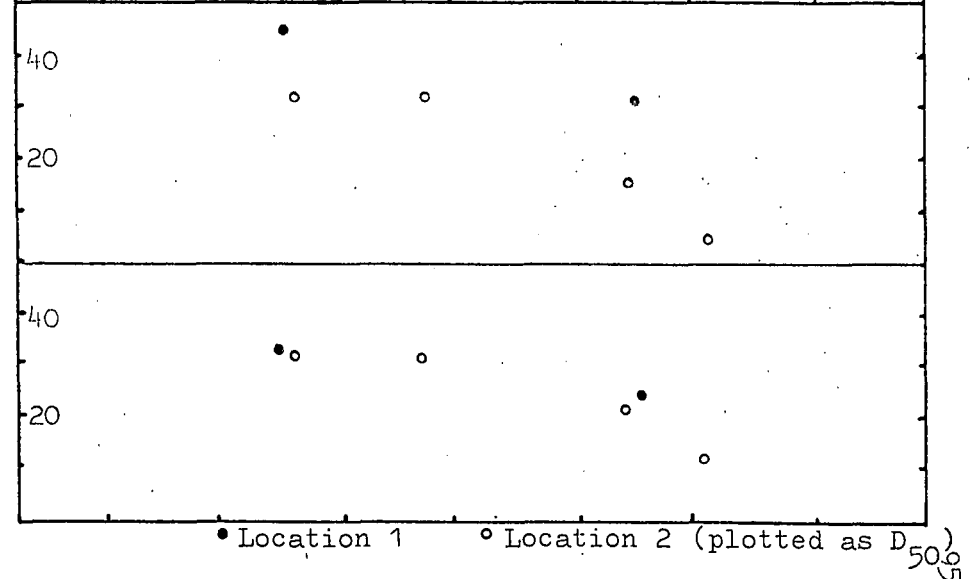
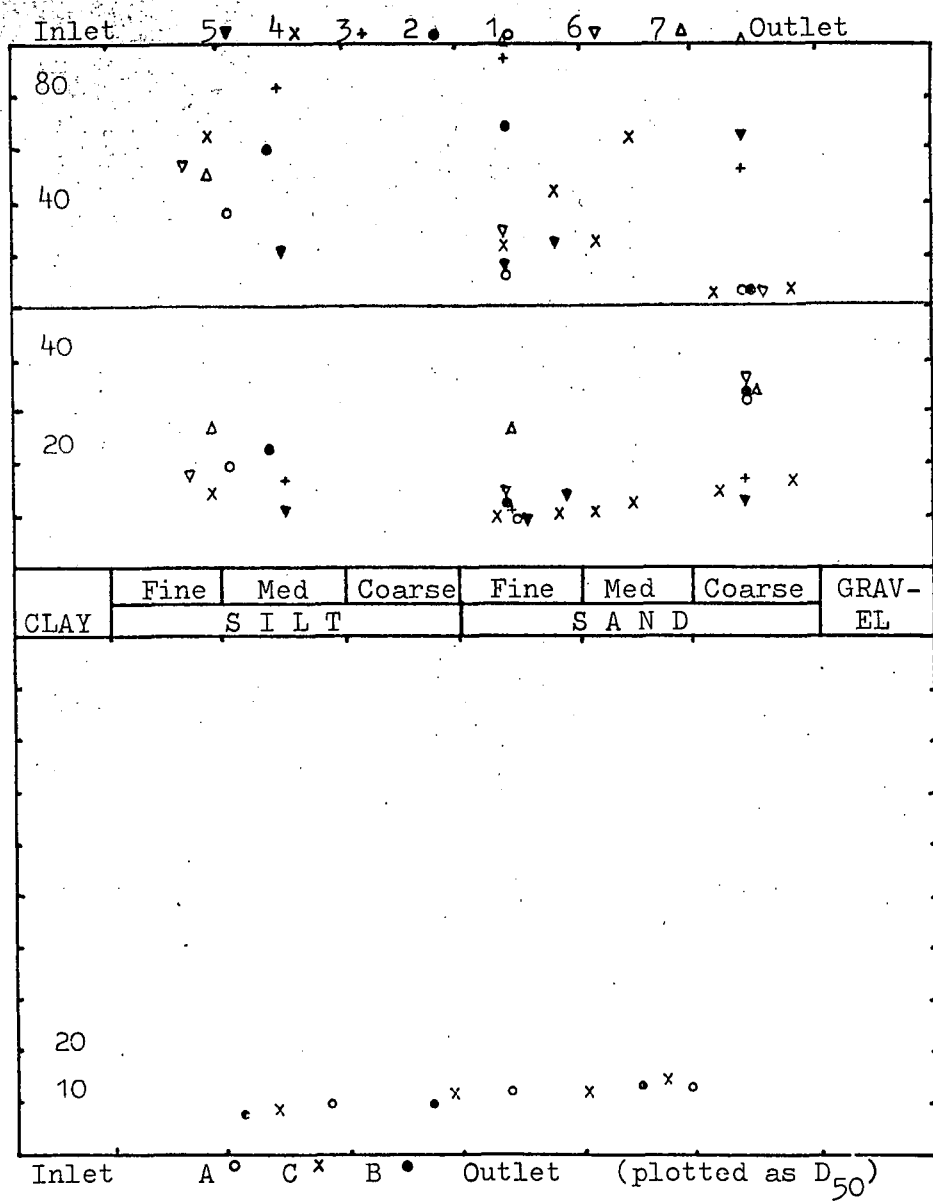


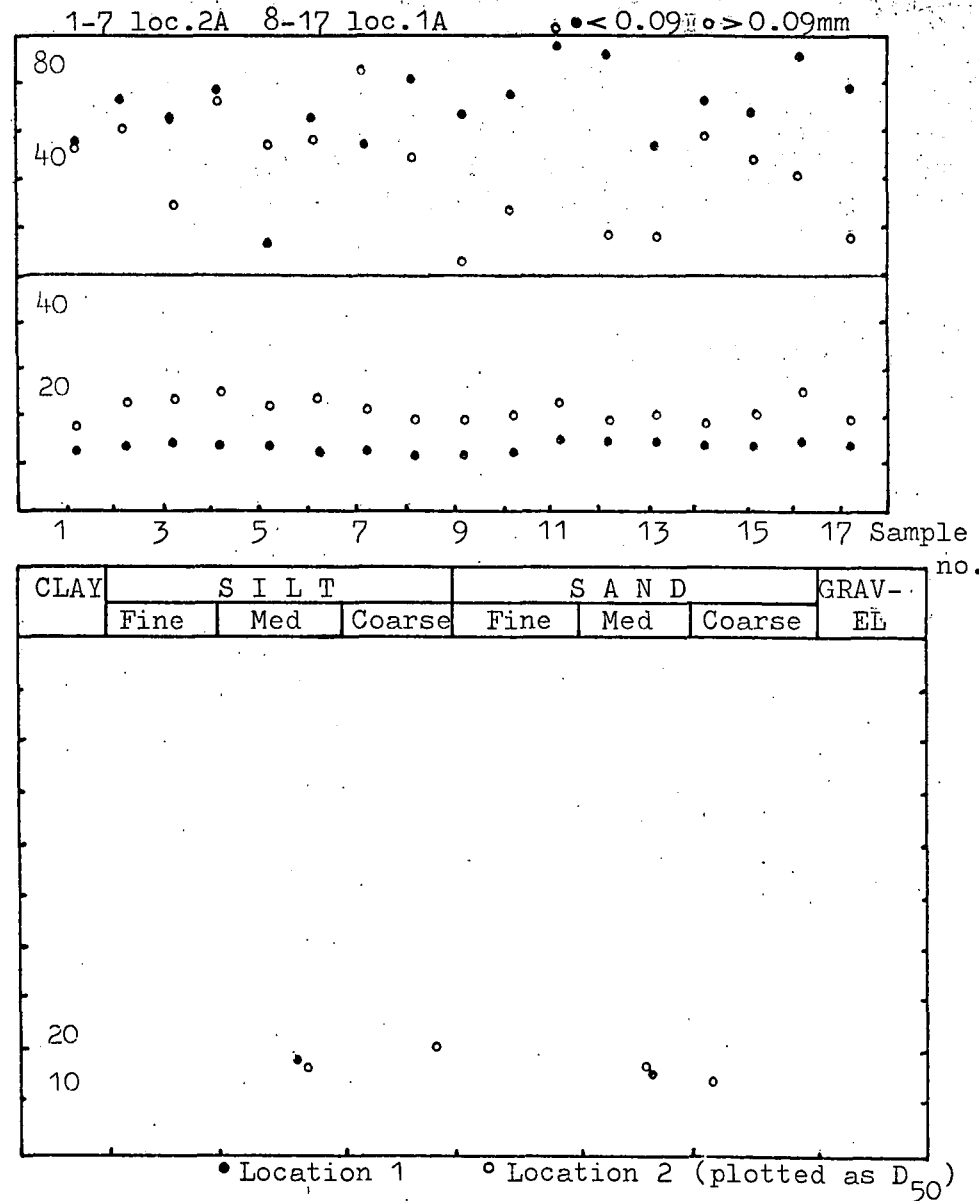
Fig.4.8 Distribution of illite (in percent) with grain size. Upper half = XRD, lower half = XRF.

a.PL6



c. EH

b.PL7



d.MA

Fig.4.9 Variation in illite composition (in percent). Upper half = mixed layer clay by XRD, lower half = paragonite recalculated from XRF.



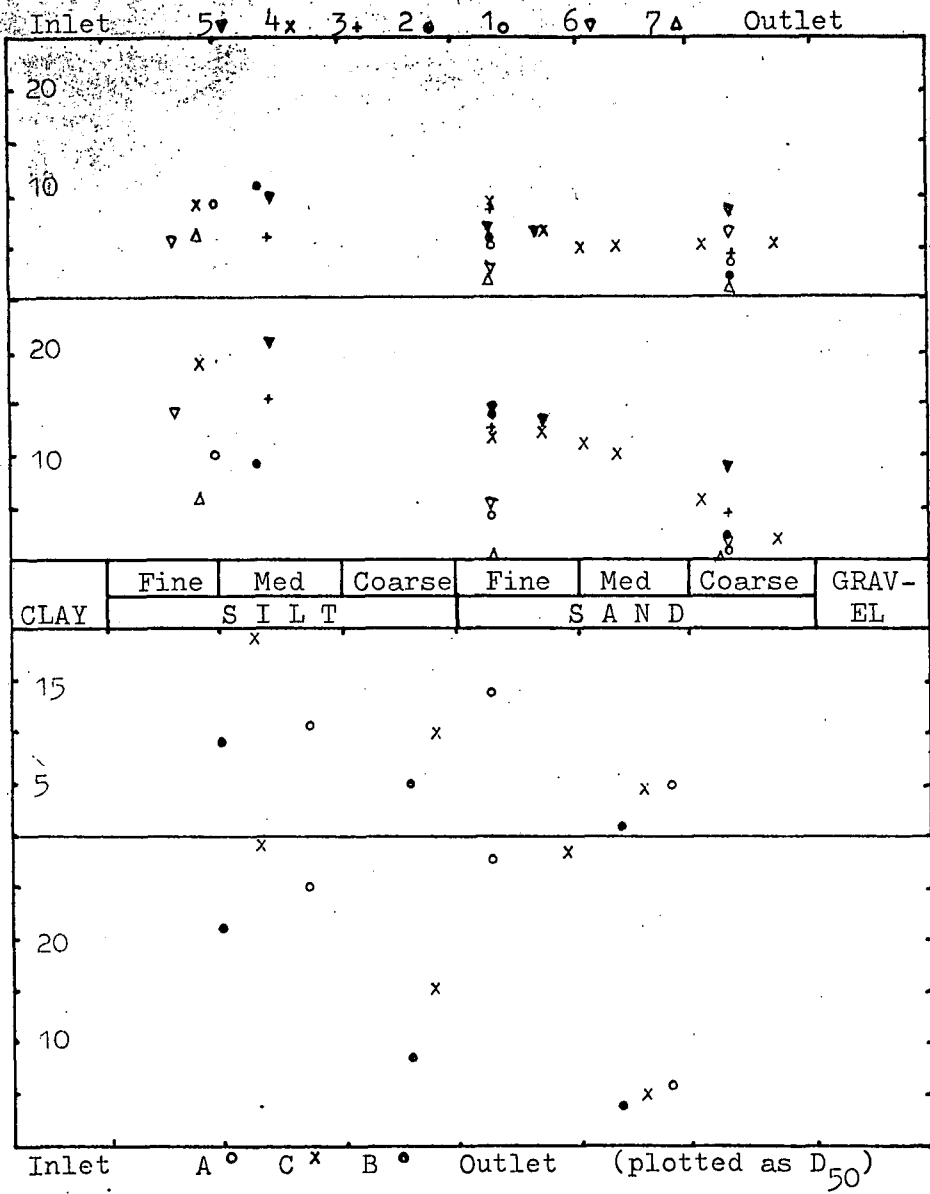
that are coarser-grained overall (cf median sizes in Fig.4.5b). At East Hetton (Fig.4.9.c) the paragonite content is very significantly lower than in the more southerly samples: this difference is not due to the dilution effect of the coal, and is therefore a real regional change. There is again an increase with grade, and possibly a slight decrease away from the inlet (cf an increase in the case of Peckfield lagoon 6), although the difference is very slight. The Maltby samples show no trend with grade; in composition they compare to the Peckfield samples.

#### 5. Kaolinite

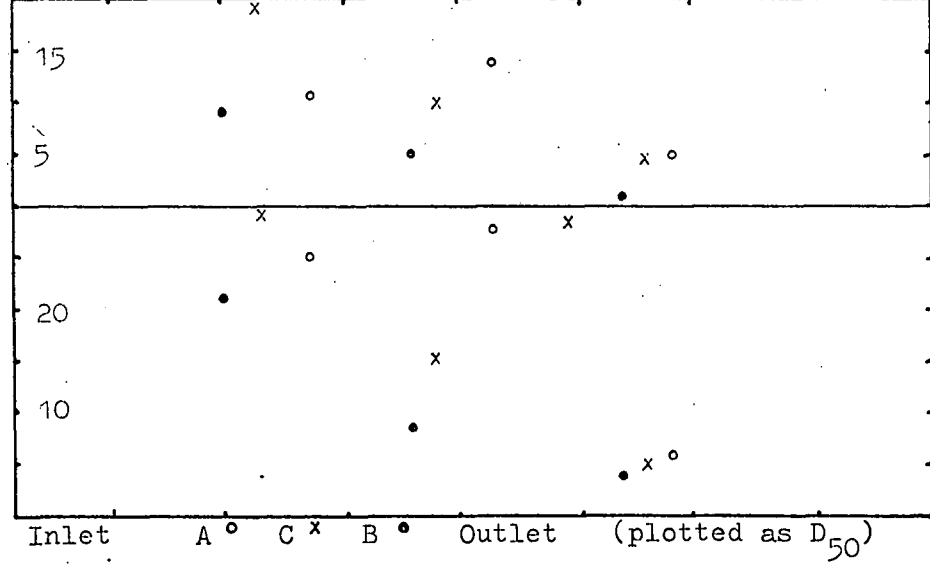
The kaolinite content of the samples generally decreases with increasing grade (Figs.4.10a-d), because of the diluting effect of the coal. In the case of Peckfield lagoon 6 (Fig.4.10a) there is a trend for decreasing kaolinite content with distance from the inlet, which is reflected much more strongly in the recalculated mineralogy; nevertheless the trend is discernible in the XRD mineralogy. From Fig.4.10b it can be seen that kaolinite is more abundant in the finer material both within individual samples and between samples (cf median sample size, Fig.4.5.b). At East Hetton, the kaolinite content again decreases with grade and away from the inlet; the Maltby material follows suit. In general the recalculated kaolinite contents are higher than the XRD determined values. This may be due to more  $Al_2O_3$  being in illite, or possibly, a small chlorite content which has not been allowed for.

The inverse relationship between coal and quartz, illite and kaolinite causes the latter three mineral species to have very similar trends, and obscures differences between them. To highlight differences the ratios of quartz/illite and kaolinite/illite have been calculated both for the XRD data and the XRF recalculated data. The quartz/illite ratio is plotted in Figs.4.11a-d, which as expected show greater clarity in the

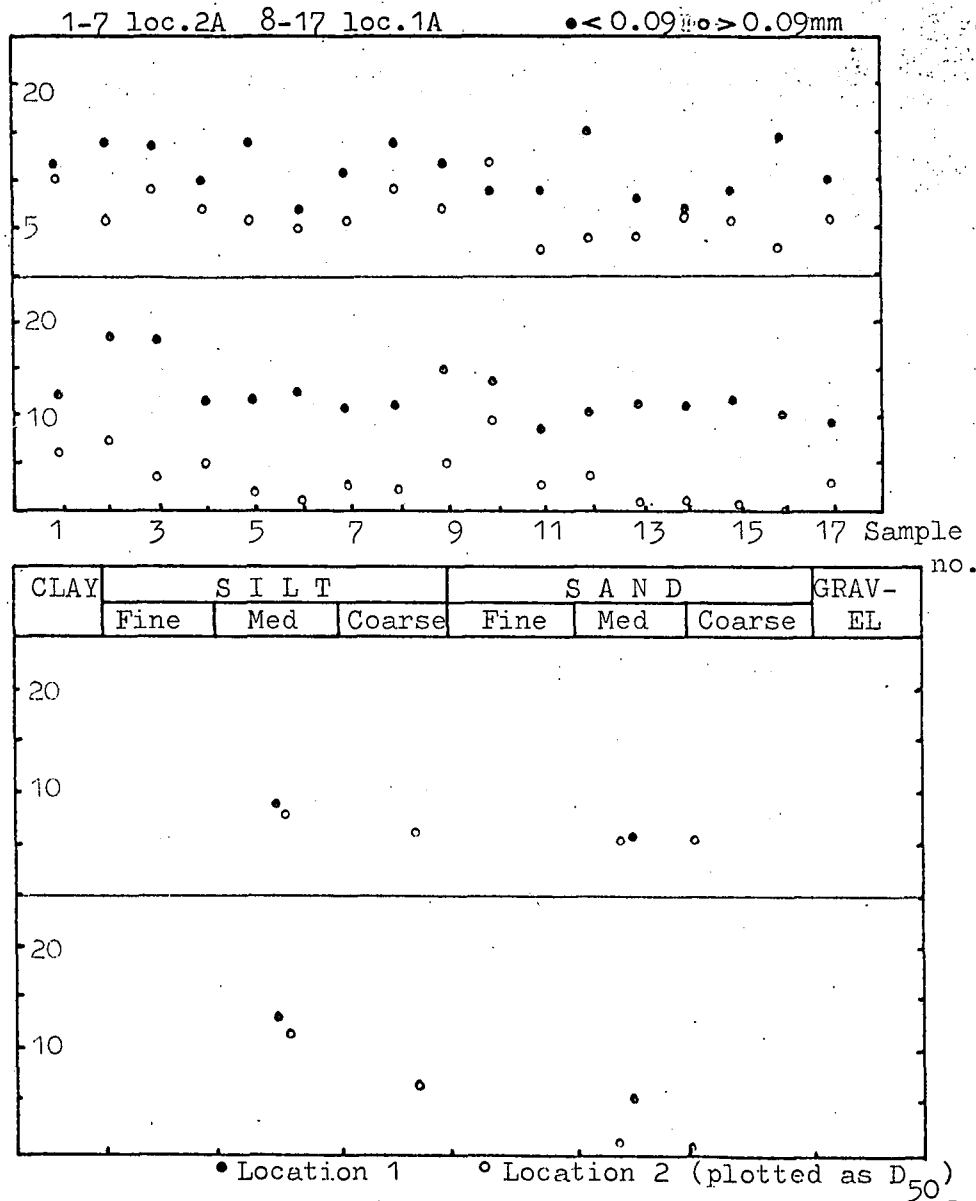
a.PL6



c. EH



b.PL7



d.MA

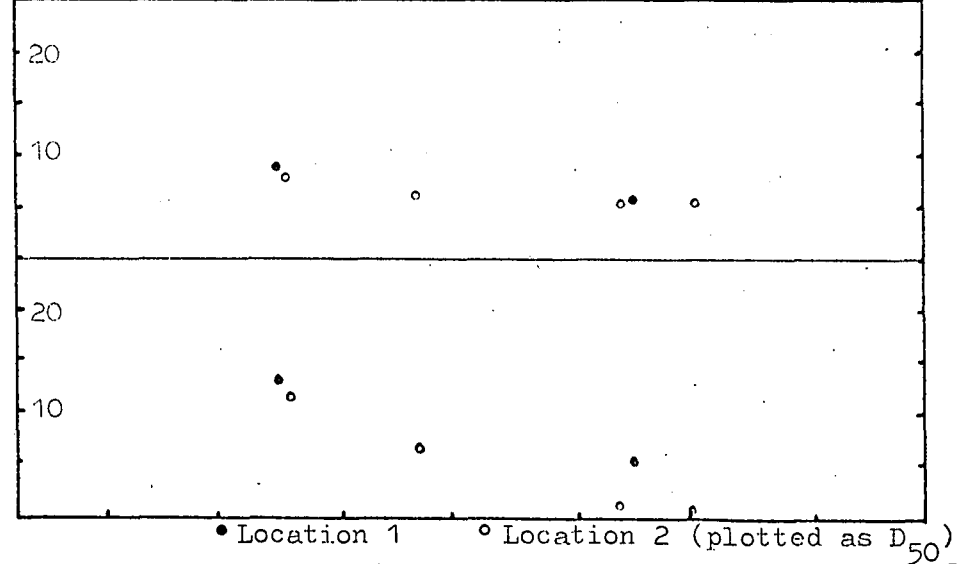
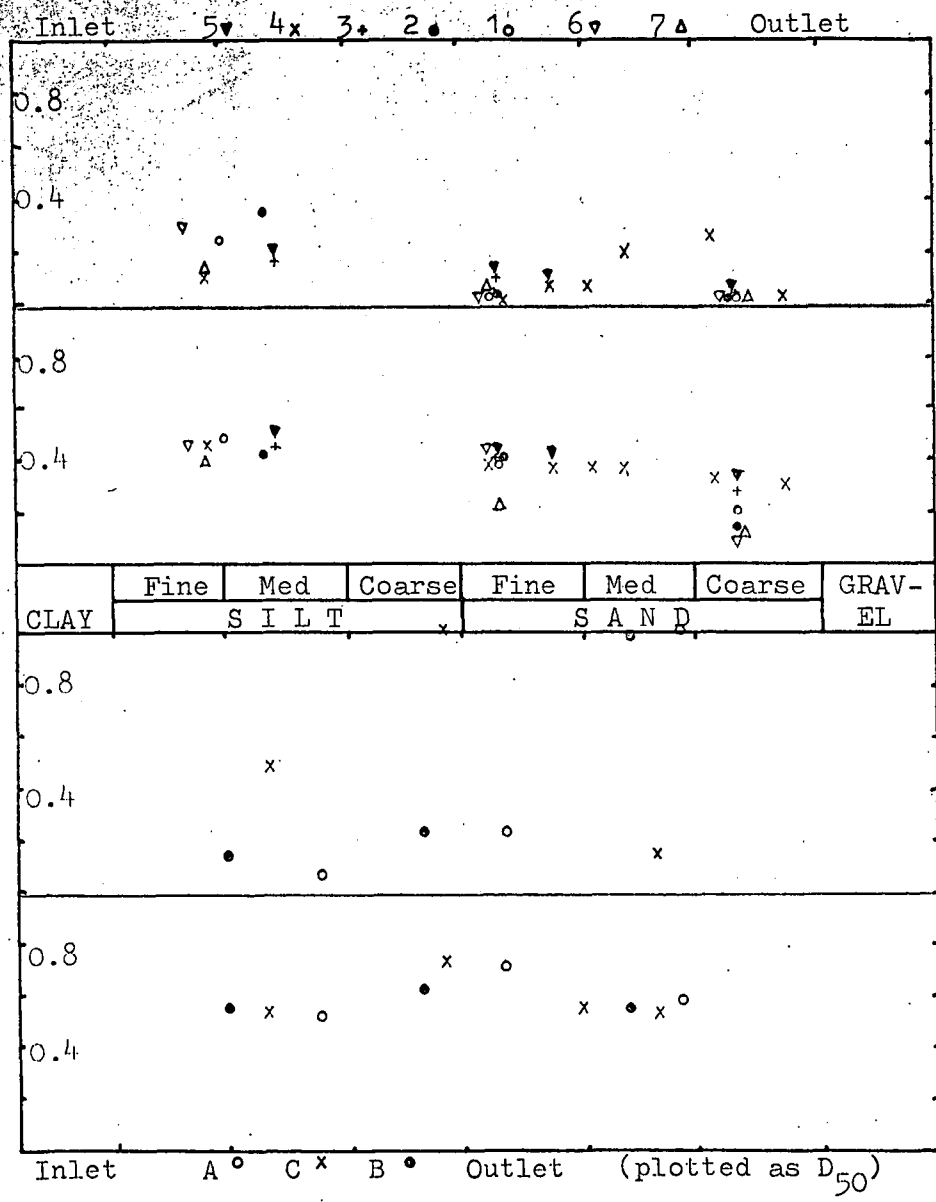
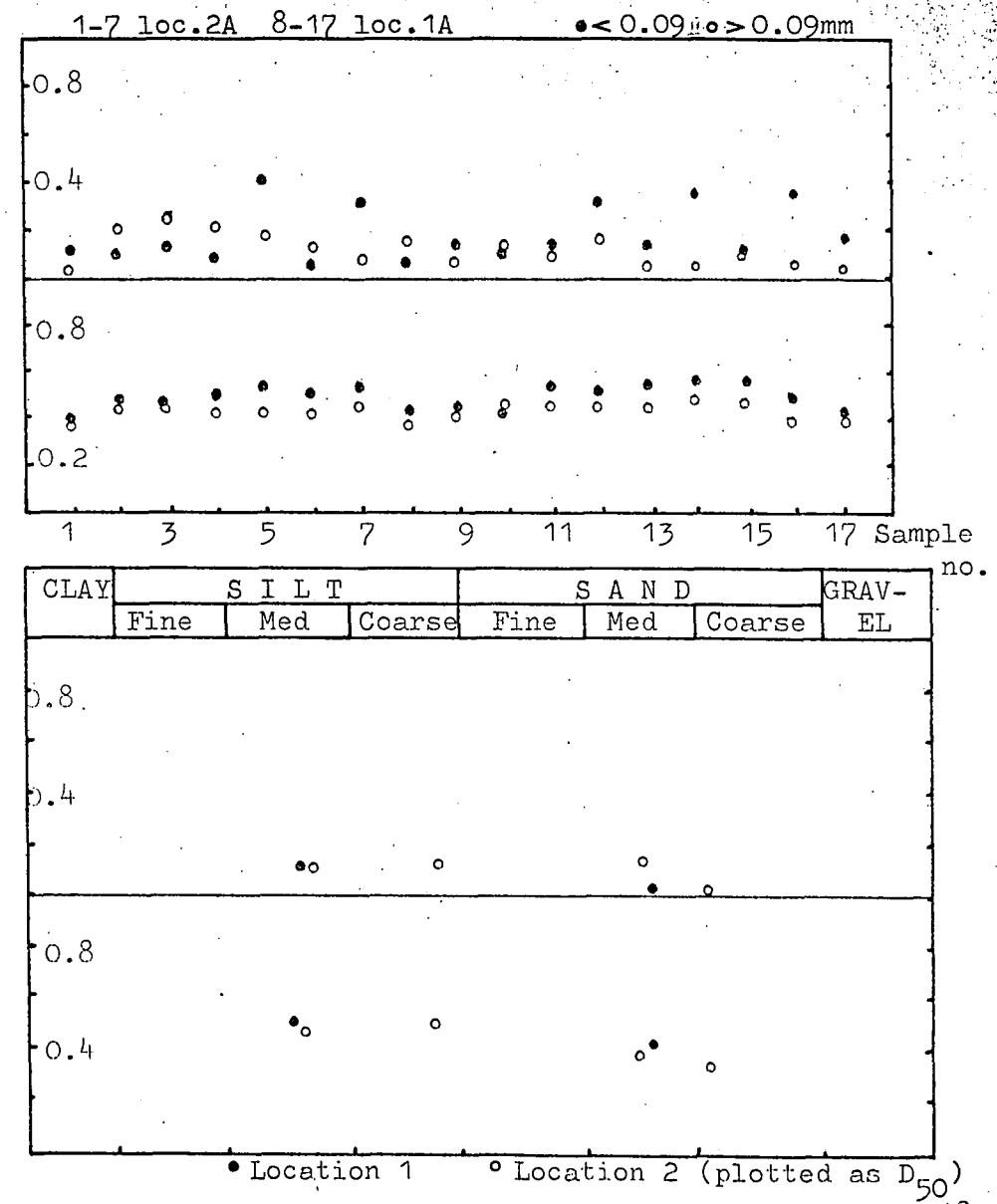


Fig.4.10 Distribution of kaolinite (in percent) with grade. Upper half = XRD, lower half = recalculated XRF.

a. PL6



b. PL7



c. EH

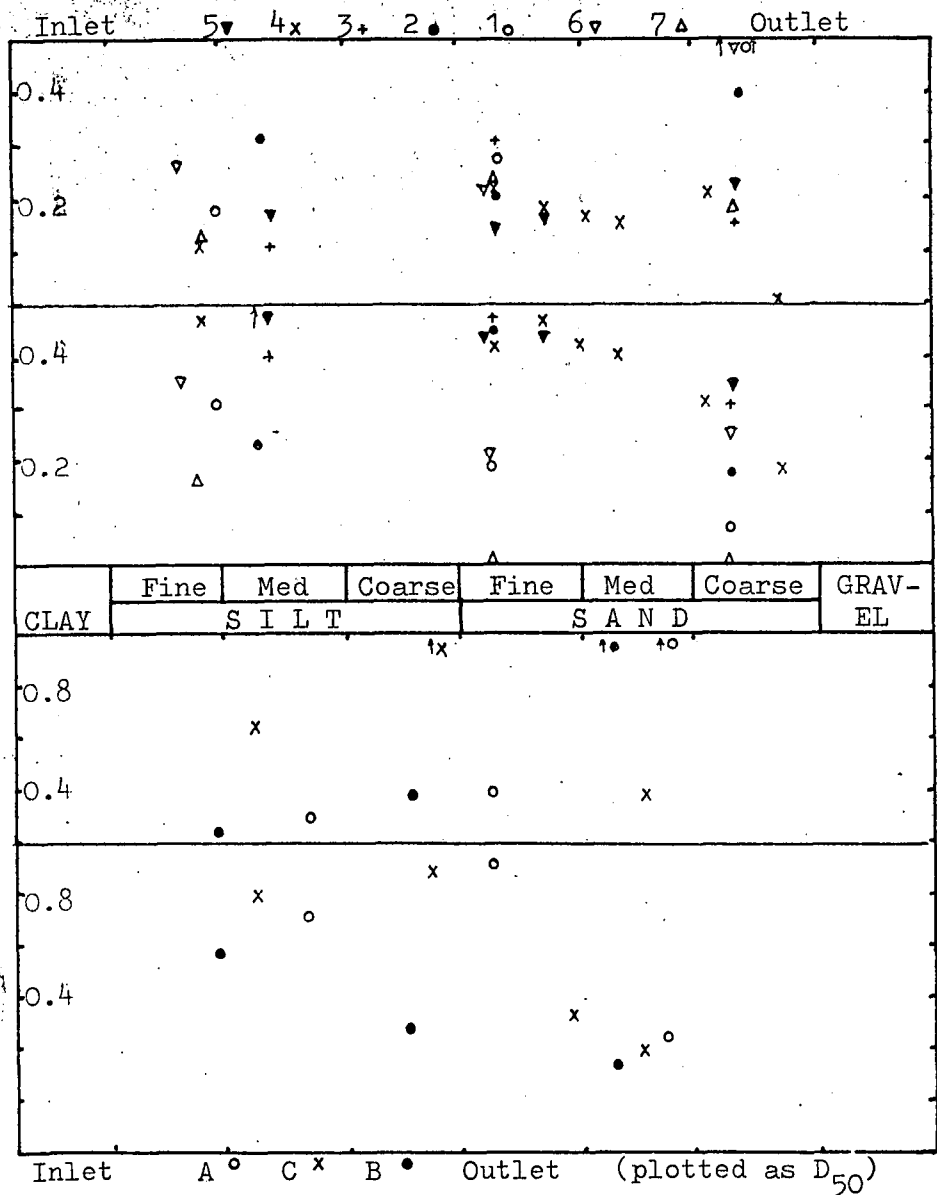
d. MA

Fig. 4.11 Variation in the quartz/illite ratio with grade. Upper half = XRD, lower half = recalculated XRF.

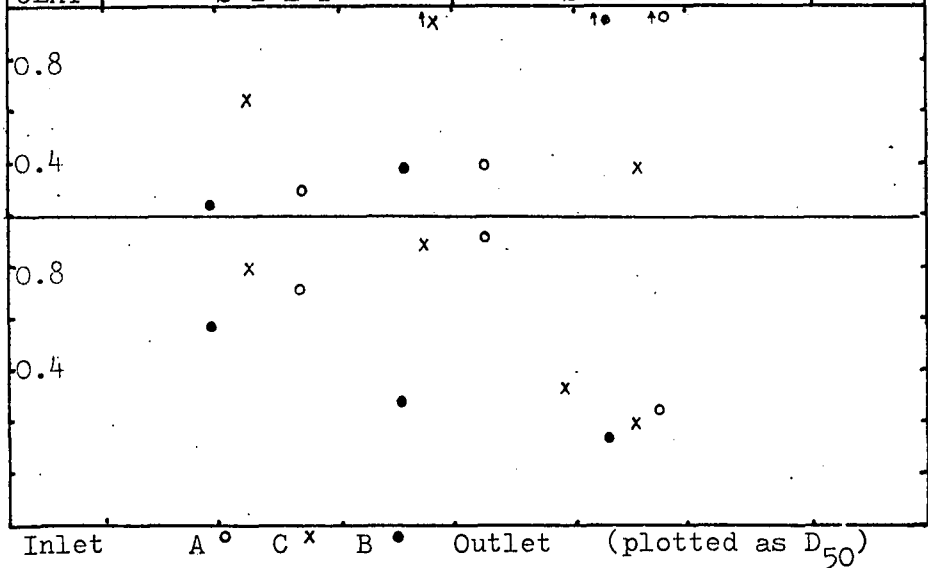
XRF recalculated graphs. At Peckfield (Figs.4.11a and 4.11b) and to some extent Maltby (Fig.4.11d) there is relatively more quartz in the finer size ranges. At East Hetton (Fig.4.11c) the amounts are approximately equal among sizes, though possibly there is a slightly greater abundance in the middle size ranges. Trends with position in the lagoon are not shown at East Hetton, and in Peckfield lagoon 6 they are only shown by the XRF recalculated data. It can be seen (Fig.4.11a) that the relative abundance of quartz decreases across the lagoon. This is most clear in the coarse sand size range, and with sample 7 (nearest to the outlet). Since the distance from inlet to sample 7 is much greater than the distances involved in the case of the East Hetton samples, it is possible that the trend had not developed in the latter lagoon.

Turning to the kaolinite/illite ratio, Figs.4.12a-d show that no relationships exist with size etc. as far as the XRD data are concerned. The random nature of the XRD data for both quartz and kaolinite ratios is probably due to the relative uncertainty of the illite determination against a high coal background. However, the XRF recalculated data display some very clear relationships. Firstly, there is always more kaolinite in the finer size fractions. The relative kaolinite abundance decreases sharply across the lagoon, particularly at Peckfield (Figs 4.12a and 4.12c). This decrease is more strongly displayed in the sand-sized fractions. The larger kaolinite <sup>containing shale particles</sup> are settling out faster than the smaller kaolinites, leaving an apparent dominance of kaolinites in the finer fractions. It should also be noted that the kaolinite/illite ratio is approximately twice as high at East Hetton as elsewhere; i.e. kaolinite is relatively more abundant in the North East area. This conclusion was reached by Taylor and Spears (1970) who considered the mineralogy of tailings and slurries across the country.

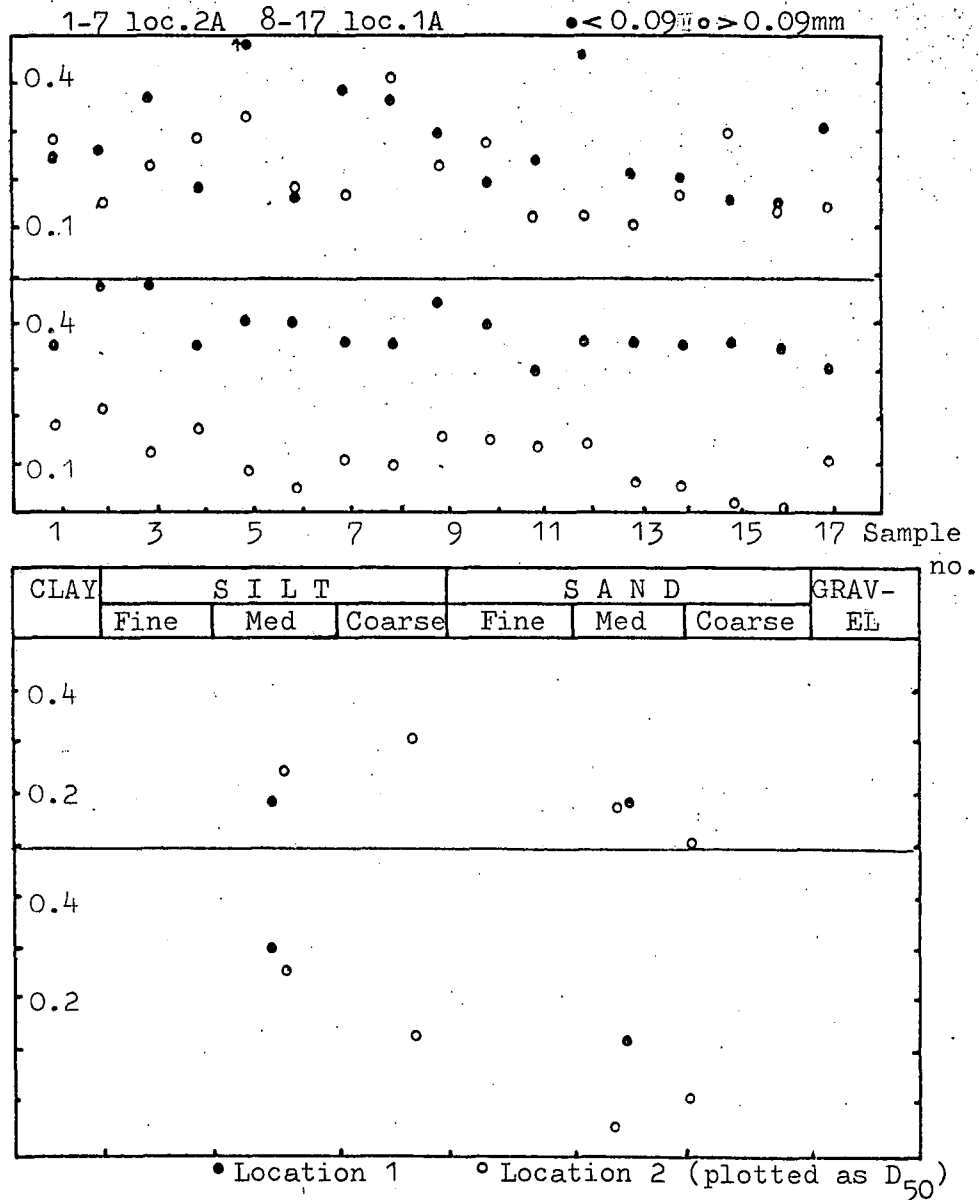
a.PL6



c. EH



b.PL7



d.MA

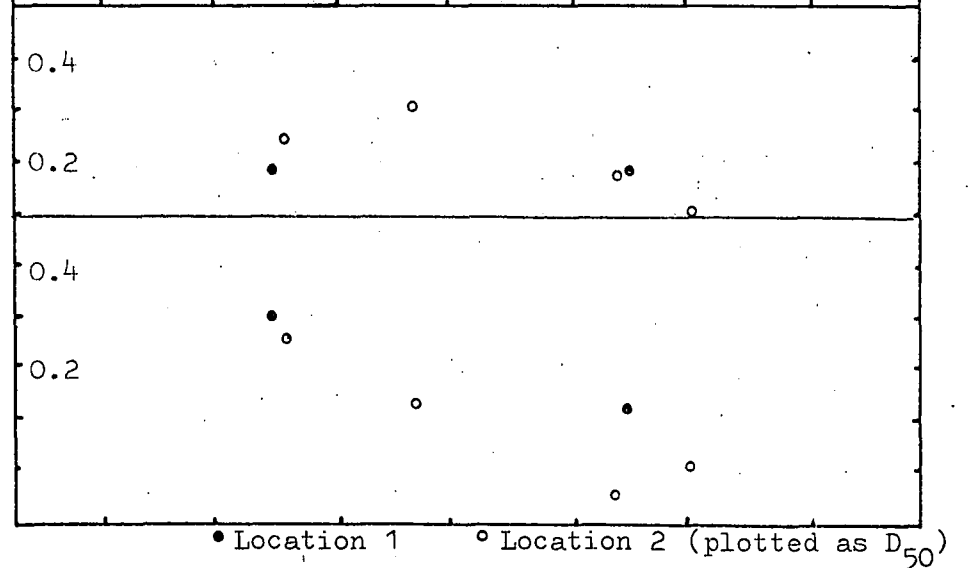
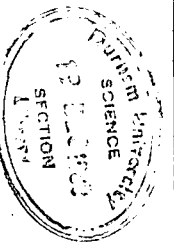


Fig.4.12 Variation in the kaolinite/illite ratio with grade. Upper half = XRD, lower half = recalculated XRF. Note scale of East Hetton.



## 6. Pyrite

There is a large and consistent discrepancy between the recalculated pyrite content and the XRD determined content, the latter being the smaller. From Fig.4.12a-d it can be seen that there is a clear trend to increased abundance of pyrite with increase in grain size for the recalculated mineral. This trend is discernible in the case of the XRD mineralogy for the Peckfield samples (Figs.4.13a and 4.13b) but is not shown for the East Hetton and Maltby samples (Figs.4.13c and 4.13d). It was pointed out in section 4.3 that the difference in the two methods of determination may be due to a high background of radiation from coal obscuring the pyrite peak in the XRD analysis. It is well known that pyrite occurs in close association with coal, Bray (1941), and this explains the close correlation of the two constituents with the greatest difference in specific gravity. (Though Bray (op.cit.) points out that the intricate association of interspersed pyrite and carbonaceous matter can cause the "apparent" S.G. of pyrite to be much lower than the value of 4.5 associated with massive forms of this mineral.)

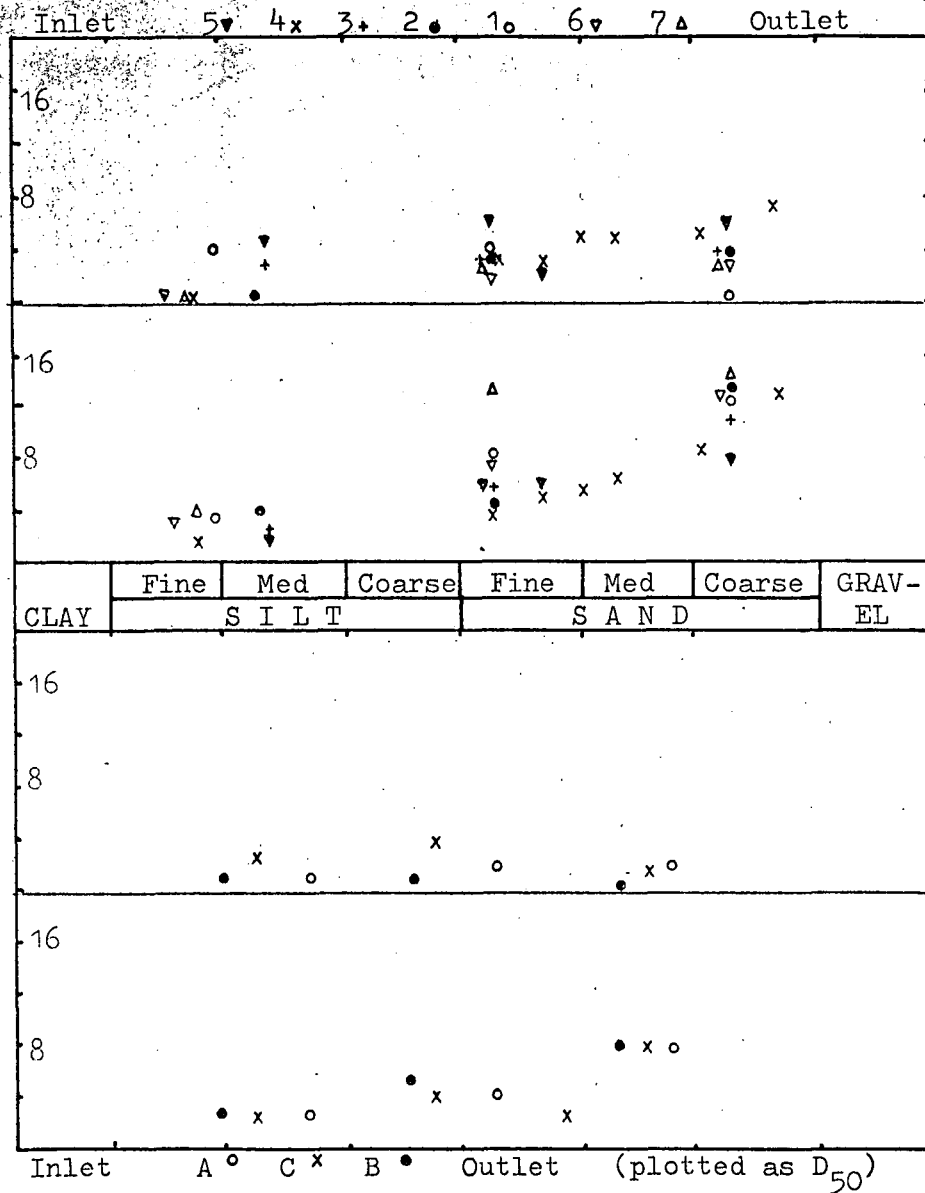
## 7. Ankerite

Ankerite or dolomite are the major carbonates found in the cleat of coal (Bray, 1941). No clear trends are shown by the XRD mineralogical data; frequently the mineral was not identified in the analysis (see Figs. 4.14.c-d). At East Hetton (Fig.4.14c) it is more abundant near the inlet. Generally the mineral is more abundant at East Hetton than in the other lagoons, possibly because sediment is washed onto the lagoon from the surrounding fields which overly limestone.

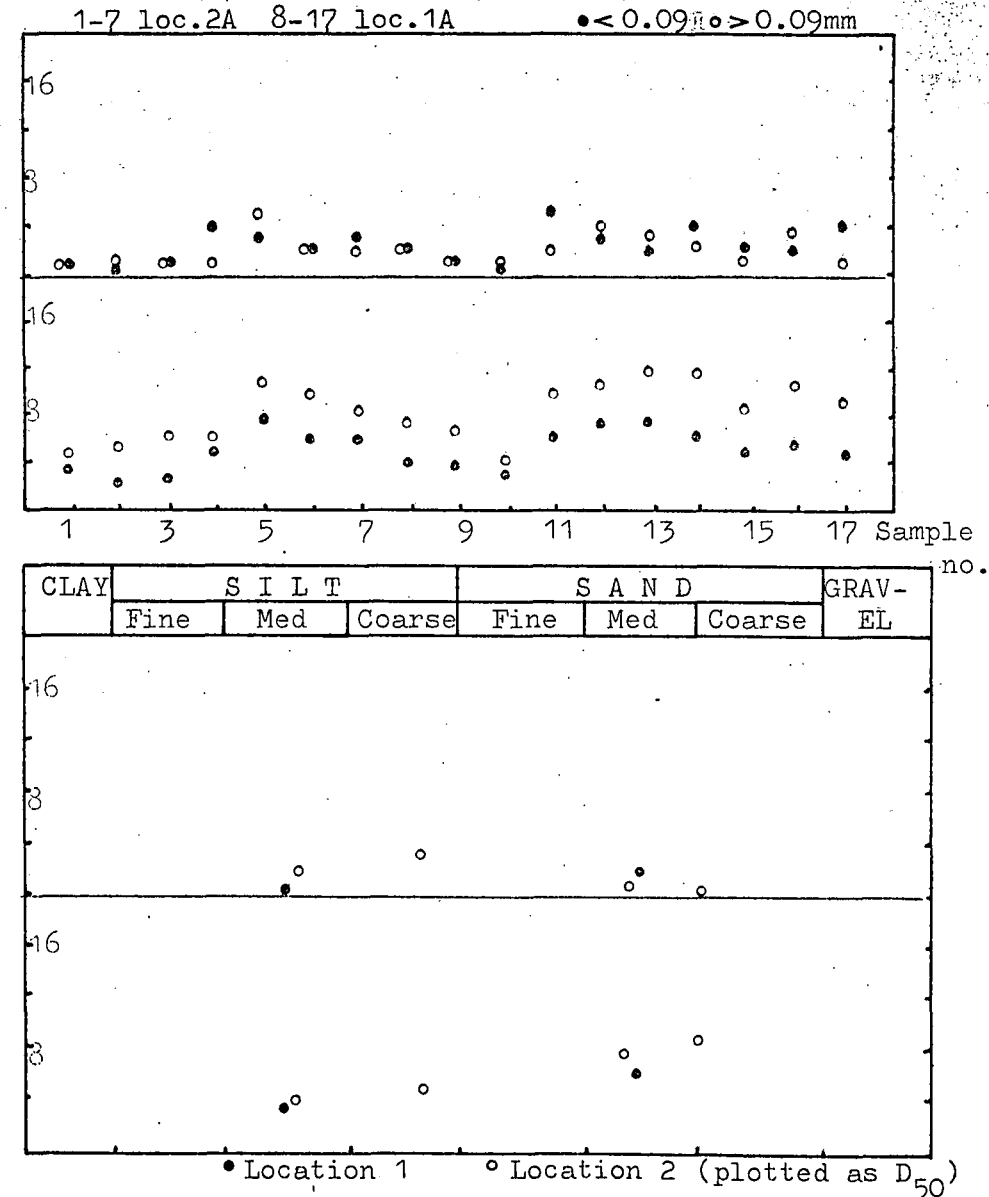
## 8. The Phosphatic mineral

From Figs.4.15a-d it can be seen that this mineral occurs preferentially in the finer grain sizes. (The actual mineral is unknown, hence only the

a.PL6



b.PL7

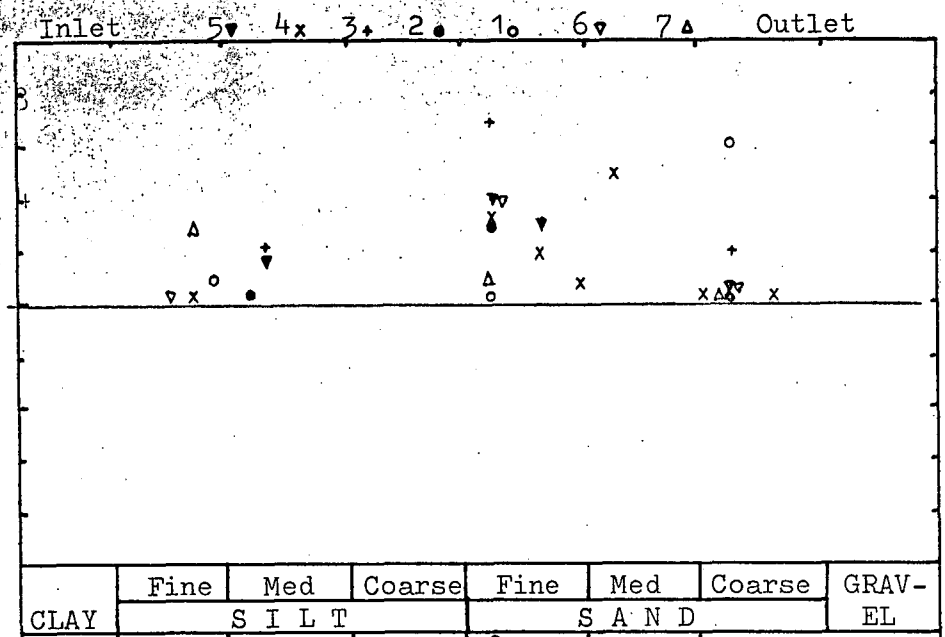


c. EH

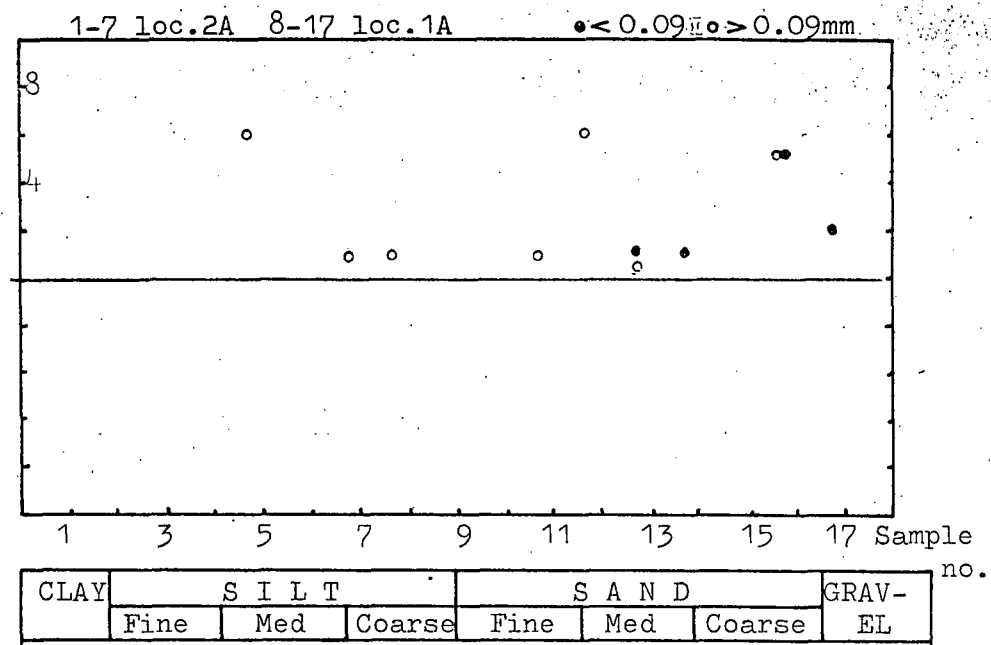
d.MA

Fig.4.13 Distribution of pyrite (in percent) with grade. Upper half = XRD, lower half = recalculated XRF.

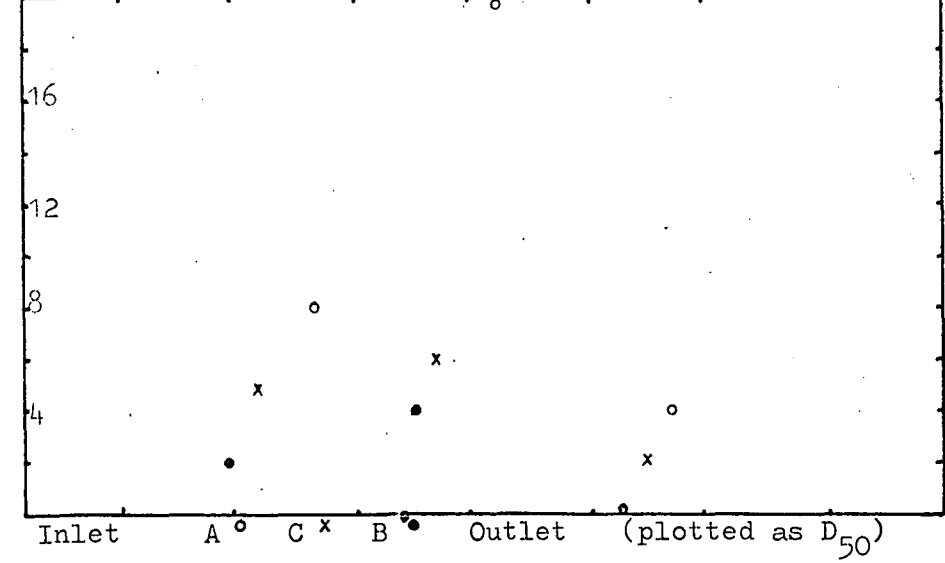
a.PL6



b.PL7



c. EH



d.MA

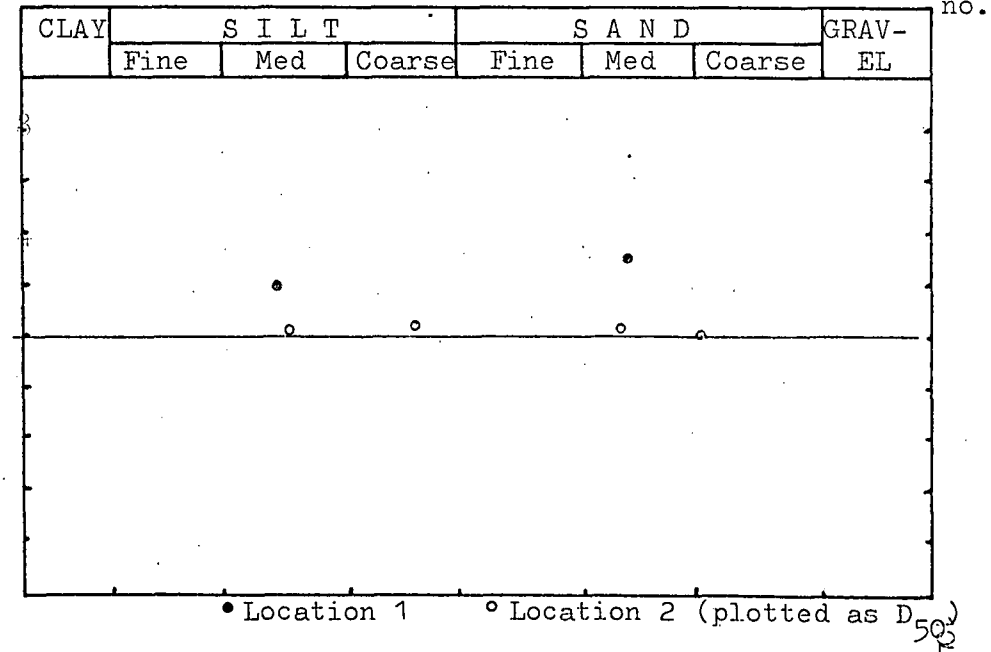
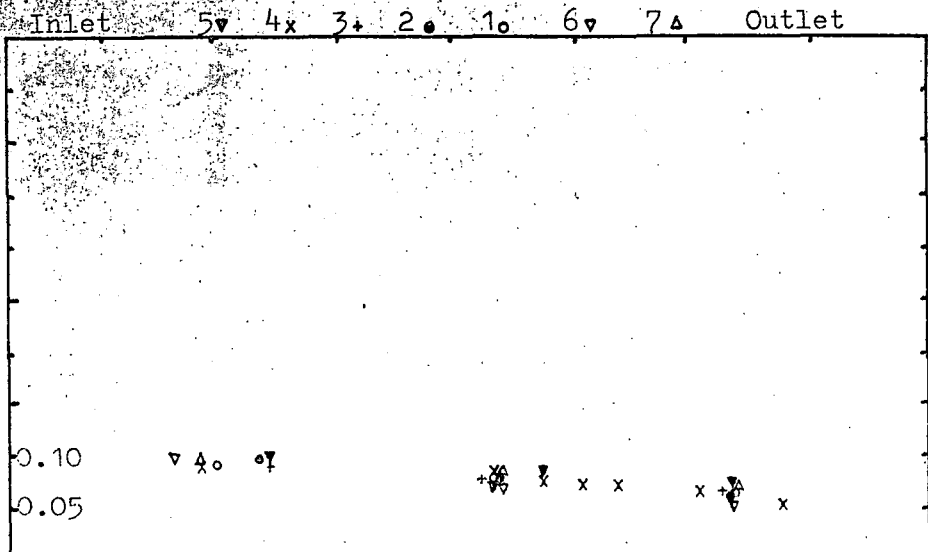


Fig.4.14 Distribution of ankerite (in percent) with grade.XRD only.

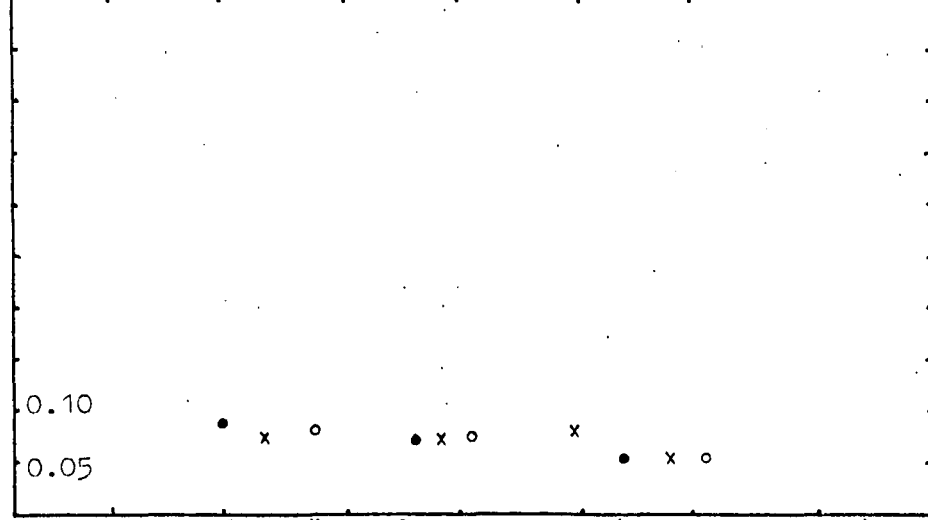


a. PL6

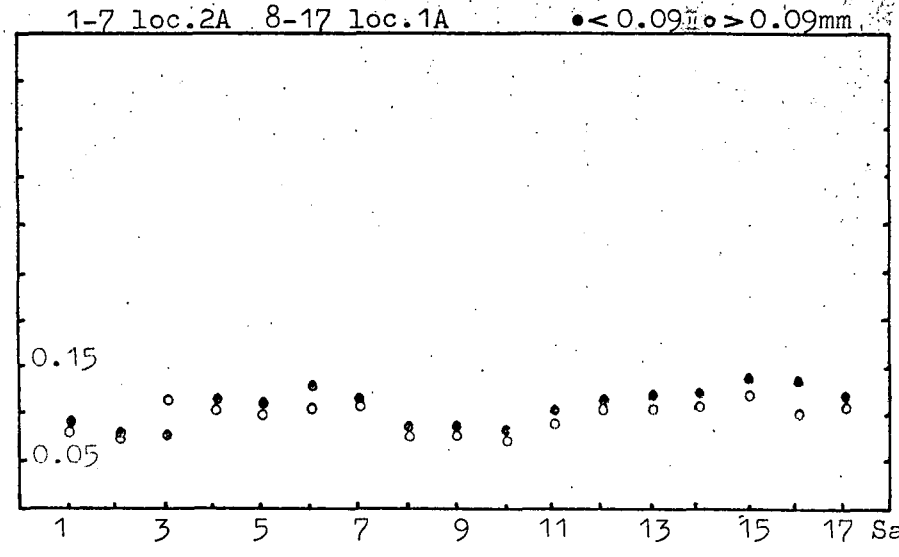


	Fine	Med	Coarse	Fine	Med	Coarse	GRAV- EL
CLAY	S I L T		S A N D				

c. EH



b. PL7



	S I L T			S A N D			GRAV- EL
CLAY	Fine	Med	Coarse	Fine	Med	Coarse	

d. MA

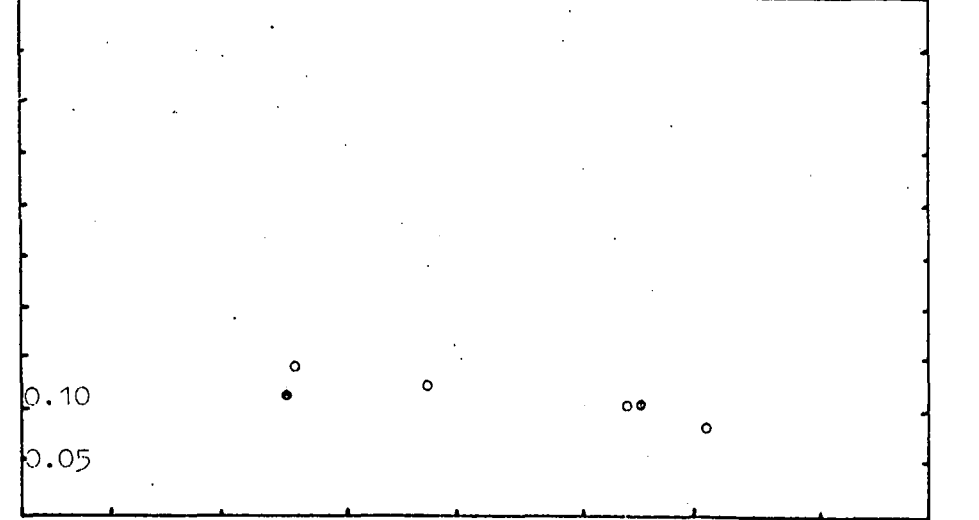


Fig.4.15 Distribution of P<sub>2</sub>O<sub>5</sub> (weight percent) with grade. XRF only.

weight percentage of  $P_2O_5$  is reported.) The East Hetton samples (Fig. 4.15.c) suggest that there is a preferential settling of larger grains near the inlet, while smaller grains occur in equal abundance everywhere. No trend with distance from the inlet can be discerned at Peckfield, however (Fig.4.15.a). The lagoon at Maltby possesses some of the highest abundances of this mineral, (Fig.4.15.d), despite the fact that the sample locations are far from the inlet. The lack of correlation with coal suggests that the phosphate is not due to phosphatic "bony" material. An apatite mineral is therefore a possibility; this supports the view of Taylor (1971.b).

#### 9. Other Minerals

Minerals other than those reported above were found in many of the XRD analyses. Chlorite was found in six samples from Peckfield lagoon 6 (Table A.4.1), followed in terms of the number of identifications by calcite (three times), goethite (twice) and siderite (once). The abundances were always less than one per cent, except for the 2 per cent calcite abundance in sample 4710. There is no trend to any of these minerals in terms of grain size or distance from the inlet.

Calcite was identified five times (all at the 1 per cent level) in the 34 samples from Peckfield lagoon 7, and chlorite once (less than 1 per cent). Calcite was also present six of the ten East Hetton samples; chlorite in four, and jarosite was identified as being possibly present in one case, and definitely present once. Of the six Maltby lagoon samples, two contain chlorite, and three contain jarosite. Again none of these three lagoons display any trends with size or distance from beach as far as these minerals are concerned.

#### 10. The chemistry and mineralogy of beach samples

Kennedy (1977) analysed the chemistry and mineralogy of two samples

representative of the inlet or "beach" area of lagoons. One of these samples was from Peckfield lagoon 6, the other from a lagoon at Abernant colliery. The chemistry, mineralogy and recalculated mineralogy of these samples is given in Table 4.4, and the grading curves are given in Fig.4.16. It is clear that these beach samples are different from samples representing the main body of the lagoon. Large particles, presumably of shale or siltstone are settling out near the inlet while coal and clay particles are swept further out. The organic carbon contents of these two samples are particularly low.

#### 11. The mineralogy of a clay layer from lagoon 16 at Silverhill Colliery

During the investigation into overtipping (see chapter 7) at Silverhill Colliery, N.Notts.Area, a particularly plastic layer of brown clay was noticed. The colour and extent of the layer was most unusual, in contrast to surrounding material which was visually similar to that found in other lagoons. The mineralogy of these layers are given in Appendix A.4.1 (no chemical determination is available). The layer has an extremely low organic carbon content (9%), but very high quartz, illite and kaolinite contents (22, 53 and 15% respectively). This is a most unusual association, yet the layer immediately below, with a coal content of 80% and very low abundances of anything else, is much more typical in comparison with the Peckfield, East Hetton and Maltby samples. Since the clay layer is extremely fine-grained (see grading curve Fig.4.17), this unusual mineralogy is not attributable to a "surge" of beach type sediment during a period of high flow. Rather it indicates a period of little or no sedimentation.

#### 4.7 The Sedimentology of Colliery Lagoons

The data presented in the previous section can be used to construct a general model of the structure of a lagoon. The sediment input into a lagoon can be divided into four main particle groups:-

Table 4.4 Beach samples from lagoons at Peckfield and Abernant. Analyses from Kennedy (1977).

Chemistry	SiO <sub>2</sub>	Al <sub>2</sub> O <sub>3</sub>	Fe <sub>2</sub> O <sub>3</sub>	MgO	CaO	Na <sub>2</sub> O	K <sub>2</sub> O	TiO <sub>2</sub>	S	P <sub>2</sub> O <sub>5</sub>
Peckfield	44.50	28.60	5.15	1.58	1.85	0.36	4.35	0.90	1.80	0.08
Abernant	46.19	29.91	3.85	1.28	1.10	0.82	4.40	1.04	0.55	0.14

Recalculated

mineralogy	Quartz	Illite	Paragonite	Kaolinite	Pyrite
Peckfield	16.73	41.29	10.75	19.38	3.38
Abernant	10.86	47.33	21.30	29.15	1.03

XRD

mineralogy	Quartz	Illite	Kaolinite	Chlorite	Ankerite	Organic carbon (thermal oxidation)
Peckfield	12	58	15	Trace	7	16.13
Abernant	5	58	8	-	-	10.71

Fig.4.16 Grading curves of the beach material from Kennedy(1978).

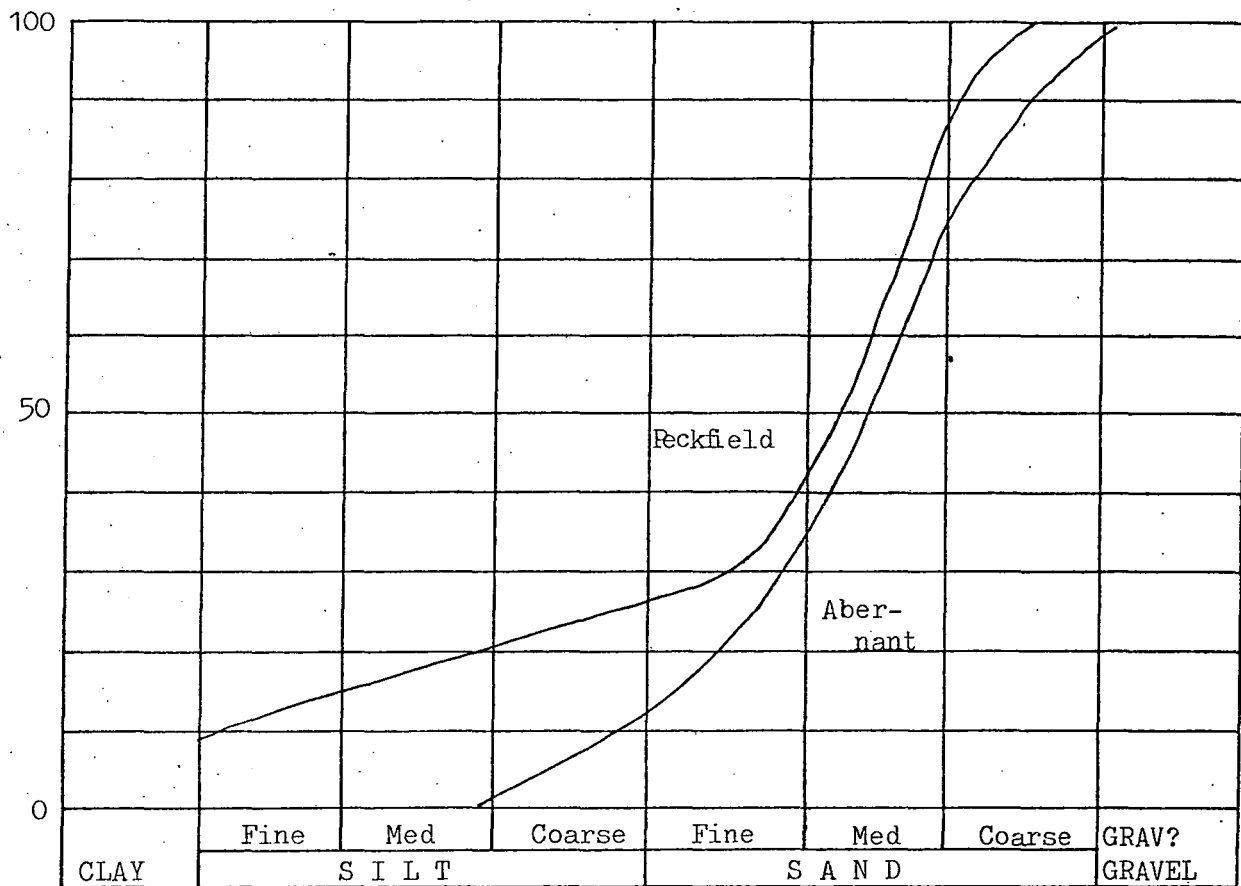
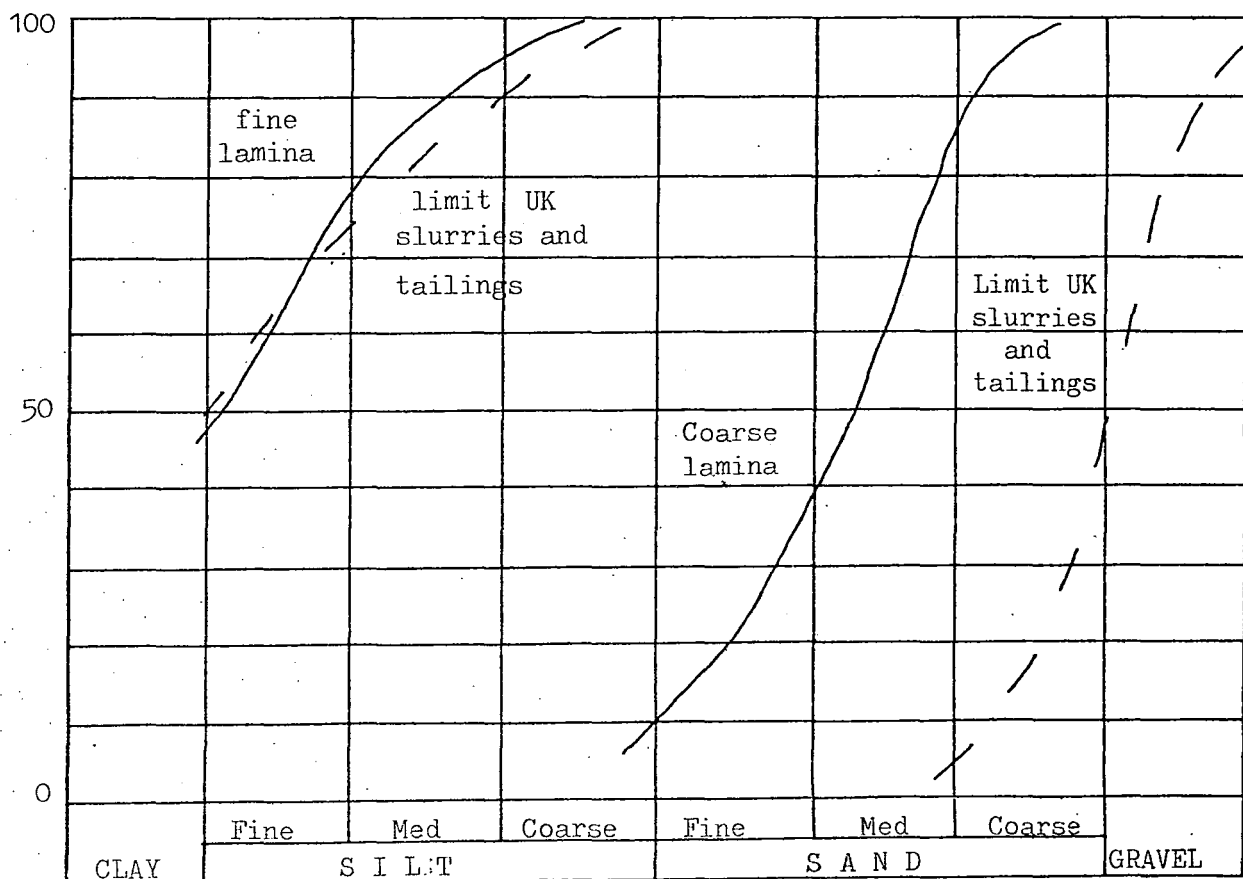


Fig.4.17 Grading curve of the fine and coarse laminae from lagoon 16, Silverhill



1. Large (sand-sized) rock particles composed mainly of quartz, illite and kaolinite which settle out quickly to form a grey-brown beach area. This beach is often raised above the rest of the lagoon.
2. Coal and included pyrite in all sizes from fine silt to coarse sand. The highest coal contents are found in the centre of the lagoon, but relatively speaking the larger particles settle out more quickly than the finer particles.
3. The quartz, illite and kaolinite particles. Again these occur in all size ranges; kaolinite and quartz settle out at an earlier stage than illite. All are more abundant near to the outlet.
4. Other minerals including carbonates and a phosphate. The abundance of these minerals in different size ranges and in different parts of the lagoon remains much more constant than with the other three groups. Although differences with size and position in the lagoon do exist, they are clearly not related to the sedimentologies of the other types.

Thus a constant input in terms of flow and composition will produce relatively coal-free beach of sand-sized shale particles, which will grade into a zone of coarse sediments with an abundance of coarse coal particles. Progressive fining towards the outlet sees a shift towards the clays and quartz, though fine coal particles remain a major constituent. However, neither the flow nor the sediment composition of the input into a lagoon is constant. The above model, with relatively low proportions of "beach" material and coarse coaly particles would reflect optimum operating conditions at the washery. However, there are frequent deviations from this optimum condition, and the effect is clearly seen in the lagoon sediments as a highly layered structure with frequent bands of coarse coaly material, present everywhere in the lagoon including the outlet. Thus in chapter 3 it was shown (Table 3.1) that

both coarse and fine layers were to be found at all three locations (i.e. A, B and C) but that the proportion of fine layers increased towards the outlet. In the previous section of this chapter it was shown that samples of all size ranges could be found in samples retrieved from any location from Peckfield lagoon 7 and Maltby lagoon 6.

There is considerable evidence to suggest that frequently any individual layer is not found everywhere in the lagoon. The cone penetration resistance profiles (Figs. 3.8 and 3.9, Chapter 3) demonstrated that many layers die-out over very short distances. It can be seen in Figs.4.18 and 4.19 that layers pinch out, and also that certain sedimentary features characteristic of braided streams are found. Braided streams are frequently observed near to the inlet: Figs.4.18 and 4.19 are from the inlet end of lagoon 109A at East Hetton. Layers dying out, and curious sedimentary features can again be observed at Peckfield, see Fig.4.20. The clay layer from Silverhill lagoon 16 which was mentioned in the preceding section was traced in a series of final pits, over all accessible parts of the lagoon (see Fig.4.21). In places it was split up by coarser laminae, but in no two trial pits were the coarse laminae quite the same (see Figs.4.22.a-d). Evidently individual coarse laminae must die-out over short distances. This is a most unusual association, as the clay layer is evidence for a long slow settling period - perhaps an annual colliery holiday - while the coarser bands reflect periods of higher sediment input. Lenticular layers and sedimentary features indicative of deltaic environments have been noticed before by Cobb,(1977, p.174).

This sedimentologically complex, layered structure seems to be the rule as far as colliery lagoons are concerned. It is found in all the lagoons reported herein, with one exception. The lagoons at Gedling Colliery (S.Notts.Area, N.C.B.) are generally visually homogenous, though

Fig.4.18 Fine laminations wedging out at the beach of lagoon 109A,  
East Hetton.

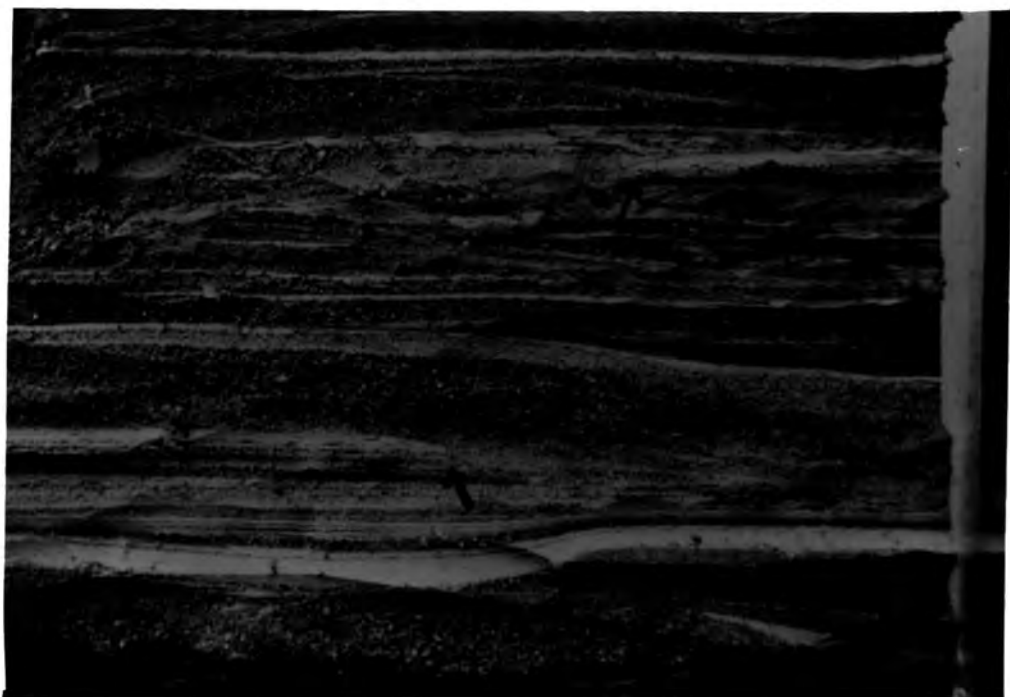


Fig.4.19 Braided stream deposit at the beach of lagoon 109A East Hetton.  
(The formation marked with the arrow is characteristic of a  
stream that is continually shifting its location, i.e. a  
braided stream.)





Fig.4.20 Sedimentary feature at the excavated face of lagoon 7 , Peckfield

Note that the fine lamination wedges out by the bunch of keys,  
as marked with the arrow.



Fig.4.21 Lagoon 16 at Silverhill, showing the locations of the trial pits. Numbered pits refer to the photograph locations of Figs.4.22.a-d.

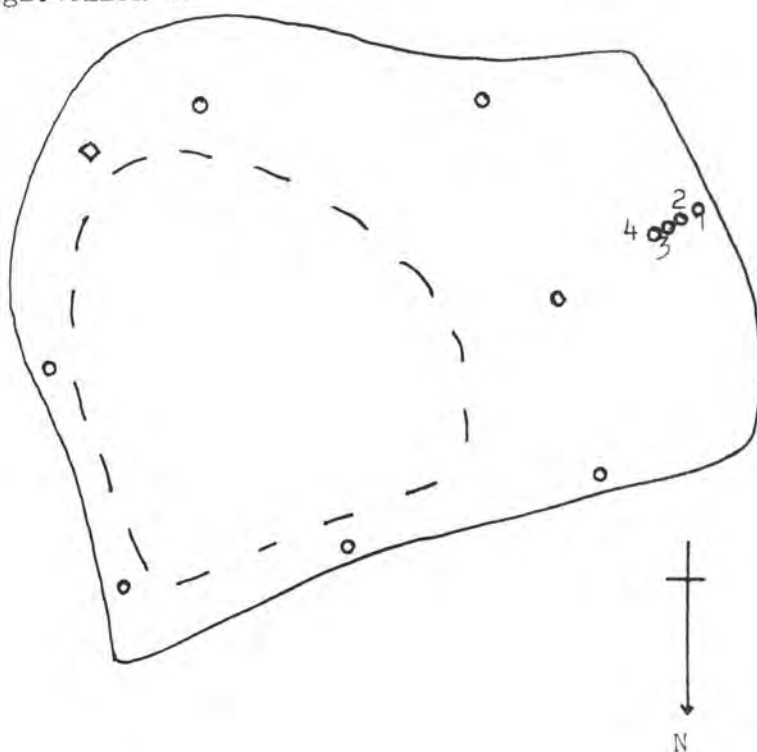


Fig.4.22 The fine lamination exposed in trial pits. For locations of the trial pits refer to Fig.4.21.

a. Trial pit 1



b. Trial pit 2 . Note that the fine lamina is interleaved with coarser material.



c. Trial pit 3. Note the distribution of the coarser material.



d. Trial pit 4. Note the distribution of the coarser material.



slightly coarser beach areas do exist. Gedling is a particularly large colliery with an efficient washery, and the ability to maintain a steady input (both in amount and composition) to the lagoons probably accounts for the structure of the lagoons. Apparently this was not always so, as National Coal Board (1972) considered it to be a layered lagoon. They also point out that homogenous lagoons do exist. Nevertheless, the layered type of lagoon seems numerically to be the more important.

#### 4.8 A Note on Sampling and Bias in Studies on Colliery Lagoons

Amongst the analyses on samples presented in section 4.6, three stand out as being very different from all the others. One is the clay layer at Silverhill, the other two are beach samples, which were taken from Kennedy (1977). Furthermore, amongst all the other samples it can be seen that the chemistry, in particular the carbon content, is highly dependent upon the grading characteristics of the layer being analysed.

It is therefore important to sample the lagoon adequately. In particular the temptation to sample only the beach area, which is elevated and therefore firm and dry, must be avoided. It is therefore recommended that the following procedure be adopted wherever possible:-

- 1) In addition to a beach samples (which are easy to collect) other parts of the lagoon must be sampled.
- 2) At each location a vertical section be inspected, either in the field or in the laboratory, and samples <sup>of</sup> representative layers of different characteristics should be taken for testing.
- 3) At each location the gross make-up of the lagoon in terms of the proportion of each representative layer type should be obtained.

This procedure will yield a highly accurate picture of the surface of the lagoon in a minimum of time. Only two further items of

information are required: firstly, are the layers laterally extensive, and secondly, does this picture hold at greater depths? The first point can be answered by trial pitting at the surface, without the need for frequent samples. The second point can be answered by some deep sounding technique, either sampling or in-situ testing (say, vane shear tests or cone penetration tests). If there is reason to suspect that the character of the lagoon has changed based on in-situ tests, samples should be obtained in any case.

#### 4.9 The Relationship Between the Organic Carbon Content and the Specific Gravity

Coal has a specific gravity of about 1.3, depending on the ash content; quartz and the clay minerals have specific gravities of about 2.65. Therefore a mixture of the two groups will result in a material having an intermediate specific gravity. The correlation between the specific gravity and coal content of fine colliery discard is thus expected to be very high, and a linear regression line fitted through the points on a graph will naturally be highly significant statistically. Taylor and Cobb (1977) show such a relationship. Now, the total specific gravity ( $SG_T$ ) will be:-

$$SG_T = \frac{\text{Mass}}{\text{Volume}} = \frac{M_c + M_o}{V_c + V_o}$$

where  $M_c$ ,  $V_c$  are the mass and volume of the coal  
 $M_o$ ,  $V_o$  are the mass and volume of all other constituents

$$SG_c = \frac{M_c}{V_c}$$

$$\text{or } V_c = \frac{M_c}{SG_c} = \frac{M_c}{1.3} = 0.769 M_c$$

$$\text{and } V_o = \frac{M_o}{2.65} = 0.377 M_o$$

$$\text{also } M_c + M_o = 1$$

$$\begin{aligned} \text{hence } SG_T &= \frac{1}{0.769M_c + 0.377M_o} = \frac{1}{0.769M_c + 0.377(1-M_c)} \\ &= \frac{1}{0.392M_c + 0.377} \end{aligned}$$

This is not the equation of a straight line. The implication of the linear statistical regression technique, that there is a linear relationship between the organic carbon content and the specific gravity is therefore not correct. The curve represented by this equation is shown as curve A in Fig.4.23, together with all the points of specific gravity and organic carbon content presented herein. In the case of the samples from Peckfield lagoons 6 and 7, the aggregate (i.e. whole sample) organic carbon contents are plotted, not the carbon contents of the individual size ranges. Also plotted are 17 points from Cobb (1977), Chapter 4, and 7 points from Taylor et al. (1978).

However, it was shown above (section 4.6) that a significant amount of pyrite is associated with the coal. If all the coal contained about 15 per cent by weight of pyrite, which is an approximate upper limit for very coal-rich samples (see Fig.4.13.a-d), then the specific gravity of the coal would be 1.45. The equation for  $SG_T$  becomes:

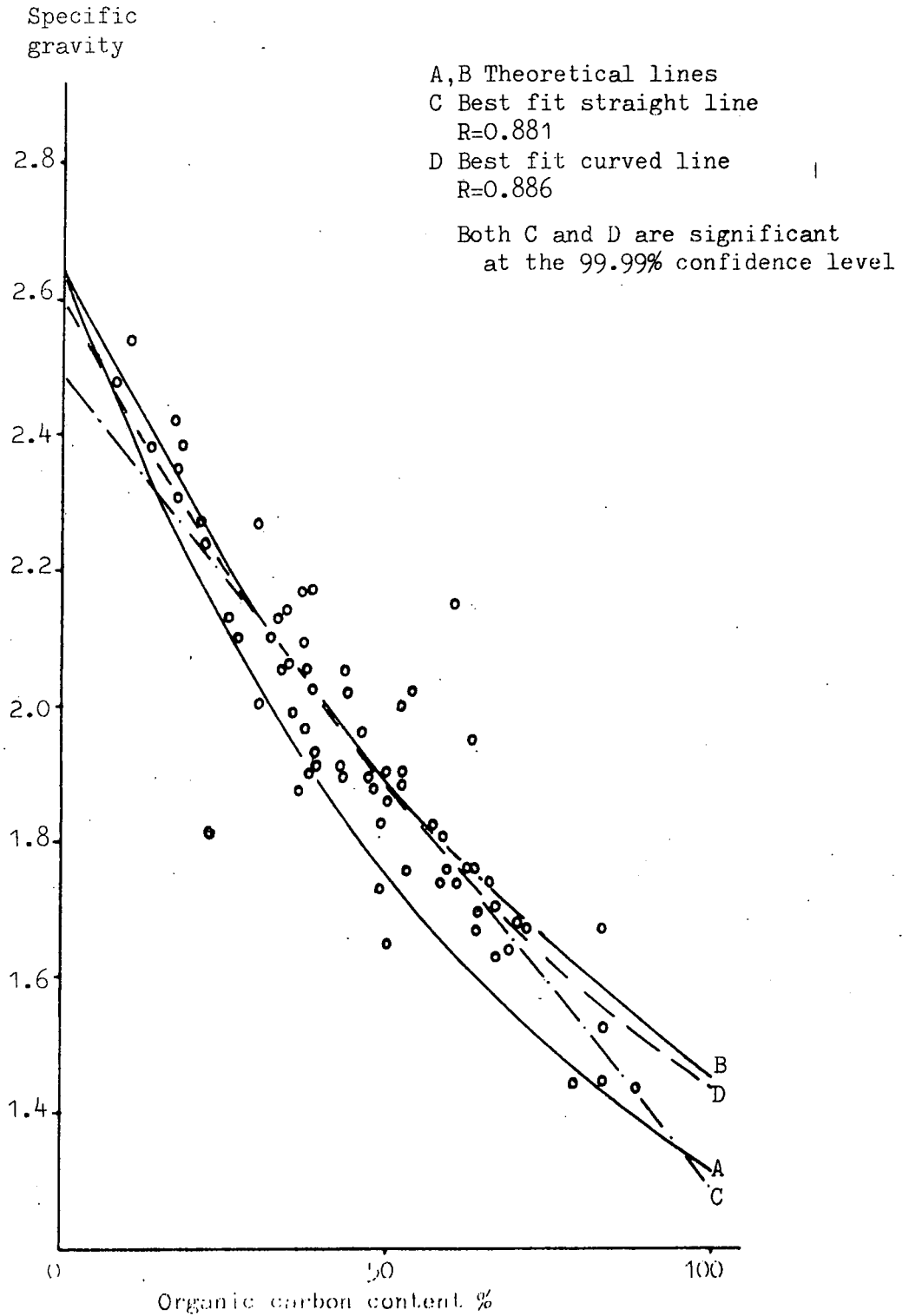
$$SG_T = \frac{1}{0.312Mc + 0.377}$$

which is shown as curve B on Fig.4.23. Curves C and D represent the best fit linear regression line and the best fit curved regression line. The curve is marginally better fit to the data, but the difference is not significant in a statistical sense. The curved fit also agrees closely with the theoretical curve B and gives a better estimate of the specific gravity at zero carbon content. In a physical sense, therefore, the curved fit is to be preferred. The average organic carbon content calculated from these analyses is 46.5.

#### 4.10 On the Difference Between Tailings and Slurry Lagoons

The fines from the washery are either pumped straight into the lagoon in the form of a slurry, or further treated by froth flotation, the rejects from this process being termed tailings. Reject wet fines is a slurry

Fig.4.23 Variation of specific gravity with organic carbon.



that has a very low coal content and is therefore often classed with tailings. Theoretically, the most coal-rich type of fines should be slurry, followed by reject wet fines, with tailings being relatively coal free. In practice there is no significant difference between the processes, as is shown quite clearly by Table 4.5. It should be noted that in nearly all cases where only one sample has been taken, the coal content is very low. In some of these cases the sample is known to be from the beach, and again the possibility of sampling bias must be considered.

This lack of a difference between slurry and tailings may be partly explained by the nature of the fine discard. Coal particles occur in all size ranges, though they are more abundant in the coarser fractions. Thus, despite a large difference in specific gravity between coal and other particles<sup>\*</sup>, they are difficult to separate in a fluid medium. In terms of settling velocity (Stokes Law), a large coal particle is equivalent to a small clay particle. Although many washeries could probably be more efficient than they are, total separation of coal from clay particles cannot be achieved.

In view of the close association of coal with the grading characteristics of the sediment shown in section 4.6. purely mechanical size separation would yield very coal-rich products in the upper size ranges. It can be seen from Figs.4.6a-d that a separation at the 200 micron size (i.e. medium sand and above) would produce a product with about 70% coal. Taking the grading curves and the volume of lagoon to which each grading curve refers into consideration, it may be calculated that for both East Hetton lagoon 109B and Peckfield lagoon 6, approximately 25% of the material in the lagoon lies

\*Footnote

The S.G. of coal is approximately 1.3; that of clays varies from about 2.4 to 2.7



Table 4.5 Organic carbon contents reported for various lagoons.

Lagoon	No. of samples	Range of determinations	Source of data
Slurry			
Peckfield*	24	31 - 62	Current work
"	1	18	GWK
Cresswell	10	34 - 73	NCB report
Blidworth	5	38 - 54	" "
Ollerton	1	50	" "
Silverhill	2	9,80	Current work
Slurry/tailings, or reject wet fines			
Orgreave	5	5 - 50	NCB report
Gedling	7	48 - 62	" "
"	3	30 - 38	T+M(1), AEC(2)
Tailings			
Maltby	6	51 - 81	Current work
"	1	23	T+M
Abernant	1	11	GWK
Elsecar	1	22	T+M
Cortonwood	1	20	AF
Manvers (ex washery)	1	38	AEC
Morrison Busty (ex washery)	1	18	AEC
Oakdale (ex washery)	2	22,22	Current work
Cadeby	33	26 - 76	AEC
East Hetton	10	14 - 83	Current work

\* The Peckfield samples are aggregate coal contents, i.e. not the individual size fractions.

Sources of data: AEC, Cobb (1977); AF, Fletcher (1976); GWK, Kennedy (1977); T+M, Taylor and Morrell (1979); NCB reports, Wimpeys (1969), Gedling, Ollerton, Blidworth, Cresswell; Wimpeys (1977b), Orgreave.

above this size. Similarly a separation at the coarse sand size (600 microns) would yield a product with about 85% coal, and remove about 10% of the material in the lagoon. Unfortunately this type of separation is probably not feasible in terms of washery processes, as the mesh sizes are too fine for a large throughput of material.

#### 4.11 Comparison of Lagoon and Tip Geochemistry

The major difference between the geochemistry of lagoons and tips is the coal content. It is very significantly higher in the case of lagoons, a point noted by Taylor and Cobb (1977). This is also true of pyrite which is closely associated with the coal.

Of the remaining constituents in tips, illite is the most important, followed by quartz and kaolinite, Taylor (1975). However, kaolinite is relatively more dominant in Northern coalfields, i.e. Scotland, Northumberland and Durham; Taylor and Spears (1970); Taylor (1974); Collins (1976). In section 4.6 the same was shown to be true in lagoons.

Taylor (1974) proposed that the coal and clay associated formed two of three major groups for coarse discard. The third major group consisted of the carbonates, and this forms a separate group in the geochemistry of lagoons. Phosphatic material also belongs to this group, which accords with the findings of Taylor (op.cit.) for English spoil heaps.

The depositional environment of lagoons, i.e. in moving water, complicates the picture by the effects of sorting, but nevertheless the three groups of Taylor (op.cit.) are readily discernible in the geochemistry of lagoons. It would have been surprising were this not so.

#### 4.12 The Stabilisation of Fine Colliery Discard with Cement

Cement stabilisation of fine colliery discard has been used as a disposal method obviating the need for lagoons, both in the U.S.A., Snyder

et al., (1977), and in South Wales (Halcrow, 1977). The material is placed directly on the tip after a curing period to allow it to develop adequate handling properties. It is well known that the presence of pyrite and its oxidation is detrimental to the action of cement (see Gratten-Bellew and Eden, 1975; Sherwood and Ryley, 1970).

In view of the high sulphur contents reported in Section 4.6, the advisability of such a practice must be questioned.

A short investigation was therefore carried out on material from the washery at Oakdale Colliery (S.Wales Area, N.C.B.). Two series of tests were carried out; the first being a leaching experiment on cement stabilised tailings; the second set of tests investigated the effect of remoulding and pyrite concentration on the strength of the material. For the leading experiment, the procedure was as follows:

1. Two samples of Oakdale washery tailings were received at 24% moisture content. Dried samples were analysed by XRF, the results being reported in Table A.4.4.d (samples OW1 and OW2). The moisture content to which the samples were made up for testing was 90%.
2. Ordinary Portland Cement (O.P.C.) was added at a concentration of 4% net weight. After thoroughly mixing the stabilised discard was allowed to stand for 24 hours. A sub-sample was taken for XRF analysis (sample OWOPC, Table A.4.4.d).
3. At the end of 24 hours the sample was placed in a steel permeameter which had been adapted for constant head conditions (see Fig.4.24). A laboratory vane test (peak and remoulded) was conducted at this stage. By interpolation a sample of rainwater thought to be typical of South Wales was made up following the tables given by Stevenson (1968), see Table 4.6. The sample was left under a 300mm head for 20 days.
4. For the period 10-20 days, the permeability was determined. At the

Fig. 4.24 Permeability apparatus for the leaching experiment.

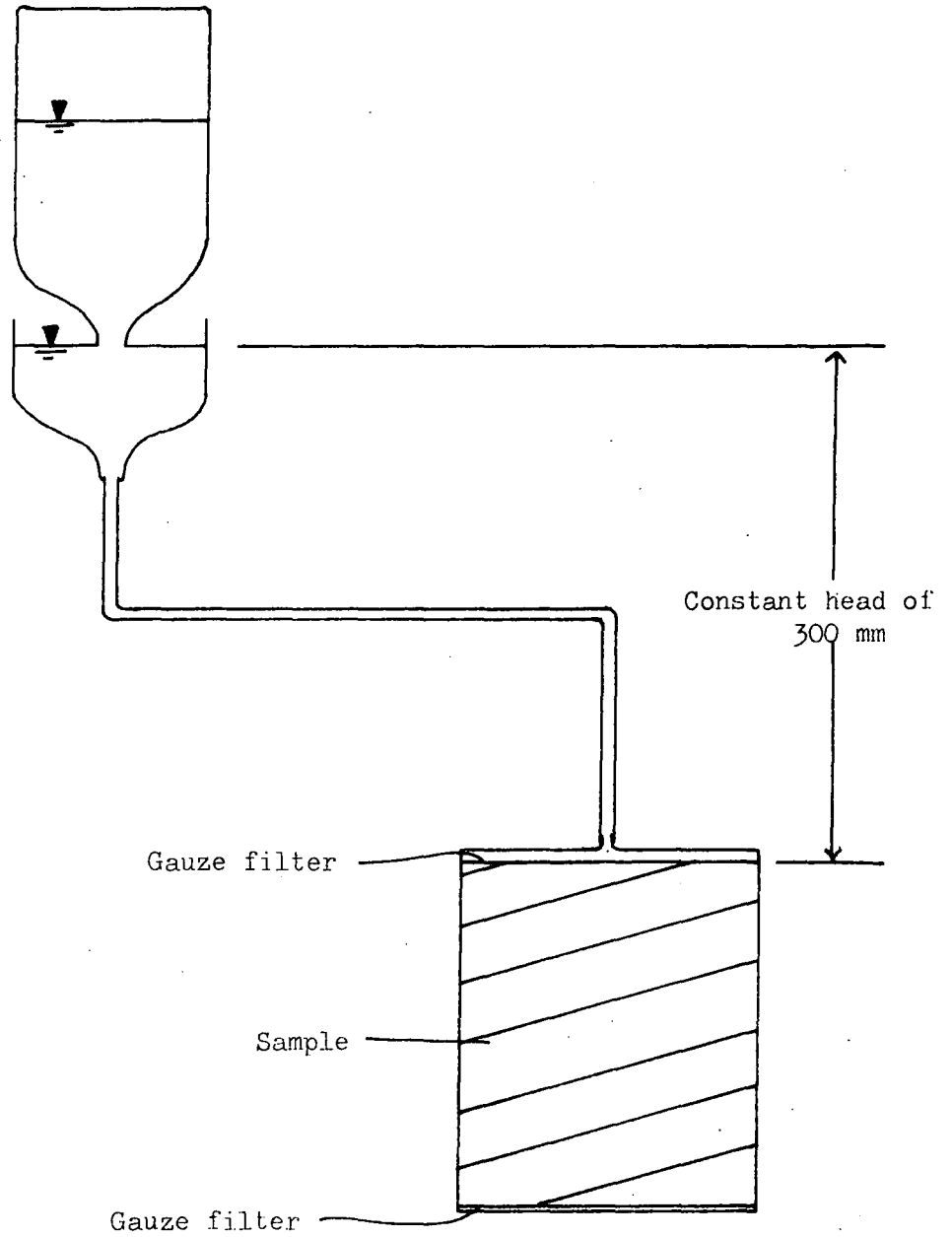


Table 4.6 Water composition for the leaching experiment.

(Concentrations in mg/l)

Cl	S	Na	K	Ca	N (as nitrate)	N (as NH <sub>4</sub> )	pH
5.0	3.0	3.1	0.6	1.0	0.7	1.4	5.0

(After Stevenson, 1968)

Table 4.7 Results of the vane test, permeability and density determinations of the leaching experiment.

	After	24 hours	20 days	30 days
1 Lab vane				
a. Average peak shear strength (3 tests)		12 kN/m <sup>2</sup>	42.5	49
b. Average remoulded strength (3 tests)		5	9	7
2 Permeability				
a. Flow rate over 10 days			0.1322 l/day	0.1225
b. Permeability			$6.8 \times 10^{-8}$ m/s	$6.3 \times 10^{-8}$
3 Density				
a. Bulk		1.435		1.418
b. Dry				0.776 *

\* N.B. This corresponds to a moisture content of 82.7%, compared to an initial moisture content of 90%. The cement takes up water on curing.

end of 20 days a further vane test was carried out.

5. A further 10 day leaching period was allowed, from which another permeability measurement was made. At the end of this period a final vane test was carried out, and the bulk density found. Samples were taken from the base and top of the permeameter for XRF analysis (samples OWB and OWT, Table A.4.4.d).

The vane test and permeability results are shown in Table 4.7. The bulk density over the thirty day period had decreased by 1.18% and indeed there seems to be a slight loss of clay mineral elements ( $\text{SiO}_2$ ,  $\text{Al}_2\text{O}_3$ ,  $\text{K}_2\text{O}$  and  $\text{Na}_2\text{O}$ ) from the bottom of the permeameter (compare sample OWB with OWT and OWOPC, Table A.4.4.d). Importantly, there is a significant loss of  $\text{CaO}$ , the principal component of cement, from the top of the permeameter and a concentration at the base. The increases in  $\text{Fe}_2\text{O}_3$  and  $\text{MgO}$  in sample OWT are probably due to contamination from the permeability apparatus. The leaching period is probably equivalent to 6 months percolation in S.Wales, assuming no run-off.

The results of the vane tests will be discussed with those from the remoulding experiment, the procedure for which was as follows:

- 1) Oakdale washery fine discard was made up to a moisture content of 75%.
- 2) Ordinary Portland Cement was added to this fine discard at a concentration of 4% wet weight. The sample was thoroughly mixed.
- 3) Six 1.5 inch tubes were filled with this mix and are referred to as sample nos.1 to 6 respectively.
- 4) The remainder of the mix was divided equally into two. To one half was added 4% dry weight of finely divided iron pyrite; to the other 2%, and emplaced in 1.5 inch tubes. The former is referred to as Sample No.7; the latter as Sample No.8.
- 5) The tubes were stood in shallow trays, and placed in sealed polythene

bags with a little water inside. The samples were thus allowed free access to water vapour.

- 6) Samples 1 to 5 were opened at intervals and tested using a laboratory vane apparatus (see Table 4.8). Peak and remoulded strengths were measured. Each sample was then physically remoulded with a rod, and tested again with the vane. The sample was then lightly remoulded once more to remove the effects of the vane test.
- 7) One week after the addition of the cement all samples were subjected to one vane test only in the top half of the sample. The bottom half of each tube was left undisturbed for further tests.

The laboratory vane test results were crudely obtained and are regarded as preliminary findings only. However, a comparison between samples is believed to be valid.

The peak strengths and the remoulded strengths before physical remoulding are shown in Table 4.9 and Fig.4.25. The results of the leaching experiment are shown, and the strengths of the samples after physical remoulding were obtained, are also entered in Table 4.9.

Table 4.10 and Fig.4.25 show the peak and remoulded strengths recorded for the vane tests conducted at the end of one week on the physically remoulded samples (1 to 5), and the control (6).

Although a comparison is not strictly valid, because of water availability and the possible effects of container size, it seems fair to state that after one week a sample stabilised at an initial moisture content of 75% is considerably stronger than one at an initial moisture content of 90%. The implications for 'quality control' at the washery are obviously important. It should be noted that the 4inch sample in the leaching experiment is stronger after 24 hours than the 1.5inch sample.

Table 4.8 Timetable of events in the leaching experiment.

Sample	Time of remoulding	Vane tests	
		At time of remoulding	After 1 week
1	3 hrs	y	y
2	7 hrs	y	y
3	24 hrs	y	y
4	48 hrs	y	y
5	1 week	y	y
6 (control)	-	-	y
7 (4% pyrite)	-	-	y
8 (2% pyrite)	-	-	y

y, test performed    -, no test

Table 4.9 Vane test shear strengths.

Time after cement addition	Vane shear strength in $\text{kN/m}^2$		
	Peak	Remoulded	Physically remoulded
3 hrs	0.7	0.3	-
7 hrs	2	1	-
24 hrs	10	4.5	2.5
48 hrs	20	6.5	3
1 week (sample 6)	47	9.5	6
1 week (sample 7)	31	7	-
1 week (sample 8)	36	8	-
Leaching experiment results			
24 hrs	12	5	-
20 days	42.5	9	-
30 days	49	7	-

Table 4.10 Strengths of remoulded samples after 1 week.

Sample	Vane shear strengths in $\text{kN/m}^2$	
	Peak	Remoulded
1	48	10.5
2	47	10
3	18.5	5
4	8	3.5
5	7.5	6
6 (control)	46	8



Fig.4.25 Cement stabilised Oakdale tailings, vane shear strength before remoulding.

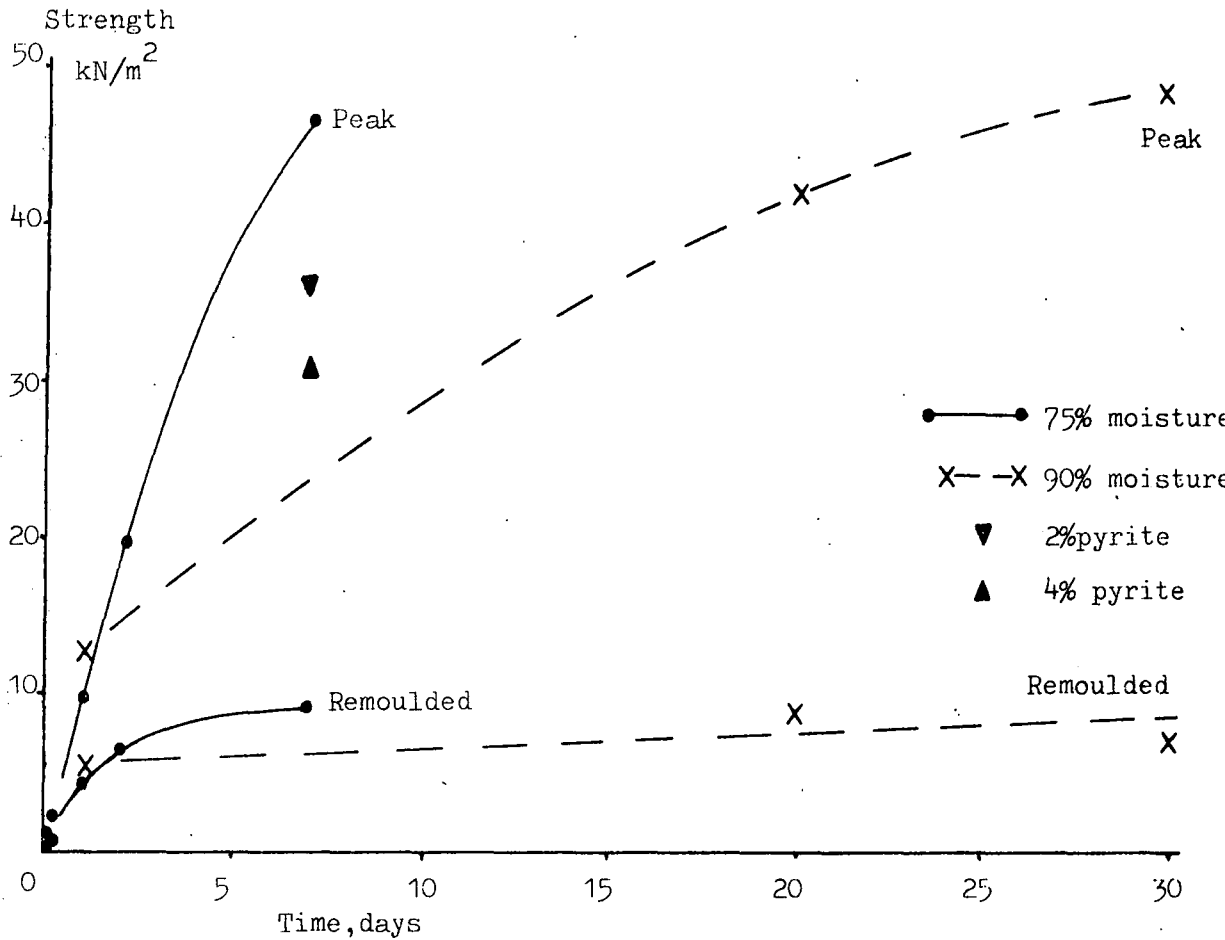
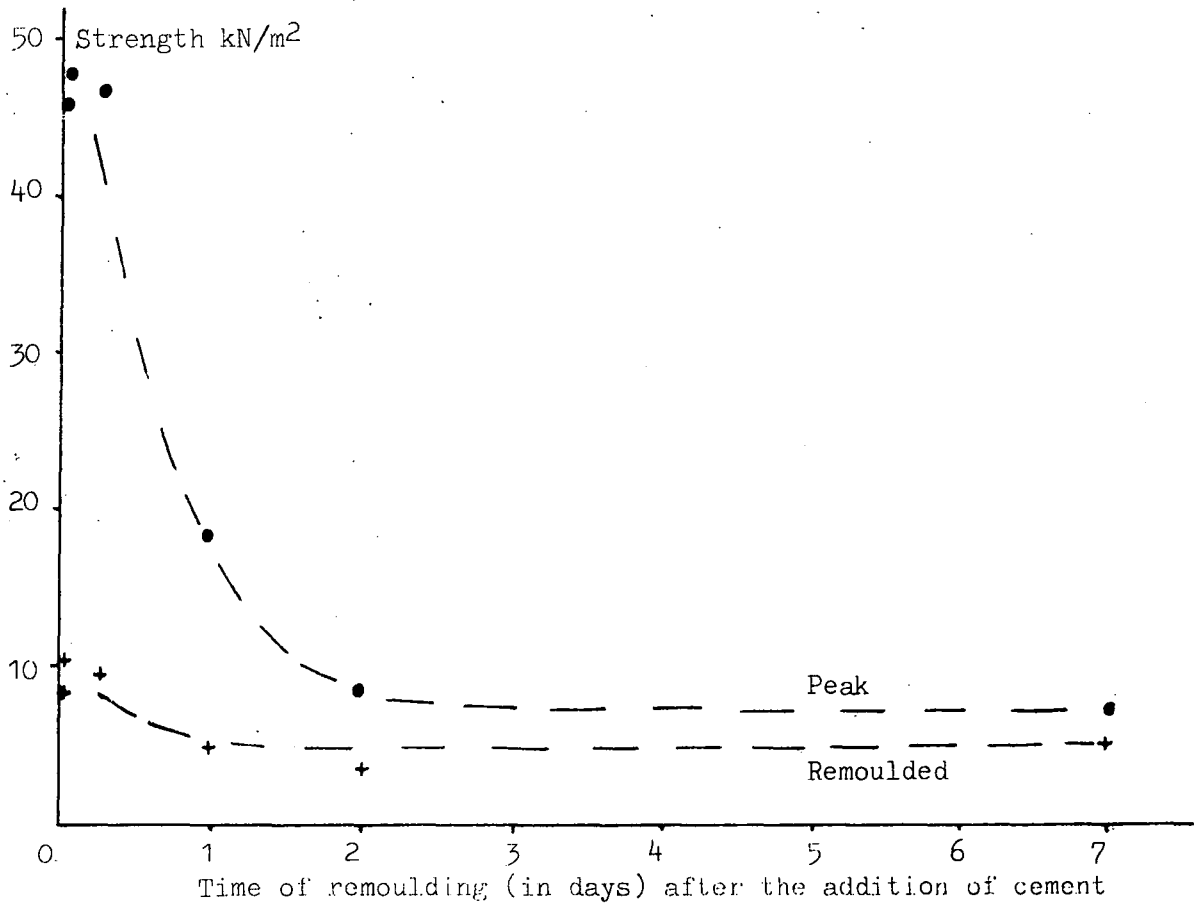


Fig.4.26 Vane shear strength of remoulded Oakdale tailings (cement stabilised) tested at the end of one week.



This could be due to faster curing of the cement in the higher temperatures generated in the larger sample, caused by the exothermic reaction of the cement itself.

It should be noted also that the leaching of cement has not in fact caused any reduction in strength. Any such trend is obscured by the general increase in strength caused by the curing of the cement.

A third point of interest is the behaviour of samples 7 and 8 with, respectively 4% and 2% dry weight of pyrite added. At the end of one week these samples show reduced strength compared to sample 6 (no remoulding, no pyrite). This is due to the action on the cement of sulphuric acid which is an oxidation product of pyrite (Gratten-Bellew and Eden, 1975). From Table A.4.4.d it can be seen that the Oakdale fine discard has a very low sulphur (and therefore pyrite) content. These vane tests are therefore of no immediate relevance to the situation at Oakdale, but where a high pyrite content is suspected it should be realised that cement addition may not yield the expected increase in strength.

Referring to Fig.4.26, it can be seen that early remoulding leads to a higher final strength, while progressively later remoulding leads to a progressively lower final strength. From the point of view of handleability a long standing time may be desirable, but the penalty is a lower final strength. The earlier the material can be handled the stronger the final product is, providing that no further remoulding occurs after emplacement on the tip. Two points should be emphasised, however. The first is that the physical remoulding carried out in the laboratory was very thorough, and represents a "worst case". Thus material handled after, say, 48 hours, may not be as weak as indicated by Fig.4.26, but will certainly be weaker than material handled immediately. Secondly, the sensitivity is much higher in the case of the early handled material; and could lead to a false sense of security.

#### 4.13 The Groundwater Chemistry of Tailings Lagoons

While much is known about acid mine drainage (Down and Stocks, 1977), relatively little work has been published on the groundwater chemistry of colliery tailings lagoons in the U.K. A considerable volume of water flows over or through lagoons, and often discharge is into a main drainage network; for instance lagoons 109A,B and C at East Hetton drain into the Kelloe Beck which ultimately discharges into the River Wear. Desiccation at the surface of lagoons raises the possibility that lagoon effluent could be highly acidic and rich with sulphates, due to the oxidation of the pyrite. Coal contains significant traces of heavy metals (Chatterjee and Pooley, 1977) and again these could be released into the groundwaters. Since the solid matter in lagoons is largely of very fine particle sizes, these processes will be enhanced, as they are related to the surface area of the particles.

A reconnaissance survey of the water chemistry of lagoons was therefore undertaken. Sixteen samples were gathered from three collieries (East Hetton, Gedling and Silverhill), the source of each sample being shown in Table 4.11. Each of the samples was analysed for pH and carbonates in the field, and for four trace metal cations (Cu, Ni, Co, Pb), four major cation (Na, K, Ca, Mg) and three anions ( $\text{SO}_4$ , Cl,  $\text{NO}_3$ ) in the laboratory. The methods employed and full results are outlined in Appendix A.4.6. It should be noted from the Appendix that the carbonate result (expressed as total alkali) is suspect, particularly for the samples from Silverhill colliery. The results are expressed graphically in Fig. 4.27.

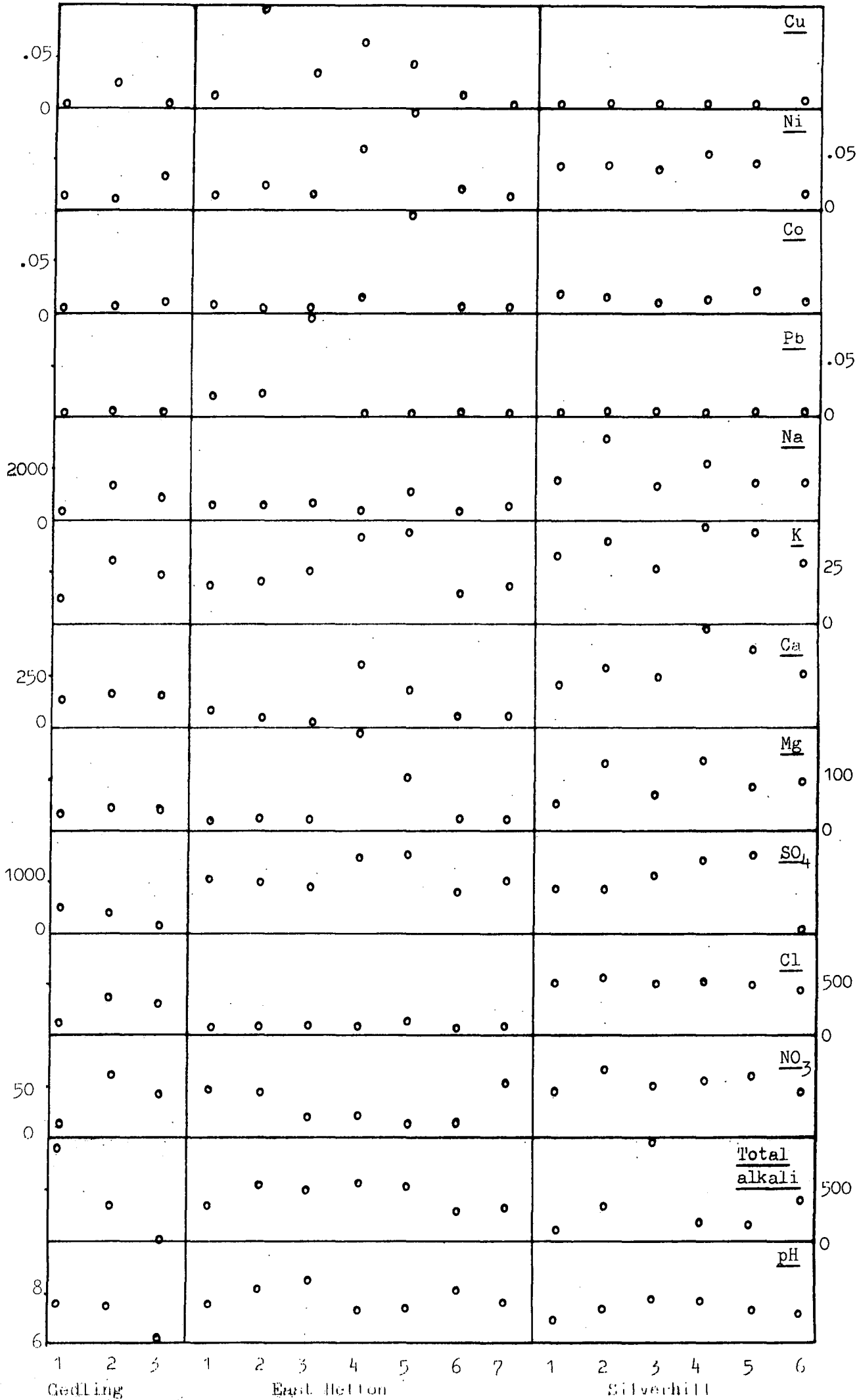
It is clear that the waters are not acid from tip (sample S5), lagoons or drainage outlets (Kelloe Beck, sample EH4). The lowest pH is 6.05 (sample G3); in contrast acid mine drainage often has a pH as low as

Table 4.11 The sources from which the groundwater samples were taken.

Sample	Description of source
Gedling	
1	Surface water, disused lagoon (no. 12)
2	Inlet water, active lagoon
3	Outlet water, active lagoon
East Hetton, lagoon 109B	
1	Inlet water
2	Outlet water
3	Piezometer, tip at 6m depth
4	Kelloe Beck, which runs in a culvert beneath the lagoon
5	Hole, dug into surface to a depth of 300mm
6	Supernatant water
7	Inlet, taken 1 hour after sample 1
Siverhill, lagoon 16	
1	Surface water / overtip seepage
2	Piezometer, tip at 3m depth
3	Outlet water
4	Surface water
5	Seepage from tip, discharge onto lagoon
6	Hole, dug into lagoon surface to a depth of 300mm

Fig.4.27 Groundwater chemistry of tailings lagoons.

All scales in mg/l except pH. Note variation in scales.



2.0 (Down and Stocks, op.cit., p.111). This could be due to the buffering \* capacity of the carbonate/bicarbonate system; sample G3 has the lowest total alkali (i.e. carbonate/Bicarbonate) concentration and also has the lowest pH; sample EH4 from Kelloe Beck has a slightly lower pH than other East Hetton samples, which could be due to a reduction in buffering capacity caused by dilution. However, it is also possible that anaerobic conditions in the lagoon prevents oxidation of the pyrite. The high levels of sulphate suggest that pyrite is in fact being oxidised in surface zones of the lagoon.

The three samples of supernatant water (G1, EH6 and S4) clearly are not like rainwater in composition (see Stevenson, 1968). In general their compositions are similar to the other samples, and for reconnaissance work samples of supernatant water may be adequate. Certainly, samples from seepage into shallow pits (EH5 and S6) would be adequate for reconnaissance.

The trace elements are present in very small amounts. However, each of the four elements is relatively abundant in a different East Hetton sample i.e. Cu in sample EH2, Ni and Co in EH5, and Pb in EH4. The reason for this is not known. Generally, however, the concentrations of copper and lead conform to the standards laid down by the World Health Organisation (Down and Stocks, 1977; cobalt and nickel are not quoted).

The major cations show more than the traces. The concentration of sodium is particularly high, being mostly 500 to 1000 mg/l; in the case of S2 it is as high as 3133 mg/l. Nicholls (1972) found concentrations of 1100-1300 mg/l in a lagoon at Markham Main colliery near Bolsover, Derbyshire, and between 1750 and 3400 mg/l in samples from the tip.

\* Footnote: A buffer is a chemical species that prevents a significant change in pH due to the addition of acid. The carbonate/bicarbonate system is such a species.

Except in the case of potassium, and also ignoring the Kelloe Beck sample (EH4) the major cations increase in concentration from East Hetton to Gedling, and Gedling to Silverhill. The waters of Kelloe Beck are different, probably because the beck is running through Magnesian Limestone country which has increased the calcium and magnesium concentration (the Magnesian Limestone contains much dolomite). It is interesting to note that potassium, unlike the other major cations, is as abundant at East Hetton as at Gedling and Silverhill. It will be recalled from section 4.6 that the potassium/sodium ratio, as determined by XRF analysis of the solid matter, was higher in the East Hetton samples than the Yorkshire and Nottinghamshire samples. Possibly, there is a casual relationship.

Turning to the anions, the sulphate concentrations are very high at East Hetton and Silverhill (about 1000mg/l), and lower at Gedling though still 160-510mg/l. Nicholls (1972) measured sulphate concentrations of 380-580 mg/l in the lagoon, but 2600-5500 mg/l on the tip. While the seepage from the tip at Silverhill (sample 55) did not have this concentration of sulphate, nevertheless it had the highest concentration (together with EH5) of any sample in the present suite. This might be evidence for more complete oxidation of the pyrite on the tip. The concentration in nearly all samples is above the acceptable level for drinking water (250mg/l, U.S.A. standard, Walton, 1970, p.457).

The chloride concentration is correlated to the sodium concentration, and is higher at Gedling and Silverhill. At these collieries the levels of up to 570 mg/l are above permissible levels (also 250 mg/l in the U.S.A.) Nicholls (1972) reports values of 2350-2750 mg/l in the lagoon and 1300-3000 mg/l in the tip at Markham Main colliery. Nicholls attributes drainage from this tip as being the cause of the pollution of Sandhall Beat public supply well by chlorides and increased hardness, which caused abandonment of

the well in 1932.

The nitrate concentration is again lower at East Hetton, and is near or above the permissible (U.S.A.) level of 45 mg/l. As explained in the Appendix A.4.6, the total alkali results are somewhat dubious.

The composition of these lagoon waters requires explanation. The high level of sulphates can reasonably be attributed to pyrite oxidation at the surface of the lagoon. The calcium, magnesium and total alkali (carbonate/bicarbonate) levels could result from the solution of ankerite which is a fairly abundant mineral (see section 4.6). The levels of sodium, potassium and chloride are not so readily explained, as leaching or breakdown of the minerals present is unlikely to lead to such high concentrations of these ions. (Except, in the case of potassium, a possible casual relationship of this type has been noted.)

Spears et al. (1970) have suggested that high concentrations of these ions in tips is due to the release of connate waters from the rocks when broken down at the surface. It is known that groundwaters in Coal Measures rocks are frequently highly saline, i.e. contain sodium, potassium and chloride ions (Downing and Howitt, 1969; Downing et al. 1970; Tate and Robertson, 1971). Frequently, they also contain high levels of sulphate (Downing et al., 1970), though this is proportionately less significant than the salinity. It is also known that deep mine waters may be saline with appreciable sulphate contents (Glover, 1973; Cairney and Frost, 1975). Minewaters are usually neutral in this country (Glover, 1973), acidity being more of a problem in the U.S.A. Glover also shows that acid minewaters are rich in sulphate from pyrite oxidation, but are not highly saline. As evidence for the connate origin of the groundwater chemistry of tips, Spears et al. (1970) compare the relative abundance of Na, K, Ca and Mg in their analysis to those presented by



Downing and Howitt (1969) for East Midlands Coal Measures sandstones. Table 4.12 compares the relative proportions of these ions in the present suite of samples with the same data from Spears et al. and Downing and Howitt. Despite being more dilute than the tip water, which itself is more dilute than the connate groundwater, the proportions of these cations is similar for all three sets of samples. (It should be noted that Table 4.12 ignores between sample variation.) That tip water, and more especially lagoon water, would be more dilute than the original groundwater is to be expected. The explanation that the chemistry derives from the groundwater is clearly plausible.

A further point of interest arises. The salinity of the lagoon waters increases from East Hetton via Gedling to Silverhill. The level of salinity in the lagoon at Markham Main Colliery is similar to that at Silverhill, which is close geographically. Downing and Howitt (1969) show that the groundwater salinity increases from the Nottingham area towards Doncaster, i.e. in the direction from Gedling to Silverhill. Although the salinity of the lagoon waters could be an accident of dilution at the washery, it is interesting to speculate that a regional trend in the groundwater has been preserved at the surface. Tip material has less contact with water at the surface than lagoon material and would thus be more likely to preserve regional groundwater trends. Again salinity increases from the tip at Silverhill (sample S5) to Yorkshire Main near Doncaster (Spears et al., 1970; see Table 4.12) which is again in the same sense as the regional groundwater trend.

Although this is only a preliminary survey, it is possible to draw a few conclusions. Acidity does not present a pollution problem, rather the salinity and sulphate rich nature of the waters is of concern. Rae (1977) also lists iron as an additional possible pollutant from minewaters

Table 4.12 Proportions of major cations by weight in the groundwaters of lagoons, tips and Coal Measures sandstones.

	Lagoons <sup>1</sup>	Tips <sup>2</sup>	Tips <sup>3</sup>	Coal Measures sandstones <sup>4</sup>
Ca	13	20	19	17
Mg	4	4	12	3
Na	81	74	68	79
K	2	2	1	1
Total Ca, Mg, Na, K by weight mg/l	1386	1962	3479	32086

1 Except EH4 (Kelloe Beck) and S5 (Siverhill tip).

2 S5.

3 Spears et al. (1970).

4 Spears et al. (1970), calculated from data in Downing and Howitt (1969).

in the Yorkshire region. In order to counter the pollution problem, dilution of these waters is necessary, and therefore it would be advantageous to discharge lagoon overflow waters into a river with as high a discharge as is possible in any locality. (Much lagoon water is in fact recycled to the washery, and is not a problem.)

Finally, it should be noted that further work on this aspect of lagoons would benefit from determining the total suspended solids concentration of surface or overflow waters, which is limited to 30 mg/l in Britain (Down and Stocks, 1977). The iron concentration and redox potential (Eh) should also be determined as these two have a bearing on pollution. The limited number of trace element determinations reported here are insufficient for positive conclusions to be drawn, though the concentrations measured are not of concern. There is much scope for extending the list of metals analysed, and relating the measurements to the metals in coal or the other minerals. These comments apply equally to lagoons, tips, minewaters or coal measures groundwaters.

#### 4.14 Conclusions

Colliery lagoons are layered sedimentary bodies. A beach area, with a low coal content but many rock fragments exists near the inlet. Away from the inlet layers vary from coarse-sands to silty-clays, and are fairly rich in coal. The proportion of finer-grained layers increases with distance from the inlet. In contrast, some lagoons are visually homogenous, notably those at Gedling colliery.

The high coal content renders XRD analysis, especially of the mixed-layer clay portion of illite, particularly difficult. Thermal oxidation at 350°C overestimates the organic carbon content, by driving off constituents other than carbon. XRF analysis of unburnt specimens is therefore strongly preferred and yields a more accurate estimation of organic carbon than does burning off organic carbon.

Three major geochemical groups are found, corresponding to those of Taylor (1974). The coal group, which includes pyrite is found more predominantly in the coarser grain sizes, though it occurs in finer-grained layers as well. The clay group includes illite, kaolinite and quartz; illite is most abundant, but kaolinite has a greater relative importance in northern coalfields. The illite composition is more sodic in the Yorkshire/Notts. coalfield than in the Northeast. The proportion of this group is inversely related to grain size and the abundance of the first group. Somewhat less abundant than the other two groups is the carbonate group, which includes a phosphatic mineral, possibly hydroxyapatite. This group is independent of grain size, and shows much less sorting than the other two groups.

The layered nature of lagoons, and the strong correlation of chemistry with grain size necessitates care when sampling to avoid bias. The distribution of grain types within the various size ranges also mitigates against efficient sorting at the washery. Consequently there is no difference in the structure or composition of lagoons fed by different types of washery. However, the size of the washery and volume of material handled may be more important (hence the uniform, non-layered lagoon at Gedling).

The high pyrite content of lagoon sediments could cause problems when cement stabilisation is undertaken, though more work is required to investigate this thoroughly. There could also be a problem with sulphur dioxide emission should fine discard ever be reclaimed on a large scale as a low grade fuel. However, this is likely to become more common with the advent of fluidised bed combustion, and sulphur emission is not a problem with this type of plant (Piper, 1977).

The pyrite content of lagoons does not lead to acid groundwaters draining

from the lagoon, though this could be due to buffering by the carbonate/bicarbonate system. Rather, the salinity and sulphate and nitrate concentrations are likely to be the main sources of pollution from lagoons. For reconnaissance studies, the supernatant waters, or just subsurface seepage water from lagoons provide adequate samples in terms of the general chemistry of lagoon waters. The sulphate content is likely to be due to pyrite oxidation, but the salinity may well be due to the original groundwater in the rock. It is possible that lagoon and tip waters reflect regional trends in the original groundwater.

## CHAPTER 5 THE SHEAR STRENGTH OF COLLIERY LAGOONS

### 5.1 Introduction

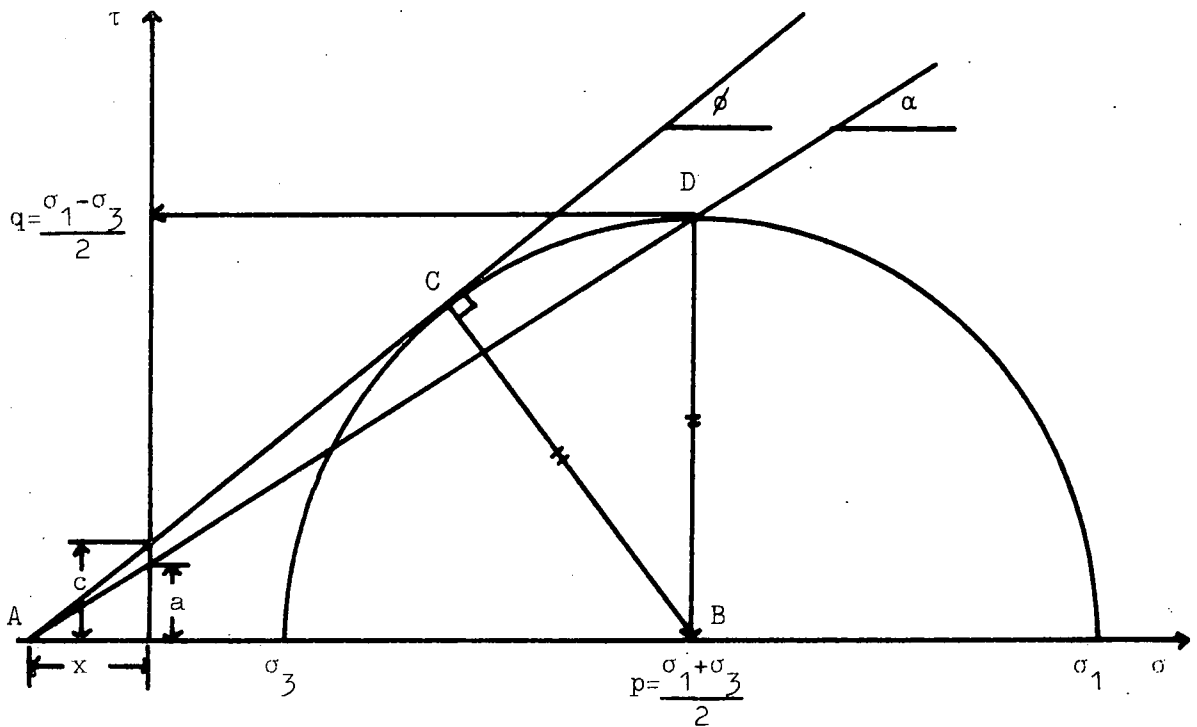
In chapters 3 and 4 it was concluded that lagoons are highly layered sedimentary bodies, in which the proportion of fines increases away from a beach area, and which contain a very high coal content. It is therefore to be expected that a marked anisotropy with respect to strength will be displayed. Furthermore it is known (Taylor, 1974) that the coal content of coarse colliery discard exercises a fundamental control on the angle of shearing resistance. In view of the high coal contents found in lagoons (chapter 4) this parameter is expected to be of importance.

In order to investigate the shear strength of lagoons with particular reference to the anisotropy, a study with field vanes and laboratory tests was carried out on Peckfield lagoon number 7. East Hetton lagoon 109B was similarly investigated but with the objective of assessing the performance of the cone penetration devices. Maltby lagoon 6 and Silverhill lagoon 16 were the sites chosen to study the performance of overtipping operations; again field and laboratory shear strengths were investigated. Finally a few reconnaissance tests were carried out on lagoon 6 at Orgreave Colliery; these are reported in Chapter 7.1.

### 5.2 A Note on Stress Paths

All the triaxial tests presented herein are shown in terms of the stress paths. The idea of stress paths arises from the desire to plot on one diagram a large number of Mohr circles, which would be somewhat confusing. With reference to Fig.5.1 it can be seen that the top point of a Mohr circle carries all the information that is contained in the complete circle, and it is therefore necessary to plot only this one point. However, it can also be seen that the axes of the diagram are redefined from the original  $\sigma, \tau$  axes to new  $p, q$  axes (where  $p = (\sigma_1 + \sigma_3)/2$  and  $q = (\sigma_1 - \sigma_3)/2$ ).

Fig.5.1 Definition of  $p, q$  point and the relation to  $c$  and  $\phi$ .



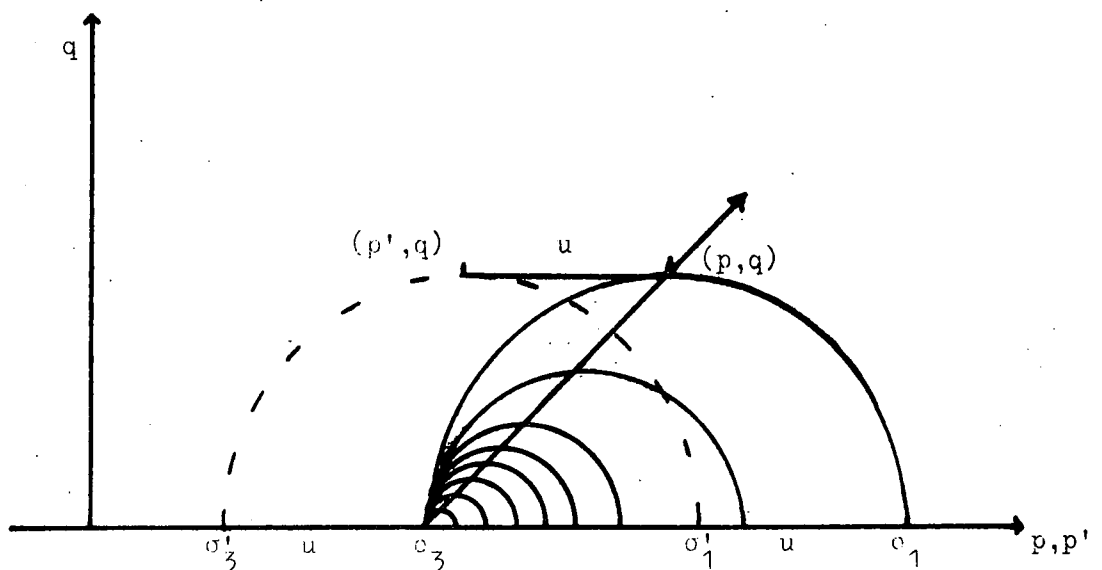
$$\sin\phi = \frac{CB}{AB} = \frac{DB}{AB} = \tan\alpha$$

$$\text{also, } \frac{c}{x} = \tan\phi, \quad \frac{a}{x} = \tan\alpha = \sin\phi$$

$$\text{hence, } x = \frac{c}{\tan\phi} = \frac{a}{\sin\phi}$$

$$c = a \cdot \frac{\tan\phi}{\sin\phi} = \frac{a}{\cos\phi}$$

Fig.5.2 Total stress paths and plot of the effective stress point.



Furthermore, the derivation of  $c$  and  $\phi$  have also changed slightly because of the redefined axes.

Plotting thus each Mohr circle as a single point allows the state of stress through which a sample passed at all stages of its history to be plotted in a very compact form. The curve joining all the  $p, q$  points that represent the history of a sample is known as a stress path. Both total and effective stresses may be plotted as stress paths. Figure 5.2 gives an example of the stress path for total stresses of a normal triaxial compression test ( $\sigma_3 = \text{const}$ ). In terms of effective stresses:-

$$p' = \frac{\sigma'_1 + \sigma'_3}{2} = \frac{\sigma_1 - u + \sigma_3 - u}{2} = \frac{\sigma_1 + \sigma_3}{2} - u$$

$$\text{i.e. } p' = p - u$$

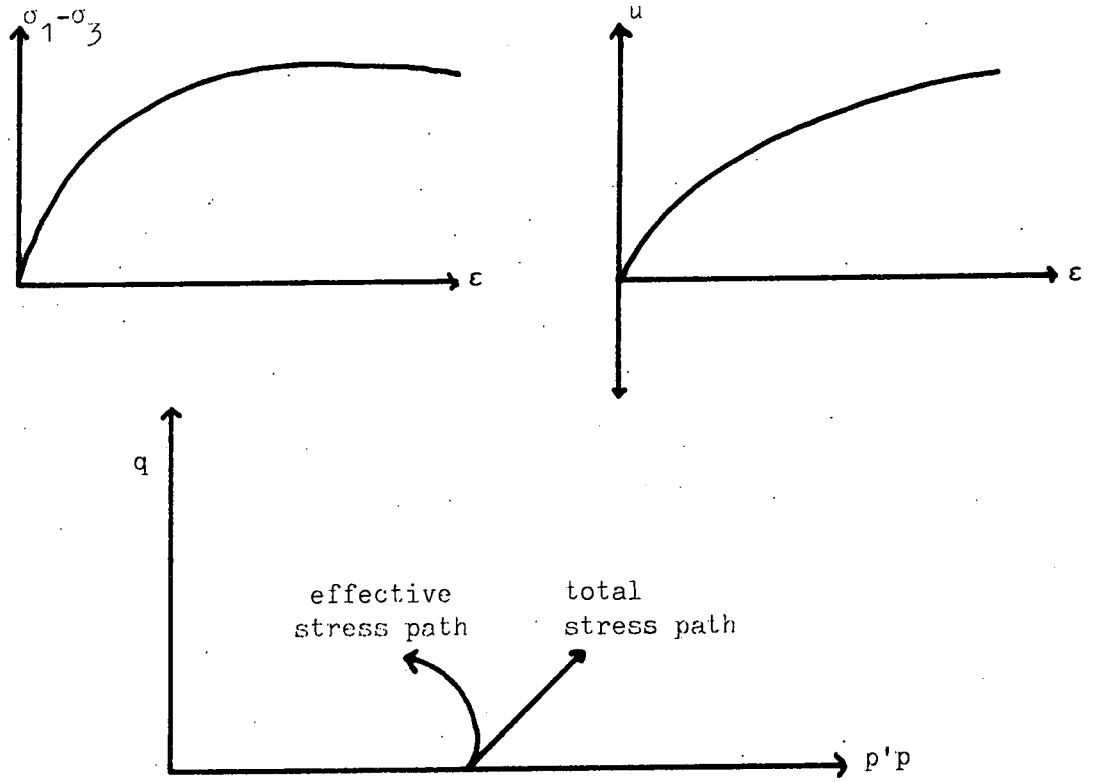
$$q' = \frac{\sigma'_1 - \sigma'_3}{2} = \frac{\sigma_1 - u - \sigma_3 + u}{2} = \frac{\sigma_1 - \sigma_3}{2}$$

$$\text{i.e. } q' = q$$

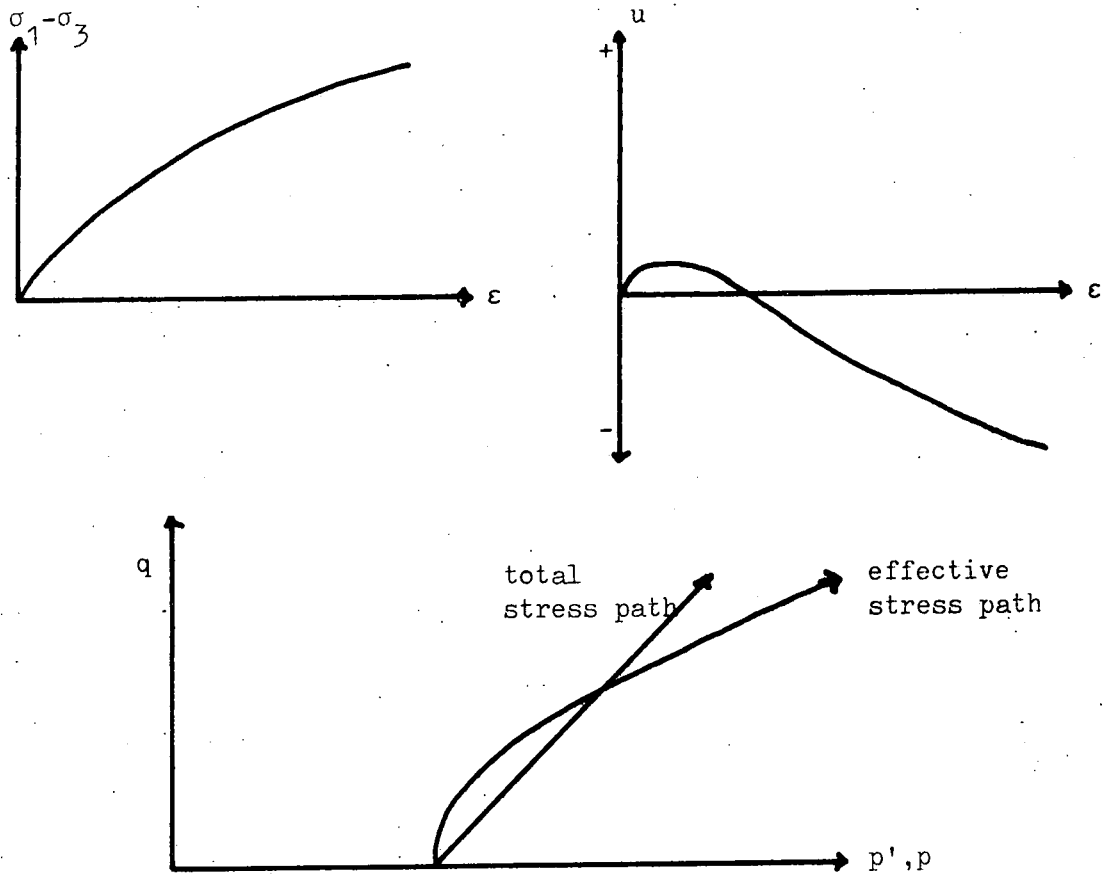
Effective stress paths are thus rapidly plotted by taking the magnitude of the pore-water pressure away from the total stress path, while keeping the value of  $q$  the same. This is shown in Fig.5.2. When the data for typical consolidated-undrained triaxial tests on loose- and dense-sands, or normally- and over-consolidated clays are plotted as effective stress paths, the difference between loose and dense states can be readily appreciated, as shown in Fig.5.3.a, b. In the figure plots of  $(\sigma_1 - \sigma_3)$  versus strain and pore pressure versus strain are shown for typical loose and dense materials, together with the form of the stress paths for each case. Loose sands can produce effective stress paths very similar to those of normally-consolidated clays, though they have to be very loose to do this.



Fig.5.3 Effective stress paths for loose and dense materials.



a. Loose sand or normally consolidated clay



b. Dense sand or overconsolidated clay

Interpretation of the angle of friction and hence cohesion on a total stress basis can be very difficult. Consider Fig.5.21.c which shows three stress paths on some fine material from East Hetton. Tests 2 and 3 failed at very similar effective stress values, but the failure points in terms of total stresses are very far removed from each other. It is not possible to plot a line through both of these points. This contradiction frequently occurs when both overconsolidated material and normally consolidated material is plotted on the same  $p, q$  graph. When there is a significant discrepancy, the failure envelope has been taken through the total stress failure points of the normally-consolidated materials only. In the case referred to above, the discrepancy was produced artificially, because the sample in test 2 was deliberately overconsolidated in the laboratory.

### 5.3 The Comparison of Field Vane Test Data and Laboratory Shear-Strength Envelopes

It was pointed out in Chapter 2.2.iii that a lack of knowledge concerning the exact state of in-situ stresses around the vane causes difficulties when relating vane-test data to laboratory shear strengths. However, on an empirical basis there is reason to believe that this may be possible. Cobb (1977) showed that the peak shear strength of colliery tailings frequently obeys the following relationship:-

$$\frac{c_u}{p'} = 0.3 \quad (c_u \text{ is the undrained vane shear strength, } p' \text{ is the effective overburden pressure)}$$

While the remoulded strength obeys:-

$$\frac{c}{p'} = 0.11 + 0.0037 \text{ PI} \quad (\text{PI is the plasticity index})$$

The former relationship was originally proposed by Terzaghi and Peck (1948), the latter by Skempton (1957).

Furthermore, it is possible that a relationship of the type:

$$\frac{c}{p'} = \tan \phi$$

may be obeyed. In order to evaluate whether or not vane test data obeys

these laws in the field it is only necessary to draw lines corresponding to these relationships on the depth versus vane shear strength plot and compare the two. However, certain complications arise. Over- or under-consolidated laminae within the sediment may obscure any trends, though it has been shown by Cobb that under favourable conditions these cases may be diagnosed. Furthermore, as was shown in Chapter 2.2.iii, and will be demonstrated again later in this chapter (section 5.4) coarse layers fail under effective stress conditions. Thus it is necessary to plot both:

$$\frac{c_d}{p'} = \tan \phi', \text{ and}$$

$$\frac{c}{p'} = \tan \phi.$$

Where  $c_d$  is the drained vane shear strength. There is apparently a contradiction in referring both the drained and the undrained strength to the effective overburden pressure. However, these relationships are empirical only, and the original definition was in terms of undrained strength and effective pressure (Skempton, 1948.a).

In order to assess the value of these relationships, four lines have been plotted on all the depth versus vane shear strength plots presented herein. They are:-

1.  $\frac{c}{p'} = .11 + .0037PI$ , where  $PI = 0$  (much fine colliery discard is non-plastic)
2.  $\frac{c}{p'} = 0.11 + 0.0037PI$  where  $PI = 15$ , a value which is towards the upper limit of  $PI$  for lagoon sediments.
3.  $\frac{c}{p'} = 0.3$  0.3 is also the tangent of 17 degrees, which is a reasonable though low value of friction (total stresses), hence this value will serve for both the second and third relationships.
4.  $\frac{c}{p'} = 1$  i.e.  $\tan 45$  degrees. This is towards the upper limit of the effective friction angle for colliery discard.

The values of the plasticity index, and friction angles are based on the various tests presented throughout the rest of this chapter. The overburden pressure is based on a bulk density of  $1.5 \text{ Mg/m}^3$ , again based on data from the rest of this chapter. When the position of the water table is known, the effective density is  $0.5 \text{ Mg/m}^3$ .

#### 5.4 The Investigation at Peckfield Colliery

The initial and most detailed investigation was carried out at Peckfield colliery. This site was chosen because lagoon no.7 was to be excavated in September 1977, and it was hoped to observe the structure of the lagoon directly. Unfortunately, field circumstances mitigated against this; the weak nature of the deposits precluded monitoring of free-standing faces.

The investigation into lagoon 7 involved both field vane tests and sampling for laboratory testing. The  $H = 2D$  and  $H = D/3$  vane combination was chosen to investigate the shear strength anisotropy because of its previous use for this purpose by Blight, (1971). Initially, tests were performed at the six locations shown in Fig.5.4. The variability of the sediments is apparent from the results, tabulated in Appendix A.5.1 and shown in Fig.5.5. Generally, the strength decreases into the lagoon (e.g. trend 1 - 4 and 5 - 4) and increases with depth. It is possible that the occasional very strong layers in profiles 1,2 and 5 are desiccation surfaces, and these are more frequent near to the beach. The R values\* shown in Fig.5.5.c show very little except the variation in the original data.

In order to obtain a more detailed picture, further tests were carried out at locations 1 and 4, and called 1A and 2A for distinction. At each

\* Note:  $R = \frac{S_v}{S_h}$ . The method of computing R from vane data is outlined in Appendix 2.2.

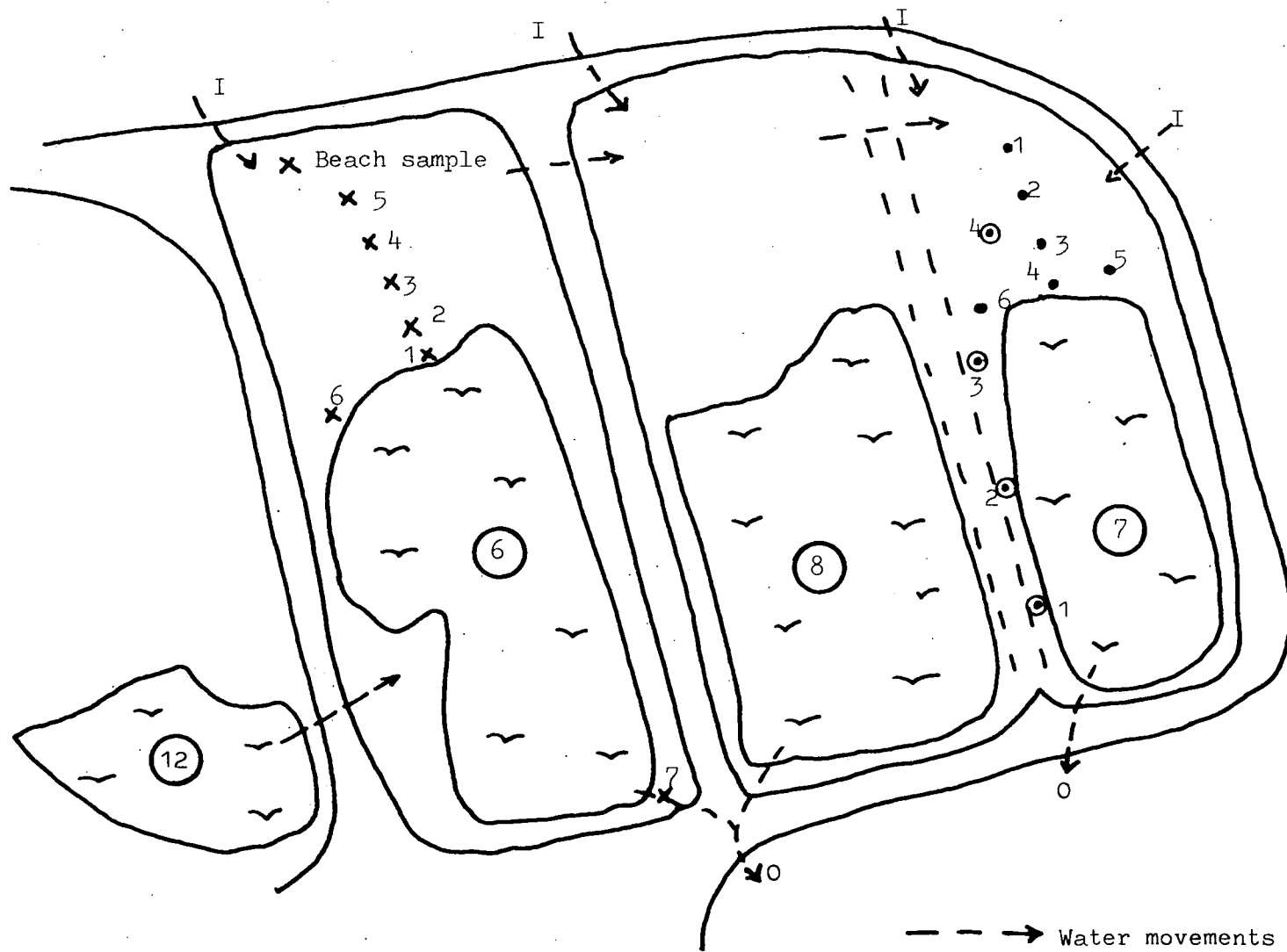








Fig.5.4 Peckfield, site layout.

-  Standing water
-  Vane testing site
-  Box sample location (samples PL1-4)
-  Sampling site, for Chap.4
-  Water movements
- I inlet
- O outlet
-  Lagoon number

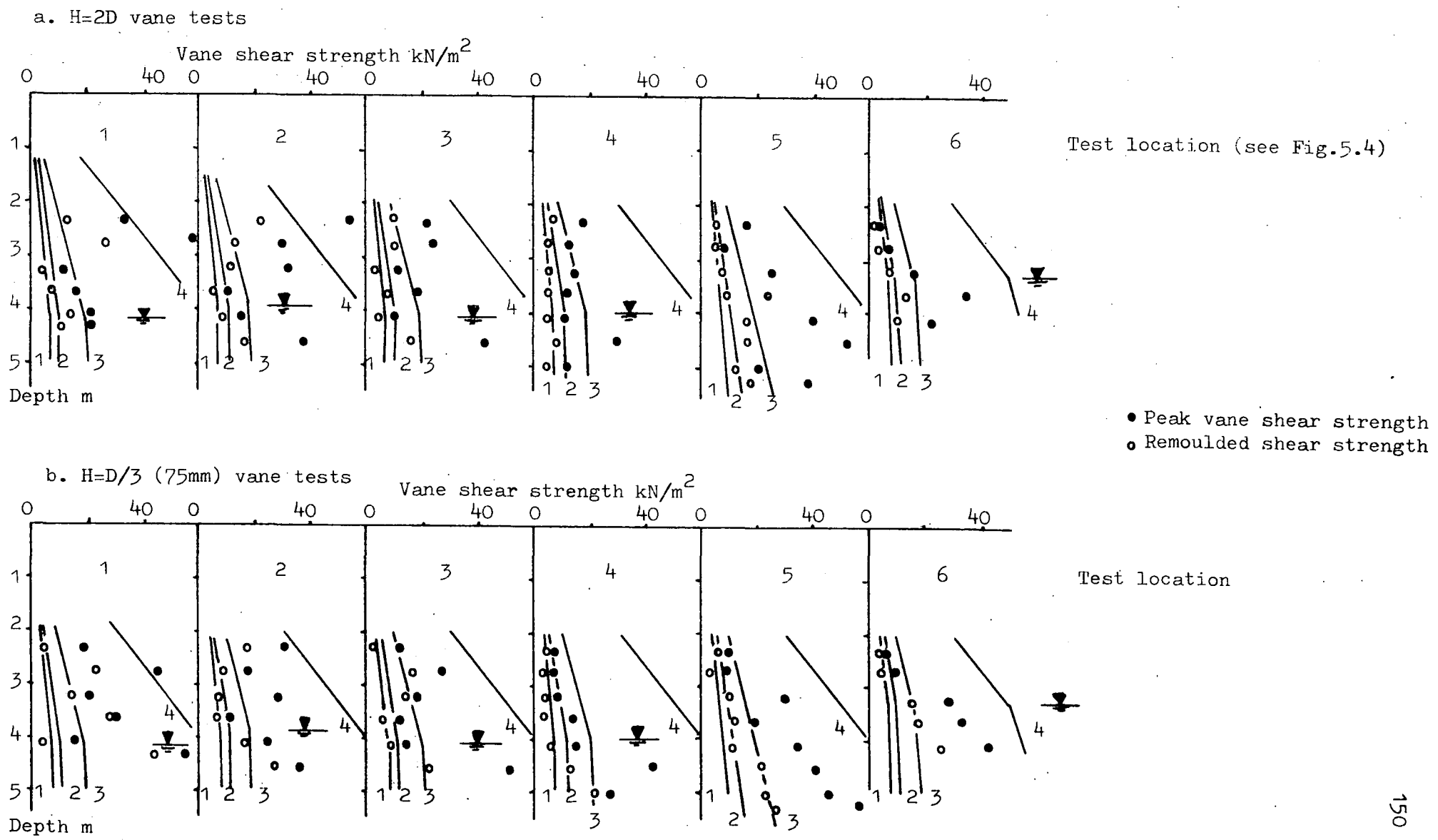
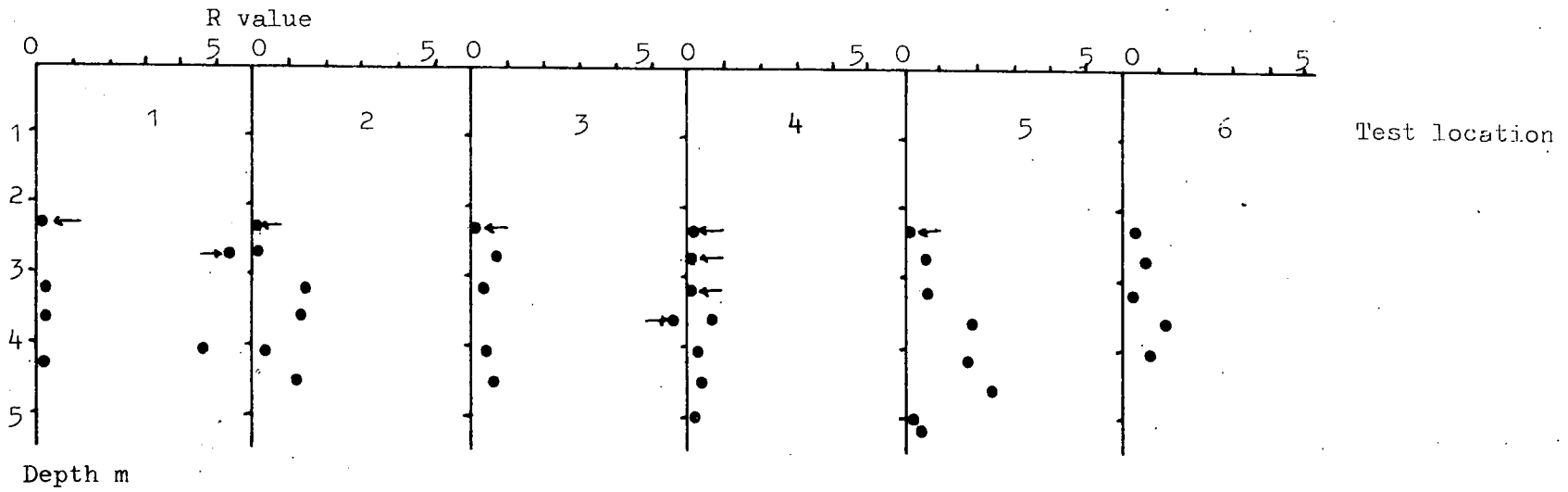


Fig.5.5 First series of vane tests in lagoon 7 at Peckfield.

c. R values



← Indicates a value of less than 0 or greater than 6

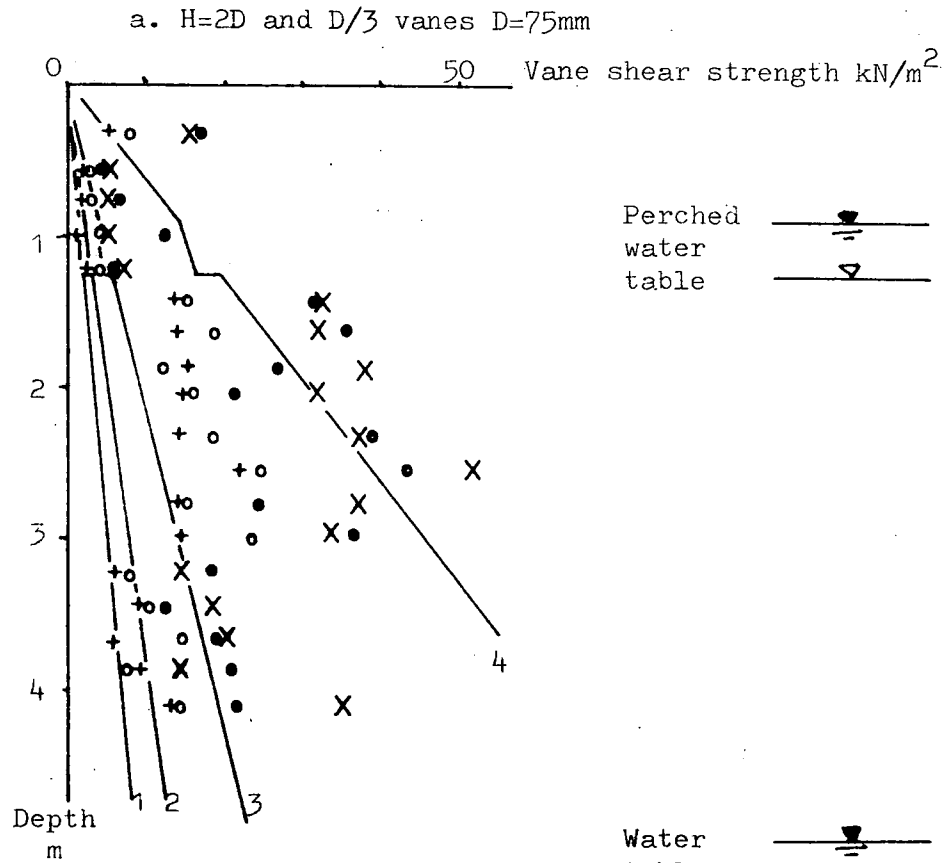
site, profiles were established using the same vanes. As described in chapter 2, inspection of the R values for these profiles led to a further series of tests being conducted at these two locations using vanes of similar heights. A vane with  $H = D/3$  and a diamond vane were used with  $D = 150\text{mm}$ , the diameter being changed from consideration of the sensitivity of the torsion head. It can be seen from Figs.5.6 and 5.7 (see also Table A.5.1) that the shear strength in each profile is extremely variable. Beneath a desiccated crust is a very weak layer. This in turn overlies a much stronger layer at between 1.5 and 3 metres depth, this layer being thicker in profile 1A. The material is then much weaker again. Profile 1A was stopped at just over 4m depth as the sediments were too strong to penetrate; profile 2A was continued to the base of the lagoon. The sediments at location 1A are both stronger and more variable than those at 2A, confirming the earlier series of tests.

The  $c/p'$  relationships are shown by lines 1 to 4 on Figs 5.5, 5.6 and 5.7. Trends are much more clearly depicted by the more detailed profiles at locations 1A and 2A (Figs.5.6 and 5.7) and it can be seen that the stronger material at 1.5 to 3 metres depth conforms approximately to the drained strength relationship, while the weaker layers above and below are better explained in terms of the undrained strength law (i.e.  $\frac{c}{p'} = 0.3 = \tan 17 \text{ degrees}$ ). In the case of the weaker layers the remoulded strength is close to relationships 1 and 2 (representing plasticity indices of 0 and 15 respectively). However, the variation in the data is such that it cannot be stated that either one of these lines is a better fit. In contrast, it is clear that the stronger sediments at 1.5 to 3 metres depth display remoulded strengths well above either of these lines. In both profiles the desiccated crust does not conform to any trend; it is not expected that it should.

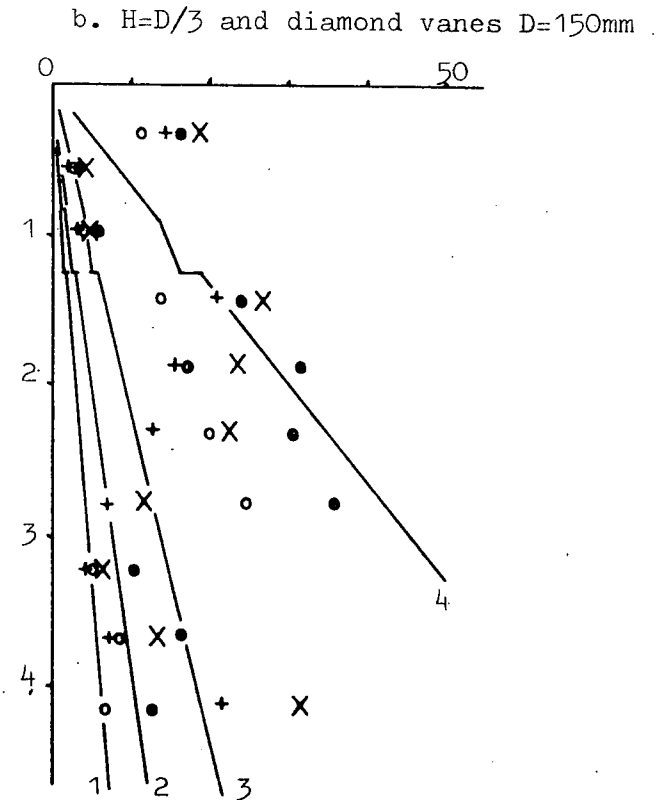
The R values for these two profiles are shown in Fig.5.8. As



Fig.5.6 Vane shear tests at location 1A, lagoon 7, Peckfield.



- X  $H=2D$  vane, peak strength
- + " " remoulded strength
- $H=D/3$  vane, peak strength
- " " remoulded strength

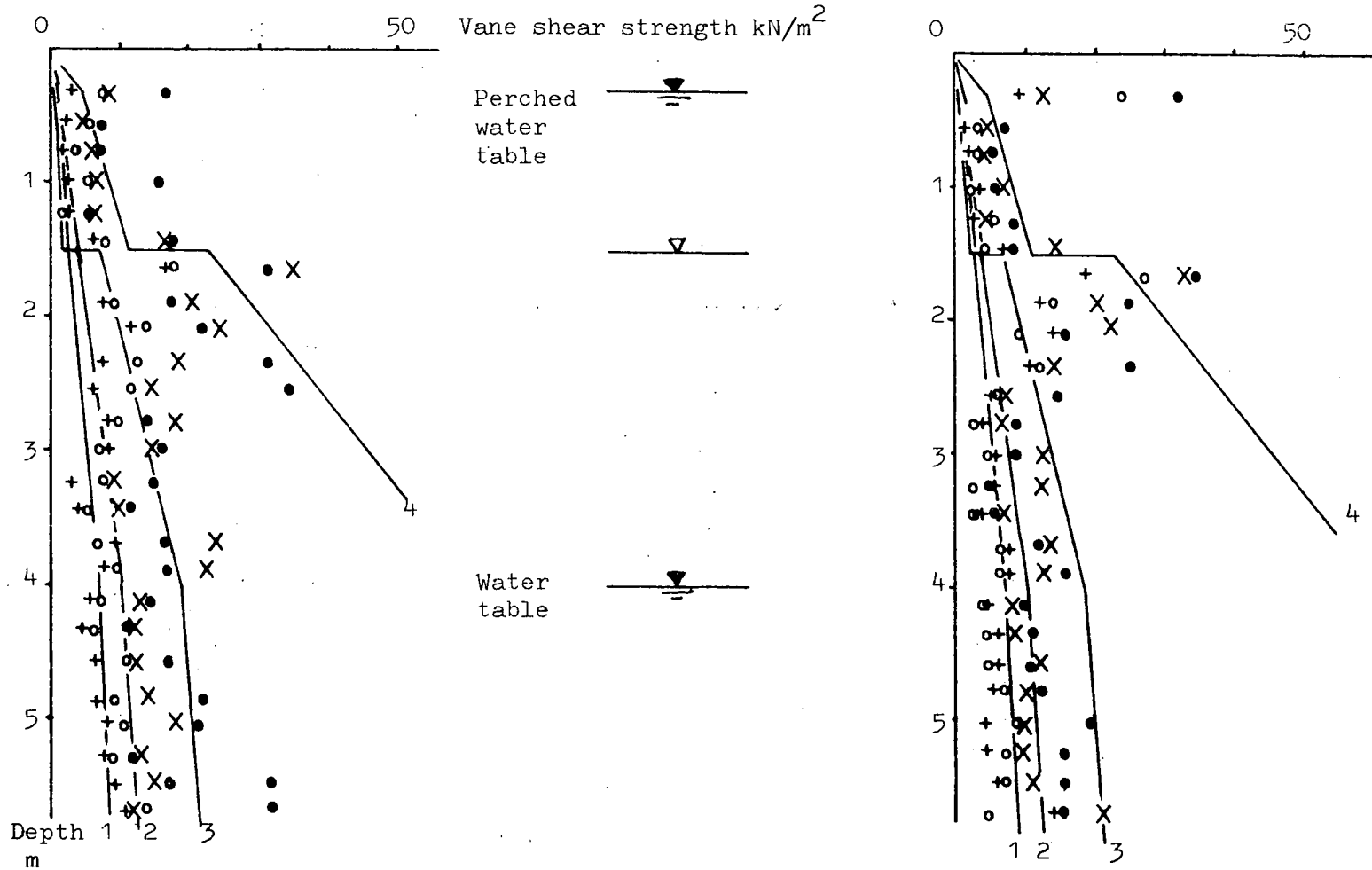


- X Diamond vane, peak strength
- + " " remoulded strength
- $H=D/3$  vane, peak strength
- " " remoulded strength

Fig.5.7 Vane shear tests at location 2A, lagoon 7, Peckfield.

a. H=2D and D/3 vanes D=75mm

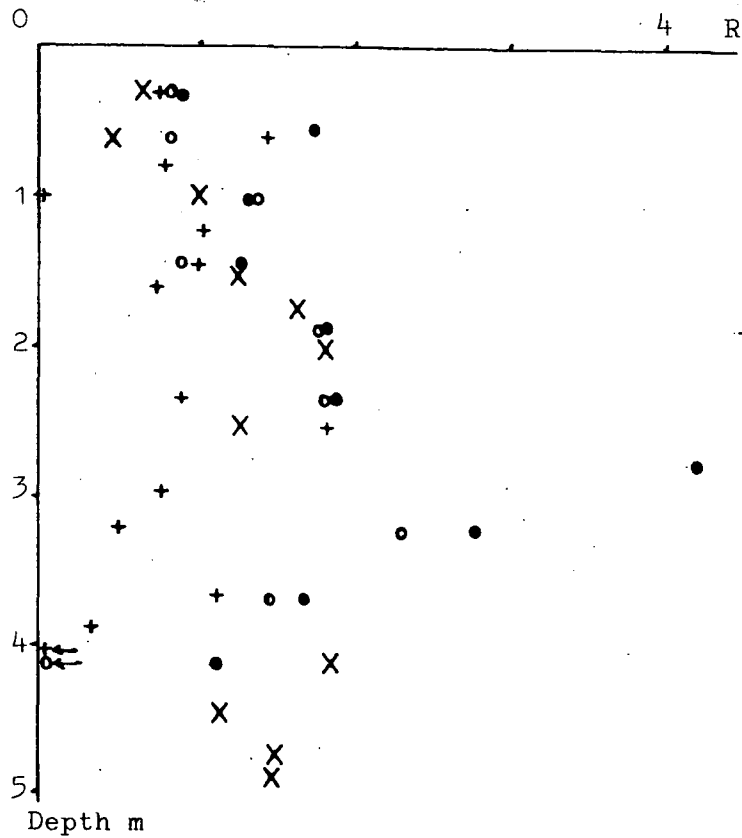
b. H=D/3 and diamond vanes D=150mm



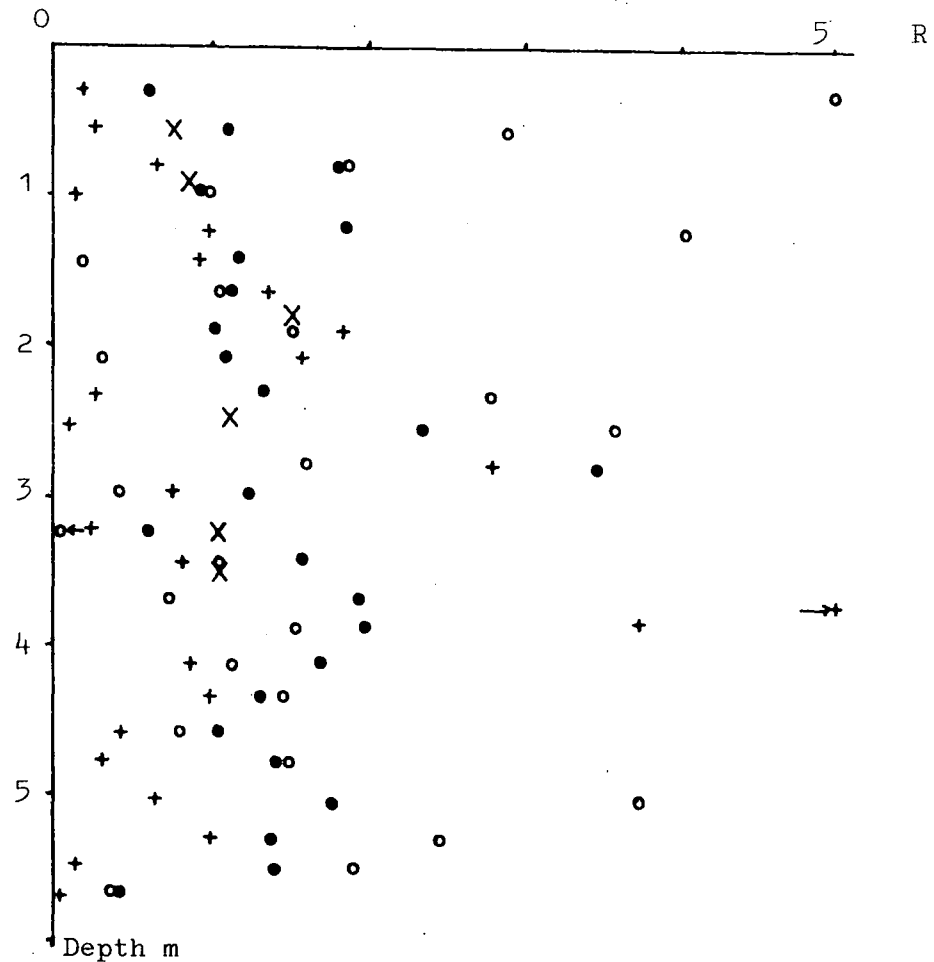
Explanation of symbols as for Fig.5.6

Fig.5.8 R values at locations 1A and 2A, lagoon 7, Peckfield.

a. Location 1A



b. Location 2A



- X Shear box tests
- + H=2D and D/3 vanes
- H=2D and diamond vanes
- o D/3 and diamond vanes

↔ Indicates a value of greater than 5 or less than 0

described in chapter 2, the profiles from the first two pairs are extremely variable, but when combined for pair 4 the profiles can be explained. The average R value is 1.56 for the two profiles, and this reflects a slightly greater strength in a vertical direction (across laminae) compared to a horizontal direction (along laminae). The particularly high R values at 2.76 m in each profile are due to a weak layer being sheared by the diamond vane while the H=2D vane was affected by the stronger sediments above and below. This high R value ( $\approx 4$ ) reflects the state of the deposit as a whole at this depth, i.e. it is very much weaker along a horizontal plane than in a vertical direction.

U100 samples were recovered at these two locations from most of the depths for which the vane shear strength is known. On cutting, these samples revealed a highly layered structure. This layered structure was also revealed by excavation (see Fig.4.20, chapter 4). Quick shear-box tests were performed on samples out from the U100's in both a vertical and horizontal orientation with respect to the original ground surface. A few tests were also conducted at 14 degrees to compare with the diamond vane. The tests were carried out with porous stones (i.e. drainage permitted) but at a strain rate equivalent to that of the field vane tests, the object being to model the field condition. The fastest available strain rate on the shear boxes was 1.22mm/min; which is a little under a half that of the smallest diameter vane turning at 6 degrees/minute. Hence this rate was adopted throughout. Average degrees of consolidation at failure can be deduced using the relationship of Gibson and Henkel (1954):-

$$U_c = 1 - \frac{h^2}{t_f \cdot c_v}$$

where  $U_c$  is the average degree of consolidation at failure

$h$  is the drainage path length

$t_f$  is the time to failure

$c_v$  is the coefficient of consolidation

From Table 5.1 it can be seen that a truly undrained condition was not achieved. In contrast it was shown in chapter 2 (Table 2.1) that in the finer material with a low  $c_v$ , very little drainage would occur, though for the coarser material conditions should be similar (i.e. both tests are drained). These tests were carried out by Van der Merwe (1977, Tables 7.1 and 7.2). He showed that very low angles of friction were recorded for some layers, indicating undrained conditions, while other layers show friction angles as high as 48 degrees, indicating that drainage is taking place. It is clear, therefore, that the vane shear test is measuring the drained strength of the coarser material, but the undrained strength of the finer material. Taylor and Cobb (1977), drew attention to this point.

Based on this argument, the shear strength of the sediment at various depths within the lagoon has been calculated according to:

either  $s = c + \sigma \tan \phi$  if  $PI \geq 9$  (i.e. an undrained strength based on total stresses).

or  $s = c' + \sigma' \tan \phi'$  if non-plastic (i.e. a drained strength based on effective stresses).

The various parameters were derived from the laboratory shear strength tests, and density measurements and index tests which are discussed below (see Table 5.3.). The laboratory shear strength has been calculated both for the horizontal and vertical mode. The strength profiles so obtained for locations 1A and 2A look very like the vane test profiles as a comparison of Fig.5.9 with Figs.5.6 and 5.7 shows. However, the correlation between the field vane shear strength profiles and the laboratory calculated shear strength profiles is only significant (at the 95% confidence level) for the  $H=2D$  and  $H=D/3$  ( $D=75\text{mm}$ ) vanes. In other words the profiles in Figs.5.6.a and 5.7.a correlate with those in Fig.5.9.a and 6, while the profiles in Figs.5.6.b and 5.7.b do not.

Table 5.1 Degree of consolidation during shear box testing.

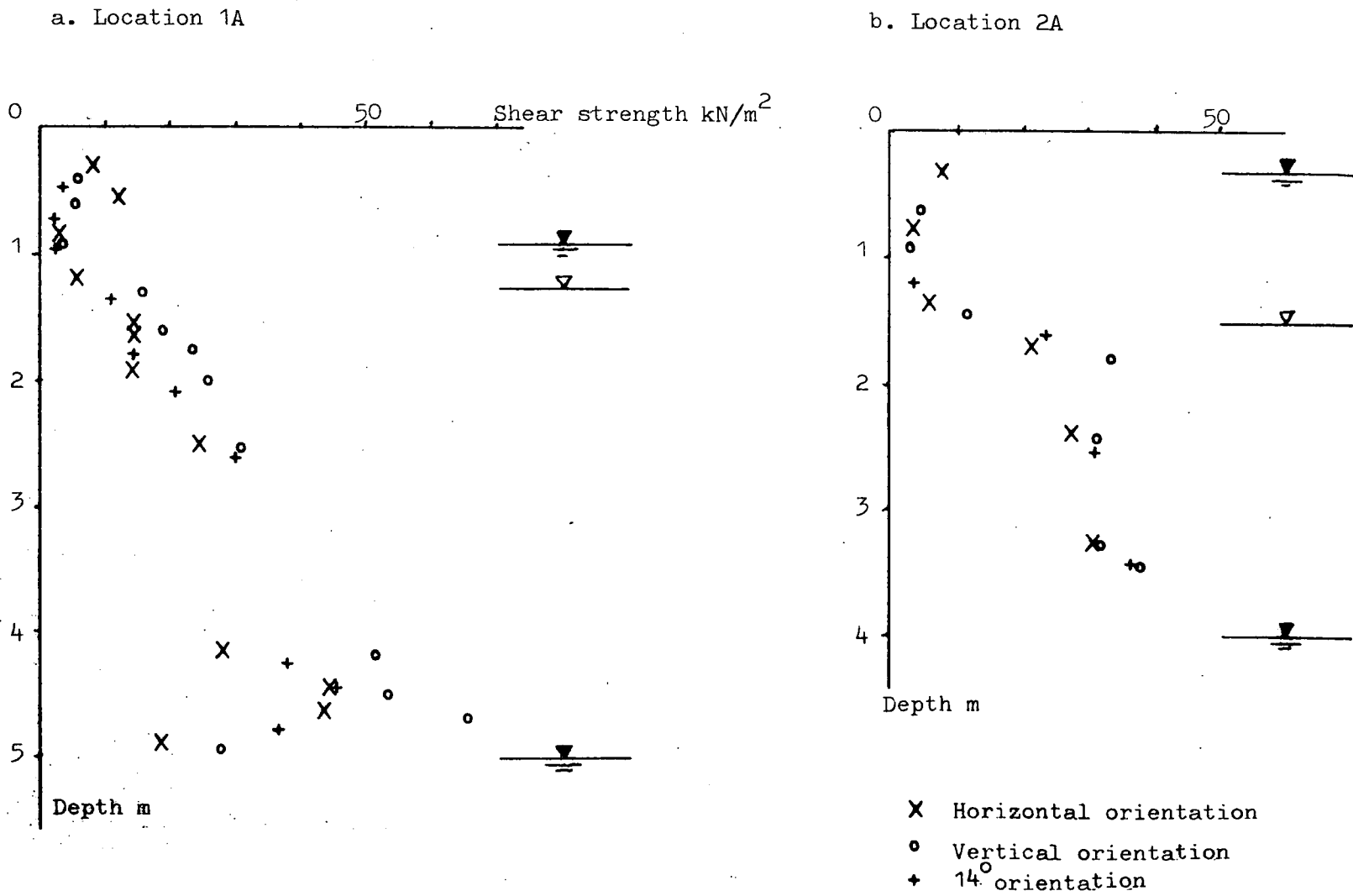
Values of  $U_c$  for shear box tests calculated from:

$$U_c = 1 - \frac{h^2}{t_f \cdot c_v} \quad (\text{Gibson and Henkel, 1954})$$

$c_v$	$t_f^*$	$U_c$
6	7.5 (fast)	0.416
6	70 (slow)	0.937
2000	7.5	0.99+
2000	70	0.99+

\* values of  $t_f$  are average values based on observations during the testing programme.

Fig.5.9 Shear box strength profiles for locations 1A and 2A, lagoon 7, Peckfield.



The shear-box test results from the two different orientations can be utilised to derive R values by:

$$R = \frac{c + \sigma \tan \phi \text{ (vertical cut)}}{c + \sigma \tan \phi \text{ (horizontal cut)}}$$

(using total or effective stress parameters as appropriate). The R values so obtained have been superimposed on Fig. 5.8, and fall in a similar range to the R values obtained from the pair 4 combination of vanes. The average of these R values is 1.20 compared to the average of the vane R values (combination 4) of 1.56. The shear-box tests thus confirm that the strength of lagoon sediments is a little greater across laminae than it is along the laminae.

In addition to the laboratory shear strength tests, various other parameters were determined. It can be seen from Fig.5.10 that the Peckfield sediments vary from clayey-silts to silty-sands. Figures 5.11 and 5.12 show that the natural moisture content is nearly always higher than the liquid limit and is highest below the perched or natural water tables. The moisture content, plasticity index and bulk density are highest in those layers that gave low vane shear strengths, and fall in the strong layer at 2 to 3 metres depth. The organic carbon content and median sediment size show the inverse of this relationship. It was shown in Chapter 4 (Figs.4.5b and 4.6.b) that the organic carbon content and grading of lagoon sediments are interdependent.

The values obtained from all the field and laboratory tests are grouped together in Table 5.2, which forms the raw data for a correlation program. Due to the presence of empty spaces in the table, a correlation program was used that gave both the coefficient and the number of pairs in the correlation. The output of the program<sup>me</sup> is shown in Table 5.3. The following statistically significant correlations may be drawn from the table, (these repeat some of the visual observations outlined above



Fig.5.10 Range of grading curves for lagoon 7, Peckfield.

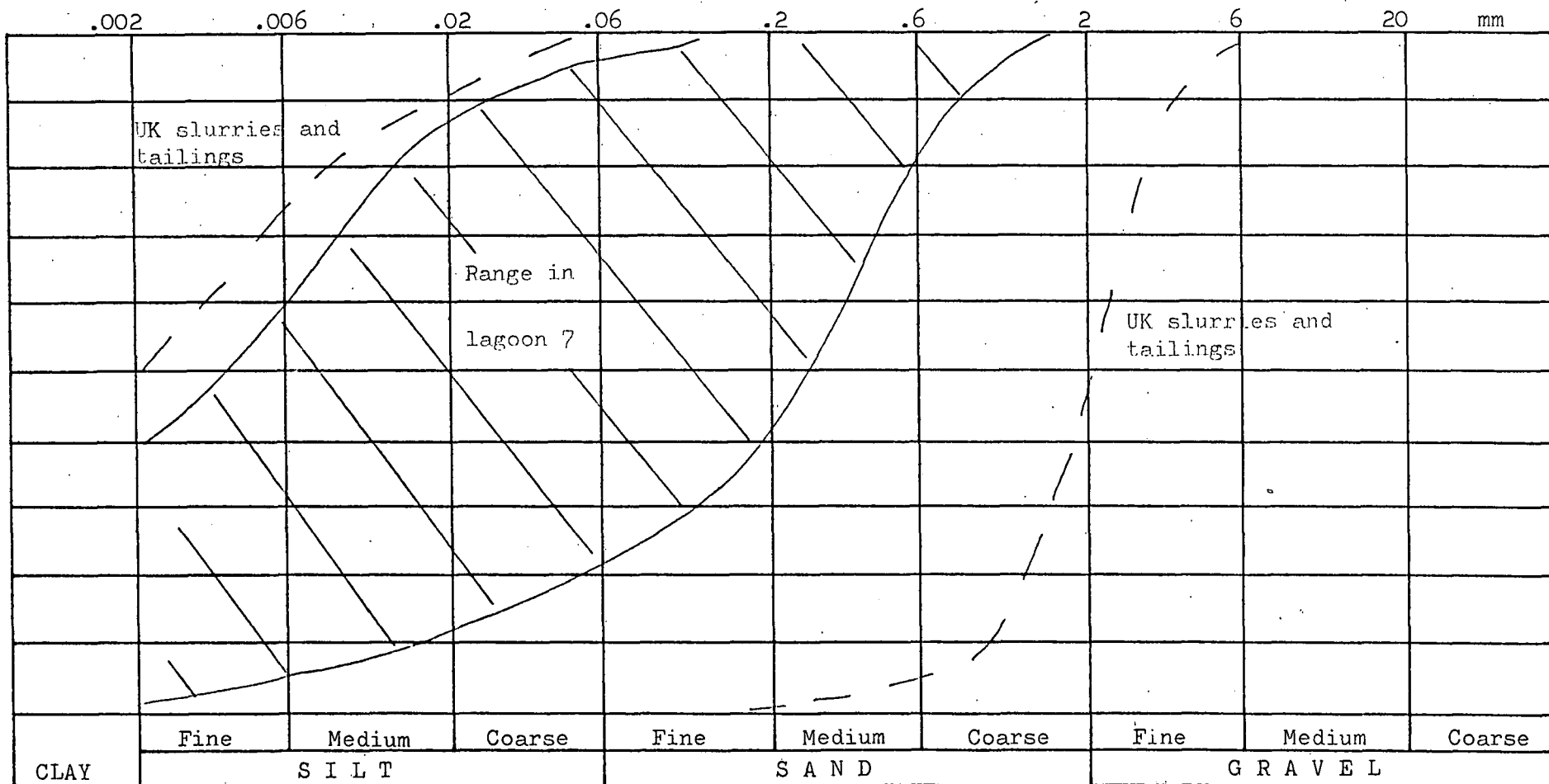


Fig. 5.11 Index parameters, profile 1A, Peckfield lagoon 7.

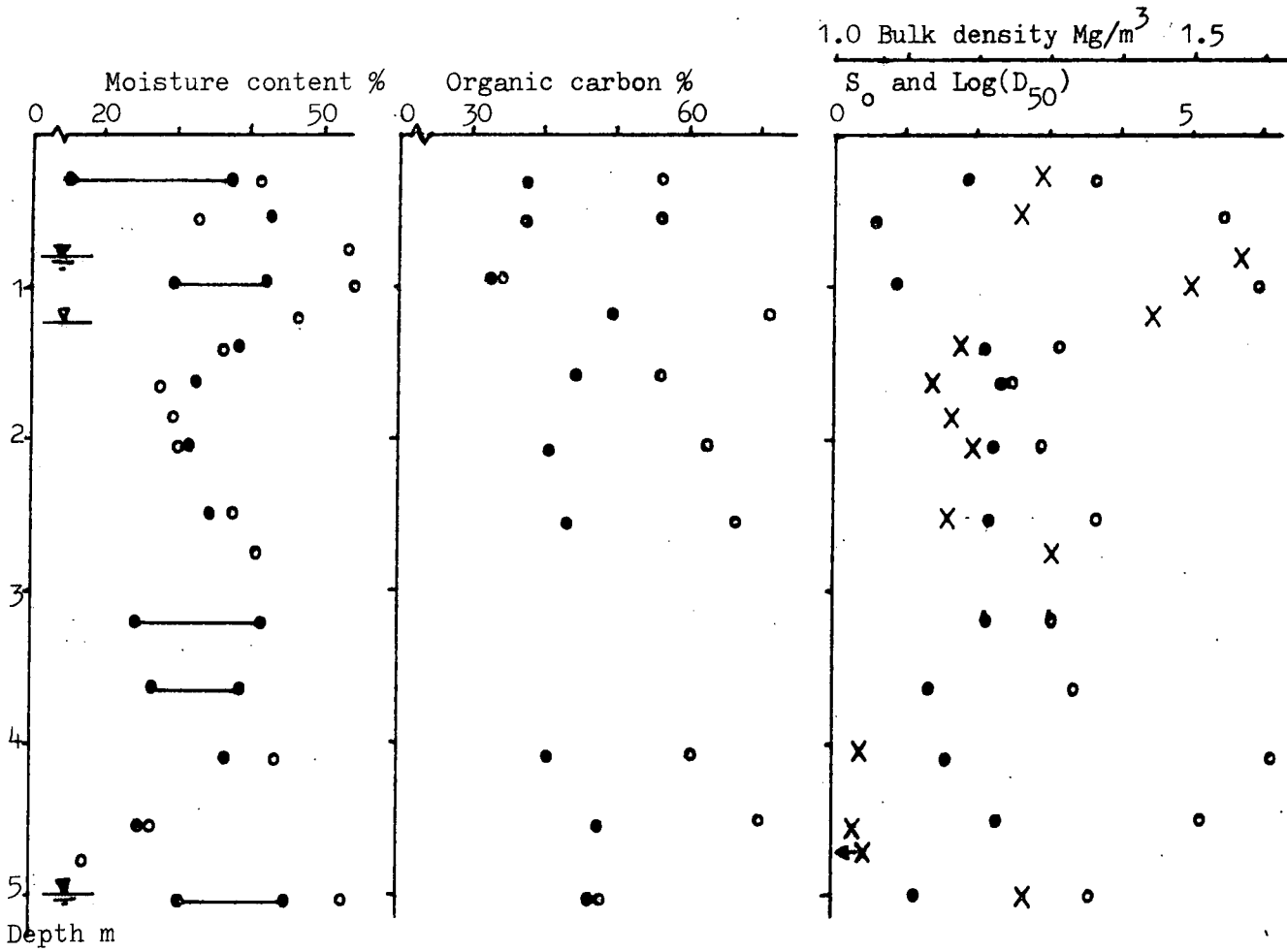
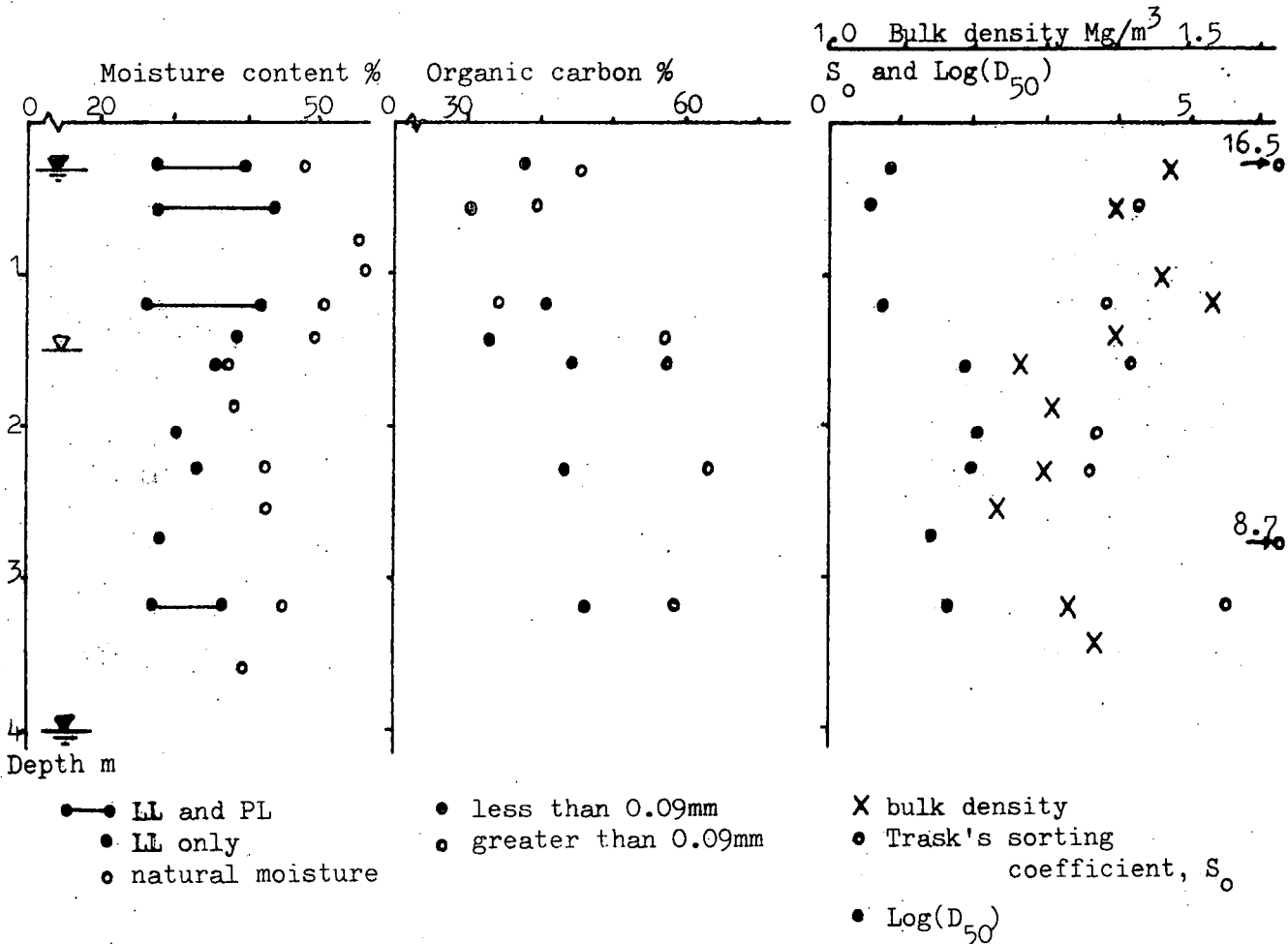


Fig. 5.12 Index parameters, profile 2, Peckfield lagoon 7.



EXPLANATION OF SYMBOLS USED IN TABLES 5.2 AND 5.3

SYMBOL	EXPLANATION
DEP.	DEPTH
S2D	STRENGTH OF 2D VANE
SD/3	" " D/3(75MM) "
R23	R VALUE FROM 2D AND D/3 VANE
SG	SPECIFIC GRAVITY
SO	TRASKS SORTING COEFFICIENT
RHOD	DRY DENSITY
RHOW	BULK DENSITY
M	MOISTURE CONTENT
E	VOIDS RATIO
PHIE	EQUIVALENT ANGLE OF FRICTION(C=0)
LL	LIQUID LIMIT
SDI	STRENGTH OF DIAMOND VANE
RD3	R VALUE FROM DIAMOND AND D/3(150MM) VANE
PL	PLASTIC LIMIT
PI	PLASTICITY INDEX
SEN2	SENSITIVITY OF 2D VANE
SEN3	" " D/3(75MM) "
SEND	" " DIAMOND "
SEN3	" " D/3(150MM) "
C<90	CARBON CONTENT OF LESS THAN 90 MICRON FRACTION
C>90	" " " GREATER " " " "
SD/3	STRENGTH OF D/3(150MM) VANE
LD50	LCG( MEDIAN SIZE)
LI	LIQUIDITY INDEX
R2D	R VALUE FROM 2D AND DIAMOND VANE
QTZ TO DOL	MINERALS IN PERCENTAGE ABUNDANCE, I.e. QUARTZ, ILLITE, KAOLINITE, PYRITE, DOLOMITE
SI TO P	ELEMENTS IN PERCENTAGE ABUNDANCE

	DEP	S20	SD/3	R23	SG	SO	RHOD	RHOW	M
1	0.300	15.021	16.483	0.770	1.823	3.708	0.910	1.287	42.250
2	0.550	5.490	4.900	1.433	2.051	5.477	0.940	1.259	33.370
3	0.770	5.731	6.237	0.787	---	---	1.020	1.573	54.360
4	0.990	5.429	12.251	0.125	2.140	5.916	0.970	1.497	55.090
5	1.210	7.239	7.128	1.049	---	---	0.980	1.444	47.770
6	1.430	32.575	32.297	1.026	1.676	3.215	0.860	1.195	37.820
7	1.630	31.972	35.639	0.733	1.803	2.433	0.850	1.138	27.760
8	1.860	37.643	26.723	4.508	---	---	0.850	1.166	30.560
9	2.070	31.731	21.383	7.394	1.759	2.944	0.920	1.200	31.703
10	2.310	37.643	33.979	.904	---	---	---	---	---
11	2.530	51.879	43.434	1.840	1.695	3.667	0.850	1.163	34.750
12	2.760	36.919	24.501	8.997	---	---	0.930	1.310	41.610
13	2.970	34.480	36.752	0.769	---	---	---	---	---
14	3.210	14.478	18.710	0.507	2.108	3.102	---	---	---
15	3.430	18.640	12.251	10.411	---	---	---	---	---
16	3.660	20.209	19.378	1.137	2.003	3.420	---	---	---
17	3.870	14.176	20.715	0.377	---	---	---	---	---
18	4.110	34.687	21.160	---	1.739	6.085	0.720	1.038	44.780
19	4.560	---	---	---	1.675	5.145	0.820	1.032	26.540
20	4.770	---	---	---	---	5.145	0.660	0.773	17.550
21	5.010	---	---	---	1.892	3.606	0.820	1.265	53.340
22	0.330	8.455	16.928	0.174	1.956	16.492	0.930	1.468	48.610
23	0.550	4.524	7.795	0.254	2.274	4.539	---	---	---
24	0.770	6.332	6.905	0.688	---	---	0.890	1.404	56.900
25	0.990	6.696	16.037	0.104	---	---	0.530	1.458	57.530
26	1.210	6.636	6.682	0.980	2.134	3.964	1.020	1.536	51.250
27	1.430	16.438	16.705	0.939	---	---	0.930	1.403	50.950
28	1.630	34.506	31.183	1.393	1.741	4.243	0.920	1.270	38.250
29	1.860	20.571	17.151	1.872	---	---	0.940	1.307	39.500
30	2.070	24.311	21.160	1.502	1.855	3.790	---	---	---
31	2.310	18.097	30.069	0.247	1.695	3.732	0.910	1.301	43.320
32	2.530	14.176	34.524	0.099	---	---	0.870	1.236	42.940
33	2.760	17.494	13.364	2.820	1.727	8.660	---	---	---
34	2.970	14.478	16.037	0.750	---	---	---	---	---
35	3.210	8.144	14.478	0.235	1.761	5.547	0.920	1.330	45.260
36	3.430	9.350	10.023	0.320	---	---	0.980	1.372	40.240
37	3.660	23.527	16.037	6.507	---	---	---	---	---
38	3.870	22.018	16.037	3.754	---	---	---	---	---
39	4.110	12.367	12.919	0.881	---	---	---	---	---
40	4.330	11.160	11.137	1.007	---	---	---	---	---
41	4.560	12.065	15.705	0.429	---	---	---	---	---
42	4.770	13.132	21.160	0.310	---	---	---	---	---
43	5.010	17.796	23.715	0.659	---	---	---	---	---
44	5.220	12.367	12.215	1.029	---	---	---	---	---
45	5.460	14.599	31.183	0.146	---	---	---	---	---
45	5.670	10.255	31.183	0.038	---	---	---	---	---

Table 5.2 Physical and chemical data correlated in Table 5.3

	E	PHIE	LL	SDI	RD3	PL	PI	SEN2	SEN3
1	1.002	40.000	37.000	12.585	0.806	---	---	2.730	2.000
2	1.180	40.000	43.000	3.512	0.918	16.000	27.000	2.270	2.200
3	1.098	15.000	---	---	---	---	---	2.710	2.330
4	1.206	8.000	43.000	4.273	1.368	30.000	13.000	3.100	2.200
5	1.179	21.000	---	---	---	---	---	2.670	1.780
6	0.949	35.000	40.000	14.165	0.869	---	---	2.350	2.160
7	1.031	39.000	33.000	---	---	---	---	2.200	1.880
8	1.020	42.000	---	20.018	1.792	---	---	2.430	2.180
9	0.912	42.000	32.000	---	---	---	---	2.150	1.370
10	---	---	---	22.242	1.809	---	---	2.600	2.080
11	0.995	49.000	35.000	---	---	---	---	2.350	1.770
12	0.823	46.000	---	11.531	6.989	---	---	2.470	1.770
13	---	---	---	---	---	---	---	2.310	1.570
14	---	---	42.000	6.322	2.313	26.000	17.000	2.220	2.330
15	---	---	---	---	---	---	---	2.060	1.220
16	---	---	39.000	13.170	1.475	27.000	120.000	3.190	1.210
17	---	---	---	---	---	---	---	1.440	2.660
18	1.410	39.000	37.000	31.315	-0.189	---	---	2.630	1.590
19	1.045	44.000	25.000	---	---	---	---	---	---
20	1.530	33.000	---	---	---	---	---	---	---
21	1.295	25.000	45.000	---	---	31.000	14.000	---	---
22	0.970	35.000	40.000	12.585	4.962	28.000	12.000	2.800	2.000
23	---	13.000	---	4.165	2.969	---	---	1.920	1.290
24	11.529	9.000	44.000	3.689	1.368	29.000	16.000	3.330	1.940
25	1.448	7.000	---	7.024	0.940	---	---	2.520	2.480
26	1.098	10.000	42.000	3.980	4.038	27.000	14.000	2.290	2.310
27	1.282	16.000	40.000	14.165	0.186	30.000	10.000	2.560	2.080
28	0.892	45.000	36.000	32.485	1.122	---	---	2.120	1.710
29	0.852	53.000	---	20.019	1.525	---	---	2.690	1.830
30	---	---	31.000	22.652	0.303	---	---	2.120	1.530
31	0.865	43.000	34.000	14.393	3.536	---	---	2.500	2.360
32	0.948	43.000	---	6.965	3.586	---	---	2.350	3.100
33	---	---	29.000	6.322	1.597	---	---	2.120	1.670
34	0.921	35.000	37.000	12.116	0.421	---	---	3.330	2.250
35	0.803	39.000	---	12.233	-0.169	28.000	9.000	2.700	1.970
36	---	---	---	6.322	1.073	---	---	2.210	2.050
37	---	---	---	13.521	0.723	---	---	2.600	2.570
38	---	---	---	12.526	1.555	---	---	2.920	1.890
39	---	---	---	8.017	1.123	---	---	2.410	1.930
40	---	---	---	8.833	1.489	---	---	2.800	2.000
41	---	---	---	11.531	0.810	---	---	2.000	1.503
42	---	---	---	9.951	1.495	---	---	2.210	2.210
43	---	---	---	9.190	3.729	---	---	2.270	2.060
44	---	---	---	9.482	2.456	---	---	1.710	1.570
45	---	---	---	10.946	1.932	---	---	1.570	1.560
45	---	---	---	20.311	0.449	---	---	1.000	2.250

Table 5.2 cont.

	SEND	SEN3	C<99	C>90	SD /3	LC50	LI	R2D	QT2
1	1.230	1.460	37.900	59.200	16.700	1.900		0.776	2.000
2	1.810	2.740	35.900	45.800	3.200	0.600	63.000	1.719	4.000
3									
4	1.330	2.250	29.200	33.500	5.010	0.950	192.000	1.338	5.000
5									
6	1.320	1.840	43.300	71.100	24.730	2.150		0.776	2.000
7			45.000	59.200		2.400			6.000
8	1.460	1.940			31.600			1.800	
9			44.000	66.200		2.260			2.000
10	1.760	1.540			30.490			1.892	
11			46.700	71.900		2.180			5.000
12	1.640	1.700			35.780			4.202	
13									
14	1.440	1.670			10.020	2.150		2.741	
15									
16	1.740	1.930			16.090	1.390		1.681	
17									
18	1.470	1.870	41.000	60.700	12.110	1.600		1.133	3.000
19			49.200	74.700		2.300			4.000
20									
21			47.000	48.000		1.150			5.000
22	1.370	1.290	38.400	48.200	32.020	0.850	167.000	0.606	4.000
23	2.220	1.770	32.700	29.600	7.520	0.600		1.109	6.000
24	2.030	1.950			5.150		175	1.816	
25	1.940	2.210			6.820			0.943	
26	1.650	1.770	30.900	35.400	8.910	0.780	171.000	1.858	5.000
27	1.320	1.840			8.350		210.000	1.191	
28	1.730	1.260	44.800	62.200	34.390	1.950		1.076	7.000
29	1.630	1.770			24.920			1.034	
30	1.540	1.630			14.760	2.000		1.090	
31	1.340	2.060	44.000	68.000	25.480	2.000		1.320	3.000
32	1.350	2.080			14.480			2.370	
33	1.660	3.350			9.070	1.420		3.478	
34	2.270	2.000			8.630			1.242	
35	1.440	1.670	46.400	63.200	4.870	1.650	189.000	0.600	5.000
36	1.960	1.960			6.540			1.607	
37	1.760	1.650			11.690			1.957	
38	1.790	2.400			15.730			1.981	
39	1.830	2.260			8.490			1.691	
40	1.480	2.290			10.260			1.328	
41	1.970	2.510			10.470			1.057	
42	1.950	1.790			12.250			1.427	
43	2.010	2.340			19.570			2.229	
44	2.250	2.070			15.590			1.381	
45	2.030	2.180			15.590			1.419	
46	1.310	3.190			14.760			0.414	

Table 5.2 cont

	ILL	KAO	PYR	DOL	SI	AL	FE	MG	CA
1	30.000	12.000	2.000	1.000	30.000	15.000	5.000	0.980	1.500
2	38.000	11.000	1.000		36.000	19.000	4.400	1.120	1.300
3									
4	48.000	9.000			39.000	20.000	3.900	1.210	1.000
5									
6	32.000	6.000	3.000		26.000	12.000	7.400	0.740	1.300
7	33.000	5.000	4.000	4.000	27.000	13.000	8.900	0.930	2.600
8									
9	37.000	5.000	3.000	1.000	26.000	12.000	9.100	0.830	2.400
10									
11	35.000	6.000	2.000	1.000	26.000	11.000	8.300	0.830	2.000
12									
13									
14									
15									
16									
17									
18	39.000	8.000	3.000		32.000	14.000	6.100	1.200	2.300
19	23.000	6.000	2.000	5.000	22.000	11.000	7.200	0.750	1.800
20									
21	34.000	10.000	4.000	2.000	33.000	16.000	5.100	1.230	1.500
22	45.000	12.000	1.000		36.000	18.000	3.800	1.120	1.100
23	53.000	14.000	1.000		44.000	22.000	2.900	1.250	0.900
24									
25									
26	38.000	14.000	1.000		44.000	22.000	2.700	1.240	1.000
27									
28	22.000	10.000	4.000	3.000	29.000	14.000	8.700	0.970	2.100
29									
30									
31	35.000	6.000	2.000		29.000	14.000	7.200	0.920	1.600
32									
33									
34	32.000	9.000	2.000	1.000	31.000	14.000	6.600	1.070	1.500
35									
36									
37									
38									
39									
40									
41									
42									
43									
44									
45									

Table 5.2 cont.

	NA	K	TI	S	P
1	0.340	3.200	0.880	3.100	0.084
2	0.320	3.600	0.900	2.500	0.089
3	-----	-----	-----	-----	-----
4	0.330	3.800	0.910	1.800	0.097
5	-----	-----	-----	-----	-----
6	0.350	2.500	0.700	4.500	0.108
7	0.350	2.700	0.700	5.200	0.113
8	-----	-----	-----	-----	-----
9	0.330	2.500	0.720	5.600	0.113
10	-----	-----	-----	-----	-----
11	0.290	2.500	0.720	5.200	0.115
12	-----	-----	-----	-----	-----
13	-----	-----	-----	-----	-----
14	-----	-----	-----	-----	-----
15	-----	-----	-----	-----	-----
16	-----	-----	-----	-----	-----
17	-----	-----	-----	-----	-----
18	0.340	3.000	0.800	3.400	0.134
19	0.360	2.300	0.710	4.700	0.117
20	-----	-----	-----	-----	-----
21	0.300	3.300	0.790	2.500	0.123
22	0.360	3.700	0.910	2.200	0.088
23	0.370	3.900	0.920	1.300	0.076
24	-----	-----	-----	-----	-----
25	-----	-----	-----	-----	-----
26	0.400	3.900	0.930	1.500	0.080
27	-----	-----	-----	-----	-----
28	0.340	2.700	0.710	5.000	0.107
29	-----	-----	-----	-----	-----
30	-----	-----	-----	-----	-----
31	0.360	2.800	0.730	4.300	0.121
32	-----	-----	-----	-----	-----
33	-----	-----	-----	-----	-----
34	0.350	3.000	0.750	3.700	0.116
35	-----	-----	-----	-----	-----
36	-----	-----	-----	-----	-----
37	-----	-----	-----	-----	-----
38	-----	-----	-----	-----	-----
39	-----	-----	-----	-----	-----
40	-----	-----	-----	-----	-----
41	-----	-----	-----	-----	-----
42	-----	-----	-----	-----	-----
43	-----	-----	-----	-----	-----
44	-----	-----	-----	-----	-----
45	-----	-----	-----	-----	-----

Table 5.2 cont.

	DEP	S2D	SD/3	R23	SG	SO	RHOD	RHC#	M
DEP	1.000	0.059 43	0.184 43	-0.032 42	-0.377 23	-0.211 21	-0.812 26	-0.653 26	-0.359 26
S2D	0.0	1.000	0.751 43	0.280 42	-0.703 13	-0.338 18	-0.595 23	-0.771 23	-0.671 23
SD/3	0.0	0.0	1.000	0.303 42	-0.693 13	-0.290 18	-0.574 23	-0.687 23	-0.550 23
R23	0.0	0.0	0.0	1.000	-0.328 17	-0.177 17	-0.042 22	-0.337 22	-0.418 21
SG	0.0	0.0	0.0	0.0	1.000	0.074 20	0.535 15	0.754 15	0.548 15
SO	0.0	0.0	0.0	0.0	0.0	1.000	0.267 16	0.255 16	0.268 16
RHOD	0.0	0.0	0.0	0.0	0.0	0.0	1.000	0.897 26	0.812 26
RHOW	0.0	0.0	0.0	0.0	0.0	0.0	0.0	1.000	0.000
M	0.0	0.0	0.0	0.0	0.0	0.0	0.0	0.0	1.000
E	0.0	0.0	0.0	0.0	0.0	0.0	0.0	0.0	0.0
PHIE	0.0	0.0	0.0	0.0	0.0	0.0	0.0	0.0	0.0
LL	0.0	0.0	0.0	0.0	0.0	0.0	0.0	0.0	0.0
SDI	0.0	0.0	0.0	0.0	0.0	0.0	0.0	0.0	0.0
RD3	0.0	0.0	0.0	0.0	0.0	0.0	0.0	0.0	0.0
PL	0.0	0.0	0.0	0.0	0.0	0.0	0.0	0.0	0.0
PI	0.0	0.0	0.0	0.0	0.0	0.0	0.0	0.0	0.0
SEN2	0.0	0.0	0.0	0.0	0.0	0.0	0.0	0.0	0.0
SEN3	0.0	0.0	0.0	0.0	0.0	0.0	0.0	0.0	0.0
SEND	0.0	0.0	0.0	0.0	0.0	0.0	0.0	0.0	0.0
SEN3	0.0	0.0	0.0	0.0	0.0	0.0	0.0	0.0	0.0
C<90	0.0	0.0	0.0	0.0	0.0	0.0	0.0	0.0	0.0
C>90	0.0	0.0	0.0	0.0	0.0	0.0	0.0	0.0	0.0
SD/3	0.0	0.0	0.0	0.0	0.0	0.0	0.0	0.0	0.0
LD50	0.0	0.0	0.0	0.0	0.0	0.0	0.0	0.0	0.0
LI	0.0	0.0	0.0	0.0	0.0	0.0	0.0	0.0	0.0
R20	0.0	0.0	0.0	0.0	0.0	0.0	0.0	0.0	0.0
QTZ	0.0	0.0	0.0	0.0	0.0	0.0	0.0	0.0	0.0
ILL	0.0	0.0	0.0	0.0	0.0	0.0	0.0	0.0	0.0
KAO	0.0	0.0	0.0	0.0	0.0	0.0	0.0	0.0	0.0
PYR	0.0	0.0	0.0	0.0	0.0	0.0	0.0	0.0	0.0
DOL	0.0	0.0	0.0	0.0	0.0	0.0	0.0	0.0	0.0
SI	0.0	0.0	0.0	0.0	0.0	0.0	0.0	0.0	0.0
AL	0.0	0.0	0.0	0.0	0.0	0.0	0.0	0.0	0.0
FE	0.0	0.0	0.0	0.0	0.0	0.0	0.0	0.0	0.0
MG	0.0	0.0	0.0	0.0	0.0	0.0	0.0	0.0	0.0
CA	0.0	0.0	0.0	0.0	0.0	0.0	0.0	0.0	0.0
NA	0.0	0.0	0.0	0.0	0.0	0.0	0.0	0.0	0.0
K	0.0	0.0	0.0	0.0	0.0	0.0	0.0	0.0	0.0
TI	0.0	0.0	0.0	0.0	0.0	0.0	0.0	0.0	0.0
S	0.0	0.0	0.0	0.0	0.0	0.0	0.0	0.0	0.0
P	0.0	0.0	0.0	0.0	0.0	0.0	0.0	0.0	0.0

Table 5.3 Correlation of the physical and chemical data from Lagoon 7 at Peckfield.

Significance levels • 99.9% • 99% +95%

First number represents product moment correlation coefficient, second number represents the number of pairs of data correlated.

	E	PHIE	LL	SDI	RD3	PL	PI	SEN2	SEN3
DEP	0.197 26	0.368 27	-0.283 21	0.119 35	-0.118 35	0.312 10	0.319 10	-0.425 43	-0.081 43
S2D	-0.160 23	0.658 24	-0.543 19	0.737 35	0.044 35	0.212 9	0.646 9	-0.024 43	0.250 43
SD/3	-0.197 23	0.626 24	-0.486 19	0.590 35	0.098 35	0.450 9	0.346 9	-0.256 43	0.082 43
R23	-0.031 22	0.373 23	-0.486 18	0.288 34	0.003 34	-0.026 9	0.450 9	0.070 42	0.035 42
SG	0.401 15	-0.235 16	0.683 19	0.629 15	0.395 15	-0.231 8	0.056 8	0.052 19	0.069 19
SO	0.020 16	0.053 17	0.042 19	-0.059 15	0.435 15	0.061 8	-0.261 8	0.255 18	0.061 18
RHOD	0.199 26	-0.303 26	0.292 17	-0.577 18	0.279 18	-0.264 8	0.030 8	0.022 23	0.211 23
RHOW	0.102 26	-0.574 26	0.652 17	0.634 19	0.278 13	0.384 8	-0.421 8	0.420 23	0.316 23
M	-0.032 26	-0.702 26	0.769 17	-0.403 18	0.039 18	0.903 8	-0.631 8	0.659 23	0.323 23
E	1.000	0.035 26	0.335 17	-0.192 18	-0.115 19	0.141 8	0.127 8	-0.231 23	0.002 23
PHIE	0.0	1.000	-0.680 17	0.552 17	0.094 19	-0.560 8	0.300 8	-0.335 24	-0.553 24
LL	0.0	0.0	1.000	0.0	0.0	0.0	0.0	-0.315 19	0.553 19
SDI	0.0	0.0	0.0	1.000	0.35	0.0	0.0	-0.094 35	0.090 35
RD3	0.0	0.0	0.0	0.0	1.000	0.370 9	0.302 9	-0.094 35	0.090 35
PL	0.0	0.0	0.0	0.0	0.0	1.000	0.090 9	-0.027 35	0.090 35
PI	0.0	0.0	0.0	0.0	0.0	0.0	1.000	0.042 43	0.042 43
SEN2	0.0	0.0	0.0	0.0	0.0	0.0	0.0	1.000	0.0
SEN3	0.0	0.0	0.0	0.0	0.0	0.0	0.0	0.0	1.000
SEND	0.0	0.0	0.0	0.0	0.0	0.0	0.0	0.0	0.0
SEN3	0.0	0.0	0.0	0.0	0.0	0.0	0.0	0.0	0.0
C<90	0.0	0.0	0.0	0.0	0.0	0.0	0.0	0.0	0.0
C>90	0.0	0.0	0.0	0.0	0.0	0.0	0.0	0.0	0.0
SD/3	0.0	0.0	0.0	0.0	0.0	0.0	0.0	0.0	0.0
LD50	0.0	0.0	0.0	0.0	0.0	0.0	0.0	0.0	0.0
LI	0.0	0.0	0.0	0.0	0.0	0.0	0.0	0.0	0.0
R20	0.0	0.0	0.0	0.0	0.0	0.0	0.0	0.0	0.0
QTZ	0.0	0.0	0.0	0.0	0.0	0.0	0.0	0.0	0.0
ILL	0.0	0.0	0.0	0.0	0.0	0.0	0.0	0.0	0.0
KAO	0.0	0.0	0.0	0.0	0.0	0.0	0.0	0.0	0.0
PYR	0.0	0.0	0.0	0.0	0.0	0.0	0.0	0.0	0.0
DOL	0.0	0.0	0.0	0.0	0.0	0.0	0.0	0.0	0.0
SI	0.0	0.0	0.0	0.0	0.0	0.0	0.0	0.0	0.0
AL	0.0	0.0	0.0	0.0	0.0	0.0	0.0	0.0	0.0
FE	0.0	0.0	0.0	0.0	0.0	0.0	0.0	0.0	0.0
MG	0.0	0.0	0.0	0.0	0.0	0.0	0.0	0.0	0.0
CA	0.0	0.0	0.0	0.0	0.0	0.0	0.0	0.0	0.0
NA	0.0	0.0	0.0	0.0	0.0	0.0	0.0	0.0	0.0
K	0.0	0.0	0.0	0.0	0.0	0.0	0.0	0.0	0.0
TI	0.0	0.0	0.0	0.0	0.0	0.0	0.0	0.0	0.0
S	0.0	0.0	0.0	0.0	0.0	0.0	0.0	0.0	0.0
P	0.0	0.0	0.0	0.0	0.0	0.0	0.0	0.0	0.0

Table 5.3 cont.

	SEND	SEN3	C<90	C>90	SD/3	LD50	LI	R2D	QTZ
DEP	0.266 35	0.338+35	0.631016	0.442 16	0.077 35	0.491+21	0.197 8	0.071 32	0.002 16
S2D	-0.217 35	-0.325 35	0.727014	0.759014	0.725*35	0.735*20	-0.399 8	0.256 32	-0.077 14
SD/3	-0.328 35	-0.140 35	0.793014	0.785014	0.667*35	0.791*20	-0.044 8	-0.022 32	0.010 14
R23	0.039 34	-0.188 34	0.253 13	0.327 13	0.293 34	0.314 19	-0.640 8	0.076 31	-0.379 13
SG	0.499 15	0.016 15	-0.887016	-0.575 16	-0.472 15	-0.733 19	-0.181 5	0.163 15	0.365 15
SO	-0.128 15	-0.011 15	-0.234 15	-0.233 16	0.248 15	-0.477 19	0.104 5	-0.073 15	-0.005 15
RHOD	0.250 18	0.039 18	-0.601+15	-0.843+15	-0.128 18	-0.523+16	0.539 8	0.147 15	0.214 15
RHOW	0.227 18	-0.027 18	-0.714018	-0.700 15	-0.303 13	-0.724 16	0.626 8	0.031 15	0.205 15
M	0.144 18	0.007 18	-0.533+15	-0.675 15	-0.481+13	-0.659 16	0.444 8	-0.054 15	0.087 15
E	0.410 18	0.065 18	-0.336 15	-0.482 15	-0.223 18	-0.414 16	-0.564 8	0.036 15	0.045 15
PHIE	-0.328 19	-0.216 19	0.735016	0.869 16	0.626 19	0.595+17	-0.279 8	0.144 16	-0.290 16
LL	0.147 16	-0.120 16	-0.549+15	-0.760 15	-0.268 19	-0.502 18	-0.641 7	-0.122 16	0.114 15
SDI	0.278 35	-0.314 35	0.616+11	0.641+11	0.576*35	0.504+17	-0.027 8	-0.322 32	0.003 11
RD3	0.016 35	-0.180 35	-0.260 11	-0.397 11	0.483 35	-0.337 17	-0.002 8	0.535 32	0.141 11
PL	-0.398 9	-0.638 9	0.203 6	-0.029 6	0.205 9	0.324 7	0.436 7	-0.272 9	0.666 6
PI	0.338 9	0.135 9	-0.260 6	-0.236 6	0.194 9	0.101 7	-0.674 7	0.176 9	-0.579 6
SEN2	-0.078 35	-0.339 35	-0.199 14	-0.048 14	-0.048 35	-0.209 20	-0.079 8	0.071 32	-0.251 14
SEN3	-0.315 35	0.051 35	-0.149 14	-0.044 14	-0.073 35	-0.124 20	0.075 8	0.094 32	-0.144 14
SEND	1.000 35	0.107 35	-0.244 11	-0.552 11	-0.246 35	-0.568+17	-0.690 8	0.136 32	0.642+11
SEN3	0.0 0	1.000 35	-0.207 11	-0.238 11	-0.420+35	-0.311 17	-0.347 8	0.143 32	-0.169 11
C<90	0.0 0	0.0 0	1.000 16	0.274 16	0.533 11	0.353 15	0.039 5	-0.571 11	-0.141 16
C>90	0.0 0	0.0 0	0.0 0	1.000 16	0.527 11	0.895 15	0.001 5	-0.484 11	-0.396 16
SD/3	0.0 0	0.0 0	0.0 0	0.0 0	1.000 35	0.367 17	-0.207 8	0.105 32	-0.084 11
LD50	0.0 0	0.0 0	0.0 0	0.0 0	0.0 0	1.000 21	0.604 5	-0.041 15	-0.249 15
LI	0.0 0	0.0 0	0.0 0	0.0 0	0.0 0	0.0 0	1.000 3	-0.574 7	0.709 5
R2D	0.0 0	0.0 0	0.0 0	0.0 0	0.0 0	0.0 0	0.0 0	1.000 32	0.215 11
QTZ	0.0 0	0.0 0	0.0 0	0.0 0	0.0 0	0.0 0	0.0 0	0.0 0	1.000 16
ILL	0.0 0	0.0 0	0.0 0	0.0 0	0.0 0	0.0 0	0.0 0	0.0 0	0.0 0
KAO	0.0 0	0.0 0	0.0 0	0.0 0	0.0 0	0.0 0	0.0 0	0.0 0	0.0 0
PYR	0.0 0	0.0 0	0.0 0	0.0 0	0.0 0	0.0 0	0.0 0	0.0 0	0.0 0
DOL	0.0 0	0.0 0	0.0 0	0.0 0	0.0 0	0.0 0	0.0 0	0.0 0	0.0 0
SI	0.0 0	0.0 0	0.0 0	0.0 0	0.0 0	0.0 0	0.0 0	0.0 0	0.0 0
AL	0.0 0	0.0 0	0.0 0	0.0 0	0.0 0	0.0 0	0.0 0	0.0 0	0.0 0
FE	0.0 0	0.0 0	0.0 0	0.0 0	0.0 0	0.0 0	0.0 0	0.0 0	0.0 0
MG	0.0 0	0.0 0	0.0 0	0.0 0	0.0 0	0.0 0	0.0 0	0.0 0	0.0 0
CA	0.0 0	0.0 0	0.0 0	0.0 0	0.0 0	0.0 0	0.0 0	0.0 0	0.0 0
NA	0.0 0	0.0 0	0.0 0	0.0 0	0.0 0	0.0 0	0.0 0	0.0 0	0.0 0
K	0.0 0	0.0 0	0.0 0	0.0 0	0.0 0	0.0 0	0.0 0	0.0 0	0.0 0
TI	0.0 0	0.0 0	0.0 0	0.0 0	0.0 0	0.0 0	0.0 0	0.0 0	0.0 0
S	0.0 0	0.0 0	0.0 0	0.0 0	0.0 0	0.0 0	0.0 0	0.0 0	0.0 0
P	0.0 0	0.0 0	0.0 0	0.0 0	0.0 0	0.0 0	0.0 0	0.0 0	0.0 0

Table 5.3 cont.

	ILL	KAO	PYR	DOL	SI	AL	FE	MG	CA
DEP	-0.416 16	-0.444 16	0.462 15	0.299 8	-0.445 16	-0.505+16	0.351 16	-0.123 16	0.388 16
S2D	-0.511 14	-0.794014	0.710013	0.200 6	-0.773014	-0.826014	0.817014	-0.693014	0.756014
SD/3	-0.528 14	-0.759014	0.678+13	0.442 6	-0.812014	-0.831014	0.829014	-0.784014	0.646+14
R23	-0.142 13	-0.409 13	0.293 12	-0.300 6	-0.387 13	-0.387 13	0.476 13	-0.443 13	0.506 13
SG	0.761016	0.762016	-0.564+15	-0.255 8	0.932016	0.960016	-0.841016	0.771016	-0.656016
SO	0.360 16	0.347 16	-0.434 15	0.074 8	0.273 16	0.282 16	-0.410 16	0.289 16	-0.354 16
RHOD	0.259 15	0.458 15	-0.454 14	-0.411 8	0.547+15	0.620+15	-0.367 15	0.196 15	-0.486 15
RHOW	0.531+15	0.695015	-0.491 14	-0.706 8	0.809015	0.818015	-0.684015	0.559+15	-0.730015
M	0.547+15	0.515+15	-0.165 14	-0.547 8	0.753015	0.674015	-0.714015	0.779015	-0.648015
E	0.377 15	0.238 15	0.097 14	0.166 8	0.413 15	0.369 15	-0.471 15	0.650015	-0.069 15
PHIE	-0.655016	-0.590+16	0.331 15	0.114 8	-0.837016	-0.827016	0.763016	-0.715016	0.665016
LL	0.559+15	0.635+15	-0.126 14	-0.545 8	0.775015	0.738015	-0.683015	0.733015	-0.621+15
SDI	-0.577 11	-0.419 11	0.882010	1.000 3	-0.621+11	-0.695+11	0.744011	-0.307 11	0.926011
RD3	0.409 11	0.377 11	-0.560 10	0.690 3	0.475 11	0.506 11	-0.470 11	0.201 11	-0.535 11
PL	0.103 6	-0.215 6	0.563 5	1.000 2	-0.050 6	-0.215 6	0.081 6	0.391 6	-0.037 6
PI	0.001 6	0.179 6	-0.272 5	1.000 2	0.136 6	0.338 6	-0.225 6	-0.029 6	0.005 6
SEN2	0.138 14	-0.013 14	-0.141 13	-0.464 6	0.030 14	0.037 14	-0.250 14	0.214 14	-0.230 14
SEN3	-0.166 14	0.054 14	-0.268 13	0.093 6	0.095 14	0.172 14	-0.251 14	0.007 14	-0.407 14
SEND	0.333 11	0.581 11	-0.287 10	0.336 3	0.586 11	0.569 11	-0.335 11	0.470 11	-0.201 11
SEN3	0.312 11	-0.222 11	-0.331 10	-0.859 3	0.195 11	0.258 11	-0.215 11	0.168 11	-0.212 11
C<90	-0.717016	-0.706016	0.652015	0.465 8	-0.877016	-0.899016	0.800016	-0.712016	0.588+15
C>90	-0.742016	-0.777016	0.430 15	0.197 8	-0.953016	-0.967016	0.846016	-0.867016	0.626015
SD/3	-0.441 11	-0.264 11	0.498 10	0.917 3	-0.535 11	-0.499 11	0.540 11	-0.597 11	0.335 11
LD50	-0.719015	-0.828015	0.759014	0.542 7	-0.929015	-0.938015	0.911015	-0.854015	0.758015
LI	0.173 5	-0.181 5	0.484 4	0.0 1	0.060 5	-0.149 5	0.074 5	0.221 5	-0.230 5
R2D	0.173 11	0.224 11	-0.298 10	0.931 3	0.521 11	0.561 11	-0.362 11	0.418 11	-0.165 11
QTZ	0.051 16	0.286 16	0.123 15	0.408 3	0.334 16	0.323 16	-0.087 16	0.373 16	-0.010 16
ILL	1.000 16	0.411 16	-0.530+15	-0.633 8	0.746016	0.702016	-0.649016	0.626016	-0.497+16
KAO	0.0 0	1.000 16	-0.536+15	-0.327 8	0.839016	0.846016	-0.854016	0.754016	-0.690016
PYR	0.0 0	0.0 0	1.000 15	0.296 8	-0.553+15	-0.582+15	0.689015	-0.274 15	0.715015
DOL	0.0 0	0.0 0	0.0 0	1.000 8	-0.522 3	-0.271 8	0.238 3	-0.312 3	0.342 3
SI	0.0 0	0.0 0	0.0 0	0.0 0	1.000 16	0.979016	-0.885016	0.883016	-0.696016
AL	0.0 0	0.0 0	0.0 0	0.0 0	0.0 0	1.000 16	-0.902016	0.840016	-0.729016
FE	0.0 0	0.0 0	0.0 0	0.0 0	0.0 0	0.0 0	1.000 16	-0.790016	0.841016
MG	0.0 0	0.0 0	0.0 0	0.0 0	0.0 0	0.0 0	0.0 0	1.000 15	-0.477 16
CA	0.0 0	0.0 0	0.0 0	0.0 0	0.0 0	0.0 0	0.0 0	0.0 0	1.000 15
NA	0.0 0	0.0 0	0.0 0	0.0 0	0.0 0	0.0 0	0.0 0	0.0 0	0.0 0
K	0.0 0	0.0 0	0.0 0	0.0 0	0.0 0	0.0 0	0.0 0	0.0 0	0.0 0
TI	0.0 0	0.0 0	0.0 0	0.0 0	0.0 0	0.0 0	0.0 0	0.0 0	0.0 0
S	0.0 0	0.0 0	0.0 0	0.0 0	0.0 0	0.0 0	0.0 0	0.0 0	0.0 0
P	0.0 0	0.0 0	0.0 0	0.0 0	0.0 0	0.0 0	0.0 0	0.0 0	0.0 0

Table 5.3 cont.



	NA	K	TI	S	P
DEP	-0.290 16	-0.479 16	-0.534+16	0.320 16	0.831*16
S2D	-0.544+14	-0.551*14	-0.783*14	0.832*14	0.692*14
SD/3	-0.430 14	-0.850*14	-0.844*14	0.837*14	0.655+14
R23	-0.314 13	-0.441 13	-0.337 13	0.607 13	0.291 13
SG	0.0291 16	0.922*16	0.874*16	-0.664 16	-0.799*16
SO	0.0167 16	0.299 16	0.435 16	-0.331 16	-0.251 16
RHOD	0.0386 15	0.523+15	0.471 15	-0.752 15	-0.786*15
RHOW	0.0333 15	0.801*15	0.703*15	-0.701*15	-0.734*15
M	0.098 15	0.738*15	0.616+15	-0.733*15	-0.265 15
E	-0.254 15	0.424 15	0.418 15	-0.527+15	0.115 15
PHIE	-0.375 16	-0.786*16	-0.684*16	0.208*16	0.577+16
LL	-0.159 15	0.779*15	0.650*15	-0.753*15	-0.431 15
SDI	-0.242 11	-0.695+11	-0.654+11	0.720+11	0.725+11
RD3	0.0678+11	0.475 11	0.405 11	-0.424 11	-0.449 11
PL	0.0070 6	-0.130 6	-0.303 6	-0.071 6	0.358 6
PI	-0.326 6	0.269 6	0.381 6	-0.169 6	-0.311 6
SEN2	-0.114 14	0.217 14	0.257 14	-0.259 14	0.023 14
SEN3	0.0203 14	0.200 14	0.170 14	-0.223 14	-0.160 14
SEND	0.0207 11	0.419 11	0.312 11	-0.385 11	-0.386 11
SEN3	-0.364 11	0.219 11	0.200 11	-0.237 11	-0.010 11
C<90	-0.340 16	-0.831*16	-0.509*16	0.202*16	0.796*16
C>90	-0.258 16	-0.950*16	-0.668*16	0.893*16	0.718*16
SD/3	0.0074 11	-0.520 11	-0.490 11	0.585 11	0.235 11
LD50	-0.296 15	-0.949*15	-0.912*15	0.933*15	0.725*15
LI	0.0440 5	-0.093 5	-0.254 5	-0.020 5	0.225 5
R2D	0.0165 11	0.419 11	0.371 11	-0.371 11	-0.238 11
QTZ	0.0029 16	0.257 16	0.068 16	-0.167 16	-0.155 16
ILL	0.0120 16	0.731*16	0.691*16	-0.677*16	-0.489 16
KAO	0.0353 16	0.856*16	0.854*16	-0.851*16	-0.747*16
PYR	-0.401 15	-0.586+15	-0.705*15	0.598+15	0.654*15
DOL	0.0525 8	-0.442 8	-0.482 8	0.252 8	0.260 8
SI	0.0372 16	0.962*16	0.884*16	-0.917*16	-0.699*16
AL	0.0387 16	0.972*16	0.910*16	-0.925*16	-0.772*16
FE	-0.349 16	-0.933*16	-0.545*16	0.927*16	0.703 16
MG	0.0146 16	0.887*16	0.778*16	-0.862*16	-0.366 16
CA	-0.309 16	-0.729*16	-0.727*16	0.815*16	0.686*16
NA	1.000 16	0.285 16	0.274 16	-0.203 16	-0.384 16
K	0.0 0	1.000 16	0.951*16	-0.658*16	-0.734*16
TI	0.0 0	0.0 0	1.000 16	-0.930*16	-0.795*16
S	0.0 0	0.0 0	0.0 0	1.000 16	0.662*16
P	0.0 0	0.0 0	0.0 0	0.0 0	0.0 0

Table 5.3 cont.

and also those in chapter 4, section 4.6).

1. The organic carbon content (coal content to a first approximation) correlates with the grain size ( $\log D_{50}$ ), friction angle and depth.

2. The specific gravity, bulk and dry densities, moisture content and liquid limit all correlate negatively with the coal content etc. The finer sediments thus contain less coal, and are wetter.

3. The field vane shear strengths all correlate one with another, and are also correlated with the coal content etc.

4. As was shown in Chapter 4 (section 4.6), the pyrite and hence iron and sulphur contents are correlated with coal, and hence with field vane shear strength etc. The clay group of minerals and chemicals show the inverse of this relationship.

All these correlations are explained in terms of the sedimentary model outlined in Chapter 4 (section 4.7) by the additional postulate that the friction angle is dependent on the coal content. Thus coarse layers are coal and pyrites rich, and have high friction angles and low bulk densities. Finer layers on the other hand are denser, wetter and show up as weak layers. Thus it can be seen that the field vane shear test is behaving in the same sense as the cone penetration test; i.e. the stronger or more resistant layers are coarse, coaly layers. The relationship between shear strength and coal content has been noted before (Taylor, 1974).

Other correlations exist in the data that are not so readily explained in terms of this model. Some of these correlations are contradictory.

5. The sensitivities of the vanes correlate with bulk density, liquid limit, depth and moisture content, and negatively with median size and plasticity index. Not all the vane sensitivities are thus correlated,

which explains the contradiction of correlations in opposite senses to depth and median size which are themselves positively related; it is from different vanes that the two correlations come. These relationships suggest that it is the wetter, more plastic layers that are the more sensitive. This is of course not an unexpected relationship.

6. Of all the R values, there are only three significant correlations; with the strength of one of the vanes used in the determination of the R value in question, with another R value, and negatively with the liquid limit. Since no other parameter in the data is related to the anisotropy of the sediments, the lack of correlation with anything else is probably a more significant conclusion.

7. The void ratio correlates with no other property, unless the 90% significance level is included when one vane sensitivity and the organic carbon content (negatively) may be mentioned.

8. The Trask sorting coefficient ( $S_o$ ) correlates negatively with the median size; i.e. the coarser sediments are more uniformly graded.

Numerical comparisons may be drawn from these data on the differences between the material at locations 1A (near the beach) and 2A (further into the lagoon). The strength and moisture content data have been compared using a Wilcoxon Matched Pairs Signed Ranks Test, which compares data in individual pairs. This is possible for those parameters for which data are available from many similar depths in the two profiles. For the other data, a Students "t" test or Fishers L.S.D. test are used where appropriate; these tests compare overall populations of data which is more appropriate when data from coincident depths are not available.

The results are presented in Table 5.4 and it can be seen that passage into the lagoon marks a transition from stronger to weaker sediments, looser to denser, coarser to finer and drier to wetter. This

Table 5.4 Comparison of physical data from locations 1A and 2A,  
lagoon 7, Peckfield.

Parameter	Test	Result	Significance level
Strength			
a. Shear box	1	Material stronger at 1A	n.s.
b. H=2D vane	1	Stronger at 1A	99.5%
c. H=D/3 vane (75mm)	1	" " "	99.5%
d. H=D/3 vane (150mm)	1	" " "	n.s.
e. Diamond vane	1	" " "	n.s.
Voids ratio	2	Higher at 1A	n.s.
Bulk density	3	Higher at 2A	95%
Log D <sub>50</sub>	2	Larger at 1A	95%
S <sub>0</sub> (Trask's sorting coeff.)	3	Larger at 2A	n.s.
Moisture content	1	Higher at 2A	99%
PL	3	Higher at 2A	n.s.
LL	2	Higher at 1A	n.s.
Organic carbon content	2	Higher at 1A	n.s.
Specific gravity	2	Higher at 2A	n.s.

n.s. Not significant i.e. less than 95%

Test 1 Wilcoxon Matched Pairs Signed Ranks Test

2 Student's t test

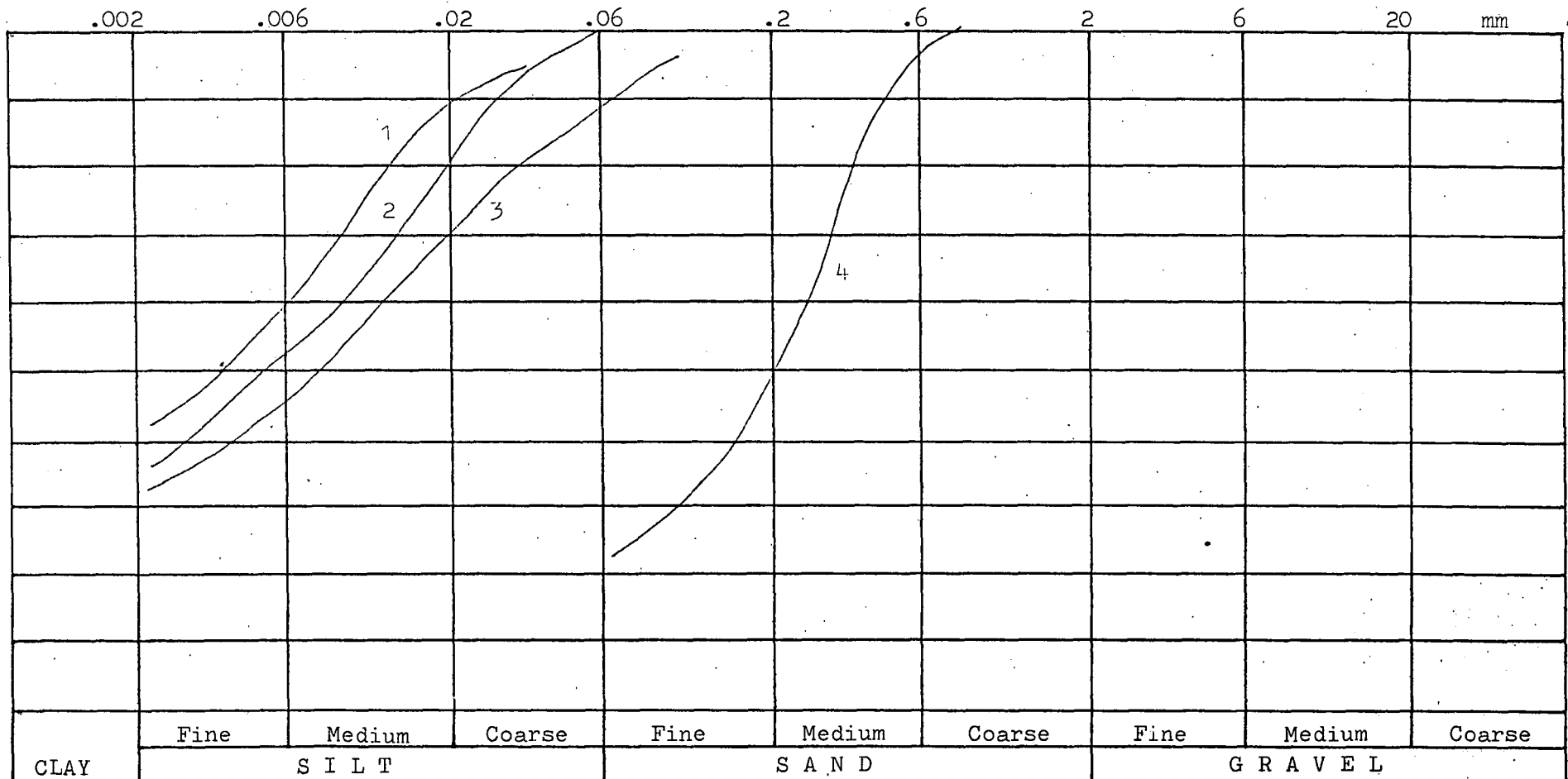
3 Fisher's L.S.D. test (i.e. F test is +ve )

is consistent with the sedimentological model proposed in chapter 4 (section 4.7). Although the other parameters are not significantly different between the two locations, it should be noted that they too are all consistent with the model with the exception of the liquid limit. Consequently it seems reasonable to suppose that the coal content decreases away from the lagoon inlet, as does the voids ratio though this parameter is not accounted for by the model. On the other hand, the density and the sorting coefficient increase away from the inlet. For consistency, the liquid limit should increase away from the inlet, but this is not so. This underlines the caution with which statistics should be used.

In addition to the U.100 samples, four undisturbed box samples were taken from the face of the excavation into lagoon No.7. The locations are shown in Fig.5.4. Figure 5.13 shows that the material fines with distance from the inlet. It can also be seen from Fig.5.13 that the organic carbon content, specific gravity and index properties conform to the trends mentioned above. Consolidated - undrained triaxial tests were performed on box samples 1 and 2, and from Figs.5.14 a and b it can be seen that the material has high effective friction angles, as expected from the high coal content. The angle of friction on a total stress basis is about 23 degrees in each case; this is higher than the shear-box test results because these samples were consolidated before shear, rather than being sheared on an immediate basis. Samples 3 and 4 were subjected to drained tests, see Figs.5.15a and b. Again the effective angle of friction is high, particularly for the coarse, coal-rich sample No.4 (at 43 degrees). Both these samples show high values of cohesion. While a true effective cohesion intercept is possible for sample 3 (Fig.5.15a), which has a clay content of about 34%, it is highly unlikely

Fig.5.13 Grading curves for samples PL71-4, lagoon 7, Peckfield.

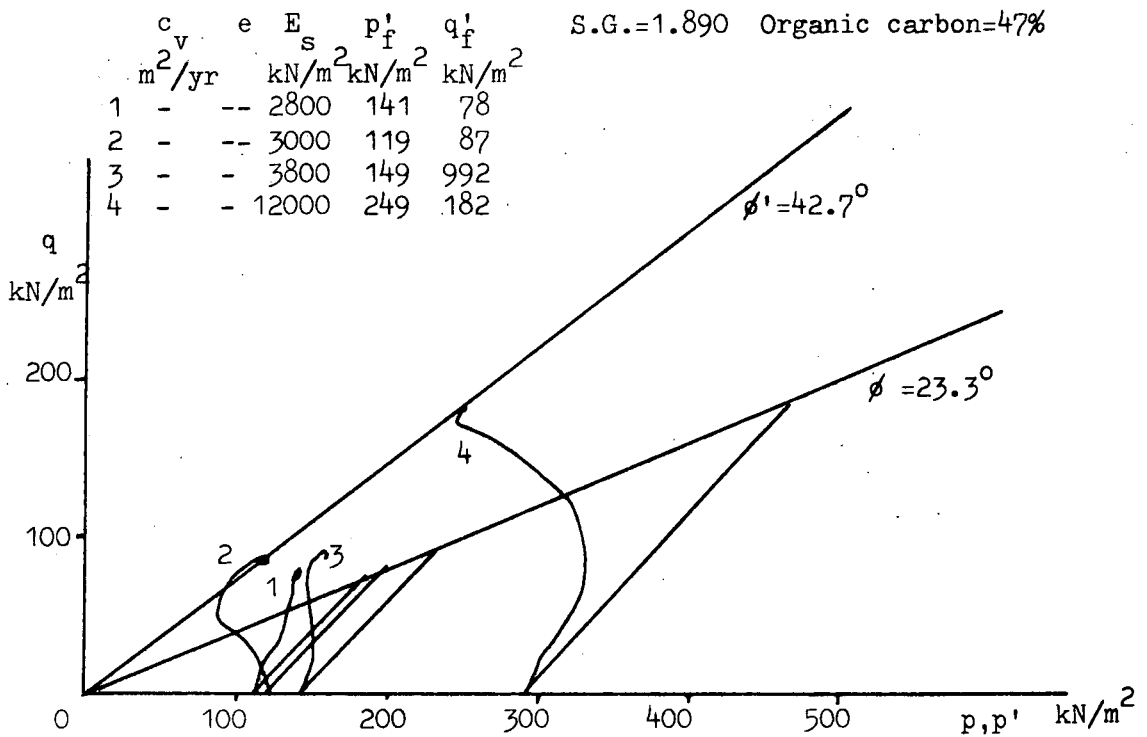
	LL	PL	PI	carbon	S.G.
PL71	53	34	19	47	1.890
PL72	59	32	27	52	1.900
PL73	51	35	16	52	1.886
PL74	-	-	-	85	1.526



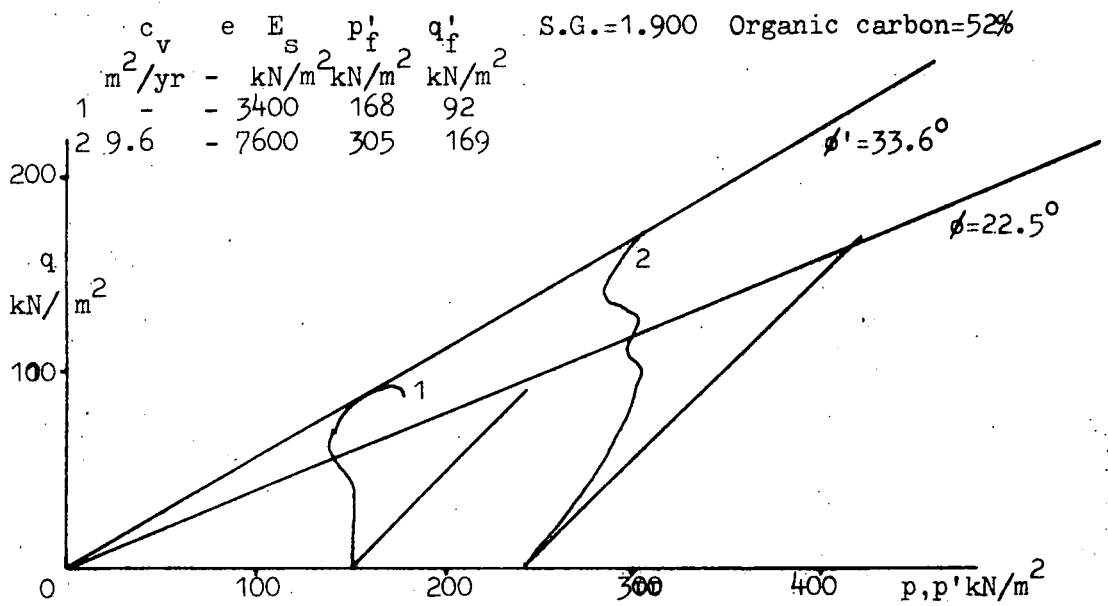
17/19

Fig. 5.14 Consolidated undrained triaxial tests on Peckfield lagoon 7.

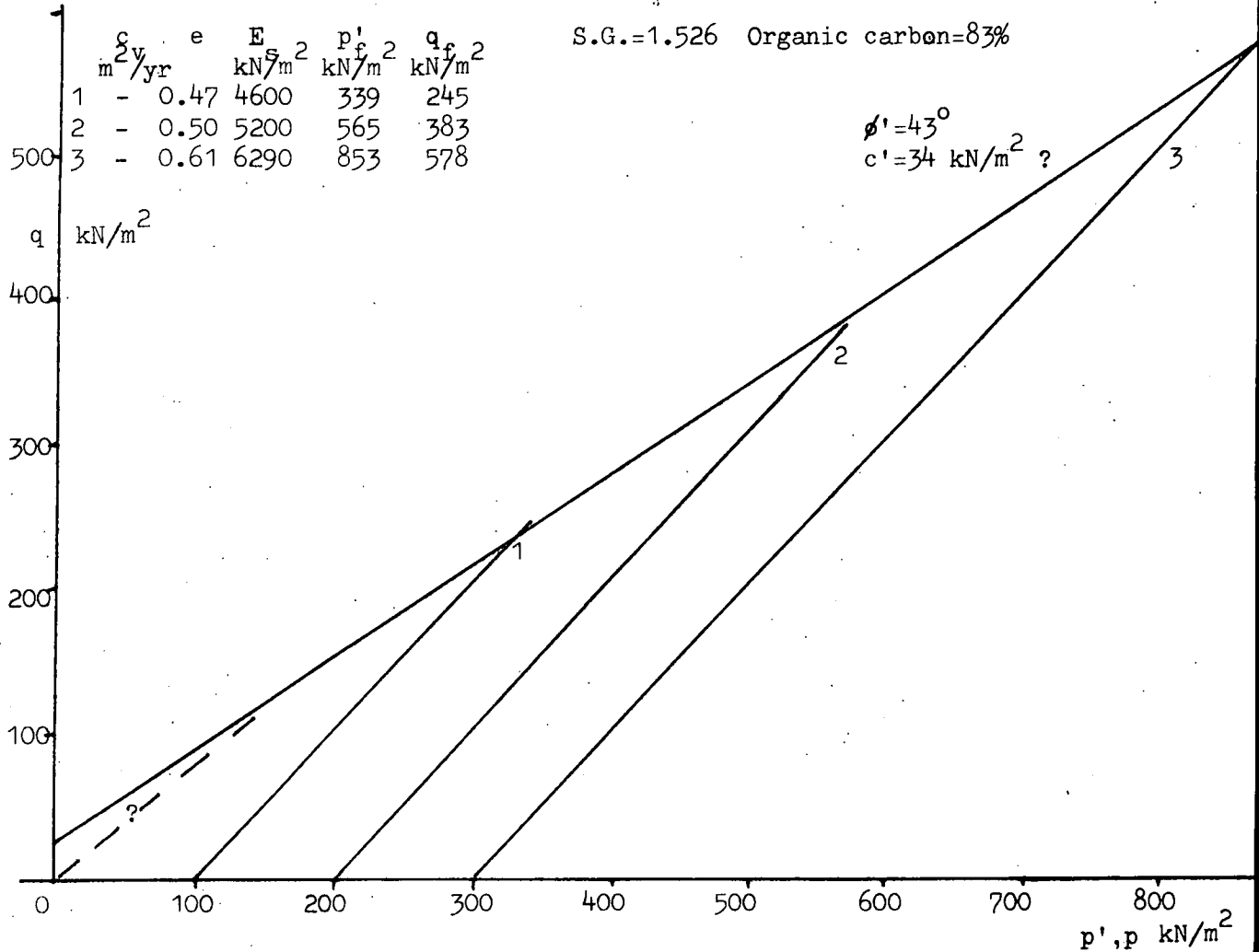
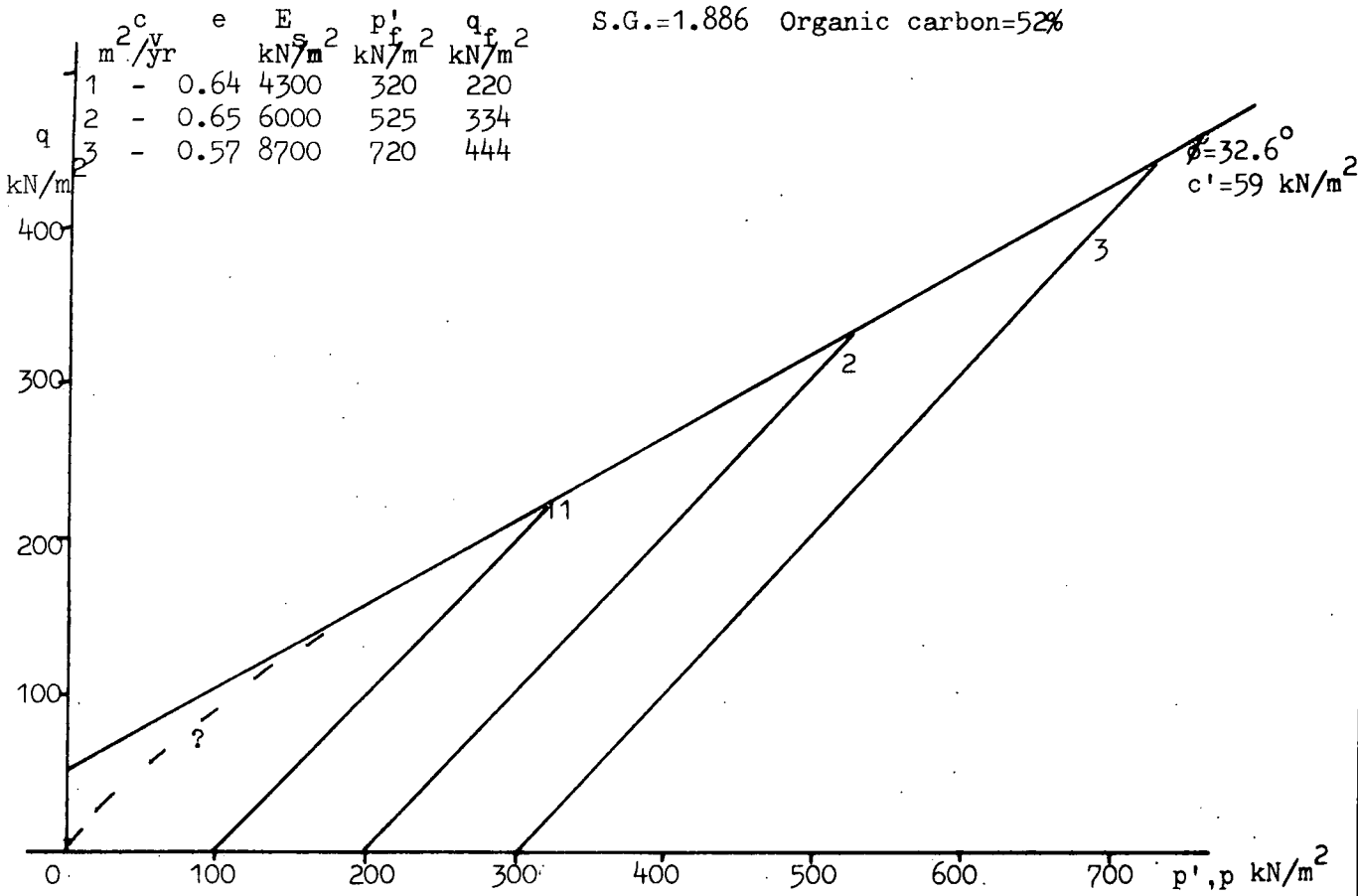
a. Sample PL71



b. Sample PL72



a. Sample PL73



b. Sample PL74

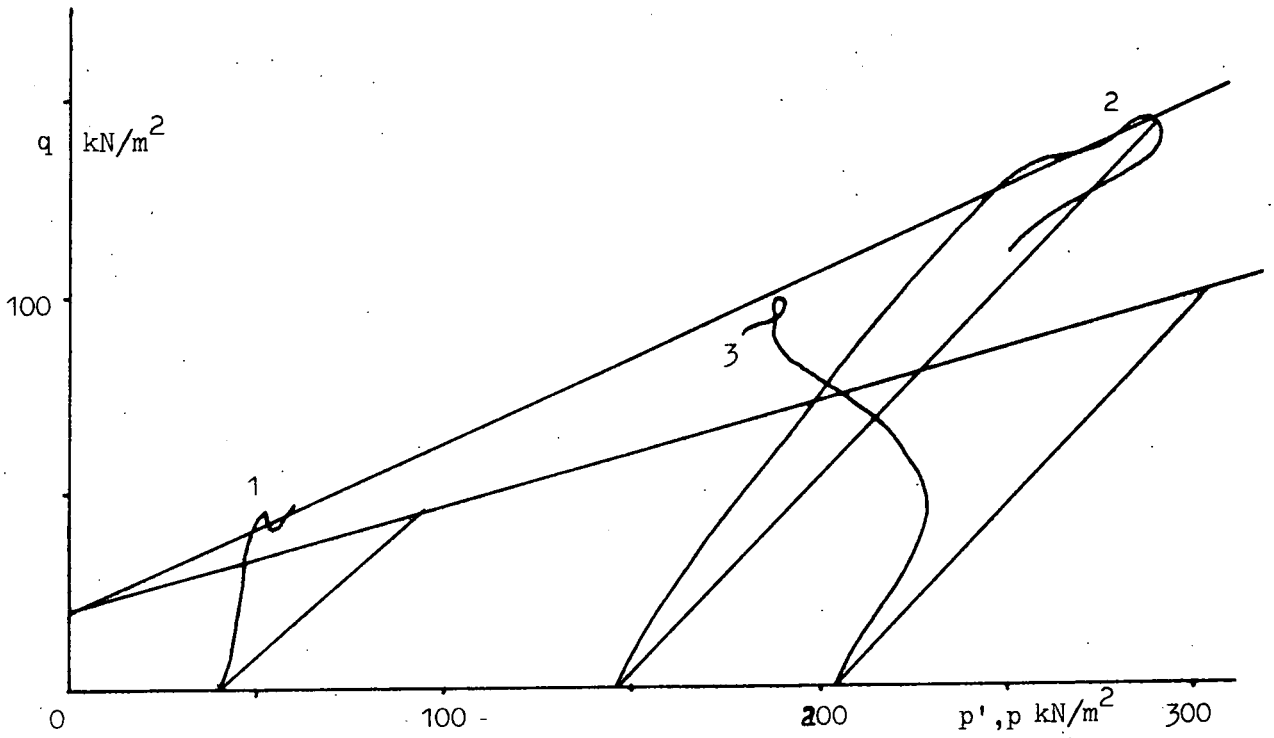


that the very coarse sample 4 has true effective cohesion. In view of the high test pressures involved compared to the in-situ effective stresses, the answer probably lies in a curved failure envelope. It is usually considered that coarse discard is cohesionless on an effective stress basis, and curved envelopes are usually postulated for the more plastic discards (Taylor and Cobb, 1977).

Two samples of material from the outlet end of lagoon No.6 at Peckfield were tested in the shear-box as described in Chapter 2.2.iv, Figures 2.14 and 2.15 show that the behaviour is essentially the same as that shown by material in lagoon 7. It is interesting to note the coarseness of the coaly layer at the outlet. A consolidated-undrained triaxial test was performed on the finer material from this location. The stress paths, Fig.5.16, show some interesting features. Sample 2 was deliberately overconsolidated in the triaxial cell to an effective cell pressure of  $600\text{kN/m}^2$ , and then unloaded to the test pressure. It exhibits a behaviour typical of overconsolidated material (see section 5.2). Sample 3 on the other hand is normally consolidated, and behaves as such. Sample 1, at a very low test pressure exhibits slightly overconsolidated behaviour, and high shearing resistance at failure. This material was evidently overconsolidated to a stress of above  $40\text{kN/m}^2$ . The effective cohesion intercept of this material is therefore almost certainly a true feature indicative of its overconsolidated state, in contrast to the two samples from lagoon 7 where the cohesion intercept may be an artefact of the test pressures involved (particularly in the case of sample 4). It will be recalled from Fig.2.15 that the fine material from lagoon 6 has a clay content in excess of 30%. The effective angle of friction is 25 degrees; shear-box tests gave an angle of 26 degrees (see Fig.2.14). The friction angle in terms of total stress is low, at 15 degrees.

Fig. 5.16 Consolidated undrained tests on Peckfield lagoon 6.

	$c_v$ $m^2/yr$	$e$	$E_s$ $kN/m^2$	$p'_f$ $kN/m^2$	$q_f$ $kN/m^2$	S.G.=2.171 Organic carbon=38%	
1	4.77	0.804	9200	52	45	$\phi' = 25^\circ$ $c' = 20 \text{ kN/m}^2$	$\phi = 15^\circ$ $c = 21 \text{ kN/m}^2$
2	5.36	0.734	11000	287	143		
3	8.86	0.773	9800	189	98		



### 5.5 East Hetton

The lagoons at East Hetton were chosen as the site for testing the use of cone penetrometers in colliery lagoons. A preliminary series of vane tests were conducted with the H=2D vane only at the locations marked, 1 2 and 3 in Fig.5.17. Location 1 represents material that was pumped into a temporary excavation (see Chapter 1.4). which is obviously much weaker than the original material at location 2, see Fig.5.18 (and Table A.5.1). Lagoon 109C was less suitable for the penetrometer study in terms of access, and the profile at location 3 represents the only vane tests conducted there. In view of the fact that the embankment of lagoon 109B is founded on these deposits, the strength below the crust is low.

The main investigation was concerned with lagoon 109B only. Testing was conducted at three locations (A, B and C, Fig.5.17); these locations involved the original lagoon material only. Vane tests at these three locations reveal a lagoon with a moderate strength at the inlet, decreasing towards the outlet (trend A - C - B in Fig.5.19, see also Table A.5.1), thus repeating the pattern found at Peckfield.

The strength versus depth relationships, depicted by the lines labelled 1 to 4 on Fig.5.19, show that the peak strength generally decreases from a drained strength relationship near to the inlet (location A), to an undrained strength relationship near to the outlet. However, as at Peckfield there is a great deal of variability in the results, which probably arises from the highly layered nature of the lagoon sediments. The remoulded shear strengths are close to relationships 1 and 2, though the variation in the strength is too great to state which relationship is the better (or indeed, if another would be more suitable). As at Peckfield, when the peak strength is nearer to the

Fig.5.17 Test locations in the lagoons at East Hetton.

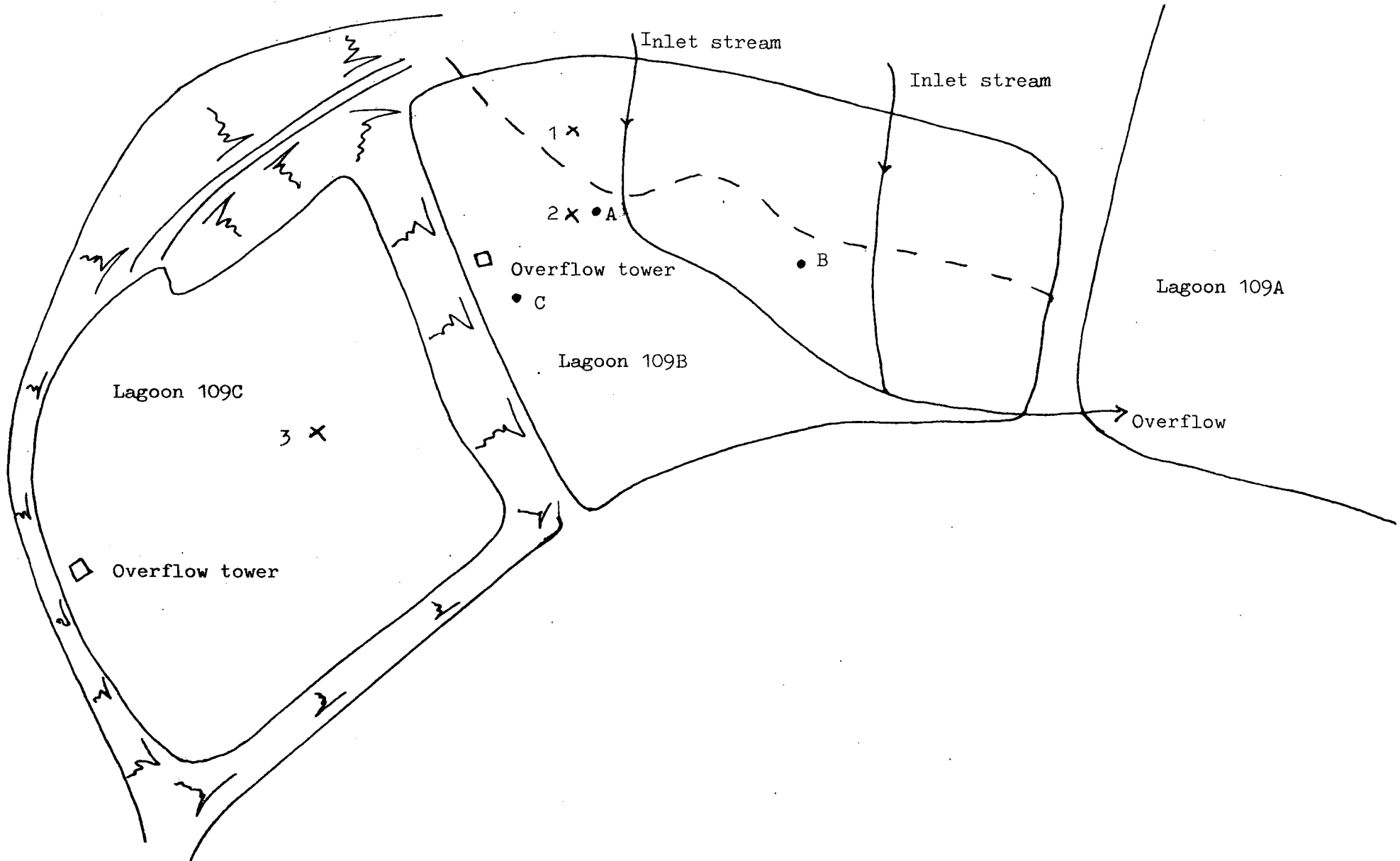
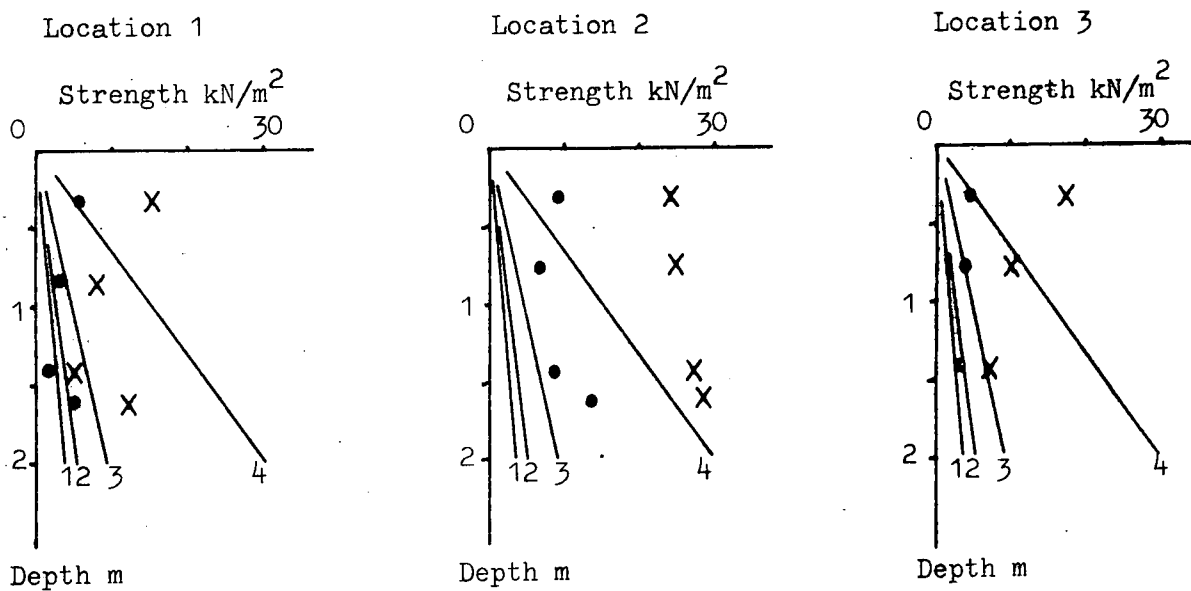
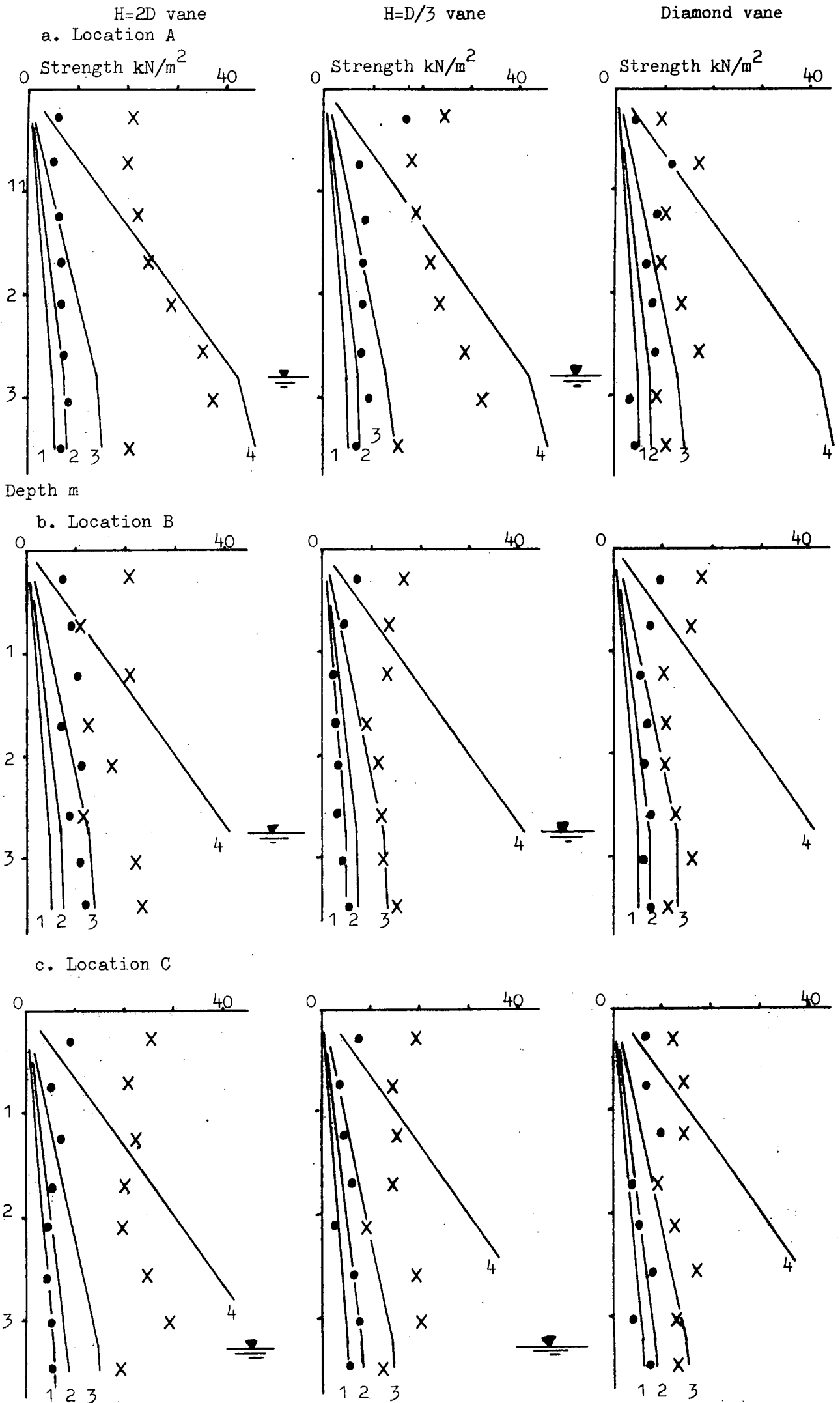


Fig. 5.18 Preliminary vane survey, East Hetton.

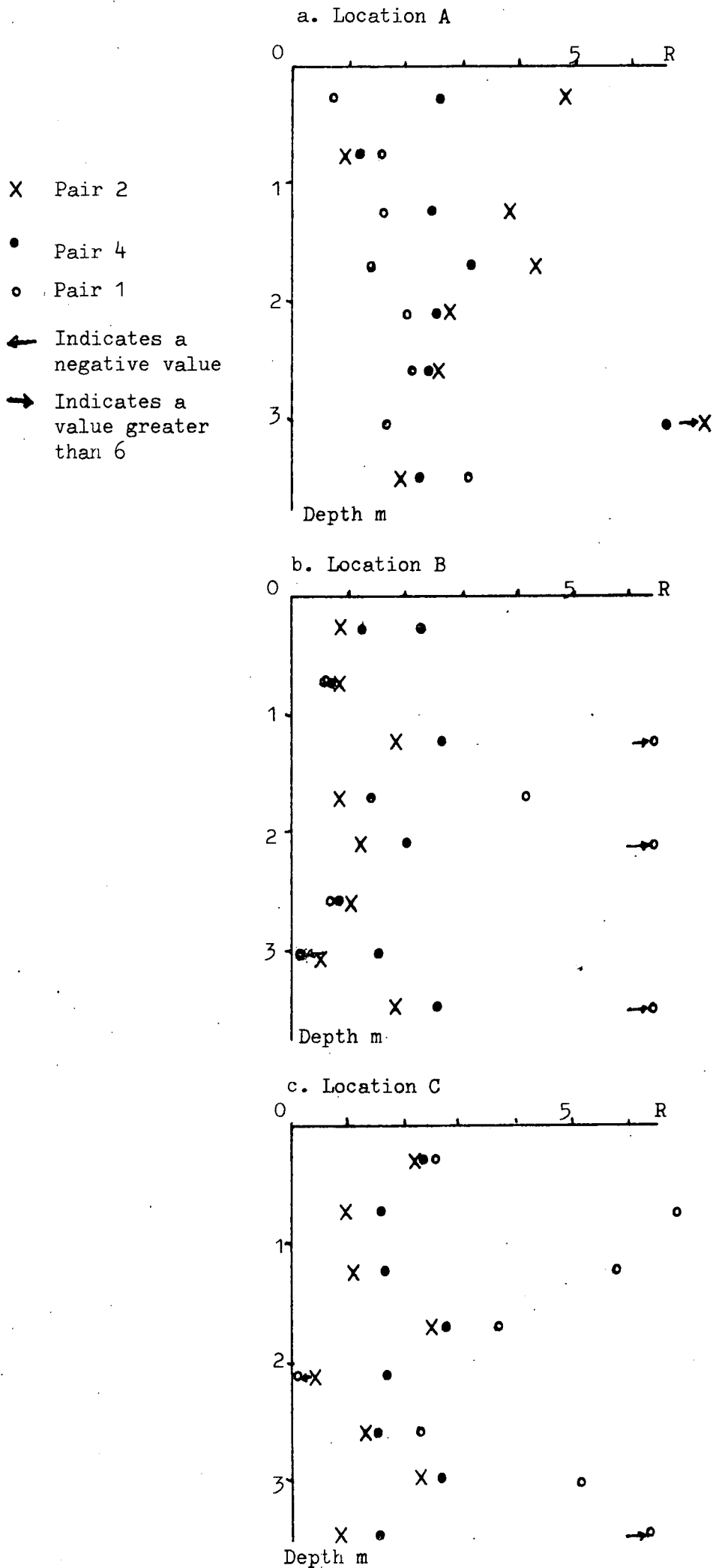




drained strength relationship the remoulded strength tends to lie above the lines defining relationships 1 and 2. The change in strength from an effective stress to total stress relationship may be explained in terms of the increasing proportion of fine grained layers with distance from the inlet (see Table 3.1).

Since the vane tests have been carried out with vanes with  $H=2D$ ,  $H=D/3$  and diamond shapes, it is possible to compare directly the R values obtained from combinations 1, 2 and 4 (as defined in chapter 2.2.iii, and Fig.2.3). From Fig.5.20 it can be seen that combination 4 gives the most consistent results, confirming the Peckfield findings (previous section). However, the results, are more variable than those at Peckfield, and the R value is higher on average. The average R value (combination 4) is 1.56 at Peckfield, compared to 2.17 at East Hetton, the standard deviations being 0.766 and 1.164 respectively. The high degree of variability of the data from East Hetton is probably due to the highly layered nature of the sediments (as was shown by the cone penetration tests, Figs.3.4 to 3.6, and the borehole logs Table 3.1). As at Peckfield, the sediments possess greater shear strength across the laminae (i.e. in a vertical orientation) than along the laminae.

U100 samples were obtained from all three locations. The logs of these samples have already been described (Table 3.1). For further analysis typical samples were taken to represent one coarse, one medium and one fine grained layer at each location, with an additional medium-fine sand at location C, (i.e. 10 specimens). The grading curves of these samples, as discussed in chapter 4, section 4.6, together with the logs, show an increase in the proportion of fines with distance from the inlet. Since the finer layers have the lowest organic carbon content (Fig.4.6.c), the proportion of coal generally decreases with distance





from the inlet. Hence the decrease in strength across the lagoon can again be explained in terms of the dependence of shear strength on the coal content, as at Peckfield.

Shear-box tests carried out on these samples show that the coarse, sand-sized material has effective friction angles of about 35 degrees (see Table 5.5). The effective friction angles of finer material is about 30 degrees as would be expected in consideration of the proportion of coal in the finer layers. The angle of friction in terms of total stresses is lower at 20 degrees. The cohesion intercept reflects the degree of consolidation, and as at Peckfield it seems probable that the finest material has a true effective cohesion intercept.

Triaxial tests were also conducted on material from East Hetton. However, the finely layered nature of the lagoon produced some difficulty in selecting only one type of material for each test. In order to obtain a sample containing only one coarse layer, a sample was taken from the beach area of lagoon 109A (the beach in lagoon 109B was obscured by overtipped material). This sample has a low coal content (9%), and as can be seen from Fig.5.21.a, it behaves as a dense material at low pressures, yet has no effective cohesion intercept. This is expected of a coarse material; the effective friction angle is 35 degrees. The friction angle in terms of total stresses is 16 degrees, the cohesion being  $21\text{kN/m}^2$  on this basis.

A layered sample from location B, containing coarse, medium and fine layers exhibits the behaviour of overconsolidated material, and has an effective cohesion intercept of  $7\text{kN/m}^2$ , and an effective friction angle of 30.5 degrees see Fig.5.21.b. The sample was from very near the surface, and was dry at the time of sampling; therefore it was almost certainly overconsolidated by desiccation. However, the form of the

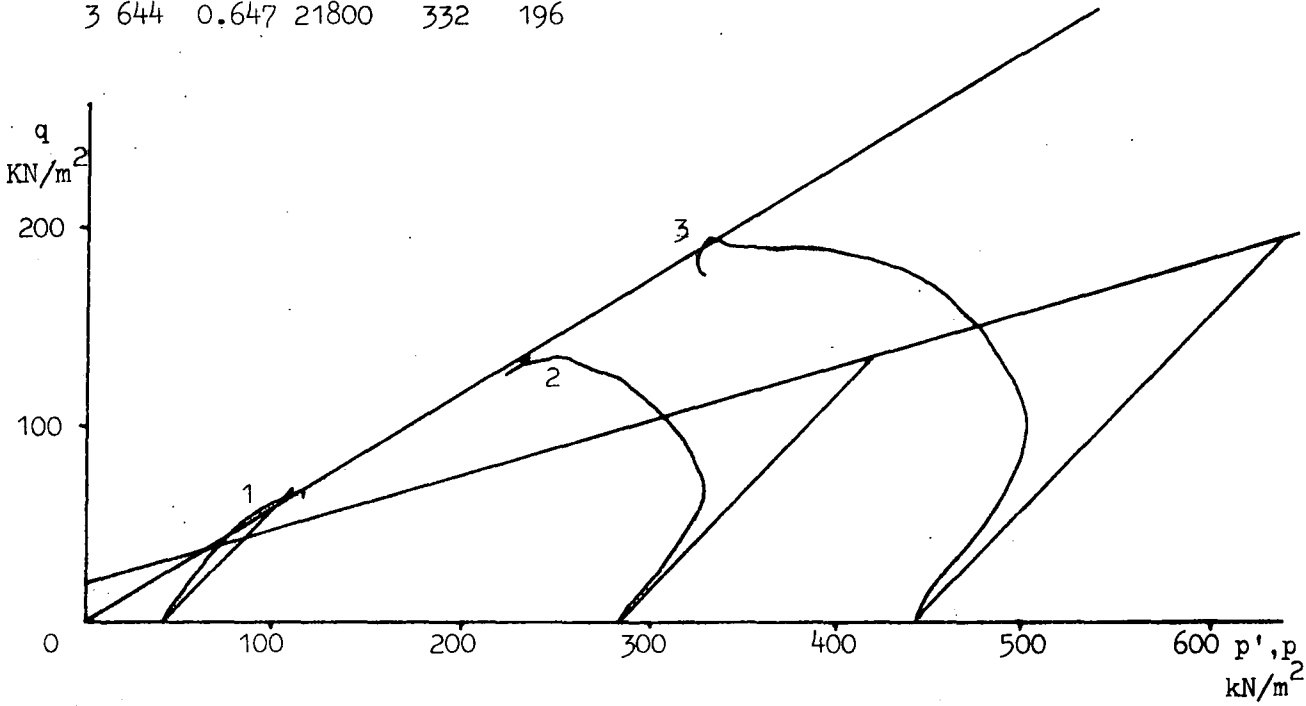
Table 5.5 East Hetton physical parameters.

Sample	Specific gravity	Organic carbon %	$\phi, \phi'$ °	c, c' kN/m <sup>2</sup>	From shear box test of type:
A Coarse	1.43	88	35	0	Drained
Medium	2.35	18	28	9	Drained
Fine	2.06	35	29	5	Consolidated undrained*
Fine	2.06	35	29	18	Consolidated undrained, desiccated sample*
B Coarse	1.44	83	36	1	Drained
Medium	1.64	69	30	0	Drained
Fine	1.90	43	19	0	Consolidated undrained
C Coarse	1.44	79	35	1	Drained
Coarse	1.44	79	35	0	Drained
Medium coarse	2.38	14	-	-	
Medium	1.83	49	18	12	Undrained
Fine	2.13	26	21	7	Consolidated undrained

\*Note. While these two samples were tested on a consolidated undrained basis, they were very dry when loaded. Insufficient time was allowed for complete saturation, and the strengths probably therefore reflect effective stress conditions.

a. Coarse sample from the beach of 109 A

	$c_v$ $m^2/yr$	$e$	$E_s$ $kN/m^2$	$p'_f$ $kN/m^2$	$q_f$ $kN/m^2$	S.G.=2.551
1	650	0.788	7300	118	68	$c'=0$ $\phi'=35^\circ$
2	650	0.703	14900	235	136	$c=21 \text{ kN/m}^2$ $\phi=16^\circ$
3	644	0.647	21800	332	196	



b. Laminated sample, generally silt.

	$c_v$ $m^2/yr$	$e$	$E_s$ $kN/m^2$	$p'_f$ $kN/m^2$	$q_f$ $kN/m^2$	$c'=7 \text{ kN/m}^2$ $\phi'=30.5^\circ$
1	-	-	3000	162	90	$c=?$ $\phi=?$
2	-	-	1600	252	132	
3	-	-	4900	589	310	

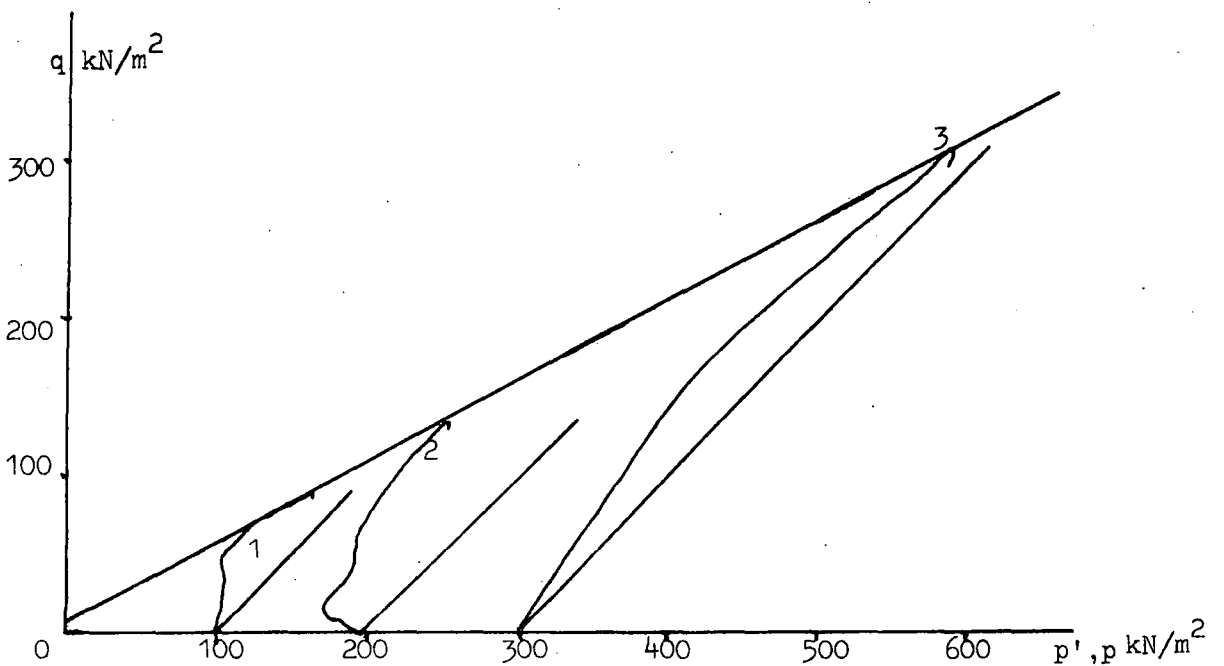
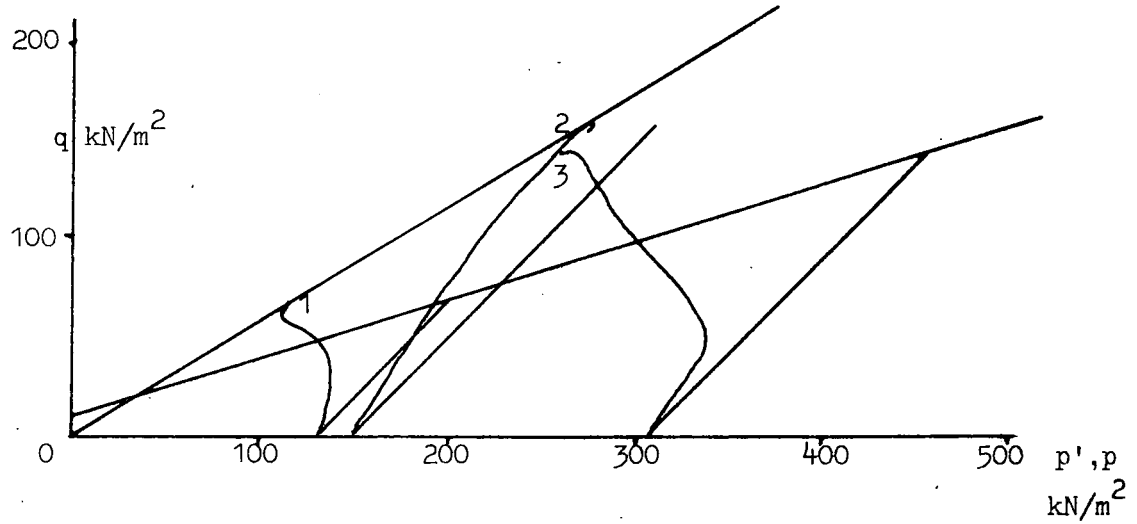


Fig. 5.21.c. Clay sample, outlet end, lagoon 109 B.

	$c_v$ m <sup>2</sup> /yr	$e$	$E_s$ kN/m <sup>2</sup>	$p'_f$ kN/m <sup>2</sup>	$q_f$ kN/m <sup>2</sup>	
1	57.2	0.62	15300	117	69	S.G.=2.093
2	31.6	0.55	21300	274	180	$c'=0$ $\phi'=40.5^\circ$
3	67.2	0.59	10800	262	167	$c=10$ kN/m <sup>2</sup> $\phi=18.7^\circ$



stress paths may be partly due to the layered nature of the sediments.

In order to obtain a layer of fine material thick enough to test, it was necessary to take a sample from very near the outlet. As can be seen in Fig.5.21.c, the sample behaves in a normally consolidated fashion. Test No.2 was deliberately overconsolidated in the triaxial cell to a pressure of  $600\text{kN/m}^2$  before being unloaded to the test pressure. The effective angle of friction is 40.5 degrees, while in terms of total stresses it is about 19 degrees. The cohesion intercept is zero in terms of effective stresses, but  $10\text{kN/m}^2$  in terms of total stresses.

### 5.6 Maltby

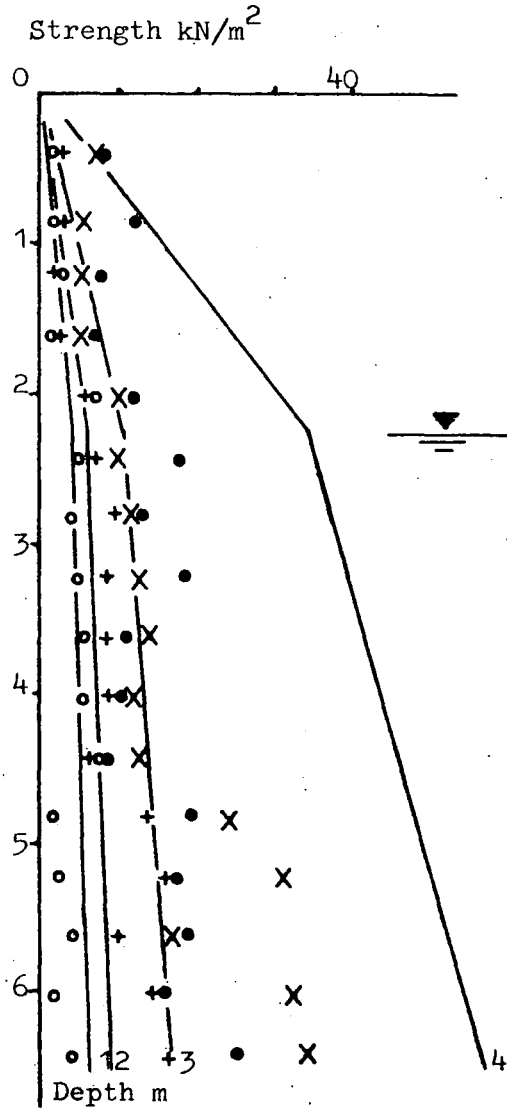
In-situ testing was carried out at Maltby lagoon No.6 using both the field vane apparatus and the first field penetrometer device. The results from the latter tests were discussed in Chapter 3.3 (Table 3.2., Fig.3.7). They show a layered lagoon with a desiccation crust at location 2 (see Fig.4.4c. for the locations). The vane tests involved the H=2D vane and the diamond vane (i.e. combination 4). The results show a lagoon that is fairly weak near the surface, particularly at location 1 which is nearer to the supernatant water of the lagoon.

The strength versus depth relationships show that peak strengths are generally following the undrained strength law, while the remoulded strengths generally follow the lines corresponding to relationships 1 and 2. The reason for the particularly weak remoulded strengths measured by the H=2D vane at about 5m depth in profile 2 is not known.

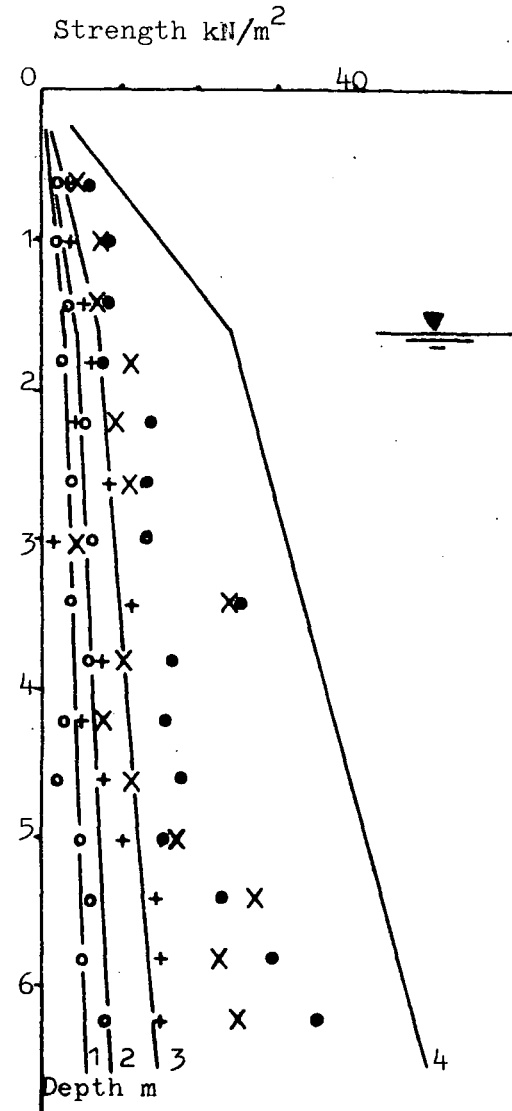
From Fig.5.23 it can be seen that the R values generally indicate a deposit which is stronger across the laminations (i.e. on a vertical plane) than along (i.e. on a horizontal plane). The average R value is 1.321 (with a standard deviation of 0.748), and is thus lower than at Peckfield or East Hetton. In the profile at location 2, Fig.5.23.a, the

Fig. 5.22 Vane shear strength profiles, Maltby lagoon 6.

a. Location 2



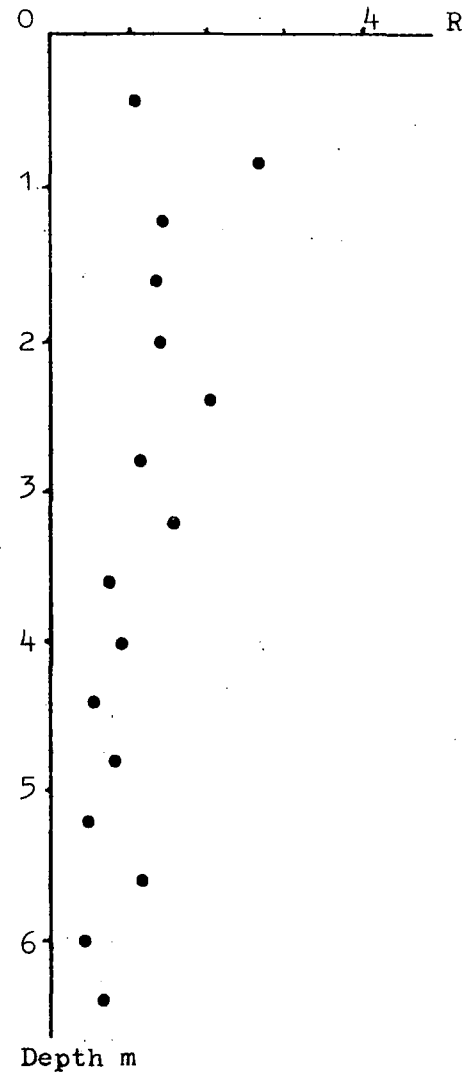
b. Location 1



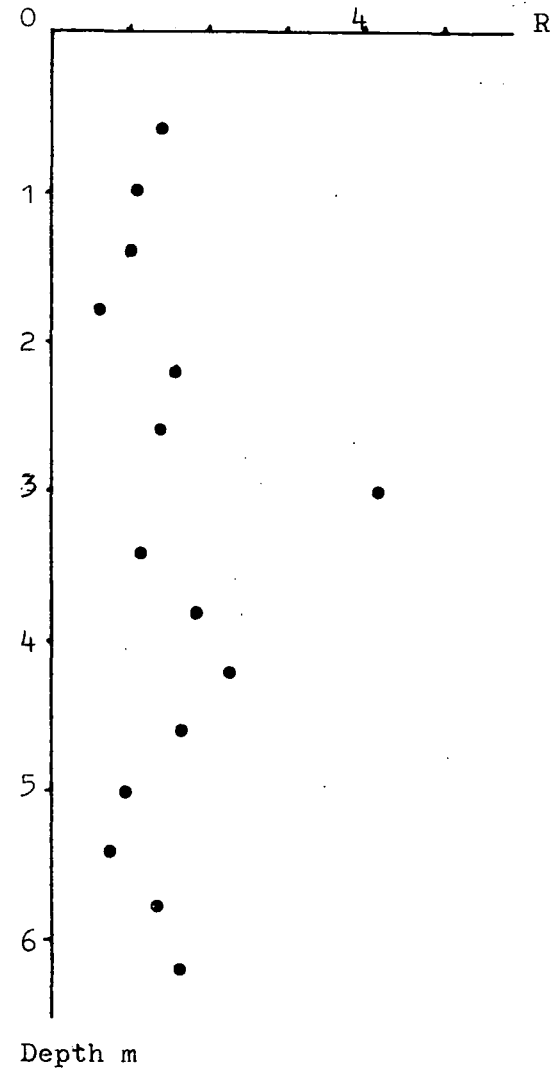
X Diamond, peak strength  
 + " remoulded  
 ● H=2D, peak strength  
 ○ " remoulded

Fig. 5.23 Rvalues Maltby lagoon 6.

a. Location 2



b. Location 1



R value is consistently very low at depths of greater than 3.5m. The reason for this is not known, though it may indicate that the H=2D vane was shearing both relatively strong and weak layers, while the diamond vane was situated mainly in the stronger layer.

This lagoon was the site of an overtipping trial (Chapter 7.2); samples were obtained both before and after tipping. Tests performed on samples obtained before tipping show that the finer material is behaving in a normally consolidated fashion (Fig.5.24.a) while the coarse material is showing a fairly loose behaviour (Fig.5.24.b). The effective cohesion intercept is zero in both cases. One sample indicated that there may be effective cohesion in some layers (Fig.5.24.c). However, this sample was composed of several layers of different characteristics and furthermore was extremely weak so consequently was heavily disturbed while being set up in the triaxial cell; this may explain the curious stress paths and apparent cohesion.

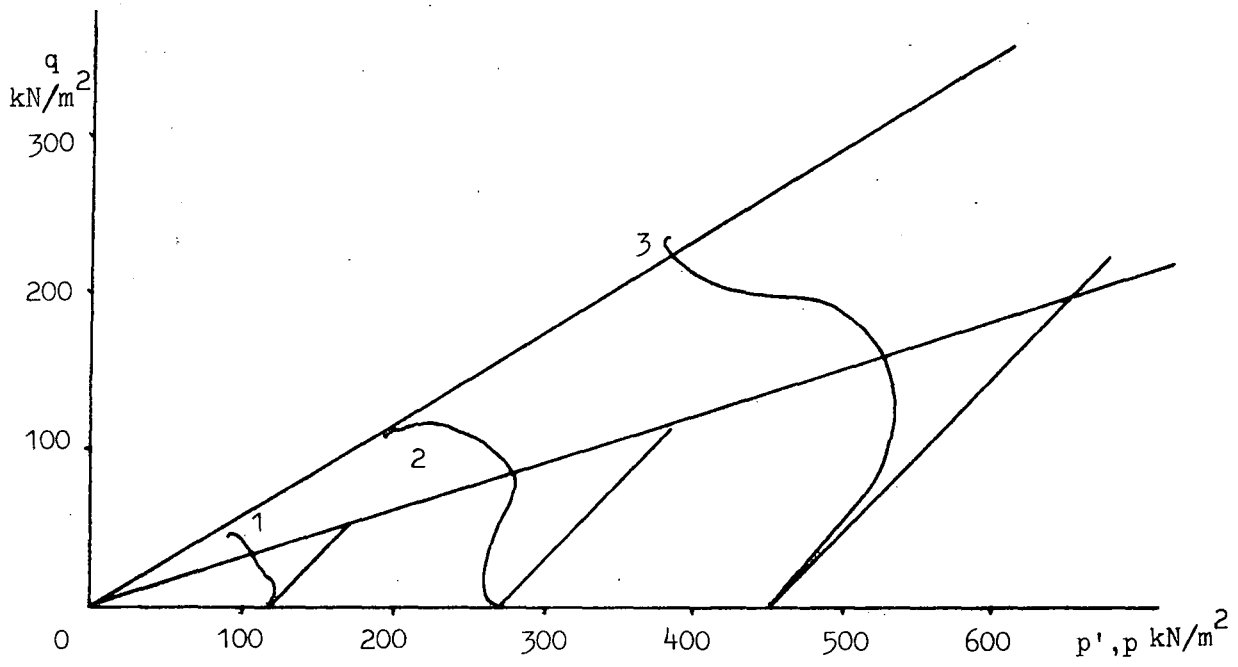
The emplacement of the embankment to a depth of 3.5 to 4 metres had the effect of increasing the overburden pressure at the sampling locations. In addition it was possible to obtain samples from great depths in the lagoon by using a shell-and-auger rig on the embankment. One consolidated-undrained triaxial test on a sample from 13.5m depth indicates that these deposits are indeed overconsolidated in terms of the stress path, and show effective cohesion; however, only one test was carried out on this material and the exact value of the cohesion is a little subjective (Fig.5.25.a). A coarser sample from 11.5 depth also exhibits fairly dense behaviour, though as expected the effective cohesion intercept is zero (Fig.5.25.b). The consolidating effect of the embankment is shown in Fig.5.25.c. This sample is from about 1 metre below the bottom of the embankment at location 1, and in the low



**Fig.5.24** Consolidated undrained triaxial tests on Maltby samples, prior to the overtopping of the lagoon.

a. Location 1, sample depth, 1.6m

	$c_v$ m <sup>2</sup> /yr	$e$	$E_s$ kN/m <sup>2</sup>	$p'_f$ kN/m <sup>2</sup>	$q_f$ kN/m <sup>2</sup>	S.G.=2.309	Organic carbon=18%
1	1.30	0.618	3917	92	47	$c'=0$	$\phi'=36^\circ$
2	2.63	0.595	6000	199	116	$c=0$	$\phi=18^\circ$
3	-	0.546	36150	381	236		



b. Location 2, sample depth, 1.1m

	$c_v$ m <sup>2</sup> /yr	$e$	$E_s$ kN/m <sup>2</sup>	$p'_f$ kN/m <sup>2</sup>	$q_f$ kN/m <sup>2</sup>	S.G.=1.907	Organic carbon=39%
1	1287	0.620	4780	158	86	$c'=0$	$\phi'=31.8^\circ$
2	3218	0.589	4540	209	109	$c=22$ kN/m <sup>2</sup>	$\phi=18^\circ$

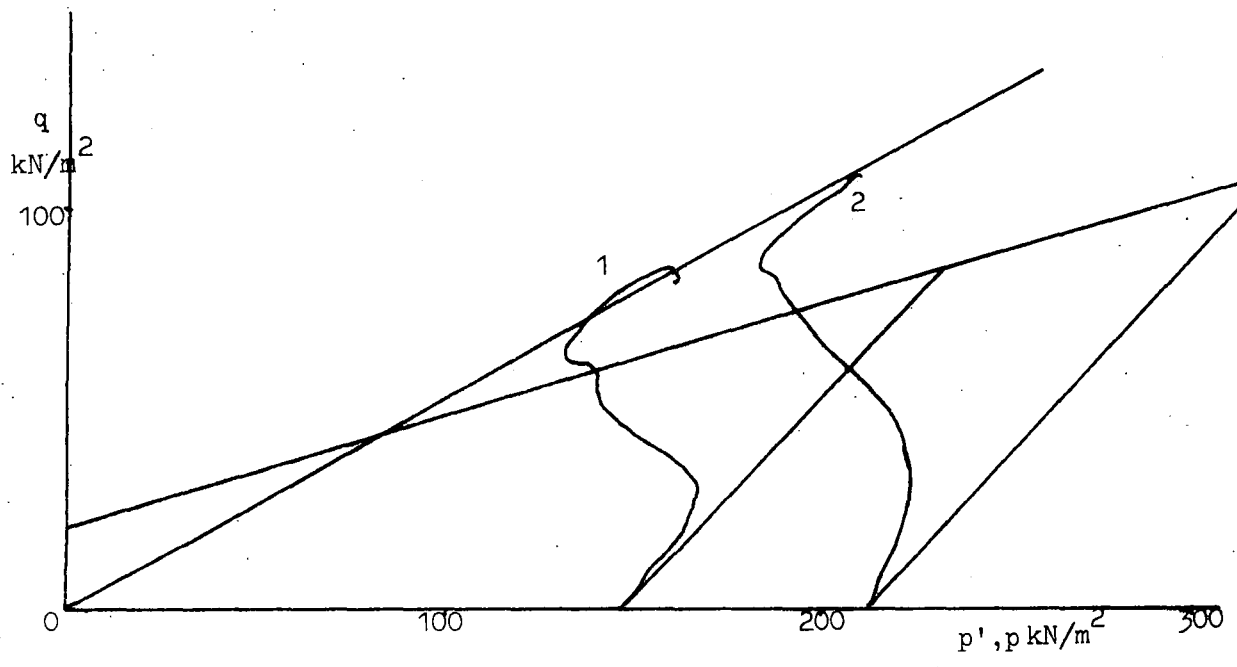
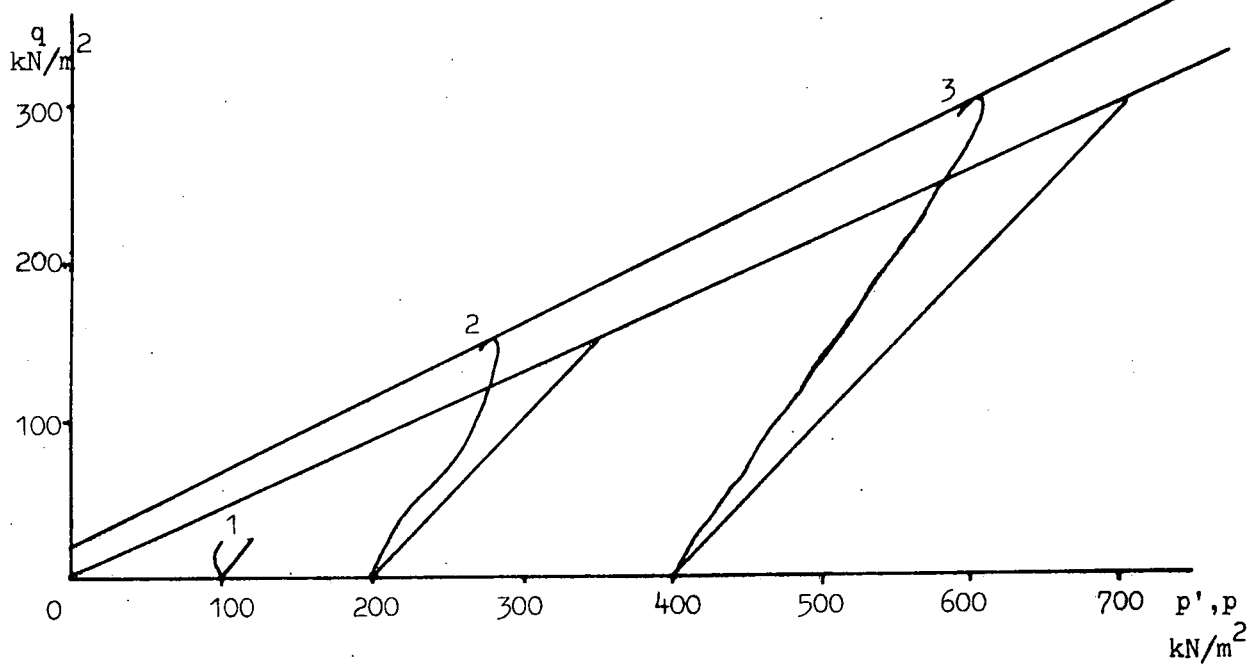


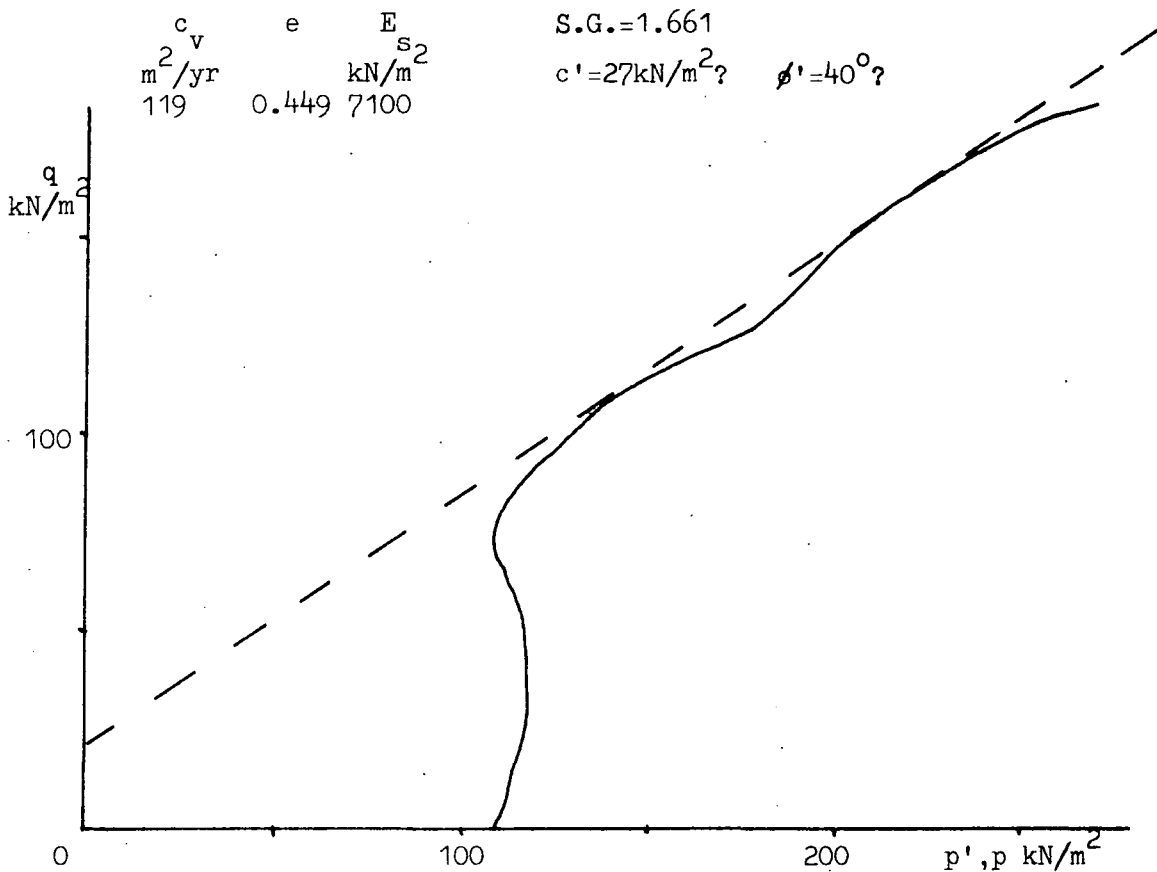
Fig.5.24.c Location 1, sample depth,0.93m

	$c_v$ $m^2/yr$	$e$	$E_s$ $kN/m^2$	$p'_f$ $kN/m^2$	$q_f$ $kN/m^2$
1.	24.4	0.72	600	100	27
2	14.5	0.71	3500	280	150
3	76.6	0.71	7200	605	302



exhibiting the dense behaviour due to overburden or overtipping.

a. Location 2, sample depth, 13.5m.



b. Location 2, sample depth 11.5m

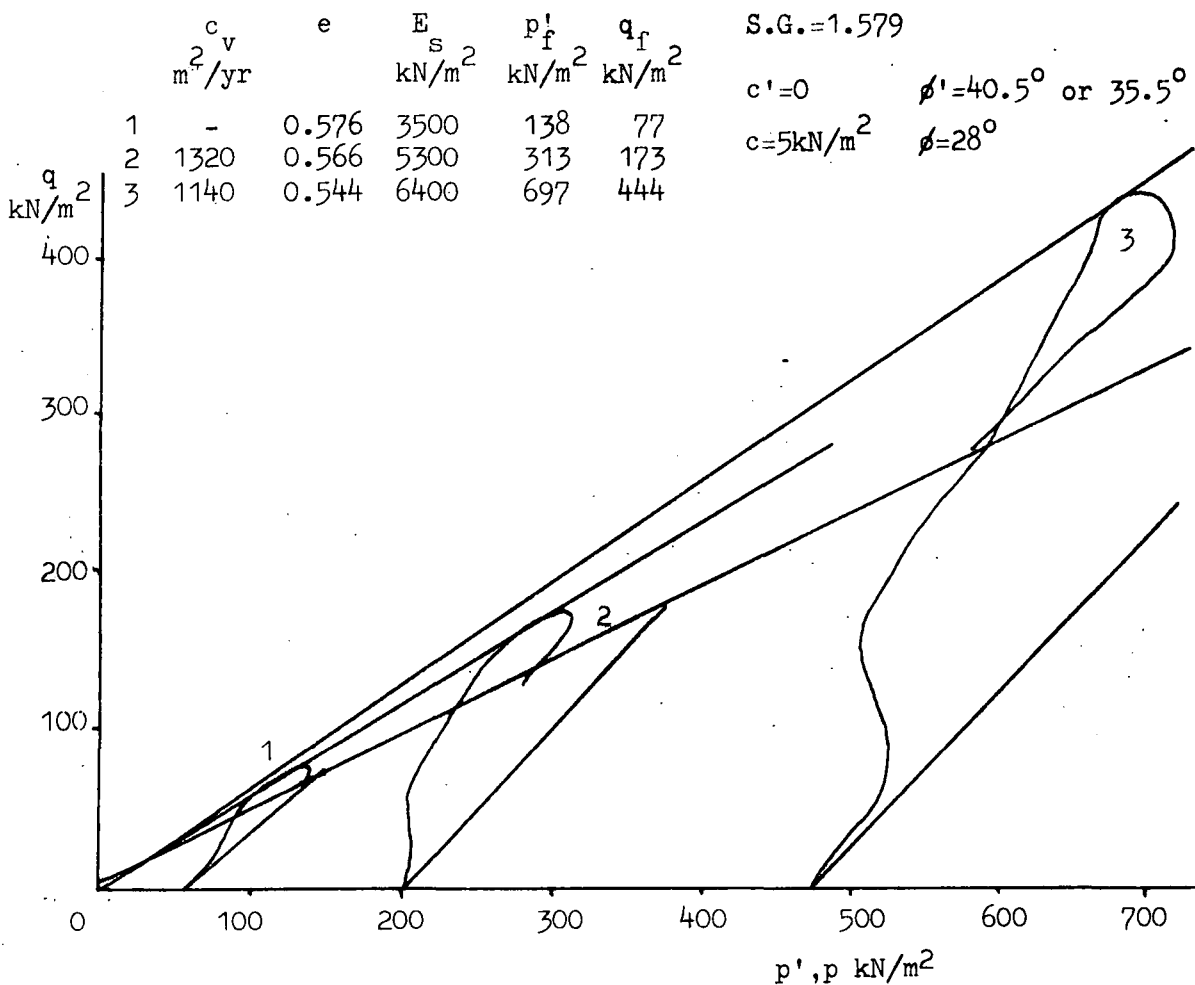
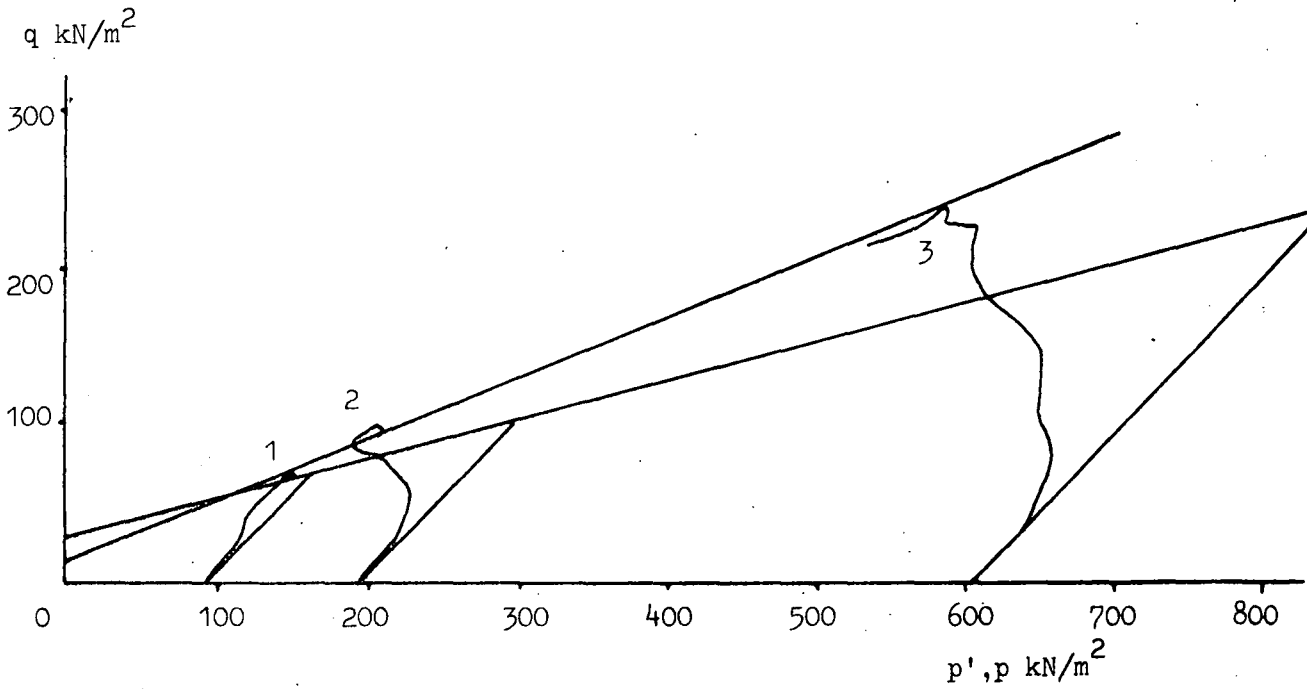


Fig.5.25.c.Location 1, sample depth, 4.0m (n.b. the depth of the embankment represents 3.4m of this)

	$c_v$ $m^2/yr$	$e$	$E_s$ $kN/m^2$	$p'_f$ $kN/m^2$	$q_f$ $kN/m^2$
1	18.6	-	2380	150	69
2	126.9	-	6400	206	100
3	53.6	-	28000	585	240



pressure tests exhibits overconsolidated behaviour and hence an effective cohesion of  $16\text{kN/m}^2$ .

### 5.7 Silverhill

Vane shear strength tests were carried out at Silverhill Colliery, lagoon No.16, while an overtipping operation was in progress (see Chapter 7.3). It is known that excess pore pressures existed widely over the lagoon at the time of this operation (Table 7.3). From Fig.5.26 it can be seen that in no case does the peak vane shear strength lie below the line representing relationship 2.Cobb (1977) however showed that this situation indicates excess pore pressures, and described a lagoon in which the minimum excess pore pressures are of the order of 2 metres head of water. Generally, the strengths at Silverhill are very weak; further discussion in the context of overtipping operations will be presented in chapter 7.3.

During the course of this investigation samples of a particularly fine-grained layer were obtained, together with coarser material immediately below. As was shown in Chapter 4 the fine grained material has a low organic carbon content (9%), whereas the coarser material is a coal-rich sediment (organic carbon is 83%) more typical of lagoon deposits. Consolidated undrained triaxial tests, Fig.5.27.a, show that the fine material has a very low effective angle of friction (22 degrees), but no cohesion as is expected from the normally-consolidated type of stress path. The angle of friction in terms of total stresses is also low at 14 degrees; again there is no cohesion. On the other hand, the coarser, coal-rich sediment exhibits stress paths indicative of a dense material, particularly at low cell pressures (Fig.5.27.b). As expected, the material is cohesionless and has a fairly high effective friction angle.

Fig.5.26 Vane shear tests in Silverhill lagoon 16.

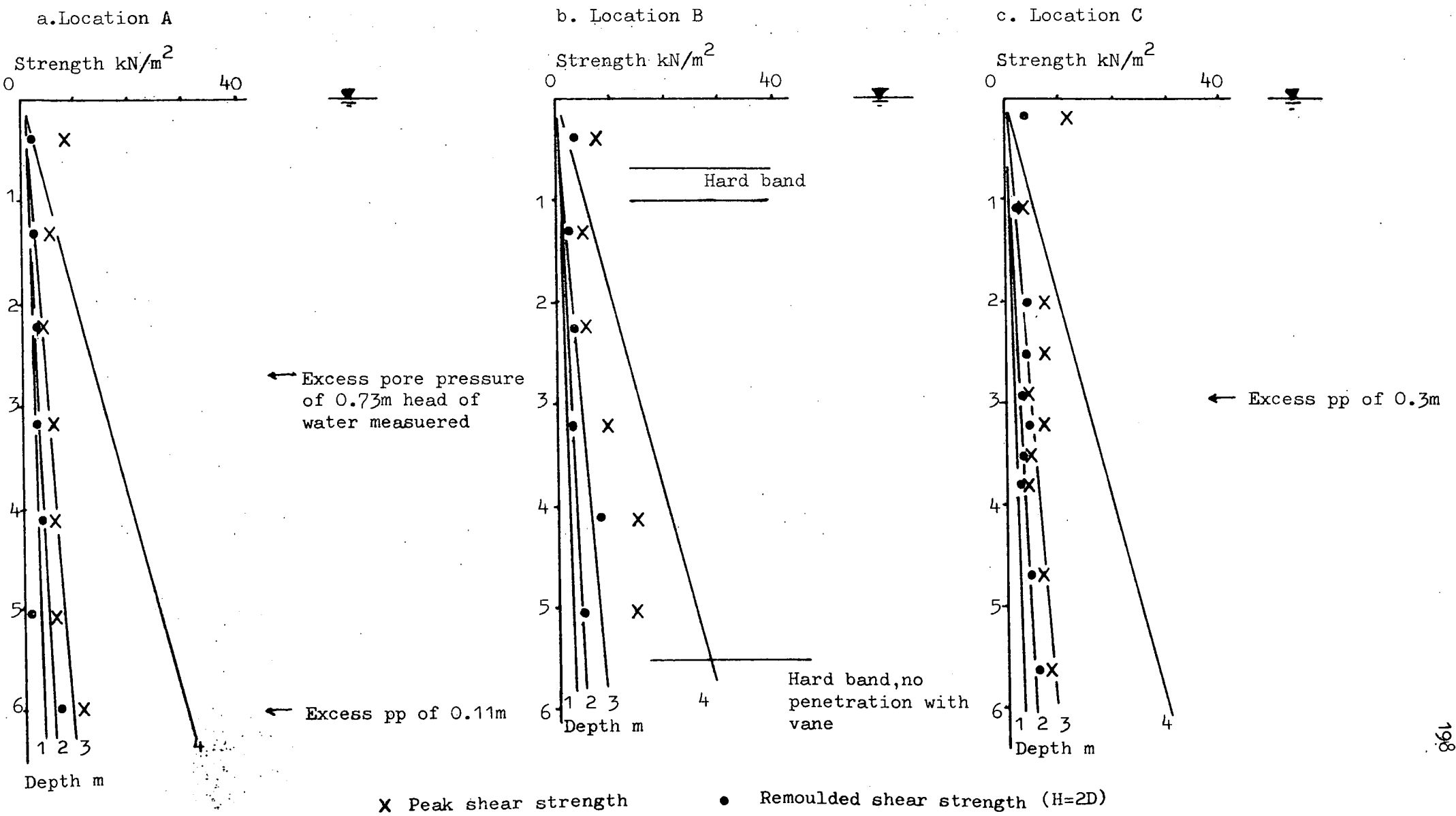
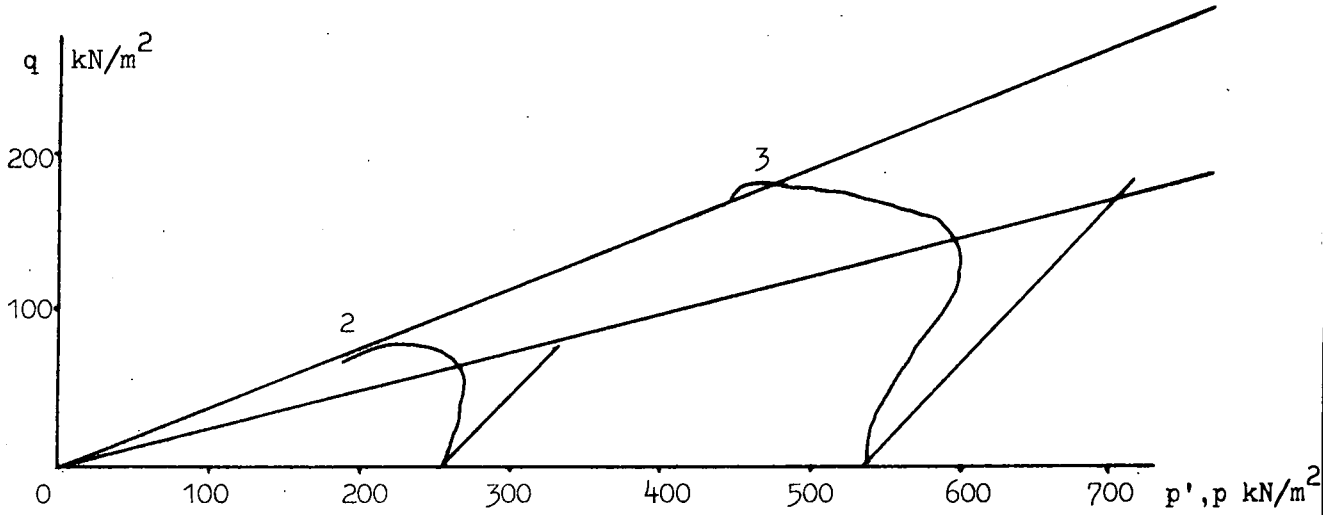


Fig.5.27 Consolidated undrained triaxial tests on Silverhill samples.

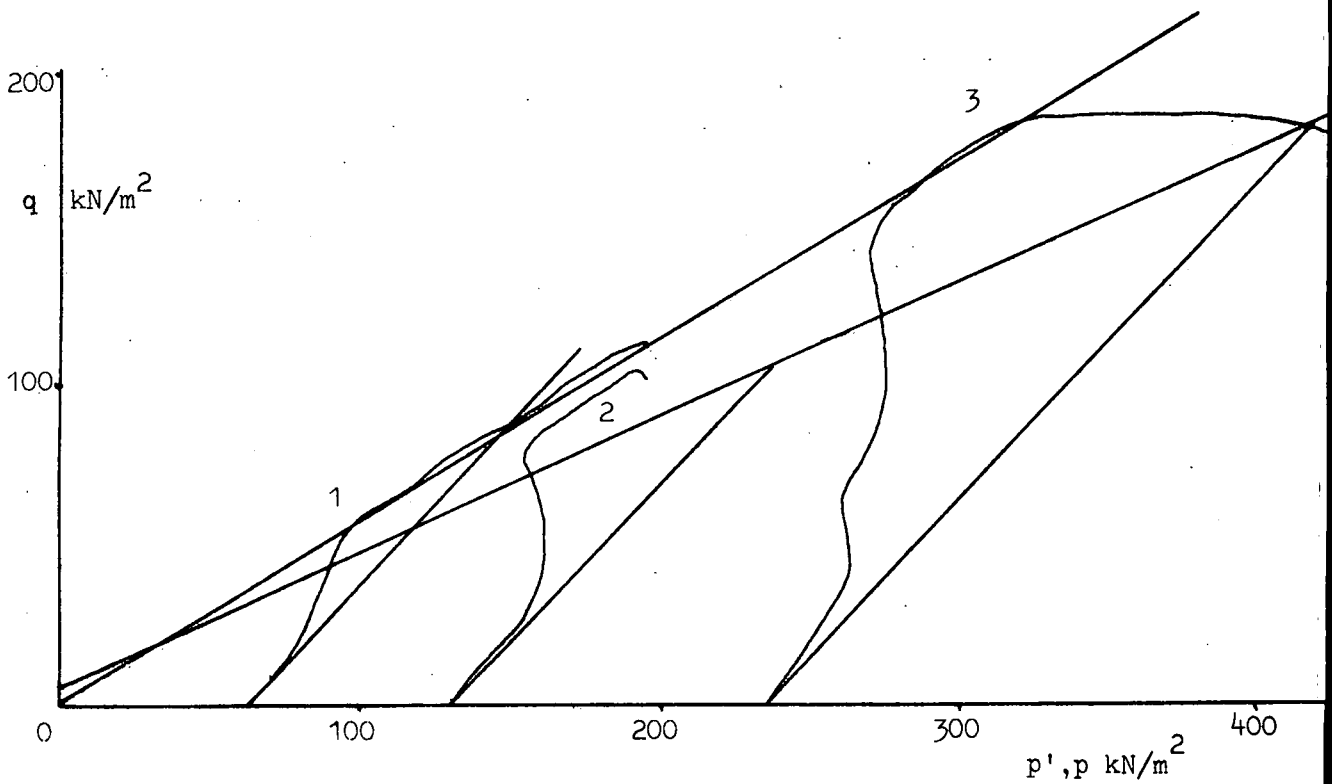
a. The clay band.

	$c_v$ m <sup>2</sup> /yr	e	$E_s$ kN/m <sup>2</sup>	$p'_f$ kN/m <sup>2</sup>	$q_f$ kN/m <sup>2</sup>	S.G.=2.476	Organic carbon=9%
1	5.5		failed			$c'=0$	$\phi'=22^\circ$
2	5.3	1.010	4600	220	77	$c=0$	$\phi=14^\circ$
3	4.4	0.971	8900	462	181		



b. Coarse layer.

	$c_v$ m <sup>2</sup> /yr	e	$E_s$ kN/m <sup>2</sup>	$p'_f$ kN/m <sup>2</sup>	$q_f$ kN/m <sup>2</sup>	S.G.=1.671	Organic carbon=8.3%
1	447	0.765	4200	194	115	$c'=0$	$\phi'=36^\circ$
2	-	0.775	5400	192	108	$c=5\text{kN/m}^2$	$\phi=26^\circ$
3	-	0.651	12700	321	188		



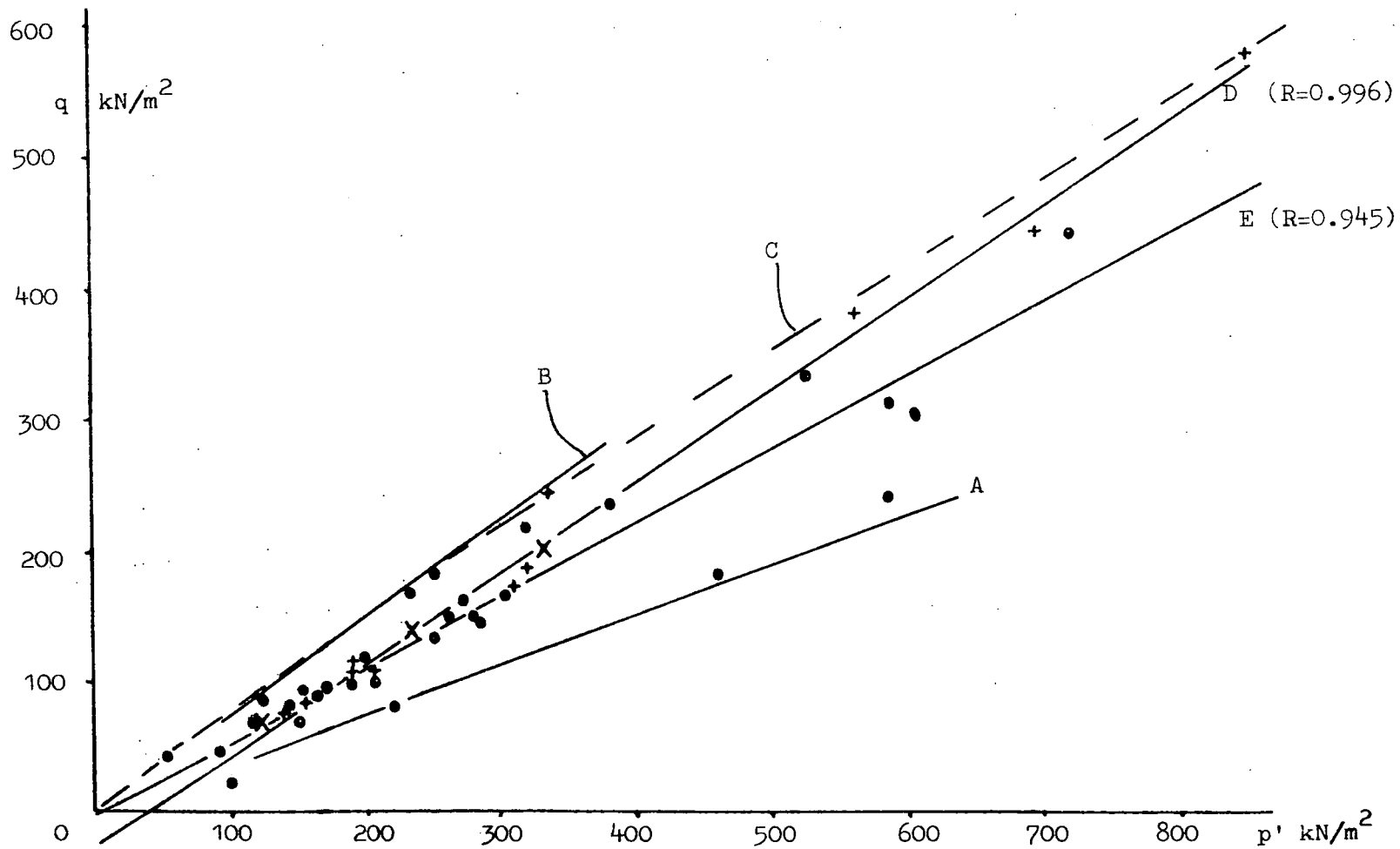
### 5.8 The Comparison of the Shear Strength of Coarse and Fine Discard

The effective stress failure points (i.e.  $p',q$ ) taken from all the triaxial tests presented herein are plotted together in Fig.5.28. All the points are bounded by envelopes equivalent to effective friction angles of 22 degrees and 49 degrees (lines A and B in Fig.5.28). There is, however, a suggestion that the top failure envelope is curved (line C). Curvature has been suggested for the less brittle coarse colliery discard shear strength envelopes, Taylor and Cobb (1977). Lines D and E represent the best fit regression lines (reduced major axis) for the coarser, coaly samples and the finer, less coaly samples respectively. The slopes of the two lines are different at the 99.99% significance level, the coarser material being the more frictional. However, both lines have negative intercepts, probably because the  $p',q$  points are derived from different samples; therefore the statistical inference must be treated with caution. Both lines represent friction angles higher than the mean angle for coarse colliery discard, which is 32.4(Taylor and Cobb, 1977). This possibility has been noted before (McKecknie Thomson and Rodin, 1972), and is probably due to the higher coal content of fine colliery discard (see chapter 4.11). McKecknie Thomson and Rodin also pointed out that the effective friction angle of tailings and slurry is inversely related to the proportion of fines in the sample. The coal content is also inversely proportional to the fines content (see chapter 4.6), and hence the same conclusion is reached: i.e. that coaly tailings are more frictional than non-coaly tailings and both are generally a little more frictional than coarse discard. This supports the conclusions of Taylor (1974) that the coal content exerts a fundamental influence on the effective friction angle. However, it should be emphasised that for both coarse and fine discard there is a significant spread of the



Fig.5.28 Effective stress failure points for lagoon sediments.

- + Coarse coaly samples (pl74, MA/2/11.5, MA/1/1.1, SI coarse)
- X Coarse non-coaly samples (EH beach)
- Fine grained samples(others)



effective friction angles, from about 22 degrees to 45+ degrees (the upper limit is difficult to define due to the curvature of failure envelopes).

Coarse colliery discard is almost universally accepted as a cohesionless material (see the various contributions to the discussion of McKecknie Thomson and Rodin, 1972). However, several fine-grained samples tested from lagoons have shown the effective cohesion, combined with stress paths typical of overconsolidated, clay-rich material. The clearest example is that of the clay from lagoon 6 at Peckfield, Fig.5.16. More work is required on this subject to establish the nature and extent of the effect; in particular low-pressure, consolidated-undrained triaxial tests should be undertaken. However, it seems reasonable to suppose that it is the clay content that is producing the effect when the material is buried at depth or alternatively desiccated at the surface.

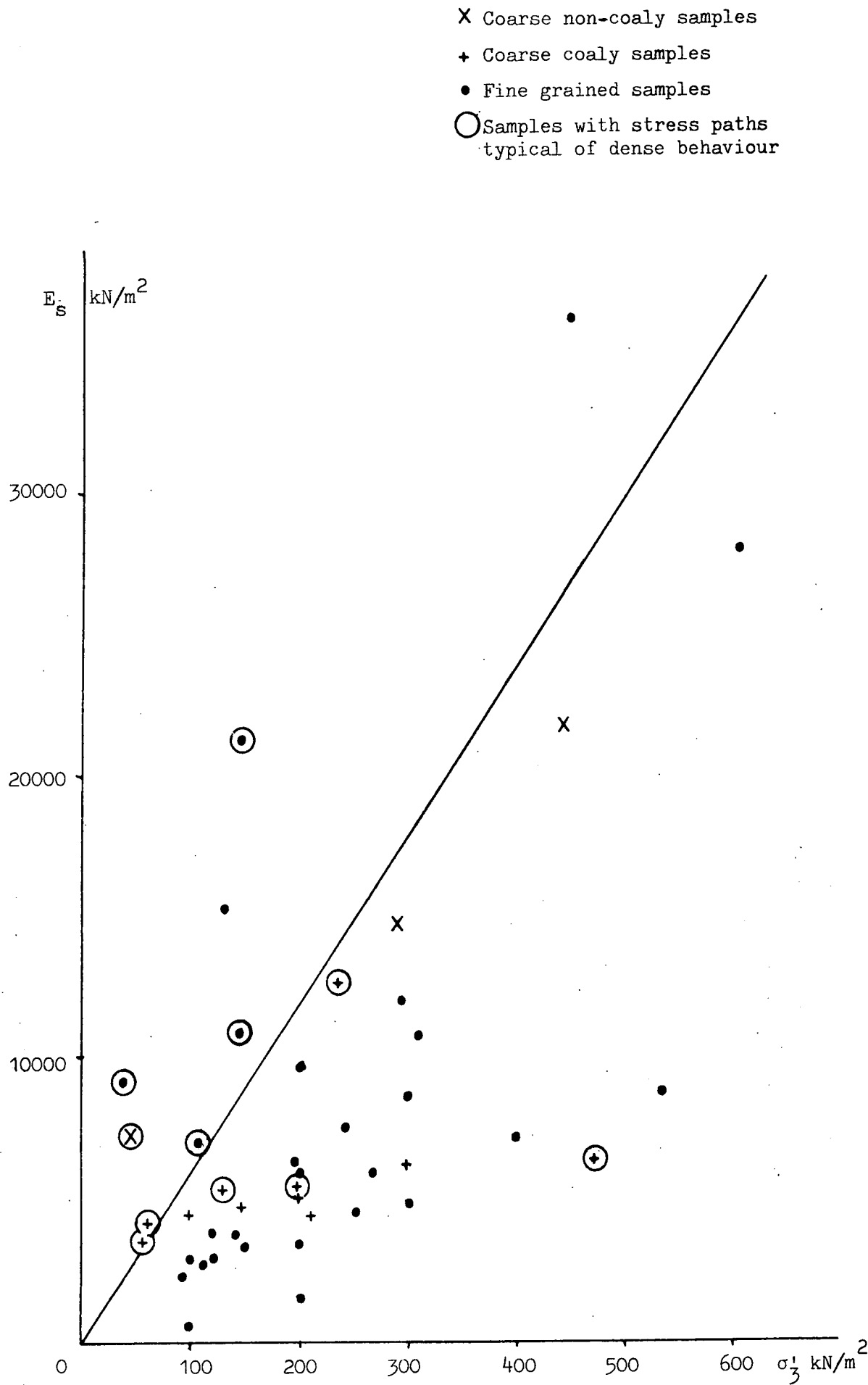
#### 5.9 A Note on the Young's Modulus of Fine Colliery Discard

The Young's modulus ( $E_s$ ) has been taken as the secant modulus to half peak deviator stress (i.e.  $\frac{1}{2}(\sigma_1 - \sigma_3)_f$ ). All the values, which are tabulated on each of the figures referring to triaxial tests, have been plotted on Fig.5.29. Scheidig (1931) showed that (see Terzaghi and Peck, 1948)

$$E_i = C \cdot \sigma_3' \quad \text{where } E_i \text{ is the initial tangent modulus.}$$

In other words, the Young's modulus of the material is directly proportional to the effective cell pressure. For loose material the value of C is approximately 100; for coarse discard from an ancient spoil heap Taylor (1971a) showed this value to be 95.4. Taylor further showed that  $E_s = 0.6 \times E_i$  at the 99.9% significance level, or in other words that for the secant modulus the value of C is 60. This relationship has been plotted as line A in Fig.29. It can be seen that in general the values

Fig.5.29, Young's Modulus from triaxial tests on lagoon sediments.



increase with the applied cell pressure, but fall well below this line. However, in the case of dense or overconsolidated materials the values are nearer to the line, and often above. Thus the low value of Young's modulus of normally consolidated lagoon sediments may be due to the very loose nature of the deposits.

#### 5.10 The Coefficient of Earth Pressure at Rest ( $K_0$ )

Figures 5.30.a-d show the results of a number of  $K_0$  tests plotted as paths in  $\sigma_3'$  versus  $\sigma_1'$  space. From this limited number of tests, no difference can be discerned between lagoons, or between materials within any one lagoon. Taken as a whole, the tests indicate a mean  $K_0$  value of 0.533, with a standard deviation of 0.080. The value of  $K_0$  is significant in triaxial, cyclic loading liquifaction studies, because the value of a correction factor for the triaxial stress ratio is dependent upon the value of  $K_0$ . Taylor et al. (1978) assumed a value of 0.4 to 0.5 for the  $K_0$  of colliery tailings lagoons, which compares with the values reported herein.

#### 5.11 Conclusions

In chapters 3 and 4 it was shown that colliery waste lagoons are layered sedimentary bodies in which there is a general trend for coarser particles to settle out near to the inlet. In chapter 4.7 it was shown that the sediments are composed of three groups of minerals; firstly, coal with pyrite; secondly, quartz, kaolinite and illite; thirdly, other minerals, the main one being ankerite. It was further shown that the coal content is related to the grain size of the sediments, coarser laminae being richer in coal. The third group of minerals is quantitatively less important than the first two.

In this chapter it has been shown that the coal content is positively correlated to the effective friction angle. Coal has a low specific gravity (about 1.3), while the clay group has a specific gravity of about

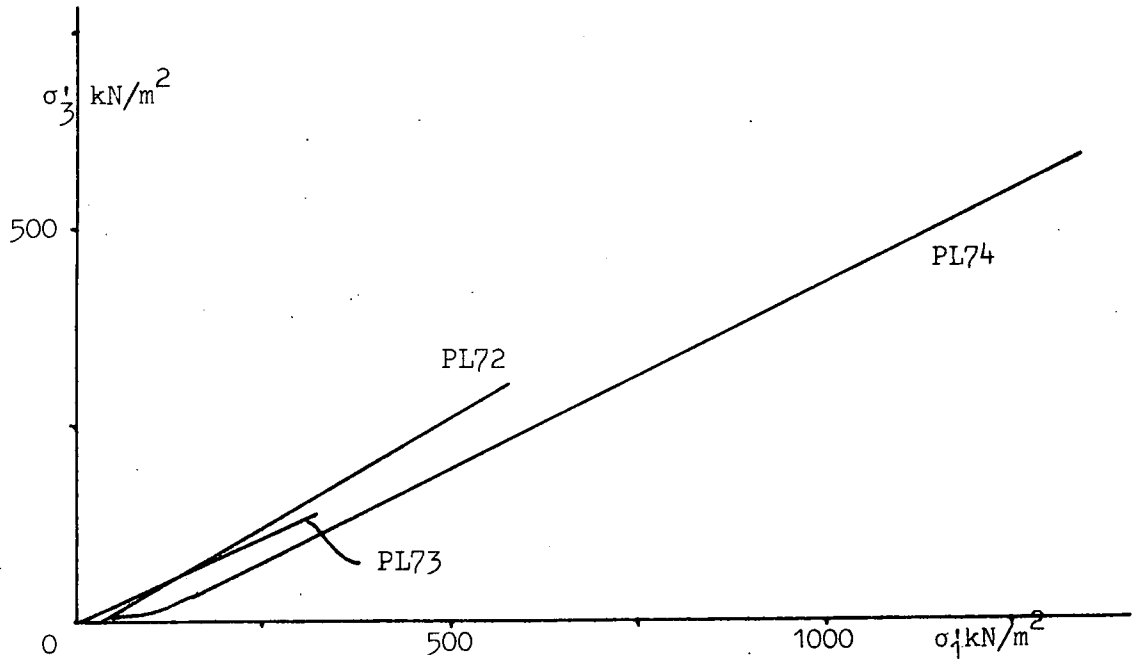
Fig.5.30  $K_o$  tests on lagoon sediments.

a. Peckfield

PL73  $K_o = 0.43$

PL72  $K_o = 0.545$

PL74  $K_o = 0.513$



b. East Hetton

1 Sandy  $K_o = 0.454$  (laboratory fabricated specimen)

2 Very coarse  $K_o = 0.600$

3 Silty  $K_o = 0.550$

4 Fine grained  $K_o = 0.545$

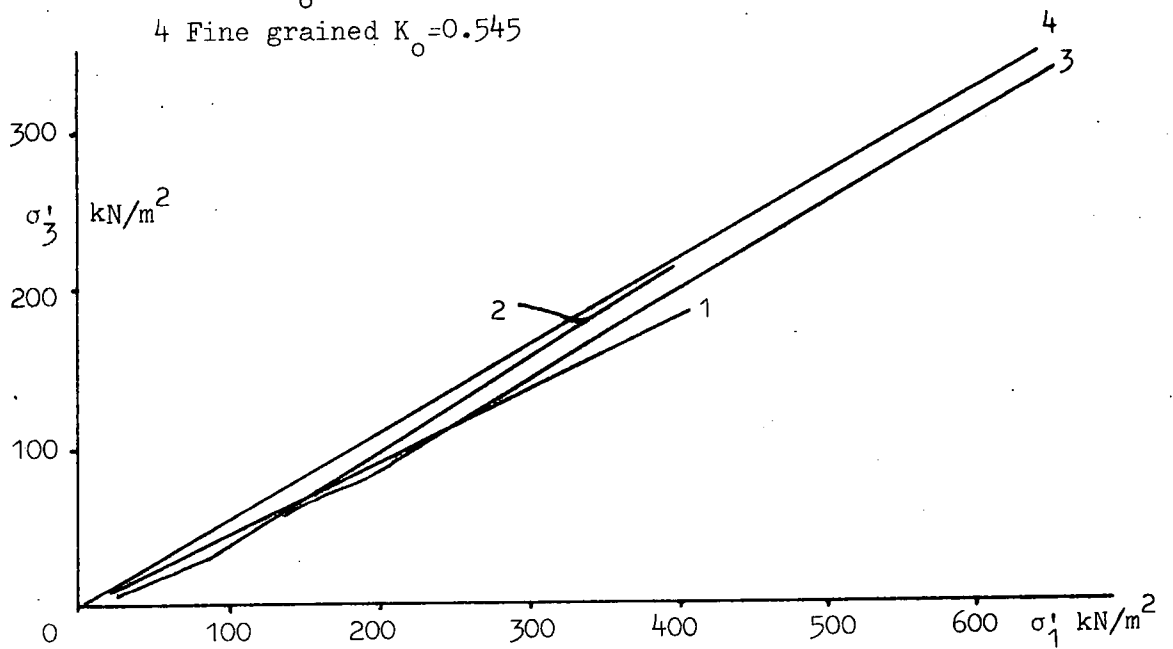
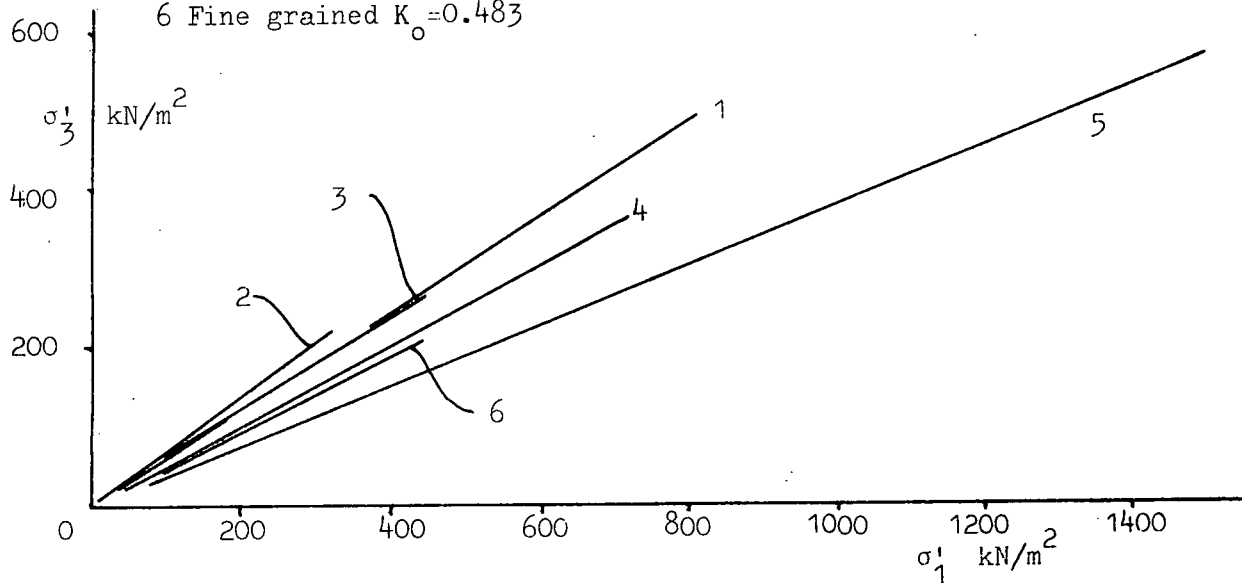
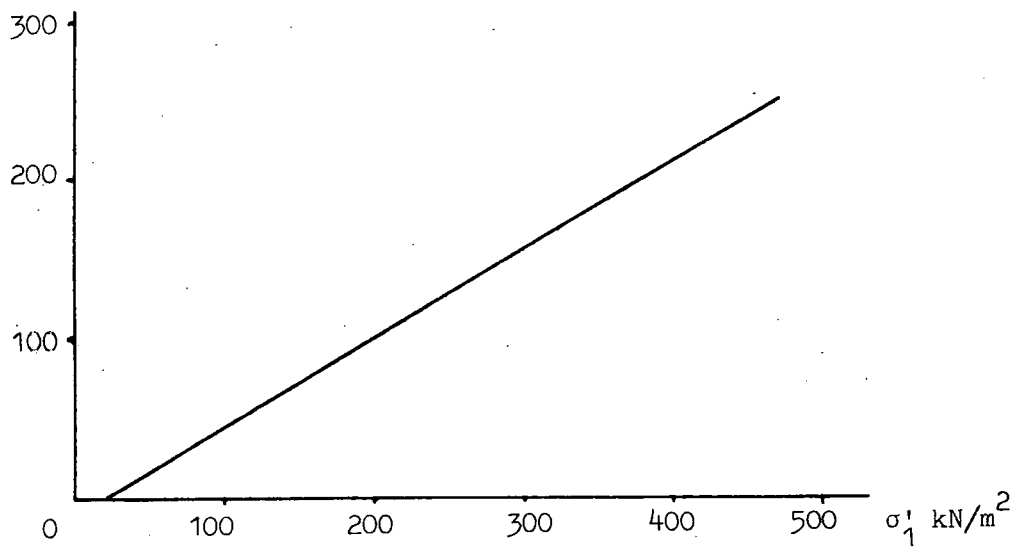


Fig.5.30.c.Maltby

- 1 Mixed layers  $K_o=0.611$
- 2 Mixed layers  $K_o=0.700$
- 3 Mixed layers  $K_o=0.573$
- 4 Coarse  $K_o=0.503$
- 5 Fine grained  $K_o=0.387$
- 6 Fine grained  $K_o=0.483$



d. Gedling  $K_o=0.559$



2.65. Thus it has been found that the coarser, more coaly layers are the more frictional and less dense materials. Finer-grained laminae exhibit lower effective angles of friction, and have higher bulk and dry densities; furthermore, they show higher natural moisture contents and liquid limits due to the higher clay contents.

The coal content of lagoon sediments is generally higher than is found in coarse discards and the effective friction angle is found to be higher, particularly in the case of the coarser, more coaly laminae from lagoons. However, some laminae with low coal contents display effective friction angles of as low as 22 degrees. In contrast to coarse colliery discard which is a cohesionless material, overconsolidated or desiccated lagoon sediments with an appreciable clay content may display true effective cohesion. More low pressure consolidated - undrained triaxial tests are required to define the extent of this effect.

The field vane shear test has been shown to measure the drained strength of the coarser laminae, but in finer-grained laminae the undrained strength is being measured. Since the coarser laminae are the more frictional, and the proportion of coarse laminae falls with distance from the inlet, there is a general fall in vane shear strength across a lagoon.

Cobb (1977) showed that the remoulded vane shear strength of lagoon sediments is related to the plasticity index by:-

$$\frac{c}{p'} = 0.11 + 0.0037 \text{ PI}$$

Furthermore, the peak shear strength will be defined by:-

$$\frac{c}{p'} = \tan \phi$$

or

$$\frac{c}{p'} = \tan \phi'$$

depending on whether the undrained strength of a fine-grained lamination,

or the drained strength of a coarse-grained lamination is being measured. If the vane is partly shearing two laminae of different drainage characteristics the measured shear strength will be intermediate between the two. These three relationships can be used to extract useful information concerning the deposits in a lagoon. If the peak shear strength lies below the remoulded strength relationship, then excess pore pressures are suspected but by no means certain; piezometers should be installed to confirm such a diagnosis. Should the peak shear strength conform to either the second or third relationships consistently into depth, then a deposit dominant in fine-grained or coarse grained laminae may be expected. In the case of Peckfield lagoon 7, it was possible to correlate both relationships to finer and coarser laminae within the deposit. However, values of shear strength intermediate to the two relationships are more usually found, in which case no positive diagnosis is possible.

It has been shown that the use of paired vane tests allows the shear strength anisotropy to be measured. A vane of  $H=2D$  shape and a diamond vane with  $H = 0.25D$  are well suited to this task in layered media. Both in the field and in the laboratory it has been found that lagoon sediments are generally stronger when sheared across the laminae than along them, by a factor of between 1.2 and 2.2. Very high or low values of  $R$  indicate laminae of markedly different properties are in juxtaposition.

Finally, it has been shown that the coefficient of earth pressure at rest is about 0.5 for lagoon deposits.



## CHAPTER 6      THE CONSOLIDATION AND DRAINAGE OF COLLIERY TAILINGS LAGOONS

### 6.1 Introduction

The consolidation and drainage characteristics of a lagoon will exert a controlling influence on the sediments in the lagoon. If a lagoon drains freely it will gain strength and increase in resistance to liquefaction; it will be easier to excavate or overtip; it will be more marketable if it is to be sold as a low-grade fuel source. Two main factors can influence the consolidation and drainage characteristics of a lagoon. These are firstly, the consolidation characteristics of the sediments in the lagoon; and secondly, the permeability of the floor and embankments of the lagoon. This work concentrates on the former, but the effects of the latter are considered.

It was shown in chapters 3.4, 4.6, 4.7 and 5.4 that lagoons are layered sedimentary bodies, in which the layers may vary from silty clays to coarse sands. The fine layers can be expected to be relatively impermeable, while the coarser layers will be relatively permeable. Therefore, it will be the distribution of the laminations and in particular the lateral extent of individual laminae that will govern the drainage of the lagoon. It has been shown (chapters 3.4 and 4.7) that individual laminations are not necessarily extensive laterally, and may well wedge out.

Previous work on the consolidation and drainage of lagoons has stressed both the importance, and the lack of, in-situ permeabilities (National Coal Board, 1972). In-situ permeabilities ranging from  $3.6 \times 10^{-5}$  to  $1.0 \times 10^{-8}$  m/s are reported. The superiority of in-situ test results over permeability measurements from laboratory tests has been noted by Murray and Symons, 1974. National Coal Board, 1972, also report

results of oedometer tests in which the  $c_v$  of lagoon sediments was found to vary from 2 to 27  $m^2/yr$ . It was also shown that, although older, loose-tipped coarse discard embankments are relatively permeable, modern thin-layer compaction techniques produce embankments with permeabilities ranging from  $3.1 \times 10^{-4}$  to  $9.5 \times 10^{-9}$  m/s.

Cobb (1977) concludes that  $c_v$  decreases from the inlet to the outlet of lagoons, whereas  $m_v$  remains fairly constant. It was also found that embankment interfaces could be highly impermeable ( $10^{-12}$  m/s), presumably due to entrainment of fines from the lagoon. Cobb (1977) further concludes that the large Rowe cell is to be preferred to the oedometer for consolidation tests due to the fact that the latter contains a sample thinner than the average thickness of laminations within the lagoon, and the tendency therefore to give low values of  $c_v$ . This effect has been noted before by Rowe and Barden (1966).

## 6.2 Theoretical Considerations

The consolidation of layered media has received attention from a number of authors. Schiffman and Stein (1970) show that one-dimensional consolidation is given by:-

$$u = \frac{c(t)}{cr}$$

where  $u$  is the degree of consolidation

$\rho_c(t)$ , the consolidation settlement is given by

$$q(t) \sum_{l=1}^n m_v^l h^l - \sum_{l=1}^n m_v^l h^l u^l(z,t) dz$$

$\rho_{cr}$  is a reference settlement and is given

$$\text{by } \rho_{cr} = \frac{\bar{q}}{\bar{q}} \sum_{l=1}^n m_v^l h^l$$

and  $q(t)$  is the load at time  $t$

$\bar{q}$  is a reference load

$m_v^l$  is the coefficient of volume compressibility of layer  $l$

$L^l$  is the height (thickness) of layer  $l$ .

$U^l(z,t)$  is the excess pore pressure of layer  $l$ , at height  $z$  and time  $t$

Essentially, therefore, the overall one-dimensional consolidation of the system is a series summation of the settlement characteristics of each layer ( $\sum_{l=1}^n m_v^l h^l$ ), the time aspects of which are governed by the pore pressure dissipation of the layer ( $u^l(z,t)$ ). The laminae with the lowest coefficients of consolidation will therefore control the overall rate of pore pressure dissipation.

Horne (1964) develops solutions for the consolidation of soil consisting of horizontal layers of low permeability interspersed by thin layers of high permeability, for the case of horizontal drainage. He shows that when

$$\frac{L^2}{H_1 H_2} \cdot \frac{k_{z1}}{k_{x2}}$$

is above a value of 1, then the rate of dissipation of pore pressure is increased by

$$\frac{k_{x1} H_1 + k_{x2} H_2}{k_{x1} H_1}$$

where  $L$  = horizontal drainage path length

$H_1, H_2$  are the laminae thicknesses ( $H_1 \gg H_2$ )

$k_{x1}, k_{x2}$  are the horizontal permeabilities.

$$(k_{x1} \ll k_{x2})$$

$k_{z1}$  is the vertical permeability of the less permeable laminae.

It will be seen in the following sections of this chapter that  $\frac{k_{z1}}{k_{x1}}$  is of the order of  $10^{-5}$ . However, even for a narrow lagoon  $\frac{L^2}{H_1 H_2}$  will be  $10^5$  or greater. For example, a lagoon 60m wide (i.e.  $L = 30m$ ), with  $H_1 = 0.1m$  and  $H_2 = 0.01m$  (in order that  $H_1 \gg H_2$ ),  $\frac{L^2}{H_1 H_2}$  is  $10^6$ ; the increase in the rate of dissipation of pore pressure is approximately 10000 times. Were the layers of more equal thickness ( $H_1 \approx H_2$ ) as would be expected in lagoons the rate of increase in dissipation would be greater, but the solution would no longer apply. Nevertheless, it is clear from Horne's work that consolidation in layered lagoon sediments is controlled by the

characteristics of the most permeable layers, providing that horizontal drainage can occur. Thus lateral continuity of the laminae is assumed. Rowe (1959) also demonstrates the importance of highly permeable laminae in controlling the consolidation of stratified soils.

The conclusion that impermeable laminae control vertical drainage and permeable laminae control horizontal drainage is also reached when considering the permeabilities of layered media. In this case the standard series and parallel resistance laws apply (see Terzaghi and Peck, 1948). In the case of the permeability measured in a vertical direction:-

$$k_v = \frac{H}{\frac{h_1}{k_1} + \frac{h_2}{k_2}} \text{ ----}$$

$k_v$  is the total vertical permeability

$k_1, k_2$  are the permeabilities of individual laminae

$h_1, h_2$  are the thicknesses of the laminae

$H$  is the overall thickness of the system.

In other words, the overall vertical permeability is a series summation of the permeabilities of the laminae. If the permeability contrast is very great, the overall permeability is governed by the least permeable laminae. In the case of permeability measured in a horizontal direction:-

$$k_h = \frac{1}{H} (h_1 k_1 + h_2 k_2 \text{ ----})$$

$k_h$  is the overall horizontal permeability.

The overall horizontal permeability is between the extremes of permeability of the individual laminae. However, when the permeability contrast is great, the overall permeability is governed by the more permeable laminae. This again refers to laminae that are continuous in a horizontal direction.

The problem of consolidation and drainage of colliery lagoons is therefore dependent upon the distribution of the laminae within it.

Consequently, it is necessary to measure the characteristics of individual laminae. Providing that the distribution of all the laminae are known in three dimensions, the overall characteristics of the lagoon can be assessed.

The type of consolidation that is outlined above applies when a superincumbent load is placed on the consolidating material. In terms of colliery lagoons this might be analogous to overtipping. However, during the active period of a lagoon, and subsequently until the lagoon is overtipped or excavated, this is not the process that is operating. Gibson (1958) presents a solution for one-dimensional consolidation of an accumulating deposit. The deposit consolidates under its own weight while it remains submerged, and actually becomes less consolidated with the progress of time. ( This is because upon the settling of the first grain no water need escape and the deposit is thus 100 per cent consolidated. As sedimentation continues, a gradient of pore water pressure is established throughout the deposit, and the material is thus less than 100 per cent consolidated). Upon cessation of sedimentation the excess pore water pressures can be quite considerable, and their decay can take a long time. Higher excess pore water pressures are generated by faster sedimentation rates, lower coefficients of consolidation and deeper lagoons. The magnitude of the excess pore water pressures and the time required for dissipation can be read from graphs presented by Gibson (1958). Mittal and Morgenstern (1976) present data from metal mine slimes ponds to prove the presence of these excess pore water pressures. However, these occur in lagoons that are some hundreds of metres in diameter, between 30 and 50 metres deep accumulating at 6 to 9 metres per year, and with coefficients of consolidation of between 3 and  $16 \text{ m}^2/\text{yr}$ . British colliery tailings lagoons are in general smaller, shallower, accumulated more

slowly and due to the presence of more permeable layers, have higher values of  $c_v$ .

In contrast to Gibson's model, Krizek and Castelleiro (1977) show that traditional consolidation models severely underestimate the settlement and consolidation in lagoons due to the effect of desiccation at the surface. This effect is of greater importance than the permeability of the floor; for instance they demonstrate that a small increase in the evapotranspiration potential can increase settlement by up to 30 per cent, whereas the change from an impermeable to a permeable floor increases the settlement by only 3 per cent. This process certainly affects much of the area of many of the lagoons in this country, although permanent free standing water exists over most of the area of active lagoons. Inactive lagoons often dry out completely, at least over the summer months.

### 6.3 The Measurement of Consolidation Parameters

In chapters 3, 4 and 5 it was shown that there exists within most lagoons a large number of laminations with widely differing properties. In the previous section it was pointed out that the consolidation and drainage characteristics of the whole lagoon will depend on the properties of the individual laminae in the lagoon. Therefore it is logical to test the consolidation parameters of individual laminae, and attempt to assess the distribution of the laminae in the lagoon. Since many laminae are very thin, this usually necessitates the use of the oedometer. This is in direct contrast to the recommendations of Cobb (1977), who preferred to use a large Rowe cell. However, the Rowe cell will give consolidation parameters representative of the lagoon only if the laminae in the Rowe cell are present in the same proportions as in the field. It is the writer's opinion here that such an occurrence would be somewhat

fortuitous.

Rowe (1959) showed that the variation in  $c_v$  over a large number of tests is quite high. In order to check the variation of  $c_v$  and  $c_r$  (vertical and radial coefficients of consolidation), a number of tests were carried out on some material from the lagoon on the west tip at Gedling Colliery, South Nottinghamshire Area, NCB. The materials from this lagoon is a visually homogenous, clayey silty sand; the grading curve is given in Fig.6.1.

The full results of the consolidation tests are given in Appendix 6.1, the  $c_v$  values being summarised in Table 6.1. From the table it can be seen that there is a variation in  $c_v$  from 8.8 to 31.8. The average values show that there is an increase in the measured  $c_v$  from the oedometer via the 6 inch Rowe cell to the 10 inch Rowe cell. However, a close inspection of the results of the oedometer tests show that this variation is due, at least in part, to variations in the tailings. The greater thickness of material being tested by the larger Rowe cells has increased the likelihood of a more permeable layer being tested, hence the higher average  $c_v$ . However, the difference between the average  $c_v$  as measured by the 10 inch Rowe cell and the oedometer is less than the variation within the material. The oedometer is to be preferred for measuring this variation in finely layered media.

The consolidation tests with drainage to a peripheral radial well also show great variation in the measured consolidation coefficient. Again there is a suggestion that this may be due to variation within the tailings itself. The variation in the values of  $c_r$  is greater than any difference between the rates of consolidation in the two different directions. It is therefore more useful to measure only the vertical consolidation parameters of different layers than it is to measure the vertical and

Fig.6.1 Grading curve of Gedling Tailings from lagoon 12/8.

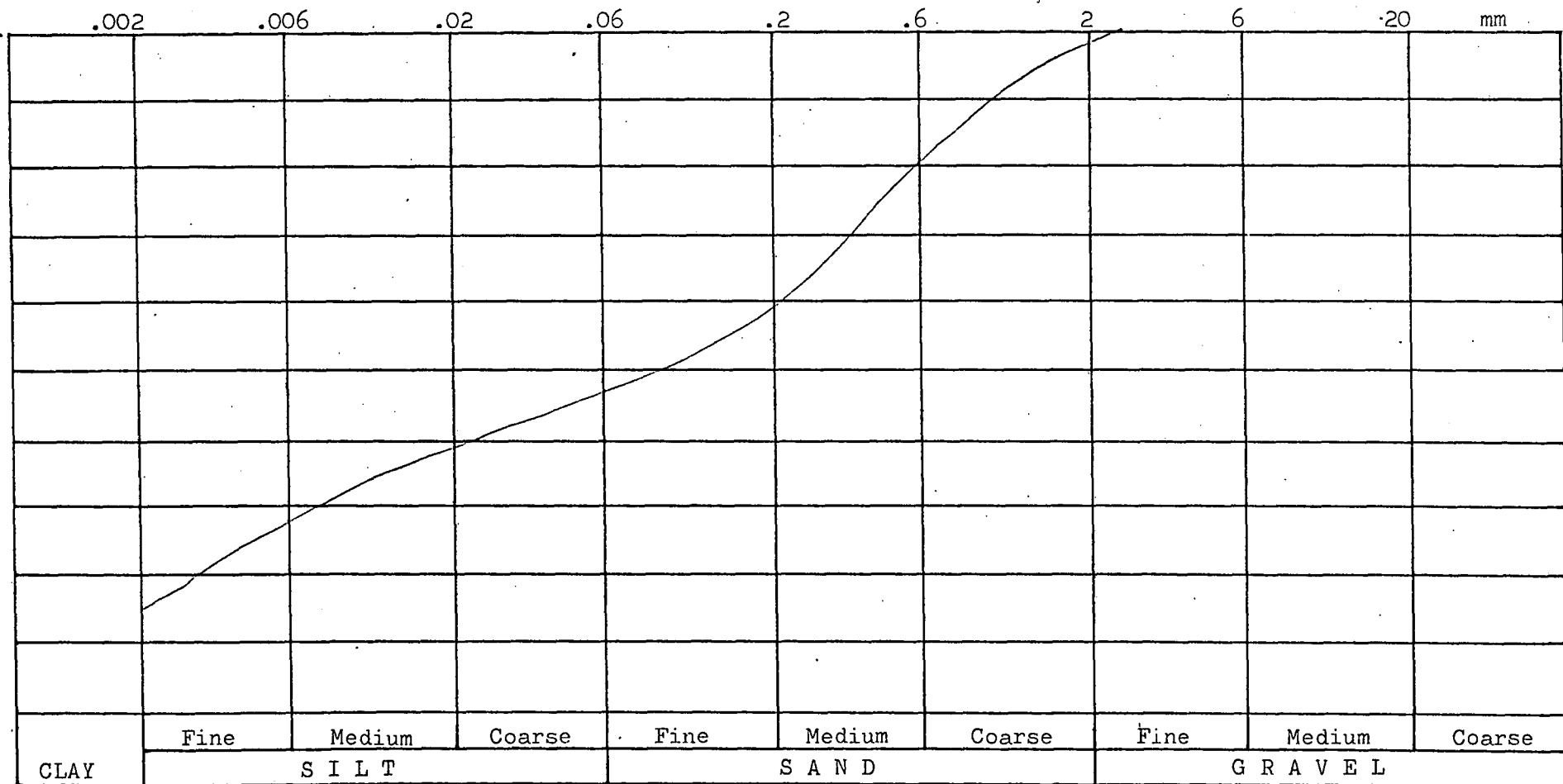




Table 6.1 Coefficients of consolidation for Gedling .

Sample	Cell	$c_v$ (m <sup>2</sup> /yr)	Comments
a. Vertical drainage			
X1	6 inch Rowe	22.0	
PR1	"	18.7	
JMK3	"	12.0	Average = 21.0
JMK7	"	22.5	
JMK19	"	30.0	
PR2	10 inch Rowe	20.9	
JMK4	"	31.8	Average = 25.2
JMK8	"	26.0	
JMK20	"	22.0	
JMK9	50mm oedometer	20.5	Average = 17.0
JMK10	"	19.1	Each of these pairs
JMK13	"	8.8	of samples were tested
JMK14	"	9.0	together, each pair
JMK17	"	21.9	coming from the same
JMK18	"	22.6	horizon.
b. Radial drainage			
PR3	6 inch Rowe	14.6	
JMK11	"	28.2	PR3 and PR4 are one pair,
PR4	10 inch Rowe	14.1	JMK11 and JMK12 are
JMK12	"	28.6	one pair.

radial consolidation parameters of individual laminae.

#### 6.4 The Measurement of Permeability In-situ

Measurement of the permeability in-situ is usually considered to yield more accurate results than measurement in the laboratory (e.g. Al-Dahir and Morgenstern, 1969; Murray and Symons, 1974). The measurement of permeability in-situ involves monitoring the flow rates or water levels in one or more observation wells. The observation wells may be auger or other boreholes, lined or unlined, or more commonly in soils, piezometers are employed. The use of only one observation piezometer has obvious advantages in terms of time and labour and for this reason has been adopted here.

Permeability tests fall into two types, either constant head or variable head (falling or rising). Although the test may be performed above the water table (Schmid, 1967), this introduces extra difficulties; in particular the degree of saturation of the soil must be known. Correct interpretation of these types of tests have not been attempted, but rather they have been treated as tests below the water table. Sufficient time was allowed for a saturated zone to develop around the piezometer, and it is not expected that very large errors result. This procedure was adopted by Mittal and Morgenstern (1975).

The basic formula for the constant head test is (see e.g. Al-Dhahir and Morgenstern, 1969):-

$$k = \frac{Q}{S.H}$$

For a variable head test the basic formula is:

$$k = \frac{A. \ln(H_o/H_t)}{S.E.}$$

where k is the permeability

Q is the rate of flow

H is the constant head

$H_0$  is the variable head at zero time

$H_t$  is the variable head at time  $t$

$t$  is the time taken for the water level to change from  $H_0$  to  $H_t$

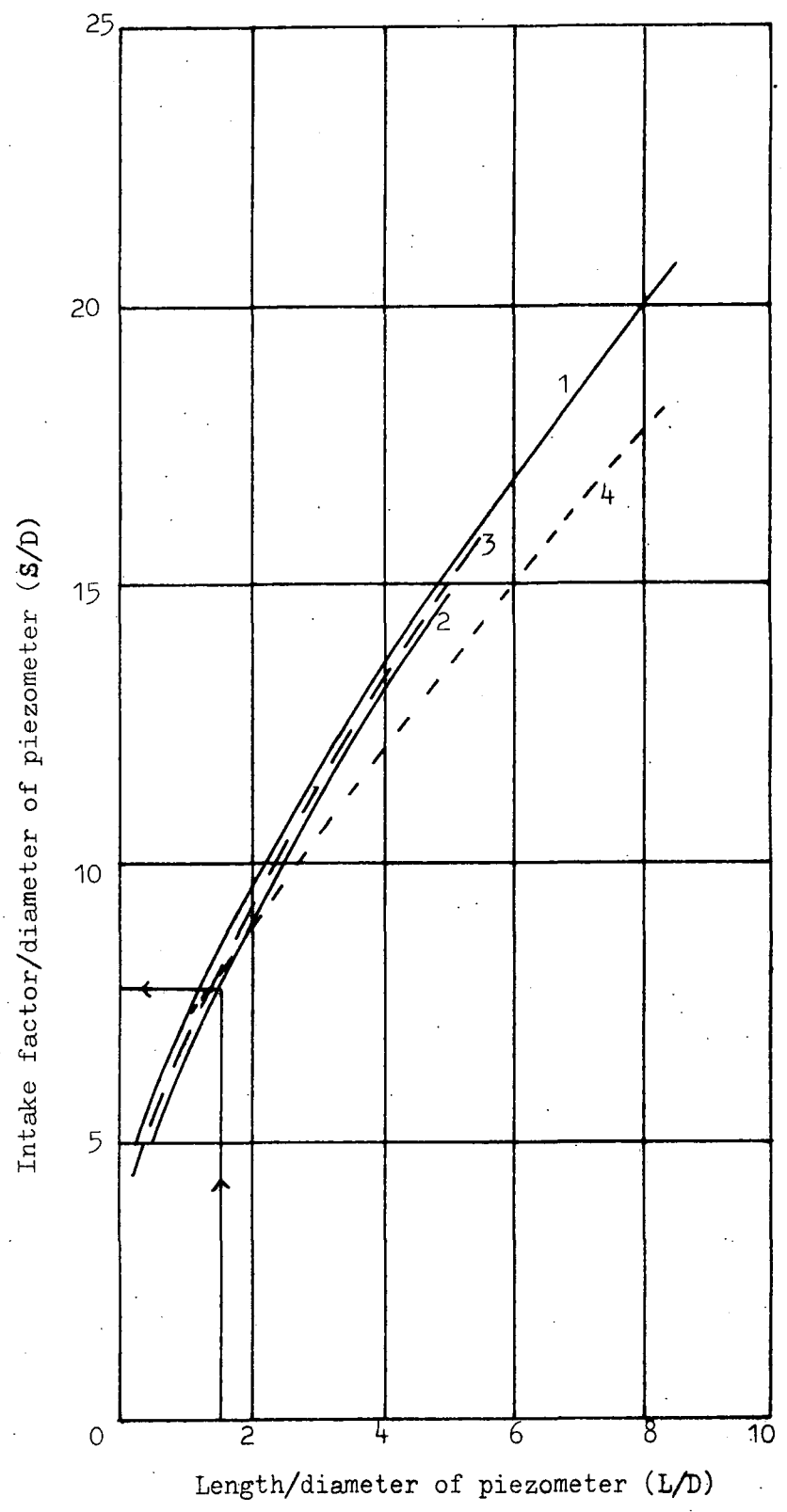
$S$  is the shape (or intake) factor. This factor has the dimensions of length.

These formulae assume that the soil is incompressible and saturated, and that there is no volume change or hydraulic loss in the measuring system. The shape factor varies according to the shape of the piezometer tip (or the borehole shape) and the permeability characteristics of the soil (including anisotropy, inhomogeneity and the presence of impermeable boundaries). Shape factors have been derived by many authors using a variety of methods. Hvorslev, (1951) empirically derived shape factors for a variety of borehole shapes and soil conditions. For a well point filter in a homogenous body of soil he gives the shape factor as:-

$$S = \frac{2L}{\ln \left[ \left( \frac{k_h}{k_v} \right)^{\frac{1}{2}} \cdot \frac{L}{D} + \left( 1 + \frac{k_h}{k_v} \cdot \frac{L^2}{D^2} \right)^{\frac{1}{2}} \right]}$$

Luthin and Kirkham (1949) and Donnan and Aravonici (1963) use an electric analogue method to derive shape factors. However, only Donnan and Aravonici include the case of a piezometer with closed ends, which is the result of interest here. Schmid (1967), Smiles and Youngs (1965) and Al-Dhahir and Morgenstern (1969) show that the above-mentioned authors underestimate the shape factors. Al-Dhahir and Morgenstern show that their finite-element method is in very close agreement with the electrical analogue study of Smiles and Youngs (see Fig.6.2). They present shape factors for the case of a piezometer with closed ends. The shape factors used herein are after Al-Dhahir and Morgenstern.

Fig.6.2 Shape factors (intake factors), after Al-Dahir and Morgenstern (1969).



- 1 One end impermeable
- 2 Both ends impermeable
- 3 Smiles and Young's result
- 4 Hvorslev's result

→ This work, shape factor for 20mm diameter is 150mm

However, the soil is not incompressible as these methods assume, and consolidation (or swell) occurs during the course of the test. Gibson (1963) presents a method of estimating both the permeability ( $k$ ) and the coefficient of consolidation or swelling ( $c$ ) from one piezometer permeability test. However, Gibson (1970) shows that unless the correct assumptions are made concerning the properties of the soil, the estimate of  $c$  can be seriously in error. The constant head test for a piezometer with a spherical tip is described by (Gibson, 1963):-

$$Q_{(t)} = 4 \pi a \cdot \frac{k \Delta u}{\gamma_w} \left( 1 + \frac{1}{(\pi \cdot T)^{\frac{1}{2}}} \right)$$

where  $Q_{(t)}$  is the volumetric flow for time  $t$   
 $a$  is the radius of the spherical tip  
 $\gamma_w$  is the density of water  
 $k$  is the permeability of the soil  
 $\Delta u$  is the constant head  
 $T$  is the time factor, and equals  $\frac{ct}{a^2}$  where  $c$  is the coefficient of consolidation or swelling.

For a cylindrical piezometer the formula can be used by taking  $a$  as the radius of a sphere with the same surface area as the piezometer filter (Parry, 1971).

The equation is of the form

$$Q_{(t)} = c_1 k \left( 1 + c_2 t^{-\frac{1}{2}} \right)$$

where  $Q_{(t)}$  and  $k$  are as above.

$t$  is the elapsed time

$c_1$  and  $c_2$  are constants.  $c_2$  is dependent on  $c$  (as above)

Therefore a plot of  $Q$  versus  $t^{-\frac{1}{2}}$  can yield the values of  $k$  and  $c$  from the intercept and slope respectively.

A great number of factors affect the results of this type of test.

Wilkinson (1968) shows that it is necessary to adopt non-linear permeability and consolidation versus stress relationships in the use of a Gibson type of analysis. Bjerrum et al. (1972) and Wilkes (1974) show that hydro-fracturing is possible when the excess head approaches 80% of the overburden pressure; though in certain cases the head may be as low as 20 per cent of the effective pressure. Hydrofracturing is characterised by a sudden increase in the permeability of 1000 times. Wilkes develops a method of estimating  $K_0$  based on an estimate of the onset of hydrofracturing. Gibson (1967) and Wilkinson (1968) show that the effect of smear at the edge of the well greatly affects the measured permeability value.

Most of the above formulae apply to homogenous media, although anisotropy may be incorporated (e.g. Hvorslev's shape factor). The interpretation of the test in non-homogenous media with highly variable permeabilities is difficult. For instance, if the piezometer is seated in a coarse-grained, highly permeable lamination which is sandwiched between two relatively impermeable laminae, then the permeability of the coarser lamina is under-estimated. This is because a much smaller volume of soil is contributing to the flow than is allowed for by the shape factors. Where the piezometer is next to an impermeable boundary most authors quote a smaller shape factor (resulting in a higher permeability) as a consequence (e.g. Hvorslev, 1951; Luthin and Kirkham, 1949). The degree of underestimation can be gauged by substituting a very large ratio of  $k_h$  to  $k_v$  into the Hvorslev shape factor formula. A ratio of  $10^4$  produces a decrease in the shape factor of 5 times; thus the permeability of the coarser lamina is underestimated by a factor of 5. However, the degree of underestimation depends on the exact geometry and permeability contrast of the laminae.

In contrast, the permeability of a fine-grained layer between two

coarser layers will if anything, be overestimated. This is due to the proximity of the more permeable laminae, which will contribute to the flow. Furthermore, if there is any hydrofracturing or other leakage through the fine grained layer, then the measured permeability will be a gross overestimate. Such a situation might be characterised by a steady increase in the flow rate during constant head test, rather than the expected decrease due to consolidation.

Finally, the piezometer tip may be seated at a layer boundary, in which case the permeability measured will be that of the more permeable layer reduced in proportion to the length of the tip in that layer. Since, in general, none of these factors can be known in detail, no corrections have been made to the results. However, it should be borne in mind that the highest permeabilities quoted are likely to be underestimates by factors of half an order of magnitude, or exceptionally more. The lowest values quoted are likely to be slight overestimates, though the error is probably less significant than for the former case.

The piezometers used in this study were simple, "home-made", push-in piezometers based loosely on the design of Parry (1971). The object was to provide a small infiltration area so that the permeability of individual laminae could be measured. The piezometer had to be of the push-in variety as it is impossible to auger a hole to any depth in very soft lagoon deposits. Furthermore, the design should be such that it minimised smearing during installation, and that the tip was at least ten times more permeable than any formation likely to be tested.

The design of the piezometer is shown in Figs.6.3 and 6.4. The first design using a geophone tip was discarded due to the possibility of water migrating around the upper sleeves and thence to the annulus left around the piezometer during installation. The second design was therefore

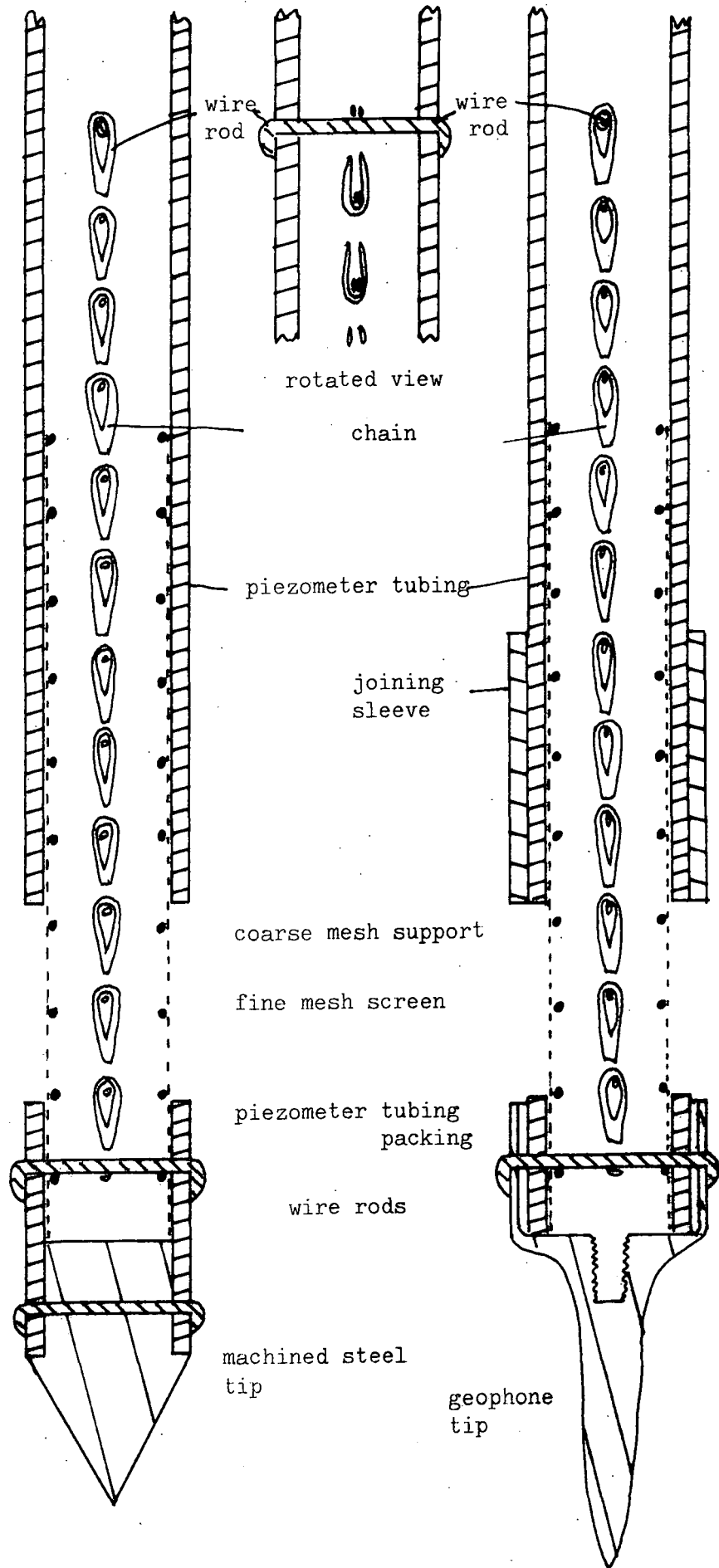
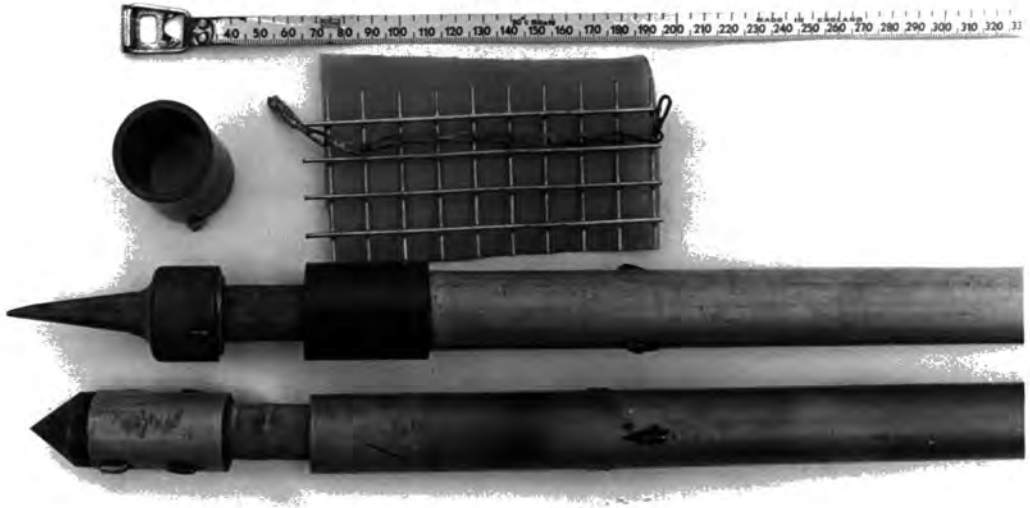


Fig.6.3 Piezometer tip construction



Fig.6.4 Piezometer tips and elements of construction.



produced, but it suffered from the problem that it required a greater installation and retraction force, <sup>h</sup> which sometimes caused distortion of the mesh and chain. It is expected that the very soft lagoon deposits being tested collapsed into the mesh; were this not so the shape factors would require correction. The shape factor for a 30mm long and 10mm diameter tip is 150mm (after Al-Dhabir and Morgernstern, 1969; see Fig. 6.2). The radius of a sphere with the same surface area is 12.2mm (this is required for the Gibson (1963) formula). Inward collapse of the material would also alleviate smear effects.

The constant head apparatus is shown in Figs. 6.5 and 6.6. The fluctuation in head caused by breaking the vacuum and recharge from the upper bottle was only 2 to 3 mm, which is negligible. The piezometer tubing used was standard 26mm O.D. (20mm I.D.). P.V.C. tubing supplied in 3m lengths by Soil Instruments Ltd. The standard connectors supplied were not robust enough for the desired purpose; therefore an alternative connector was made by enlarging one end of each tube (gently heated) on a steel mandril to form a 26mm I.D. female end. These connectors were extremely strong.

#### 6.5 The Consolidation and Drainage of Lagoon 109B at East Hetton Colliery

This lagoon is deep compared to its width. Two sides of the lagoon are limestone, while the floor is clay (chapter 1.4). It was shown in chapters 3, 4 and 5 that this lagoon is finely laminated, with both coarse and fine grained laminae found in all parts of the lagoon. It was further shown that many of the laminae are not continuous laterally. It is therefore to be expected that drainage in this lagoon would be predominantly in a horizontal direction, but that some vertical movement of water could take place. Some water could escape beneath the southwestern embankment into lagoon 109A (see Fig. 1.6).

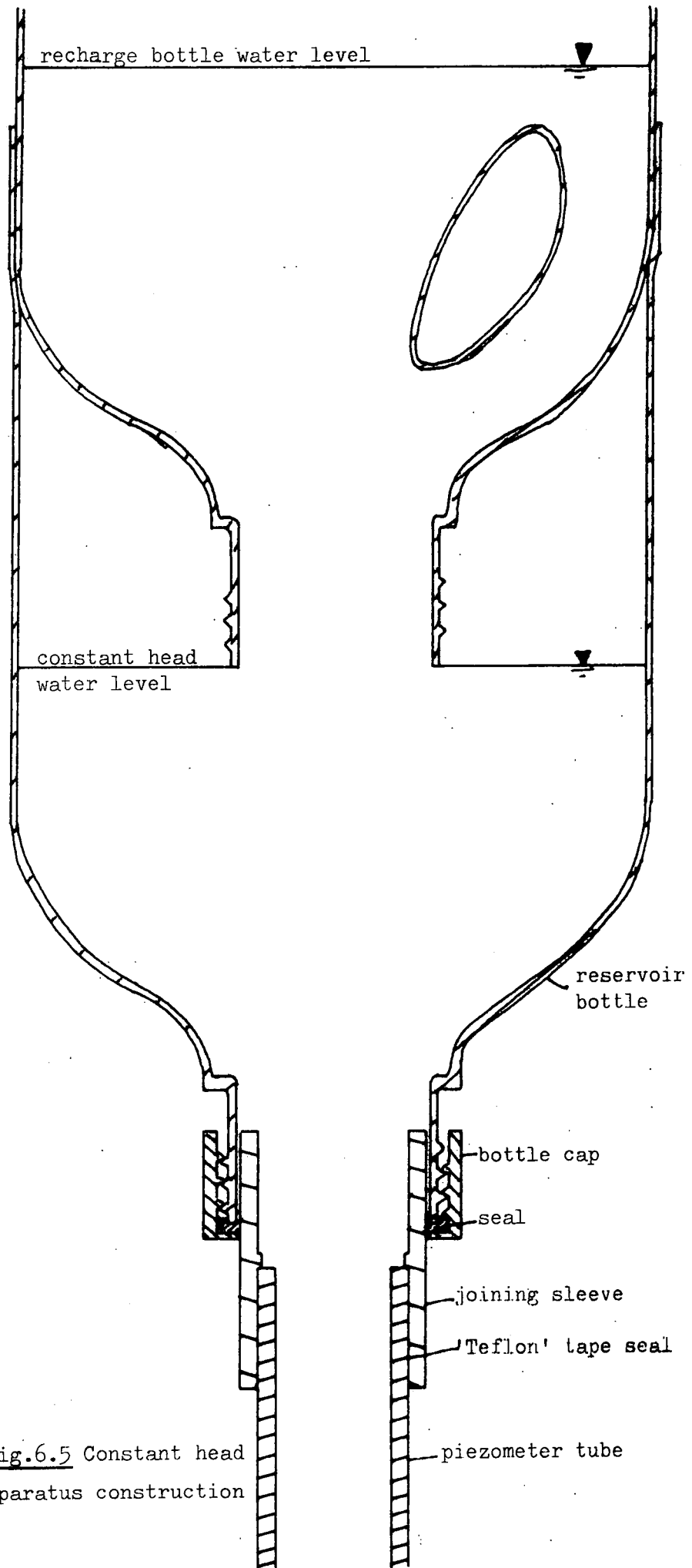


Fig.6.5 Constant head apparatus construction

Fig.6.6 Constant head permeability test set up.



Laboratory consolidation tests were carried out on East Hetton material from the locations sketched in Fig.6.7. The beach samples were taken from lagoon 109A because the beach of 109B was covered by a layer of overtipped material, as described in chapter 1. The results are given in Appendix 6.1, and are summarised in Fig.6.8 and Table 6.2. The following points should be noted.

1. The fine lamina at the beach is as impermeable as any in the lagoon. Conversely the coarse lamina at the outlet is as permeable as any other (in fact it is more permeable).
2. The actual range of measured  $c_v$ 's is very large, from 2.87 to 1432  $m^2/yr$ .
3. The calculated permeabilities are very low, the highest being  $7.82 \times 10^{-8}$  m/s.
4. The void ratios are very high, being between 0.75 and 1.35.
5. Generally the material is relatively incompressible, compression indices being below 0.25, for most samples. However, some of the samples with a low coal content (evidenced by a higher specific gravity) have higher compressibilities. There is no significant trend of compressibility across the lagoon.

Preliminary observations in the summer of 1978 suggested that the water table was some  $2\frac{1}{2}$  m below the surface even near the overflow tower near the south-western embankment, see Fig.s 3.4, 3.5 and 3.6. During the summer of 1979 the number of observations was considerably extended and in addition, in-situ permeability tests were carried out. The full results are contained in Appendix 6.2, Tables A.6.2.1 and A.6.2.2. The data were collected by Henderson (1979), but the current writer's interpretation differs slightly from that of Henderson, as explained in the Appendices. The results are summarised in Fig.6.9. It is apparent that most of the in-situ permeability measurements have yielded values several orders of

Fig.6.7 Sample locations of consolidation samples at East Hetton.

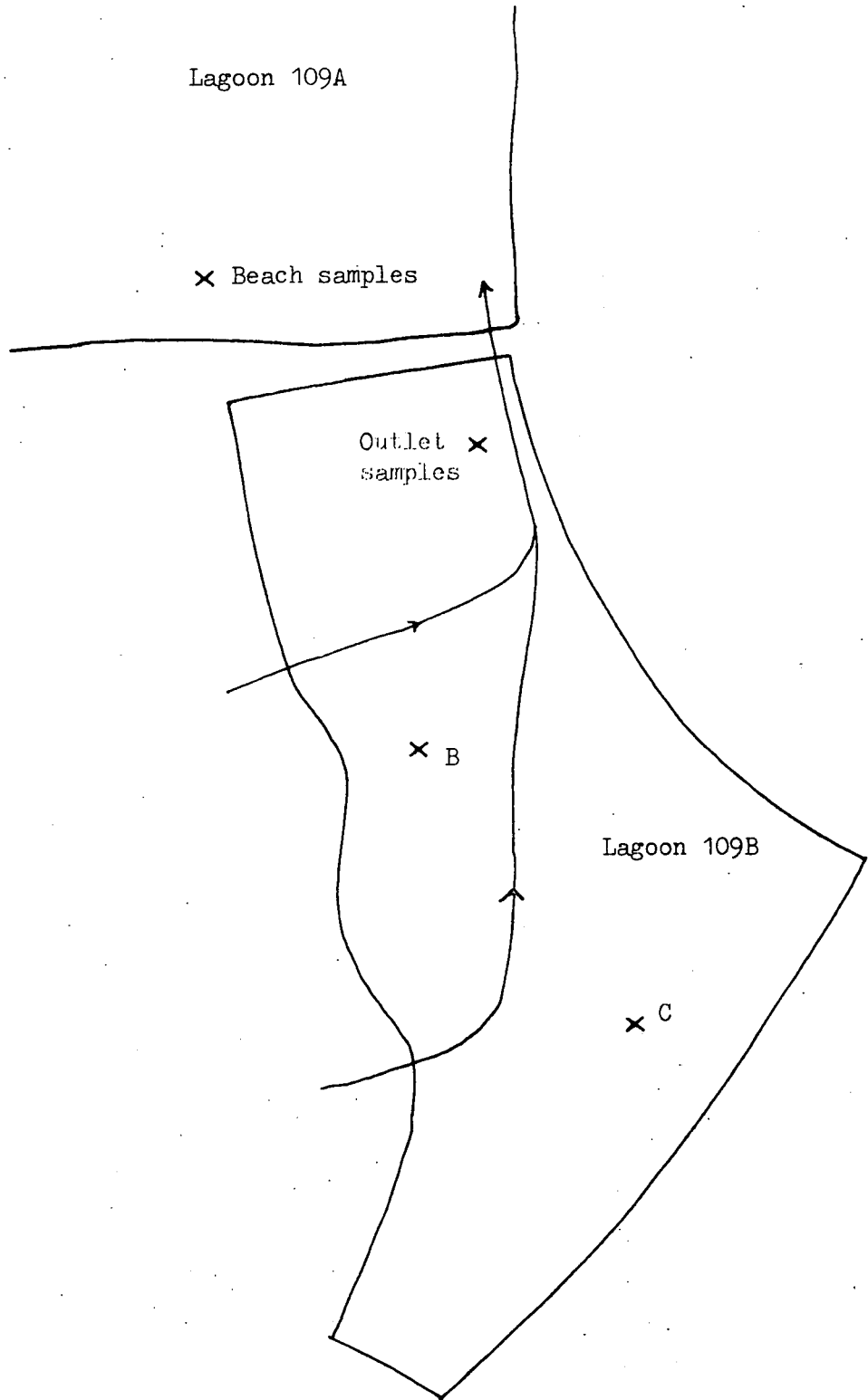


Fig.6.8 Void ratio - log pressure curves for East Hetton samples.

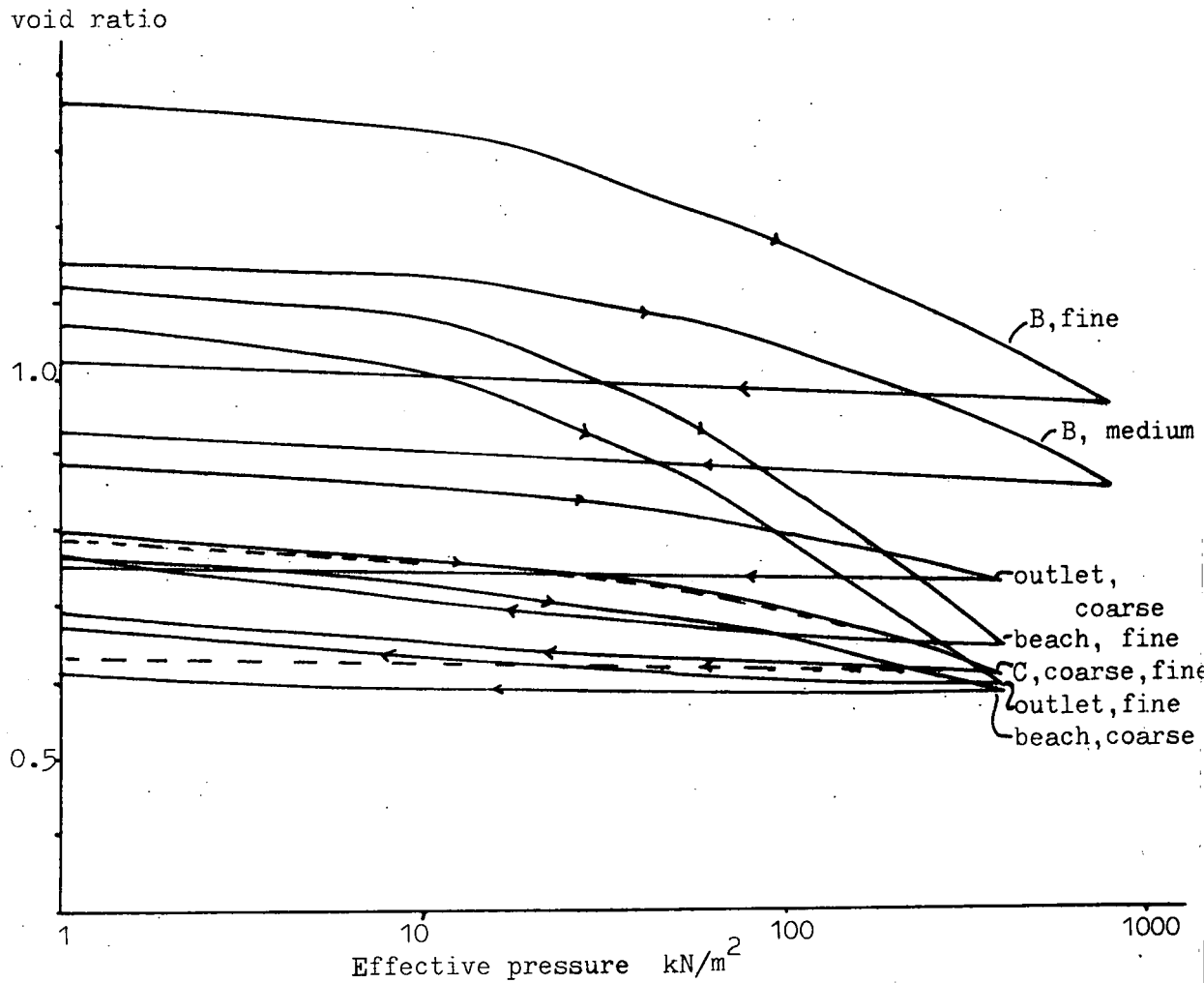
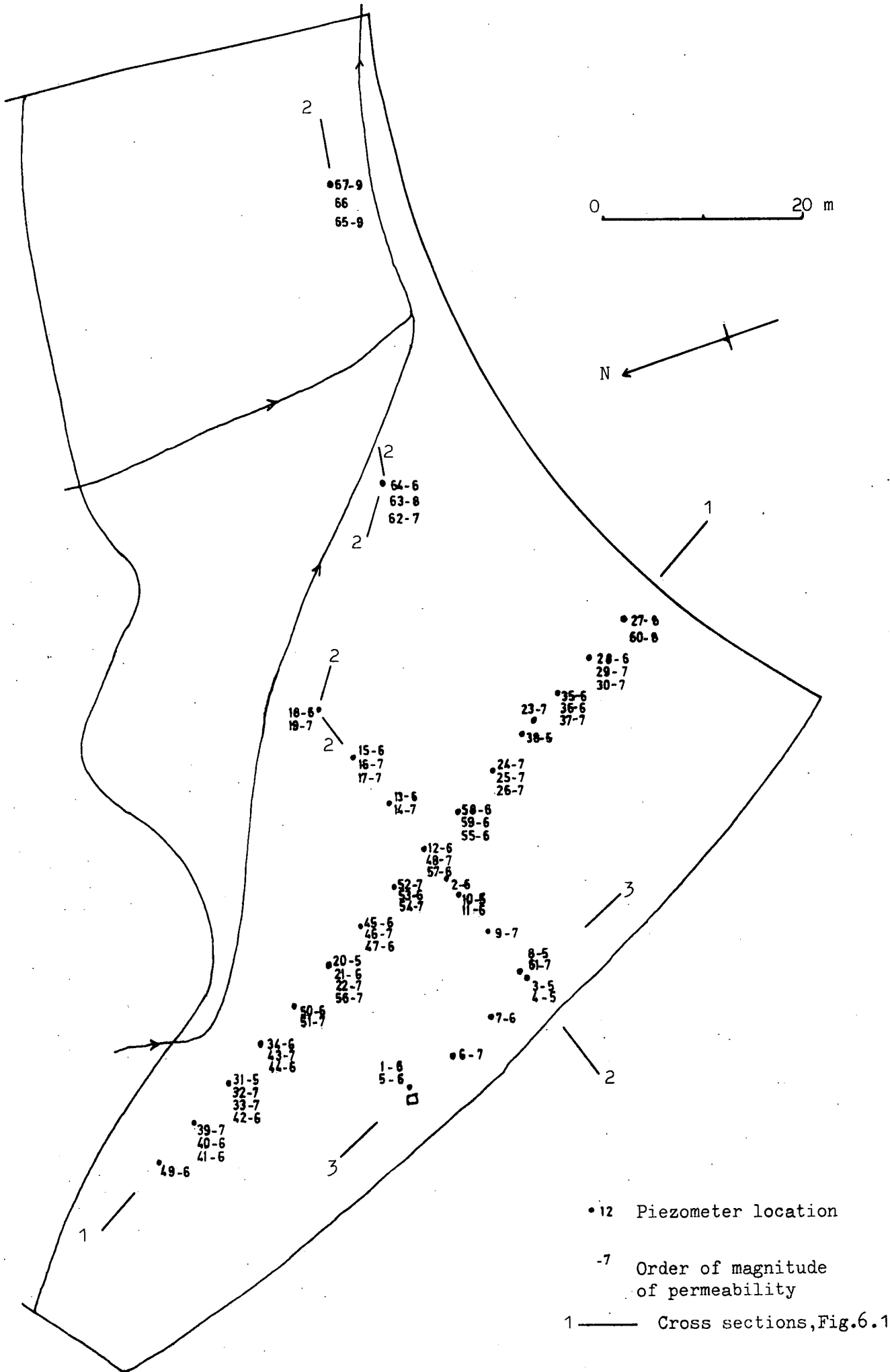


Table.6.2 Consolidation data, East Hetton.

Sample (Oedometer)	$c_v$ (m <sup>2</sup> /yr)*	$K$ (m/s)* ( $\times 10^{-7}$ )	$C_c$	$C_r$	S.G.
Beach, fine	3.61	6.42 -10	0.329	0.037	2.546
coarse	536	3.68 -8	0.238	0.010	2.551
C, fine	9.24	6.07 -10	0.161	0.036	2.124
coarse	90.7	5.62 -8	0.149	0.010	1.390
B, fine	10.5	9.48 -10	0.217	0.023	1.900
medium	245	1.47 -8	0.205	0.026	1.640
Outlet, fine	2.87	9.41 -10	0.284	0.025	2.093
coarse	1432	7.82 -8	0.115	0.011	1.787
(Triaxial)					
Beach, coarse	648	-	-	-	2.551
Outlet, fine	52.0	-	-	-	2.093

\* averaged over linear section

Fig.6.9 In-situ permeability, lagoon 109B, East Hetton.





magnitude higher than those derived from the oedometer tests. It is also clear that there is a considerable variation of permeability at any one location. However, there is a general trend to lower permeability values with distance from the inlet, values lower than  $10^{-8}$  m/s being found only at distances greater than 80 m from the inlet. This contradicts the results of the oedometer tests and other observations, which suggests that the finer material at the outlet is not less permeable than fine laminae anywhere in the lagoon, and similarly with coarser laminae. However, it is possible that at the outlet there is an increased probability of the piezometer being seated well in the centre of a thick fine-grained lamination, such that the nearest permeable layer has no influence on the measured value of permeability. (It will be recalled from chapter 3.3 that fine-grained laminae were thicker near the outlet, and from chapter 5.3 that only at the outlet could a fine-grained layer thick enough for a triaxial test be found.) Thus a value of  $10^{-8}$  to  $10^{-9}$  m/s is probably a reasonable estimate for the permeability of all the fine-grained horizons.

The in-situ  $c_v$  values (Table A.6.2.2) also show considerable variation across the lagoon, see Fig.6.10. Again it should be noted that the very low values occur only near the outlet, for the reason explained above. The general range of values is somewhat lower than found in the oedometer, being from 0.055 to 364, compared to 2.87 to 1432  $m^2/yr$ . As with the oedometer values, widely different  $c_v$ 's can be found in the sediments at one location.

The piezometric head is fairly complex, as can be seen in Fig.6.11. In general the deeper levels in the lagoon have lower piezometric surfaces than levels above. It is suggested that surface recharge (via the stream, rainfall and probably also run-off from the tip and neighbouring fields) creates a perched water table near the surface. The less permeable layers

Fig.6.10 Coefficients of consolidation, lagoon 109B, East Hetton.

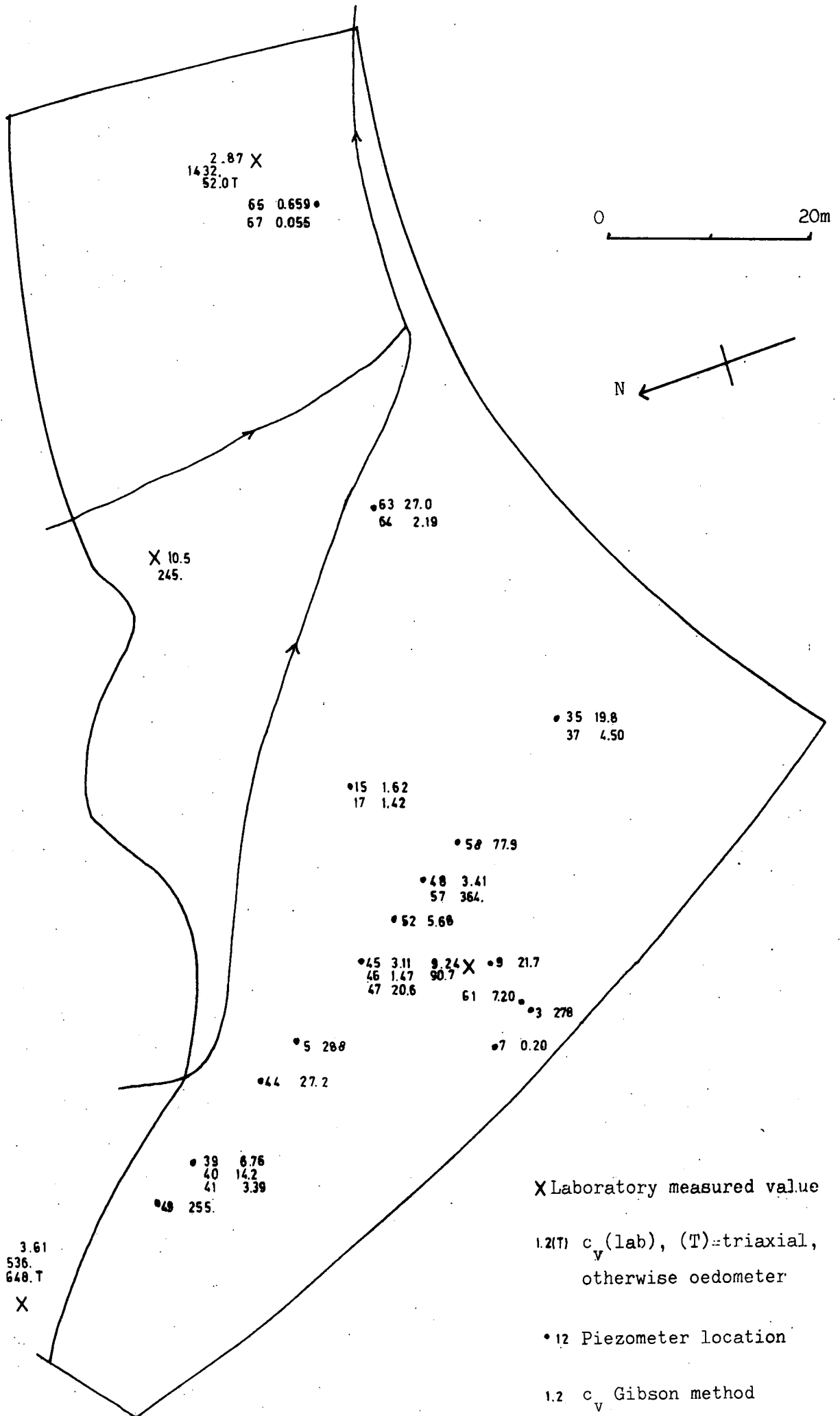


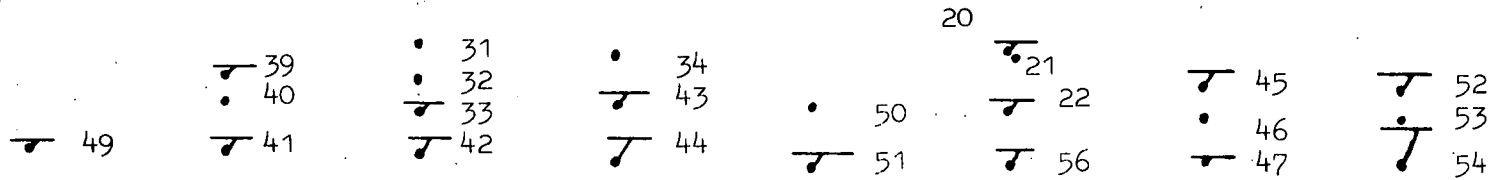
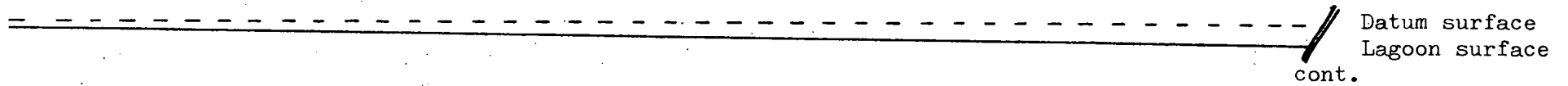
Fig.6.11 Piezometric head variation in lagoon 109B, East Hetton.

a. Section 1 (see Fig.6.9)

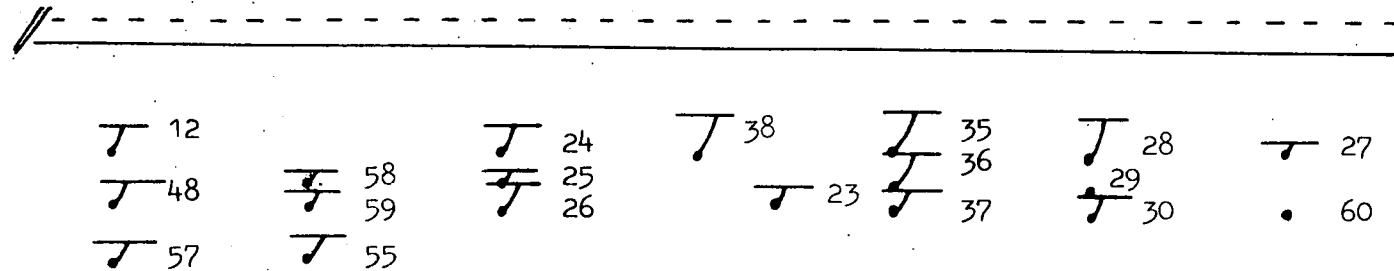
Scale 10mm=2m (no vertical exaggeration)

• Piezometer tip (dry)

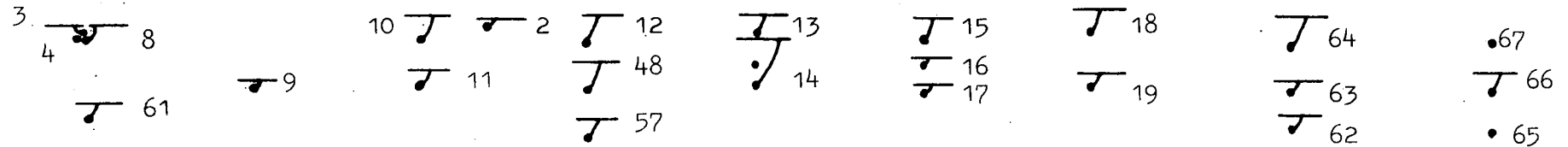
└ Piezometr tip and water level



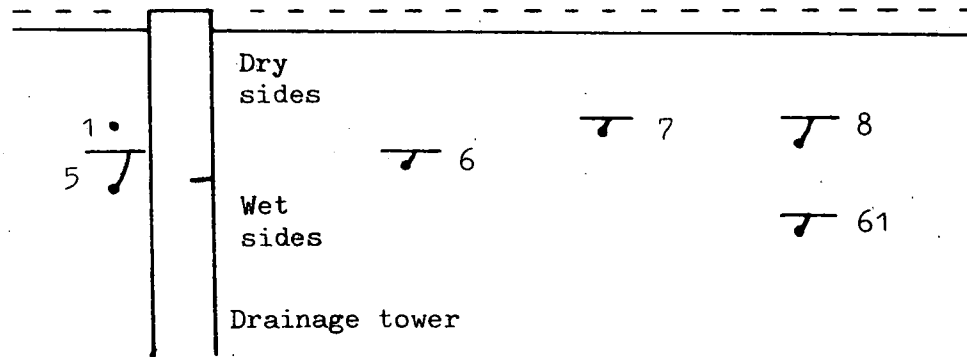
cont.



b. Section 2



c. Section 3



in the lagoon serve as aquitards, and the poor supply to layers beneath is rapidly drained to the sides of the lagoon thus causing the lower piezometric head. The lowering of the piezometric head with deeper levels in the lagoon has been noted before (NCB, 1972).

The general form of the water table shows a lowering towards the inlet, more dry layers being found here. There will be fewer aquitards in this region, and a generally more permeable deposit obviously enhances drainage. At the other end of the lagoon, piezometers 27 and 60 (Fig.6.11a) and 65, 66 and 67 (Fig.6.11b) are nearest to the limestone walls and show evidence of enhanced drainage. Piezometers 64 and 18 (Fig.6.11b) are the nearest to the stream, and the elevated heads suggest recharge in these regions. However, piezometers close to the stream of the inlet end of the lagoon do not show this, perhaps because of more rapid drainage.

#### 6.6 The Consolidation and Drainage of Lagoon 16 at Silverhill Colliery

Observations of the level of the water table and in-situ permeability in this lagoon were carried out at the same time as the lagoon was being overtipped. Observations and conclusions pertinent to the overtipping operation are confined to chapter 7.

Two oedometer tests were carried out, on specimens of the fine-grained layer and underlying coarser band that have been described in chapter 4.6. From Fig.6.12 and Table 6.3 it can be seen that the fine-grained material has a very low coefficient of consolidation, while the coarse materials as expected, consolidate very rapidly. The finer material is highly compressible compared to other lagoon sediments; it will be recalled from chapter 4.6 that this material has a very low organic carbon content but is rich in illite and kaolinite. The coarser sample is very incompressible.

Permeability tests have been carried out in-situ in this lagoon, and are summarised in Fig.6.13 from the data in Appendix 6.3. Table A.6.3.1.

Fig.6.12 Void ratio-log pressure curves for Silverhill samples.

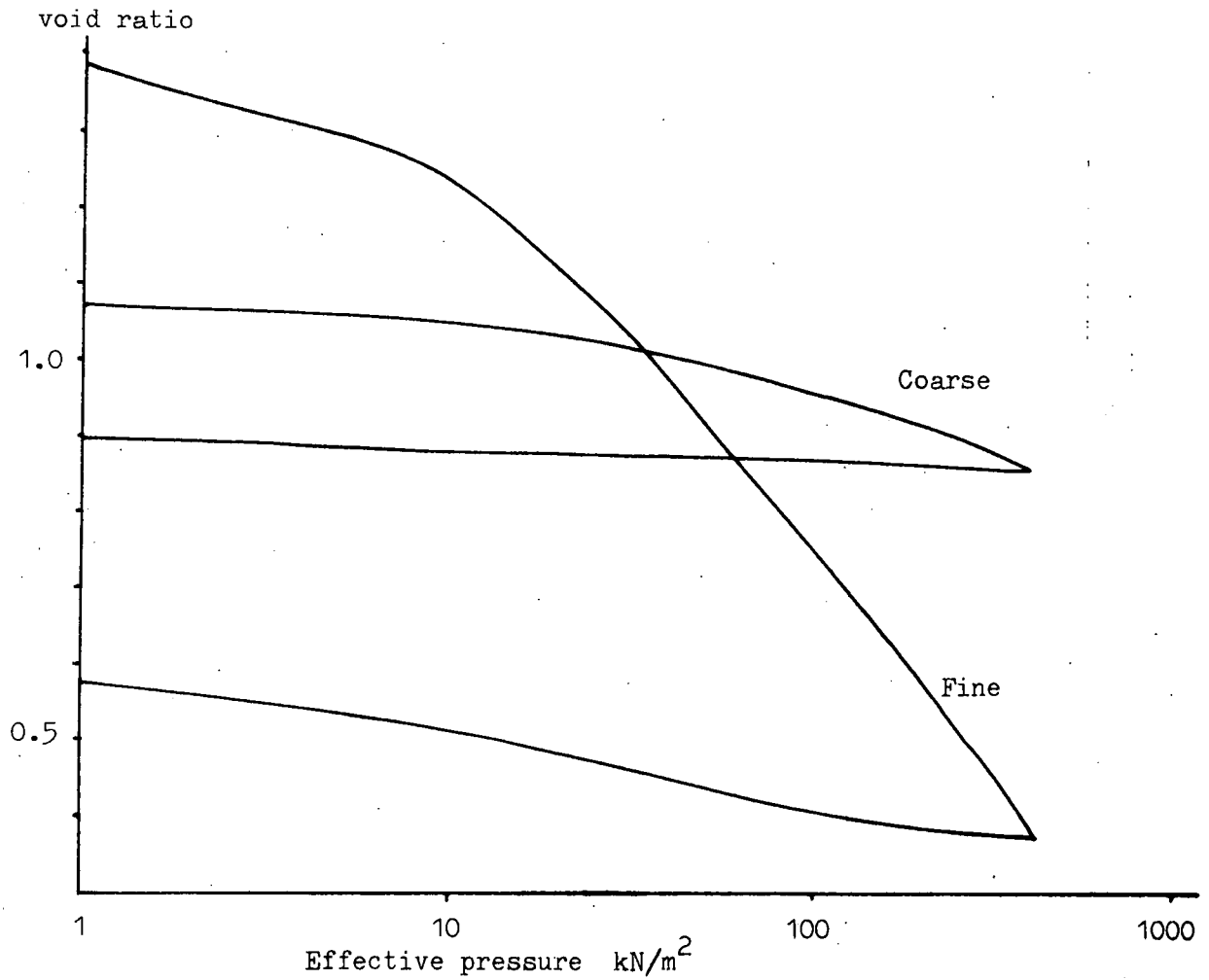
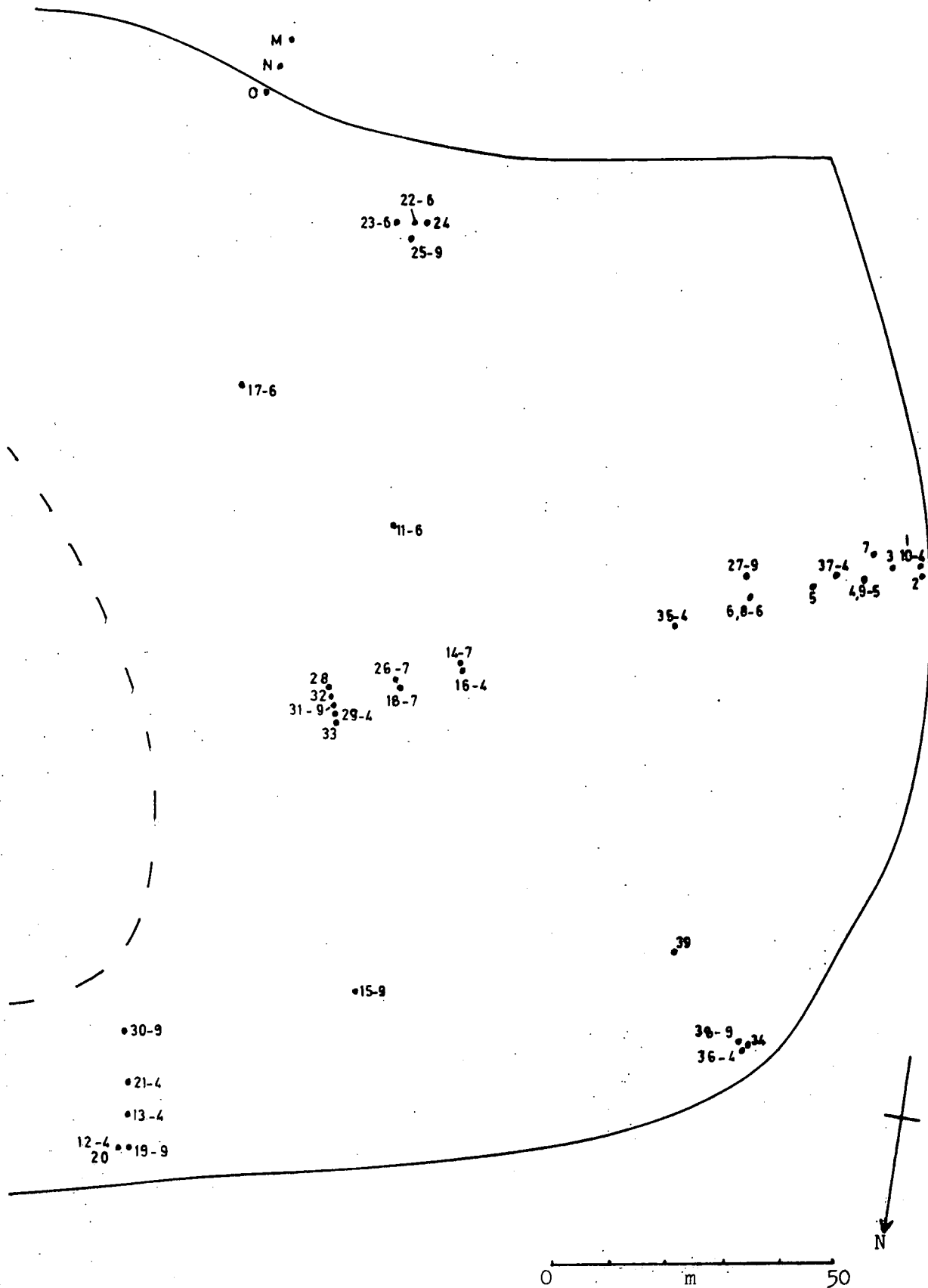


Table 6.3 Consolidation data, Silverhill.

Sample	$c_v$ (m <sup>2</sup> /yr)*	$K$ (m/s)* ( $\times 10^{-}$ )	$C_c$	$C_r$	S.G.
(Oedometer)					
Fine	2.33	1.45 -9	0.541	0.085	2.476
Coarse	594	7.96 -7	0.202	0.017	1.671
(Triaxial)					
Fine	5.1	-	-	-	2.476
Coarse	447	-	-	-	1.671

\*averaged over the linear section



- Piezometer location
- Order of magnitude of permeability

From the figure, no systematic trends emerge; however it is a large lagoon and too few tests have been performed for this purpose.

Furthermore, the location of the inlet has been moved throughout the history of this lagoon, thus making it less likely that any trends exist across the lagoon. The range of measured permeabilities is higher than at East Hetton, and is characterised by fewer mid-range values and more high permeability values (see Fig.6.14). However, there are too few tests at Silverhill in particular to compare the distributions accurately, nor have similar areas of each lagoon been sampled. Since the contrast between the most permeable and least permeable layers at Silverhill is five orders of magnitude, drainage will be almost entirely in a horizontal direction unless there is vertical interconnection between the more permeable layers. However, it is known (chapter 4.6) that at least one of the less permeable bands is continuous across the entire lagoon.

During one visit to this lagoon, a particularly heavy thunderstorm occurred. It was noticed that run-off drained onto the lagoon from an area of tip that was almost twice the area of the lagoon itself. Run-off was almost total on some of the compacted tip haulage roads, but in other less well compacted areas there was a great deal of infiltration. Seepage from the tip onto the lagoon in fact occurs at several places along the southern side of the lagoon, along the line of an old berm. One stream was estimated to flow continuously at  $5\text{m}^3$ /day, even in very dry weather. Three piezometers placed in the tip at the location shown in Fig.6.13 show that a flow net transfers water to the southern part of the lagoon, see Fig.6.15. Thus, although it is now inactive, this lagoon receives a considerable recharge of water throughout the year. Discharge can only take place through the



Fig.6.14 Distribution of measured permeability values.

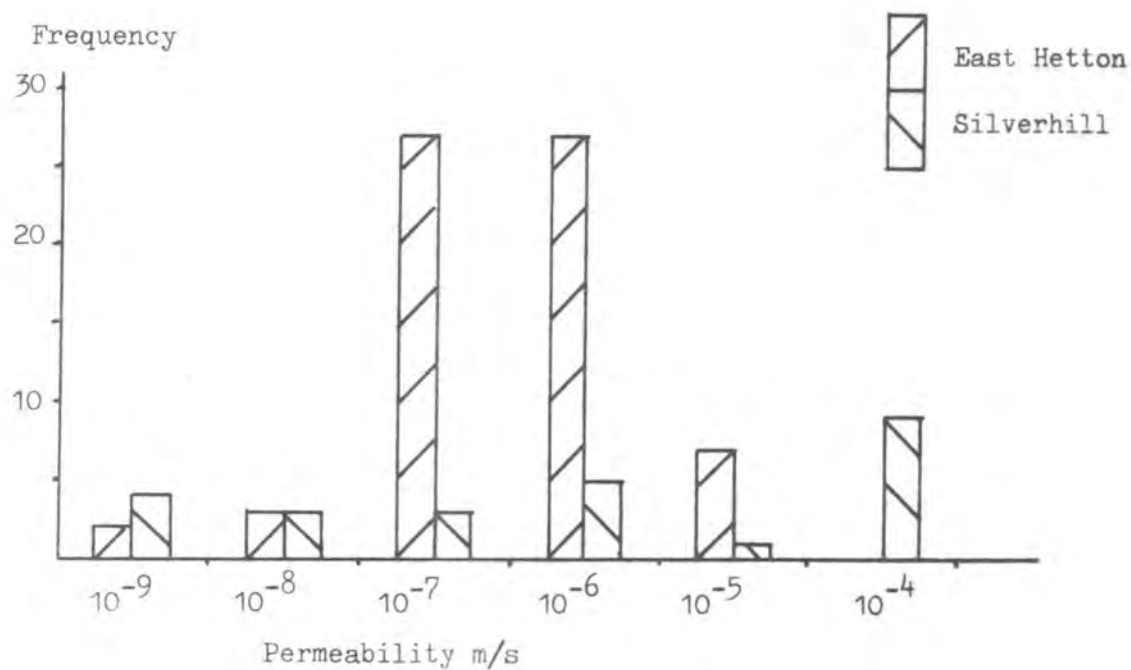
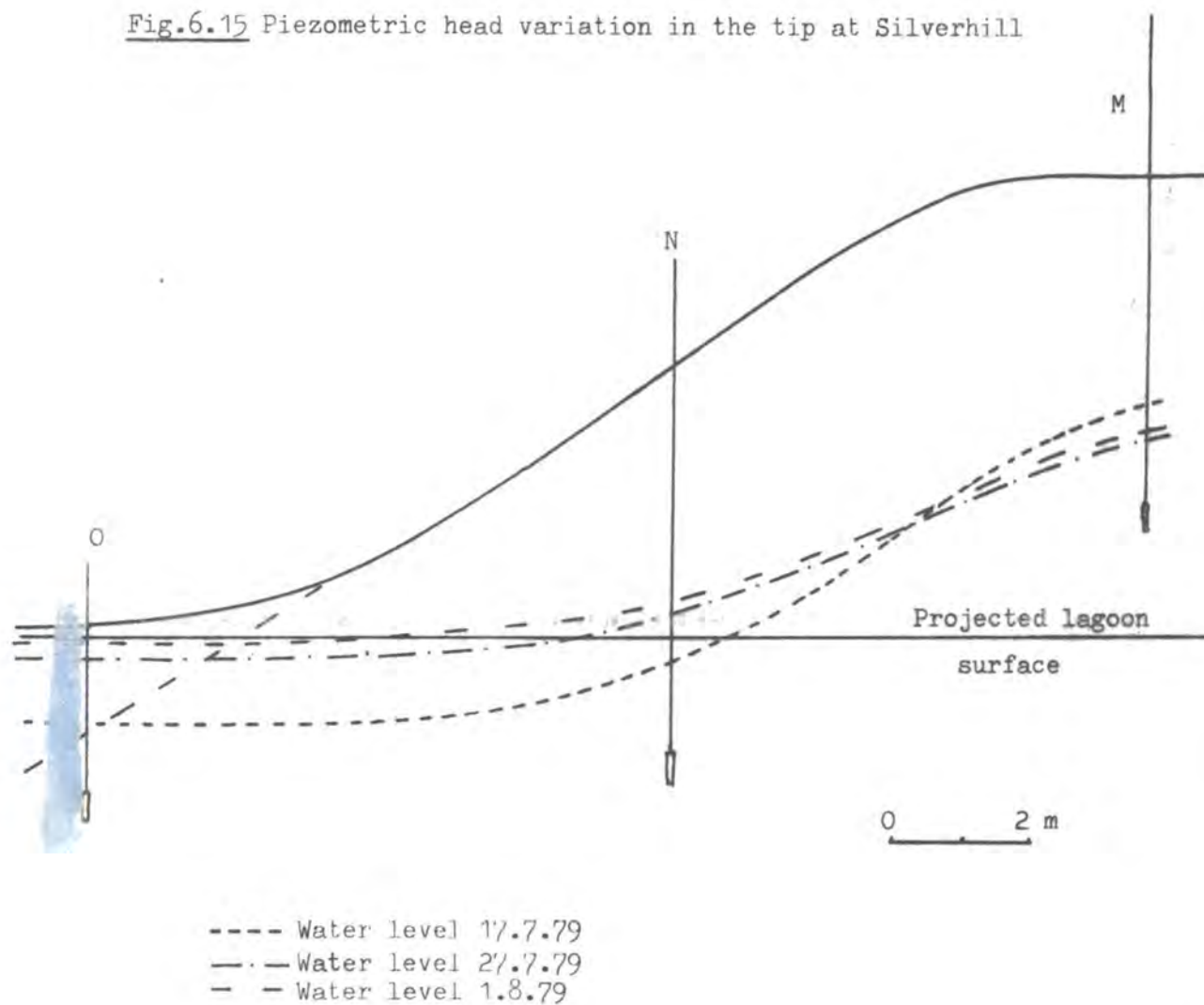


Fig.6.15 Piezometric head variation in the tip at Silverhill



overflow tower, or through the permeable western half of the floor. However, because of the extensive, impermeable layers the latter mode of discharge is probably not quantitatively significant. A small volume of water seeps through the face of the southern embankment. Whether this reflects a general flow net or the position of an older berm is not known. Piezometers were installed by the National Coal Board during construction of this embankment, but subsequent monitoring revealed no water; they are now blocked. The means of discharge of water from a lagoon is important in the context of overtipping operations. This will be discussed further in Chapter 7.

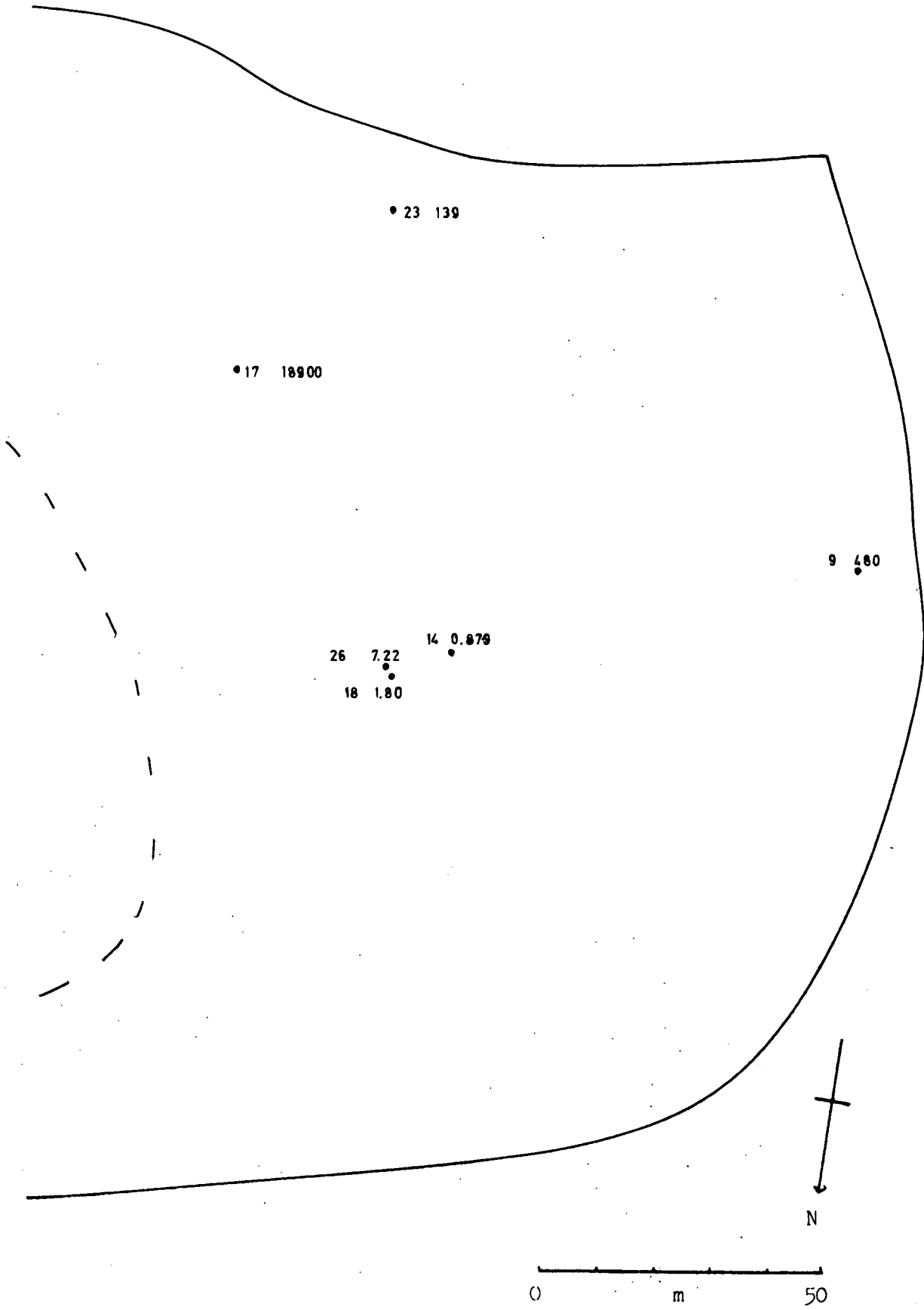
Measurements of the coefficient of consolidation in-situ were not obtained at many points (Table A.6.3.2). The available values are shown in Fig.6.16. The range of values is very great being from 0.879 to  $18900 \text{ m}^2/\text{yr}$ .

#### 6.7 A Note on Gibson's Consolidation Model for an Accreting Deposit

It was mentioned in Section 6.2 that Gibson's (1958) model does not account for all the factors operating in a lagoon. However, in view of the fact that it predicts the existence of excess pore pressures in such a deposit, which have been shown to exist in the field (Mittal and Morgernstern,1976), the applicability of the model is worth investigating.

The lagoon at East Hetton contains many very permeable layers, and has comparatively short drainage paths to permeable sides. It is not expected that excess pore pressures of any magnitude ever existed within this lagoon. In contrast, the lagoon at Silverhill Colliery is much larger, and though very permeable in a lateral direction much of the embankment in particular and floor is relatively impermeable. From data supplied by the Area Civil Engineers for the North East and North Nottinghamshire Areas (written communications) the average pumping rate

Fig.6.16 In-situ coefficients of consolidation (Gibson method).



- 1 Piezometer location
- 1.2 Coefficient of consolidation

at East Hetton was  $4600 \text{ m}^3/\text{yr}$ , compared to  $59000 \text{ m}^3/\text{yr}$  at Silverhill. This represents rates of accumulation of approx.  $0.7 \text{ m}/\text{yr}$  and  $1.7 \text{ m}/\text{yr}$  respectively; the former rate at East Hetton is roughly constant with time, while the latter rate refers to later life only of the Silverhill lagoon. The rate of accumulation varies at Silverhill because of the shape of the lagoon; it is much wider at the present surface of the deposit.

The rate of accumulation at Silverhill is given in Fig. 6.17, from which it can be seen to decrease with time until the summer of 1970 after which it is nearly constant. Gibson's model requires that the rate shall fit either a constant or square-root versus time law, neither of which it does particularly well. Therefore the value of the constant rate in later life is assumed. The coefficient of consolidation of the lagoon in a vertical direction is also required. Since a layered structure will consolidate essentially at the speed of the least permeable layers, the lagoon can be considered to behave as if it were shallower, but with one low value of  $c_v$ . From the data on in-situ permeabilities and in-situ coefficients of consolidation (Figs. 6.14 and 6.16), it can be seen that approximately one-third of the layers are of very low permeability and  $c_v$ . Therefore, an equivalent lagoon 7m deep, accumulating at approximately  $0.5 \text{ m}/\text{yr}$  is assumed, with a  $c_v$  of  $2.33 \text{ m}^2/\text{year}$  (from the oedometer test on the fine layer). If the base was impermeable, and all flow of water was in a vertical direction, the maximum excess pore pressure would be approximately 2.2m head of water in the deepest part of the lagoon (read from Fig. 3. of Gibson, 1958), at the cessation of pumping. This would have dissipated almost completely by the summer of 1979 (Fig. 5, Gibson, 1958).

For this calculation, no evaporation is assumed, which has been shown to play an important effect (Krizek and Casteiliero, 1977). Furthermore, some of the floor is probably permeable. Lateral flow will take place to this and other parts of the embankment, through which some water is known to be discharged (see previous section). Therefore, the values

Fig.6.17 Level of the deposits in lagoon 16, Silverhill.

Data from the Area Civil Engineer (written communication).

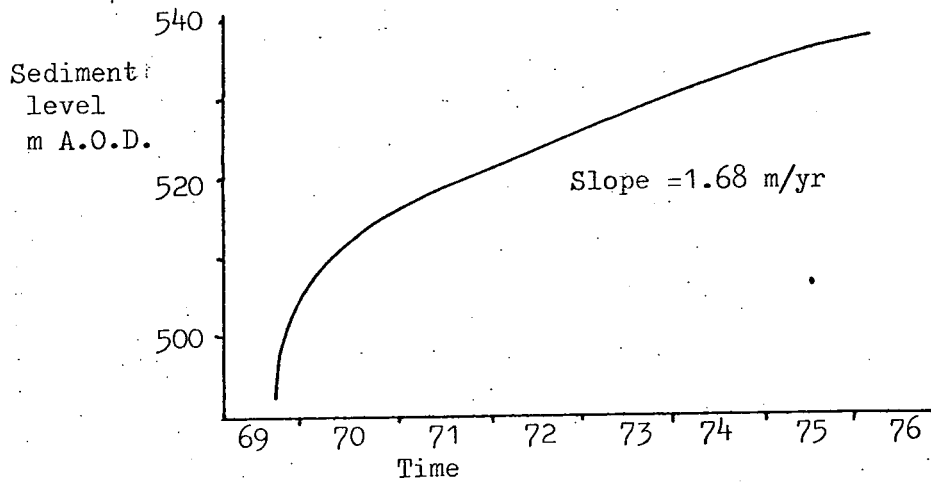
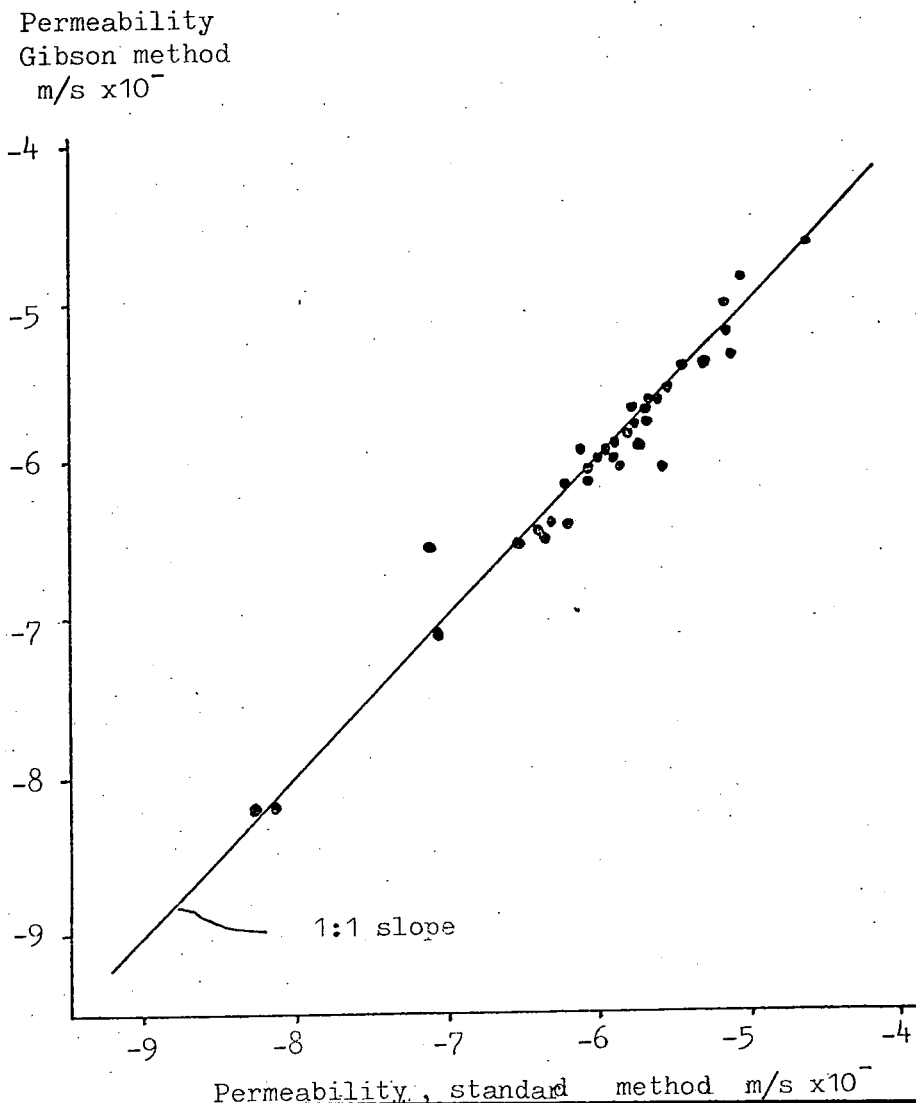


Fig.6.18 Comparison of in-situ permeability methods of analysis.



of excess head calculated are probably gross overestimates, and refer to the deepest part of the lagoon. Excess pore pressures in all other parts of the lagoon will be negligible. Given also that this is a fairly large lagoon in terms of British collieries, then this effect can be neglected in most cases, particularly those with permeable sides. However, some excess pore pressures could exist at the cessation of pumping in any lagoon that has uniform, impermeable deposits, with a large input of sediments.

#### 6.8 The Comparison of In-situ Measured Permeability Values for East Hetton and Silverhill Lagoons

The measurement of permeability in-situ has been accomplished by two distinct types of method. Firstly methods which assume the soil skeleton to be incompressible and secondly methods which assume consolidation to take place (see Section 6.4). All the permeability values quoted in Sections 6.5 and 6.6 are those from the former method (both constant and variable head types). For some of the constant head tests sufficient data were gathered for the second (Gibson) type of analysis, which also yielded the  $c_v$  values quoted in Sections 6.5 and 6.6. The full results are quoted in Tables A.6.2.2 and A.6.3.2. From Fig.6.18 it can be seen that the two methods compare very closely indeed, the greatest deviation being about half an order of magnitude. Considering the known errors introduced by applying these methods to layered media (see Section 6.4), there is no significant difference between the results of the methods. This fact adds a measure of confidence as to the accuracy of the determinations.

#### 6.9 The Consolidation and Drainage of Lagoons 6 and 7 at Peckfield Colliery

Six-inch Rowe cell tests were conducted on the four box samples described in Chapter 5. The Rowe Cell was used in this case because in each sample the thickness of the lamina under test was sufficient for

this apparatus. The voids ratio versus log pressure curves are shown in Fig.6.19 together with the summary consolidation data in Table 6.4. As expected from the grading curves (Fig.5.13), sample PL74 has a relatively high  $c_v$ , whilst the other three samples are much less permeable. The void-ratios of the samples are very high, reflecting the loose nature of the deposits. The compressibility of all four samples is very similar, despite the much greater proportion of fines in samples 1 to 3. The permeabilities of all samples are very low. No in-situ permeability measurements were undertaken in these lagoons, but from sections 6.5 and 6.6 it is suspected that the true permeabilities are much higher than those indicated in Table 6.4.

The results of the consolidation tests indicate that in lagoon 7 at least, drainage will take place in a horizontal direction along the coarser-grained laminae. Vertical movement of water will take place only where clay laminae wedge out (see Fig.4.20). Since these lagoons are relatively narrow, and the sides are formed of limestone (either in-situ rock, or in embankments, see chapter 1.), much drainage will therefore be through the sides.

A general sketch of the lagoons and the piezometer locations is given in Fig.6.20. In chapter 5 it was shown that lagoon 7 possesses a weak layer of fine material to approximately 1 to 1.5m depth, above a layer of much coarser, sand-sized material. The water levels shown in Fig. 6.21 indicate that a perched water table of some 200-300mm exists within the top, fine-grained layer. Once the existence of this water table was established, the piezometers were emplaced at deeper levels in the lagoon, and a second water table was discovered at approximately 4m depth. However, while the upper water table has an approximately constant level everywhere, the lower water table is found at greater depths away from

Fig.6.19 Void ratio-log pressure curves for Peckfield lagoon 7 samples.

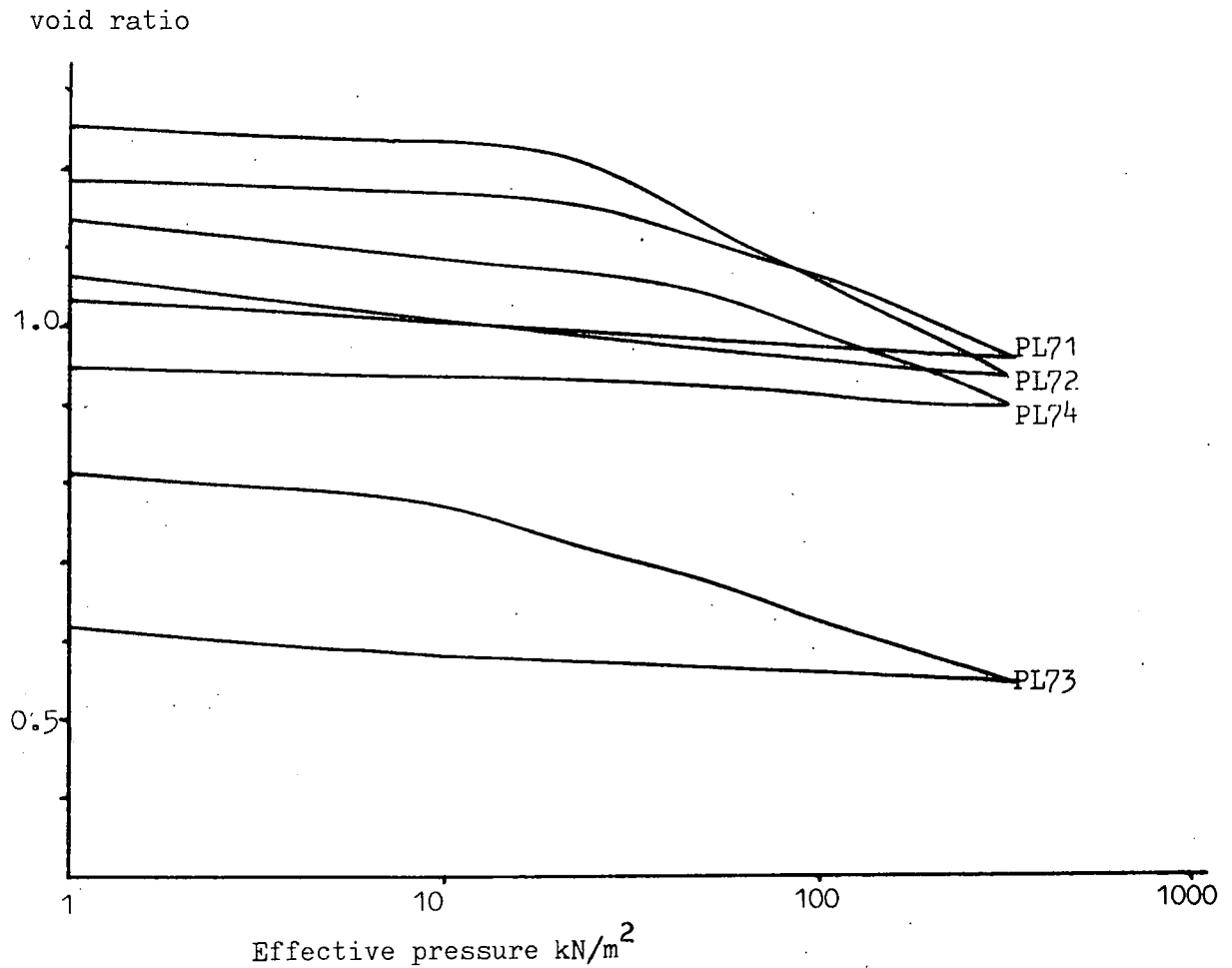


Table 6.4 Consolidation data, Peckfield.

Sample	$c_v$ ( $\text{m}^2/\text{yr}$ )*	$K$ ( $\text{m/s}$ )* ( $\times 10^{-7}$ )	$C_c$	$C_r$	S.G.
(6" Rowe cell)					
PL71	25.3	3.80 -9	0.189	0.029	1.890
PL72	6.81	1.25 -9	0.229	0.033	1.900
PL73	22.4	5.45 -9	0.148	0.024	1.886
PL74	2258	2.29 -7	0.165	0.026	1.526
(Triaxial)					
PL72	9.6	-	-	-	1.900
PL6 (lagoon 6, fine material see Fig.2.15)	6.3	-	-	-	2.171
(Shear box)					
PL6	5.6	-	-	-	2.171

\* averaged over the linear section



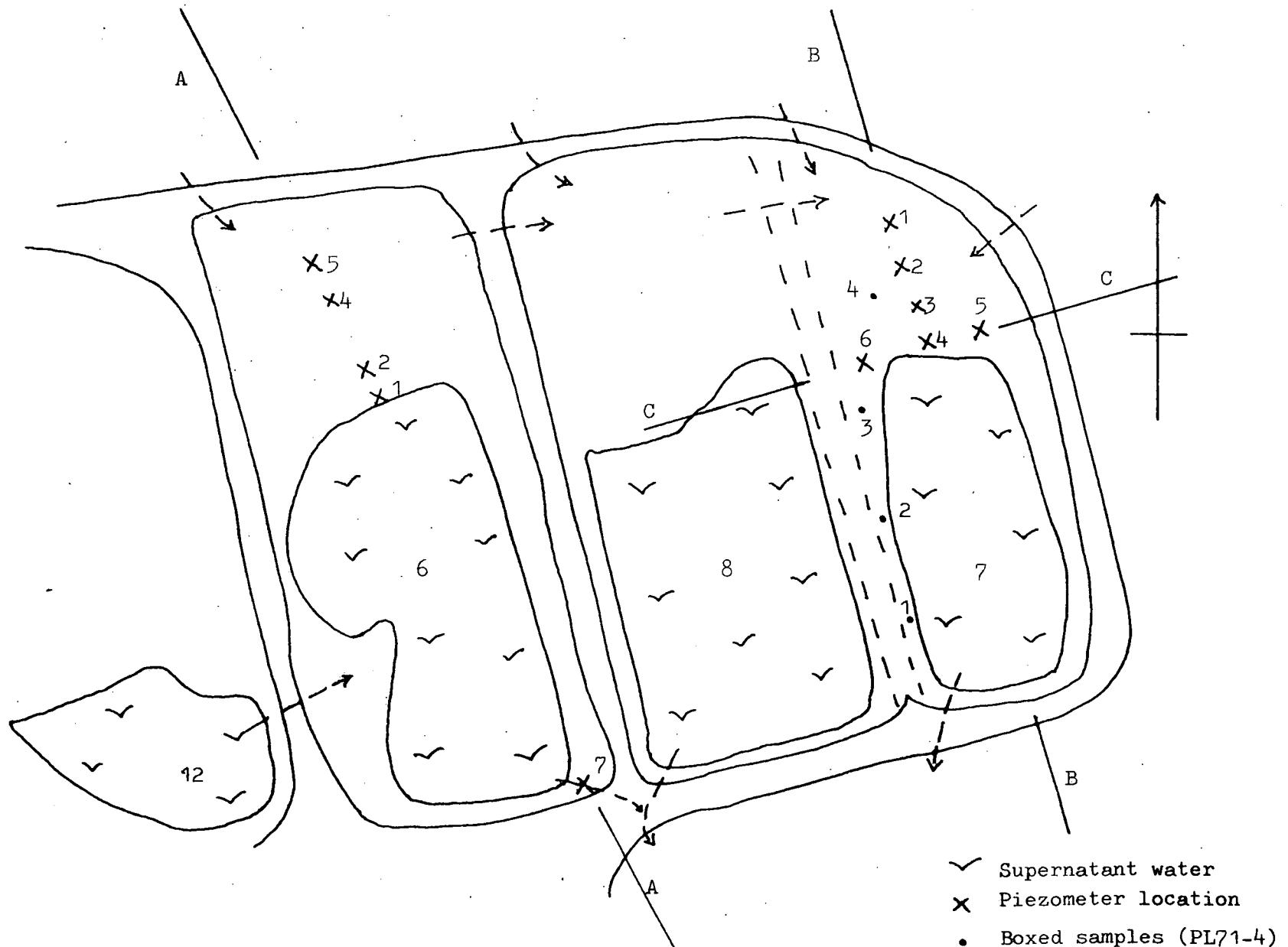
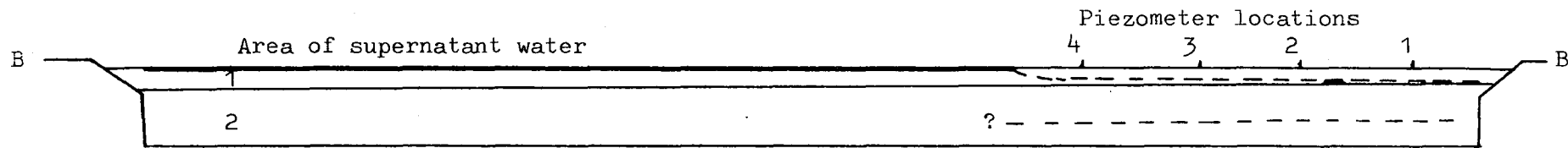
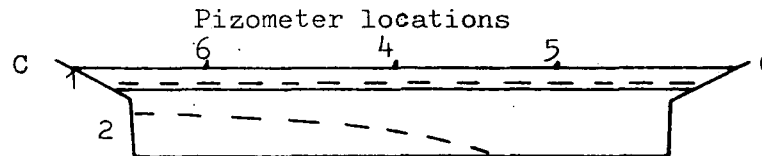


Fig.6.20 Piezometer locations at Peckfield showing the cross sections in Figs.6.21 and 22.

Fig.6.21 Cross-section of Peckfield lagoon 7.



- 1 Fine layer with perched water table. in this layer water presumably seeped to layer 2, but much also seems to flow to the sides.
- 2 Coarser layer, much flow through base see section C C below.

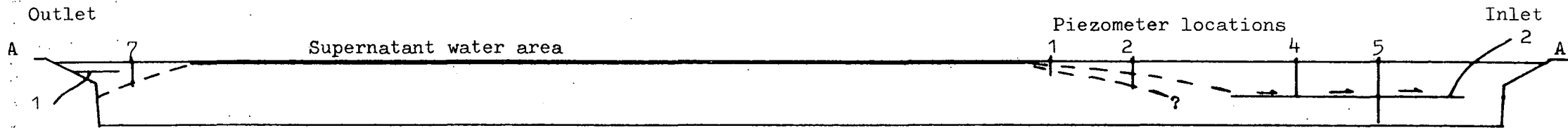


the western wall (dividing this lagoon from lagoon 8), and no water table exists some 25 m away from this wall. The form of the water table suggests that water is entering the lagoon through the western wall, presumably from lagoon 8, and is seeping away through the limestone floor. Further evidence was provided for this hypothesis when lagoon No.7 was excavated. The floor of the lagoon was always very wet during this operation, and the water levels in lagoons 6 and 8 lowered dramatically.

Lagoon 6 contrasts with lagoon 7 in that there was no large scale lamination, though small scale features were in evidence. The water levels recorded in the piezometers suggest that perched water tables are not generally present, rather that water seeps away through the floor as shown by Fig.6.22. However, a very wet layer was encountered at 3m depth while augering for the piezometer holes (push in piezometers were not used here). Piezometer 4 was emplaced in this layer but remained dry for most of the time. However, this layer probably represents a water table supported by an aquiclude. This hypothesis is supported by the fact that the water level rose in this piezometer after a period of heavy rain.

Observations of the piezometers in lagoon 6 continued throughout the summer of 1977, while lagoon 7 was being excavated. From the levels recorded in these piezometers, together with the rainfall data presented in Table 6.5 and Fig.6.23, it can be seen that the water-levels responded to periods of heavy rain, but generally fell when excavation of lagoon 7 started. The areas of supernatant water in lagoons 6 and 8 receded over this period by about 5m horizontal distance from each edge. Thus these lagoons seemed to be supplying water to lagoon 7.

Fig.6.22 Cross-section of lagoon 6 at Peckfield.



1 Site of coarse layer, see Fig.2.13.

2 Wet layer observed during the augering of piezometer holes 4 and 5. This is transmitting water to the sides of the lagoon. Generally at the inlet end of the lagoon flow is through the floor, but at the outlet end short flow paths exist to the sides of the lagoon and much flow will be via the sides. This is shown by the fact that the excavation of lagoon 6 de-watered both lagoons 6 and 8.

Table 6.5 Piezometer readings in lagoon 7, Peckfield, and rainfall data.

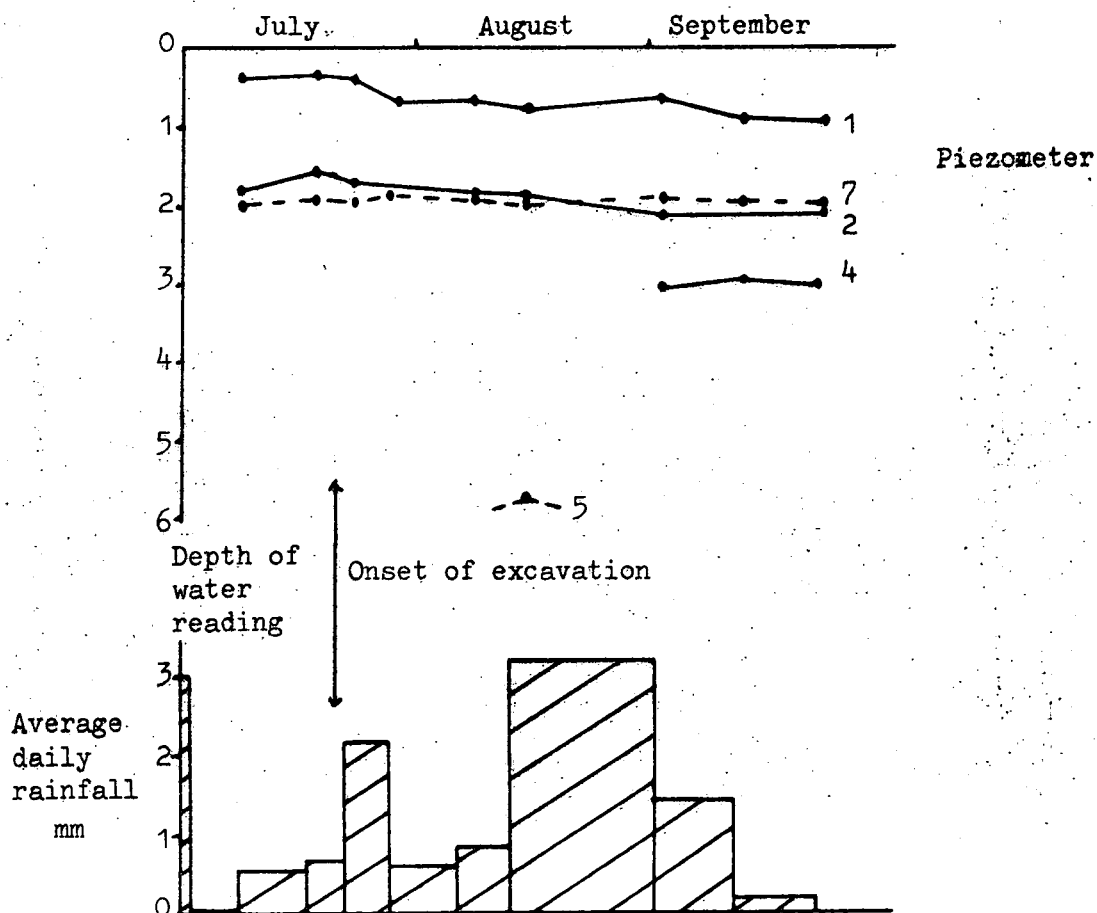
a. Piezometer readings

Piezometer	July					August		September		
	1	9	18	23	29	8	15	2	13	24
1		0.34	0.33	0.42	0.68	0.69	0.80	0.66	0.89	0.92
2		1.80	1.55	1.70	-	1.83	1.90	2.08	-	2.10
4		d	d	d	d	d	d	3.04	2.93	3.00
5		d	w	d	d	d	w	d	d	d
7		2.00	1.94	1.93	1.87	1.90	1.96	1.92	1.97	2.00

b. Rainfall data, average for the period preceeding the date shown, mm

3.00	0	0.57	0.68	2.16	0.59	0.81	3.19	1.45	0.19
------	---	------	------	------	------	------	------	------	------

Fig.6.23 Piezometer readings and rainfall data, lagoon 7, Peckfield.



#### 6.10 The Consolidation and Drainage of Lagoon 6 at Maltby Colliery

The water levels in this lagoon were measured only in the vicinity of the embankment but as part of the overtipping experiment described in chapter 7. They were everywhere about 2-2½ m from the surface, rising towards the area of supernatant water. Four samples of material were taken from the two locations sampled in the lagoon (see Fig.4.4.c). It can be seen from Fig.6.24 and Table 6.6 that values of  $c_v$  range from approximately 2 to 2000 m<sup>2</sup>/yr, as determined both by oedometer and triaxial tests. The material is generally incompressible, though one sample with a relatively low carbon content (as evidenced by a specific gravity of 2.309) proved to be highly compressible.

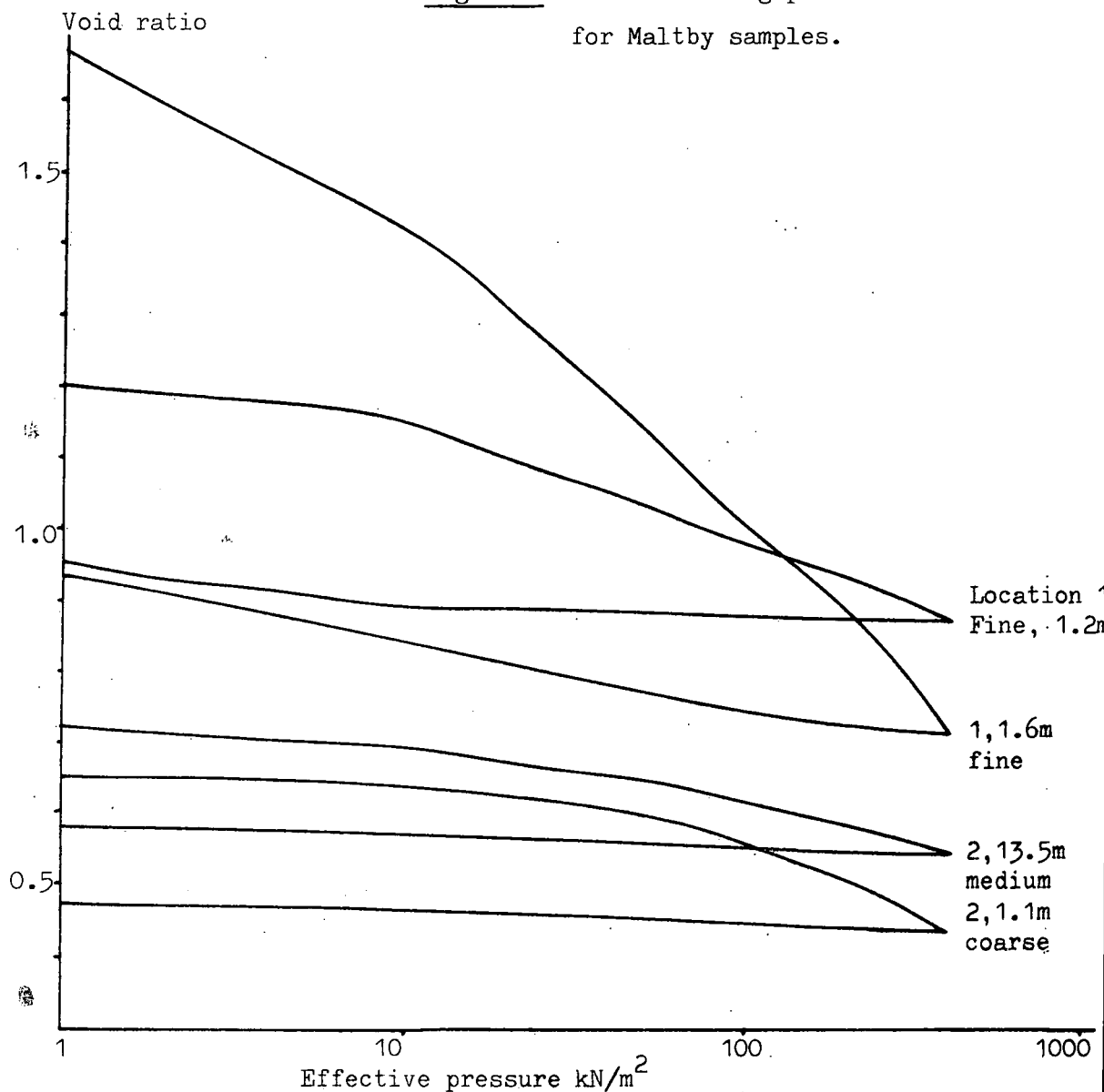
There is insufficient data on the distribution of the laminae in this lagoon to comment on the pattern of drainage. However, in view of the range of permeabilities of the various laminae, flow of water in a horizontal direction will certainly be of considerable importance.

#### 6.11 The Compressibility of Colliery Lagoon Sediments

In the preceding sections it has been shown that while most samples tested in the oedometer were relatively incompressible, a few had much higher compressibilities. Figure 6.25 shows the compression and swell indices plotted against the specific gravity. It is apparent that the more compressible material ( $C_c > .25$  and  $C_s > .03$ ) is always low in coal (as evidenced by the higher specific gravities) and impermeable (i.e. fine-grained). Coarser-grained material is less compressible, and carbon (coal) rich material is less compressible whether it be coarse or fine-grained.

Other authors have also reported low compression indices for coal-rich lagoon sediments. N.C.B, 1972 report values of between 0.02 and 0.27, all on materials with low values of  $c_v$ . Cobb (1977) reports

Fig.6.24 Void ratio-log pressure curves  
for Maltby samples.

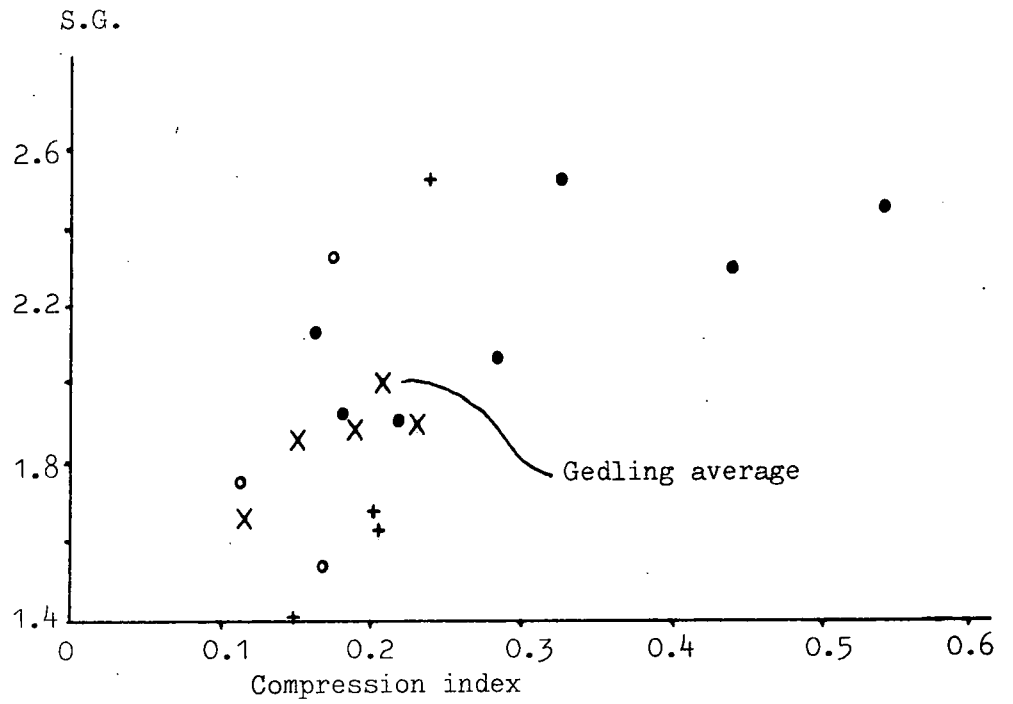


Location and sample	Depth	$c_v$ ( $m^2/yr$ )*	$k$ ( $m/s$ )* ( $\times 10^{-9}$ )	$C_c$	$C_r$	S.G.
1 coarse	1.1	1065	1.14 -7	0.172	0.016	2.329
2 medium	13.5	92.5	4.74 -9	0.117	0.016	1.661
1 fine	1.2	8.56	2.33 -9	0.178	0.015	1.927
1 fine	1.6	3.58	1.77 -9	0.438	0.082	2.309
(Triaxial)						
1 fine	1.2	38.5	-	-	-	1.927
2 medium	13.5	119	-	-	-	1.661
1 fine	1.6	1.97	-	-	-	2.309
2 coarse	1.6	2252	-	-	-	1.907
2 coarse	11.7	1230	-	-	-	1.579
1 fine	4.0	66.4	-	-	-	-

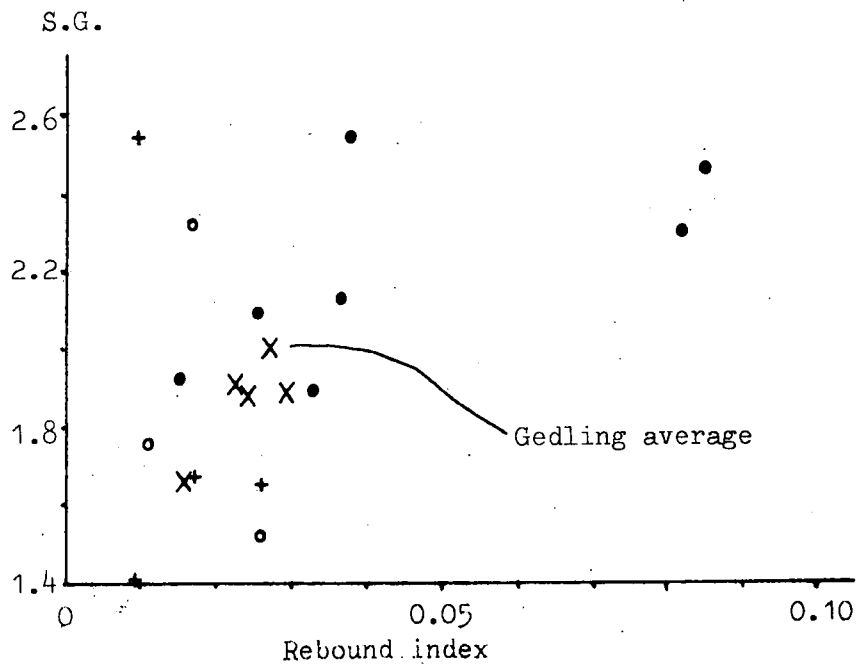
\* Averaged over the linear section

Fig.6.25 Compression characteristics of tailings.

a. Compression index



b. Rebound index



- 0-10
  - X 10-100
  - + 100-1000
  - o 1000+
- }  $c_v$  m<sup>2</sup>/yr



values between 0.160 (SG = 1.99,  $c_v = 45.1$ ) and 0.246 (SG = 2.10,  $c_v = 408$ ). Holubec (1976) reports  $C_c$  values of 0.20 to 0.30 for Appalachian colliery tailings dams, while Büsch et al. (1974) and Busch et al. (1975) report tests from which values of 0.080 to 0.312 may be calculated with one high value of 0.568; no  $c_v$  values are reported for this material.

The compressibility of lagoon sediments is therefore controlled both by the coal content and the grain size. In chapter 4.6 it was shown that the finer-grained sediments contain the least coal, and in chapter 3.3. and 3.4 it was shown that the proportion of finer grained laminae increases away from the inlet. Thus it is to be expected that the overall compressibility will increase away from the inlet. However it is difficult to estimate the extent of the effect unless the compressibility of every layer at any location is known. Referring to the borehole logs of East Hetton (Table 3.1), it can be assumed that all the fine-grained layers have an average compression index of 0.277 (which is the average of the oedometer values for East Hetton, Table 6.2, leaving out the anomalous value from one overconsolidated sample) while the other layers have an average  $C_c$  of 0.177. For location A, with 28 per cent fine laminae, the gross  $C_c$  becomes 0.205 (i.e.  $0.28 \times 0.277 + 0.78 \times 0.177$ ); that of location B is 0.236 and location C is 0.199. Thus the gross compressibility of the lagoon is increasing slightly away from the inlet. However, this is based on assumptions rather than facts and the effect is not great. For most practical purposes the compressibility can reasonably be assumed to be constant across a lagoon. This conclusion was reached by Cobb (1977).

#### 6.12 The Drainage of Colliery Lagoons

The manner in which water flows through colliery lagoons will depend on a variety of factors, which will include the following:-

1. The permeability of the base and embankments that contain the lagoon. Lagoon embankments are frequently built from coarse colliery discard. According to N.C.B. (1972) spoil placed in an uncompacted fashion leads to permeabilities ranging from  $10^{-4}$  m/s to  $10^{-6}$  m/s (as determined by in-situ tests). However, modern, thin-layer compaction techniques reduce the permeability of coarse discard to as low as  $10^{-8}$  m/s, though several values around  $10^{-7}$  and one as high as  $10^{-5}$  m/s are reported.

The base of the lagoon on the other hand depends on the choice of site for the lagoon. Some lagoons are placed on coarse discard, in which case the above values will apply. Some lagoons (such as those at Peckfield) have floors of a permeable rock (in the case of Peckfield the rock is Lower Magnesian limestone). Others again have floors of impermeable clays; for instance the lagoons at East Hetton are situated in a valley with a floor of alluvial clay.

2. The relative importance of horizontal and vertical permeabilities in the lagoon sediment. The layered nature of colliery lagoons necessitates application of the series and parallel resistance formulae (see section 6.2). Based on the borehole logs at East Hetton given in Table 3.1, a reasonable approximation of horizontal and vertical permeabilities may be made as shown in Table 6.7. Although the values are approximations, Table 6.7 does show that the horizontal and vertical permeabilities do not vary as much across the lagoon as would be suggested by the relative proportions of coarse and fine layers. However Table 6.7 does not take into account the effect of discontinuities in the layers, which will enhance vertical drainage. It is therefore reasonable to assume that  $2 \times 10^{-9}$  m/s is an approximate lower bound to the vertical permeability.

3. The extent of the supernatant water. When the supernatant water is very close to the embankment the proportion of flow through the

Table 6.7 Horizontal and vertical permeabilities in East Hetton lagoon 109B. Based on the logs in Table 3.1.

N.B.  $k_h = \frac{1}{H}(k_1 h_1 + k_2 h_2 + k_3 h_3 + \dots)$

$$k_v = \frac{H}{(h_1/k_1 + h_2/k_2 + h_3/k_3 + \dots)}$$

Location A	28% medium fine to fine, say $k = 10^{-9}$ m/s
	43% medium, mixed $10^{-7}$
	29% medium coarse to coarse $10^{-5}$

$$k_h = 2.94 \times 10^{-6} \text{ m/s} \quad k_v = 3.52 \times 10^{-9} \text{ m/s} \quad k_h/k_v = 835$$

Location B	59% medium fine to fine, say $k = 10^{-9}$ m/s
	25% medium mixed $10^{-7}$
	16% medium coarse to coarse $10^{-5}$

$$k_h = 1.63 \times 10^{-6} \text{ m/s} \quad k_v = 1.68 \times 10^{-9} \text{ m/s} \quad k_h/k_v = 970$$

Location C	22% medium fine to fine, say $k = 10^{-9}$ m/s
	61% medium, mixed $10^{-7}$
	17% medium coarse to coarse $10^{-5}$

$$k_h = 1.76 \times 10^{-6} \text{ m/s} \quad k_v = 4.42 \times 10^{-9} \text{ m/s} \quad k_h/k_v = 398$$

Note. The assignment of permeability values to the various layers is based on the ranges of values obtained from the in-situ tests. Although this approach leaves something to be desired, it allows for changes in the sediment in a consistent fashion.

embankment will be relatively high. The presence of supernatant water implies extensive layers of relatively low permeability. For instance, the lagoons at Peckfield receive about 1m of water per year in rainfall; taking run-off into account this is equivalent to about 2m per year over the area of supernatant water. However, allowing for evaporation, the input is approximately 1m per year over the area of supernatant water. This area forms a constant head boundary, where the head is approximately 300mm. Assuming that this head is dissipated through a layer 150mm thick, then the permeability of the layer would be:-

$$k = \frac{Q}{i.A} = \frac{1.0}{2.1. 1.365. 24.60.60} \text{ m/s}$$

$$= 1.6 \times 10^{-8} \text{ m/s}$$

Although all the values have been assumed, they are all reasonable, and the value of permeability is therefore a reasonable assumption also. Furthermore, the order of magnitude calculated for the permeability is insensitive to changes in the assumed parameters.

Flow through lagoons is a complex problem in detail, involving many boundary conditions, perched water tables, overflow towers and a varying sedimentology within the lagoon itself. An accurate assessment of the flow in a lagoon would therefore require a complex three-dimensional analysis (say by finite-element analysis) which in turn would require very detailed and accurate knowledge of the relevant parameters. Very seldom will these be available, and in any event the results would be useful only on an individual lagoon basis. It was therefore thought desirable to analyse the flow in a simplified manner which, with reasonable judgement, could be applied to a wide variety of lagoons without the necessity for expensive and difficult computations. For this reason an electrical analogue using "Teledeltos" paper and a

field plotter were chosen for the analysis.

The main parameter of interest is the relative proportion of flow that is to be expected through the base and the sides. Any action that could be taken in terms of lagoon design would be related to controlling flow through one or the other. It is possible to determine the relative proportions quickly and directly with the analogue by reversing the boundary conditions and determining the equipotential at the junction of the floor and sides. This is explained diagrammatically in Fig.6.26, from which it can be seen that a direct read-out from a one point determination gives the required information.

The electrical analogue is isotropic with respect to electrical flow whereas it is required to model an anisotropic water flow condition. This is accomplished in seepage and flow net analysis by transforming the horizontal scale of the analogue after Samsioe (see Craig, 1974, p.46):-

$$x_t = x \cdot \frac{k_z}{k_x}$$

where  $x$  is a natural length

$x_t$  is the transformed scale length

$k_x, k_z$  are the permeabilities in the  $x$   
 $z$  directions

The equivalent isotropic permeability,  $k'$ , given by:

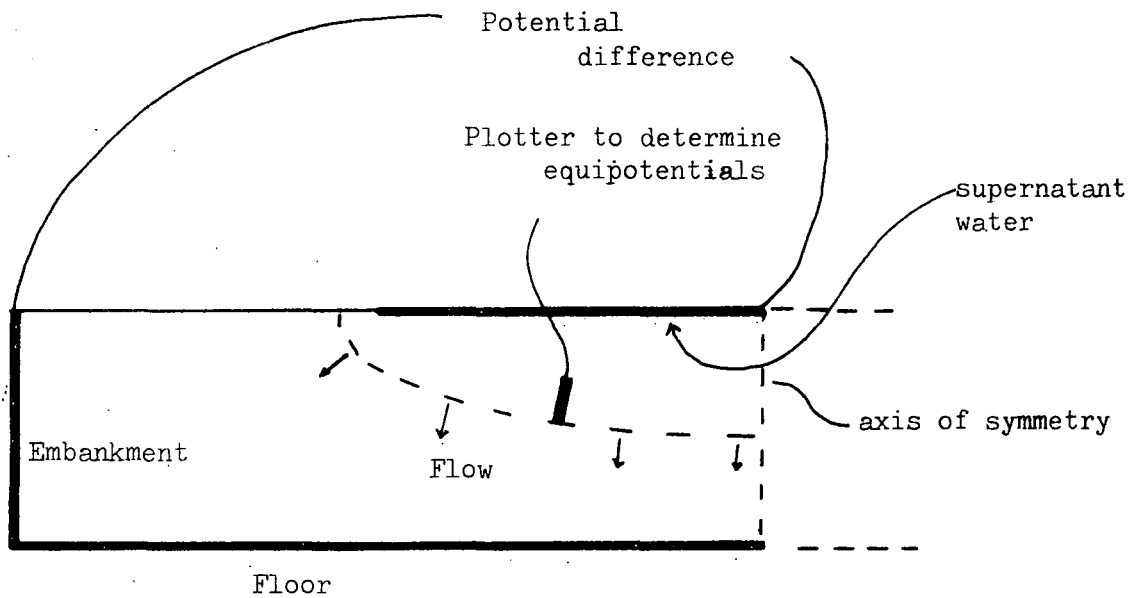
$$k' = \sqrt{k_x \cdot k_z}$$

Therefore, any geometrical shape analysed by this analogue method can be regarded as several combinations of geometric shapes and permeability ratios. It is useful to define a flow shape as:-

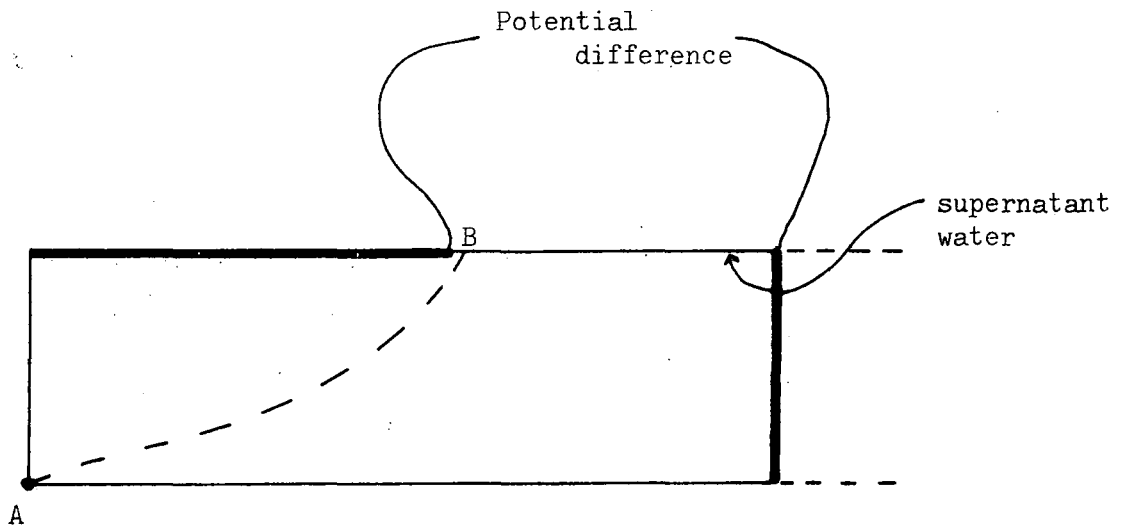
$$F.S. = \frac{L/D}{\sqrt{k_h/k_v}}$$

Fig.6.26 Analogue set-up for lagoon flow analysis.

a. Normal boundary condition



b. Reversed boundary conditions, as used in the analysis.



The equipotential AB is equivalent to a flow line with the normal boundary condition. Therefore determining the potential at A as a percentage of the potential difference automatically gives the proportion of the flow at the divide between the floor and the embankment. The field plotter used was calibrated in percentages.

where F.S. is the flow shape, is the shape of the analogue section.

L is the length of the lagoon section being analysed

D is the depth

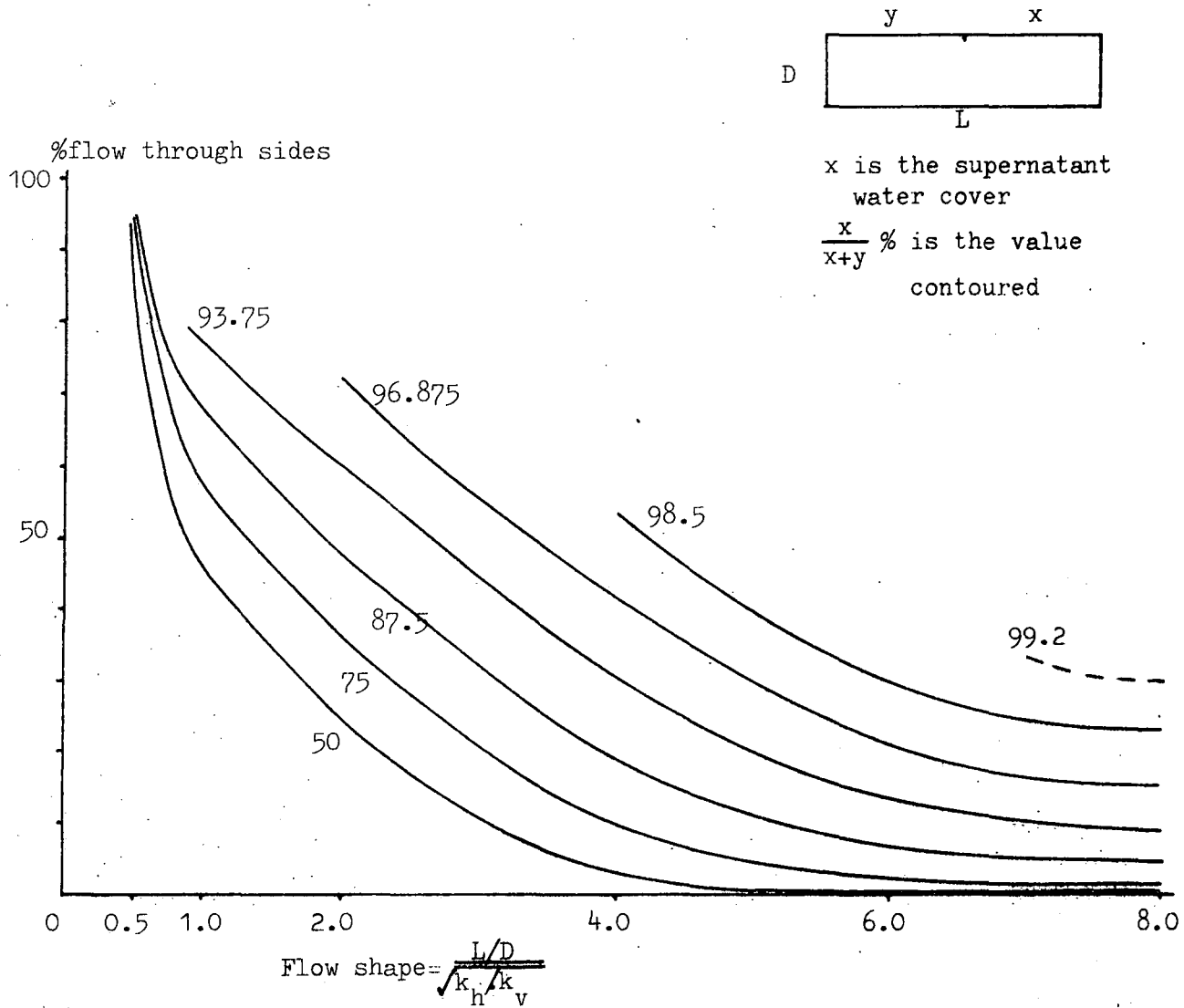
$k_h, k_v$  are the horizontal and vertical permeabilities

Thus an analogue shape of 10 long to 1 deep could represent a lagoon section 10 long to 1 deep with isotropic permeability, or one of 100 long to 1 deep with a permeability ratio (horizontal to vertical) of 100 to 1.

In the analysis, rectangular shapes only were analysed as shown in Fig.6.26.b. There are two sources of error introduced by this simplification. The first is that while many lagoons have a fairly flat floor, most have sloping embankments. In fact, due to the transformation of horizontal scale mentioned above, the slope in the analogue is frequently nearly vertical. The second source of error is that the phreatic surface is not incorporated correctly. The error is not serious when the supernatant water is close to the embankment in relation to the depth of the lagoon, because the phreatic surface will be close to the actual lagoon surface. Nor is the error serious when the flow shape number is high (i.e. a very wide, shallow lagoon) because very little water flows through the sides in this case. The error is only noticeable when the flow shape number is small and the supernatant water is far from the sides, in which case the proportion of flow through the sides is overestimated.

Bearing these simplifications in mind, Fig.6.27 shows the variation in the proportion of flow through the sides of the lagoon for different flow shapes and degrees of supernatant water cover. It can be seen that very little water flows through the sides for lagoons with a large flow number unless the lagoon is almost completely covered by supernatant

Fig.6.27 The proportion of flow through the sides of a lagoon with equally permeable sides and base.





water. Thus designing efficient filters for the embankments of such a lagoon to encourage rapid drainage through the sides would not be an economic measure.

Peckfield lagoons 6 and 7 can be modelled with Fig.6.27. Lagoon 6 in half cross section has a length to depth ratio of about 5, and supernatant water cover of about 75 per cent (see Figs.6.20 and 6.22). The ratio of horizontal to vertical permeability is not known; however the existence of the supernatant water implies extensive low permeability zones, while coarse permeable laminae are known to exist (see Fig.2.13). Assuming that the permeability ratio is on the order of 100, the flow shape is

$$F. S. = \frac{5}{\sqrt{100}} = 0.5$$

which, from Fig.5.26 gives the flow to the sides as being about 95 per cent. However, in the region of the lagoon inlet the general form of the phreatic surface (Fig.6.22) suggests that most of the flow is through the floor, although the picture is complicated by a perched water table. Thus overall, probably some 80 per cent of the flow is through the sides. The actual amount of flow can be assessed from an estimate of the inflow into the lagoon in terms of run-off and rainfall, and is about  $1 \text{ m}^3/\text{yr}$  per  $\text{m}^2$  of supernatant water or about  $3500 \text{ m}^3$  per year.

In contrast, lagoon 7 possesses an upper layer with a perched water table, which must be treated separately. In half-section this layer is 21m wide and 1.5 m deep, a length to depth ratio of 14. The area of supernatant water and the presence of a perched water table implies both impermeable laminae and a high permeability ratio. Assuming therefore that the permeability ratio is again 100, the flow shape is

$$F. S. = \frac{14}{\sqrt{100}} = 1.4$$

and the supernatant water cover is about 70 per cent. From Fig. 6.27, the flow to the sides is about 45 per cent, despite the thin nature of the layers. The total volume of flow at  $1\text{ m}^3/\text{yr}$  per  $\text{m}^2$  of supernatant water is about  $2000\text{ m}^3/\text{yr}$ .

However, not all lagoons have sides of equal permeability. The electrical analogue can be used to analyse approximately the case of a lagoon with an impermeable base, as is shown in Fig.6.28. This introduces the limitation that the permeability ratio (i.e.  $k_h/k_v$ ) should be the same in the lagoon and the base, but nevertheless it gives a measure of the effect of an impermeable base. Only the case in which the flow path is as long through the base as it is vertically through the lagoon has been analysed, simulating a thin layer of relatively impermeable clay. Thicker layers of impermeable clay would require additional analyses. The resulting variation of flow through the sides versus flow shape is shown in Fig.6.29. A comparison with Fig.6.27 shows that, as expected, very much more water flows through the sides.

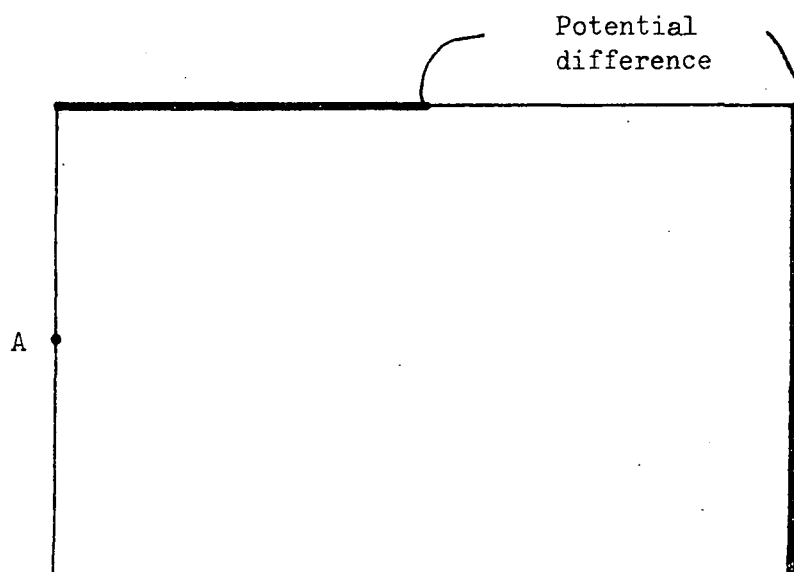
The lagoons at East Hetton have limestone sides (presumed to be permeable) and a base of 1m of alluvial clay (presumed to be relatively impermeable). Lagoon 109B is about 70m wide, i.e. 35m wide from the centre line to the edge. It is 13m deep but the water table is 3m down and hence it can be treated as being 10m deep. The permeability ratio is as high as 1000 (see Table 6.7), but may be lower. The flow shape is therefore:

$$\text{F.S.} = \frac{L/D}{\sqrt{1000}} = \frac{35/10}{\sqrt{1000}} = 0.11$$

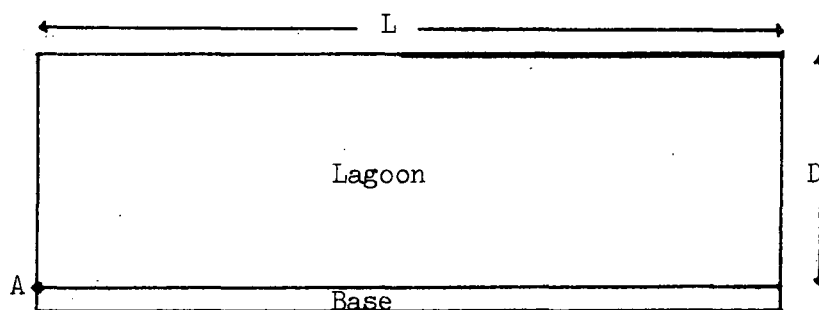
Figure 6.29 shows that virtually all the water flows through the sides, irrespective of the area covered by the supernatant water. Even if the permeability ratio is as low as 25, which gives a flow shape of 0.70, the flow through the sides will still be in excess of 90 per cent.

Fig.6.28 Analysis of flow in a lagoon with an impermeable base.

a. Analogue. The potential at point A is measured as a percentage.



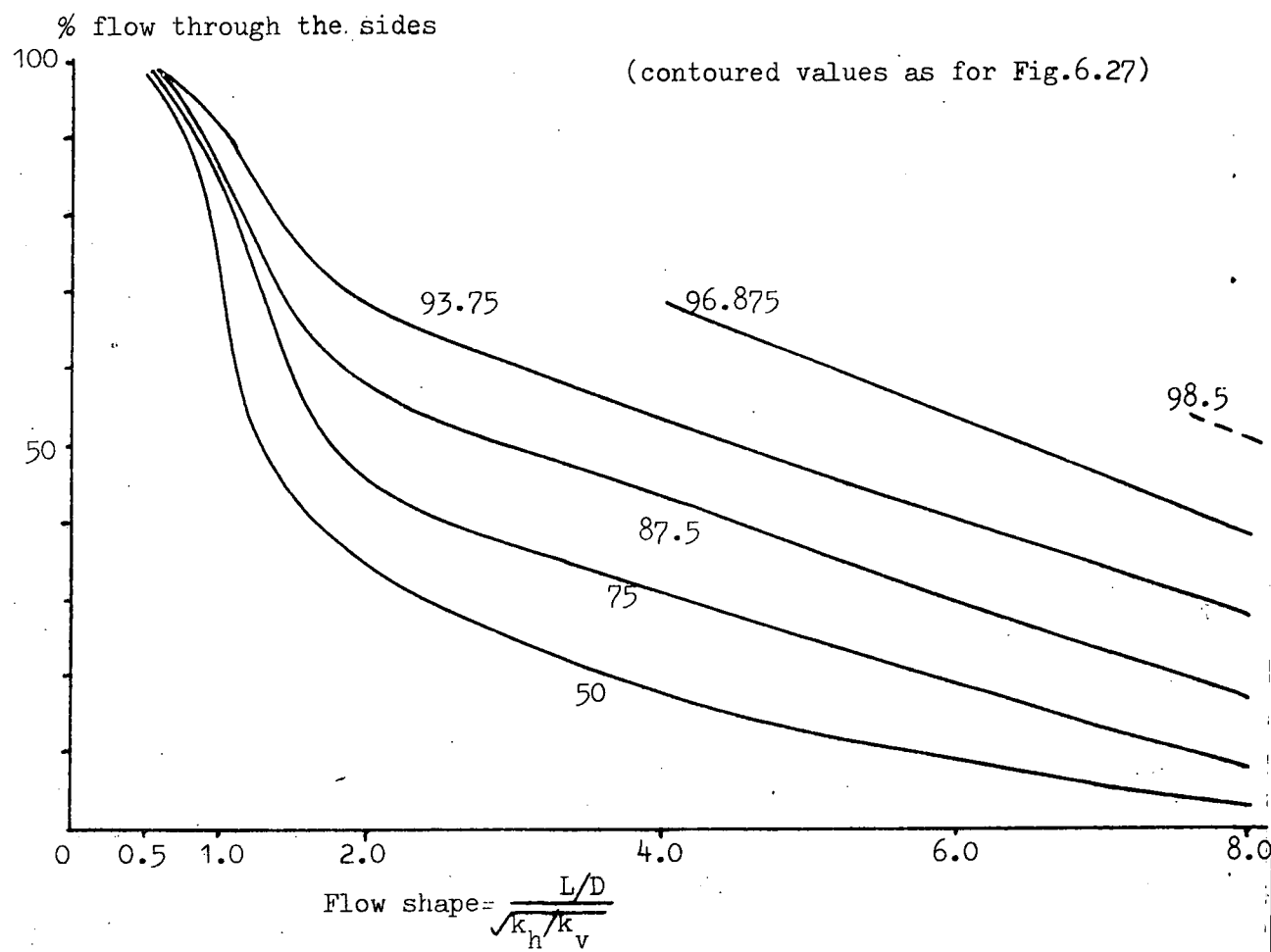
b. The lagoon



In this case the flow path through the base is as long as a vertical flow path in the lagoon. For instance, this could be a layer of clay  $1/10$ th as thick as the lagoon, but with a permeability of  $1/10$ th that of the lagoon sediments.

Strictly speaking this only applies if the flow lines are normal to the boundary between the two materials.

Fig.6.29 The proportion of flow to the sides of a lagoon with a less permeable base.



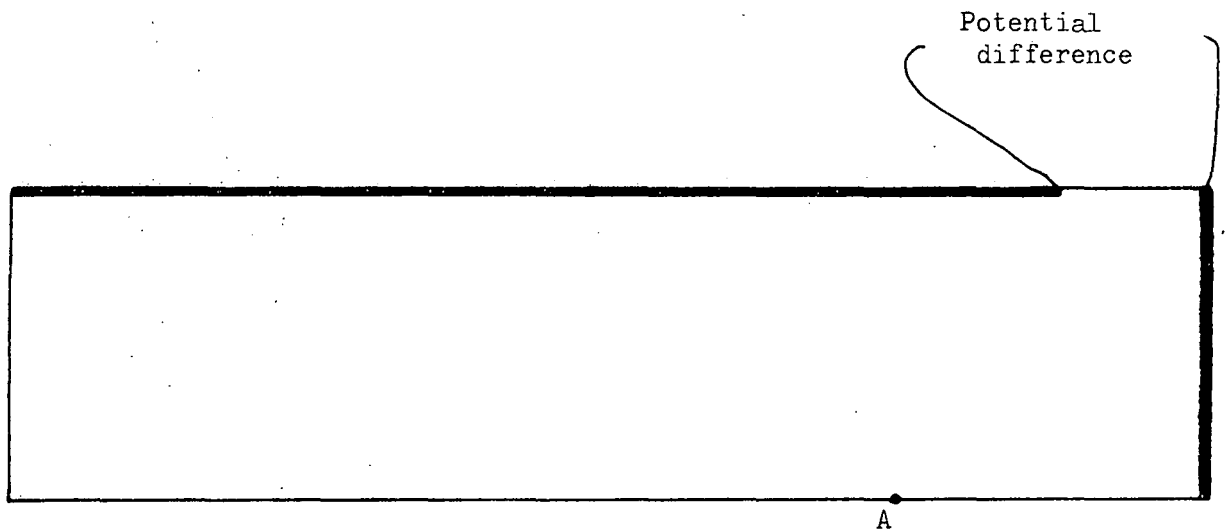
Furthermore, Fig.6.27 shows that even if the base of the lagoon were permeable, virtually all the water would nevertheless flow through the sides. Thus if it had been felt necessary to prevent water flowing into the limestone walls, little would have been achieved by laying a permeable blanket on the floor of the lagoon. Rather, the limestone walls of the lagoon would have to be lined with an impermeable material.

Using similar reasoning to the above, the case of a lagoon with an impermeable embankment can be analysed. The analogue model is shown in Fig.6.30, and the resulting variation in flow through the sides with flow shape is shown in Fig.6.31. It can be seen that only in a lagoon with a very low flow shape number is there any appreciable flow through the sides. In applying this model, it should be remembered that the effective isotropic permeability of the lagoon in transformed section is not  $k_h$ , but  $\sqrt{k_h \cdot k_v}$ ; this will be of the order of  $10^{-8}$  m/s for most lagoons. Therefore a coarse colliery discard embankment built by thin layer compaction techniques will usually not be less permeable than the lagoon in transformed section, despite the fact that the horizontal permeability of the lagoon greatly exceeds that of the embankment. No case corresponding to this condition is known to the writer. However Cobb (1977) produces evidence for very impermeable lagoon embankment interfaces, which Fig.6.31 could be used to analyse.

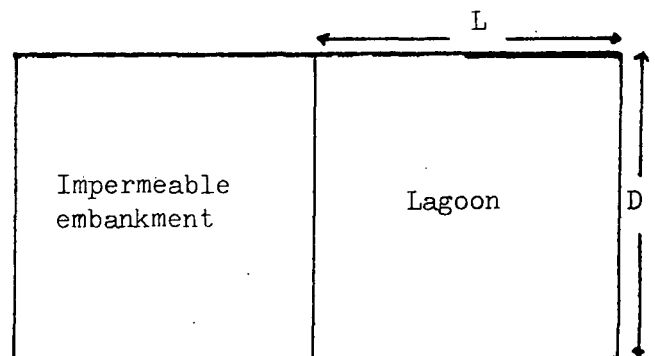
The method outlined could easily be extended to more cases, such as lagoons with a different cross-sectional form. It is a quick method which requires very little computation. The method is not highly accurate, because of some of the simplifying assumptions. However, it is doubtful whether a more rigorous method would greatly improve the position unless very accurate data concerning the permeabilities of the floor and embankments are available. Even then the occurrence of

Fig.6.30 Analysis of flow in a lagoon with impermeable sides.

- a. Analogue. The potential at A is measured as a percentage.



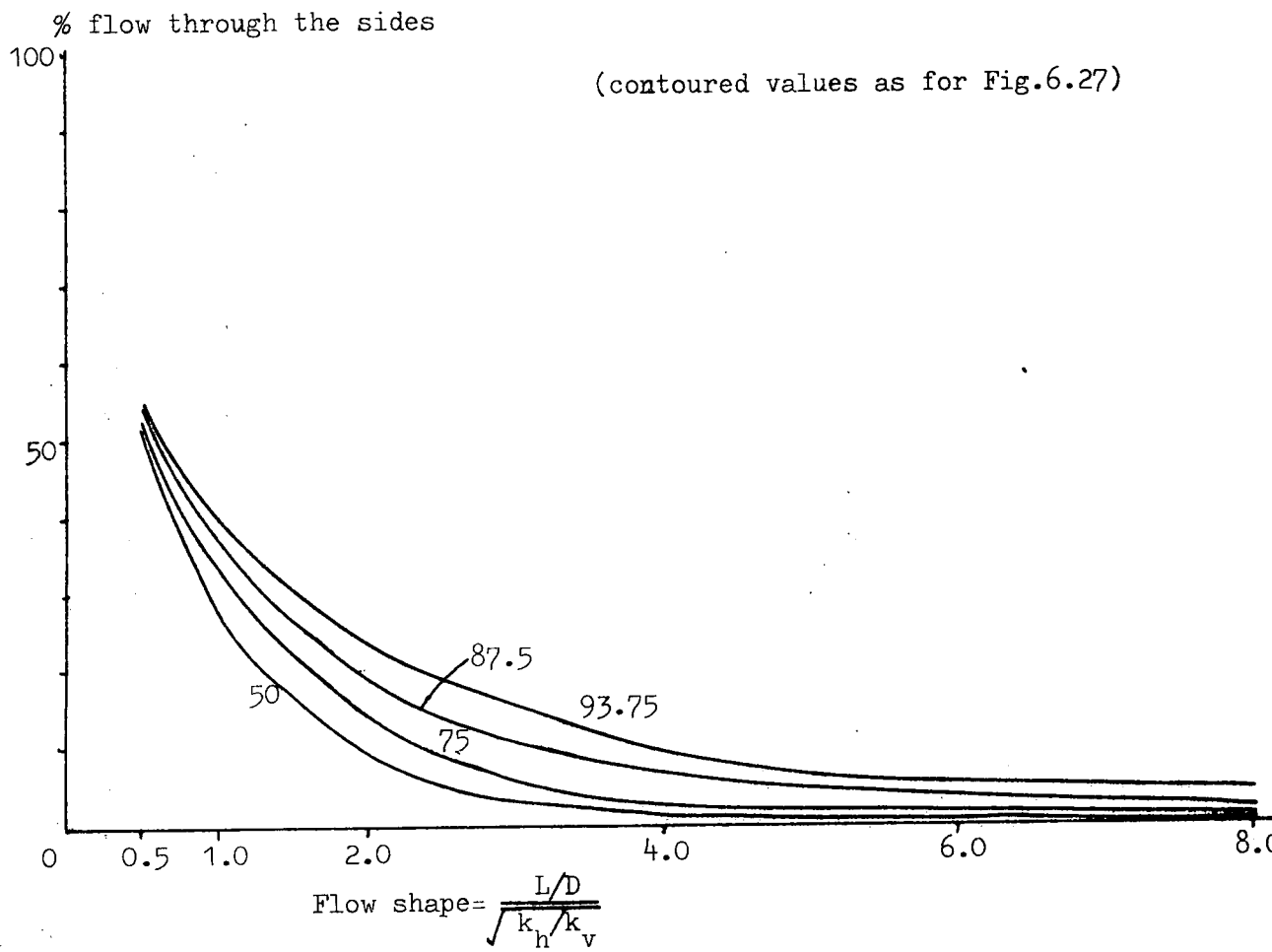
- b. The lagoon



In this case the flow path through the embankment is three times the length of a horizontal flow path in the lagoon. For instance, this could be an embankment as wide as the transformed lagoon, but with a permeability of only  $1/3$ rd that of the lagoon.

Strictly speaking this only applies if the flow lines are normal to the material boundary.

Fig.6.31 The proportion of flow to the sides of a lagoon with less permeable sides.



perched water tables, and the complexity of the sedimentology in the lagoon would be difficult to model accurately. Therefore it is felt that the method outlined is accurate enough for a rapid assessment of flow through a lagoon.

### 6.13 Conclusions

Colliery lagoons consist of thin laminae with widely varying consolidation and permeability parameters. It has been shown that recognition of this fact has implications both for measuring the characteristics of the sediment and for determining overall patterns of drainage of the lagoon.

In the laboratory, oedometer tests have been used to determine the consolidation parameters. This method is preferred to the use of Rowe cells, in contrast to usual practice, because the parameters of individual laminae can be tested in the smaller oedometer. It has been shown that for any particular type of lamination the consolidation parameters do not vary across the lagoon. Thus a fine grained layer will have a similar coefficient of consolidation and compression index everywhere it occurs. Hence, in terms of time and effort, it is efficient to test the consolidation parameters of characteristic horizons, and to assess the contribution of each type of sediment by trial pitting or borehole logging in several parts of the lagoon. With experience, it is probable that this could be applied from lagoon to lagoon as well.

The coefficient of consolidation has been shown to vary from about  $2 \text{ m}^2/\text{yr}$  for fine-grained laminae to  $2000 + \text{m}^2/\text{yr}$  for coarser horizons. In this type of sediment the consolidation will take place by horizontal drainage via the more permeable horizons, and the effective coefficient of consolidation will tend towards that of the more permeable sediments, as has been shown by Rowe (1959) and Horne (1964).

The compression index is generally fairly low, and is dependent



on two features of the lamination under test. Firstly all carbon (coal)-rich laminae have compression indices of about 0.2. Secondly, of carbon (coal)-lean samples, the fine-grained examples have higher compression indices of up to 0.54. However, coarse-grained, coal-lean samples also have low compression indices. The compression index is therefore controlled both by the carbon (coal) content and by the sediment size.

In-situ piezometer tests have been used for determination of permeabilities. A simple home-made, push-in piezometer of cheap and easy construction has been shown to perform very well for this type of test. The permeability values so obtained have been found to be consistently similar by two methods of interpretation. Furthermore, the values are consistently two orders of magnitude or more higher than the values determined from oedometer tests, which are generally considered to be inferior for measuring this property of soils. The permeability of lagoon sediments varies from  $10^{-9}$  m/s to  $10^{-4}$  m/s, and at East Hetton and Silverhill the full spectrum from permeable to relatively impermeable sediments is found. Although the in-situ permeability measurements have not been directly correlated with particular laminae within the lagoons, it is suggested that with reasonable judgement the overall permeability of the lagoon can be assessed from borehole logs or trial pits. This is based on the assumption that the range of permeabilities measured is directly correlated to the range of different laminae found within the lagoon, which is of course to be expected.

The piezometric head has been studied in four lagoons. At Silverhill the position is complicated by an overtipping operation, and this is discussed in the following chapter. The other three lagoons (East Hetton, 109B; Peckfield, 6 and 7) all show the presence of perched water tables. This is clearly a consequence of the layered structure of lagoon sediments

where there is an alternative of coarse and fine (i.e. permeable and impermeable) laminae.

The analysis of flow through a lagoon is a complex problem, because of the variety of shapes and boundary conditions, perched water tables and complex sedimentology. A simple approach has been outlined which allows a very rapid approximate assessment of the proportion of flow through the floor and embankments of the lagoon. Using this approach the importance of the layering in the sediments in controlling the flow of water is underlined. In the case of East Hetton virtually all the water flows through the sides, and the permeability of the floor is virtually irrelevant because of the layering. Lagoon 6 at Peckfield also discharges much of the water to the embankments, despite having a permeable floor. Even the upper, 1.5 metre thick, weak layer in lagoon 7 at Peckfield discharges half of its flow to the embankment. It is possible using this approach to analyse the effect of a less permeable base or embankment to the lagoon in a very quick and simple fashion, though the answers are approximate. The method used does not involve drawing a complete flow net, and therefore quantities of flow cannot be computed. However, these can be assessed from rainfall, inflow and draw-off rates, making an allowance for evaporation. Thus it is possible to decide whether it is necessary to take action to control the flow through the lagoon and how best to approach the design of any control measures.

## CHAPTER 7 THE OVERTIPPING OF COLLIERY LAGOONS

### 7.1 Introduction

Ultimately a lagoon must either be excavated for re-use or overtipped. The latter practice is attractive because it both increases the volume of waste that can be disposed of in a given area, and disguises an unsightly hazard, permitting easier landscaping. The dangers and uncertainties inherent in the practice have dictated caution. Current National Coal Board recommendations (N.C.B., 1970) limit the maximum depth of overtip to three metres.

The possible sources of danger in an overtipping operation fall into four categories:-

- a) 'Static short-term' - bearing capacity failure of the sediment being overtipped.
- b) 'Static long-term' - slope failure of the final composite tip heap.
- c) 'Dynamic short-term' - local liquefaction; collapse and failure due to vehicle (plant) vibrations.
- d) 'Dynamic long-term' - general failure of the final tip complex due to mobility of the embodied lagoon during earth tremors.

While procedures exist for calculating bearing capacities, these cannot confidently be applied to the extremely soft, compressive sediments found in lagoons without a field trial. Furthermore, laboratory liquefaction work should always be checked against field data (Peck, 1979). The pore pressures generated by overtipping and their subsequent dissipation would need to be monitored in order to arrive at Codes of Practice. As lagoon sediments in general have higher angles of friction than coarse discard, the long term stability will be ensured if the lagoon drains adequately. Adequate drainage will also ensure against

liquefaction to a degree.

The problems of overtipping are highlighted by a few instances that have come to the writer's attention. At Gedling Colliery there exists within the tip heap a lagoon which was successfully overtipped and is now completely enclosed. On the other hand, at the same colliery an embankment built into another lagoon displaced material to a depth of 12 m before it was stable. At Bilsthorpe Colliery (North Nottinghamshire region, N.C.B.) the writer has observed a small lagoon that was overtipped on all sides. Material was displaced towards the centre, where it welled up and now exists in a semi-liquid state.

The lack of knowledge about pore pressure behaviour during overtipping came to light during a series of vane tests carried out during a reconnaissance of lagoon No.7 at Orgreave Colliery (S.Yorkshire Area, N.C.B.). At the time of these tests part of the perimeter was being overtipped by a D6 and a D8 caterpillar vehicle. The line of overtip and the position of the vane tests is shown in Fig.7.1. At position A, near the outlet, the sediment failed and heaved at the toe of the overtip under the weight of a D6 vehicle (see Fig.7.2). From cracks in this heaved material water seeped out onto the lagoon surface. At B however, even the D8 vehicle was able to overtip safely (see Fig.7.3). While the vehicles were active the  $H=D/3$  vane profile in Fig.7.4 was put down, the vehicles had moved to another part of the tip several hundred yards away. The second profile is obviously very much stronger. Without adequate instrumentation the reason for this can only be assumed, but the possibility of high pore pressures caused by vehicle activity cannot be ruled out.

## 7.2 The Maltby Overtipping Trial

### 1. Introduction

In view of these findings a full-scale field overtipping trial was

Fig.7.1 Sketch of the outlet end of lagoon 6, Orgreave.

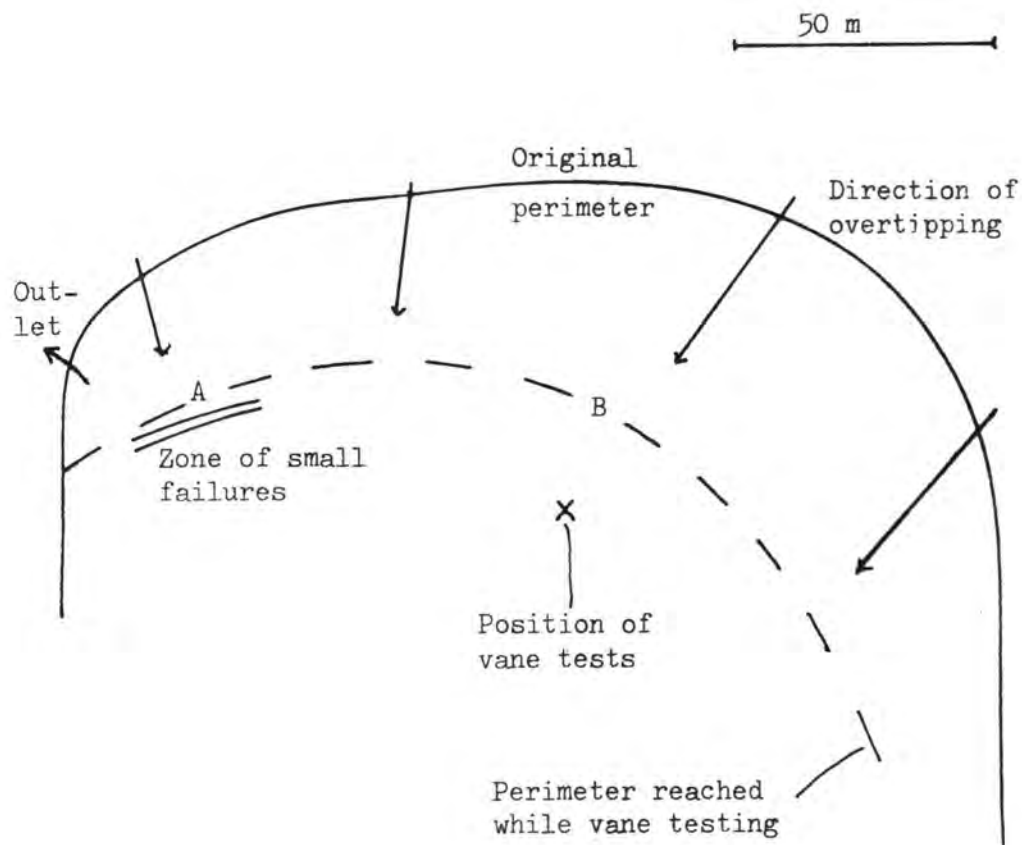


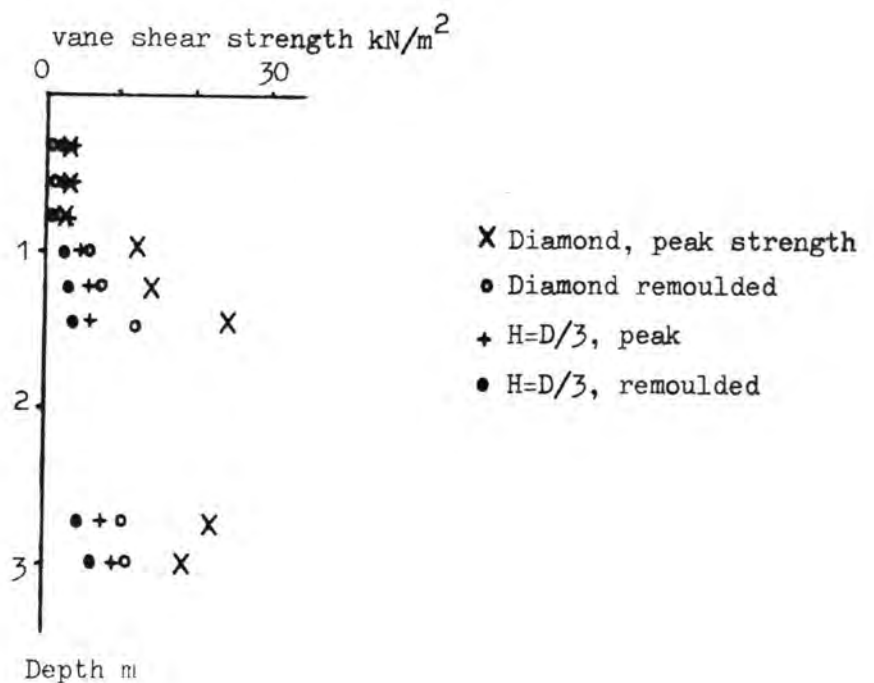
Fig.7.2 Overtipping at A by a D6; note heave at the toe of the overtipped embankment.



Fig.7.3 Overtipping at B by a D6 and a D8; note that there is no cracking of the surface of the lagoon.



Fig.7.4 Vane tests in lagoon 6 at Orgreave.



conducted (Taylor, Kirby and Lucas, 1980). The aims of this trial were to investigate the effect of overtipping on:-

- a) the shear strength of the lagoon sediments
- b) the pore pressures within the lagoon
- c) the liquefaction susceptibility of the lagoon sediments.

Previous work (Taylor et al., 1978; Taylor and Morrell, 1978) using a laboratory triaxial cyclic loading apparatus indicates that whereas undisturbed (in-situ) lagoon sediments generally show fair resistance to cyclic mobility, remoulded samples (i.e. laboratory fabricated) tend to have a much lower resistance (at the same void ratio). Kennedy (1977) showed the same to be true under monotonic loading conditions. The possibility that remoulding due to overtipping might decrease liquefaction resistance could not be ruled out.

In addition the susceptibility of the sediments to earth tremors (simulated by explosives) could be monitored directly in the field. In conjunction with laboratory triaxial cyclic loading tests, the conflict of "in-situ versus remoulded" samples (Yoshimi, 1977) might be resolved.

Finally it was hoped that positive recommendations of methods of overtipping, factors of safety etc. might emerge from such a trial.

The lagoon chosen for this study was lagoon no.6 at Maltby Colliery, South Yorkshire Area, NCB. Earlier field vane testing in this lagoon by the writer and by Messrs.Wimpey had revealed a high average sensitivity (4.2). It was thought that this might indicate a high susceptibility to liquefaction. In addition triaxial cyclic loading tests by Taylor et al., (1978) had indicated a fairly high degree of susceptibility to liquefaction. Site access was also suitable.

## 2 Pre-Construction Phase

The trial centred around the construction of an embankment of fresh

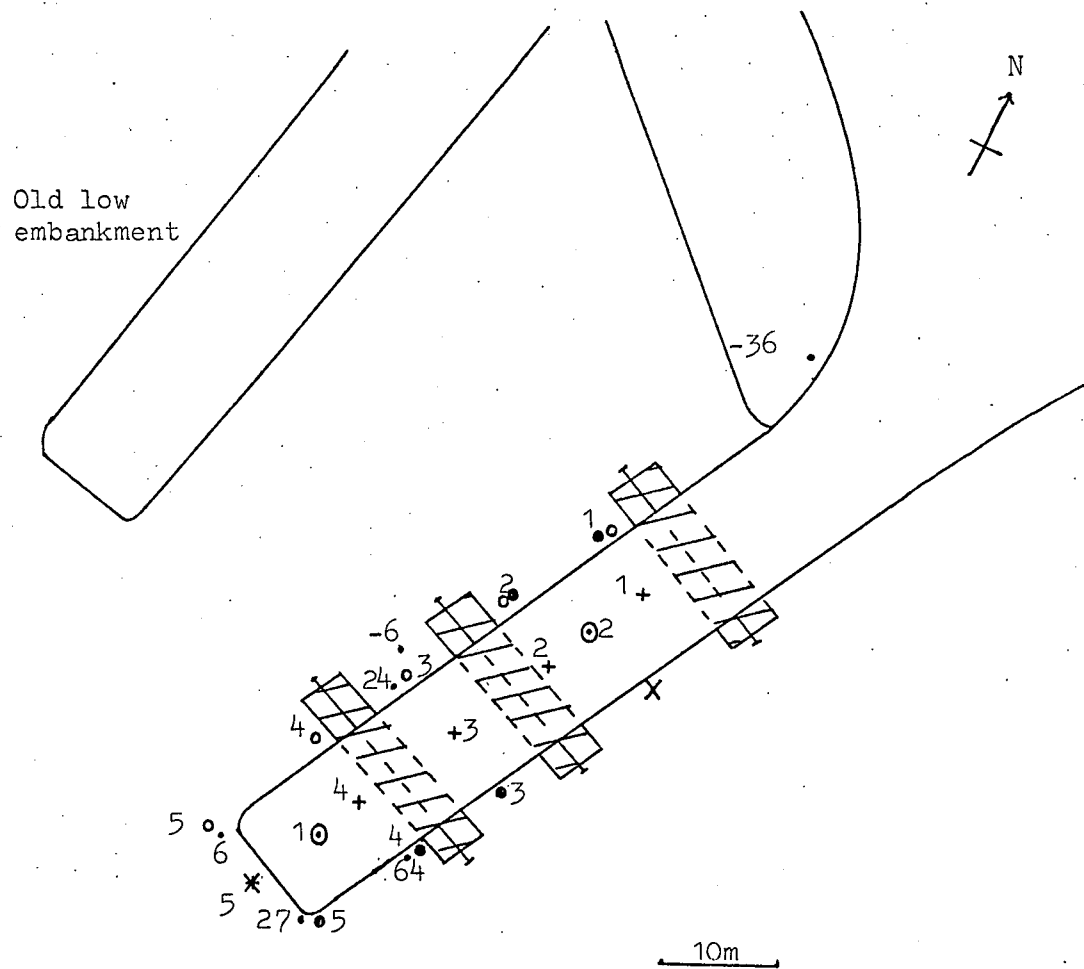
colliery discard 3m high, 10m wide and 50 m long across part of the 12m deep lagoon, as shown in Fig.7.5. (The depth of the lagoon was known from the Wimpey site investigation report, Wimpey 1977a). It was decided to use a caterpillar D6 earth-moving vehicle for the project, because plant of this size had previously been shown to be operationally effective, while at the same time keeping sediment disturbance within tolerable limits. The original proposal was to construct a 3m high embankment in three layers, each nominally of 1m thickness (see Fig.7.6). From the proposed orientation (Fig.7.5) it was expected that a transition would be encompassed from a safe operation at the edge of the lagoon, to one of marginal safety in the wetter material adjacent to the supernatant water.

A grid of pegs was set out on the lagoon surface, and levelled to enable monitoring of the surface settlements. Settlements underneath the embankment were to be estimated from lateral extension wires strung across the centreline of the embankment and covered by three sections of the filter fabric "Terra m" as shown in Fig.7.5 and 7.6. Apparent shortening of the wires was monitored during construction.

For measuring pore water pressure changes, 15 piezometers were installed: 5 pneumatic piezometers being placed 4m deep below the centre line of the embankment. Five Casagrande type piezometers, together with five drive-in type were installed around the periphery of the proposed embankment as indicated in Fig.7.5. Two vibrating wire piezometers were also installed later for the blasting trials.

In Fig.7.5, positions 1 and 2 represent locations where in-situ vane shear and static cone penetrometer tests were conducted. The fourth vane pair combination was used in these tests. From Figs.3.7a and 3.7b it can be seen that the vane shear strengths were approximately





- ⊙ 1,2 sampling and testing locations
- + Pneumatic piezometers, locations 1-5
- Drive in piezometers, locations 1-5
- Casagrande piezometers, locations 1-5
- X Vibrating wire piezometers
- 6 Height change of surveyed peg (mm)

▨ Terram filter fabric overlying lateral extension wire

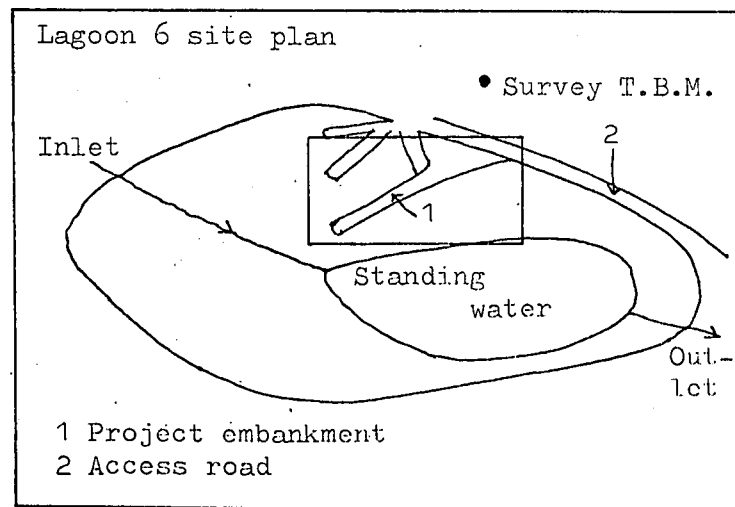


Fig.7.5 Site plan showing details of instrumentation and surface level changes following construction.

Fig. 7.6 Construction of the embankment at Maltby.  
Note "Terram", and minor shear failures.



the same at both locations although at 2 the sediments were weaker with depth. The average sensitivity for both locations was 4.9.

The cone penetrometer was also used at these two locations, though time permitted only the 30 degree cone to be used. The two profiles shown in Figs. 3.7a and 3.7b demonstrate that the relative changes with depth are not dissimilar to the vane profiles. However, at 2 there exists a zone of desiccation to 0.7m which cannot be so readily defined at 1. It was therefore expected that the factor of safety against bearing capacity failure would be higher at 2.

At locations 1 and 2, U100 undisturbed samples were taken to be water table, the depth of which is shown in Figs.3.7a and 3.7b. On cutting, the U100 samples showed a very laminated structure; individual layers ranged from plastic, clayey silts to medium-to-coarse coaly material. Triaxial tests showed the variation in the sediment type (see Figs.5.24 and 5.25), though  $K_0$  tests showed a variation of  $K_0$  from 0.39 to 0.70 irrespective of sediment type.

Triaxial cyclic loading tests were carried out on a number of undisturbed samples (Table 7.1). Test conditions were standardised to an initial effective stress of  $115 \text{ kN/m}^2$  and a triaxial stress ratio of 0.15 (peak acceleration = 0.08g). The triaxial stress ratio was derived from relationships of acceptable accuracy used by other (e.g. Seed, 1977). Fifteen cycles at the prescribed stress ratio were considered by Taylor *et al.* (1978) to be a satisfactory model for a British earthquake of MMS Intensity VI on a 200-year return period prediction. The effective confining stress used is that which would be expected at 12m depth in the lagoon, following an overtip of 3m of coarse discard, with the water table at the original lagoon surface. The test results given in Table 7.1 show a very large variability in the susceptibility to cyclic

Table 7.1 Triaxial cyclic loading test results.

Position	Depth m	Void ratio post consol.	Specific gravity	Cycles to		Sample description
				5% $\epsilon$	10% $\epsilon$	
Before overtipping						
2	0.7	0.67	1.67	150	160	Coaly specimen
2	2.4	0.40	1.91	33	41	Mixed coal and cly
2	2.4	0.49	1.91	30	38	Mixed coal and clay
1	0.2	0.72	1.75	29	48	Laminated coal and clay
1	0.7	0.65	1.67	113	122	Coaly specimen
1	0.7	0.63	1.67	92	107	Coaly specimen
1	2.2	0.43	1.79	76	99	Laminated coal and clay
1	2.2	0.38	1.79	19	26	Laminated coal and clay
1	2.2	0.54	1.79	27	35	Laminated coal and clay
After overtipping						
2	2.7	0.56	1.56	70	87	Clayey with coaly bands
2	2.7	0.45	1.56	66	77	Clayey with coaly bands
1	0.8	0.56	1.75	22	57	Laminated coal and clay
1	2.8	0.49	1.80	63	83	Coaly with pure clay band
1	2.8	0.60	1.80	231	260	Coaly with pure clay band
1	2.8	0.52	1.80	130	145	Coaly with pure clay band

Table 7.2 Vibration measurements.

Source	Wht. explosive kg	Max. acceleration RMS	No. of significant cycles	Observed rise in pore pressure m
D6 vehicle	-	0.006g	-	0.3
D8 vehicle	-	0.03g	-	N.D.
4-2-1*	1.23	0.033g	16	0.0
5-3-1 $\frac{1}{2}$ *	1.84	0.04g	11	0.0
3-6-2	2.81	0.16g	2 <sup>+</sup>	0.0
30*	5.27	0.25g	+	1.5-1.8

\* no. of sticks of gelegnite + incomplete record N.D. not determined

mobility, but none of the specimens exhibit significant shear strains ( $\epsilon$ ) within the prescribed 15 cycles.

### 3 The Construction Phase

The embankment was in fact largely constructed of two layers each of which, because of settlement, was nominally of 1.5 m thickness decreasing to 1 at the distal end. Settlement, which to a large extent was conditioned by passage of the construction vehicle, resulted in an additional 1m thick layer being emplaced over the distal 20m of the embankment. The total thickness of the discard varied from 3.96m at 2 to 3.40m at location 1. The measured embankment bulk density was 2.01 Mg/M<sup>3</sup> at a moisture content of 10 per cent.

#### a) Ground movements

Throughout the construction phase the ground movements were monitored. No general failure was observed, although minor local shear failure was recorded on the wetter side of the embankment (Fig.7.6). Similarly, no major movement of the lagoon surface was measured, the maximum heave around the embankment periphery being 0.13m (c.f. Orgreave, where heave of up to 1m was noticed, Fig.7.2). Heave and local shear failure occurred only when the D6 vehicle was progressively placing spoil.

Relevelling of the survey grid, after construction, demonstrated that only the pegs close to the embankment had moved at all (Fig.7.5). Movement of the lateral extension wires showed that considerable settlement had occurred under the embankment. After the first lift, the near, middle and far wires respectively showed that 0.63, 1.19 and 1.15m of settlement had taken place under the centreline of the embankment. After the second lift the settlements were calculated to be 0.94, 1.23 and 1.23 m respectively. Most of the settlement thus appears to have occurred on the first lift, except at the near end where extra passage of the vehicle may have caused extra settlement. Post-construction boreholes through

the embankment showed 1.09 m at location 1, confirming the result of the wire measurements. However, at 2 the borehole indicated 1.66 m of settlement which is far more than exhibited by the wire.

b) Piezometric measurements

The results of the rapid acting pneumatic piezometers are typified by the record of P1, which is displayed in Fig.7.7 (see Fig.7.5 for location). It can be seen that the maximum piezometric head changes occurred whilst the piezometer was being overtipped. Only small changes were recorded prior to and after this event. Head rises were consistent with the excess pore pressures generated by the weight of material being overtipped, taking account of the pressure bulb effect at 4 m depth. A piezometric head rise of 0.30 m was recorded in P1 when the D6 was stationary with the engine revving close to location 2. This rise, shown in Fig.7.7 can reasonably be attributed to the weight of the vehicle and induced ground vibrations. When stationary close to location 1 however, the D6 appeared to produce a change in head over a wider area, with 0.10 to 0.15 m being measured at distances of over 10m (see Fig. 7.7 piezometers 3 and 5). This effect may have been largely due to vehicle vibrations.

The stand-pipe piezometers did not react so quickly as the pneumatic type, due to the time required for infiltration of the water. The final piezometric head changes recorded by these were, however, similar to those recorded by the pneumatic type. The drive in piezometers seem to offer no advantages over the Casagrande type; reaction times were no faster, as shown by Fig.7.8.

Following the overtipping of a layer, pore pressures fell and full equilibrium was attained after 3 days, though only small excess pore pressures persisted after twenty-four hours.

Fig.7.7. Response of the pneumatic piezometers during the Maltby overtipping operation.

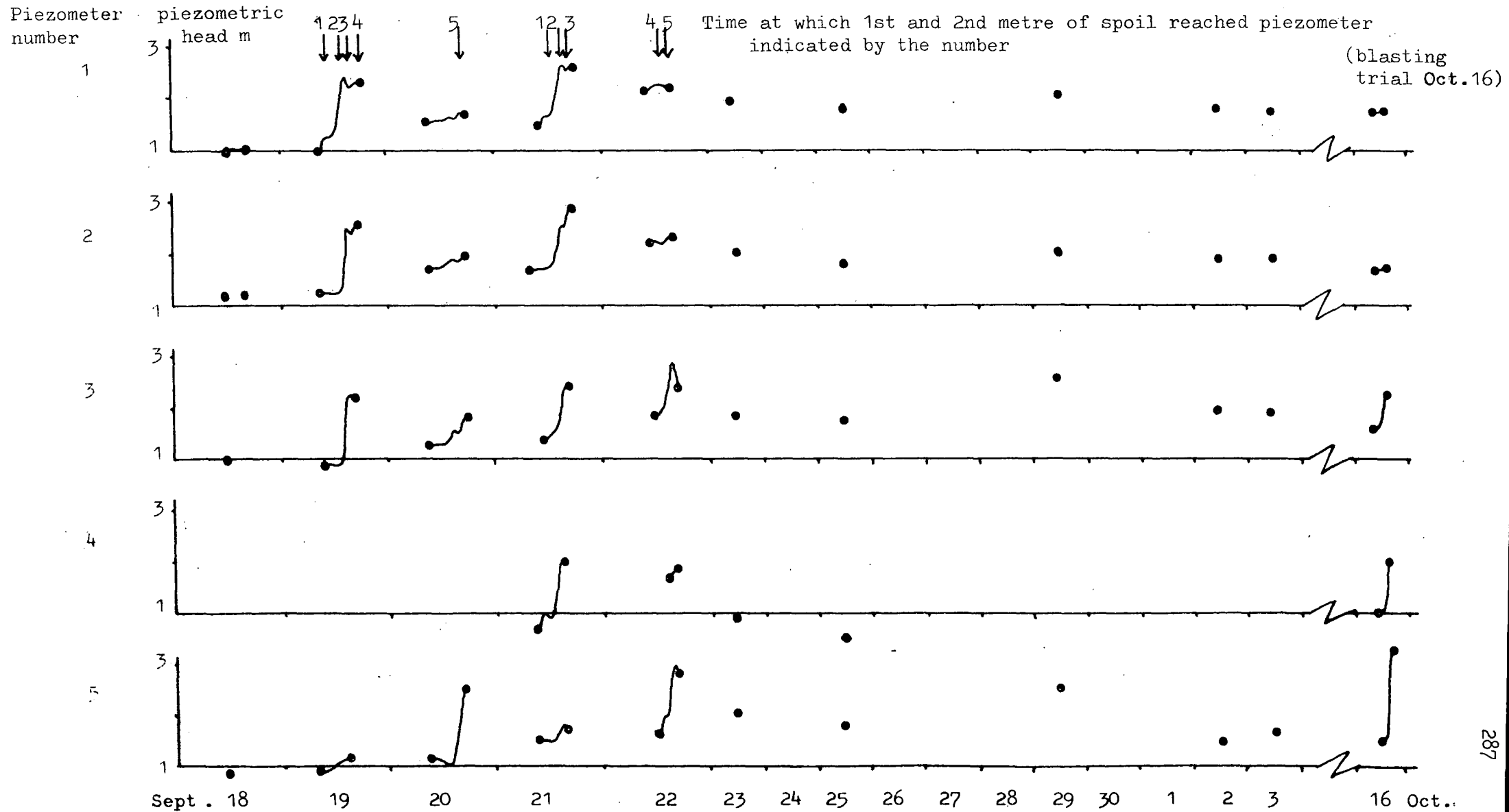
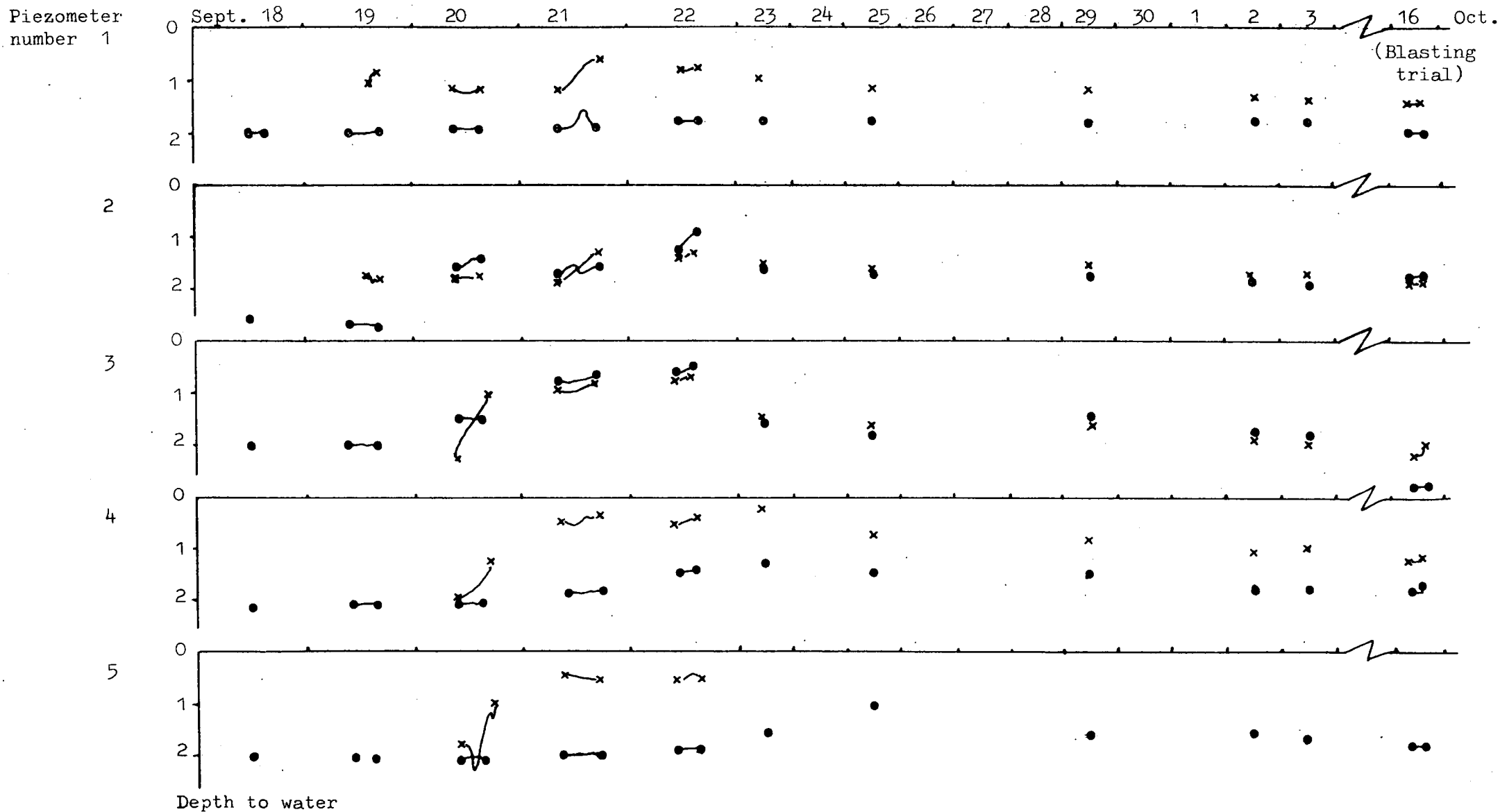


Fig.7.8 Response of the standpipe piezometers during the Maltby overtipping operation.

● Drive in  
 × Casagrande





c) Field shear strength determinations during construction

During construction of the first 1.5m layer, the operation was stopped just before position 2 was reached in order to conduct repeat vane tests. The D6 remained on the end of the embankment with its engine revving. From Fig.7.9 it can be seen that a general rise in strength was recorded at this location.

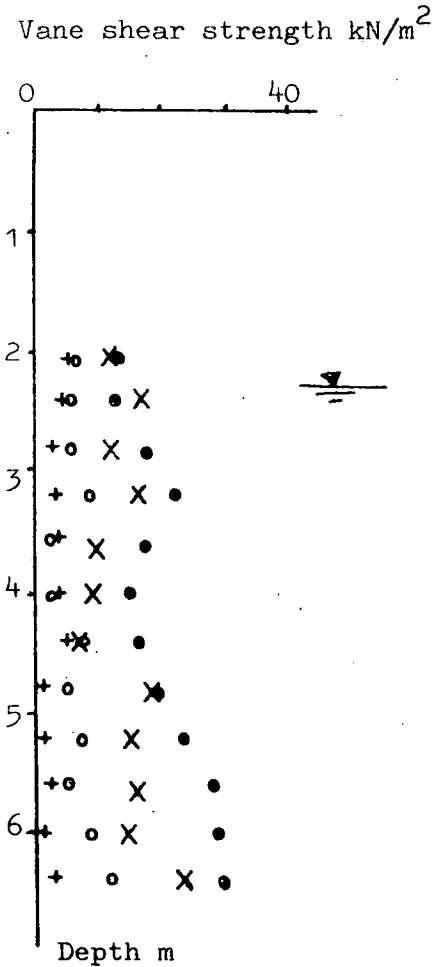
Construction was also halted at position 1 and in this case a general fall in strength was recorded. Previous lagoon investigations and the work of others imply that this is the expected result where pore pressure increases are registered. Also at 1 a repeat penetration test shows a small drop in cone resistance, especially at 5m depth (see Fig. 7.10). The increase in strength at location 2 is somewhat enigmatic, but it is believed that it may be due to consolidation involving collapse of the sediments' metastable fabric. Over the same range of depths the sensitivity does decrease (3.2 in retest, compared with 4.1 in initial test). Moreover, the pore water pressure did not necessarily change at 2. Although piezometer P1 showed a rise of 0.3m as mentioned previously, no pore pressure change was recorded in P2 whilst the D6 was at 2.

d) Vibration measurements

Vehicle vibrations were measured from the output of an array of velocity sensitive geophones situated 1m from the edge of the embankment and buried to a depth of 0.30m. One orthogonal array and 3 vertical geophones were used. From the output of the orthogonal array the maximum velocity vector was calculated and this was used to give an estimate of accelerations produced.

From Table 7.2 it can be seen that the maximum acceleration cycle recorded for the Caterpillar D6 vehicle had an R.M.S. value of 0.006g. After completion of the overtip operation a Caterpillar D8 was driven

Fig.7.9 Repeated vane shear tests at location 1, Maltby.

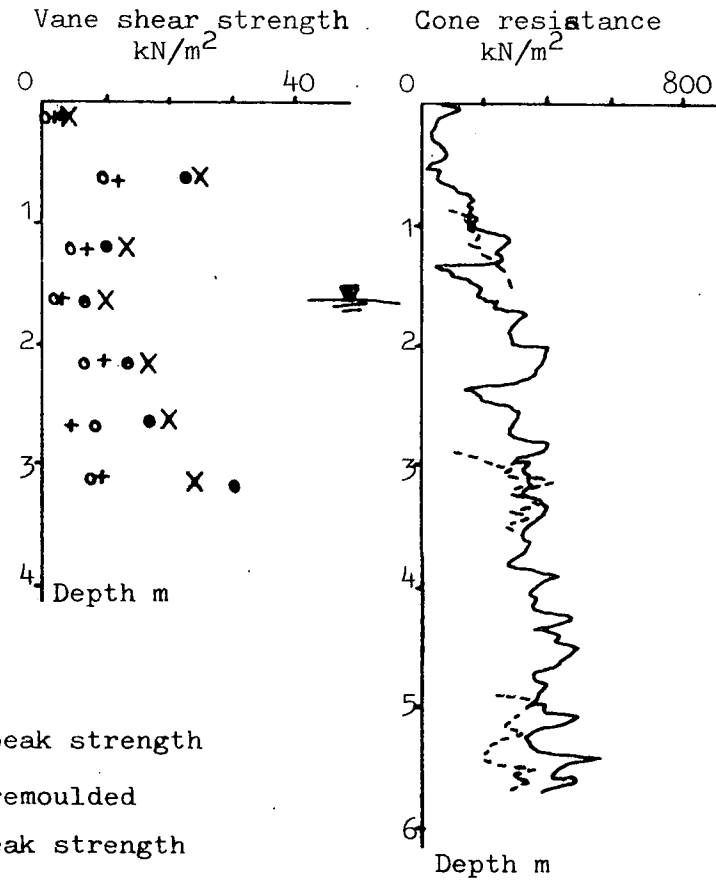


- X Initial tests, peak strength
- + Initial tests, remoulded
- Repeat tests, peak strength
- Repeat tests, remoulded

Fig.7.10 Repeated hand vane and cone penetration tests at location 2, Maltby.

a. Hand vane

b. Cone penetration



- Initial tests
- - - Repeated tests

onto the embankment for a short time. The vibration levels recorded for this larger machine were considerably greater, with a maximum single cycle R.M.S. value of 0.03g. This is much less however, than the level allowed for in the model earthquake (0.08g).

#### 4. Post-Construction Blasting Trials

These tests took place 1 month after completion of the embankment. Just prior to the trials 2 vibrating wire piezometers with a readout time of approximately 10 seconds were installed (Fig.7.5). Four series of explosions were used to simulate increasingly intense ground shaking events. The first three each consisted of detonating 3 charges separated by 5 second delays in order to produce a total ground shaking episode of about 13 seconds.

The first series comprised 4, 2 and 1 sticks of Special Gelignite 80, the second of 6, 3 and  $1\frac{1}{2}$  and the third of 8, 6 and 2 sticks. Each stick contained 0.176kg of explosive. These were all detonated at a distance of 20 to 30m from the embankment. A fourth explosion was detonated in a borehole which had been put down at location 1 (Fig.7.5) and which penetrated the floor of the lagoon.

The observed vibration levels are given in Table 7.2. The number of significant cycles was taken as the number having an amplitude 60% of the maximum recorded for each series. Because the records for the third series and the fourth blast were incomplete, the number of significant cycles are unknown for these cases. It would be expected that for the third series, however, this would be 10-15. Importantly, no pore water pressure changes were detected in any piezometer as a result of the first three series of ground shaking events. The fourth explosion produced an increase in piezometric head of 1.8m in P5 and 1.5m in the distal vibrating wire piezometer founded at 3.6m depth. Piezometers within

15m of location B showed some rise in pore pressure (e.g. 0.6m in P3). Despite the fact that acceleration levels were at least 0.25g, the pore pressure response was essentially local.

During the blasting trials no surface manifestations of any liquefaction phenomena were observed and there was no major disruption of the embankment. The embankment lifted slightly during the fourth explosion and afterwards the distal end was found to have cracked and settled by 0.5m.

#### 5. Post-Construction Cyclic Loading Tests

Prior to the blasting trials 2 boreholes were put down through the embankment at A and B to obtain further, relatively undisturbed U100 samples of the underlying lagoon materials.

Both standard triaxial tests and cyclic loading tests similar to those carried out prior to construction were conducted. The estimated additional consolidation stress that the post-construction samples had experienced were estimated to be  $75 \text{ kN/m}^2$ . From Table 7.1 it will be observed that there is no discernible difference between samples tested before or after construction. The inherent sedimentological variation between samples is almost certainly greater than any effect produced by consolidation and remoulding due to embankment construction. In the case of the standard triaxial tests, it was shown (Chapter 5.5) that the compacting effect of the embankment produced a small cohesion intercept in the case of fine-grained laminae at shallow depth. The  $K_0$  values proved to be too variable to discern any differences before and after construction.

#### 7.3 The Overtipping Operation at Silverhill

It was shown in chapters 4 and 6 that lagoon no.16 at Silverhill possesses extensive layers of weak clay. The permeability of all

sediments ranges from  $10^{-4}$  to  $10^{-9}$  m/s. When this site was first visited on 10 May 1979 overtipping was already in progress, a covering of 1 to 1.5m having been placed in the western and northern parts of the lagoon (see Fig. 7.11). The lagoon had failed over a long perimeter beneath the overtip, though the failures comprised only small slips, (see Figs. 7.12 and 7.13), with some heave at the toe. Considerable cracking of the lagoon surface occurred at the toe, and water was seeping continuously from the cracks on to the lagoon surface.

At the failure marked as "failure 1" (Fig. 7.11) two vane profiles were put down at locations A and B. With reference to the more detailed sketch in Fig. 7.14, profile A was just beyond the zone of disturbance by heave, and profile B was sited just at the limit of visible cracking at the surface (presumably the factor of safety against failure was approximately 1). A further profile was put down at location C; the three profiles are shown in Fig. 5.26.a-c. The weakness of the deposits, particularly at location C should be noted.

The progress of the overtipping operation and response of the pore-water pressure was monitored throughout the summer of 1979. The piezometer locations and movement of the overtipping front is shown in Fig. 7.15. The water levels in piezometers is shown in Table 7.3. Piezometers 1 to 6 were installed in a line from the zone of greatest overtipping activity. Concern at the excess pore pressures found caused operations to be halted until 27 June. These six piezometers were moved before full permeability tests could be conducted, in order that the extent of excess pore water pressure in the lagoon could be investigated. Permeability tests were conducted at all other locations though some were abandoned due to lack of response in the time available.

Table 7.3. indicates that excess pore water pressures existed over wide

Fig.7.11 Location of failures in the overtip embankment at Silverhill

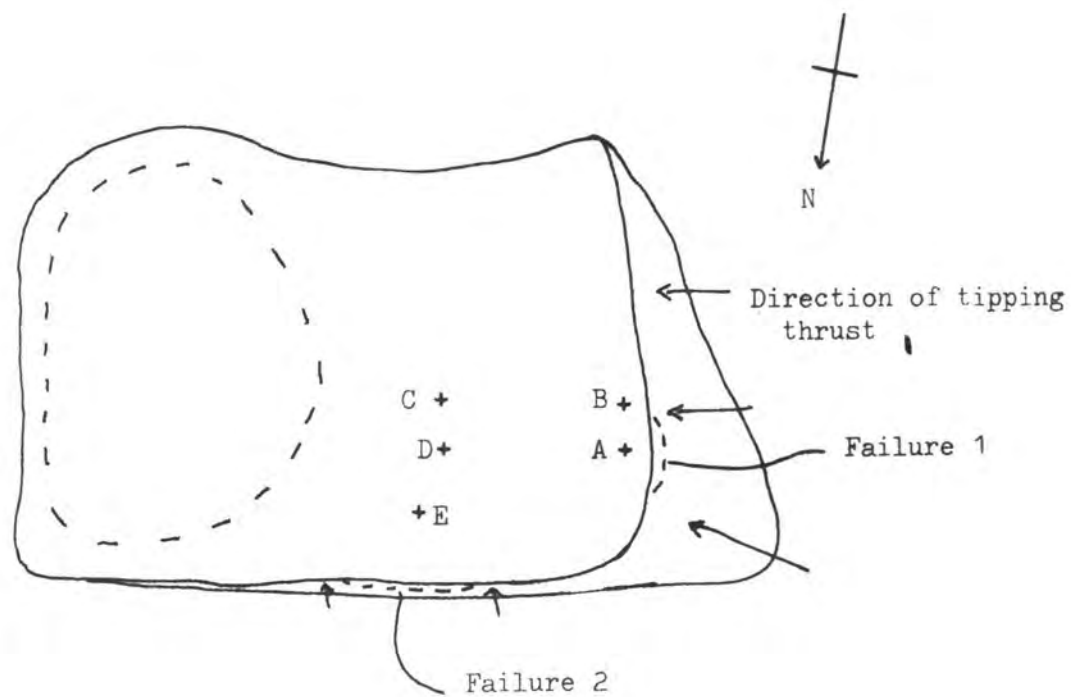


Fig.7.12 Failure 1



Fig.7.13 Failure 2.



Fig.7.14 Sketch of failure 1.

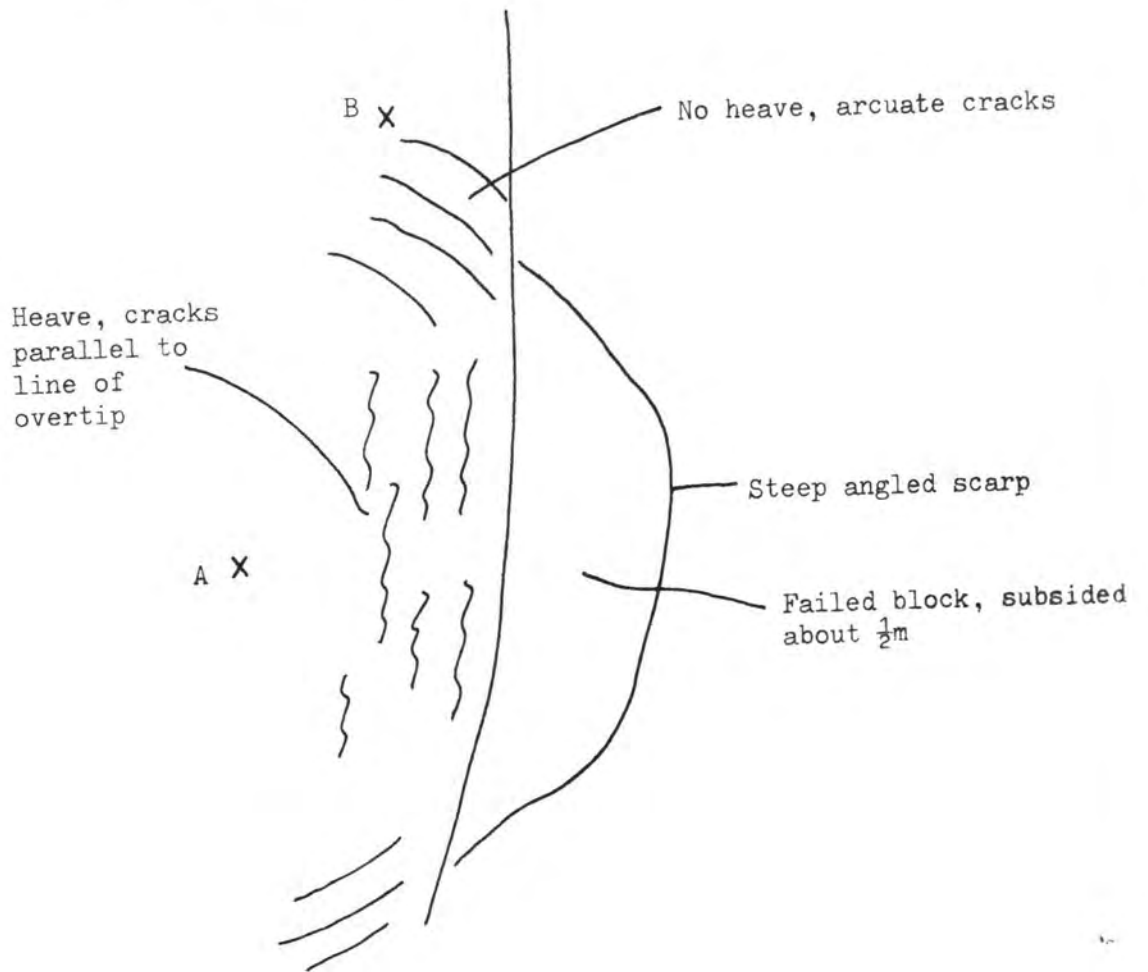
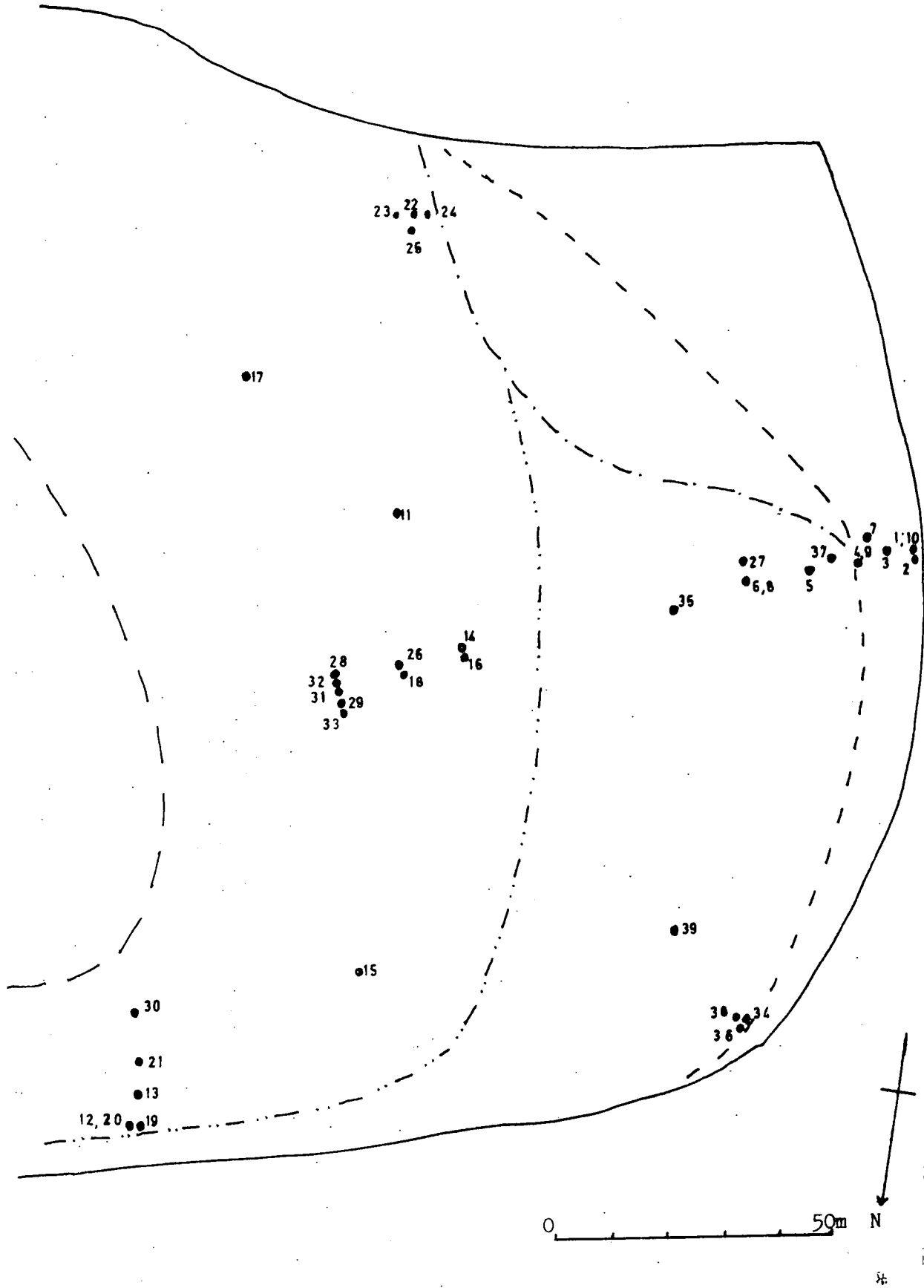


Fig.7.15 Piezometer locations and overtipping progress at Silverhill.



Limit of overtip

- 27.6.79
- - - 9.7.79
- · - · 17.7.79
- · · · 10.79

● Piezometer location





areas of the lagoon, furthermore pore pressures were influenced by the over tipping operation. For instance, piezometer 16 had an excess head of 200mm on 20 June, which fell to 60mm excess by the 27 June; this piezometer was 80m from the nearest overtipping. On 28 June overtipping 85m away produced a small rise in head, while further reaction occurred at this location between 5 July and 9 July when a rise of 133mm was recorded; the nearest overtipping was then 80m away. Piezometers at a similar depth show decreasing excess head away from the overtip; e.g. P9 and P8 on 7 June were 13 and 83m respectively from the overtip, their placement depths were 4.58 and 4.62m, P9 showed an excess head of 960mm, while P8 showed an excess head of 670mm. (With permeabilities of  $2.82 \times 10^{-5}$  and  $7.63 \times 10^{-6}$  m/s respectively, they appear to be in the same or similar layers.) The general trend in all piezometers is for decreasing head with distance from the overtip; were these observations referenced to a horizontal datum the difference would be exaggerated because the ground slopes away (perhaps by 1 in 100) from the overtip.

The reactions of piezometers 36 and 38 during this period are interesting. These two piezometers were placed on 26 June some 5m away from the limit of overtipping, in the northwest corner of the lagoon. By 19 July overtipping had advanced nearly to the two piezometers, P36 (in material with  $k = 7.74 \times 10^{-4}$  m/s) had a head of +340mm at this stage, having risen before P38. P38 on the other hand (in material with  $k = 2.14 \times 10^{-9}$  m/s) reacted more slowly but by 9 July had reached +1058mm. By 27 July overtipping had progressed some 5m beyond the two piezometers, P36 recorded a high of +760mm, while P38 was at +2000mm. This approaches the 2.3m equivalent head of the estimated 1.5m of discard, which had a bulk density measured at  $1.53 \text{ Mg/m}^{-3}$  when first placed.

The effect of pressure relief by seepage to the surface was also recorded

in P36. Nearby piezometer 34 was removed on 27 July, and on the 28 July seepage was noticed from the hole. On the 29th the hole was plugged, and the seepage stopped; the water level in P36 rose 60mm in four hours, despite the fact that the only overtipping that took place that day was in a far corner of the lagoon.

Overtipping continued throughout the summer and autumn of 1979. By October the limit of advance had nearly reached piezometer 16. To the south of that piezometer the operation was generally successful. To the north the operation had been held up by many minor failures; the estimated 1.5m of overtip in fact only projected a few centimetres above the lagoon surface. Two hand vane profiles were put down at this time at the position marked D and E on Fig.7.15. At D there was general failure and at E failure and considerable settlement. From the vane profiles (Fig.7.16) it can be seen that the sediment is weak at D and very weak indeed at E. Comparing these two profiles with those at A, B and C (Fig.5.30), it would seem that a vane shear strength of  $3\text{kN/m}^2$  marks the reasonable limit of advance, while strengths greater than  $5\text{kN/m}^2$  will allow rapid progress without even minor failures (providing that the depth of overtip is 1.5m or less).

#### 7.4 The Bearing Capacity of Lagoon Sediments

Any lagoon to be overtipped must be capable of carrying the load placed upon it by the overtipping operation. The most dangerous period for stability is just as the vehicle being used for spreading reaches the limit of advance of the embankment. The weights and track dimensions of some vehicles are shown in Table 7.4. Assuming that the material used for overtipping has a bulk density of  $2.0\text{ Mg/m}^3$  and that there is a 2:1 spread of the vehicle ground pressure through the embankment, then the pressure exerted in the surface of the lagoon is as shown in Fig.7.17.

Fig.7.16 Hand vane shear tests at Silverhill.

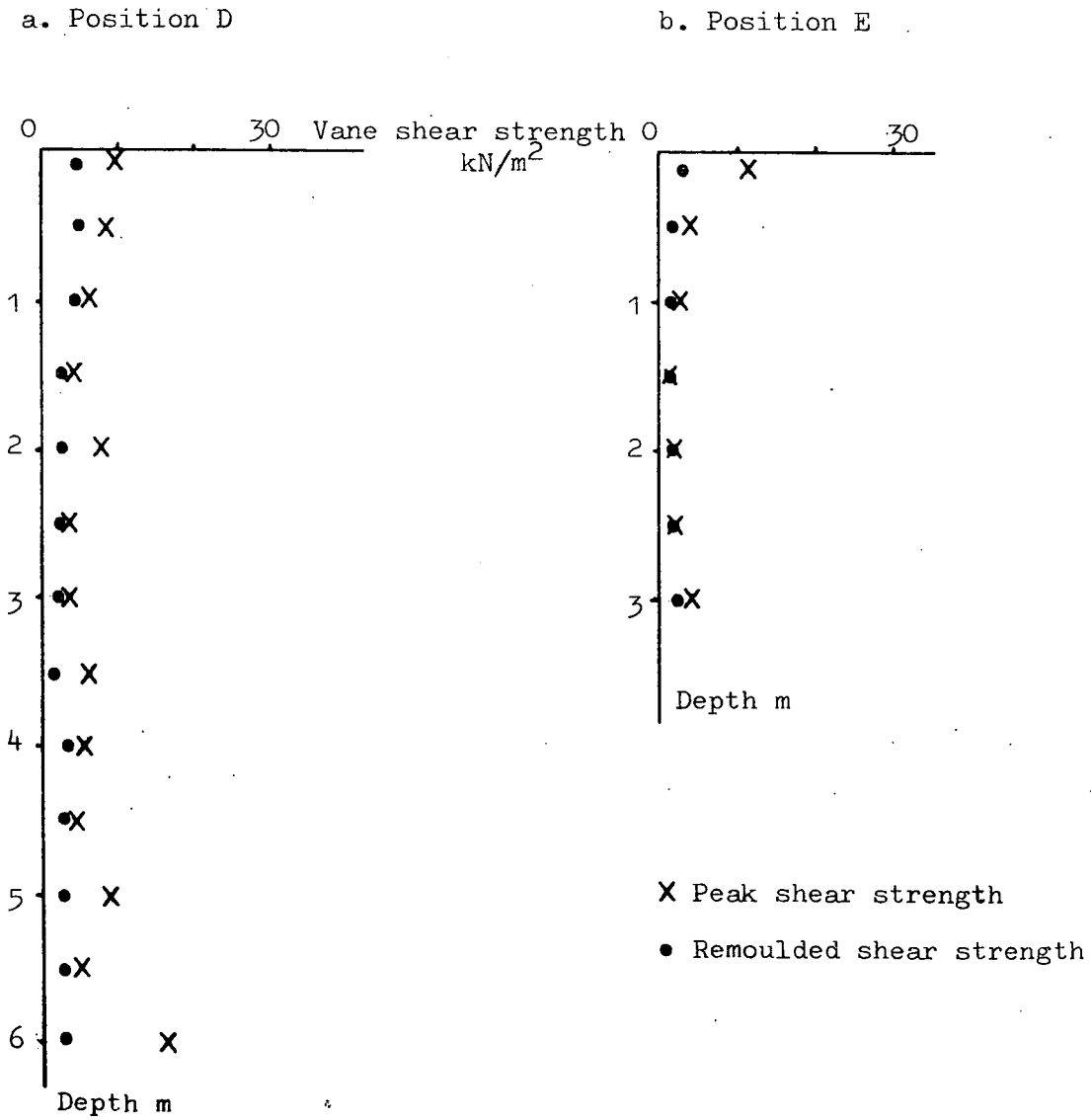


Table 7.4 Weights of vehicles used for overtippng.

	Shipping weight +fuel kg	Track length m	Width of each track m	Overall width m	Area of tracks m <sup>2</sup>
D6	13700	2.37	0.455	2.36	2.17
D6 (wide tracks)	13700	2.37	0.510	2.99	2.41
D8	28200	2.90	0.560	2.70	2.41

Fig.7.17 Bearing pressure on a lagoon surface.

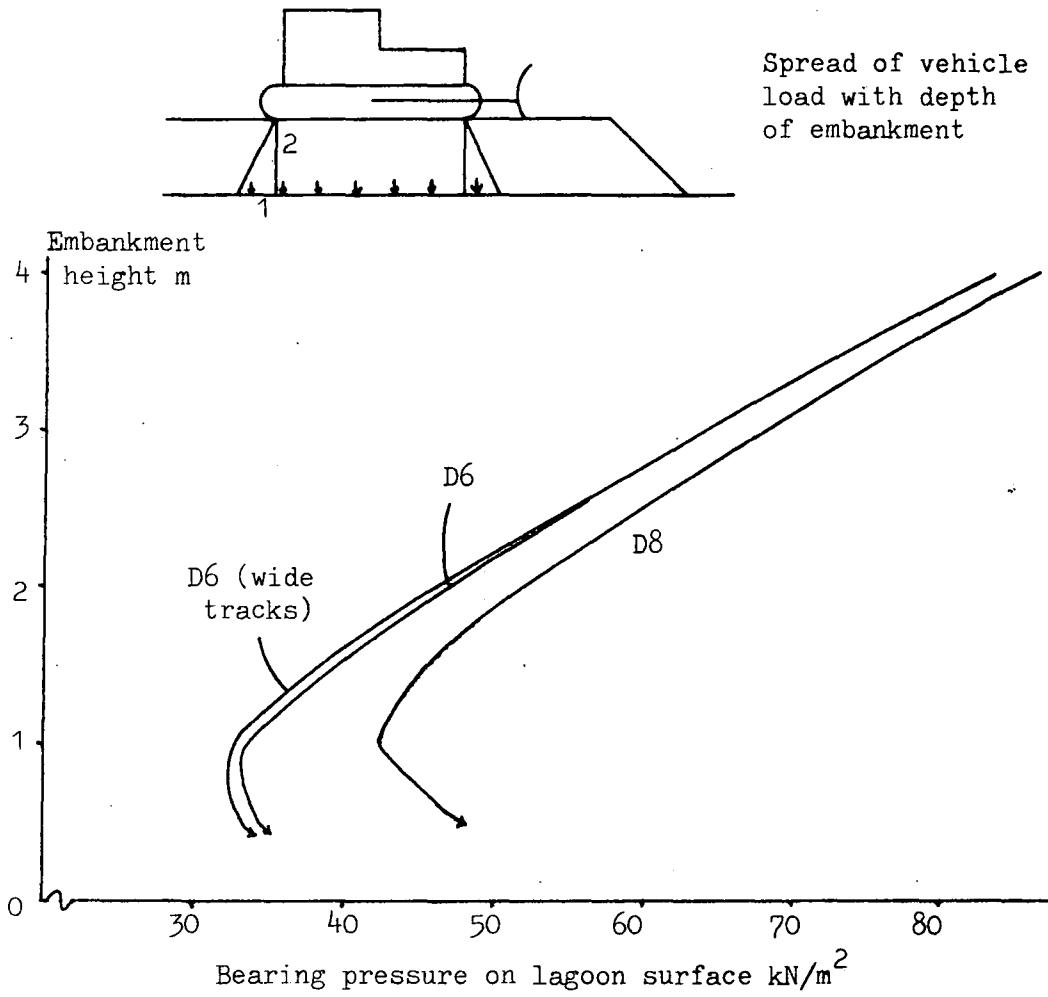
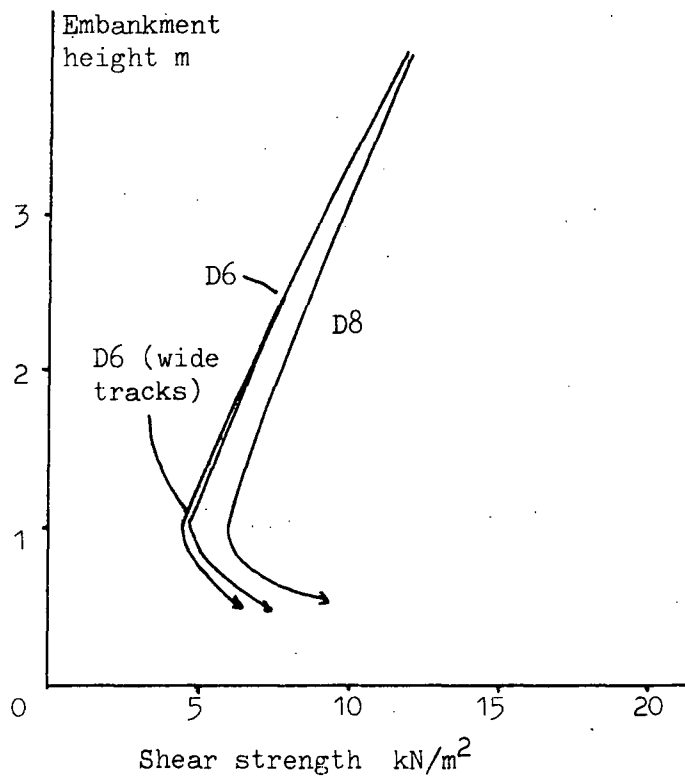


Fig.7.18 Minimum shear strength required to prevent failure.



These are the loads that the lagoon must accommodate.

Many options are available for assessing the bearing capacity of embankments on soft sediment. Davis and Booker (1973) suggest that a Prandtl type bearing capacity analysis is applicable to soils with various types of strength vs depth profile. The equation

$$q = (\pi + 2) C_{\min}$$

gives the bearing capacity at the limit of advance ( $q$ ) in terms of the minimum undrained shear strength in the profile. Rearranging -

$$C_{\min} = q / (\pi + 2)$$

However, the embankment can be expected to supply some resistance to failure, and therefore

$$C_{\min} = q - \frac{\text{(resistance due to embankment)}}{\text{spread area under vehicle}} / (\pi + 2)$$

is more applicable. The resistance due to the embankment is taken as  $\sigma \tan \phi'$  where  $\phi' = 30^\circ$  and  $\sigma$  is due to the self weight of the discard and the vehicle. The necessary  $C_{\min}$  at limiting equilibrium ( $F=1$ ) is plotted in Fig.7.18, taking  $q$  values from Fig.7.17. For a given depth of overtip and type of vehicle the necessary minimum undrained strength can be found from Fig.7.18. The figure also shows the importance of allowing pore pressure dissipation, as the minimum strength must increase before more material is emplaced.

The experience at Maltby and Silverhill suggests that while one metre of material exerts the minimum pressure on the ground, drivers nevertheless prefer (or the height of the blade dictates) to place 1.5m in the first lift. Furthermore, it is clear that materials with much lower strengths than indicated by Fig.7.18 can be safely overtipped providing care is exercised, and minor failures are tolerated.

Lambe and Whitman (1969) suggest that a moment arm slope stability analysis is applicable for total stress analyses of the bearing capacity of layered soils. The factor of safety is given by

$$F = \frac{(\text{resisting strengths}) \times \text{radius of circle}}{\text{Embankment load} \times \text{moment arm}}$$

This method is applicable only to circular failures in which the centre of the circle is near ground level. Menzies and Simons (1976) suggest that both circular and non-circular methods of slices may be used for this problem, for both total and effective stress analyses. The factors of safety are as follows:

Shape of failure arc	Method	Total Stress	Effective Stress
Circular	Bishop Simplified	$F = \frac{(S_u \cdot b / \cos \alpha)}{(W \sin \alpha)}$	$F = \frac{c' \cdot b + (W - ub) \tan \phi' / M \alpha}{(W \sin \alpha)}$ $M \alpha = \frac{\cos \alpha (1 + \tan \alpha \tan \phi')}{F}$
Non-circular	Janbu Simplified	$F = \frac{f_0 \cdot (S_u \cdot b / \cos^2 \alpha)}{(W \tan \alpha)}$	$F = \frac{f_0 (c' \cdot b + (W - u \cdot b) \tan \phi') / n \alpha}{(W \tan \alpha)}$ $n \alpha = \frac{\cos^2 \alpha (1 + \tan \alpha \tan \phi')}{F}$

in which  $W$  is the weight of slice

$\alpha$  is the slope at mid point of base of slice

$S_u$  is the undrained strength

$c$  is the cohesion

$\phi'$  is the friction angle

$u$  is the pore water pressure

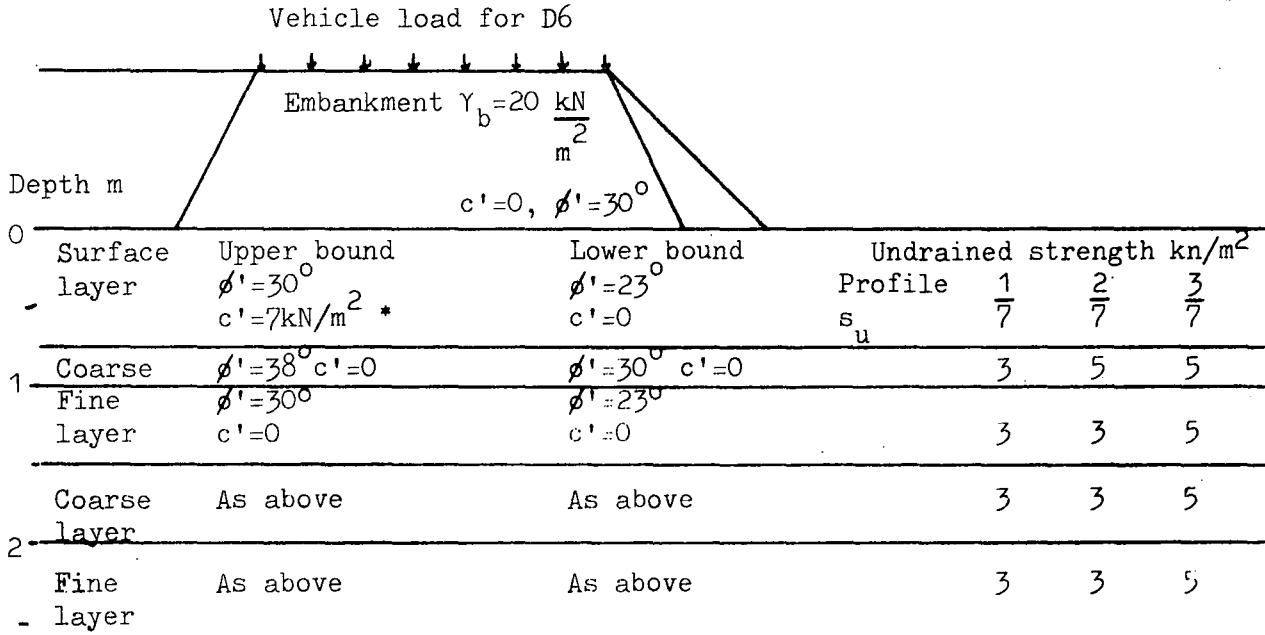
$b$  is the width of slice

These equations have been applied to the overturning operation depicted in Fig. 7.19. The problem involves a 1 or 1.5m embankment being placed by a D6 vehicle on the soil profile shown. The layers



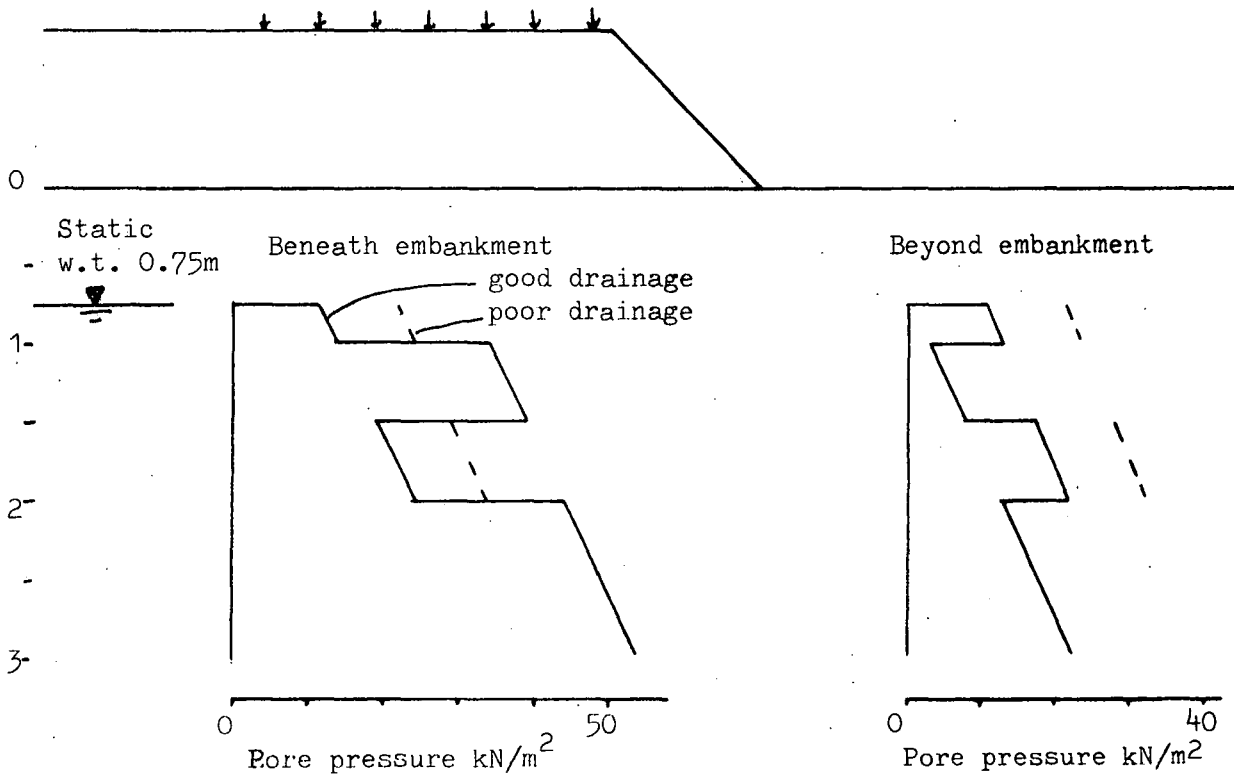
Fig.7.19 Hypothetical lagoon used for bearing capacity (slip circle) analysis.

a. Distribution of layers and shear strength assumed



\* In the overconsolidated state, i.e. not with the embankment load

b. Pore pressure distribution for a 1m embankment



of sediment are arbitrarily assigned approximate upper or lower band  $c'$   $\phi'$  values from the range found in Chapter 5 for the effective stress analysis. The pore water pressure distribution used to calculate the effective stresses is based on the behaviour at Maltby and Silverhill; impermeable layers exhibit an excess pore water pressure equivalent to the applied load (if any); permeable layers drain well, and the pore water pressure is everywhere 1/3 of the applied load (as observed at Silverhill; see previous section). As a worst case, the problem was also considered with the excess pore water pressure of the free draining layer as 2/3 of the applied load, which might correspond to the situation when an embankment is being approached and the water is confined in the free draining layer.

The total stress analysis assumed the vane profiles outlined in Fig. 7.19. These correspond to the safer and marginal ( $F=1$ ) profiles found at Silverhill.

1 ) Bishop analysis

Trial surfaces 1 and 2 shown in Fig. 7.20 were analysed, and the factors of safety are shown in Table 7.5, from which it can be seen that:-

a) There is a large difference between the total and effective stress analyses, the former giving a lower factor of safety in all cases. This is because  $\sigma \tan \phi'$  is greater than  $S_u$  for most slices, especially in the free draining layers.

b) The total stress analysis for profile 3 with a 1m embankment gives  $F=1$  for both the shallow and the deeper circle. The minimum strength in this profile is  $5\text{kN/m}^2$ , which is close to the  $4.6\text{kN/m}^2$  obtained from the Prandtl analysis.

c) The total stress analysis suggests that the deeper circle is the more critical; the effective stress analysis contradicts this.

d) The problem of negative ( $W - u_b$ ) terms (which are set to zero)

Fig.7.20 Trial failure surfaces for Bishop Simplified Method of Slices, to estimate embankment stability.

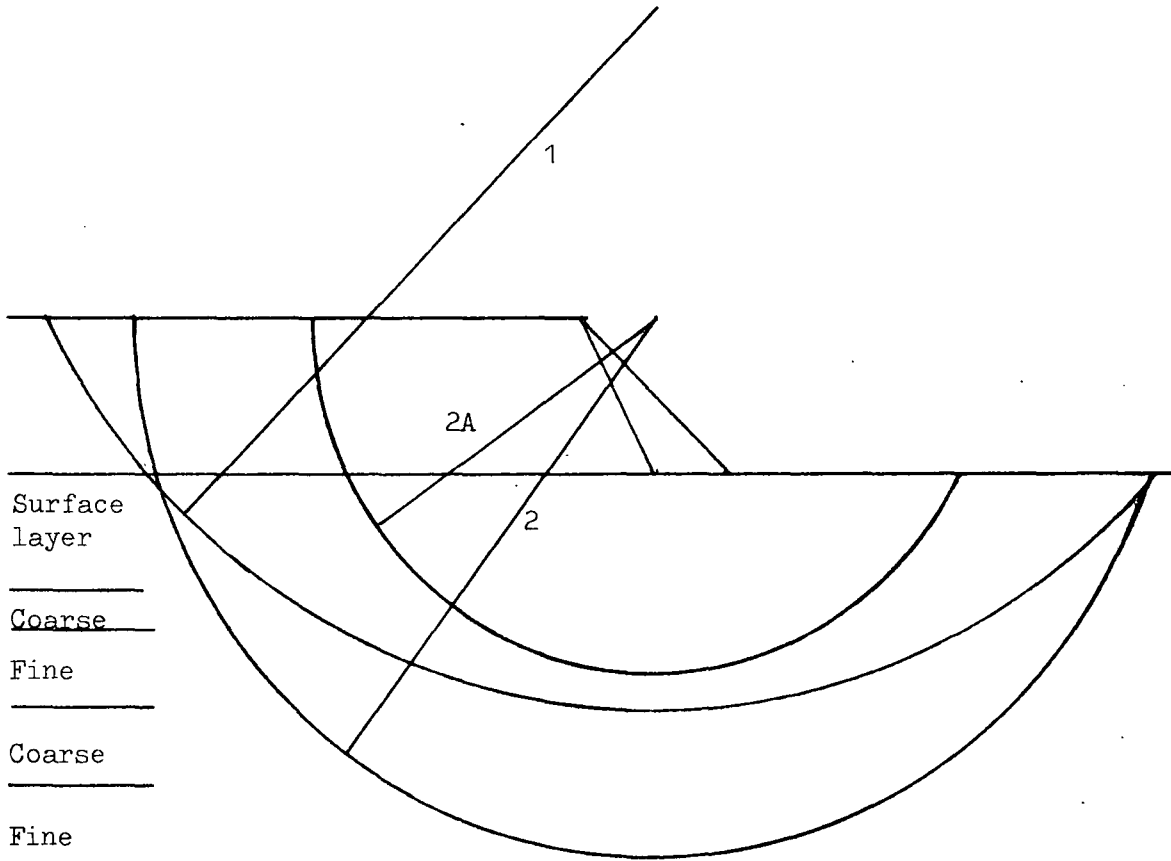


Fig.7.21 Sketch of three-dimensional failure involving surfaces 2 and 2A in Fig.7.20 above.

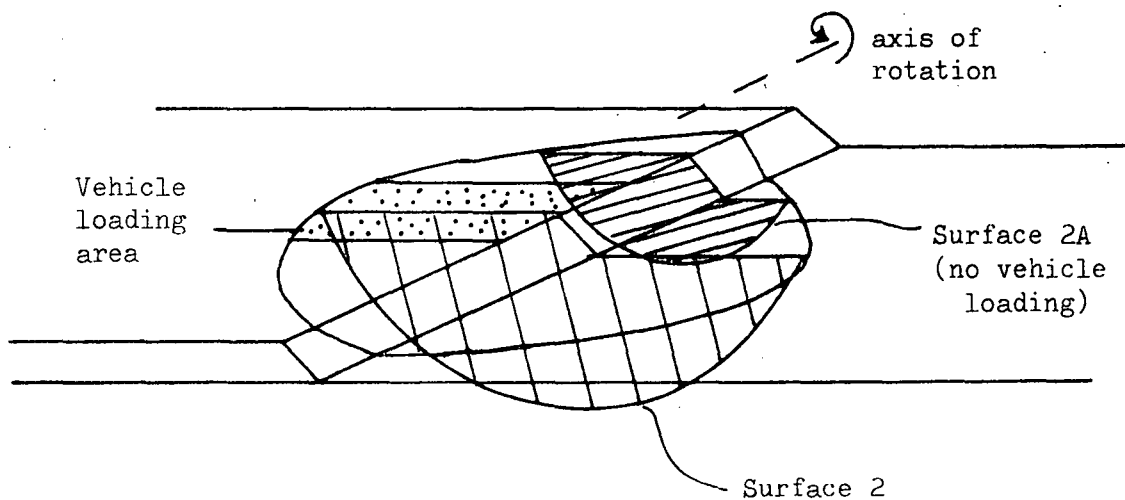


Table 7.5 Overtipping factors of safety (Bishop). (Refer to figs.7.21 and 7.22)

Trial surface	Stress analysis	1 metre fill height			1.5 metre fill height			
		Profile 1	2	3	1	2	3	
1	Total	F	0.86	0.91	1.10	0.62	0.66	0.79
	Effective							
	a. good drainage	$\phi'_u, c'=7$	$\phi'_u, c'=0$	$\phi'_1, c'=0$	$\phi'_u, c'=0$	$\phi'_1, c'=7$	$\phi'_1, c'=0$	
	F	1.93	1.68	1.26	1.34	1.22	1.01	
b. poor drainage	F			$\phi'_1, c'=0$	Problems with high pore pressure terms			
	F			1.08				
1 Clay (unlaminated)	Total	As for above			As for above			
	Effective		$\phi'_1, c'=7$	$\phi'_1, c'=0$	$\phi'_1, c'=7$	$\phi'_1, c'=0$		
	F		1.45	1.19	1.21	0.97		
2	Total	F			3	0.97		
	Effective							
	a. good drainage	$\phi'_u, c'=7$	$\phi'_u, c'=0$	$\phi'_1, c'=0$	$\phi'_u, c'=7$	$\phi'_u, c'=0$		
	F	2.31	2.08	1.53	1.94	1.75		
b. poor drainage	F			$\phi'_1, c'=0$	Problems with high pore pressure terms			
	F			1.21				
2A	Total	F			3	1.56		
	Effective							
	a. good drainage	$\phi'_u, c'=7$						
	F	2.22						

N.B. Not all permutations were considered necessary.

Note  $\phi'_u$  refers to the upper bound effective angle of friction.

$\phi'_1$  refers to the lower bound effective angle of friction,

see Fig.7.21 for definition of upper and lower bounds.

$c'$  in  $\text{kN/m}^2$ .

because of high pore water pressures means that many of the values in the "poor drainage" boxes are suspect. By extrapolation from other cases, however, they seem to be not unreasonable. This is true also of the Janbu analysis (see below).

e) Generally results have been calculated for the lower bound effective strength assumptions. An indication of the upper bound assumptions is included for completeness.

The small trial surface 2A was analysed for two conditions only to assess the end effect. This surface is the mid-point surface for the ends (see Fig.7.21). Lambe and Whitman (1969) suggest that the overall factor of safety is given by:-

$$F = \frac{F_1 A_1 + F_2 A_2}{A_1 + A_2} \quad (A_1, A_2 \text{ are the areas of circles 1 and 2})$$

which leads to:-

$$F = \frac{1.09 \times 63 + 1.56 \times 23}{63 + 23} = 1.22 \quad (\text{total stress})$$

$$F = \frac{1.93 \times 63 + 2.22 \times 23}{63 + 23} = 2.01 \quad (\text{effective stress})$$

(the areas are in arbitrary units).

These factors of safety are 11% (total stress) and 4% (effective stress) greater than the two dimensional values. This slight conservatism is desirable, and hence end effects have been ignored for all other cases.

2. Consideration of the distribution of sediments within the model suggests that a non-circular failure arc is more likely. The failure surfaces shown in Fig.7.22 have therefore been analysed according to the Janbu method, on the same basis as before, and are shown in Table 7.6. The same comments regarding total vs effective stress results, negative (w - u.b) terms, etc., apply as for the Bishop analysis. However, in this case the effective stress analysis also suggests that the deeper

Fig.7.22 Trial surfaces for Janbu Simplified Method of Slices, to estimate embankment stability.

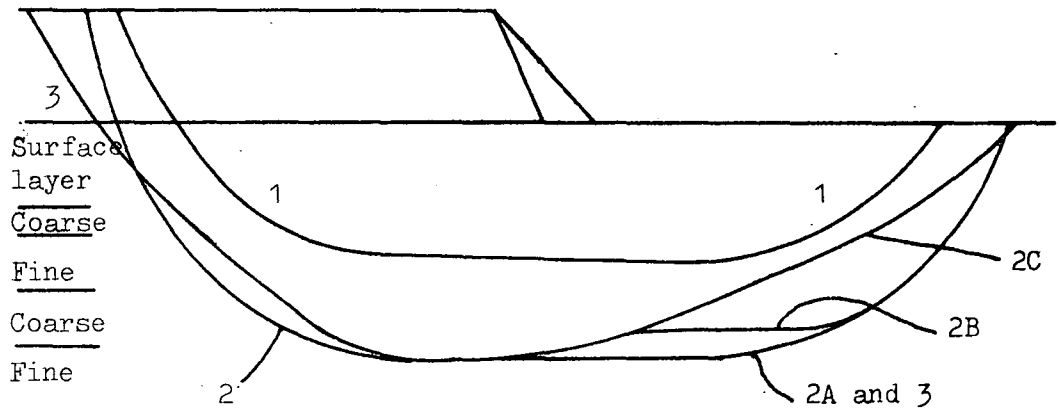


Fig.7.23 Height of a free standing cut.

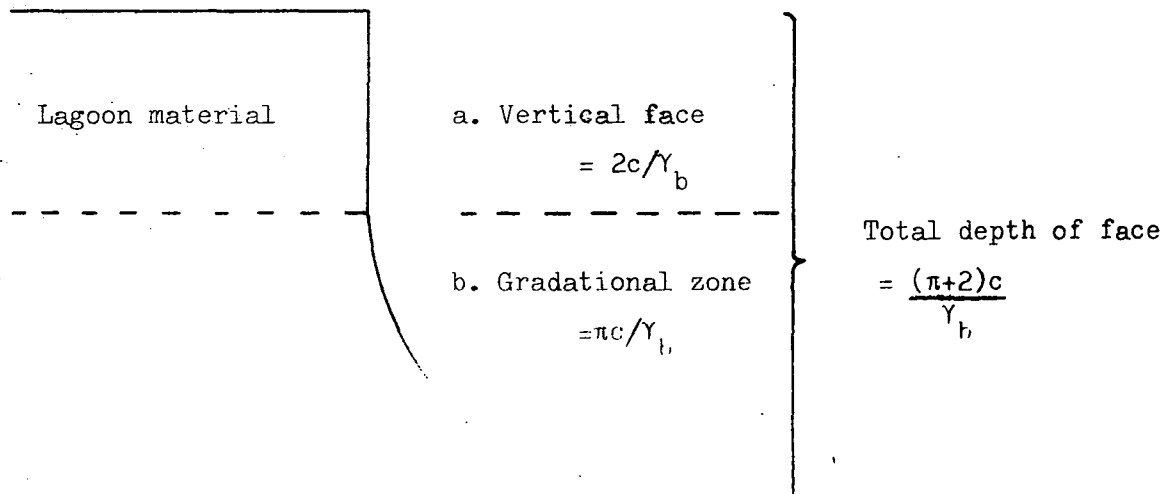


Table 7.6 Overtipping factors of safety (Janbu). (Refer to Figs. 7.21 and 7.22)

Trial surface	Stress analysis	1 metre fill height		1.5 metre fill height		
1	Total	Profile 1	3			
		F	1.56	1.76		
	Effective					
	a. good drainage	$\phi'_1, c'=7$	$\phi'_1, c'=0$			
		F	2.97	2.61		
2A	Total	Profile 1	3	1	3	
		F	1.33	1.56	0.88	1.03
	Effective					
	a. good drainage	$\phi'_1, c'=7$	$\phi'_1, c'=0$	$\phi'_1, c'=7$	$\phi'_1, c'=0$	
		F	2.44	2.12	1.77	1.54
	b. poor drainage	$\phi'_1, c'=7$	$\phi'_1, c'=0$	Results invalid due to high pore pressures		
		F	2.29	1.96		
2B	Total	Profile 1	3	1	3	
		F	1.47	1.70	0.93	1.10
	Effective					
	a. good drainage	$\phi'_1, c'=7$	$\phi'_1, c'=0$	$\phi'_1, c'=7$	$\phi'_1, c'=0$	
		F	2.58	2.24	1.90	1.65
	b. poor drainage	$\phi'_1, c'=7$	$\phi'_1, c'=0$	Results invalid due to high pore pressures		
		F	2.15	1.78		
2C	Total	Profile 1	3	1	3	
		F	1.41	1.64	0.79	0.92
	Effective					
	a. good drainage	$\phi'_1, c'=7$	$\phi'_1, c'=0$	$\phi'_1, c'=7$	$\phi'_1, c'=0$	
		F	2.15	1.96	1.42	1.31
	b. poor drainage	$\phi'_1, c'=7$	$\phi'_1, c'=0$	Results invalid due to high pore pressures		
		F	1.99	1.80		
3	Total	Profile 1	3	1	3	
		F	0.95	1.22	0.60	0.78
	Effective					
	a. good drainage	$\phi'_1, c'=7$	$\phi'_1, c'=0$	$\phi'_1, c'=7$	$\phi'_1, c'=0$	
		F	1.52	1.29	1.03	0.85
	b. poor drainage	$\phi'_1, c'=7$	$\phi'_1, c'=0$	Results invalid due to high pore pressures		
		F	1.12	0.84		
3 Clay (unlaminated)	Total	As for above (3)		As for above (3)		
	Effective	$\phi'_1, c'=7$	$\phi'_1, c'=0$	$\phi'_1, c'=7$	$\phi'_1, c'=0$	
		F	1.39	1.16	0.98	0.81

(See notes for Table 7.5)

failure surface is the more critical (in contrast to the previous calculations).

In both the Bishop and Janbu analyses the most critical surface was re-analysed assuming the lagoon to be a homogenous clay with a lower bound  $\phi'$  value ( $23^{\circ}$ ), and with or without a desiccated crust (i.e.  $c'=0$  or  $7\text{kN/m}^2$ ).

With reference to the most critical surfaces from both the Bishop (surface 1, Table 7.5) and Janbu methods (surface 3, Table 7.6), the following conclusions can be drawn concerning the bearing capacity of lagoon sediments:-

1. The use of a total stress analysis with strengths obtained from the field vane is very conservative. The method of slices and bearing capacity approaches suggest that a minimum strength of  $4.6\text{kN/m}^2$  is required for the lagoon sediments. It is known from field evidence that the limit of overtipping advance will occur when the minimum strength is nearer to  $3\text{kN/m}^2$ .
2. Based on the results of an effective stress analysis using the method of slices, overtipping with 1m of coarse discard should be relatively straightforward in all parts of the lagoon that have a firm crust.
3. The tendency for vehicle drivers to put down 1.5m of discard means that in addition to a firm crust good drainage is required (see surface 3, Table 7.6;  $F = 1.03$  where a crust exists and there is good drainage beneath 1.5m of fill).
4. Where the water table is at less than 0.75 m depth, the operation will become very difficult for 1.5m lifts, although 1m lifts should be possible to nearer to the supernatant water.
5. When the far side of the lagoon is reached (from the start of operations), the confinement of the water in coarse layers will lead to



problems with excess pore pressures.

It is therefore suggested that overtipping only be attempted using D6 vehicles putting down 1 to 1.5 lifts. A firm crust is required for adequate safety of the operation and time must be allowed during the operation in order to allow the dissipation of excess pore water pressures. In terms of vane shear strengths, a factor of safety of 1.5 leads to a figure of  $4.5\text{kN/m}^2$  as the minimum strength for any layer that can be overtipped. It is emphasised that these recommendations are for careful, controlled overtipping.

So far no consideration has been given to settlement. This will consist of two parts; consolidation settlement, and settlement due to soft material being displaced ahead of the overtipping operation. Consolidation can be determined from the data in Chapter 6. The compression index is usually about 0.20 (see chapter 6.11); the load caused by 1.5m of discard (density,  $2.0\text{ Mg/m}^3$ ) is  $30\text{kN/m}^2$  (the vehicle weight is removed quickly in terms of consolidation). The total consolidation settlement caused by this load will thus be about 0.27m for a 5m deep lagoon, 0.43m for a 10m deep lagoon and 0.63m for a 20m deep lagoon. In the firmer parts of the lagoon, settlement will be of this order. However, in weaker parts the settlement will be much greater due to forward displacement of the lagoon sediments, as observed at Silverhill and Orgreave (see Fig.7.2). This effect will tend to decrease the stability of an overtipping operation, and reaffirms the general conclusion that overtipping will only be successful where the lagoon has a firm crust.

#### 7.5 The Stability of an Excavated Face in a Lagoon

In general, there is no danger to life or property on excavation by dragline. However, if a vehicle is to work the face from the floor of the lagoon, there could be considerable danger, not to mention costly

delay, if conditions are adverse. In particular, it is important to know the horizontal strength of weak laminae as this will control failure modes. The diamond vane with  $H=0.25D$  is suitable for this purpose.

In the short-term an excavated face will behave in an undrained fashion, and the depth to which a free standing vertical cut can be made will be defined by:-

$$z = \frac{2c_{\min}}{\gamma} \approx 0.13 c_{\min}$$

where  $z$  is the depth of the free vertical face

$c_{\min}$  is the minimum strength (vane)

$\gamma$  is the bulk density ( $15\text{kN/m}^3$  is a reasonable figure, see chapter 5).

However, below the vertical face will be a zone in which the face grades from horizontal to vertical (see Fig.7.23). The limiting depth is (Schofield and Wroth, 1968, p.282):-

$$z' = \frac{\pi c_{\min}}{\gamma}$$

Thus the total limiting depth of cut is:-

$$z = \frac{(\pi + 2)c_{\min}}{\gamma} > \frac{c_{\min}}{3}$$

These relationships have been found to roughly predict the depth of cut in two cases. Cobb (1977) reports vane tests in Cadeby lagoon 9, which show a strength of  $20\text{kN/m}^3$  at a depth of 5m. The lagoon sediment would thus be expected to stand up approximately 7m in total for a short period, which was found to be the case. At Peckfield lagoon 7, the weak layer near the surface exhibited strengths as low as  $3\text{kN/m}^2$  (as measured by the vane, see chapter 5.4). Thus, it would not be expected that a cut of any depth could be made in this material. In fact, this layer did continually slump towards the floor of the lagoon maintaining a very shallow gradient and causing some problems for the face shovel.

Even below this layer, the sediments were too weak to support a free-face until the inlet was nearly reached, as would be predicted from the vane profiles (Figs.5.6 and 5.7).

#### 7.6 Conclusions

An embankment was built at Maltby in a region of the lagoon where the vane shear strengths were generally not less than  $7 \text{ kN/m}^2$ . The embankment was found to be stable in a static sense although minor shear failures occurred around the periphery. No general settlement of the lagoon surface occurred, but considerable compaction and consolidation took place immediately below the embankment. The induced pore pressures conformed with the embankment loading. Although full dissipation took 3 days, pore pressure equilibrium was practically re-established in 24 hours.

Machine vibrations, although sustained, produced little change in pore pressures and no adverse change in strength. Significantly, vibrations were well below the levels considered applicable to a British 200-year return period earthquake. Furthermore, stability during such an earthquake does not appear to pose a problem; induced shocks well in excess of the  $0.08g$  accelerations representing such an earthquake produced no liquefaction in the lagoon. The largest explosion produced rises in pore pressure of 1.5 to 1.8 m, but these only occurred within a distance of 15m and no liquefaction effects were observed.

Laboratory cyclic loading tests showed that no discernible change in the cyclic mobility potential of the sediments was produced by the overtipping operation. The tests showed the sediments to be generally resistant to liquefaction, which confirms the field observations.

At Silverhill it was observed that overtipping was possible where the minimum vane shear strength in the sediments was as low as  $3 \text{ kN/m}^2$ , although

care was necessary to maintain progress. Where the minimum strength was as high as  $5\text{kN/m}^2$  overtipping was relatively easy. The overtipping operation produced pore pressure increases in the sediments. The effects of these increases were transmitted along free-draining layers and could be observed at distances of 80m from the area of overtipping. Due to this drainage, permeable horizons never attained the increase expected from the load imposed by the embankment. In contrast, impermeable horizons only displayed pore pressure increases when overtipped, and the amount of the increase conformed to the embankment loading.

An analysis of overtipping using a bearing capacity and a method of slices approach suggests that vane shear strengths produce very conservative estimates of the bearing capacity of lagoon sediments. In contrast, an effective stress method of slices approach suggests that the overtipping of lagoon sediments is possible where there is a firm crust of limited depth providing that the depth of overtip is not more than 1.5m. Also, where there are free-draining horizons, the excess pore pressures transmitted ahead of the embankment should not be excessive, as will probably be the case when the layer is confined against a nearby lagoon embankment. In this situation, overtipping is unlikely to progress in a controlled fashion; embankments with drainage facilities would render the operation more successful, but may be uneconomic on other grounds.

Finally, lagoons that are to be excavated using a face shovel will require an investigation of the sediment shear strength using in-situ vane tests. The maximum depth of cut is approximately  $c_{\text{min}}/3$ , which seems to confirm the very limited amount of field evidence available.

Overtipping and excavation operations will continue to be used for some time. The experience gained to date, especially for overtipping operations, provides a reasonable basis for predicting how and where successful progress

may be expected. However, it is probable that continued experience and records will allow refinement of the predictions outlined in this chapter, and it is recommended that such records be kept and analysed.

## CHAPTER 8    CONCLUSIONS

The behaviour of lagoons is explained by their mineralogical composition and sedimentological structure. Therefore a considerable portion of this work has concentrated on these aspects of lagoons. It is difficult to elucidate the mineralogy of coal-rich sediments by XRD techniques, and therefore the major element chemistry has also been studied using XRF equipment. The more quantitative nature of the latter method allows sedimentological trends to be measured. Using this method it has been found that thermal oxidation of coal-rich sediments at 350°C overestimates the organic carbon content, and unless it is determined by wet chemistry the indirect XRF determination yields a better estimate. Pyrite is also oxidised at the temperature necessary to remove coal, and the sulphur driven off. Therefore, the XRF determinations were performed using un-oxidised specimens. It should be mentioned that for coarse discards wet chemical analyses of organic carbon have shown good agreement with oxidation. Coal contents are generally lower, however.

Coal has a much lower specific gravity than the other minerals in lagoon sediments, and therefore the overall specific gravity of any sample is directly related to the coal content. This has been noted before by Taylor and Cobb, 1977. However, this previous interpretation is apparently in error, because it implies a linear relationship between the specific gravity and the coal content. While the error is not significant in a statistical sense, the current writer shows that the true relationship is a curve, and develops a theoretical and a statistical expression for the curve in chapter 4.

Based on studies of the chemistry and mineralogy of lagoons, a model is proposed which accounts for the structure and can therefore be used

to explain and predict the behaviour of lagoons. The model postulates that the flow into lagoons can be divided into two different regimes.

The first regime, presumably the normal condition at the washery, is a period of steadyflow with a suspended load of fine-grained particles. The sediment mainly consists of silt and clay-sized particles with a fairly low coal content. (The actual coal content will vary from washery to washery.) On discharge at the inlet of the lagoon the water flows as a stream to the supernatant water area. Little of the sediment is lost from this stream which is energetic enough to retain all the fine grained particles. When the stream reaches the supernatant water it loses energy and progressively deposits particles of similar Stokesian settling velocities. Thus at first only the coarse silt quartz and clay particles will be deposited, followed by finer silt quartz and clays, together with coarse silt-sized coal particles. Progressive fining away from the inlet yields sediments which are always coal-rich in their coarser fractions. It is observed that the sediment as a whole becomes more coal-rich into the lagoon, due to the early depletion of non-coal particles.

The second regime is presumed to result from an abnormal condition at the washery, such as starting up following the weekend break, overloading or breakdown of the plant. This results in a flush of water and coarse particles which are predominantly coal. Although this condition is transient, the actual volume of sediment released into the lagoon is of the same order as the long, steady, normal periods between. This sediment undergoes the same type of changes as did the finer sediment. That is, the sediment fine away from the inlet and is more coal-rich in the coarser fractions, and becoming more coal-rich overall.

The two regimes alternate on a short-term basis, perhaps daily or weekly (not necessarily in a regular fashion). The resultant lagoon is

therefore highly laminated, with an alternation of coarse and fine laminae. The proportion of coarse laminae decreases away from the inlet because the particles are deposited very rapidly from the water, whereas the finer-grained particles of the normal washery regime are dispersed more evenly throughout the lagoon. Therefore, while individual layers are becoming more coal-rich away from the inlet, the lagoon as a whole is becoming less coal-rich. This is really a delta formation with low-angle foreset beds. With this model the observed characteristics of lagoons with respect to many properties are readily explained. The model is obviously a gross over-simplification, in particular the sediment input will not be either one type or the other, but will vary between them. Furthermore the exact distribution curves of particle size and composition are not known exactly and will vary from washery to washery.

Coal is a material of low specific gravity; thus, the coarse coaly layers are less dense than the finer layers. Pyrite is associated with the coal, at least in those areas studied in this thesis, and there is therefore more pyrite in the coarse sediments. Coal is a highly frictional material (Taylor, 1974) and therefore the coarse laminae have higher effective friction angles than the finer laminae. The friction angle of lagoon sediments is also higher than that of many coarse colliery discards because of the higher coal content of the former. The average coal contents for lagoons is 46.5 per cent (range 9-81) compared to 13.5 per cent for coarse discards (range 0-40, see Taylor, 1979). In this context it is interesting to note the following statistics extracted from various site investigation and research reports to the NCB for a computer database system being established at Durham University, (D.J.Kirby, written communication). A plot of 142  $p', q$  points (effective stresses) gave a



cohesion of zero, and a friction angle of 35.3 degrees; the correlation coefficient was 0.988, which is significant at the 99.9 per cent level. A similar plot for coarse discard based on 422 points gave an effective cohesion of  $21\text{kN/M}^2$ , a friction angle of 31.4 degrees; the correlation coefficient and significance level were 0.976 and 99.9 per cent respectively. The cohesion intercept of the coarse discard is due to the curved nature of the envelope (Taylor and Cobb, 1977). The difference in friction angle is highly significant, however, and can be attributed to the difference in coal content. The same data set reveals that fine discard has an average ash content of 51 per cent (86 points), while for coarse discard it is 72 per cent (90 points). It should be noted that ash contents are not available for all the samples of the  $p',q$  points.

In lagoons it is observed that the in-situ shear strength decreases away from the inlet, due to the decrease in the proportion of coarse, frictional laminae. A decrease in the number of desiccated surfaces might also be expected, and would have the same effect. The vane shear test has proved useful in the measurement of the in-situ shear strength. It is shown in chapter 2 that paired vane tests can be used to measure the shear strength on horizontal and vertical surfaces within the lagoon. It is further shown from field evidence and a theoretical study that a vane of  $H=2D$  shape and a vane of diamond shape with  $H=D/4$  are suited to this purpose in laminated sediments. From field trials with this combination and also a laboratory study it is found that lagoon sediments are stronger on a vertical plane than on a horizontal plane, and it is therefore expected that failures in overtip embankments or excavated faces would be controlled by horizontal planes of weakness. It is further shown, following Blight (1967) that the vane shear test can be used to determine the drained strength in more permeable horizons. Consequently it is expected that the drained strength is measured for the coarser laminae within lagoons;

this is justified because this would be the failure mode in the field.

The coefficient of consolidation is high for the coarser laminae, 2000 m<sup>2</sup>/yr or more being measured for some very coarse bands. Values of as low as 2m<sup>2</sup>/yr are measured for the finest laminae. It is expected that the horizontal laminations in most lagoons will cause consolidation by predominantly horizontal drainage. However, lagoons that are very wide compared to their depth will consolidate partially by vertical drainage. It is shown that excess pore pressures generated by sedimentation (Gibson, 1958; Mittal and Morgenstern, 1976) will not be significant in most British colliery tailings lagoons. In terms of compressibility it is found that only fine-grained, coal-free laminations are compressible. Coarser laminae (including the coal-free beach area) or coal-rich laminae (in this respect, more than about 30 per cent coal) have compression indices of 0.20-0.25; for the finest grained, coal-free laminae the index may be as high as 0.50. It is suggested that this fact is due to the natural habit and a low compressibility of the coal particles themselves. Being of equant habit, particle reorientation due to an imposed load may be negligible, and bending and cracking of these relatively brittle particles may require heavy loads. It is speculated that this accounts for the high curvature of the voids ratio versus log (pressure) graphs of these sediments. This is one area that may repay further study.

Estimates of permeability have been obtained both from laboratory (consolidation) tests and in-situ permeability tests. Following the recommendations of various authorities, greater reliance is placed on the in-situ measurement despite the known errors that can arise from the estimation of this property in layered media. The in-situ tests give higher values of permeability and a greater range of values than the

consolidation tests ( $10^{-4}$  to  $10^{-9}$  m/s compared to  $10^{-7}$  to  $10^{-10}$  m/s for the consolidation tests). A lightweight, plastic piezometer, not dissimilar to the Cambridge push-in has proved most useful for work in colliery lagoons. It has both a weight and a cost advantage (being "home-produced") over the Cambridge piezometer. In layered media the horizontal permeability is expected to be several orders of magnitude higher than the vertical permeability. For many lagoons this means that the embankments are considerably more important in draining the lagoon than is the floor. However, for wide, shallow lagoons, or lagoons with homogenous deposits, or lagoons with extensive interlinking of the coarser laminations by vertical drainage paths the floor of the lagoon will assume greater importance. Currently there is a lack of data concerning the permeabilities of the materials that form the walls and floor of lagoons, and the way in which the entrainment of fines will affect these permeabilities.

The problem of the behaviour of any particular lagoon in respect of the properties outlined above is thus resolved by estimating the distribution of the laminations within it, and the permeability of the walls and floor of the lagoon. In general it would not be necessary to test more than a few samples in the laboratory; coal content and particle size analysis would serve as useful indicators of most other parameters. In the field it would be necessary to estimate the degree of layering of the lagoon in various places and the proportions of the various types of layer present. This might be accomplished by observations in trial pits, which enables information to be gathered very quickly. In particular, it is easy to trace the lateral extent of individual laminations. However, no information is gained concerning the structure at depth.

For deep sounding, a lightweight cone penetrometer has been developed

which has great potential (Peace, 1980). It provides a continuous record of all laminations penetrated, based on an electrical load cell system at the tip. Attempts to interpret penetration records by conventional foundation failure type theories proved to be unsuccessful. However, Vesic's (1972) theory of expanding cavities, together with both direct and indirect observational evidence suggests that it is possible to interpret a penetration profile in terms of coarse and fine laminae. It is not possible to derive directly soil mechanics parameters, but the knowledge of the structure allows prediction of the behaviour of the lagoon. Inclusion of a pore pressure transducer at the tip will allow the penetration records to be interpreted with greater confidence, and will allow the identification of overconsolidated laminations, which is not possible at present.

The information gathered to date concerning the detailed structure of lagoons is somewhat incomplete and equivocal. On the one hand it is known that many lagoons are highly laminated. However, some lagoons are more homogenous in appearance; lagoon 12 at Gedling colliery is one example, but there is some suggestion (chapter 6.3) that even this lagoon is laminated to an extent. This generally homogenous character may be due to the size and tailings output of this large mine.

Concerning laminated lagoons themselves, there is evidence both to show that individual laminae may be continuous, and again that they may not be. The brown clay layer at Silverhill is a particularly good example of a very continuous layer, while being fairly thin and on occasion interleaved with other laminae. The perched water table in the upper zone of lagoon 7 at Peckfield implies that at least one fine-grained lamina is fairly continuous. The existence of supernatant water over parts of most lagoons implies extensive, low permeability horizons.

Against this, layers that are not continuous have been noted at East Hetton in trial pits in lagoon 109A (Figs.4.18 and 4.19), and by deep sounding by cone penetration (Fig.3.9). Cobb (1977) also describes large and small scale deformations which have dislocated laminations. The inter-leaved sediments in the clay band at Silverhill are clearly not continuous; a clay band was noted to wedge out in the excavated face of lagoon 7 at Peckfield (Fig.4.20). The beach area of most lagoons is a braided stream deposit, and it is expected that laminae would be discontinuous due to continual shifting of the stream; erosion and deposition would occur contemporaneously along the stream. In the supernatant water region of the lagoon, it would normally be expected that the more even depositional environment would allow the slow formation of fine-grained laminations. Coarser laminae in this region reflect a sudden flush of energetic water.

A preliminary study has been made of the chemistry of the pore water of lagoon sediments. In view of the high pyrite contents of many lagoons, it was expected that acid waters would be encountered, but this is not so. The waters were always neutral or slightly basic. The major cation is sodium, of the anions chloride and sulphate are significant. While the levels of these chemical species were too high in the lagoons studied for direct use, dilution alone would be sufficient to improve the quality of the water. Provided that discharge were after dilution, pollution by lagoon waters should not cause a hazard. However, it is emphasised that this is only a preliminary study which did not involve many chemical species. This is a topic for further work, which would attempt to relate the groundwater chemistry to the resultant lagoon and tip water chemistry.

The problem of overtipping colliery lagoons has been investigated,

mainly in the field but also with a theoretical stability study. In the field, observations have shown that it is possible to overtip to an in-situ shear strength limit of  $3\text{kN/m}^2$ , as measured by the field vane test. This is the lowest strength of any lamination to a depth of 5m that can be overtipped. To include a margin for safety however, a lower limit of  $4.5\text{kN/m}^2$  would be advisable. A theoretical study using a method of slices approach to embankment stability has shown that a total stress analysis does not yield sensible answers when compared to known field performance. This approach would suggest that an undrained shear strength of about  $5\text{kN/m}^2$  is the limiting condition. In contrast the effective stress approach suggests that overtipping with 1m of coarse discard is possible where a firm crust exists and the water table is 0.75m or more below the surface. Overtipping with 1.5m of discard further requires that the coarser layers are able to drain the area of overtipping. The need for a firm crust agrees with field observations. Obviously it is also necessary for pore pressures to dissipate between lifts.

This study suggests that it would be extremely difficult, if not impossible, to overtip across a lagoon with supernatant water. Certainly, an adequate factor of safety could not be maintained. It would, of course, be possible to constrain tipping to one area of the lagoon, and displace the sediments in front of the overtipped coarse discard. There are two objections to this. Firstly, although coarse discard is disposed of, the displaced fine discard becomes a more pressing problem, being soft and "mobile". Secondly, the fine discard is remoulded and therefore weaker (the sensitivity as measured in-situ is usually 2 or more). In order to cover a lagoon with a layer of coarse discard it is therefore necessary to remove the supernatant water and allow the surface of the lagoon to desiccate in fine weather. Bearing in mind the vagaries of

the British weather, the best timing for the operation would be to draw-off the supernatant water in the early spring in anticipation of overtipping in the summer and autumn. The operation might require several seasons.

The final stages of overtipping present further problems. Consolidation beneath the overtip embankment will displace water, mainly into the looser sediments yet to be overtipped. In the end, the water will have nowhere to escape and the pore water pressure will rise. There are three ways in which this problem could be countered. Firstly, lagoons could be designed and managed such that short drainage paths exist to free-draining embankments. In most lagoons the short drainage paths exist in the form of the coarse laminations. Secondly, the practice of drawing-off water and allowing desiccation will create an unsaturated zone at the surface into which the displaced water could flow. Thirdly, since an unsaturated zone usually exists at the beach end of lagoons, it would be advantageous to progress towards this area; the natural tendency is to start in this area because it is safer and often nearer to colliery haul roads. This practice would have the effect of delaying the start of overtipping until the wetter end of a lagoon had dried out.

Liquefaction of these sediments is a potential danger that has been studied by Kennedy (1977) and Taylor et al. (1978). This danger is a serious concern during overtipping operations due to plant vibrations, or subsequently should an earth tremor mobilise an overtipped lagoon to cause collapse of a composite tip structure. This study suggests that plant vibrations are not of a sufficient level to be a concern. Furthermore, large-scale tremors produced by explosives failed to cause liquefaction, despite vibration levels that would greatly exceed all experience of earthquakes in the U.K. Therefore, liquefaction does not

seem to be a problem from the field evidence. Nevertheless, laboratory tests (Taylor et al., 1978) suggest that mobility could occur in some lagoon sediments, and caution should be observed. The minimum freeboard of 1m around the lagoon would mitigate against disaster during the operation itself. The final tip profile would be stable so long as the lagoon was drained within the composite tip.

Overtipping is a practical problem, and solutions will come through the continued refinement of techniques. It is therefore important that records of overtipping operations be kept, ideally in the form of a short report indicating the state and strength of the lagoon, piezometer observations, and the timing and level of success of the operation. It is interesting to note that following the Maltby exercise and the early part of the Silverhill overtipping operation, the writer was of the opinion that a vane shear strength of  $5\text{kN/m}^2$  was the limiting value. Later experience at Silverhill allowed this to be refined to  $3\text{kN/m}^2$ .

It is apparent from the preceding discussion that a critical feature of lagoons is their ability to drain rapidly. The free-draining lagoon will be (relatively) strong, easy to overtip, and stable in terms of the final tip profile. Producing a free draining lagoon involves two processes. The first is the actual lagoon itself; can the free-draining laminae be encouraged, or distributed better throughout the lagoon by changing washery and pumping practices? The second process involves the design and construction of free-draining floors and embankments. While designs involving materials with the correct filter properties could almost certainly be produced, it is questionable whether it would be economic to do so. However, can the usual embankment material (coarse discard) be used more efficiently in this respect? For instance, would an uncompacted zone lining the embankment on the upstream side produce a



cheap permeable filter? (This would require some sort of drain through the embankment as well.) This again raises the problem of the lack of data on this aspect of lagoons and design studies would necessarily start with the collection of more permeability data from embankments.

Finally, it should be noted that a great deal of data exists on various aspects of coarse and fine discard. This is contained in research and site investigation reports held by various branches of the National Coal Board, and research reports and theses from Durham University and elsewhere (including Cambridge, Leeds, Strathclyde and Surrey universities). Each report or thesis is concerned with a particular lagoon (or tip) or topic. The information has never been gathered together and viewed as a whole. This is now being undertaken at Durham University, where the information is being stored in a central data bank on the Northumbrian Universities Multiple Access IBM 360/70 Computer. The system is amenable to data retrieval for statistical analysis. The successful completion of this data bank, and analysis of the information for design studies or specification of testing in future site investigations, is, in the opinion of the writer, the single most useful and cost effective topic which merits further attention.

REFERENCES

- AAS, G., 1965. 'A study of vane shape and the rate of shear on the measured values of the in-situ shear strength of clays'. Proc. 6th Int. Conf. Soil Mech. Found. Engng. Montreal, Vol.1, 141-145.
- AAS, G., 1967 'Vane tests for the investigation of anisotropy of the undrained shear strength of clays.' Proc. Geotech. Conf. Oslo, Vol.1, 3-8.
- AL-DAHIR, Z.A. and MORGENSTERN, N.R., 1969. 'Intake factors for cylindrical piezometer tips.' Soil Science, Vol.107, 17-21.
- BACHELIER, M. and PAREZ, L., 1965. 'Contribution a l'etude de la compressibilite des soils a l'aide du penetrometre a cone. Proc. 6th Int. Conf. Soil Mech. Found. Engng., Montreal, Vol.2, 3-7.
- BEGEMANN, H.K.S., 1969. 'The Dutch static penetration test with the adhesion jacket cone.' Delft Laboratory for Soil Mechanics, L.G.M. Mendelingen Publications, Vol.12, pt 4.
- BEGEMANN, H.K.S., 1974. 'Reports on discussions.' Proc. European Symp. Penetration Testing, Stockholm, Vol.2, 29-39.
- BILLAM, J., 1977. 'Correlations between cone resistance and vane shear strength in some Scandinavian soft to medium stiff clays.' Discussion, Can. Geotech. Journ., Vol 14, 272-4.
- BISHOP, A.W. and HENKEL, D.J., 1962. 'The measurement of soil properties in the triaxial test.' 2nd edition, E. Arnold, London.
- BJERRUM, L., 1972. 'Embankments on soft ground.' Proc. A.S.C.E. Speciality Conf. on 'Performance of earth and earth supported structures.' Vol.2., 1-54.
- BJERRUM, L., NASH, J.K.T.L., KENNARD, R.M. and GIBSON, R.E., 1972. 'Hydraulic fracturing in field permeability testing.' Geotechnique, Vol.22, 319-32.
- BLIGHT, G.E., 1968. 'A Note on field vane testing of silty soils.' Can. Geotech. Journ., Vol.5, 142-9.
- BLIGHT, G.E., 1970. 'In-situ strength of rolled and hydraulic fill.' Journ. Soil Mech. Found. Engng. Div. Proc. A.S.C.E., Vol.99, 881-99.
- BRAY, A. 1941. 'The sulphide and carbonate constituents of coal seams.' Proc. Geol. Ass., Vol.52, 183-93.
- BRITISH STANDARDS INSTITUTION, BS 1377, 1975. 'Methods of test for soils for civil engineering purposes.' B.S.I., London, 143pp
- BUSCH, R.A., BACKER, R.R. and ATKINS, L.A., 1974. 'Physical property data on coal waste embankment materials.' U.S. Bureau of Mines Report on Investigations 7964, 142pp.

- BUSCH, R.A., BACKER, R.R., ATKINS, L.A. and KEALY, C.D., 1975. 'Physical property data on fine coal refuse.' U.S. Bureau of Mines Report on Investigations 8062, 40pp.
- CADLING, L. and ODENSTAD, S., 1950. 'The vane borer.' Roy. Swedish Geotech. Inst. Stockholm, Proc.No.2, 88pp.
- CAIRNEY, T. and FROST, R.C., 1975. 'A case study of mine water quality deterioration, Mainsforth colliery, County Durham.' Journ. Hydrology, Vol.25, 275-93.
- CASAGRANDE, A. and CARILLO, N., 1944. 'Shear failure of anisotropic materials.' Journ. Boston Soc. Civ. Engrs., Vol.31, 74-87.
- CHATTERJEE, P.K. and POOLEY, F.D., 1977. 'An examination of trace elements in some South Wales coals.' Proc. Australian Inst.Min. Metall., Vol.263, 19-30.
- COBB, A.E., 1977. 'Stability and degradation of colliery shale embankments and properties of tailings lagoon deposits.' Ph.D. thesis, Univ. Durham.
- COX, J.B., 1967. 'A review of the vane test.' Proc. Site Investigation Symp., Australian Inst. Civ. Engrs., Sydney, Vol.CE 9, 19-30.
- CRAIG, R.F., 1974. 'Soil Mechanics.' Van Nostrand Reinhold Publishing Co., London, 275pp.
- DAVIS, E.H. and BOOKER, J.R., 1973. 'The effect of increasing strength with depth on the bearing capacity of clays.' Geotechnique, Vol.23, 551-63.
- DAVIS, J.C., 1973. 'Statistics and data analysis in geology.' John Wiley and Sons, New York.
- DE BEER, E.E., 1948. 'Données concernant la résistance en cisaillement déduites des essais de pénétration en profondeur.' Geotechnique, Vol.1, 22-40.
- DE BEER, E.E. and MARTENS, A., 1957. 'A method of computation of an upper limit of the effect of the heterogeneity of sand layers on the settlements of bridges.' Proc. 4th Int.Conf.Soil Mech. Found. Engng., Vol.1, 275-82.
- DONALD, I.B., JORDAN, D.O., PARKER, R.J. and TOH, C.T., 1977. 'The vane test - a critical appraisal.' Proc. 9th Int. Conf. Soil Mech. Found. Engng., Tokyo, Vol.1, 81-8.
- DONNAN, W.W. and ARONOVICI, V.S., 1961. 'Field measurements of hydraulic mining.' Applied Science Publishers Ltd., London, 371pp.
- DOWNING, R.A. and HOWITT, F., 1969. 'Saline ground waters in the Carboniferous rocks of the English East Midlands in relation to geology.' Quarterly Journ.Engng. Geol., Vol.1, 241-69.
- DOWNING, R.A., LAND, D.H., ALLENDER, R., LOVELOCK, P.E.R. and BRIDGE, L.R., 1970. 'The hydrogeology of the River Trent basin.' Hydrogeology report No.5, Water supp.pap., Inst.Geol.Sci., 104pp.

- DURGONOGLU, H.T., 1972. 'Static penetration resistance of soils.' Ph.D. thesis, Univ. Calif.
- DURGONOGLU, H.T. and MITCHELL, J.K., 1975. 'Static penetration resistance of soils. I Analysis. II Evaluation of theory and implications for practice.' Proc. A.S.C.E. Speciality Conf. 'In-situ measurement of soil properties.' Raleigh, N.Carolina, Vol.1, 151-70(I), 171-89(II).
- FISHER, R.A. and YATES, F., 1948. 'Statistical tables for biological, agricultural and medical research.' Oliver and Boyd, Edinburgh, 112pp.
- FLETCHER, A.J., 1976. 'The vane test in lagoon deposits.' Unpublished M.Sc. dissertation, Univ. Durham.
- GIBSON, R.E. 1958. 'The progress of consolidation in a clay layer increasing in thickness with time.' Geotechnique, Vol.8, 171-82.
- GIBSON, R.E., 1963. 'An analysis of system flexibility and its effects on time lag in pore water pressure measurements.' Geotechnique, Vol.13, 1-11.
- GIBSON, R.E., 1966. 'A note on the use of the constant head test measure soil permeability in-situ'. Geotechnique, Vol.16, 256-9.
- GIBSON, R.E., 1970. 'An extension to the constant head in-situ permeability test.' Geotechnique, Vol.20, 193-7.
- GIBSON, R.E. and HENKEL, D.J., 1954. 'Influence of the duration of tests at constant rate of strain on the measured "drained" strength.' Geotechnique, Vol.4, 3-15.
- GLOVER, H.G., 1973. 'Acid and ferruginous mine drainages.' Paper presented at an International Symposium on Degraded Environments and Resources Renewal, Univ. Leeds, England.
- GRATTAN-BELLEW, P.E. and EDEN, W.J., 1975. 'Concrete deterioration and floor heave due to bigeochemical weathering of underlying shale.' Can. Geotech. Journ., Vol.12, 372-8.
- HALLCROW, SIR WILLIAM AND PARTNERS, 1977. 'Interim report on cement stabilised tailings with special reference to Oakdale colliery.' Internal report to the National Coal Board.
- HANSEN, J.B. and GIBSON, R.E., 1949. 'Undrained shear strength of anisotropically clays.' Geotechnique, Vol.1, 189-204
- HENDERSON, M.J., 1979. 'Permeability studies in two constrasting colliery lagoons.' Unpublished M.Sc. dissertation, Univ. Durham.
- HOLDEN, J.C., 1974. 'Reports on discussions.' Proc. European Symp. Penetration Testing, Stockholm, Vol.2, 100-7.
- HOLLAND, J.G. and BRINDLE, D.W., 1966. 'A self consistent mass absorption correction for silicate analysis by X-ray flourescence.' Spectrochim. Acta, Vol.22, 2083-93.

- HOLUBEC, I., 1976. 'Geotechnical aspects of coal waste embankments.' Can. Geotech. Journ., Vol.13, 27-39.
- HORNE, M.R., 1964. 'Consolidation of stratified soil with vertical and horizontal drainage.' Int. Journ. Mech. Sci., Vol.6, 187-97.
- HUGHES, J.M. and WINDLE, D., 1976. 'Some geotechnical properties of mineral waste tailings lagoons.' Gnd. Engng., Vol.9, pt.1, 23-8.
- HVORSLEV, M.J., 1951. 'Time lag and soil permeability in groundwater observations.' Bull.no.36, Waterways Experimental Station, U.S. Army Corps of Engineers, Vicksburg, Miss.
- KEELING, P.S., 1962. 'Some experiments on the low temperature removal of carbonaceous materials from clays.' Clay Min. Bull. Min. Soc. Lond., Vol.5, 155-8.
- KENNEDY, G.W., 1977. 'The response of coarse and fine coal-mine discards under controlled load triaxial testing.' M.Sc. Thesis. Univ. Durham.
- KRIZEK, R.J., CASTELEIRO, M. and EDIL, T.B., 1977. 'Desiccation and consolidation of dredged materials.' Journ. Geotech. Div. Proc. A.S.C.E., Vol.103, 1399-1418.
- LAMBE, T.W. and WHITMAN, R.V., 1969. 'Soil Mechanics.' John Wiley and Sons, New York, 553pp.
- LUNNE, T., EIDE, O. and DE RUITER, J., 1976. 'Correlations between cone resistance and vane shear strength in some Scandinavian soft to medium stiff clays.' Cam. Geotech. Journ. Vol.13, 430-41.
- LUTHIN, J.N. and KIRKHAM, D., 1949. 'A piezometer method for measuring permeability of soil in-situ below the water table.' Soil Sci., Vol.68, 349-58.
- McKECHNIE THOMSON, G. and RODIN, S., 1972. 'Colliery spoil heaps after Aberfan.' Inst. Civ. Engrs., London, Pap.7522.
- MENZIES, B.K. and MAILEY, L.K., 1976. 'Some measurements of strength anisotropy in soft clays using diamond shaped vanes.' Geotechnique Vol.16, 631-4.
- MENZIES, B.K. and SIMONS, N.E. 1978. 'Stability of embankments on soft ground.' In 'Developments in soil mechanics I.' Ed. C.R.Scott, Applied Science Publishers, London, 393-435.
- MITTAL, H.K. and MORGENSTERN, N.R., 1975. 'Parameters for the design of tailings dams.' Can. Geotech. Journ., Vol.12, 235-61.
- MITTAL, H.K. and MORGENSTERN, N.R., 1976. 'Seepage control in tailings dams.' Can. Geotech. Journ., Vol.13, 277-93.
- MURRAY, R.T. and SYMONS, E.F., 1974. 'Embankments on soft foundations: settlement and stability study at Tickton.' Transp. Road Res. Lab., L.R. 643, Crowthorne.
- NATIONAL COAL BOARD, 1970. 'Technical handbook - spoil heaps and lagoons.' 2nd draft, National Coal Board, London.

- NATIONAL COAL BOARD, 1972. 'Review of research on properties of spoil tip materials.' Headquarters Research Report, Wimpey Laboratories Ltd., Hayes.
- NICHOLLS, G.D., 1962. 'A scheme for recalculating the chemical analysis of argillaceous rocks for comparative purposes.' The American Mineralogist, Vol.47, 34-46.
- NICHOLLS, G.D., 1972. 'Pollution affecting weels in the Bunter Sandstone.' Water Res. Assoc. Conf. Groundwater Pollution in Europe, Ed. J.A. Cole, Reading, 116-25.
- NIE, N.H., HALL, C.H., JENKINS, J.G., STEINBRENNER, K. and BENT, D.H. 1974. 'Statistical package for the Social Sciences.' McGraw-Hill, New York, 674pp.
- PARRY, R.M.G., 1971. 'A simple driven piezometer.' Geotechnique, Vol.21, 163-7.
- PEACE, G.A., 1980. 'A miniature electric cone penetrometer for the investigation of colliery tailings lagoons.' Unpublished M.Sc. dissertation, Univ. Durham.
- PECK, R.B., 1979. 'Liquefaction potential: science versus practice.' Journ. Geotech. Engng. Div., Proc. A.S.C.E., Vol.105, 393-8.
- PIPER, A., 1977. 'A Major step forward in coal fluidisation.' Queensland Govt. Mining Journ., Vol.78, 157-8.
- PLANTEMA, G., 1957. 'The influence of density on sounding results in dry, moist and saturated sands.' Proc. 4th Int. Conf. Soil Mech. Found. Engng., London, Vol.1, 237-40.
- RAE, G., 1977. 'Computer analysis of information on mine drainage waters.' Int. Assoc. Hydrogeol. Congress, Birmingham, U.K., Vol.XIII, pt.1, B39-50.
- ROWE, P.W., 1959. 'Measurement of the coefficient of consolidation of lacustrine clay.' Geotechnique, Vol.9, 107-18.
- ROWE, P.W. and BARDEN, L., 1966. 'A new consolidation cell.' Geotechnique Vol.16, 162-70.
- SCHIFFMAN, R.L. and STEIN J.R., 1970. 'One-dimensional consolidation of layered systems.' Journ. Soil Mech. Found. Engng. Div. Proc. A.S.C.E., Vol.96, 1499-1504.
- SCHMERTMAN, J.H., 1970. 'Static cone to compute static settlement over sand.' J. Soil Mech. Found. Eng. Div. Proc. A.S.C.E., Vol.96, 1011-43.
- SCHMID, W.E., 1967. 'The field determination of permeability by the infiltration test.' In 'Permeability and capillarity of soils.' A.S.T.M., spec. Tech. Publ. 417, 141-57.
- SCHOFIELD, A.N. and WROTH, P. 1968. 'Critical state soil mechanics.' McGraw-Hill, New York, 310pp.
- SCHULTZE, E. and METZER, K.J., 1965. 'The determination of the density and modulus of compressibility of non-cohesive soils by soundings.' Proc. 6th Int. Conf. Soil Mech. Found. Engng., Montreal, Vol.1, 354-8.

- SEED, H.B., 1976. 'Evaluation of soil liquefaction effects on level ground during earthquakes.' In: Liquefaction Problems in Geotechnical Engineering - A.S.C.E. National Convention, Philadelphia, 1-104.
- SHERWOOD, P.T. and RYLEY, M.D., 1970. 'The effect of sulphates in colliery shale and its use for road making.' Road Res. Lab., L.R. 324, Crowthorne.
- SIEGEL, S., 1956. 'Non-parametric statistics for the behavioural sciences.' McGraw-Hill, New York.
- SKEMPTON, A.W., 1948. 'A study of the geotechnical properties of some post glacial clays.' Geotechnique, Vol.1, 7-22.
- SKEMPTON, A.W. 1957. 'The planning and design of the New Hong Kong Airport. Discussion, Proc. Inst. Civil Engrs. Vol.7, 305-7.
- SMILES, D.E. and YOUNG, E.G., 1965. 'Hydraulic conductivity determinations by several field methods in a sand tank.' Soil Science, Vol.99, 83-7.
- SMITH, G.N. 1978. 'Elements of soil mechanics for civil and mining engineers.' Granada Publishing, 424pp.
- SNYDER, G.A., ZUHL, F.A. and BURCH, E.F., 1977. 'Solidification of fine coal refuse.' Mining Congress Journ., Vol.63, 43-6.
- SPEARS, D.A., TAYLOR, R.K. and TILL, R., 1970. 'A mineralogical investigation of a spoil heap at Yorkshire Main colliery.' Quart. Journ. Eng. Geol., Vol.3, 239-52.
- STEVENSON, C.M., 1968. 'Analysis of the chemical composition of rainwater and air over the British Isles and Eire for the years 1959-64.' Quart. Journ. Roy. Met.Soc., Vol.94, 56-70.
- TATE, T.K. and ROBERTSON, A.S., 1971. 'Investigations into the high salinity groundwater at the Woodfield pumping station, Wellington, Shropshire.' Res.Rep.No.6, Water Supp.Pap., Inst.Geol.Sci., 21pp
- TAYLOR, R.K., 1971a. 'The deformational and physico-chemical properties of certain sediments with particular reference to colliery spoil.' Ph.D. Thesis, Durham Univ.
- TAYLOR, R.K., 1971b. 'Petrography of the Mansfield Marine Band, Tinsley Park, Sheffield.' Proc.Yorks. Geol.Soc., Vol.38, 299-328.
- TAYLOR, R.K., 1974. 'Influence of the coal content on the peak shear strength of colliery shales.' Geotechnique, Vol.24, 683-8.
- TAYLOR, R.K., 1975. 'English and Welsh colliery spoil heaps - mineralogical and mechanical interrelationships.' Eng. Geol., Vol.9, 39-52.
- TAYLOR, R.K. and SPEARS, D.A., 1970. 'The breakdown of British Coal Measures rocks.' Int. J. Rock Mech. Min.Sci. Vol.7, 481-501.
- TAYLOR, R.K. and COBB, A.E., 1977. 'Mineralogical and geotechnical controls on the storage and use of British coal mine wastes.' Proc. 9th Int.Conf. Soil Mech. Found. Engng., Tokyo., Vol.2, 373-88.

- TAYLOR, R.K., MACMILLAN, G.L. and MORRELL, G.R., 1978. 'The liquefaction response of coal mine tailings to earthquakes.' Proc.3rd Int. Conf. Int.Assoc. Eng.Geol., Madrid, Spec.Sess.3, 79-90.
- TAYLOR, R.K. and MORRELL, G.R., 1979. 'Fine grained colliery discard and its susceptibility to liquefaction and flow under cyclic stress.' Eng. Geol.,Vol.14, 219-29.
- TAYLOR, R.K. and KIRBY, J.M. and LUCAS, J.M., 1980. 'An investigation of overtipping a colliery lagoon.' In, Int.Conf. Engng. Protection from Natural Disasters, Bangkok, Eds.,Balasubramaniam, A.S., Karasudhi,P. and Kanok-Nukulchai, W., Asian Institute of Technology, 629-42.
- TERZAGHI,K. and PECK, R.B., 1948.'Soil mechanics in engineering practice.' John Wiley and Sons, New York.
- TILL,R.,1974. 'Statistical methods for the earth scientist - and introduction.' Macmillan.
- VAN DER MERWE, J. 1977. 'The shear strength study of a mine tailings lagoon incorporating the field vane.' Unpublished M.Sc. dissertation, Univ. Durham.
- VESIC, A.S. 1972. 'The expansion of cavities in an infinite soil mass.' Journ. Soil Mech. Found. Engng.Div. Proc. A.S.C.E.,Vol.98, 265-90.
- WALTON, W.C.,1970. 'Groundwater resource evaluation.' McGraw-Hill, New York, 664pp.
- WEISEL , C.E., 1973. 'Some factors influencing in-situ vane test results.' Proc. 8th.Int. Conf. Soil Mech.Found.Engng.,Moscow, Vol.1, 475-9.
- WILKES, P.F., 1974. 'Permeability tests in alluvial deposits and the determination of  $k_o$ .' Geotechnique, Vol.24, 1-11.
- WILKINSON, W.B.,1968. 'Constant head in-situ permeability tests in clay strata.' Geotechnique, Vol.18, 172-84.
- WIMPEY LABORATORIES, 1969. 'Headquarters research project: study of the properties of slurry and tailings in lagoons.' Lab. ref. S/6732/1, Hayes.
- WIMPEY LABORATORIES, 1977. 'Investigation of lagoon deposits and retaining banks at Maltby Colliery, Yorkshire. Vol.1, factual report.' Lab. ref. S/12182, Hayes.
- WIMPEY LABORATORIES, 1977. 'Investigation of tailings lagoons 6 and 7, Orgreave Colliery. Vol.1, factual report.' Lab.ref. S/11219, Hayes.
- YOSHIMI, Y.,1977. 'Liquefaction and cyclic deformation of soils under undrained conditions.' Proc. 9th Int. Conf. Soil Mech. Found. Engng., Tokyo, Vol.2, 613-23.
- ZWECK, H.,1974. 'Reports on discussion.' Proc. European Symp.Penetration Testing, Stockholm,Vol.2, 53-5.
- ZUSSMAN, J. 1967. 'Physical methods in determinative mineralogy.' Academic Press, London, 514pp.



APPENDIX 2.1 THE STRESS DISTRIBUTION AT THE ENDS OF A VANE

In order to assess the stress distribution at the ends of the vane the following procedure was adopted:

- a) A shear force vs displacement graph is assumed.
- b) For any angular rotation, the displacement of any point along the top or side edge is calculated. This is then translated into a shear force by reading the value from the shear force vs displacement graph.
- c) For the point, the contribution to the torque mobilised by the vane is calculated by the shear force multiplied by the moment arm.
- d) The total torque is calculated as the integral of all such points.
- e) For all rotations, a maximum torque is found. It is the stress distribution that produces this peak torque that is of interest.

The scheme is represented in Fig. A.2.1.

The shear force vs displacement graph can be assumed from shear box tests. Unfortunately the limited displacement precludes the full development of residual strength in most cases, though sample F11 in Fig.3.12 (Chaper 3) shows some fall to residual. For calculation purposes this curve has been described approximately by a straight line portion followed by a sine wave, as shown in Fig. A.2.2. Also shown are the resultant stress distributions at peak torque.

It can be seen that the stress distribution along the top and bottom edges is curved, and that the form of the curve is the same as the assumed failure curve (this can also be seen by inspection of Fig. A.2.1). It can also be seen that the position of peak stress shifts towards the axis of rotation (i.e. the vane shaft) in the decreasing height of the vane (i.e. less shear on a vertical surface). Since a real shear force versus displacement graph is curved rather than straight over the initial portion (compare Fig. A.2.2. with sample F11, Fig.3.12) then the actual stress distribution will be curved upwards slightly more than those shown in Fig.A.2.2. A representative curve is sketched in Fig. A.2.3. It is

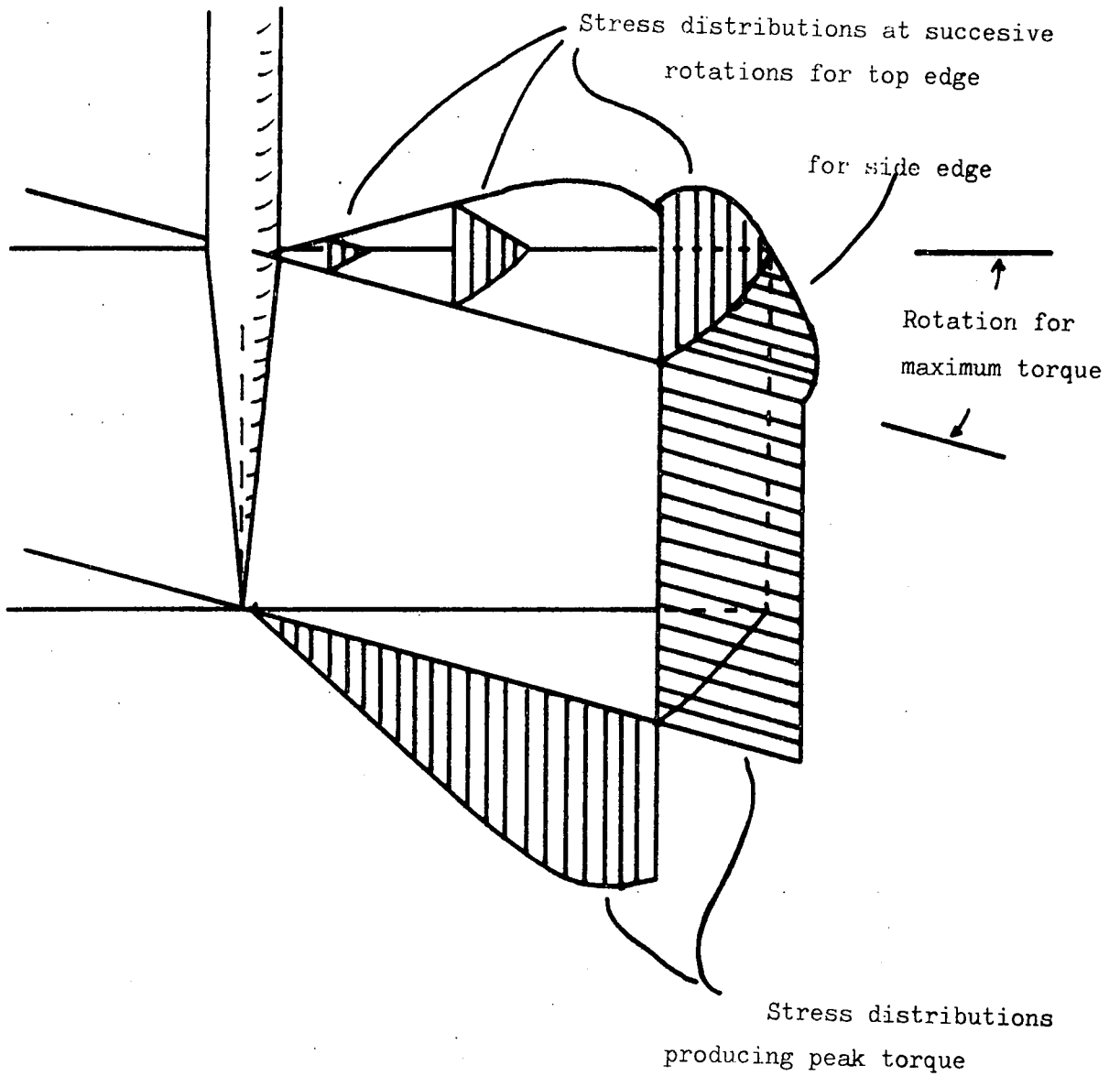
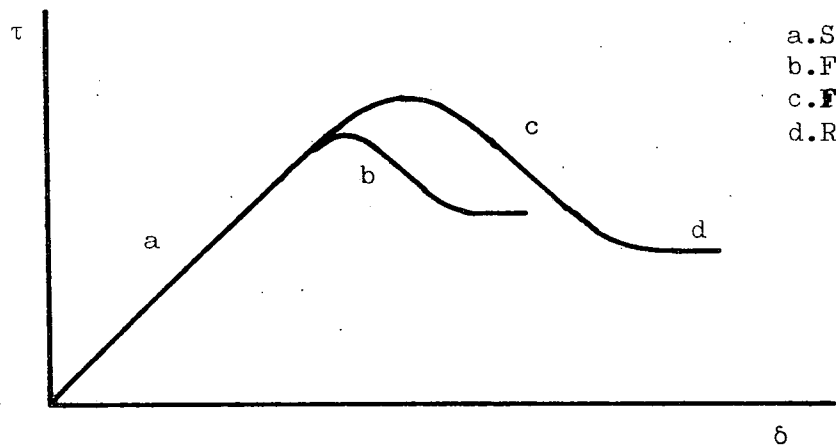
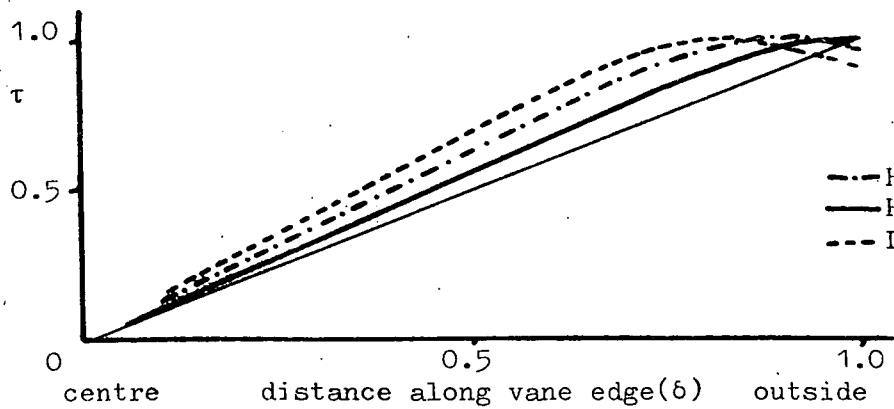


Fig. A.2.1 Shear stress distribution around a rectangular vane.

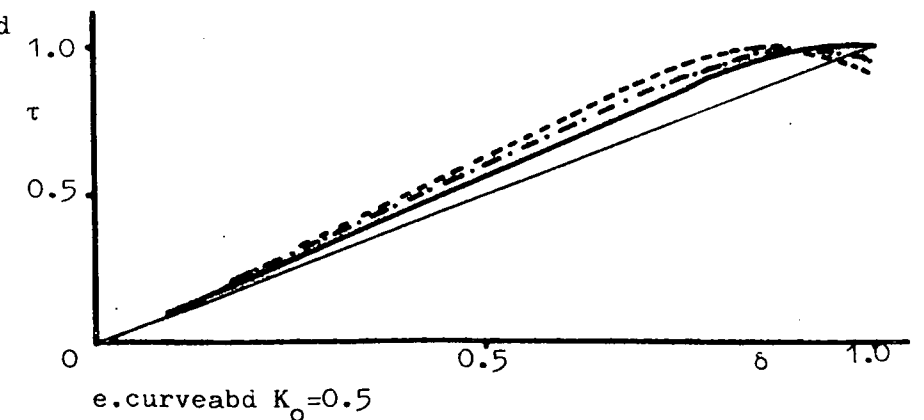
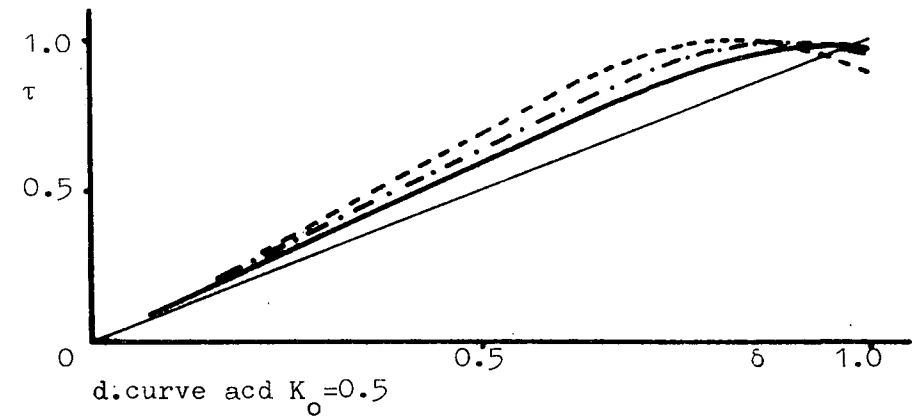
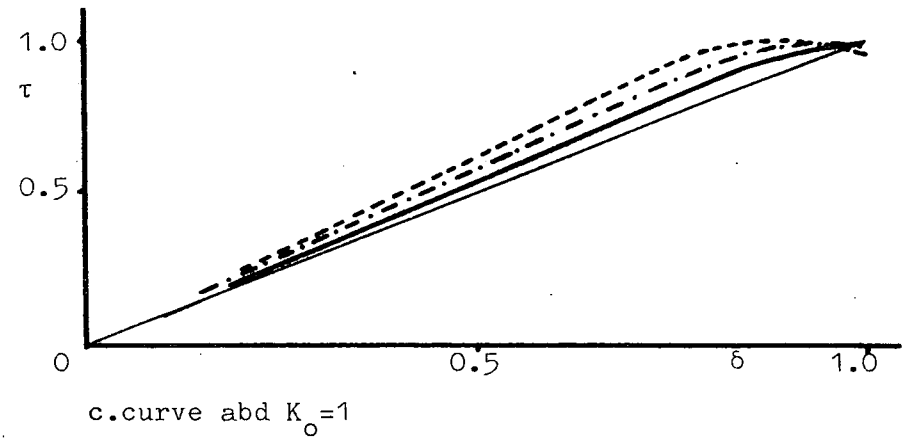


a. Shear stress-displacement curves.



b. curve  $a$  and  $K_0=1$

Fig. A.2.2 Shear stress at failure along vane edge, calculated from an assumed failure curve for the soil.



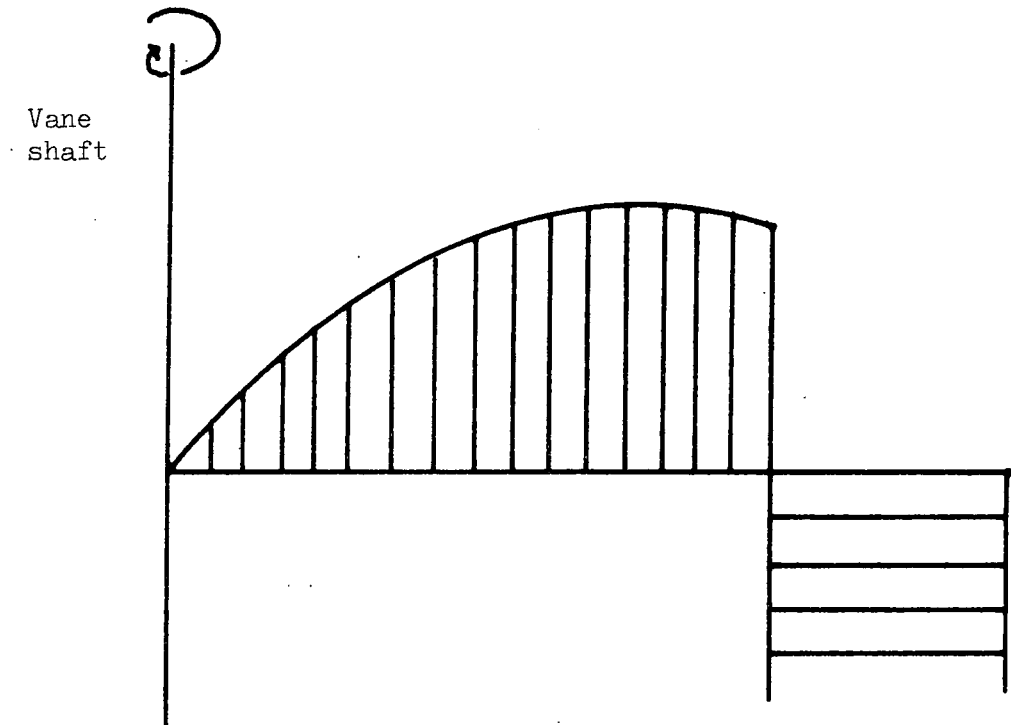


Fig. A.2.3 Approximate shear stress distribution at failure, rescaled from failure curve of sample F11, Fig. 3.12.

further apparent that the exact state of in-situ stress has very little effect on the form of the failure stress distribution. Critical examination of Fig.A.2.2. shows that the stress curves shift slightly towards the axis of rotation with decreasing value of  $K_o$ , though the difference is negligible.

Now for a rectangular vane, the equation of torque generated along the top and bottom edges of the vanes is equivalent to the shear stress multiplied by the movement of the solidus of revolution of the stress distribution. For a uniform stress distribution this is:-

$$T = \pi c. \frac{D^3}{6}$$

T = torque along top and bottom edge

D = diameter of vane

c = shear stress (strength)

For a triangular stress distribution:-

$$T = \pi c. \frac{D^3}{8}$$

For the curved stress distribution the equation will depend on the exact form of the shear force displacement graph. It will also vary slightly from vane to vane, as shown in Fig. A.2.2. However, the exact form of the stress at failure is not known because many of the field vane measurements presented herein refer to tests in layered media. More than one layer will frequently be sheared, with the consequent superposition of two different shear stress versus displacement curves. Consequently the following equation has been adopted for all measurements:

$$T = \pi c. \frac{D^3}{7}$$

which is the value suggested by Donald et al. (1977). Donald et al. (op cit) also suggest that a curved stress distribution is to be expected in strain softening (e.g. normally consolidated) soils. They further suggest that the stress distribution along the vertical edges of a rectangular vane is not quite uniform, but the effect is neglected as being small.

APPENDIX 2.2 EQUATIONS OF TORQUE FOR VANES

(See Fig.2.3 for definition of combination of pairs of vanes.)

1. Uniform Stress Distribution

$$\text{For a rectangular vane } T = \frac{\pi D^2 H S_v}{2} + \frac{\pi D^3}{6} S_h \dots\dots\dots 1$$

$$\text{For a diamond vane } T = \frac{\pi D^3}{6} \cdot s \cdot \sec \alpha \dots\dots\dots 2$$

Where T is the torque

$\alpha$  is the inclination of the vane edge to the horizontal

D is the diameter of the vane

H is the height

$S_h$  is the shear strength in a horizontal plane

$S_v$  is the shear strength on a vertical plane

s is the average shear strength

Several authors (Menzies and Mailey, 1976; Casagrande and Carillo, 1944)

have suggested that:

$$s = S_h + (S_v - S_h) \cos^2 (90 - \alpha) \dots\dots\dots 3$$

$$\text{hence } T = \frac{\pi D^3}{6} \cdot \sec \alpha \left[ S_h + (S_v - S_h) \cos^2 (90 - \alpha) \right] \dots\dots\dots 4$$

Thus for vane pair combination 1 :-

$$\frac{T_{2D}}{T_{D/3}} = X = \frac{\pi D^3 (S_v + \frac{1}{6} S_h)}{\frac{\pi D^3}{6} (S_v + S_h)} \dots\dots\dots 5$$

$$= \frac{6 S_v + S_h}{S_v + S_h} \dots\dots\dots 6$$

putting  $R = \frac{S_v}{S_h}$  i.e.  $S_v = R.S_h$  and solving for R:-

$$R = \frac{X - 1}{6 - X} \dots\dots\dots 7$$

The substitution  $S_v = R S_h$  is now made into equation 1, and hence  $S_v$  and  $S_h$  found.

For pair combination 2:-

$$X = \frac{T}{D_i} \quad , \quad \text{and as above}$$

$$R = \frac{\cos^2 \alpha \cdot \sec \alpha - X}{X - \sin^2 \alpha \cdot \sec \alpha} \quad \dots\dots \quad 8$$

For pair combination 3:-

$$X = \frac{T_{D/3}}{T_{D/2}} \quad , \quad \text{and}$$

$$R = \frac{27 - X}{12X - 27} \quad \dots\dots \quad 9$$

For pair combination 4:-

$$X = \frac{T_{2D}}{T_{D_i}} \quad , \quad \text{and}$$

$$R = \frac{\sec \alpha \cdot \cos^2 \alpha \cdot X - 1}{6 - \sec \alpha \cdot \sin^2 \alpha \cdot X} \quad \dots\dots \quad 10$$

For the triangular stress distribution, the equation of torque for a rectangular vane is:-

$$T = \frac{\pi D^2 H}{2} S_v + \frac{\pi D^3}{8} S_h \quad \dots\dots \quad 11$$

and for a diamond vane:-

$$T = \frac{\pi D^3}{8} \cdot \sec \alpha \cdot \left[ S_h + (S_v - S_h) \cos^2(90 - \alpha) \right] \quad \dots\dots \quad 12$$

Equations 8-10 become:-

$$R = \frac{3}{4} \cdot \frac{X - 1}{6 - X} \quad \dots\dots \quad 13$$

$$R = \frac{\sec \alpha \cdot \cos^2 \alpha - X}{\frac{4}{3} X - \sec \alpha \cdot \sin^2 \alpha} \quad \dots\dots \quad 14$$

$$R = \frac{27 - 8X}{16X - 32} \quad \dots\dots 15$$

$$R = \frac{\sec\alpha \cdot \cos^2\alpha - X}{8 - \sec\alpha \cdot \sin^2\alpha \cdot X} \quad \dots\dots 16$$

3. For a parabolic stress distribution, the equation of torque for a rectangular vane is (see Appendix A.2.1):-

$$T = \frac{\pi \cdot D^2 \cdot H}{2} \cdot S_v + \frac{\pi \cdot D^3}{7} S_h \quad \dots\dots 17$$

and for a diamond vane:

$$T = \frac{\pi \cdot D^3}{7} \left[ \sec\alpha S_h + (S_v - S_h) \cos^2(90-\alpha) \right] \quad \dots\dots 18$$

Equations 8-10 become:-

$$R = \frac{X - 1}{7 - \frac{7}{6} X} \quad \dots\dots 19$$

$$R = \frac{\sec\alpha \cdot \cos^2\alpha - X}{\frac{7}{6} X - \sec\alpha \cdot \sin^2\alpha} \quad \dots\dots 20$$

$$R = \frac{54 - 16X}{28X - 63} \quad \dots\dots 21$$

$$R = \frac{\sec\alpha \cdot \cos^2\alpha \cdot X - 1}{7 - \sec\alpha \cdot \sin^2\alpha \cdot X} \quad \dots\dots 22$$

The results reported in this thesis, unless otherwise stated, are in terms of the parabolic stress assumption. The equations for all three are quoted to give the reader an appreciation of the differences caused by a change in assumption. In this context it is worth noting that the horizontal shear strength calculated from field torque readings will vary considerably according to the assumption.



Table A.4.1.1

	QTZ	ILL	KAC	PYR	ANK	OTHER	COAL	TOTAL	
1<90	11	47	8	4	1	CHL X -	35	106	
190	1	18	5	4	X	CHL X -	76	104	
1710	-	X	3	-	6	GOE X -	89	98	
2<90	12	35	11	1	-	CC X -	36	95	
290	1	28	6	3	3	- - -	55	96	
2710	-	5	2	4	-	- - -	91	102	
3<90	10	54	6	3	2	- - -	31	106	
390	3	25	8	3	7	- - -	47	93	
3710	X	24	4	4	2	GOE X -	76	110	
4<90	9	64	8	5	-	- - -	22	103	
490	1	37	8	3	3	- - -	44	96	
4150	3	35	7	3	2	- - -	44	94	
4212	3	26	5	5	1	CHL X -	51	91	
4300	6	27	5	5	5	- - -	49	97	
4710	6	22	5	5	X	CC 2 CHL X	67	107	
4104	X	?	5	7	X	CHL X -	81	93	
5<90	12	54	10	5	2	CHL XSID X	27	108	
590	5	36	6	6	4	- - -	43	100	
5150	4	37	7	3	3	- - -	43	97	
5710	2	32	8	6	X	- - -	45	93	
6<90	11	34	9	X	X	- - -	38	92	
690	X	27	6	2	4	- - -	68	107	
6710	-	X	3	3	-	- - -	93	99	
7<90	9	53	7	X	3	CC X -	33	105	
790	X	8	2	3	1	- - -	85	99	
7500	X	10	2	3	-	- - -	81	96	
	QTZ	ILL	KAC	PYR	ANK	OTHER	COAL	TOTAL	
PL71<90	5	48	12	1	-	CC 1 -	38	105	
PL72<90	6	54	14	-	-	- - -	31	105	
PL73<90	5	38	14	1	-	CHL X -	41	99	
PL74<90	5	53	10	4	-	- - -	34	106	
PL75<90	10	25	14	3	-	CC 1 -	44	95	
PL76<90	2	42	7	2	-	- - -	44	97	
PL77<90	8	28	11	3	-	- - -	47	97	
PL78<90	2	38	14	2	-	- - -	39	95	
PL79<90	5	40	12	1	-	- - -	38	96	
PL710<90	5	48	9	-	-	- - -	33	95	
PL711<90	5	38	9	5	-	- - -	50	107	
PL712<90	10	33	15	3	-	- - -	45	106	
PL713<90	5	39	8	2	1	- - -	41	96	
PL714<90	12	35	7	4	1	- - -	44	103	
PL715<90	5	56	9	2	-	- - -	41	103	
PL716<90	9	27	14	2	5	- - -	49	105	
PL717<90	5	33	10	4	2	- - -	47	101	
PL71>90	1	36	10	1	-	CC 1 -	46	95	
PL72>90	8	40	6	X	-	- - -	40	94	
PL73>90	10	40	9	1	-	- - -	34	94	
PL74>90	5	24	7	1	-	- - -	58	95	
PL75>90	3	18	6	5	6	- - -	58	96	
PL76>90	4	28	5	2	-	- - -	64	103	
PL77>90	3	36	6	2	1	- - -	59	106	
PL78>90	3	22	9	2	1	- - -	57	94	
PL79>90	2	30	7	1	-	CC 1 -	57	98	
PL710>90	5	43	12	X	-	CC 1 -	34	95	
PL711>90	2	26	3	2	1	- - -	71	105	
PL712>90	5	34	4	4	6	- - -	57	107	
PL713>90	1	37	4	3	X	- - -	63	108	
PL714>90	1	35	6	2	-	- - -	67	105	
PL715>90	2	24	7	1	-	- - -	61	95	
PL716>90	1	22	3	3	5	- - -	70	104	
PL717>90	1	42	6	1	-	- - -	48	98	
	QTZ	ILL	KAC	PYR	ANK	OTHER	COAL	TOTAL	
EHCCCL	15	30	19	3	5	JAR X -	26	98	
EHCMS	NOT DETERMINED								
EHCSI	9	18	10	4	10	CC 1 -	49	101	
EHCSA	2	13	5	2	2	- - -	79	103	
EHBCL	6	37	8	1	2	CC 1 -	43	98	
EHBSI	3	13	5	1	4	CHL ? -	69	95	
EHBSA	X	X	1	X	X	JAR ?CHL ?	83	84	
EHAACL	2	41	12	1	8	CC X -	35	101	
EHASI	8	35	14	2	20	CC X -	18	93	
EHASA	1	X	5	2	4	CC X CHL X	88	100	
	QTZ	ILL	KAC	PYR	ANK	OTHER	COAL	TOTAL	
MA1/5F	6	45	9	-	2	CHL X -	51	113	
MA1/5C	1	32	6	2	3	CHL X -	61	105	
MA2/10C	X	5?	5	-	-	- - -	81	91	
MA2/5F	4	32	8	2	-	JAR X -	54	100	
MA2/5M	5	32	6	3	X	JAR X -	53	99	
MA2/5C	2	16	5	1	-	JAR X -	69	93	
MACOARSE	15	60	6	-	?	CHL 4JAR X	12	97	
	QTZ	ILL	KAC	PYR	ANK	OTHER	COAL	TOTAL	
SILCL	22	53	15	2	?	SID XCHL ?	9	101	
SILSA	3	X	3	1	?	SID X -	80	89	

APPENDIX A.4.2 : STANDARDS CALIBRATIONS AND THE REGRESSION EQUATIONS USED TO DETERMINE THE COMPOSITIONS OF THE SAMPLES

Figure A.4.2.1.a-j represents the "raw counts" plotted against the composition for 33 standards. Based on these results a stepwise multiple regression model available in the Statistical Package for the Social Sciences (Nie et al., 1975) was used to obtain the following regression equations.

Composition, weight percent = counts ÷ 100 x regression coefficient

(NB counts were divided by 100, so that the last two digits were ignored. Otherwise greater precision is implied in the XRF analysis than is possible.)

$$\text{SiO}_2 = \text{SiO}_2 \times 0.0124 + \text{Al}_2\text{O}_3 \times 0.00130 + \text{Na}_2\text{O} \times 0.00270 \\ - (\text{SiO}_2)^2 \times 3.57 \times 10^{-7} - 0.0139$$

$$\text{Al}_2\text{O}_3 = \text{Al}_2\text{O}_3 \times 0.00476 + \text{Fe}_2\text{O}_3 \times 1.36 \times 10^{-4} + \text{Na}_2\text{O} \times 0.00721 - 0.360$$

$$\text{Fe}_2\text{O}_3 = \text{Fe}_2\text{O}_3 \times 459 \times 10^{-3} + \text{P}_2\text{O}_5 \times 1.52 \times 10^{-3} + (\text{Fe}_2\text{O}_3)^2 \times 7.11 \times 10^{-8} \\ - (\text{Fe}_2\text{O}_3)^4 \times 5.09 \times 10^{-17} + 0.457$$

$$\text{MgO} = \text{MgO} + 6.78 \times 10^{-3} + 0.018$$

$$\text{CaO} = \text{CaO} \times 0.00250 - (\text{MgO})^2 \times 5.97 \times 10^{-7} - (\text{CaO})^2 \times 2.64 \times 10^{-8} \\ + 0.318$$

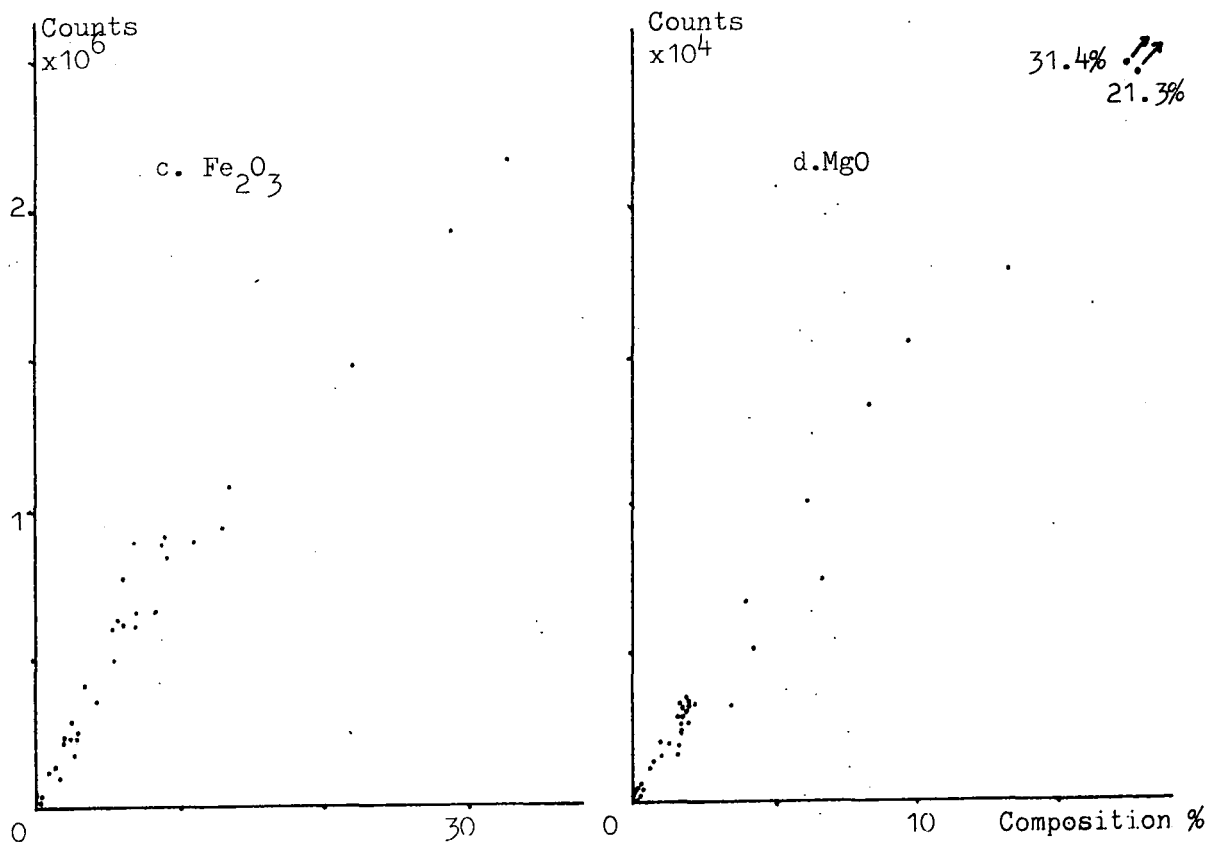
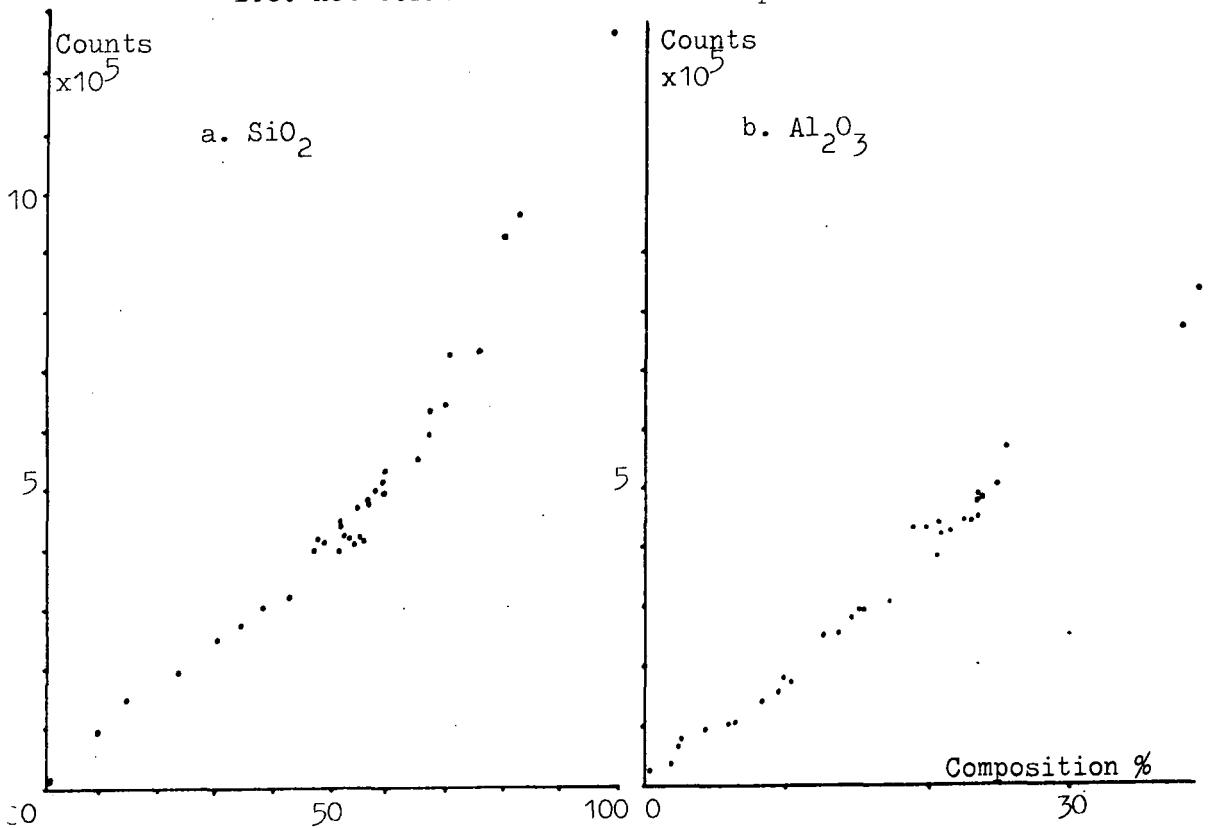
$$\text{Na}_2\text{O} = \text{Na}_2\text{O} + 0.00433 + (\text{Na}_2\text{O})^3 \times 2.64 \times 10^{-10} + 0.049$$

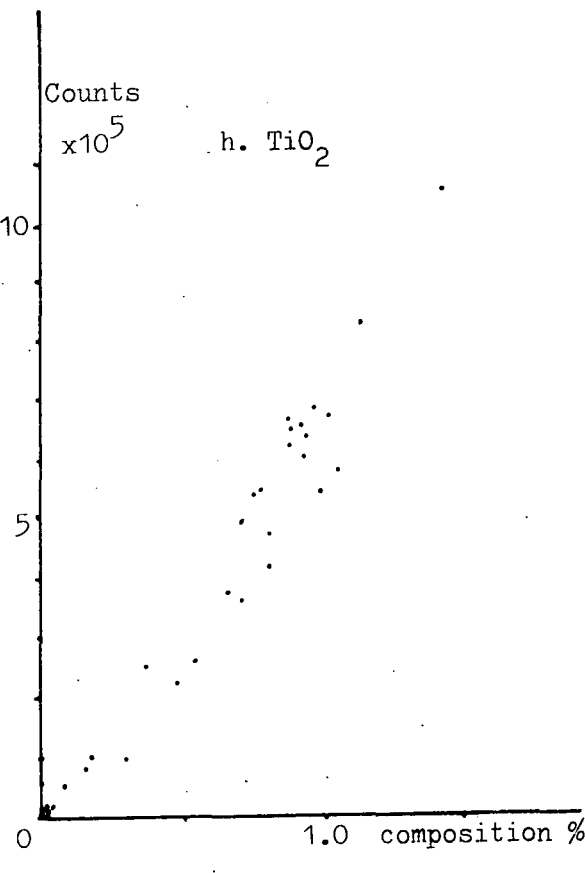
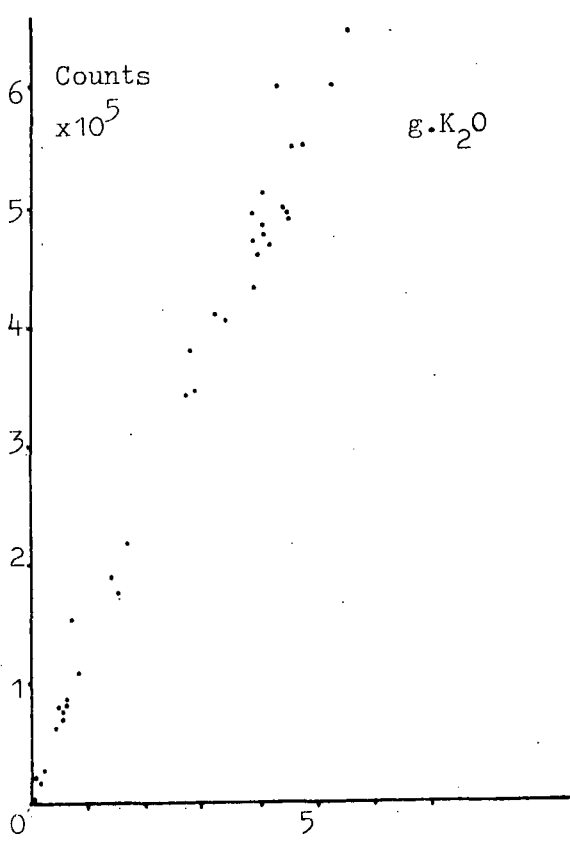
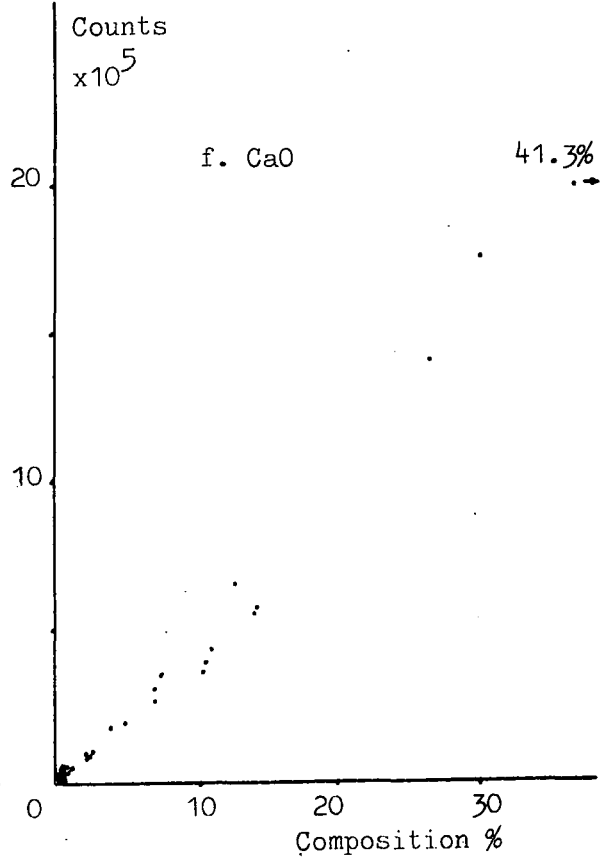
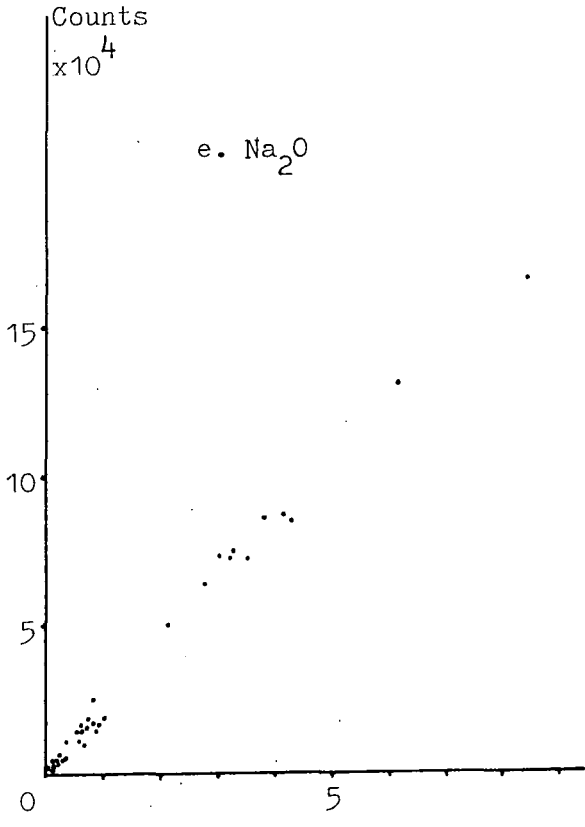
$$\text{K}_2\text{O} = \text{K}_2\text{O} \times 9.18 \times 10^{-4} - \text{CaO} \times 3.48 \times 10^{-5} - \text{TiO}_2 \times 1.41 \times 10^{-5} + \\ (\text{MgO})^2 \times 4.55 \times 10^{-8} - (\text{K}_2\text{O})^2 \times 1.49 \times 10^{-8} - 0.008$$

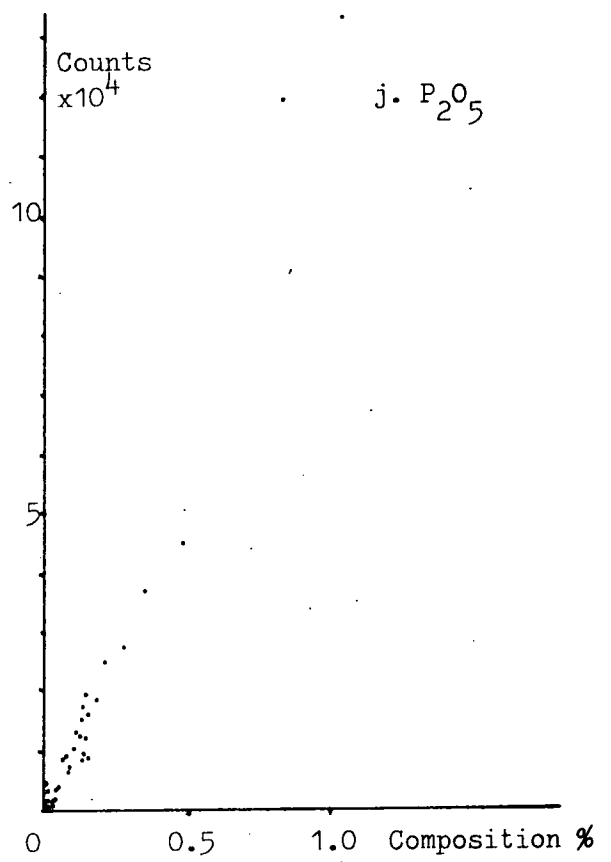
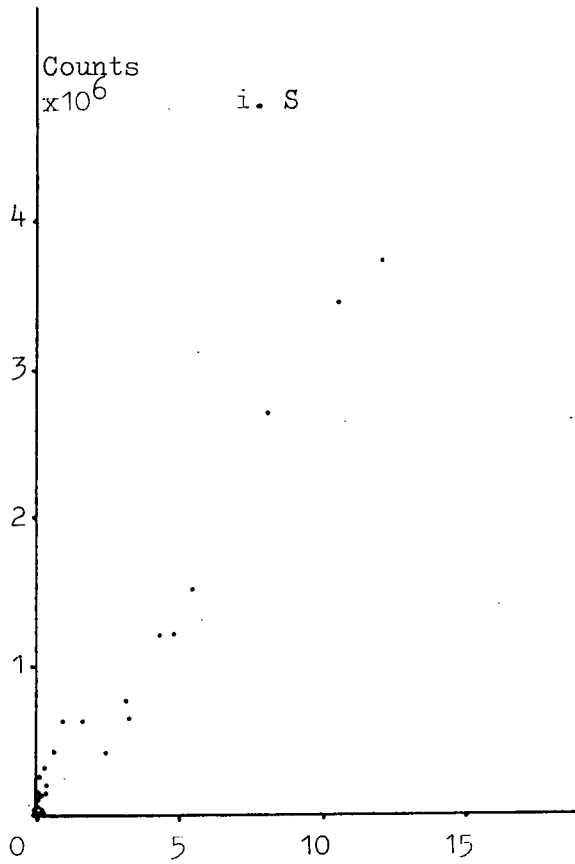
$$\text{TiO}_2 = \text{TiO}_2 \times 1.70 \times 10^{-4} + \text{P}_2\text{O}_5 \times 1.92 \times 10^{-3} - (\text{Al}_2\text{O}_3) \times 6.84 \times 10^{-9} \\ + (\text{S})^2 \times 8.69 \times 10^{-16} - (\text{TiO}_2)^4 \times 3.18 \times 10^{-18} - 0.008$$

$$\text{S} = \text{S} \times 3.23 \times 10^{-4} + \text{Al}_2\text{O}_3 \times 9.63 \times 10^{-5} + \text{Na}_2\text{O} \times 3.22 \times 10^{-4} \\ + (\text{MgO})^2 \times 3.84 \times 10^{-8} - 0.590$$

Fig.A.4.2.1 Calibration charts for the XRF analysis. (N.B. 'raw' data, i.e. not corrected for mass absorption.)







$$P_{25}O_5 = P_{25}O_5 \times 1.22 \times 10^{-3} - (P_{25}O_5)^2 \times 9.3 \times 10^{-7} + (P_{25}O_5)^4 \times 3.26 \times 10^{-12} \\ + 0.003$$

The criterion for the number of coefficients to include in the regression was semi-subjective, but based on the principle that improvement in the correlation coefficient was negligible when further regression terms were added.

APPENDIX A4.3: THE REPEATABILITY OF COUNTS OBTAINED FROM THE XRF EQUIPMENT

One major problem encountered during operation of this prototype equipment was the maintenance of a good vacuum. The pressure obtained when running samples was approximately  $20 \text{ N/m}^2$ , (or .002 atmospheres), which was greater than the machine specifications, which was as low as  $4 \text{ N/m}^2$  or better. This pressure was insufficient to trigger the "VACUUM ERROR" warning, though subsequent to the analysis presented here the vacuum deteriorated to  $50 \text{ N/m}^2$  or worse, and the "VACUUM ERROR" warning was obtained. In order to check the effects of the poor vacuum, one standard (BR1) was repeatedly run as a monitor. The variation of counts with the state of the vacuum is shown in Fig.A.5.3.1, from which it can be seen that only sodium and magnesium counts were affected greatly.

However, all the standards and samples were run under the same conditions with a vacuum of about  $20 \text{ N/m}^2$ , and it is therefore believed that internal consistency has been maintained. The chemistries should therefore be reliable, with the possible exception of  $\text{MgO}$  and  $\text{Na}_2\text{O}$ .

A further check on repeatability was obtained by repeating the analysis of samples MA15 CU and MA15 CB (high and low carbon respectively) twelve times. The range of counts so obtained is shown in Table A.5.3.1. It can be seen that the reproducibility is poor for  $\text{MgO}$ ,  $\text{Na}_2\text{O}$  and  $\text{P}_2\text{O}_5$  in particular, though only  $\text{Fe}_2\text{O}_3$  and  $\text{TiO}_2$  are repeated to better than 0.5% in both samples. The sample with the higher coal content (MA15 CU) has the poorer results, probably because all the determinations are nearer to the sensitivity threshold.

Fig.A.4.3.1 The effect of the vacuum on

XRF counts

+ Vacuum good

o poor

● very poor

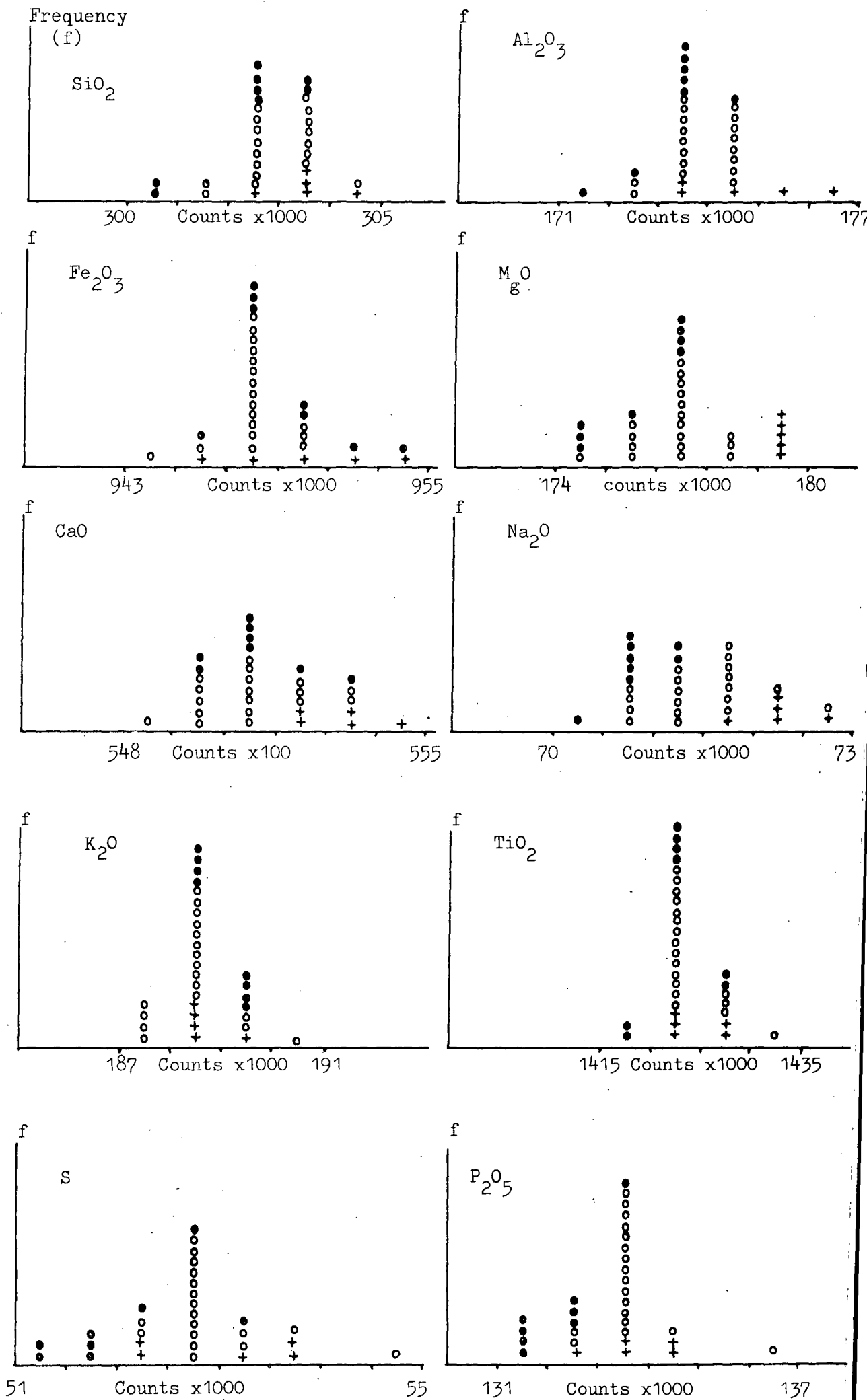




Table A.4.3.1 Variability of counts of one coal rich and one coal free sample.

Note 12 repeat determinations on each sample, all run under 'poor vacuum' conditions of approximately 20 N/m<sup>2</sup>.

Sample	MA15CU		MA15CB	
	Upper and lower limit	Range%	Upper and lower limit	Range%
SiO <sub>2</sub>	194500 193200	0.7	387510 385480	0.5
Al <sub>2</sub> O <sub>3</sub>	241950 239430	1.1	554290 551230	0.6
Fe <sub>2</sub> O <sub>3</sub>	695600 692800	0.4	849270 846740	0.3
MgO	10260 10120	3.4	23610 23040	2.5
CaO	43400 42700	1.6	63060 59640	1.2
Na <sub>2</sub> O	5830 5430	7.4	13810 13490	3.0
K <sub>2</sub> O	30230 30000	0.8	50170 49890	0.6
TiO <sub>2</sub>	43880 43610	0.4	63500 63220	0.4
S	117200 116700	0.4	37800 37510	0.8
P <sub>2</sub> O <sub>5</sub>	92110 88710	3.8	202760 198900	1.9

Table A.4.4.1 Peckfield lagoon 6.

	SI02	AL203	FE203	MGO	CAU	NA2O	K2O	TI02	S	P2O5	TOTAL
1<90	38.451	17.748	4.204	1.131	1.073	0.486	3.442	0.894	1.961	0.082	69.473
190	18.749	9.267	6.469	0.642	1.654	0.183	2.080	0.731	4.490	0.069	44.333
1>710	4.856	2.945	8.893	0.181	0.809	0.179	0.565	0.451	6.689	0.064	25.621
2<90	39.078	18.964	4.191	1.164	1.040	0.707	3.573	0.882	2.089	0.090	71.679
290	33.380	17.565	5.343	1.307	2.422	0.265	3.256	0.795	2.804	0.072	67.209
2710	4.827	3.177	10.708	0.174	0.883	0.187	0.538	0.487	7.382	0.057	28.421
3<90	43.566	21.901	3.489	1.300	1.043	0.504	3.939	0.912	1.729	0.081	78.464
3>90	30.368	16.154	5.763	1.232	2.718	0.218	2.998	0.771	3.379	0.072	63.673
3710	12.751	7.308	9.004	0.391	0.964	0.170	1.436	0.653	6.299	0.061	39.046
4<90	45.395	22.833	3.072	1.361	0.947	0.439	4.050	0.926	1.266	0.080	80.368
490	31.312	16.592	5.335	1.232	2.417	0.231	3.151	0.909	3.129	0.074	64.281
4150	30.570	16.355	5.257	1.212	2.386	0.226	3.017	0.779	3.179	0.069	63.049
4212	27.321	14.535	5.837	1.083	2.598	0.209	2.752	0.755	3.767	0.072	58.931
4300	25.372	13.499	5.741	0.954	2.005	0.205	2.586	0.753	4.029	0.069	55.212
4710	18.870	10.236	7.982	0.615	1.253	0.196	2.064	0.748	5.530	0.069	47.563
4>1.4	11.882	6.490	10.576	0.337	0.952	0.166	1.408	0.620	6.924	0.053	39.408
5<90	45.692	22.786	3.307	1.368	1.212	0.309	3.925	0.936	1.323	0.084	80.942
590	33.190	17.550	5.512	1.300	2.750	0.252	3.273	0.821	3.149	0.073	67.870
5150	31.660	16.680	5.614	1.266	2.988	0.235	3.123	0.801	3.346	0.072	65.785
5710	26.135	13.954	5.839	0.900	1.698	0.231	2.747	0.792	4.262	0.079	56.636
6<90	41.280	19.934	3.776	1.226	0.939	0.504	3.693	0.906	1.677	0.085	74.021
690	22.007	10.764	6.164	0.778	2.055	0.192	2.379	0.745	4.172	0.070	49.325
6710	3.614	2.605	10.516	0.127	0.891	0.144	0.408	0.455	7.552	0.053	26.365
7<90	37.226	17.745	3.437	2.474	4.721	0.842	3.318	0.758	1.963	0.091	72.575
790	5.835	3.244	8.680	0.249	1.492	0.174	0.725	0.520	6.752	0.070	27.741
7150	4.172	2.540	10.520	0.167	1.211	0.166	0.504	0.431	7.656	0.074	27.441

APPENDIX A.4.4 : CHEMISTRY DETERMINED BY X-RAY FLOURESCENCE.

	SIO2	AL2O3	FE2O3	MGO	CAO	NA2O	K2O	TI02	S	P2O5	TOTAL
1<90U	37.097	18.932	3.822	1.158	1.112	0.326	3.758	0.920	2.020	0.090	69.235
2<90U	43.955	21.953	2.888	1.246	1.009	0.374	3.888	0.919	1.343	0.076	77.550
3<90U	43.722	22.174	2.741	1.239	0.968	0.404	3.941	0.930	1.494	0.080	77.692
4<90U	36.222	17.088	5.239	1.070	0.867	0.322	3.338	0.837	2.599	0.116	67.696
5<90U	34.009	15.954	7.694	1.158	1.871	0.274	3.026	0.731	4.166	0.111	68.992
6<90U	35.678	17.103	6.340	1.070	1.419	0.274	3.262	0.771	3.353	0.131	69.401
7<90U	35.035	16.114	6.093	1.151	1.536	0.278	3.182	0.772	3.205	0.119	67.485
8<90U	34.078	17.238	4.365	1.110	1.245	0.270	3.466	0.907	2.194	0.090	64.962
9<90U	37.175	19.048	4.263	1.171	1.226	0.270	3.594	0.900	2.103	0.091	69.840
10<9U	38.611	19.592	3.894	1.212	0.957	0.330	3.782	0.910	1.778	0.087	71.153
11<9U	33.181	14.971	6.726	0.913	1.072	0.304	3.045	0.773	3.384	0.106	64.474
12<9U	33.830	15.797	7.053	1.049	1.674	0.300	3.077	0.756	3.841	0.120	67.499
13<9U	34.542	15.652	7.377	1.117	1.880	0.304	3.065	0.801	3.955	0.123	68.816
14<9U	34.032	15.253	6.657	1.124	1.806	0.274	3.033	0.767	3.644	0.123	66.710
15<9U	36.694	16.628	5.590	1.363	2.219	0.291	3.305	0.816	2.561	0.144	69.616
16<9U	32.814	15.668	6.017	1.117	1.648	0.296	3.109	0.806	3.045	0.141	64.660
17<9U	32.769	15.990	5.148	1.232	1.509	0.300	3.305	0.792	2.519	0.123	63.688
1>90U	32.253	16.121	3.996	0.988	1.236	0.447	3.453	0.865	2.651	0.081	62.091
2>90U	39.481	18.577	3.355	1.015	1.599	0.668	3.707	0.860	3.007	0.074	72.343
3>90U	30.552	13.976	5.620	0.893	0.913	0.556	2.958	0.800	3.338	0.116	59.721
4>90U	30.459	14.291	5.601	0.927	0.878	0.590	2.807	0.769	3.475	0.109	59.906
5>90U	24.224	10.833	9.702	0.791	2.301	0.413	2.433	0.697	5.927	0.102	57.423
6>90U	23.020	10.433	8.174	0.717	1.813	0.447	2.357	0.691	5.328	0.112	53.091
7>90U	27.090	12.007	7.119	0.900	1.500	0.421	2.670	0.733	4.482	0.113	57.026
8>90U	25.785	12.407	5.498	0.852	1.701	0.395	2.871	0.836	3.979	0.078	54.402
9>90U	32.679	15.871	4.787	0.968	1.519	0.491	3.454	0.876	3.615	0.081	64.339
10>9U	39.251	18.749	3.256	1.042	1.180	0.556	3.713	0.929	2.244	0.090	71.001
11>9U	22.340	10.034	7.907	0.629	1.377	0.378	2.135	0.659	5.290	0.094	50.843
12>9U	25.180	11.612	9.488	0.886	3.145	0.361	2.544	0.685	5.605	0.110	59.674
13>9U	21.556	9.575	9.946	0.703	2.633	0.343	2.258	0.677	6.288	0.109	54.088
14>9U	20.985	9.016	9.254	0.662	2.080	0.296	2.186	0.687	6.138	0.111	51.414
15>9U	26.156	11.096	6.747	0.920	2.352	0.404	2.700	0.757	4.564	0.122	55.829
16>9U	17.254	7.767	7.840	0.581	1.830	0.391	1.965	0.679	5.528	0.104	43.939
17>9U	29.205	13.652	6.507	1.003	2.455	0.426	3.133	0.781	4.816	0.113	62.096

/Cont. Peckfield lagoon 7.

	SI02	AL2O3	FE2O3	MGO	CAO	NA2O	K2O	TIO2	S	P2O5	TOTAL
1<90B	50.472	28.817	3.258	1.694	0.931	0.430	4.533	0.954	0.832	0.105	92.075
2<90B	52.994	27.923	2.550	1.544	0.863	0.443	4.340	0.961	0.811	0.091	92.520
3<90B	53.058	28.655	2.339	1.538	0.806	0.491	4.461	0.970	0.688	0.086	93.091
4<90B	51.763	27.322	5.324	1.653	0.797	0.452	4.171	0.905	0.825	0.147	93.358
5<90B	49.702	25.599	8.286	1.734	1.993	0.382	3.917	0.817	1.179	0.147	93.756
6<90B	50.455	26.846	6.494	1.660	1.500	0.400	4.023	0.819	1.010	0.160	93.367
7<90B	50.293	25.716	6.439	1.809	1.647	0.395	4.002	0.845	1.015	0.159	92.320
8<90B	49.277	28.108	4.241	1.639	1.214	0.378	4.378	0.961	0.799	0.107	91.103
9<90B	50.124	28.221	3.495	1.714	0.368	0.447	4.449	0.935	0.760	0.096	91.109
10<9B	51.738	27.942	2.558	1.531	0.772	0.486	4.409	0.953	0.647	0.091	91.126
11<9B	49.942	24.880	7.057	1.477	1.107	0.456	3.974	0.863	1.433	0.128	91.318
12<9B	48.672	25.238	7.836	1.612	1.934	0.417	3.882	0.823	1.571	0.153	92.137
13<9B	50.027	25.150	7.918	1.680	2.939	0.430	3.864	0.823	1.564	0.154	93.650
14<9B	50.841	25.555	7.033	1.836	1.968	0.400	3.925	0.843	1.029	0.159	93.589
15<9B	50.137	25.275	5.652	2.087	2.415	0.413	3.956	0.861	1.309	0.174	92.289
16<9B	49.680	26.927	7.301	1.897	1.837	0.473	4.028	0.999	1.003	0.511	94.706
17<9B	44.928	24.133	5.326	1.870	1.668	0.408	3.987	0.846	1.196	0.152	84.515
1>90B	48.021	27.069	3.886	1.592	1.114	0.677	4.352	0.971	1.301	0.107	89.091
2>90B	51.674	27.235	2.569	1.510	0.820	0.807	4.308	0.949	0.916	0.085	90.874
3>90B	53.072	28.705	2.320	1.538	0.804	0.799	4.442	0.962	0.877	0.090	93.607
4>90B	49.838	26.176	5.790	1.612	0.865	0.851	4.038	0.919	1.429	0.155	91.674
5>90B	47.558	25.103	9.598	1.877	2.386	0.873	3.700	0.862	2.165	0.178	94.301
6>90B	48.346	26.338	8.340	1.707	2.242	1.073	3.812	0.889	1.926	0.194	94.869
7>90B	50.380	26.236	7.332	1.938	1.722	0.790	3.961	0.881	1.471	0.172	94.884
8>90B	47.322	26.717	5.134	1.700	1.674	0.729	4.109	0.993	1.886	0.117	90.381
9>90B	50.291	28.162	3.775	1.721	0.992	0.755	4.391	0.937	1.245	0.102	92.372
10>9B	52.627	28.063	2.571	1.544	0.801	0.777	4.394	0.957	0.920	0.092	92.747
11>9B	49.329	25.519	8.212	1.517	1.457	1.025	3.842	0.935	1.688	0.086	93.609
12>9B	45.813	24.862	9.395	1.578	3.237	0.668	3.663	0.864	2.023	0.193	92.297
13>9B	46.864	24.522	9.493	1.680	3.041	0.825	3.609	0.889	2.179	0.209	93.310
14>9B	49.062	25.363	9.412	1.795	2.307	0.868	3.739	0.932	1.890	0.211	95.580
15>9B	47.878	23.775	6.716	2.019	2.825	0.781	3.726	0.902	2.360	0.199	91.180
16>9B	47.132	26.425	8.621	1.884	2.209	0.986	3.698	1.000	2.035	0.231	94.222
17>9B	49.112	27.157	4.974	2.019	1.745	0.803	4.147	0.841	1.468	0.153	92.419

/cont. Peckfield lagoon 7, oxidised samples.

	S102	AL203	FE203	MGO	CAO	NA2O	K2O	TIO2	S	P2O5	TOTAL
EHCCL	41.725	22.200	3.435	1.097	2.957	0.218	3.025	0.947	1.643	0.072	77.317
EHCMS	41.768	20.461	4.788	2.379	7.122	0.209	2.570	0.702	1.501	0.080	81.578
EHCSI	31.138	15.173	4.607	0.981	3.886	0.222	2.427	0.833	2.469	0.075	61.817
EHCSA	15.144	6.987	5.805	0.479	3.054	0.144	1.302	0.633	4.650	0.056	38.254
EHBCL	36.073	18.231	3.720	0.846	2.263	0.166	2.873	0.959	1.632	0.084	66.896
EHBSI	22.721	10.145	4.525	0.574	2.704	0.118	1.919	0.784	2.934	0.071	46.495
EHBSA	13.676	6.075	5.572	0.378	2.536	0.101	1.213	0.607	4.518	0.052	34.779
EHACL	38.869	20.469	3.864	1.083	2.898	0.205	2.910	0.908	1.633	0.083	72.922
EHASI	40.758	20.345	4.963	2.236	7.205	0.200	2.566	0.733	1.960	0.075	81.043
EHASA	15.683	7.084	5.375	0.513	3.628	0.118	1.304	0.600	4.178	0.054	38.538

	S102	AL203	FE203	MGO	CAO	NA2O	K2O	TIO2	S	P2O5	TOTAL
MA15B	51.925	27.515	6.202	1.734	1.111	0.694	4.266	0.897	0.859	0.158	95.363
M15CB	48.459	27.248	7.640	1.605	1.784	0.642	4.104	0.900	1.206	0.211	93.799
210CB	46.161	28.204	7.540	1.321	1.624	0.595	3.736	1.102	1.110	0.297	91.689
25FB	51.046	28.289	5.669	1.700	1.224	0.521	4.316	0.905	0.786	0.182	94.637
25MB	50.967	25.444	7.358	1.714	1.448	0.751	4.105	0.954	1.002	0.185	93.928
25CB	44.417	25.219	9.941	1.416	1.971	0.721	4.376	0.981	1.891	0.242	91.175
15FU	37.671	18.053	5.366	1.158	1.167	0.430	3.252	0.748	2.068	0.119	70.037
15CU	24.431	12.029	7.709	0.703	1.398	0.296	2.550	0.726	3.430	0.106	53.378
210CU	10.737	5.449	5.543	0.296	0.808	0.136	1.286	0.529	4.919	0.086	29.789
25FU	35.071	17.127	5.497	1.063	1.232	0.387	3.236	0.778	2.232	0.142	66.762
25CU	17.244	8.152	7.768	0.473	1.302	0.257	1.946	0.664	4.357	0.104	42.266
25MU	31.050	14.332	7.087	0.913	1.307	0.456	2.845	0.777	2.585	0.126	61.479
COU	47.829	21.570	4.644	1.639	1.283	0.543	3.958	0.916	0.882	0.068	83.331
COB	53.623	25.256	4.658	1.836	1.344	0.651	4.224	0.926	0.760	0.075	93.355

	S102	AL203	FE203	MGO	CAO	AN2O	K2O	TIO2	S	P2O5	TOTAL
OW1	44.213	25.695	2.225	1.205	1.455	0.395	3.598	1.027	0.459	0.173	80.446
OW2	45.521	26.578	2.145	1.219	1.507	0.421	3.707	1.050	0.446	0.174	82.767
OWOPC	42.912	23.790	2.138	1.253	5.773	0.369	3.485	0.914	0.641	0.176	81.452
OW3	41.996	22.930	2.225	1.259	6.680	0.326	3.294	0.901	0.743	0.176	80.531
OWT	43.744	24.396	2.244	1.307	4.412	0.349	3.383	0.950	0.655	0.163	81.602

/Cont. East Hetton lagoon 109B, Maltby lagoon 6 (including oxidised samples), and Oakdale washery samples.

Table A.4.5.1

	QTZ	ILL	PARAG	KAG	PYR
1<90	17.57	35.14	17.04	10.48	3.59
190	7.85	19.87	11.35	4.03	8.42
1>710	1.39	6.99	31.55	0.56	12.54
2<90	16.89	38.97	22.36	9.47	3.92
290	12.72	30.84	10.59	14.31	5.26
2710	1.09	6.86	33.59	1.27	13.84
3<90	17.80	39.57	15.70	16.57	3.24
3>90	11.36	28.07	9.57	13.45	6.34
3710	4.15	14.26	14.70	4.54	11.81
4<90	12.53	39.71	13.62	18.93	2.37
490	11.79	29.53	9.64	13.14	5.97
4150	11.23	28.33	9.83	13.71	5.36
4212	10.22	25.88	9.95	11.50	7.05
4300	9.49	24.42	10.34	10.29	7.55
4710	6.83	19.33	12.14	6.45	10.37
4>1.4	4.25	13.97	14.64	2.75	12.98
5<90	18.83	37.04	10.28	21.46	2.43
590	12.54	30.82	10.08	14.30	5.90
5150	12.04	29.34	9.87	13.54	6.27
5710	9.72	26.11	10.90	9.79	7.99
6<90	17.83	37.43	16.57	15.72	3.14
690	9.34	22.51	10.51	5.24	7.82
6710	0.55	5.23	33.93	1.43	14.16
7<90	16.35	38.47	26.97	7.05	3.53
790	2.02	8.23	25.83	0.06	12.66
7150	1.18	6.31	32.40	0.20	14.35
	QTZ	ILL	PARAG	KAO	PYR
1<90U	14.82	35.24	11.21	12.87	3.79
2<90U	18.13	37.53	12.28	18.85	2.52
3<90U	17.63	38.35	12.98	18.59	2.80
4<90U	16.12	32.23	12.31	11.72	4.87
5<90U	15.24	29.00	11.64	12.02	7.81
6<90U	15.56	31.00	10.89	12.98	6.29
7<90U	16.08	30.37	11.23	11.09	6.01
8<90U	13.80	32.58	10.13	11.69	4.11
9<90U	14.77	33.76	9.85	15.22	3.34
10<9U	15.55	35.09	11.27	14.30	3.33
11<9U	15.57	29.53	12.69	9.00	6.34
12<9U	15.25	29.75	12.42	10.88	7.20
13<9U	15.13	29.70	12.61	10.56	7.42
14<9U	16.09	29.06	11.62	10.19	6.93
15<9U	17.13	31.57	11.36	11.21	4.30
16<9U	14.38	29.97	12.17	10.34	5.71
17<9U	13.96	31.68	11.67	9.49	4.72
1>90U	13.29	34.75	15.85	6.76	4.97
2>90U	17.63	39.62	20.77	8.13	5.64
3>90U	4.11	31.90	21.48	4.05	6.26
4>90U	13.65	31.04	23.42	5.67	6.52
5>90U	11.48	25.69	19.81	2.21	11.11
6>90U	10.75	25.47	21.63	1.40	9.99
7>90U	12.96	27.80	18.66	3.13	8.40
8>90U	11.19	29.13	16.68	2.81	7.45
9>90U	14.01	35.30	17.14	5.57	6.73
10>9U	17.19	38.29	17.89	9.91	4.21
11>9U	10.54	22.74	20.49	3.08	9.92
12>9U	11.52	25.99	17.12	3.92	10.62
13>9U	10.29	23.35	18.10	1.34	11.79
14>9U	10.38	22.15	16.46	1.11	11.51
15>9U	13.10	27.84	17.88	0.79	8.56
16>9U	8.12	21.46	22.45	-1.42	10.36
17>9U	13.14	31.78	16.52	3.42	9.03
	QTZ	ILL	PARAG	KAO	PYR
EHCCCL	15.61	28.30	9.49	28.52	3.08
EHCMS	17.70	24.34	10.58	27.98	2.81
EHCSI	13.28	23.29	11.75	15.64	4.63
EHCSA	6.92	12.80	13.86	5.15	3.72
EHBSCL	14.57	26.37	7.75	20.51	3.05
EHBSI	10.79	17.70	8.21	8.39	5.50
EHBSA	6.53	11.52	10.81	4.12	8.47
EHACL	14.79	27.17	9.30	25.25	3.06
EHASI	16.82	24.19	10.19	27.84	3.57
EHASA	7.35	12.50	11.64	5.71	7.93
15FU	16.43	32.84	16.14	13.53	3.88
15CU	10.28	25.24	14.45	5.73	6.43
210CU	4.33	12.57	13.34	1.50	9.22
25FU	14.92	32.17	14.82	11.84	4.13
25CU	7.65	19.55	15.12	1.39	3.17
25MU	14.19	29.71	18.91	7.13	4.95
CDU	22.45	40.21	16.64	15.19	1.65

APPENDIX 4.6: ANALYSIS AND RESULTS OF THE WATER CHEMISTRY OF LAGOONS

All sampling bottles (which were polythene) and other apparatus used in this exercise were washed in 0.1 molar hydrochloric acid, and thoroughly rinsed in double-distilled water. Each sample was collected in one clean polythene bottle, and then filtered through Whatmans No.4 filter paper into a second clean bottle. About 150-200ml. was collected for each sample. A 50ml portion of this was extracted, the temperature and pH were taken. A titration was then performed using 0.1 or 0.01 molar  $H_2SO_4$  to a pH of 4.5, then to pH 4.2. The total alkali was expressed as  $CaCO_3$  in mg/l and is equal to

$$\frac{(2C - D) \times N \times 50000}{\text{vol sample}}$$

where N = normality of acid

C = titre to pH = 4.5

D = titre to pH = 4.2

These titrations were performed as far as possible at the point of sampling; however, at Gedling colliery samples G2 and G3 were transported a short distance involving an elapse of about five minutes. All the samples at Silverhill lagoon were transported from the tip to the car park, involving elapses of up to half-an-hour between sampling and titration. This elapse of time could allow a change in the carbonate/bicarbonate balance due to solution of carbon dioxide from the atmosphere. Furthermore, 0.1M acid was used as the titre in some cases and the very small amounts involved could lead to large errors in the estimate of total alkali. The use of 0.01M acid in all cases would have been more accurate. Therefore the total alkali results are somewhat dubious, those at East Hetton lagoon probably being the most reliable; they were all

done at the time of sampling.

The samples were then delivered to Dr.D.A.Spears at the Geology Department of Sheffield University, who very kindly analysed for the following chemical species:

Trace metals; Cu, Ni, Co, Pb, by atomic absorption with a heated graphite atomiser.

Major elements; Na, K, Ca, Mg, by flame atomic absorption.

Sulphate by atomic absorption.

Chloride by a colorimetric method using a thiocyanate complex.

Nitrate by ion-selective electrode.

The results are reported in Table 4.6.1. The final column of the table indicates the balance between the anions and cations analysed, in meq/l (i.e. the value in mg/l divided by the atomic weight of the species in question). The results for Gedling and more particularly Silverhill indicate a considerable imbalance (cation excess, usually). This is probably due to the poor total alkali results.



Table A.4.6.1 The chemistry of lagoon waters. Samples collected jointly with Mr. J.F.Bell; analysis (except total alkali,pH and temperature) by Dr.D.A.Spears, Sheffield University.

Sample	Trace elements mg/l				Major elements mg/l				Anions mg/l			Total alkali mg/l	pH	Temp. °C	Cation excess meq/l
	Cu	Ni	Co	Pb	Na	K	Ca	Mg	SO <sub>4</sub>	Cl	NO <sub>3</sub>				
G1	0.002	0.013	0.004	0.002	277	13.5	134	34.8	510	126	15.4	888	7.6	8.5	-22.0
G2	0.023	0.008	0.007	"	1136	30.8	165	45.4	400	375	61.2	336	7.45	14'	31.1
G3	0.003	0.033	0.011	"	857	24.1	157	40.1	160	312	40.4	16	6.05	11	35.8
EH1	0.014	0.011	0.007	0.022	614	18.9	76	22.8	1040	84	46.5	360	7.6	7.5	-4.0
EH2	0.106	0.023	0.006	0.024	637	20.5	39	24.3	1000	85	44.4	536	8.2	10	-9.6
EH3	0.032	0.015	0.003	0.164	667	25.6	19	22.0	930	91	19.3	500	8.5	11	-6.6
EH4	0.064	0.061	0.017	0.002	416	43.7	310	193.6	1500	90	21.8	560	7.3	8.5	-2.1
EH5	0.043	0.223	0.153	"	1115	45.4	176	98.3	1550	120	14.2	504	7.4	8	13.9
EH6	0.010	0.020	0.007	"	389	15.6	47	21.2	800	60	13.5	286	8.15	8	-6.8
EH7	0.003	0.013	0.007	"	624	18.6	45	21.0	1020	81	52.4	360	7.6	7.5	-4.8
S1	0.002	0.042	0.021	"	1606	32.9	203	57.0	900	516	46.2	114	6.9	8	48.0
S2	"	0.043	0.017	"	3133	40.3	297	130.3	860	570	67.2	342	7.4	8	116.5
S3	"	0.040	0.011	"	1333	26.5	251	65.0	1120	510	50.0	1060	7.7	8	2.7
S4	"	0.055	0.015	"	2248	48.1	502	136.7	1440	515	53.5	190	7.6	8	83.5
S5	0.003	0.046	0.024	"	1452	44.8	382	83.2	1550	492	58.3	146	7.25	8	38.0
S6	0.006	0.014	0.010	"	1528	28.9	254	93.4	52	444	43.5	394	7.0	8	60.1

APPENDIX A.5.1 In-situ vane test shear strength data.

PECKFIELD LAGOON NO. 7. VANE TESTS

1st PAIR VANE TESTS, MAY 1977, JMK J VD M

ALL STRENGTHS IN KN/M\*\*2

PARABOLIC STRESS DISTRIBUTION

TEST DEPTH	PEAK STRENGTH	H=2D		H=1/3D		SENSITIVITY		HORIZ	VERTICAL	R(=5V/S)
		H=2D	H=1/3D	H=2D	H=1/3D	H=2D	H=1/3D			
1.000	2.310	33.179	18.933	13.573	3.787	2.444	5.000	-3.877	38.484	-9.925
1.000	2.760	64.849	43.656	27.146	22.719	2.399	1.922	9.722	72.743	7.442
1.000	3.210	11.894	20.492	4.162	15.169	2.855	1.333	34.263	8.680	0.254
1.000	3.660	16.167	30.292	8.144	28.956	1.985	1.046	52.891	10.922	0.206
1.000	4.110	20.812	14.701	13.573	3.564	1.533	4.125	4.914	23.089	4.609
1.000	4.330	22.320	55.239	11.462	43.434	1.947	1.272	107.908	10.094	0.094
2.000	2.310	52.724	30.515	22.320	17.151	2.362	1.779	-5.045	60.995	-12.090
2.000	2.760	30.464	17.819	11.271	8.241	2.295	2.162	-2.428	35.173	-14.483
2.000	3.210	31.972	23.284	11.160	6.682	2.365	4.233	22.343	33.348	1.490
2.000	3.660	10.436	9.578	5.007	5.568	2.084	1.720	8.201	10.757	1.312
2.000	4.110	15.383	24.501	9.350	16.705	1.645	1.467	39.098	11.998	0.307
2.000	4.560	38.005	35.638	17.193	26.728	2.211	1.333	31.841	38.892	1.221
3.000	2.310	22.320	12.251	9.954	2.227	2.242	5.500	-3.472	26.070	-6.732
3.000	2.760	24.130	27.197	10.255	16.037	2.353	1.708	32.619	21.921	0.703
3.000	3.210	11.462	18.042	3.197	14.032	1.585	1.285	28.568	9.019	0.316
3.000	3.660	14.701	11.582	7.541	6.237	2.480	1.857	0.185	21.352	-115.682
3.000	4.110	10.255	13.810	4.162	8.464	2.464	1.632	19.495	8.936	0.458
3.000	4.560	43.253	51.229	15.985	23.387	2.706	2.190	63.984	40.247	0.630
4.000	2.310	18.399	8.464	6.937	4.677	2.652	1.810	-7.444	22.094	-2.969
4.000	2.760	11.763	7.128	5.067	3.118	2.321	2.296	-0.295	13.490	-45.724
4.000	3.210	15.202	8.909	5.912	4.009	2.571	2.222	-1.166	17.545	-15.053
4.000	3.660	11.763	14.032	4.524	6.905	2.600	2.032	17.661	10.922	0.619
4.000	4.110	8.626	14.478	3.619	6.237	2.383	2.321	23.319	6.454	0.271
4.000	4.560	29.559	43.434	6.937	13.364	4.261	3.250	65.629	24.409	0.372
4.000	5.010	11.884	26.728	4.223	22.274	2.814	1.200	50.479	6.371	0.126
5.000	2.310	15.503	8.909	5.007	6.014	3.096	1.431	-1.649	17.959	-10.894
5.000	2.760	7.842	10.023	3.740	3.341	2.097	3.000	13.511	7.033	0.521
5.000	3.210	24.733	30.515	7.239	11.137	3.417	2.740	39.761	22.589	0.868
5.000	3.660	24.130	20.046	8.506	11.805	2.837	1.698	13.505	25.653	1.909
5.000	4.110	40.417	34.524	15.684	12.251	2.577	2.814	25.083	42.617	1.699
5.000	4.560	51.879	40.761	17.193	23.387	3.018	1.743	22.954	50.024	2.441
5.000	5.010	20.209	44.547	11.763	23.347	1.718	1.805	83.488	11.170	0.134
5.000	5.220	39.211	57.912	16.891	24.501	2.321	2.364	87.827	32.270	0.367
6.000	2.310	3.318	5.346	1.810	3.118	1.833	1.714	8.590	3.565	0.299
6.000	2.760	7.239	8.909	3.318	4.455	2.182	2.000	11.581	6.620	0.572
6.000	3.210	15.684	28.956	6.756	16.705	2.321	1.733	50.139	10.756	0.214
6.000	3.660	34.043	33.411	14.176	17.319	2.404	1.875	32.325	34.341	1.062
6.000	4.110	21.225	43.434	9.169	26.728	2.322	1.625	78.855	13.073	0.166
1.100	0.300	15.021	16.483	5.490	8.241	2.736	2.000	18.818	14.481	1.443
1.100	0.550	5.490	4.900	2.413	2.227	2.275	2.200	3.956	9.710	1.443
1.100	0.770	5.731	6.237	2.111	2.573	2.714	2.333	7.045	5.544	0.737
1.100	0.990	5.429	12.251	1.749	5.568	3.103	2.200	23.164	2.896	0.125
1.100	1.210	7.239	7.128	2.715	4.009	2.557	1.778	6.948	7.292	1.043
1.100	1.410	32.575	32.297	13.875	14.923	2.348	2.164	31.843	32.686	1.024
1.100	1.630	31.972	35.638	13.875	18.933	2.304	1.882	41.497	30.616	0.734
1.100	1.860	37.643	26.728	15.503	12.251	2.428	2.182	9.251	41.709	4.504
1.100	2.070	31.731	21.383	14.740	15.542	2.147	1.371	4.313	35.585	7.394
1.100	2.310	37.643	34.979	14.478	18.710	2.600	2.083	41.108	37.154	0.904
1.100	2.530	51.879	43.434	22.018	24.501	2.356	1.773	29.905	55.030	1.840
1.100	2.760	36.919	24.501	14.961	13.810	2.468	1.774	4.618	41.544	8.997
1.100	2.970	33.440	36.752	14.478	23.387	2.312	1.571	41.979	32.271	0.769
1.100	3.210	14.478	18.710	6.515	8.019	2.222	2.333	25.479	12.908	0.507
1.100	3.430	18.640	12.251	9.049	10.023	2.060	1.222	2.019	21.020	10.411
1.100	3.660	20.209	19.378	6.334	15.146	3.190	1.279	18.044	20.522	1.137
1.100	3.870	14.176	20.715	9.833	7.796	1.442	2.657	31.174	11.749	0.377
1.100	4.110	34.687	21.160	13.211	13.364	2.626	1.583	-0.499	34.725	-79.670
2.100	0.300	8.445	16.928	3.016	8.464	2.800	2.000	30.499	5.295	0.174
2.100	0.550	4.524	7.796	2.353	6.014	1.923	1.296	13.030	3.310	0.254
2.100	0.770	6.032	6.905	1.810	3.564	3.333	1.938	8.299	5.709	0.683
2.100	0.990	6.696	16.037	2.654	6.459	2.523	2.483	30.982	3.227	0.104
2.100	1.210	6.636	6.632	2.896	2.896	2.292	2.308	6.755	6.620	0.980
2.100	1.410	16.348	16.705	6.394	8.019	2.557	2.083	17.273	16.219	0.939
2.100	1.630	34.506	31.183	16.289	18.264	2.119	1.707	25.857	35.749	1.383
2.100	1.860	20.571	17.151	7.661	9.355	2.685	1.833	11.672	21.346	1.872
2.100	2.070	24.311	21.160	11.462	13.810	2.121	1.532	16.112	25.487	1.582
2.100	2.310	18.097	30.069	7.239	12.696	2.500	2.368	49.223	13.652	0.277
2.100	2.530	14.176	34.524	6.032	11.137	2.350	3.100	67.030	6.619	0.099
2.100	2.760	17.474	13.364	8.264	8.019	2.117	1.667	6.750	19.033	2.870
2.100	2.970	14.478	16.037	4.343	7.128	3.333	2.250	18.529	13.901	0.750
2.100	3.210	8.144	14.478	3.016	7.350	2.700	1.970	24.612	5.792	0.235
2.100	3.430	9.350	10.023	4.223	4.900	2.214	2.045	11.098	9.102	0.820
2.100	3.660	23.527	16.037	9.049	6.237	2.600	2.571	4.044	26.317	6.507
2.100	3.870	22.018	16.037	7.541	8.464	2.920	1.895	6.459	24.247	3.754
2.100	4.110	12.757	12.919	5.128	6.682	2.412	1.933	13.799	12.164	0.841
2.100	4.330	11.160	11.137	3.981	5.588	2.803	2.000	11.097	11.171	1.007
2.100	4.560	12.065	16.705	6.032	11.137	2.000	1.500	24.128	10.343	0.429
2.100	4.330	13.332	21.160	6.032	9.578	2.210	2.209	33.634	10.425	0.310
2.100	5.010	17.796	20.715	7.842	10.023	2.269	2.067	25.381	16.715	0.659
2.100	5.270	12.367	12.251	7.239	7.796	1.708	1.571	12.062	12.412	1.029
2.100	5.460	14.599	31.183	9.290	16.705	1.571	1.467	57.718	3.439	0.146
2.100	5.670	10.255	31.183	10.255	13.810	1.000	2.258	64.658	2.482	0.034

ALL STRENGTHS IN KN/M\*\*2

PARABOLIC STRESS DISTRIBUTION

TEST DEPTH	PEAK STRENGTH	REM STRENGTH		SENSITIVITY		HORIZ	VERTICAL	R(=SV)		
		DIAMOND	H=D/3	DIAMOND	H=D/3				DIAMOND	H=D/3
1.100	0.300	18.438	16.705	14.399	11.415	1.280	1.463	18.652	15.037	0.805
1.100	0.550	3.512	3.202	1.932	1.169	1.818	2.738	3.550	2.903	0.819
1.100	0.990	4.273	5.012	3.219	2.227	1.327	2.250	4.184	5.721	1.364
1.100	1.410	26.457	24.780	20.018	13.504	1.322	1.835	26.666	23.163	0.869
1.100	1.860	23.179	31.601	15.921	16.288	1.456	1.940	22.157	39.696	1.792
1.100	2.310	22.242	30.487	12.643	19.796	1.759	1.540	21.242	38.412	1.808
1.100	2.760	11.531	35.777	7.024	24.501	1.642	1.460	8.578	59.092	6.889
1.100	3.210	6.322	10.023	4.390	5.986	1.440	1.674	5.872	13.582	2.313
1.100	3.660	13.170	16.093	7.551	8.353	1.744	1.927	12.816	18.901	1.475
1.100	4.110	31.315	12.111	21.189	6.459	1.478	1.875	33.654	-6.354	-0.149
2.100	0.300	12.585	32.019	9.131	24.640	1.378	1.299	10.218	50.705	4.962
2.100	0.550	4.156	7.517	1.873	4.232	2.219	1.776	3.747	10.749	2.869
2.100	0.770	3.698	5.151	1.815	2.645	2.032	1.947	3.510	6.557	1.868
2.100	0.990	7.024	6.821	3.629	3.090	1.935	2.207	7.050	6.626	0.940
2.100	1.210	3.940	8.910	2.400	5.012	1.659	1.778	3.380	13.649	4.038
2.100	1.410	14.165	8.353	6.790	4.232	2.086	1.974	14.875	2.762	0.186
2.100	1.630	32.486	34.385	18.789	27.285	1.729	1.260	32.260	36.207	1.122
2.100	1.860	20.018	24.919	12.292	14.060	1.629	1.772	19.425	29.628	1.525
2.100	2.070	22.652	14.756	14.692	9.077	1.542	1.626	23.617	7.162	0.303
2.100	2.310	14.399	25.476	10.770	12.390	1.337	2.056	13.052	36.125	2.768
2.100	2.530	6.365	14.478	5.151	6.361	1.352	2.080	6.051	21.701	3.586
2.100	2.760	6.322	8.074	3.805	2.645	1.662	3.053	6.109	9.759	1.597
2.100	2.970	12.116	8.631	5.326	4.316	2.275	2.000	12.543	5.278	0.421
2.100	3.210	12.233	4.872	5.151	3.341	2.375	1.458	13.130	-2.206	-0.168
2.100	3.430	6.322	6.543	3.219	3.341	1.964	1.958	6.296	6.755	1.073
2.100	3.660	13.521	11.694	7.668	7.100	1.763	1.647	13.746	9.935	0.723
2.100	3.870	12.526	15.731	6.965	6.543	1.798	2.404	12.138	18.811	1.550
2.100	4.110	8.019	8.492	4.390	3.759	1.827	2.259	7.963	8.945	1.123
2.100	4.330	8.838	10.859	5.970	4.733	1.480	2.294	8.594	12.800	1.487
2.100	4.560	11.531	10.469	5.853	4.176	1.970	2.507	11.662	9.446	0.810
2.100	4.770	9.951	12.251	5.092	6.849	1.954	1.789	9.672	14.461	1.495
2.100	5.010	9.190	19.573	4.566	8.353	2.013	2.343	7.926	29.557	3.729
2.100	5.220	9.482	15.592	4.214	7.517	2.250	2.074	8.740	21.465	2.456
2.100	5.460	10.946	15.592	5.385	7.155	2.033	2.179	10.382	20.058	1.932
2.100	5.670	20.311	14.756	15.453	4.622	1.314	3.193	20.991	9.413	0.448

EAST HETTON LAGOONS 109B, 109A  
H=2D VANE TESTS, OCT 1977

ALL STRENGTHS IN KN/M2

TEST	DEPTH	PEAK	REM	SENS
1	0.33	15.0	5.1	2.97
1	0.77	18.5	13.2	12.63
1	1.41	5.3	11.9	12.82
1	1.63	12.3	14.4	12.81
2	0.33	24.2	19.0	12.68
2	0.77	25.6	16.9	13.72
2	1.41	27.9	15.7	13.12
2	1.63	29.9	13.6	12.19
3	0.33	17.4	14.8	13.64
3	0.77	10.7	13.6	12.95
3	1.41	7.8	13.4	12.30

EAST HETTON, VANE TESTS, APR.-MAY 1978

2ND PAIR VANE TESTS, LOCATION A=1.B=2.C=3

ALL STRENGTHS IN KN/M\*\*2

PARABOLIC STRESS DISTRIBUTION

TEST DEPTH	PEAK STRENGTH	REM STRENGTH		SENSITIVITY		HORIZ	VERTICAL	R(=SV)		
		DIAMOND	H=D/3	DIAMOND	H=D/3				DIAMOND	H=D/3
1.000	1.000	9.680	24.245	4.346	17.385	2.227	1.395	7.907	38.249	4.837
1.000	2.000	17.779	17.761	11.458	7.513	1.552	2.362	17.746	17.739	0.997
1.000	3.000	10.668	19.170	8.495	3.833	1.256	2.170	9.534	27.344	2.834
1.000	4.000	9.482	22.083	6.322	4.551	1.500	2.592	7.949	34.190	4.302
1.000	5.000	13.611	24.245	7.309	4.227	1.465	2.716	12.341	34.448	2.791
1.000	6.000	17.582	29.225	8.495	9.021	2.070	3.249	16.157	40.418	2.509
1.000	7.000	4.495	32.702	2.963	9.867	2.867	3.314	5.546	55.979	10.099
1.000	8.000	10.865	15.505	4.544	6.860	2.391	2.260	10.332	19.965	1.238
2.000	1.000	17.779	16.727	9.877	7.142	1.900	2.342	17.911	15.712	0.877
2.000	2.000	15.304	13.720	7.704	4.323	2.051	3.174	16.061	11.713	0.729
2.000	3.000	9.245	12.968	5.531	2.255	1.679	5.750	8.338	16.508	1.868
2.000	4.000	9.285	8.833	2.766	3.101	3.357	2.448	9.342	8.398	0.809
2.000	5.000	10.272	11.559	6.717	2.537	1.529	4.556	10.118	12.793	1.264
2.000	6.000	12.341	12.404	7.112	3.477	1.806	3.568	12.847	11.982	0.923
2.000	7.000	16.001	12.404	6.124	4.041	2.613	3.070	16.443	8.943	0.544
2.000	8.000	11.063	15.317	7.704	5.638	1.436	2.717	10.547	19.406	1.840
3.000	1.000	12.643	19.734	6.717	7.518	1.882	2.625	11.742	26.550	2.253
3.000	2.000	14.026	14.096	6.914	3.353	2.029	3.659	14.021	14.160	1.010
3.000	3.000	14.618	15.505	2.432	4.793	1.542	3.235	14.514	15.355	1.127
3.000	4.000	8.840	14.942	4.148	6.390	2.143	2.333	8.154	20.759	2.546
3.000	5.000	12.441	9.585	5.926	2.819	2.167	3.400	13.240	6.453	0.487
3.000	6.000	16.389	19.358	8.099	6.390	2.098	3.027	16.704	21.633	1.295
3.000	7.000	12.441	20.298	4.149	7.424	3.095	2.734	11.935	27.466	2.301
3.000	8.000	13.236	12.498	7.112	6.014	1.861	2.078	13.329	11.787	0.844

ALL STRENGTHS IN KN/M\*\*2

PARABOLIC STRESS DISTRIBUTION

TEST DEPTH	PEAK STRENGTH		REM	STRENGTH		SENSITIVITY		HORIZ	VERTICAL	R(=S)
	DIAMOND	H=20		DIAMOND	H=20	DIAMOND	H=20			
1.000	1.000	9.680	21.415	4.346	6.274	2.227	3.413	8.840	23.212	2.622
1.000	2.000	17.779	20.329	11.458	5.128	1.552	3.365	17.598	20.720	1.177
1.000	3.000	10.668	22.079	8.495	6.394	1.256	3.453	9.951	23.926	2.410
1.000	4.000	9.482	24.431	6.322	7.179	1.500	3.403	8.412	26.720	3.177
1.000	5.000	13.631	24.680	7.309	6.937	1.365	4.278	12.482	32.136	2.575
1.000	6.000	17.542	36.195	8.495	7.360	2.070	4.919	16.250	34.944	2.400
1.000	7.000	8.495	37.944	2.963	8.506	2.867	4.461	6.395	42.453	6.604
1.000	8.000	10.470	20.691	4.148	6.817	2.524	3.035	9.739	22.256	2.299
2.000	1.000	17.779	20.872	9.877	7.541	1.800	2.768	17.560	21.346	1.214
2.000	2.000	15.804	10.858	7.704	9.049	2.051	1.200	16.160	10.101	0.622
2.000	3.000	9.295	20.933	5.531	10.798	1.679	1.939	8.451	22.716	2.684
2.000	4.000	9.295	12.306	2.766	9.506	3.357	1.447	9.069	12.769	1.479
2.000	5.000	10.272	18.278	6.717	11.543	1.529	1.570	9.700	19.504	2.011
2.000	6.000	12.841	11.824	7.112	9.043	1.396	1.307	12.915	11.668	0.903
2.000	7.000	16.001	22.340	6.124	11.160	2.313	2.005	15.546	23.357	1.502
2.000	8.000	11.063	23.768	7.704	12.065	1.476	1.970	10.153	25.713	2.532
3.000	1.000	12.843	25.639	6.717	9.471	1.892	2.707	11.713	27.627	2.359
3.000	2.000	14.026	20.812	6.914	5.912	2.029	3.520	13.541	21.851	1.614
3.000	3.000	14.518	22.501	9.482	7.420	1.542	3.033	14.055	23.708	1.687
3.000	4.000	8.890	20.450	4.148	5.067	2.143	4.036	8.062	22.220	2.756
3.000	5.000	12.841	19.605	5.326	4.747	2.167	3.963	12.357	20.641	1.570
3.000	6.000	16.989	24.311	8.099	4.524	2.098	5.373	16.466	25.431	1.544
3.000	7.000	12.841	29.076	4.148	5.309	3.095	5.477	11.679	31.562	2.731
3.000	8.000	13.236	19.002	7.112	5.490	1.861	3.462	12.824	19.995	1.551

MALTBY LAGOON 6 OVERTIPPING PROJECT 13.9.78

4TH PAIR VANE TESTS, POSITIONS AB +DE

ALL STRENGTHS IN KN/M\*\*2

PARABOLIC STRESS DISTRIBUTION

TEST DEPTH	PEAK STRENGTH		REM	STRENGTH		SENSITIVITY		HORIZ	VERTICAL	R(=S)
	DIAMOND	H=20		DIAMOND	H=20	DIAMOND	H=20			
1.000	0.400	6.717	7.541	2.963	1.448	2.267	5.208	6.658	7.667	1.151
1.000	0.800	5.334	11.944	3.556	1.905	1.580	13.200	4.861	12.856	2.666
1.000	1.200	5.334	7.118	1.975	1.327	2.700	5.364	5.266	7.391	1.421
1.000	1.600	5.136	6.515	2.173	1.810	2.764	3.600	5.138	6.726	1.101
1.000	2.000	9.285	12.015	3.051	5.072	2.350	2.010	9.091	12.421	1.366
1.000	2.400	9.285	17.072	7.389	4.888	1.297	4.494	9.091	12.421	1.366
1.000	2.800	11.063	12.306	9.887	3.439	1.217	3.579	8.975	12.496	2.133
1.000	3.200	12.445	18.218	8.099	4.162	1.537	4.377	8.333	19.182	1.587
1.000	3.600	13.631	10.557	8.297	4.886	1.643	2.160	11.552	10.886	0.728
1.000	4.000	11.063	9.652	9.285	4.585	1.191	2.185	11.165	9.436	0.825
1.000	4.400	11.055	7.058	6.124	6.093	1.083	1.158	9.086	6.354	0.593
1.000	4.800	23.311	19.304	13.236	0.603	1.761	32.000	23.600	18.698	0.074
1.000	5.200	30.226	16.594	16.594	8.870	1.821	8.839	31.249	14.432	0.462
1.000	5.600	16.160	18.309	9.877	3.559	1.640	5.169	18.043	18.736	1.168
1.000	6.000	31.518	15.684	13.631	3.206	2.319	13.000	32.752	23.246	0.644
1.000	6.400	33.983	24.552	15.804	3.016	2.125	8.800	23.344	23.160	0.677
1.000	6.800	4.741	6.636	3.161	1.116	1.580	3.300	6.336	6.336	1.084
1.000	7.200	6.636	6.636	3.161	1.116	1.580	3.300	6.336	6.336	1.084
1.000	7.600	7.112	7.118	5.334	2.715	1.333	2.200	7.112	7.112	1.101
1.000	8.000	11.260	7.058	6.717	2.353	1.676	3.000	11.260	6.414	0.558
1.000	8.400	19.285	13.573	4.346	5.188	2.136	2.200	18.978	14.220	1.130
1.000	8.800	19.285	13.513	8.692	4.102	1.250	3.294	18.677	13.918	1.304
1.000	9.200	13.148	13.211	1.185	6.093	3.300	2.168	13.508	14.508	4.172
1.000	9.600	23.113	25.457	11.260	3.318	2.853	7.673	22.948	25.815	1.122
1.000	10.000	16.075	16.710	7.389	5.731	1.378	2.910	16.681	17.726	1.844
1.000	10.400	7.704	15.202	4.939	2.413	1.560	6.300	7.168	16.350	2.222
1.000	10.800	11.260	17.012	7.704	1.740	1.462	9.724	16.849	17.892	1.064
1.000	11.200	16.594	15.684	14.865	1.102	1.527	8.824	16.661	15.845	0.934
1.000	11.600	27.064	22.320	14.223	5.731	1.903	3.805	27.487	21.593	0.730
1.000	12.000	22.125	29.016	14.616	4.524	1.493	6.413	22.487	20.971	1.150
1.000	12.400	24.101	34.928	14.816	7.360	1.627	4.746	23.638	36.585	1.566
1.000	12.800	0.000	13.211	0.000	9.046	1.805	1.718	0.000	0.000	0.000
1.000	13.200	0.000	20.550	0.000	8.498	2.364	2.321	0.000	0.000	0.000
1.000	13.600	0.000	27.412	0.000	14.325	1.714	1.833	0.000	0.000	0.000
1.000	14.000	0.000	34.722	0.000	14.346	2.000	1.182	0.000	0.000	0.000
1.000	14.400	0.000	28.143	0.000	5.391	1.733	2.321	0.000	0.000	0.000
1.000	14.800	0.000	23.940	0.000	5.826	1.875	2.404	0.000	0.000	0.000
1.000	15.200	0.000	26.041	0.000	11.513	1.625	3.322	0.000	0.000	0.000
1.000	15.600	0.000	28.763	0.000	12.234	2.000	2.736	0.000	0.000	0.000
1.000	16.000	0.000	36.823	0.000	10.518	2.200	2.275	0.000	0.000	0.000
1.000	16.400	0.000	44.499	0.000	9.137	2.333	2.714	0.000	0.000	0.000
1.000	16.800	0.000	46.235	0.000	14.894	2.200	3.113	0.000	0.000	0.000
1.000	17.200	0.000	47.514	0.000	20.650	1.778	2.667	0.000	0.000	0.000

SILVERHILL LAGOON NO. 16

H=20 VANE TESTS, MAY 1979

ALL STRENGTHS IN KN/M\*\*2

PARABOLIC STRESS DISTRIBUTION

TEST DEPTH	PEAK STRENGTH	REM	STRENGTH	SENSITIVITY
	H=20	H=20	H=20	H=20
1.100	0.40	8.083	1.508	5.360
1.100	1.33	5.067	2.051	2.471
1.100	2.26	3.921	2.895	1.438
1.100	3.19	5.610	2.111	2.657
1.100	4.12	5.731	3.499	1.638
1.100	5.07	5.791	1.327	4.364
1.100	6.00	10.798	6.274	1.721
2.100	0.40	7.118	2.654	2.682
2.100	1.33	4.964	2.051	2.412
2.100	2.26	5.489	2.946	1.857
2.100	3.19	9.109	2.473	3.683
2.100	4.12	14.357	7.771	1.859
2.100	5.07	14.533	4.826	3.013
3.100	0.18	11.023	3.559	3.322
3.100	1.10	3.680	2.051	1.794
3.100	2.02	7.601	3.981	1.909
3.100	2.51	7.329	3.499	2.069
3.100	2.94	3.851	2.835	1.362
3.100	3.22	7.329	4.223	1.714
3.100	3.55	4.464	2.835	1.574
3.100	3.82	4.223	3.197	1.321
3.100	4.70	6.997	4.964	1.415
3.100	5.62	8.385	5.851	1.433

APPENDIX A.6.1 Laboratory consolidation data.

GEDLING TAILINGS LAGOON 12/8, SAMPLE X1

VERTICAL, HIGHER PRESSURE, 6" CELL

ANALYSIS OF CONSOLIDATION DATA

INITIAL MOISTURE CONTENT= 46.604  
 FINAL MOISTURE CONTENT = 31.408  
 INITIAL VOIDS RATIO = 0.933  
 NATURAL BULK DENSITY= 1.518  
 NATURAL DRY DENSITY= 1.036  
 FINAL BULK DENSITY= 1.541  
 FINAL DRY DENSITY= 1.173  
 SPECIFIC GRAVITY= 2.002

LOAD NO.	PRESSURE (KN/M**2)	VOIDS RATIO	STRAIN PERCENT	CV (M**2/YR)	MV (M**2/MN)	CC	K M/SEC
1	37.5	0.863	-3.619	12.591	0.965	0.000	3.77E-09
2	75.0	0.854	-4.081	19.874	0.128	-0.030	7.97E-10
3	150.0	0.778	-8.025	16.395	0.548	-0.253	2.89E-09
4	300.0	0.712	-11.405	30.764	0.245	-0.217	2.34E-09
5	600.0	0.658	-14.242	16.033	0.107	-0.182	5.30E-10
6	1200.0	0.601	-17.187	24.319	0.057	-0.189	4.31E-10
7	120.0	0.628	-15.785	0.000	0.016	-0.027	0.00E+00
8	12.0	0.670	-13.584	0.000	0.242	-0.043	0.00E+00
9	0.0	0.707	-11.704	0.000	1.813	0.000	0.00E+00

GEDLING 12/8 TAILINGS LAGOON SAMPLE PR1 JANUARY 1977

VERTICAL DRAINAGE, 6 INCH ROWE CELL

ANALYSIS OF CONSOLIDATION DATA

INITIAL MOISTURE CONTENT= 47.777  
 FINAL MOISTURE CONTENT = 31.573  
 INITIAL VOIDS RATIO = 0.956  
 NATURAL BULK DENSITY= 1.512  
 NATURAL DRY DENSITY= 1.023  
 FINAL BULK DENSITY= 1.597  
 FINAL DRY DENSITY= 1.214  
 SPECIFIC GRAVITY= 2.002

LOAD NO.	PRESSURE (KN/M**2)	VOIDS RATIO	STRAIN PERCENT	CV (M**2/YR)	MV (M**2/MN)	CC	K M/SEC
1	10.0	0.954	-5.214	13.215	5.214	0.000	2.14E-08
2	20.0	0.797	-8.166	30.351	3.115	-0.192	2.93E-08
3	40.0	0.749	-10.621	14.413	1.337	-0.160	5.97E-09
4	80.0	0.692	-13.499	18.721	0.805	-0.197	4.67E-09
5	160.0	0.649	-15.728	17.126	0.322	-0.145	1.71E-09
6	320.0	0.597	-18.347	12.903	0.194	-0.170	7.77E-10
7	110.0	0.603	-18.067	0.000	0.016	-0.012	0.00E+00
8	40.0	0.615	-17.467	0.000	0.105	-0.027	0.00E+00
9	0.0	0.649	-15.707	0.000	0.533	0.000	0.00E+00

GEDLING 12/8 TAILINGS LAGOON SAMPLE PR2 JANUARY 1977

VERTICAL DRAINAGE 10 INCH CELL

ANALYSIS OF CONSOLIDATION DATA

INITIAL MOISTURE CONTENT= 52.458  
 FINAL MOISTURE CONTENT = 32.854  
 INITIAL VOIDS RATIO = 1.050  
 NATURAL BULK DENSITY= 1.489  
 NATURAL DRY DENSITY= 0.976  
 FINAL BULK DENSITY= 1.510  
 FINAL DRY DENSITY= 1.129  
 SPECIFIC GRAVITY= 2.002

LOAD NO.	PRESSURE (KN/M**2)	VOIDS RATIO	STRAIN PERCENT	CV (M**2/YR)	MV (M**2/MN)	CC	K M/SEC
1	10.0	0.999	-2.546	15.204	2.546	0.000	1.20E-08
2	20.0	0.876	-8.503	19.951	2.039	-0.203	1.26E-08
3	40.0	0.841	-10.204	29.555	0.465	-0.116	4.26E-09
4	80.0	0.789	-12.750	17.516	0.354	-0.173	1.92E-09
5	160.0	0.727	-15.790	18.673	0.217	-0.206	1.12E-09
6	320.0	0.673	-18.244	0.000	0.030	-0.024	0.00E+00
7	110.0	0.737	-15.244	0.000	0.122	-0.034	0.00E+00
8	40.0	0.752	-14.523	0.000	0.242	0.000	0.00E+00
9	0.0	0.775	-13.420	0.000	0.323	0.000	0.00E+00

GEDLING 12/8 TAILINGS LAGOON SAMPLE PR3 FEBRUARY 1977

RADIAL DRAINAGE 6 INCH ROWE CELL

ANALYSIS OF CONSOLIDATION DATA

INITIAL MOISTURE CONTENT= 41.104  
 FINAL MOISTURE CONTENT = 34.603  
 INITIAL VOIDS RATIO = 0.835  
 NATURAL BULK DENSITY= 1.562  
 NATURAL DRY DENSITY= 1.107  
 FINAL BULK DENSITY= 1.712  
 FINAL DRY DENSITY= 1.272  
 SPECIFIC GRAVITY= 2.031

LOAD NO.	PRESSURE (KN/M**2)	VOIDS RATIO	STRAIN PERCENT	CV (M**2/YR)	MV (M**2/MN)	CC	K M/SEC
1	10.0	0.985	-9.120	160.677	8.120	0.000	4.04E-07
2	20.0	0.665	-9.242	13.054	1.221	-0.068	4.94E-09
3	40.0	0.635	-10.809	16.810	0.919	-0.102	4.79E-09
4	80.0	0.600	-12.820	13.054	0.536	-0.116	2.17E-09
5	160.0	0.544	-15.355	12.690	0.437	-0.136	1.72E-09
6	320.0	0.481	-19.292	16.541	0.255	-0.209	1.31E-09
7	110.0	0.491	-18.754	0.000	0.032	-0.021	0.00E+00
8	40.0	0.510	-17.354	0.000	0.246	-0.058	0.00E+00
9	0.0	0.597	-12.959	0.000	1.329	0.000	0.00E+00

GEDLING 12/8 TAILINGS LAGOON SAMPLE PR 4 FEBRUARY 1977  
 RADIAL DRAINAGE 10 INCH ROWE CELL  
 ANALYSIS OF CONSOLIDATION DATA

INITIAL MOISTURE CONTENT= 58.885  
 FINAL MOISTURE CONTENT = 32.570  
 INITIAL VOIDS RATIO = 1.179  
 NATURAL BULK DENSITY= 1.460  
 NATURAL DRY DENSITY= 0.919  
 FINAL BULK DENSITY= 1.571  
 FINAL DRY DENSITY= 1.185  
 SPECIFIC GRAVITY= 2.002

LOAD NO.	PRESSURE (KN/M**2)	VOIDS RATIO	STRAIN PERCENT	CV (M**2/YR)	MV (M**2/MN)	CC	K M/SEC
1	10.0	0.079	-4.560	485.309	4.560	0.000	6.86E-07
2	20.0	0.918	-11.985	53.923	7.779	-0.537	1.30E-07
3	40.0	0.830	-16.018	13.491	2.291	-0.292	9.58E-09
4	80.0	0.792	-17.763	13.728	0.519	-0.126	2.21E-09
5	160.0	0.732	-20.522	13.007	0.419	-0.200	1.69E-09
6	320.0	0.674	-23.145	16.116	0.206	-0.190	1.03E-09
7	110.0	0.686	-22.630	0.000	0.032	-0.024	0.00E+00
8	40.0	0.689	-22.492	0.000	0.026	-0.007	0.00E+00
9	0.0	0.689	-22.489	0.000	0.001	0.000	0.00E+00

GEDLING LAGOON 12/8, JMK3  
 VERTICAL DRAINAGE, 6" ROWE CELL  
 ANALYSIS OF CONSOLIDATION DATA

INITIAL MOISTURE CONTENT= 41.910  
 FINAL MOISTURE CONTENT = 34.535  
 INITIAL VOIDS RATIO = 0.839  
 NATURAL BULK DENSITY= 1.545  
 NATURAL DRY DENSITY= 1.088  
 FINAL BULK DENSITY= 1.584  
 FINAL DRY DENSITY= 1.178  
 SPECIFIC GRAVITY= 2.002

LOAD NO.	PRESSURE (KN/M**2)	VOIDS RATIO	STRAIN PERCENT	CV (M**2/YR)	MV (M**2/MN)	CC	K M/SEC
1	10.0	0.813	-1.413	205.781	1.413	0.000	9.02E-08
2	20.0	0.794	-2.457	13.225	1.054	-0.064	4.34E-09
3	40.0	0.767	-3.909	27.513	0.744	-0.089	6.35E-09
4	80.0	0.728	-6.031	23.829	0.552	-0.130	4.08E-09
5	160.0	0.684	-8.410	12.227	0.317	-0.145	1.20E-09
6	320.0	0.627	-11.495	12.035	0.210	-0.199	7.85E-10
7	110.0	0.642	-10.709	0.000	0.042	-0.031	0.00E+00
8	40.0	0.644	-10.594	0.000	0.018	-0.005	0.00E+00
9	10.0	0.665	-9.439	0.000	0.431	-0.035	0.00E+00
10	0.0	0.700	-7.579	0.000	2.054	0.000	0.00E+00

GEDLING LAGOON 12/8, JMK4  
 VERTICAL DRAINAGE, 10" ROWE CELL  
 ANALYSIS OF CONSOLIDATION DATA

INITIAL MOISTURE CONTENT= 45.106  
 FINAL MOISTURE CONTENT = 33.693  
 INITIAL VOIDS RATIO = 0.903  
 NATURAL BULK DENSITY= 1.526  
 NATURAL DRY DENSITY= 1.052  
 FINAL BULK DENSITY= 1.519  
 FINAL DRY DENSITY= 1.136  
 SPECIFIC GRAVITY= 2.002

LOAD NO.	PRESSURE (KN/M**2)	VOIDS RATIO	STRAIN PERCENT	CV (M**2/YR)	MV (M**2/MN)	CC	K M/SEC
1	10.0	0.896	-0.379	73.221	0.379	0.000	8.59E-09
2	20.0	0.954	-2.549	47.111	2.179	-0.137	3.18E-08
3	40.0	0.836	-3.522	71.291	0.499	-0.061	1.10E-08
4	80.0	0.804	-5.204	85.906	0.436	-0.106	1.16E-08
5	160.0	0.762	-7.419	32.204	0.292	-0.140	2.91E-09
6	320.0	0.703	-10.521	31.769	0.209	-0.136	2.06E-09
7	110.0	0.710	-10.116	0.000	0.022	-0.017	0.00E+00
8	40.0	0.729	-9.136	0.000	0.156	-0.042	0.00E+00
9	10.0	0.736	-8.748	0.000	0.142	0.000	0.00E+00

GEDLING TAILINGS LAGOON 12/8, JMK 7  
 VERTICAL LONG TERM, 6" ROWE CELL  
 ANALYSIS OF CONSOLIDATION DATA

INITIAL MOISTURE CONTENT= 41.357  
 FINAL MOISTURE CONTENT = 33.481  
 INITIAL VOIDS RATIO = 0.829  
 NATURAL BULK DENSITY= 1.548  
 NATURAL DRY DENSITY= 1.095  
 FINAL BULK DENSITY= 1.502  
 FINAL DRY DENSITY= 1.125  
 SPECIFIC GRAVITY= 2.002

LOAD NO.	PRESSURE (KN/M**2)	VOIDS RATIO	STRAIN PERCENT	CV (M**2/YR)	MV (M**2/MN)	CC	K M/SEC
1	10.0	0.823	-0.244	4695.023	0.244	0.000	3.55E-07
2	20.0	0.821	-0.347	1415.318	0.103	-0.006	4.51E-08
3	40.0	0.814	-0.704	102.845	0.210	-0.025	6.62E-09
4	80.0	0.802	-1.403	77.113	0.162	-0.039	3.88E-09
5	160.0	0.773	-2.395	24.233	0.138	-0.090	1.42E-09
6	320.0	0.739	-4.353	22.476	0.127	-0.120	8.95E-10
7	110.0	0.746	-4.477	0.000	0.020	-0.015	0.00E+00
8	40.0	0.757	-3.903	0.000	0.036	-0.024	0.00E+00
9	10.0	0.763	-3.393	0.000	0.242	-0.021	0.00E+00
10	0.0	0.779	-2.585	0.000	0.534	0.000	0.00E+00

GEDLING TAILINGS LAGOON 12/8, JMK 8  
 VERTICAL LONG TERM, 10" ROWE CELL  
 ANALYSIS OF CONSOLIDATION DATA

INITIAL MOISTURE CONTENT= 46.248  
 FINAL MOISTURE CONTENT = 33.631  
 INITIAL VOIDS RATIO = 0.926  
 NATURAL BULK DENSITY= 1.520  
 NATURAL DRY DENSITY= 1.039  
 FINAL BULK DENSITY= 1.547  
 FINAL DRY DENSITY= 1.158  
 SPECIFIC GRAVITY= 2.002

LOAD NO.	PRESSURE (KN/M**2)	VOIDS RATIO	STRAIN PERCENT	CV (M**2/YR)	MV (M**2/MN)	CC	K M/SEC
1	10.0	0.929	0.164	0.000	-0.164	0.000	0.00E+00
2	20.0	0.922	-0.169	30.697	0.332	-0.021	3.16E-09
3	40.0	0.906	-1.039	31.580	0.436	-0.056	4.27E-09
4	80.0	0.873	-2.750	27.318	0.432	-0.109	3.66E-09
5	160.0	0.825	-5.232	30.075	0.319	-0.159	2.97E-09
6	320.0	0.722	-10.596	26.032	0.354	-0.343	2.86E-09
7	110.0	0.729	-10.232	0.000	0.015	-0.015	0.00E+00
8	40.0	0.743	-9.570	0.000	0.117	-0.032	0.00E+00
9	10.0	0.755	-8.849	0.000	0.240	-0.021	0.00E+00
10	0.0	0.768	-8.179	0.000	0.735	0.000	0.00E+00

GEDLING TAILINGS LAGOON 12/8, JMK 9  
 VERTICAL, OEDOMETER  
 ANALYSIS OF CONSOLIDATION DATA

INITIAL MOISTURE CONTENT= 48.941  
 FINAL MOISTURE CONTENT = 34.313  
 INITIAL VOIDS RATIO = 0.980  
 NATURAL BULK DENSITY= 1.506  
 NATURAL DRY DENSITY= 1.011  
 FINAL BULK DENSITY= 1.471  
 FINAL DRY DENSITY= 1.095  
 SPECIFIC GRAVITY= 2.002

LOAD NO.	PRESSURE (KN/M**2)	VOIDS RATIO	STRAIN PERCENT	CV (M**2/YR)	MV (M**2/MN)	CC	K M/SEC
1	9.8	0.969	-0.579	16.133	0.589	0.000	2.95E-09
2	19.6	0.953	-1.335	15.045	0.777	-0.050	3.62E-09
3	39.2	0.927	-2.680	39.436	0.695	-0.088	8.50E-09
4	78.5	0.885	-4.783	19.169	0.551	-0.138	1.32E-09
5	158.0	0.824	-7.851	15.091	0.405	-0.200	1.90E-09
6	319.7	0.752	-11.478	25.953	0.243	-0.235	1.76E-09
7	93.2	0.765	-10.863	0.000	0.031	-0.023	0.00E+00
8	39.2	0.778	-10.181	0.000	0.142	-0.036	0.00E+00
9	9.8	0.800	-9.064	0.000	0.423	-0.037	0.00E+00
10	0.0	0.828	-7.662	0.000	1.572	0.000	0.00E+00

GEDLING TAILINGS LAGOON 12/8, JMK 10  
 VERTICAL, OEDOMETER  
 ANALYSIS OF CONSOLIDATION DATA

INITIAL MOISTURE CONTENT= 42.345  
 FINAL MOISTURE CONTENT = 32.829  
 INITIAL VOIDS RATIO = 0.840  
 NATURAL BULK DENSITY= 1.542  
 NATURAL DRY DENSITY= 1.083  
 FINAL BULK DENSITY= 1.564  
 FINAL DRY DENSITY= 1.177  
 SPECIFIC GRAVITY= 2.002

LOAD NO.	PRESSURE (KN/M**2)	VOIDS RATIO	STRAIN PERCENT	CV (M**2/YR)	MV (M**2/MN)	CC	K M/SEC
1	9.8	0.820	-1.518	16.927	1.548	0.000	8.12E-09
2	19.6	0.804	-2.337	22.500	0.848	-0.050	5.91E-09
3	39.2	0.783	-3.469	25.318	0.591	-0.059	4.64E-09
4	78.5	0.749	-5.356	18.736	0.498	-0.116	2.92E-09
5	159.9	0.699	-8.015	20.370	0.345	-0.159	2.18E-09
6	319.7	0.640	-11.217	19.110	0.218	-0.177	1.29E-09
7	93.2	0.652	-10.601	0.000	0.031	-0.021	0.00E+00
8	39.2	0.663	-10.012	0.000	0.122	-0.029	0.00E+00
9	9.8	0.681	-9.000	0.000	0.382	-0.031	0.00E+00
10	0.0	0.700	-7.978	0.000	1.145	0.000	0.00E+00

GEDLING TAILINGS LAGOON 12/8, SAMPLE JMK 11  
 RADIAL DRAINAGE, LONG TERM, 6" ROWE CELL  
 ANALYSIS OF CONSOLIDATION DATA

INITIAL MOISTURE CONTENT= 49.760  
 FINAL MOISTURE CONTENT = 35.784  
 INITIAL VOIDS RATIO = 0.996  
 NATURAL BULK DENSITY= 1.502  
 NATURAL DRY DENSITY= 1.003  
 FINAL BULK DENSITY= 1.552  
 FINAL DRY DENSITY= 1.143  
 SPECIFIC GRAVITY= 2.002

LOAD NO.	PRESSURE (KN/M**2)	VOIDS RATIO	STRAIN PERCENT	CV (M**2/YR)	MV (M**2/MN)	CC	K M/SEC
1	10.0	0.995	-0.042	964.192	0.042	0.000	1.26E-08
2	20.0	0.929	-3.362	10.912	3.321	-0.220	1.12E-09
3	40.0	0.882	-5.704	38.568	1.212	-0.155	1.48E-09
4	80.0	0.832	-8.237	35.658	0.671	-0.168	7.42E-09
5	150.0	0.770	-11.307	27.837	0.418	-0.204	3.52E-09
6	320.0	0.694	-15.125	27.937	0.269	-0.253	2.33E-09
7	110.0	0.701	-14.795	0.000	0.019	-0.014	0.00E+00
8	40.0	0.712	-14.233	0.000	0.094	-0.026	0.00E+00
9	10.0	0.735	-13.095	0.000	0.442	-0.038	0.00E+00
10	0.0	0.751	-12.262	0.000	0.958	0.000	0.00E+00

GEDLING TAILINGS LAGOON 12/8. SAMPLE JMK 12  
 RADIAL DRAINAGE, LONG TERM, 10" ROWE CELL  
 ANALYSIS OF CONSOLIDATION DATA

INITIAL MOISTURE CONTENT= 57.944  
 FINAL MOISTURE CONTENT = 36.110  
 INITIAL VOIDS RATIO = 1.160  
 NATURAL BULK DENSITY= 1.464  
 NATURAL DRY DENSITY= 0.927  
 FINAL BULK DENSITY= 1.471  
 FINAL DRY DENSITY= 1.081  
 SPECIFIC GRAVITY= 2.002

LOAD NO.	PRESSURE (KN/M**2)	VOIDS RATIO	STRAIN PERCENT	CV (M**2/YR)	MV (M**2/MN)	CC	K M/SEC
1	10.0	1.160	0.000	0.030	0.000	0.030	0.00E+00
2	20.0	1.012	-6.827	49.172	6.827	-0.490	1.04E-07
3	40.0	0.976	-8.529	62.212	0.912	-0.122	1.75E-08
4	80.0	0.932	-10.566	81.222	0.557	-0.146	1.40E-08
5	160.0	0.867	-13.576	37.198	0.421	-0.216	4.85E-09
6	320.0	0.789	-17.161	20.098	0.259	-0.257	1.62E-05
7	110.0	0.796	-16.861	0.000	0.017	-0.014	0.00E+00
8	40.0	0.814	-15.929	0.000	0.148	-0.042	0.00E+00
9	10.0	0.833	-15.134	0.000	0.343	-0.031	0.00E+00
10	0.0	0.852	-14.269	0.000	1.020	0.030	0.00E+00

GEDLING TAILINGS LAGOON 12/8. SAMPLE JMK 13  
 VERTICAL DRAINAGE, LONG TERM, OEDOMETER  
 ANALYSIS OF CONSOLIDATION DATA

INITIAL MOISTURE CONTENT= 49.240  
 FINAL MOISTURE CONTENT = 34.577  
 INITIAL VOIDS RATIO = 0.986  
 NATURAL BULK DENSITY= 1.504  
 NATURAL DRY DENSITY= 1.008  
 FINAL BULK DENSITY= 1.525  
 FINAL DRY DENSITY= 1.133  
 SPECIFIC GRAVITY= 2.002

LOAD NO.	PRESSURE (KN/M**2)	VOIDS RATIO	STRAIN PERCENT	CV (M**2/YR)	MV (M**2/MN)	CC	K M/SEC
1	5.8	0.931	-2.747	11.803	2.801	0.030	1.02E-08
2	19.6	0.899	-4.344	7.364	1.675	-0.105	3.82E-09
3	39.2	0.859	-6.361	10.370	1.075	-0.133	3.46E-09
4	78.5	0.801	-9.291	5.393	0.798	-0.193	2.32E-09
5	156.9	0.765	-11.098	9.786	0.254	-0.119	7.70E-10
6	318.7	0.702	-14.301	7.080	0.223	-0.207	4.89E-10
7	109.8	0.709	-13.927	0.000	0.021	-0.016	0.00E+00
8	39.2	0.721	-13.343	0.000	0.096	-0.026	0.00E+00
9	0.0	0.767	-11.016	0.000	0.685	0.000	0.00E+00

GEDLING TAILINGS LAGOON 12/8. SAMPLE JMK 14  
 VERTICAL DRAINAGE, LONG TERM, OEDOMETER  
 ANALYSIS OF CONSOLIDATION DATA

INITIAL MOISTURE CONTENT= 53.800  
 FINAL MOISTURE CONTENT = 35.300  
 INITIAL VOIDS RATIO = 1.077  
 NATURAL BULK DENSITY= 1.482  
 NATURAL DRY DENSITY= 0.964  
 FINAL BULK DENSITY= 1.505  
 FINAL DRY DENSITY= 1.112  
 SPECIFIC GRAVITY= 2.002

LOAD NO.	PRESSURE (KN/M**2)	VOIDS RATIO	STRAIN PERCENT	CV (M**2/YR)	MV (M**2/MN)	CC	K M/SEC
1	9.8	0.992	-4.099	4.152	4.180	0.300	5.38E-09
2	19.6	0.944	-6.419	7.493	2.466	-0.160	5.73E-09
3	39.2	0.900	-8.524	9.046	1.147	-0.145	3.22E-09
4	78.5	0.855	-10.706	6.341	0.608	-0.151	1.20E-09
5	156.9	0.797	-13.453	11.194	0.392	-0.130	1.36E-09
6	318.7	0.727	-16.842	10.954	0.242	-0.229	8.22E-10
7	109.8	0.737	-16.380	0.000	0.027	-0.021	0.00E+00
8	39.2	0.750	-15.730	0.000	0.110	-0.030	0.00E+00
9	0.0	0.800	-13.351	0.000	0.720	0.000	0.00E+00

GEDLING TAILINGS LAGOON, 12/8, SAMPLE JMK 17  
 VERTICAL, OEDOMETER, HIGH PRESSURE  
 ANALYSIS OF CONSOLIDATION DATA

INITIAL MOISTURE CONTENT= 54.283  
 FINAL MOISTURE CONTENT = 28.496  
 INITIAL VOIDS RATIO = 1.087  
 NATURAL BULK DENSITY= 1.490  
 NATURAL DRY DENSITY= 0.959  
 FINAL BULK DENSITY= 1.548  
 FINAL DRY DENSITY= 1.204  
 SPECIFIC GRAVITY= 2.002

LOAD NO.	PRESSURE (KN/M**2)	VOIDS RATIO	STRAIN PERCENT	CV (M**2/YR)	MV (M**2/MN)	CC	K M/SEC
1	10.0	0.746	-0.745	7.355	6.745	0.000	1.54E-08
2	25.0	0.891	-9.379	16.111	1.883	-0.138	9.40E-09
3	49.0	0.851	-11.090	19.395	0.879	-0.136	5.28E-09
4	98.0	0.803	-13.044	16.384	0.528	-0.159	2.68E-09
5	196.0	0.750	-16.116	37.005	0.289	-0.175	3.43E-09
6	392.0	0.691	-19.035	14.535	0.172	-0.135	7.73E-10
7	784.0	0.629	-21.935	10.946	0.094	-0.208	5.84E-10
8	1568.0	0.564	-25.028	16.079	0.050	-0.214	2.51E-10
9	392.0	0.579	-24.306	0.000	0.008	-0.025	0.00E+00
10	98.0	0.600	-23.303	0.000	0.045	-0.035	0.00E+00
11	0.0	0.662	-20.355	0.000	0.392	0.000	0.00E+00



GEDLING TAILINGS LAGOON, 12/8, SAMPLE JMK 18  
VERTICAL, CEDDMETER, HIGH PRESSURE  
ANALYSIS OF CONSOLIDATION DATA

INITIAL MOISTURE CONTENT= 60.954  
FINAL MOISTURE CONTENT = 28.604  
INITIAL VOIDS RATIO = 1.220  
NATURAL BULK DENSITY= 1.451  
NATURAL DRY DENSITY= 0.902  
FINAL BULK DENSITY= 1.475  
FINAL DRY DENSITY= 1.147  
SPECIFIC GRAVITY= 2.002

LOAD NO.	PRESSURE (KN/M**2)	VOIDS RATIO	STRAIN PERCENT	CV (M**2/YR)	MV (M**2/MN)	CC	K M/SEC
1	10.0	1.102	-5.336	12.195	5.336	0.000	2.02E-08
2	25.0	1.044	-7.926	19.542	1.824	-0.144	1.11E-08
3	49.0	0.998	-10.011	21.078	0.943	-0.158	6.15E-09
4	98.0	0.935	-12.857	18.761	0.645	-0.210	3.75E-09
5	196.0	0.869	-15.819	21.237	0.347	-0.218	2.28E-09
6	392.0	0.810	-18.474	19.867	0.161	-0.196	9.91E-10
7	784.0	0.740	-21.627	21.236	0.099	-0.232	6.49E-10
8	1568.0	0.667	-24.903	31.688	0.053	-0.241	5.23E-10
9	392.0	0.682	-24.216	0.000	0.008	-0.025	0.00E+00
10	98.0	0.701	-23.354	0.000	0.038	-0.031	0.00E+00
11	0.0	0.745	-21.403	0.000	0.261	0.000	0.00E+00

GEDLING TAILINGS LAGOON 12/8, SAMPLE JMK 19  
VERTICAL, LONG TERM, 6" CELL  
ANALYSIS OF CONSOLIDATION DATA

INITIAL MOISTURE CONTENT= 69.155  
FINAL MOISTURE CONTENT = 33.793  
INITIAL VOIDS RATIO = 1.384  
NATURAL BULK DENSITY= 1.420  
NATURAL DRY DENSITY= 0.840  
FINAL BULK DENSITY= 1.412  
FINAL DRY DENSITY= 1.056  
SPECIFIC GRAVITY= 2.002

LOAD NO.	PRESSURE (KN/M**2)	VOIDS RATIO	STRAIN PERCENT	CV (M**2/YR)	MV (M**2/MN)	CC	K M/SEC
1	10.0	1.165	-9.188	30.659	9.188	0.000	8.73E-08
2	20.0	1.090	-12.345	54.249	3.476	-0.250	5.84E-08
3	40.0	1.032	-14.767	39.636	1.382	-0.192	1.70E-08
4	80.0	0.958	-17.884	19.161	0.914	-0.247	5.43E-09
5	160.0	0.857	-22.122	23.727	0.645	-0.336	4.75E-09
6	320.0	0.767	-25.901	13.094	0.303	-0.299	1.23E-09
7	110.0	0.777	-25.469	0.000	0.028	-0.022	0.00E+00
8	40.0	0.807	-24.189	0.000	0.245	-0.069	0.00E+00
9	10.0	0.953	-22.299	0.000	0.331	-0.075	0.00E+00
10	0.0	0.896	-20.465	0.000	2.359	0.000	0.00E+00

GEDLING TAILINGS LAGOON 12/8, SAMPLE JMK 20  
VERTICAL, LONG TERM, 10" CELL  
ANALYSIS OF CONSOLIDATION DATA

INITIAL MOISTURE CONTENT= 57.722  
FINAL MOISTURE CONTENT = 33.545  
INITIAL VOIDS RATIO = 1.155  
NATURAL BULK DENSITY= 1.465  
NATURAL DRY DENSITY= 0.929  
FINAL BULK DENSITY= 1.539  
FINAL DRY DENSITY= 1.152  
SPECIFIC GRAVITY= 2.002

LOAD NO.	PRESSURE (KN/M**2)	VOIDS RATIO	STRAIN PERCENT	CV (M**2/YR)	MV (M**2/MN)	CC	K M/SEC
1	1.0	1.047	-5.041	2970.756	50.411	0.000	4.64E-05
2	10.0	0.989	-7.735	390.134	3.152	-0.058	3.31E-07
3	20.0	0.907	-11.510	6.077	4.092	-0.270	7.71E-09
4	40.0	0.865	-13.492	20.906	1.120	-0.142	7.22E-09
5	80.0	0.817	-15.602	31.565	0.636	-0.157	6.22E-09
6	160.0	0.763	-18.199	27.226	0.372	-0.180	3.14E-09
7	320.0	0.691	-21.537	23.978	0.256	-0.239	1.90E-09
8	110.0	0.703	-21.005	0.000	0.032	-0.025	0.00E+00
9	40.0	0.719	-20.226	0.000	0.141	-0.038	0.00E+00
10	10.0	0.728	-19.832	0.000	0.165	-0.014	0.00E+00
11	0.0	0.737	-19.405	0.000	0.533	0.000	0.00E+00

EAST HETTON LAGOON 109A, BEACH FINE  
VERTICAL OEDOMETER  
ANALYSIS OF CONSOLIDATION DATA

INITIAL MOISTURE CONTENT= 43.953  
FINAL MOISTURE CONTENT = 30.302  
INITIAL VOIDS RATIO = 1.119  
NATURAL BULK DENSITY= 1.730  
NATURAL DRY DENSITY= 1.201  
FINAL BULK DENSITY= 1.873  
FINAL DRY DENSITY= 1.437  
SPECIFIC GRAVITY= 2.546

LOAD NO.	PRESSURE (KN/M**2)	VOIDS RATIO	STRAIN PERCENT	CV (M**2/YR)	MV (M**2/MN)	CC	K M/SEC
1	9.8	1.083	-1.709	5.642	1.744	0.000	3.05E-09
2	19.6	1.034	-3.994	5.417	2.372	-0.151	3.92E-09
3	49.0	0.943	-8.323	2.579	1.534	-0.230	1.23E-09
4	98.0	0.855	-12.447	3.201	0.918	-0.290	9.11E-10
5	196.0	0.756	-17.128	3.663	0.546	-0.330	6.20E-10
6	392.0	0.645	-22.348	3.957	0.321	-0.367	3.94E-10
7	198.0	0.651	-22.107	0.000	0.016	-0.017	0.00E+00
8	9.8	0.724	-18.633	0.000	0.237	-0.056	0.00E+00
9	0.0	0.771	-16.404	0.000	2.796	0.000	0.00E+00

EAST HETTON LAGOON 109A, BEACH COARSE  
VERTICAL OEDOMETER  
ANALYSIS OF CONSOLIDATION DATA

INITIAL MOISTURE CONTENT= 30.450  
FINAL MOISTURE CONTENT = 22.821  
INITIAL VOIDS RATIO = 0.777  
NATURAL BULK DENSITY= 1.873  
NATURAL DRY DENSITY= 1.436  
FINAL BULK DENSITY= 1.942  
FINAL DRY DENSITY= 1.581  
SPECIFIC GRAVITY= 2.551

LOAD NO.	PRESSURE (KN/M**2)	VOIDS RATIO	STRAIN PERCENT	CV (M**2/YR)	MV (M**2/MN)	CC	K M/SEC
1	9.8	0.762	-0.858	423.803	0.875	0.000	1.15E-07
2	19.6	0.745	-1.766	416.321	0.935	-0.054	1.21E-07
3	49.0	0.719	-3.229	406.377	0.507	-0.065	6.38E-08
4	98.0	0.686	-5.096	594.732	0.394	-0.110	3.26E-08
5	196.0	0.653	-6.963	571.788	0.201	-0.110	3.56E-08
6	392.0	0.581	-10.999	536.433	0.221	-0.238	3.68E-08
7	98.0	0.587	-10.695	0.000	0.012	-0.009	0.00E+00
8	9.8	0.597	-9.091	0.000	0.077	-0.011	0.00E+00
9	0.0	0.614	-9.183	0.000	1.031	0.000	0.00E+00

EAST HETTON LOCATION C, FINE  
VERTICAL OEDOMETER  
ANALYSIS OF CONSOLIDATION DATA

INITIAL MOISTURE CONTENT= 37.036  
FINAL MOISTURE CONTENT = 32.928  
INITIAL VOIDS RATIO = 0.787  
NATURAL BULK DENSITY= 1.629  
NATURAL DRY DENSITY= 1.189  
FINAL BULK DENSITY= 1.669  
FINAL DRY DENSITY= 1.255  
SPECIFIC GRAVITY= 2.124

LOAD NO.	PRESSURE (KN/M**2)	VOIDS RATIO	STRAIN PERCENT	CV (M**2/YR)	MV (M**2/MN)	CC	K M/SEC
1	9.8	0.774	-0.710	6.295	0.725	0.000	1.41E-09
2	19.6	0.762	-1.373	8.450	0.681	-0.039	1.78E-09
3	49.0	0.733	-2.983	7.610	0.555	-0.072	1.31E-09
4	98.0	0.702	-4.735	9.075	0.369	-0.104	1.04E-09
5	196.0	0.659	-7.150	9.085	0.259	-0.143	7.28E-10
6	392.0	0.605	-10.190	9.402	0.167	-0.180	4.85E-10
7	9.8	0.663	-6.913	0.000	0.095	-0.036	0.00E+00
8	0.0	0.692	-5.303	0.000	1.765	0.000	0.00E+00

EAST HETTON LOCATION C, COARSE  
VERTICAL OEDOMETER  
ANALYSIS OF CONSOLIDATION DATA

INITIAL MOISTURE CONTENT= 57.452  
FINAL MOISTURE CONTENT = 48.971  
INITIAL VOIDS RATIO = 0.799  
NATURAL BULK DENSITY= 1.217  
NATURAL DRY DENSITY= 0.773  
FINAL BULK DENSITY= 1.270  
FINAL DRY DENSITY= 0.853  
SPECIFIC GRAVITY= 1.390

LOAD NO.	PRESSURE (KN/M**2)	VOIDS RATIO	STRAIN PERCENT	CV (M**2/YR)	MV (M**2/MN)	CC	K M/SEC
1	9.8	0.780	-1.054	1080.009	1.075	0.000	3.57E-07
2	19.6	0.756	-2.380	1034.891	1.367	-0.079	4.35E-07
3	49.0	0.729	-3.932	1004.006	0.541	-0.070	1.68E-07
4	98.0	0.698	-5.509	971.578	0.356	-0.100	1.07E-07
5	196.0	0.657	-7.898	931.536	0.247	-0.137	7.15E-08
6	392.0	0.609	-10.595	882.392	0.149	-0.151	4.09E-08
7	9.8	0.625	-9.666	0.000	0.027	-0.010	0.00E+00
8	0.0	0.630	-9.349	0.000	0.358	0.000	0.00E+00

EAST HETTON, LOCATION B, FINE  
VERTICAL DRAINAGE, OEDOMETER  
ANALYSIS OF CONSOLIDATION DATA

INITIAL MOISTURE CONTENT= 71.851  
FINAL MOISTURE CONTENT = 38.997  
INITIAL VOIDS RATIO = 1.365  
NATURAL BULK DENSITY= 1.381  
NATURAL DRY DENSITY= 0.803  
FINAL BULK DENSITY= 1.303  
FINAL DRY DENSITY= 0.935  
SPECIFIC GRAVITY= 1.900

LOAD NO.	PRESSURE (KN/M**2)	VOIDS RATIO	STRAIN PERCENT	CV (M**2/YR)	MV (M**2/MN)	CC	K M/SEC
1	9.8	1.325	-1.714	8.393	1.749	0.000	4.55E-09
2	19.6	1.301	-2.715	8.165	1.040	-0.079	2.63E-09
3	98.0	1.164	-8.489	8.230	0.757	-0.195	1.93E-09
4	196.0	1.113	-10.642	8.196	0.240	-0.169	6.10E-10
5	392.0	1.038	-13.831	13.722	0.182	-0.251	7.75E-10
6	784.0	0.962	-17.039	16.124	0.095	-0.252	4.75E-10
7	98.0	0.985	-16.081	0.000	0.017	-0.025	0.30E+00
8	9.8	1.006	-15.202	0.000	0.119	-0.021	0.00E+00
9	0.0	1.026	-14.324	0.000	1.057	0.000	0.00E+00

EAST HETTON, LOCATION B, COARSE  
VERTICAL DRAINAGE, OEDOMETER  
ANALYSIS OF CONSOLIDATION DATA

INITIAL MOISTURE CONTENT= 70.277  
FINAL MOISTURE CONTENT = 41.949  
INITIAL VOIDS RATIO = 1.153  
NATURAL BULK DENSITY= 1.297  
NATURAL DRY DENSITY= 0.762  
FINAL BULK DENSITY= 1.224  
FINAL DRY DENSITY= 0.862  
SPECIFIC GRAVITY= 1.640

LOAD NO.	PRESSURE (KN/M**2)	VOIDS RATIO	STRAIN PERCENT	CV (M**2/YR)	MV (M**2/MN)	CC	K M/SEC
1	9.8	1.133	-0.897	149.304	0.916	0.000	4.24E-08
2	19.6	1.114	-1.768	260.737	0.896	-0.062	7.24E-08
3	49.0	1.076	-3.563	321.141	0.622	-0.077	6.19E-08
4	98.0	1.039	-5.285	198.170	0.364	-0.123	2.24E-08
5	196.0	0.988	-7.624	38.427	0.252	-0.167	3.03E-08
6	392.0	0.929	-10.434	179.533	0.155	-0.201	8.64E-09
7	784.0	0.853	-13.897	167.366	0.095	-0.248	5.12E-09
8	98.0	0.875	-12.909	0.000	0.017	0.000	0.00E+00
9	9.8	0.903	-11.613	0.000	0.169	-0.028	0.30E+00
10	0.0	0.933	-10.199	0.000	1.633	0.000	0.00E+00

EAST HETTON OUTLET, FINE  
VERTICAL, OEDOMETER  
ANALYSIS OF CONSOLIDATION DATA

INITIAL MOISTURE CONTENT= 51.386  
FINAL MOISTURE CONTENT = 31.300  
INITIAL VOIDS RATIO = 1.076  
NATURAL BULK DENSITY= 1.527  
NATURAL DRY DENSITY= 1.008  
FINAL BULK DENSITY= 1.641  
FINAL DRY DENSITY= 1.250  
SPECIFIC GRAVITY= 2.093

LOAD NO.	PRESSURE (KN/M**2)	VOIDS RATIO	STRAIN PERCENT	CV (M**2/YR)	MV (M**2/MN)	CC	K M/SEC
1	9.8	1.014	-2.975	1.222	3.035	0.000	1.15E-09
2	19.6	0.944	-6.353	2.058	3.553	-0.233	2.27E-09
3	68.6	0.847	-11.011	2.072	1.015	-0.178	6.52E-10
4	117.7	0.766	-14.934	2.372	0.898	-0.347	7.99E-10
5	196.0	0.679	-19.119	3.588	0.628	-0.392	6.99E-10
6	392.0	0.598	-23.021	3.746	0.246	-0.269	2.86E-10
7	98.0	0.603	-22.749	0.000	0.012	-0.009	0.30E+00
8	9.8	0.643	-20.843	0.000	0.280	-0.040	0.30E+00
9	0.0	0.674	-19.331	0.000	1.950	0.000	0.00E+00

EAST HETTON OUTLET, COARSE  
VERTICAL, OEDOMETER  
ANALYSIS OF CONSOLIDATION DATA

INITIAL MOISTURE CONTENT= 49.253  
FINAL MOISTURE CONTENT = 35.715  
INITIAL VOIDS RATIO = 0.880  
NATURAL BULK DENSITY= 1.419  
NATURAL DRY DENSITY= 0.950  
FINAL BULK DENSITY= 1.385  
FINAL DRY DENSITY= 1.020  
SPECIFIC GRAVITY= 1.787

LOAD NO.	PRESSURE (KN/M**2)	VOIDS RATIO	STRAIN PERCENT	CV (M**2/YR)	MV (M**2/MN)	CC	K M/SEC
1	9.8	0.862	-0.957	1343.506	0.976	0.000	4.07E-07
2	19.6	0.848	-1.712	1326.494	0.778	-0.047	3.19E-07
3	68.6	0.815	-3.474	1297.013	0.366	-0.061	1.64E-07
4	117.7	0.793	-4.633	1248.715	0.244	-0.033	9.46E-08
5	196.0	0.769	-5.942	1540.024	0.175	-0.111	8.37E-08
6	392.0	0.726	-8.208	1432.443	0.123	-0.142	5.65E-08
7	98.0	0.732	-7.855	0.000	0.013	-0.011	0.30E+00
8	9.8	0.744	-7.251	0.000	0.074	-0.011	0.30E+00
9	0.0	0.751	-6.848	0.000	0.443	0.000	0.00E+00

SILVERHILL LAGOON 16. FINE  
 VERTICAL OEDOMETER  
 ANALYSIS OF CONSOLIDATION DATA

INITIAL MOISTURE CONTENT= 55.731  
 FINAL MOISTURE CONTENT = 23.423  
 INITIAL VOIDS RATIO = 1.380  
 NATURAL BULK DENSITY= 1.620  
 NATURAL DRY DENSITY= 1.040  
 FINAL BULK DENSITY= 1.934  
 FINAL DRY DENSITY= 1.567  
 SPECIFIC GRAVITY= 2.476

LOAD NO.	PRESSURE (KN/M**2)	VOIDS RATIO	STRAIN PERCENT	CV (M**2/YR)	MV (M**2/MN)	CC	K M/SEC
1	9.8	1.233	-6.164	2.034	6.289	0.000	3.97E-09
2	19.6	1.110	-11.331	1.531	5.619	-0.409	2.67E-09
3	49.0	0.912	-19.664	1.800	3.196	-0.498	1.78E-09
4	98.0	0.744	-26.712	2.235	1.791	-0.557	1.24E-09
5	196.0	0.598	-32.843	3.709	0.854	-0.485	9.31E-10
6	392.0	0.370	-42.437	2.676	0.725	-0.753	6.05E-10
7	98.0	0.406	-40.910	0.000	0.090	-0.050	0.00E+00
8	9.8	0.515	-36.351	0.000	0.875	-0.109	0.00E+00
9	0.0	0.580	-33.607	0.000	4.400	0.000	0.00E+00

SILVERHILL LAGOON 16. COARSE  
 VERTICAL OEDOMETER  
 ANALYSIS OF CONSOLIDATION DATA

INITIAL MOISTURE CONTENT= 63.817  
 FINAL MOISTURE CONTENT = 48.978  
 INITIAL VOIDS RATIO = 1.066  
 NATURAL BULK DENSITY= 1.325  
 NATURAL DRY DENSITY= 0.809  
 FINAL BULK DENSITY= 1.314  
 FINAL DRY DENSITY= 0.982  
 SPECIFIC GRAVITY= 1.671

LOAD NO.	PRESSURE (KN/M**2)	VOIDS RATIO	STRAIN PERCENT	CV (M**2/YR)	MV (M**2/MN)	CC	K M/SEC
1	9.8	1.041	-1.206	461.993	1.231	0.000	1.76E-07
2	19.6	1.021	-2.219	451.737	1.046	-0.070	1.47E-07
3	49.0	0.992	-3.618	667.598	0.487	-0.073	1.01E-07
4	98.0	0.954	-5.451	645.557	0.388	-0.126	7.77E-08
5	196.0	0.911	-7.525	615.405	0.224	-0.142	4.30E-08
6	392.0	0.850	-10.468	586.619	0.162	-0.202	2.95E-08
7	98.0	0.858	-10.092	0.000	0.015	-0.013	0.00E+00
8	9.8	0.878	-9.117	0.000	0.122	-0.020	0.00E+00
9	0.0	0.894	-8.346	0.000	0.867	0.000	0.00E+00

PECKFIELD LAGOON 7, SAMPLE 1  
 VERTICAL DRAINAGE 6" CELL  
 ANALYSIS OF CONSOLIDATION DATA

INITIAL MOISTURE CONTENT= 62.744  
 FINAL MOISTURE CONTENT = 26.704  
 INITIAL VOIDS RATIO = 1.186  
 NATURAL BULK DENSITY= 1.497  
 NATURAL DRY DENSITY= 0.865  
 FINAL BULK DENSITY= 1.181  
 FINAL DRY DENSITY= 0.931  
 SPECIFIC GRAVITY= 1.890

LOAD NO.	PRESSURE (KN/M**2)	VOIDS RATIO	STRAIN PERCENT	CV (M**2/YR)	MV (M**2/MN)	CC	K M/SEC
1	20.0	1.164	-0.998	19.271	0.499	0.000	2.98E-09
2	40.0	1.127	-2.708	16.372	0.863	-0.124	4.38E-09
3	80.0	1.074	-5.118	28.834	0.619	-0.175	5.54E-09
4	160.0	1.020	-7.571	37.423	0.323	-0.178	3.75E-09
5	320.0	0.956	-10.503	34.401	0.199	-0.213	2.12E-09
6	110.0	0.969	-9.929	0.000	0.031	-0.027	0.00E+00
7	10.0	1.001	-8.469	0.000	0.162	-0.031	0.00E+00
8	0.0	1.031	-7.083	0.000	1.514	0.000	0.00E+00

PECKFIELD LAGOON 7, SAMPLE 2  
 VERTICAL, 6" ROWE CELL  
 ANALYSIS OF CONSOLIDATION DATA

INITIAL MOISTURE CONTENT= 66.156  
 FINAL MOISTURE CONTENT = 28.645  
 INITIAL VOIDS RATIO = 1.257  
 NATURAL BULK DENSITY= 1.399  
 NATURAL DRY DENSITY= 0.842  
 FINAL BULK DENSITY= 1.184  
 FINAL DRY DENSITY= 0.921  
 SPECIFIC GRAVITY= 1.900

LOAD NO.	PRESSURE (KN/M**2)	VOIDS RATIO	STRAIN PERCENT	CV (M**2/YR)	MV (M**2/MN)	CC	K M/SEC
1	10.0	1.242	-0.646	5.552	0.646	0.000	1.11E-09
2	20.0	1.212	-1.974	5.443	1.337	-0.100	2.22E-09
3	40.0	1.161	-4.233	5.247	1.152	-0.169	1.87E-09
4	80.0	1.072	-8.209	5.529	1.038	-0.298	1.78E-09
5	160.0	1.018	-10.597	7.902	0.325	-0.179	7.97E-10
6	320.0	0.936	-14.201	7.032	0.252	-0.270	5.45E-10
7	110.0	0.949	-13.653	0.000	0.030	-0.027	0.00E+00
8	10.0	0.988	-11.920	0.000	0.201	-0.038	0.00E+00
9	0.0	1.064	-8.553	0.000	3.823	0.000	0.00E+00

PECKFIELD LAGOON 7, SAMPLE 3  
 VERTICAL DRAINAGE 6" CELL  
 ANALYSIS OF CONSOLIDATION DATA

INITIAL MOISTURE CONTENT= 42.928  
 FINAL MOISTURE CONTENT = 24.848  
 INITIAL VOIDS RATIO = 0.810  
 NATURAL BULK DENSITY= 1.490  
 NATURAL DRY DENSITY= 1.042  
 FINAL BULK DENSITY= 1.455  
 FINAL DRY DENSITY= 1.166  
 SPECIFIC GRAVITY= 1.886

LOAD NO.	PRESSURE (KN/M**2)	VOIDS RATIO	STRAIN PERCENT	CV (M**2/YR)	MV (M**2/MN)	CC	K M/SEC
1	10.0	0.766	-2.394	780.570	2.384	0.000	5.77E-07
2	20.0	0.715	-5.231	14.528	2.917	-0.171	1.31E-08
3	40.0	0.678	-7.290	14.377	1.086	-0.124	4.84E-09
4	80.0	0.635	-9.664	22.656	0.640	-0.143	4.50E-09
5	160.0	0.587	-12.278	27.438	0.362	-0.157	3.08E-09
6	320.0	0.544	-14.671	32.901	0.171	-0.144	1.73E-09
7	160.0	0.549	-14.465	0.000	0.015	-0.012	0.00E+00
8	40.0	0.565	-13.539	0.000	0.090	-0.028	0.00E+00
9	10.0	0.583	-12.512	0.000	0.396	-0.031	0.00E+00
10	0.0	0.618	-10.600	0.000	2.185	0.000	0.00E+00

PECKFIELD LAGOON 7, SAMPLE 4  
 VERTICAL DRAINAGE 6" CELL  
 ANALYSIS OF CONSOLIDATION DATA

INITIAL MOISTURE CONTENT= 74.267  
 FINAL MOISTURE CONTENT = 22.934  
 INITIAL VOIDS RATIO = 1.133  
 NATURAL BULK DENSITY= 1.247  
 NATURAL DRY DENSITY= 0.715  
 FINAL BULK DENSITY= 0.964  
 FINAL DRY DENSITY= 0.784  
 SPECIFIC GRAVITY= 1.526

LOAD NO.	PRESSURE (KN/M**2)	VOIDS RATIO	STRAIN PERCENT	CV (M**2/YR)	MV (M**2/MN)	CC	K M/SEC
1	20.0	1.068	-3.047	2403.939	1.523	0.000	1.14E-04
2	40.0	1.040	-3.953	2398.370	0.467	-0.064	3.35E-07
3	80.0	1.009	-5.814	2242.539	0.484	-0.132	3.17E-07
4	160.0	0.957	-8.271	2141.291	0.326	-0.174	2.17E-07
5	320.0	0.900	-10.947	2392.993	0.182	-0.170	1.35E-07
6	160.0	0.905	-10.634	0.000	0.015	-0.012	0.00E+00
7	40.0	0.924	-9.794	0.000	0.083	-0.032	0.00E+00
8	0.0	0.945	-8.818	0.000	0.271	0.000	0.00E+00

VERTICAL OEDOMETER

ANALYSIS OF CONSOLIDATION DATA

INITIAL MOISTURE CONTENT= 27.974  
 FINAL MOISTURE CONTENT = 21.424  
 INITIAL VOIDS RATIO = 0.652  
 NATURAL BULK DENSITY= 1.805  
 NATURAL DRY DENSITY= 1.410  
 FINAL BULK DENSITY= 1.914  
 FINAL DRY DENSITY= 1.576  
 SPECIFIC GRAVITY= 2.329

LOAD NO.	PRESSURE (KN/M**2)	VOIDS RATIO	STRAIN PERCENT	CV (M**2/YR)	MV (M**2/MN)	CC	K M/SEC
1	9.8	0.635	-1.003	1229.135	1.136	0.000	4.33E-07
2	19.6	0.622	-1.789	1207.128	0.814	-0.043	3.05E-07
3	49.0	0.595	-3.421	1177.571	0.565	-0.068	2.06E-07
4	98.0	0.559	-5.632	1131.571	0.467	-0.121	1.64E-07
5	196.0	0.512	-8.474	1072.573	0.307	-0.156	1.02E-07
6	392.0	0.439	-12.842	990.979	0.244	-0.240	7.48E-08
7	98.0	0.448	-12.316	0.000	0.021	-0.014	0.00E+00
8	9.8	0.465	-11.316	0.000	0.129	-0.017	0.00E+00
9	0.0	0.478	-10.527	0.000	0.908	0.000	0.00E+00

MALTY LOCATION 2, 1.35M, 11.11.78

VERTICAL OEDOMETER

ANALYSIS OF CONSOLIDATION DATA

INITIAL MOISTURE CONTENT= 42.799  
 FINAL MOISTURE CONTENT = 29.712  
 INITIAL VOIDS RATIO = 0.711  
 NATURAL BULK DENSITY= 1.386  
 NATURAL DRY DENSITY= 0.971  
 FINAL BULK DENSITY= 1.362  
 FINAL DRY DENSITY= 1.050  
 SPECIFIC GRAVITY= 1.661

LOAD NO.	PRESSURE (KN/M**2)	VOIDS RATIO	STRAIN PERCENT	CV (M**2/YR)	MV (M**2/MN)	CC	K M/SEC
1	9.8	0.687	-1.375	95.798	1.403	0.000	4.34E-09
2	19.6	0.671	-2.304	24.374	0.961	-0.053	7.26E-09
3	49.0	0.636	-4.371	128.693	0.720	-0.089	7.87E-09
4	98.0	0.613	-5.727	178.800	0.285	-0.077	1.60E-09
5	196.0	0.578	-7.756	88.002	0.220	-0.115	5.99E-09
6	392.0	0.543	-9.842	97.607	0.115	-0.119	3.45E-09
7	98.0	0.551	-9.330	0.000	0.019	-0.015	0.00E+00
8	9.8	0.567	-8.401	0.000	0.116	-0.016	0.00E+00
9	0.0	0.582	-7.557	0.000	0.940	0.000	0.00E+00

MALTY LOCATION 1, 1.2M, 11.11.78

VERTICAL OEDOMETER

ANALYSIS OF CONSOLIDATION DATA

INITIAL MOISTURE CONTENT= 62.479  
 FINAL MOISTURE CONTENT = 28.103  
 INITIAL VOIDS RATIO = 1.204  
 NATURAL BULK DENSITY= 1.421  
 NATURAL DRY DENSITY= 0.874  
 FINAL BULK DENSITY= 1.261  
 FINAL DRY DENSITY= 0.984  
 SPECIFIC GRAVITY= 1.927

LOAD NO.	PRESSURE (KN/M**2)	VOIDS RATIO	STRAIN PERCENT	CV (M**2/YR)	MV (M**2/MN)	CC	K M/SEC
1	9.8	1.154	-2.278	4.540	2.324	0.000	3.27E-09
2	19.6	1.093	-5.038	6.937	2.883	-0.202	6.11E-07
3	49.0	1.028	-7.981	8.148	1.054	-0.163	2.56E-09
4	98.0	0.978	-10.268	10.055	0.507	-0.167	1.58E-09
5	196.0	0.930	-12.427	8.719	0.246	-0.158	6.64E-10
6	392.0	0.870	-15.142	13.033	0.158	-0.199	6.39E-10
7	98.0	0.876	-14.860	0.000	0.011	-0.010	0.00E+00
8	9.8	0.895	-14.013	0.000	0.113	-0.019	0.00E+00
9	0.0	0.958	-11.170	0.080	3.373	0.000	0.00E+00

MALTY 1.6-1.9M, FINE

VERTICAL OEDOMETER

ANALYSIS OF CONSOLIDATION DATA

INITIAL MOISTURE CONTENT= 72.398  
 FINAL MOISTURE CONTENT = 48.759  
 INITIAL VOIDS RATIO = 1.672  
 NATURAL BULK DENSITY= 1.490  
 NATURAL DRY DENSITY= 0.864  
 FINAL BULK DENSITY= 1.779  
 FINAL DRY DENSITY= 1.196  
 SPECIFIC GRAVITY= 2.309

LOAD NO.	PRESSURE (KN/M**2)	VOIDS RATIO	STRAIN PERCENT	CV (M**2/YR)	MV (M**2/MN)	CC	K M/SEC
1	9.8	1.408	-3.361	3.269	10.062	0.000	1.02E-08
2	19.6	1.316	-13.320	3.001	3.916	-0.337	3.64E-09
3	49.0	1.142	-19.825	3.028	2.553	-0.437	2.40E-09
4	98.0	0.997	-25.245	3.039	1.380	-0.481	1.32E-09
5	196.0	0.870	-29.995	4.738	0.648	-0.422	9.52E-10
6	392.0	0.703	-36.087	4.055	0.444	-0.541	5.58E-10
7	98.0	0.745	-34.693	0.000	0.074	-0.052	0.00E+00
8	9.8	0.845	-30.924	0.000	0.654	-0.101	0.00E+00
9	0.0	0.931	-27.723	0.000	4.728	0.000	0.00E+00

APPENDIX A.6.2    IN-SITU PERMEABILITY DETERMINATION

The data for in-situ permeability determinations were collected by Mr.M.J.Henderson, with some assistance from the current writer. The complete data and results are presented by Henderson (1979). However, the interpretation of the data is apparently in error, and consequently so too are the permeability values quoted by Henderson. Therefore amended values are quoted herein. In the case of the constant and falling head tests, the shape factor used by Henderson is after Donnan and Aravanici (1961) and has a value of 130mm. As shown in chapter 6.3. Al-Dahir and Morgenstern(1969) and others show that the work of Donnan and Aravanici is in error, and the shape factor used herein is 150mm after Al-Dahir and Morgenstern. Therefore the in-situ permeability values in Tables A.6.2.1 and A.6.3.1 differ from those of Henderson by a constant factor of 130/150.

In the case of the interpretation after Gibson (1963), Henderson (1979) uses as the radius of the piezometer a value of 10mm, which is the radius of the cylindrical piezometer. However, the radius used should be that of a sphere with the same infiltration surface area, which gives a value of 12mm. This difference is more serious than the error involved in the constant and falling head tests, because the radius appears to the power of four in the calculation of the in-situ coefficient of consolidation. The results in Tables A.6.2.2. and A.6.3.2 therefore also differ from those quoted by Henderson by a constant factor.

Table A.6.2.1 Constant head in-situ permeability determinations, lagoon 109B  
East Hetton.

Loc- ation	Permeability m/s x 10 <sup>-</sup>		Loc- ation	Permeability m/s x 10 <sup>-</sup>		Loc- ation	Permeability m/s x 10 <sup>-</sup>	
1	8.57	-6	23	8.93	-7	45	1.28	-6
2	6.99	-6	24	4.55	-7	46	6.26	-7
3	1.53	-5	25	1.72	-7	47	1.76	-6
4	1.10	-5	26	5.14	-7	48	4.18	-7
5	9.71	-6	27	5.36	-8	49	1.17	-6
6	1.40	-7	28	9.36	-5	50	1.01	-6
7	2.70	-6	29	4.00	-7	51	5.48	-7
8	1.59	-5	30	1.31	-7	52	5.88	-7
9	7.76	-7	31	1.49	-5	53	3.93	-7
10	1.98	-5	32	1.96	-7	54	3.18	-7
11	1.88	-6	33	2.03	-7	55	2.08	-6
12	4.71	-6	34	2.94	-6	56	5.10	-7
13	2.01	-6	35	5.01	-6	57	2.46	-6
14	8.67	-7	36	6.20	-6	58	3.66	-6
15	1.92	-6	37	1.46	-7	59	2.36	-6
16	5.48	-7	38	1.27	-5	60	2.96	-8
17	3.94	-7	39	4.50	-7	61	8.75	-7
18	8.75	-6	40	2.11	-6	62	8.84	-7
19	2.34	-7	41	1.37	-6	63	8.42	-8
20	1.53	-5	42	5.05	-6	65	7.57	-6
21	2.86	-6	43	5.62	-7	65	7.07	-9
22	9.19	-7	44	1.59	-6	66	- no flow -	
						67	5.36	-9

Table A.6.2.2 In-situ permeability and coefficient of consolidation,  
after Gibson(1963).

Loc- ation	Permeability m/s x 10 <sup>-</sup>		c <sub>v</sub> m <sup>2</sup> /yr	Loc- ation	Permeability m/s x 10 <sup>-</sup>		c <sub>v</sub> m <sup>2</sup> /yr
3	1.41	-5	278	47	2.74	-6	23.3
7	8.85	-7	0.200	47*	1.48	-6	17.9
9	1.16	-6	21.7	48	3.29	-7	3.41
15	1.23	-6	1.62	49	1.11	-6	255
17	3.46	-7	4.22	50	9.92	-7	288
21	2.79	-6	-	52	6.99	-7	5.68
23	8.69	-7	-	54	3.09	-7	-
35	4.06	-6	19.8	55	2.03	-6	-
37	1.27	-7	4.50	57	2.23	-6	364
39	4.04	-7	4.23	58	4.02	-6	77.9
39*	4.49	-7	9.28	59	2.34	-6	-
40	1.70	-6	14.2	61	6.97	-7	7.20
41	9.34	-7	3.39	63	7.84	-8	27.0
44	1.48	-6	27.2	64	4.55	-6	2.19
45	1.01	-6	3.11	65	6.54	-9	0.659
46	3.88	-7	1.47	67	6.30	-9	0.0547

\* Two interpretations possible, the former is referred to in the text.



APPENDIX A.6.3 IN-SITU PERMEABILITY MEASUREMENTS, SILVERHILL.

Table A.6.3.1 Constant and variable head test results.

a. Constant head.

Loc- ation	Permeability m/s x 10 <sup>-7</sup>	Loc- ation	Permeability m/s x 10 <sup>-7</sup>
8	6.61 -6	21	5.07 -4
9	2.44 -5	22	1.34 -6
10	5.25 -4	23	1.76 -6
11	3.07 -6	26	3.10 -7
12	7.15 -4	26*	7.71 -8
13	4.00 -4	29	1.66 -4
14	4.69 -7	31	8.05 -4
14*	1.53 -7	35	6.71 -4
16	4.11 -4	36	5.09 -4
17	9.96 -6	37	1.55 -8
17*	3.73 -6	39	8.65 -8
18	4.90 -7		

Retests carried out at later dates.

16*	5.50 -4	36*	2.32 -5
16*	5.38 -4		
16*	1.29 -3		

b. Variable head tests.

15	1.87 -8	27	8.41 -9
19	1.19 -8	31	2.56 -8
25	1.97 -9	38	1.85 -9
25*	1.33 -9		

\* Where more than one interpretation is possible, or there has been a retest, the first value is that referred to in the text.

Table A.6.3.2 In-situ permeability and coefficient of consolidation, after Gibson (1963).

Loc- ation	Permeability m/s x 10 <sup>-7</sup>	$c_v$ m <sup>2</sup> /yr.
8	6.47 -6	-
9	2.30 -5	480
14	3.08 -7	0.879
17	9.67 -6	18900
18	3.99 -7	1.80
22	1.30 -6	-
23	1.61 -6	139
26	2.97 -7	7.22

